

11-02

Experimental Studies of Shock-Wave/ Wall-Jet Interaction in Hypersonic Flow

**Michael S. Holden
Kathleen Rodriguez**

**CALSPAN-UB RESEARCH CENTER
Buffalo, New York 14225**

(NASA-CR-195957) EXPERIMENTAL
STUDIES OF SHOCK-WAVE/WALL-JET
INTERACTION IN HYPERSONIC FLOW,
PART A Final Report (Calspan-State
Univ. of New York Joint Venture)
226 p

N94-34964

Unclassified

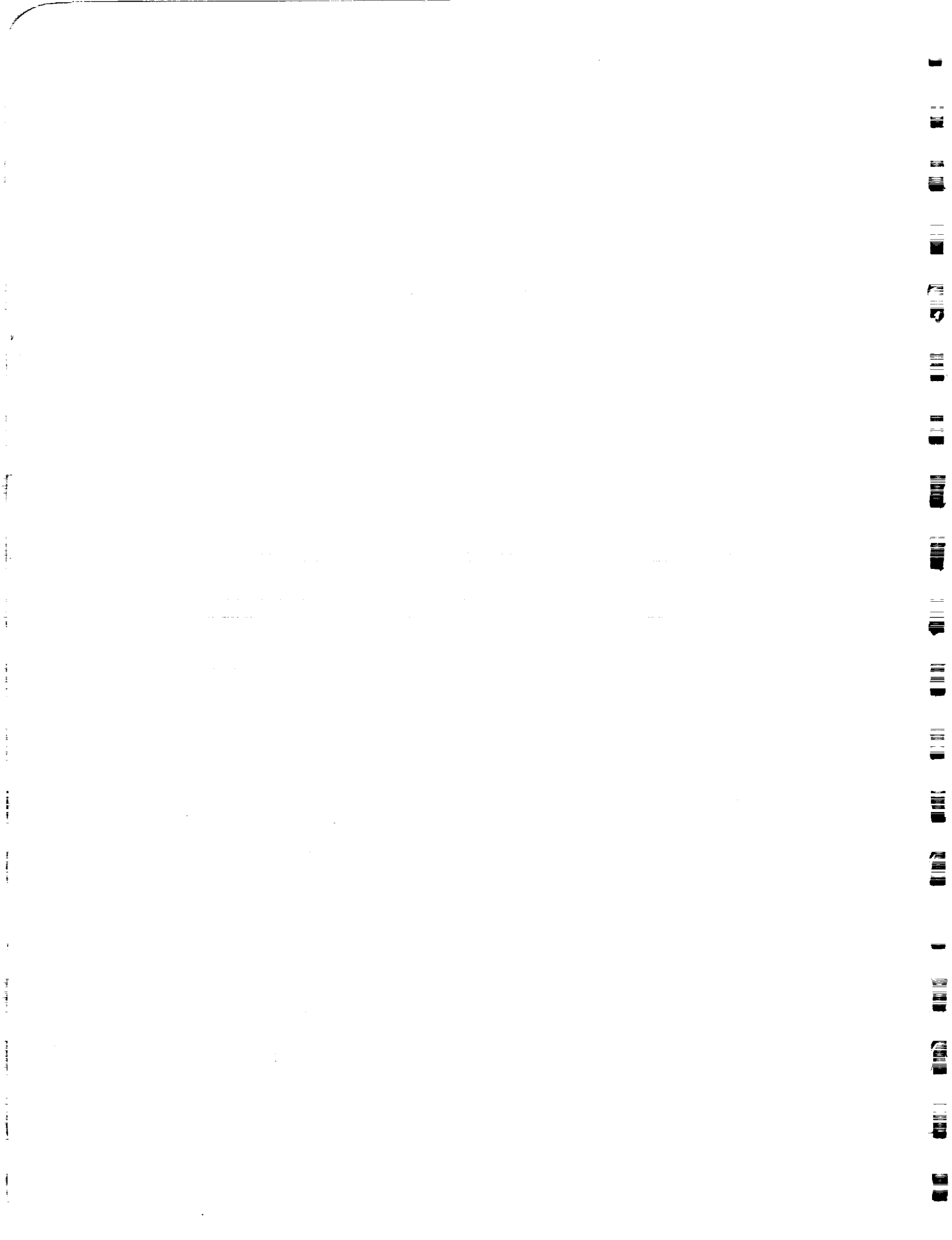
G3702 0010565

**Final Report Part A
Grant Number NAG 1-790
May 1994**



National Aeronautics and
Space Administration

Langley Research Center
Hampton, Virginia 23665-5225





Experimental Studies of Shock-Wave/ Wall Jet Interaction in Hypersonic Flow

MAY 1994

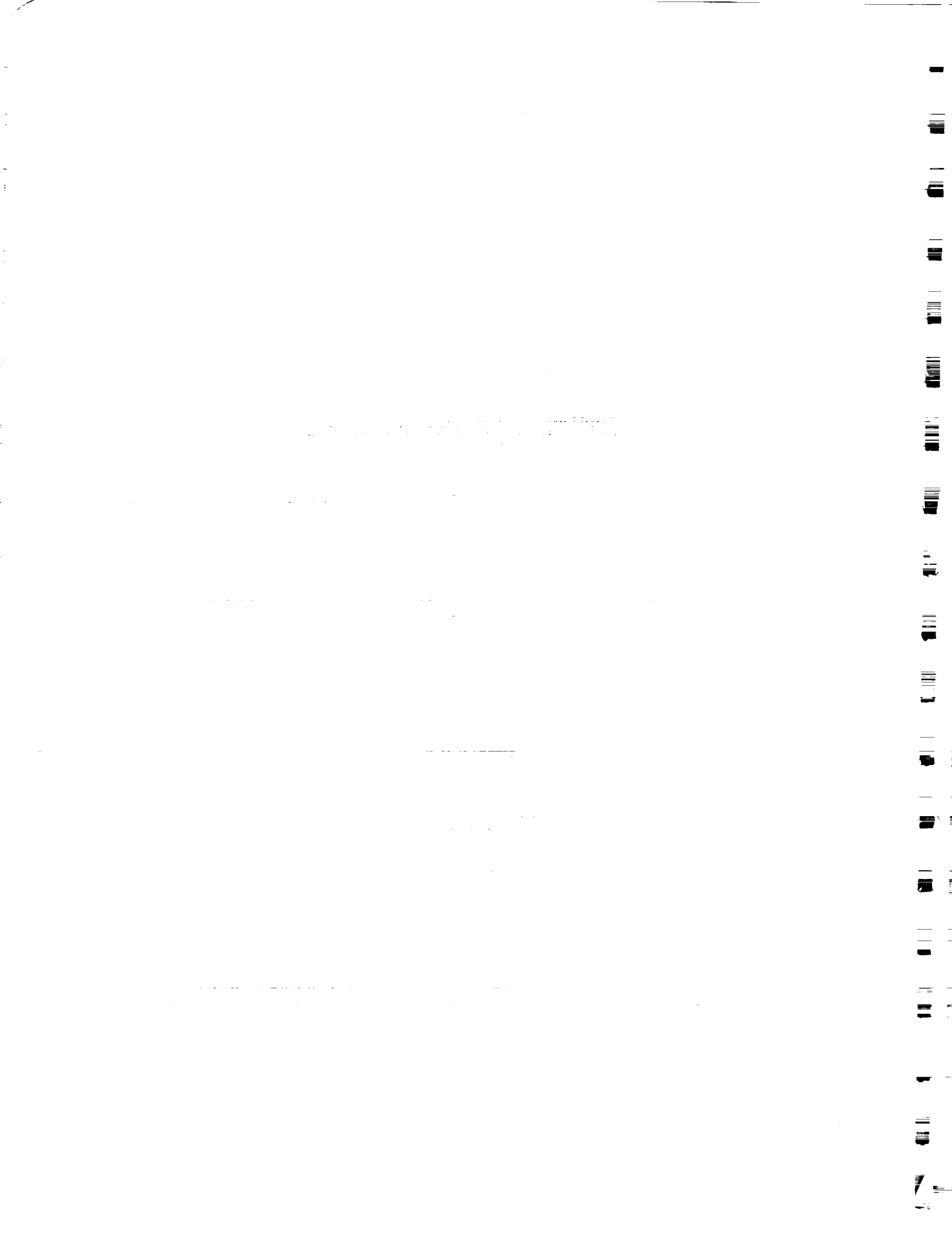
This experimental program was conducted under Grant Number NAG 1-790. The analysis and publication of measurements was funded internally and with the contract with UDRI.

Prepared By:

**Michael S. Holden
Kathleen Rodriguez
Calspan-UB Research Center
P.O. Box 400
Buffalo, NY 14225**

Prepared For:

**NATIONAL AERONAUTICS AND SPACE ADMINISTRATION
Langley Research Center
Hampton, Virginia 23665-5225**



ABSTRACT

Experimental studies have been conducted to examine slot film cooling effectiveness and the interaction between the cooling film and an incident planar shock wave in turbulent hypersonic flow. The experimental studies were conducted in the 48-inch shock tunnel at Calspan at a freestream Mach number of close to 6.4 and at a Reynolds number of 35×10^6 based on the length of the model at the injection point. The Mach 2.3 planar wall jet was generated from 40 transverse nozzles (with heights of both 0.080 inch and 0.120 inch), producing a film that extended the full width of the model. The nozzles were operated at pressures and velocities close to matching the freestream, as well as at conditions where the nozzle flows were over- and under-expanded. A two-dimensional shock generator was used to generate oblique shocks that deflected the flow through total turnings of 11, 16, and 21 degrees; the flows impinged downstream of the nozzle exits. Detailed measurements of heat transfer and pressure were made both ahead and downstream of the injection station, with the greatest concentration of measurements in the regions of shock-wave/boundary layer interaction. The major objectives of these experimental studies were to explore the effectiveness of film cooling in the presence of regions of shock-wave/boundary layer interaction and, more specifically, to determine how boundary layer separation and the large recompression heating rates were modified by film cooling. Detailed distributions of heat transfer and pressure were obtained in the incident-shock/wall-jet interaction region for a series of shock strengths and impingement positions for each of the two nozzle heights. Measurements were also made to examine the effects of nozzle lip thickness on cooling effectiveness. The major conclusion from these studies was that the effect of the cooling film could be readily dispersed by relatively weak incident shocks, so the peak heating in the recompression region was not significantly reduced by even the largest levels of film cooling. For the case studies in the absence of film cooling, the interaction regions were unseparated. However, adding film cooling resulted in regions of boundary layer separation induced in the film cooling layer—the size of which regions first increased and then decreased with increased film cooling. Surprisingly, the size of the separated regions and the magnitude of the recompression heating were not strongly influenced by the thickness of the cooling film, nor by the point of shock impingement relative to the exit plane of the nozzles. The lip thickness was found to have little effect on cooling effectiveness. Measurements with and in the absence of shock interaction were compared with the results of earlier experimental studies and correlated in terms of the major parameters controlling these flows.

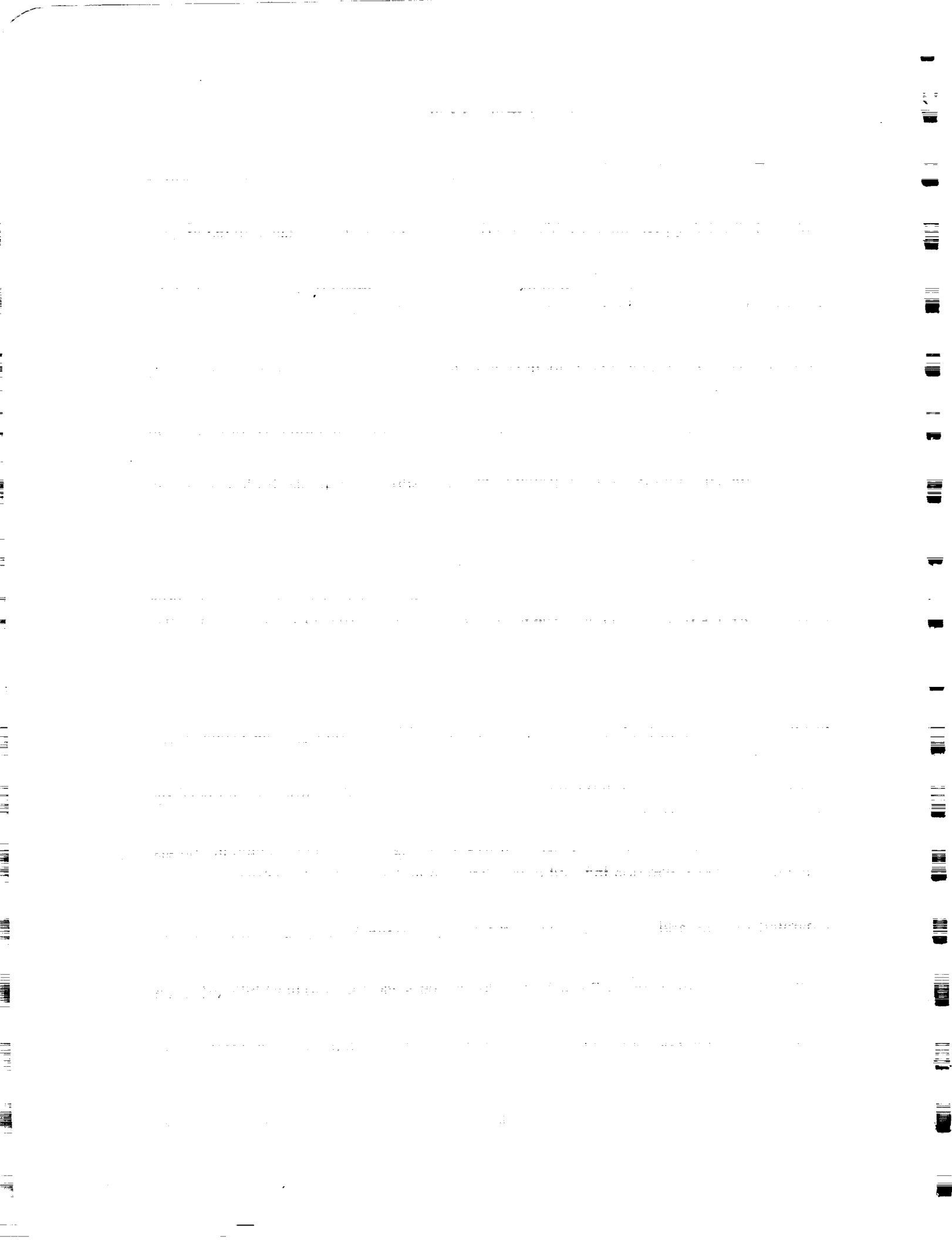


Table of Contents

<u>Section</u>	<u>Page</u>
ABSTRACT.....	ii
NOMENCLATURE.....	x
1 INTRODUCTION.....	1
2 EXPERIMENTAL PROGRAM	7
2.1 PROGRAM OBJECTIVES AND DESIGN.....	7
2.1.1 Program Objectives.....	7
2.1.2 Design of the Experiment.....	7
2.2 EXPERIMENTAL FACILITIES AND TEST CONDITIONS.....	8
2.2.1 Experimental Facilities	8
2.2.2 Evaluation of Test Conditions.....	11
2.2.3 Accuracy of Test Conditions	13
2.2.4 Airflow Calibrations of the "A" Nozzle	13
2.3 MODEL AND INSTRUMENTATION	13
2.3.1 Film-Cooling/Shock-Interaction Model.....	13
2.3.2 Calculation of Coolant Rates	19
2.3.3 Heat Transfer Instrumentation.....	21
2.3.4 Pressure Instrumentation.....	22
2.3.5 Measurement Recording System.....	24
2.3.6 Holographic Interferometry.....	24
2.3.7 Flow Visualization.....	25
3 RESULTS AND DISCUSSION.....	26
3.1 INTRODUCTION.....	26
3.2 MEASUREMENTS TO SELECT FREESTREAM CONDITIONS.....	26
3.3 BOUNDARY LAYER PROFILE MEASUREMENTS UPSTREAM OF SLOT INJECTION	29
3.4 MEASUREMENTS IN REGIONS OF SHOCK-WAVE/BOUNDARY LAYER INTERACTION ON FLAT PLATE CONFIGURATION WITHOUT FILM COOLING.....	29
3.5 BASELINE MEASUREMENTS WITH FILM COOLING IN THE ABSENCE OF SHOCK INTERACTION.....	30
3.5.1 Measurements of Film Cooling Effectiveness.....	30
3.5.2 Lip Thickness Effect on Slot-Cooling Effectiveness	37

Table of Contents (continued)

<u>Section</u>		<u>Page</u>
3.6	STUDIES OF SHOCK-WAVE/WALL-JET INTERACTION.....	41
3.6.1	Purpose and Scope of Studies.....	41
3.6.2	Studies with 0.080-Inch Slot Configuration.....	41
3.6.3	Studies with 0.120-Inch Slot Configuration.....	50
3.6.4	Lip Thickness Effects on Slot Cooling in Regions of Shockwave Boundary Layer Interaction	64
4	CONCLUSIONS	66
5	REFERENCES	68
	Appendix A.....	A-1
	Appendix B.....	B-1
	Appendix C.....	C-1

List of Figures

Figure	Page
1 Wall Pressure and Wall Heat Transfer Distributions (Alzner and Zakkay)	4
2 Heat Transfer Distributions for Air Injection (Alzner and Zakkay)	4
3 Heat Transfer Distributions for Hydrogen Injection (Alzner and Zakkay).....	5
4 Effect of Film Cooling on Shock-Impingement Heating (Ledford and Stollery).....	5
5 Performance Map of Calspan's Shock Tunnels.....	9
6 Wave Diagram for Tailored-Interface Condition	9
7 Test Time Available for Tailored-Interface Operations of Shock Tunnel.....	10
8 Mach Number Distribution for "A" Nozzle, $M_\infty=6.4$	15
9 Mach Number Distribution for "A" Nozzle, $M_\infty=7.9$	15
10 Model Assembly Showing Generator and Injector Nozzles	16
11 View of Model Showing Nozzle Slots and Highly Instrumented Flat Plate	16
12 Film-Cooling/Shock-Interaction Model Installed in Calspan's 48-Inch Shock Tunnel.....	17
13 Schematic Diagram of Injector Section of Model	18
14 Instrumentation Positions on Film-Cooling/Shock-Interaction Model	20
15a Boundary Layer Survey Rake Installed Upstream of Nozzle Exit	23
15b Schlieren Photograph of Flow Over Survey Rake.....	23
16a Comparison Between Flat-Plate Heat Transfer Measurements and Simple Predictions.....	28
16b Pressure Measurements on Flat Plate.....	28
17 Schlieren Photographs of Slot-Cooling Runs for 0.120-Inch Slot With a Range of Injection Ratios	31
18a Heat Transfer Variation With Mass Addition for 0.080-Inch Slot	33
18b Heat Transfer Variation With Mass Addition for 0.120-Inch Slot	33
19a Effective Efficiency" of Film Cooling for 0.080-Inch Slot	34

List of Figures (cont.)

Figure				
19b Effective Efficiency" of Film Cooling for 0.120-Inch Slot				34
20a Correlation of Film-Cooling Effective Efficiency With Simple Scaling Parameters				35
20b Correlation of Film-Cooling Effective Efficiency With Simple Scaling Parameters				35
21a Correlations of Effective Efficiency of Film Cooling.....				36
21b Correlations of Effective Efficiency of Film Cooling.....				36
21c Correlations of Effective Efficiency of Film Cooling.....				36
22a Heat Transfer Variation with Lip Thickness fpr 0.120-Inch Slot, Matched Pressure Condition ($\lambda=0.094$)				38
22b Heat Transfer Variation with Lip Thickness for 0.120-Inch Slot, "Over-Matched" Pressure Condition ($\lambda=0.222$)				39
23a Heat Transfer Measurements in Shock-Interaction Region, Without Film Cooling.....				40
23b Pressure Measurements in Shock-Interaction Region, Without Film Cooling.....				40
24a Range of Compression Angles for Present Study Compared With Those to Induce Incipient Separation (Holden AIAA Paper 77-45)				30
24b Correlation of Maximum Heating Rate in Wedge- and Externally Generated Shock-Induced Turbulent Separated Flows (Holden AIAA Paper 77-45).....				42
25a Heat Transfer Distribution in Regions of Incident-Shock/Wall-Jet Interaction ($\Theta_{sg}=10.5$ Degrees, Slot Height = 0.080 Inch)				42
25b Pressure Distribution in Regions of Incident-Shock/Wall-Jet Interaction ($\Theta_{sg}=10.5$ Degrees, Slot Height = 0.080 Inch)				43
26 Schlieren Photographs for Incident-Shock/Wall-Jet Interactions ($\Theta_{sg}=10.5$ Degrees, Slot Height = 0.080 Inch)				44
27a Unseparated Shock-Wave/Cooling-Film Interaction				45
27b Separated Shock-Wave/Cooling-Film Interaction.....				45

List of Figures (cont.)

Figure		Page
28	Heat Transfer Distribution in Separation Region (Θ_{sg} = 10.5 Degrees, Slot Height = 0.080 Inch)	46
29	Typical Distributions of Heat Transfer and Pressure in Interaction Region (Θ_{sg} = 10.5 Degrees, Slot Height = 0.080 Inch)	46
30a	Heat Transfer Distribution in Regions of Incident-Shock/Wall-Jet Interaction (Θ_{sg} = 8.0 Degrees, Slot Height = 0.080 Inch).....	48
30b	Pressure Distribution in Regions of Incident-Shock/Wall-Jet Interaction (Θ_{sg} = 8.0 Degrees, Slot Height = 0.080 Inch).....	48
31	Schlieren Photographs for Incident-Shock/Wall-Jet Interactions (Θ_{sg} = 8.0 Degrees, Slot Height = 0.080 Inch).....	49
32	Heat Transfer Distribution in Separation Region (Θ_{sg} = 8.0 Degrees, Slot Height = 0.080 Inch)	51
33	Typical Distributions of Heat Transfer and Pressure in Separated Interaction Region (Θ_{sg} = 8.0 Degrees, Slot Height = 0.080 Inch)	51
34	Heat Transfer Distribution in Regions of Incident-Shock/Wall-Jet Interaction (Θ_{sg} = 5.5 Degrees, Slot Height = 0.080 Inch).....	52
35	Pressure Distribution in Regions of Incident-Shock/Wall-Jet Interaction (Θ_{sg} = 5.5 Degrees, Slot Height = 0.080 Inch).....	52
36	Schlieren Photographs for Incident-Shock/Wall-Jet Interactions (Θ_{sg} = 5.5 Degrees, Slot Height = 0.080 Inch).....	53
37	Heat Transfer Distribution in Separation Region (Θ_{sg} = 5.5 Degrees, Slot Height = 0.080 Inch)	54
38	Typical Distributions of Heat Transfer and Pressure in Separated Interaction Region (Θ_{sg} = 5.5 Degrees, Slot Height = 0.080 Inch)	54
39	Variation of Separated Flow Length With Blowing Rate for Various Incident-Shock Strengths (Slot Height = 0.080 Inch).....	55
40	Variation of Maximum Heating Rate With Film-Coolant Flow Rate (Slot Height = 0.080 Inch)	55

List of Figures (cont.)

Figure	Page
41 Heat Transfer Distribution in Regions of Incident-Shock/Wall-Jet Interaction ($\Theta_{sg} = 8.0$ Degrees, Slot Height = 0.120 Inch).....	57
42 Pressure Distribution in Regions of Incident-Shock/Wall-Jet Interaction ($\Theta_{sg} = 8.0$ Degrees, Slot Height = 0.120 Inch).....	57
43 Schlieren Photographs for Incident-Shock/Wall-Jet Interactions ($\Theta_{sg} = 8.0$ Degrees, Slot Height = 0.120 Inch).....	58
44 Heat Transfer Distribution in Separation Region ($\Theta_{sg} = 8.0$ Degrees, Slot Height = 0.120 Inch)	59
45 Typical Distributions of Heat Transfer and Pressure in Separated Interaction Region ($\Theta_{sg} = 8.0$ Degrees, Slot Height = 0.120 Inch)	59
46 Heat Transfer Distribution in Regions of Incident-Shock/Wall-Jet Interaction ($\Theta_{sg} = 5.5$ Degrees, Slot Height = 0.120 Inch).....	60
47 Pressure Distribution in Regions of Incident-Shock/Wall-Jet Interaction ($\Theta_{sg} = 5.5$ Degrees, Slot Height = 0.120 Inch).....	60
48 Schlieren Photographs for Incident-Shock/Wall-Jet Interactions ($\Theta_{sg} = 5.5$ Degrees, Slot Height = 0.120 Inch)	61
49 Heat Transfer Distribution in Separation Region ($\Theta_{sg} = 5.5$ Degrees, Slot Height = 0.120 Inch)	61
50 Typical Distribution of Heat Transfer and Pressure in Separated Interaction Region ($\Theta_{sg} = 5.5$ Degrees, Slot Height = 0.120 Inch).....	62
51 Variation of Separated Flow Length With Blowing Rate for Various Incident-Shock Strengths (Slot Height = 0.120 Inch).....	63
52 Variation of Maximum Heating Rate With Film-Coolant Flow Rate (Slot Height= 0.120 Inch)	63
53 Heat Transfer Variation with Lip Thickness in Regions of Incident-Shock/Wall-Jet Interaction ($\Theta_{sg}=10.5$ Degrees, Slot Height=0.080 Inch $\lambda=0.100$).....	65

List of Tables

Table		Page
1	Test Conditions	14
2	Model and Blowing Configurations.....	27

NOMENCLATURE

C_H	=	$q/(\rho_\infty u_\infty (H_0 - H_w))$, Stanton Number
C_p	=	Pressure Coefficient ($= p/(1/2 \rho_\infty u_\infty^2)$)
H	=	Total Enthalpy
h	=	Heat Transfer Constant
l	=	Flow Length
M	=	Mach Number
p	=	Static Pressure
q, Q	=	Heat Transfer Rate
Re	=	Reynolds Number
Re_x	=	$(\rho u x)/\mu$
Re_δ	=	$\frac{\rho u \delta}{\mu}$
S	=	Slot Height
T	=	Static Temperature
u, U	=	Velocity
X	=	Downstream Distance

GREEK SYMBOLS

α	=	Compression Angle
γ	=	Specific Heat Ratio
δ	=	Boundary Layer Thickness
η	=	Cooling Effectiveness, Equation 1
θ	=	Shock-Generator Angle
λ	=	Blowing Parameter = $\frac{\rho_c U_c}{\rho_e U_e}$

μ = Viscosity

ρ = Density

SUBSCRIPTS

0 = Stagnation Value

aw = Adiabatic Wall

b = Boundary Layer

c = Coolant

e = Edge of Boundary Layer

fp = Flat Plate

i = Incident Shock

max = Point of Maximum Pressure/Heating

nc = No Cooling

r = Reference Value

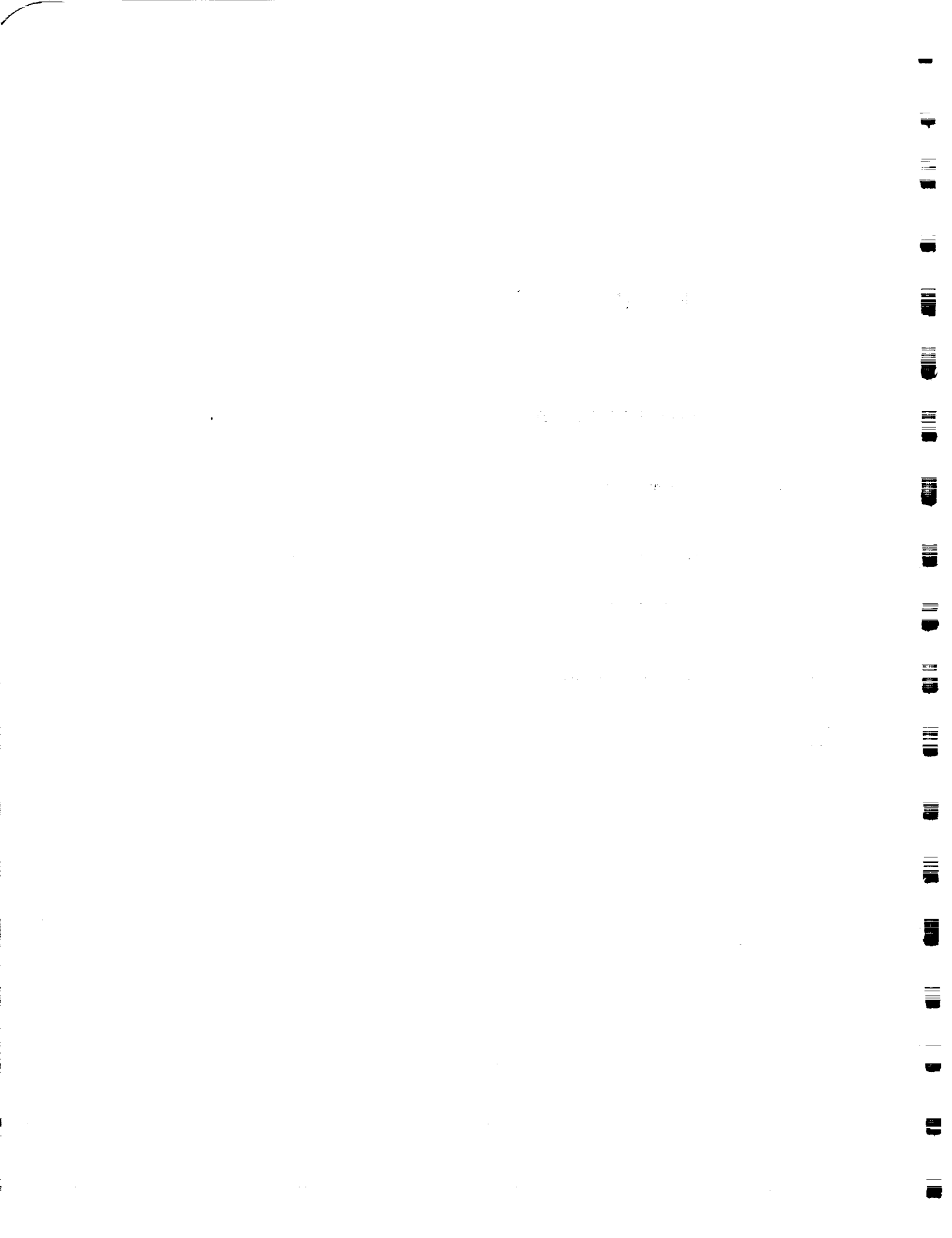
sep = Separated Region

$surf$ = Surface (Appendix)

t = Total

w = Wall

∞ = Freestream Value



Section 1 INTRODUCTION

A key technology in the development of supersonic-combustion ramjet (scramjet) propulsion is associated with the active cooling of the walls of the inlet, combustor, and nozzle of the engine. To develop an effective and efficient coolant system, the relative merits of film and transpiration cooling must be evaluated against complications associated with the combustion of the coolant and the interaction between the coolant layer and shock waves generated by the compression ramp and the cowl, and induced by vectored injection or injector struts. Although there is a significant body of information on constant-pressure film and transpiration cooling, and on regions of shock-wave/boundary layer interaction, on smooth surfaces in supersonic and hypersonic flows, there is little information on shock-wave/cooling-layer interaction. In fact, the only studies that have been performed of this latter phenomenon yielded conflicting conclusions, as discussed later. For the specific application of scramjets, film cooling has recently been favored over the relatively more efficient transpiration cooling, because the injectant momentum contributes directly to thrust, and mechanical construction of the system is intrinsically simpler. In low-speed turbulent flows, rapid mixing between the freestream and the injectant limits the effectiveness of the film-cooling technique. However, for supersonic and hypersonic flows where the velocity and the static pressure of the coolant can be matched to those of the freestream and there is a significant difference in Mach number between the coolant and the freestream, film cooling may become a more efficient technique. This, in part, may result from a reduction in spreading rate in shear layer mixing with increased convective Mach number, which reduction may be associated with compressibility effects¹.

While the literature is rich in studies of film cooling, there is relatively little information for high-temperature flows, where there exist significant differences in density and Mach number between the freestream and the injectant. A good review of both experimental efforts and analyses covering work up to the late sixties was published by Goldstein². The principal emphasis of the earlier experimental work was on subsonic flow. Analysis of the measurements centered principally around "control volume" energy balances to define a cooling effectiveness (η) and the parameters upon which it depended. Subsequent work on film cooling has been directed more toward the supersonic and hypersonic flow regimes. There has also been increasing use of computational techniques based on numerical solutions to the full or reduced Navier-Stokes equations. Observations of the increased effectiveness of film cooling in high supersonic and hypersonic flows have been made in a number of studies, including those by Parthasarathy and Zakkay³ and by

Cary and Hefner^{4,5} for a Mach 6 flow, although these two data sets do not correlate well. Further studies in high-speed flow, including works by Richards and Stollery⁶, pointed out the important role of film transition in cooling effectiveness. The important effects of the specific heat and molecular weight of the injectant as well as the relative Mach number between the two streams have yet to be fully understood. Also, the effects of lip thickness on cooling effectiveness have yet to be quantified experimentally in hypersonic flows. Although there are still efforts to correlate the performance of film cooling well downstream of the slot in terms of non-dimensional parameters controlling the effectiveness parameter, such efforts are increasingly being replaced by numerical solutions to the full or reduced time-averaged Navier-Stokes equations. The work of Cary, Bushnell, and Hefner⁷ typifies the early work in this area, where numerical computational solutions were obtained for the boundary layer equations, and a multicomponent (five) mixing-length model was used to describe the mixing between the freestream and the coolant. These solutions were, in principle, capable of describing the flow from the slot to the far wake. While some aspects of the arbitrary nature of the turbulence model are removed when two-equation models (such as the k- ϵ model) are employed (for example, Baker, et al.⁸), selection of the numerical constants and description of compressibility and low Reynolds number effects in high Mach number flows become the key and controversial issues. Such studies have predicted that lip thickness has a significant effect on cooling effectiveness, a prediction that has yet to be supported by experimental studies. Recent sets of studies where both correlation and parabolized Navier-Stokes (PNS) computations were employed to describe window film cooling are those reported by Swigert et al.⁹ and Majeski and Weatherford¹⁰. Three sets of experimental studies were performed in three different hypersonic facilities with the basic objective of investigating flows with significant differences in stagnation temperature between the freestream and the coolant. However, although the freestream Mach number was hypersonic, the local boundary layer edge Mach number was typically 4, with injectant Mach numbers of 1.9 to 4.45. The correlations and predictions made in these studies suggest that, in high-temperature flows, the effects of large stagnation temperature differences and compressibility play a significant, and as yet poorly understood, role in controlling the structure of the mixing, and hence heating levels in the core and wall-jet regions of the slot flows.

The small amount of information on the effects of shock impingement on the effectiveness of film cooling is conflicting. To the author's knowledge, there are only three studies (Alzner and Zakkay¹¹, Ledford and Stollery¹², and Baryshev, Leontyev, and Rozhdestvenskiy¹³) that specifically investigated the effects of shock impingement on the

local flowfield structure and effectiveness of a cooling film. The studies by Alzner and Zakkay were conducted at Mach 6 on an axisymmetric configuration employing either air or hydrogen, which was injected at sonic velocity. Measurements obtained in these studies of the distributions of heat transfer and pressure through an interaction region are shown in Figures 1, 2, and 3 for a 10° shock generator angle. Figure 1 indicates that the flow is separated in the absence of injection, with the separated region increasing in size with increased mass flow rate. It can be seen that there is a significant reduction in heating rate in the recompression region with injection, for both air and hydrogen injection. The injection rates in these studies were from one-third to three-quarters of the freestream mass flow rate. The studies of Ledford and Stollery were conducted at Mach 8.2 for a shock-generator angle of 5° ; however, the expansion fan from the trailing edge of the shock generator significantly decreased the strength of the interaction. Figure 4 shows the distribution of heat transfer through the interaction regions with and without coolant for $\lambda = 0.15$. Here, we see that, in contrast to the Alzner and Zakkay study, coolant has little effect on the peak heating, despite the weak strength of the interaction. The Baryshev *et al.* study, which was conducted at Mach 2.2, also shows little reduction in heating resulting from film cooling in a shock-interaction region. Although the blowing rates in the Alzner studies were larger than those in the other investigations, this was offset, in part, because the shock strength in this study was significantly larger than in the other two studies. There appears to be no simple explanation for the differences in the basic results from these investigations.

The principal objective of the present studies was to determine whether film cooling is an effective way of reducing the peak heating in regions of shock-wave/turbulent boundary layer interaction in hypersonic flows. We also sought to provide a detailed set of measurements to describe the key features of these flows against which to evaluate the turbulent modeling for flows where compressibility and large total temperature effects could be important. A third objective was to investigate the effect of the thickness of the injector lip on the cooling effectiveness. In the following section, we discuss the objectives and the design of the experimental program. The experimental facilities, the model, and the instrumentation are then described in detail, together with the test conditions and model configurations at which the studies were conducted. In Section 3, the results of the experimental studies are presented, together with comparisons and correlations with measurements made in earlier studies. The major flowfield characteristics of separated regions of shock-wave/wall-jet interactions are discussed, together with the associated

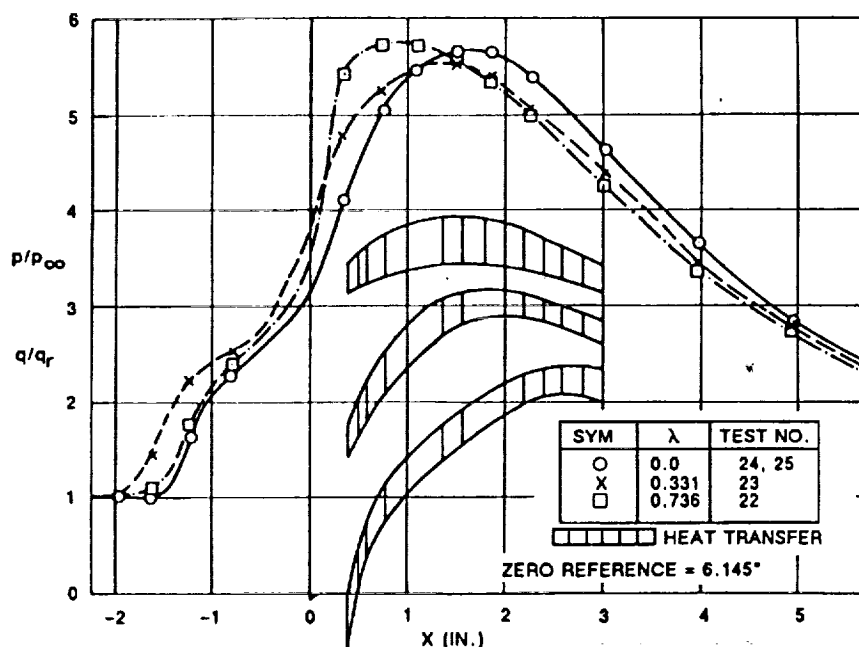


Figure 1 WALL PRESSURE AND WALL HEAT TRANSFER DISTRIBUTIONS (ALZNER AND ZAKKAY)

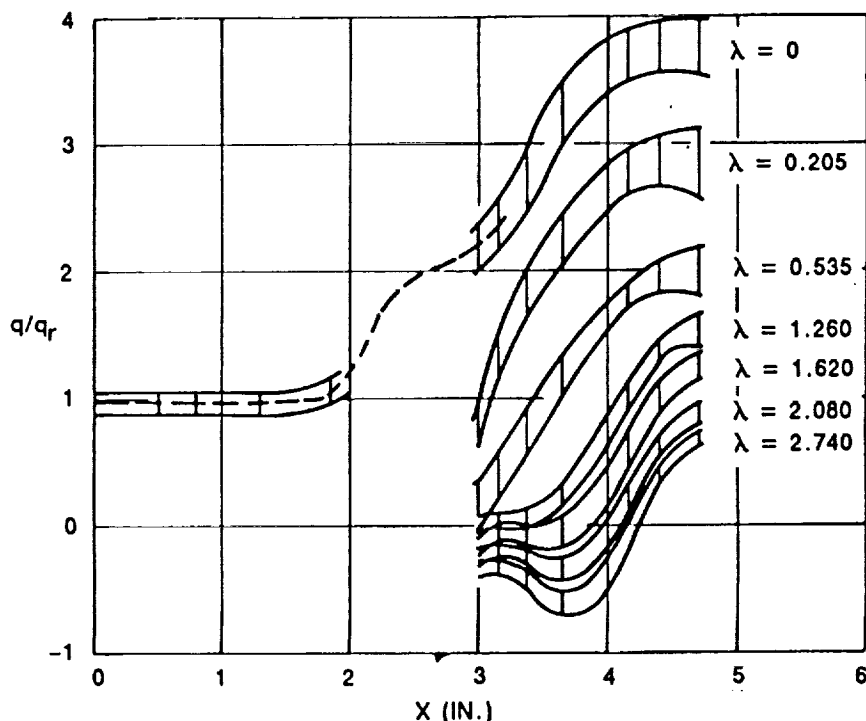
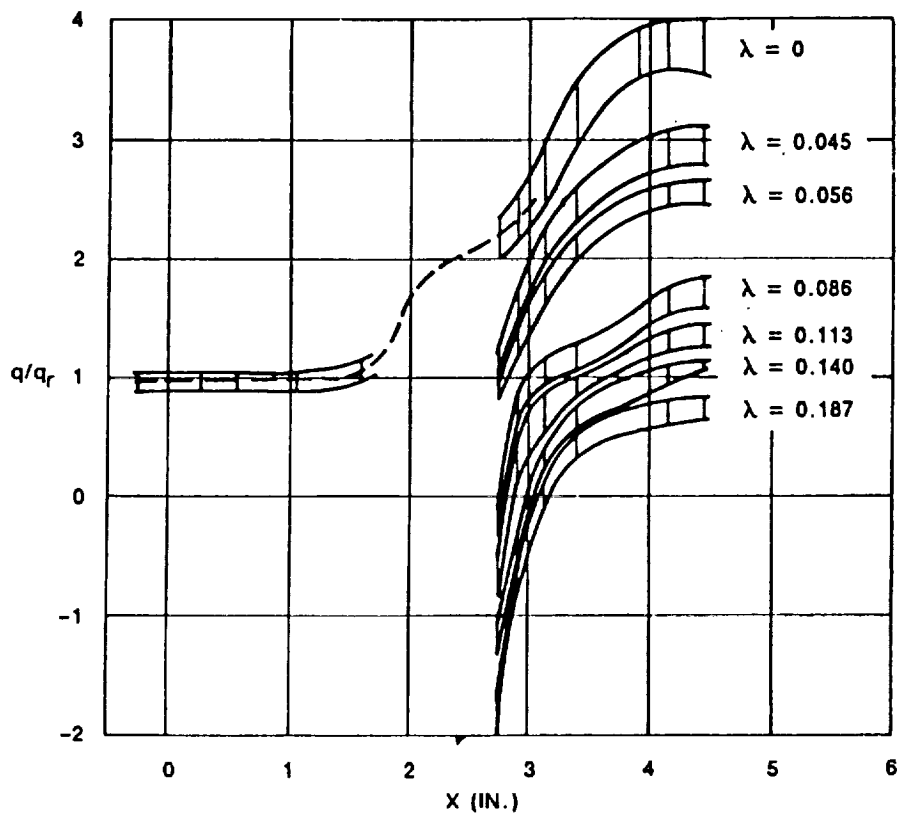
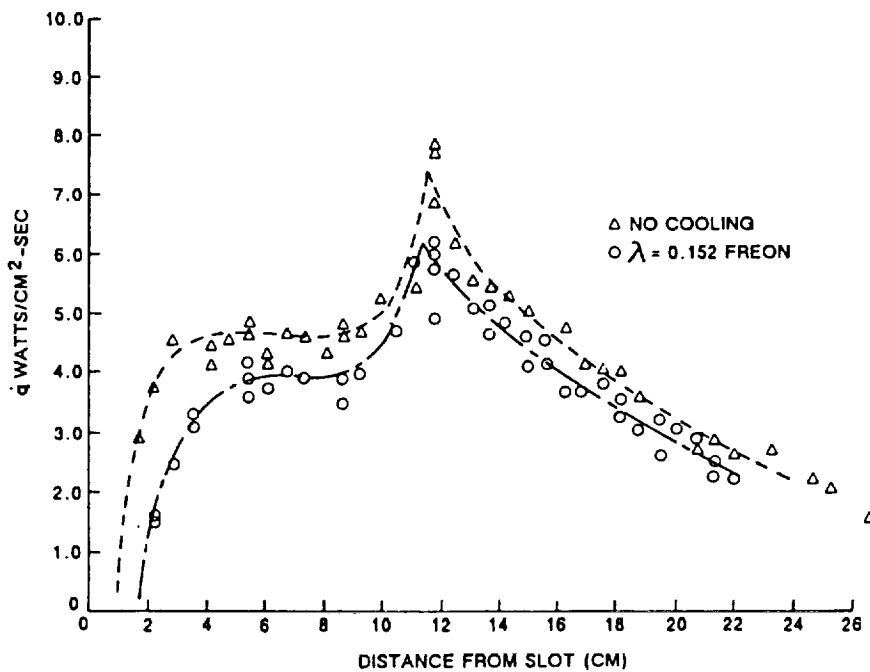


Figure 2 HEAT TRANSFER DISTRIBUTIONS FOR AIR INJECTION (ALZNER AND ZAKKAY)



**Figure 3 HEAT TRANSFER DISTRIBUTIONS FOR HYDROGEN INJECTION
(ALZNER AND ZAKKAY)**



**Figure 4 EFFECT OF FILM COOLING ON SHOCK-IMPINGEMENT HEATING
(LEDFORD AND STOLLERY)**

distributions of surface pressure and heat transfer. Next, we discuss the effects of the lip thickness on cooling effectiveness and the characteristics of shock/film interaction regions. The major conclusions from these studies are then presented.

Section 2

EXPERIMENTAL PROGRAM

2.1 PROGRAM OBJECTIVES AND DESIGN

2.1.1 Program Objectives

The principal objective of this program was to design and conduct an experimental program to provide definitive surface and flowfield measurements defining how cooling films produced by a supersonic wall jet were influenced by shock-wave interaction. In hypersonic flow over a flat surface, we sought to determine whether the shock would induce separated interaction regions in the coolant flow, and for which model, injector, and flow configurations the heating in the recompression region was reduced by film cooling. The second important objective was to obtain surface and flowfield measurements having sufficient resolution to provide a data set with which to evaluate the turbulence modeling and detailed performance of the time-averaged Navier-Stokes codes, as well as the semi-empirical correlation techniques.

2.1.2 Design of the Experiment

The experimental studies were conducted at a freestream Mach number of 6.4 with a Mach 2.3 wall jet, a representative cooling configuration for scramjet combustor designs that might be employed in the high hypersonic speed range. To simulate the fluid dynamics at the injector, a fully developed turbulent boundary layer that had a thickness of 0.44 inch (three to five injector heights) was generated over the flat plate upstream of the injector station. Helium was used as the injectant so as to be representative of a low-density, high-specific-heat coolant such as hydrogen. The injector nozzles were designed to be run so that the velocity and pressure at the exit plane matched those in the local freestream. However, we also ran at both under- and over-expanded conditions, where the pressures in the exit plane of the nozzles were respectively, above and below local freestream levels. A sharp, flat-plate shock-generator system was used to generate sets of planar oblique shocks representative of wall pressure rises of 4 to 12 through the interaction region. The point of shock impingement was positioned to provide measurements close to, in addition to well downstream of, the slot to examine the effect of wall-jet structure on the characteristics of the interaction regions.

2.2 EXPERIMENTAL FACILITIES AND TEST CONDITIONS

2.2.1 Experimental Facilities

This experimental program was conducted in Calspan's 48-inch shock tunnel at a nominal freestream Mach number of 6.4 and at Reynolds numbers up to 24×10^6 based on the distance from the leading-edge to the injector station. At these high Reynolds number conditions, boundary layer transition was complete on the flat plate within 6 inches of its leading edge. The wall-to-freestream stagnation temperature ratio in these studies was close to 0.3. The test conditions at which the experimental studies were conducted are listed in Table 1 and shown on the Reynolds number/Mach number map of the shock tunnel in Figure 5.

The Calspan 48-inch shock tunnel is essentially a blow-down tunnel with a shock compression heater. A wave diagram depicting tunnel operation for tailored-interface conditions is shown in Figure 6. The flow in the tunnel is initiated by rupturing a double diaphragm, permitting high-pressure helium from the driver section to expand rapidly into the driven section. This sudden release of pressure generates a normal shock, which propagates through the low-pressure air, producing a region of high-temperature, high-pressure air between this normal-shock front and the gas interface (the contact surface) between the driver and driven gases. When the primary, or incident, shock strikes the end of the driven section, it is reflected, leaving a region of almost stationary, high-pressure, heated air. This air is then expanded through a nozzle to the desired freestream conditions in the test section. The duration of the flow in the test section is controlled by the interactions between the reflected shock, the interface, and the leading expansion wave generated by the non-stationary expansion process occurring in the driver section. It is standard operating procedure to control the initial conditions of the gases in the driver and driven sections so that the gas interface becomes transparent to the reflected-shock interaction. This is known as operating under "tailored-interface" conditions. Under these conditions, for incident shock Mach numbers of around 3, the test time is controlled by the time taken for the driver/driven interface to reach the throat, or the leading expansion wave to decrease the reservoir of pressure behind the reflected shock. Thus, the flow duration is either driver-gas-limited or expansion-wave-limited, respectively. Figure 7 shows the flow duration in the test section as a function of the Mach number of the incident shock. For operation at low-incident-shock Mach numbers, running times of over 25 milliseconds can easily be obtained with a long driver section in the 48-inch shock tunnel.

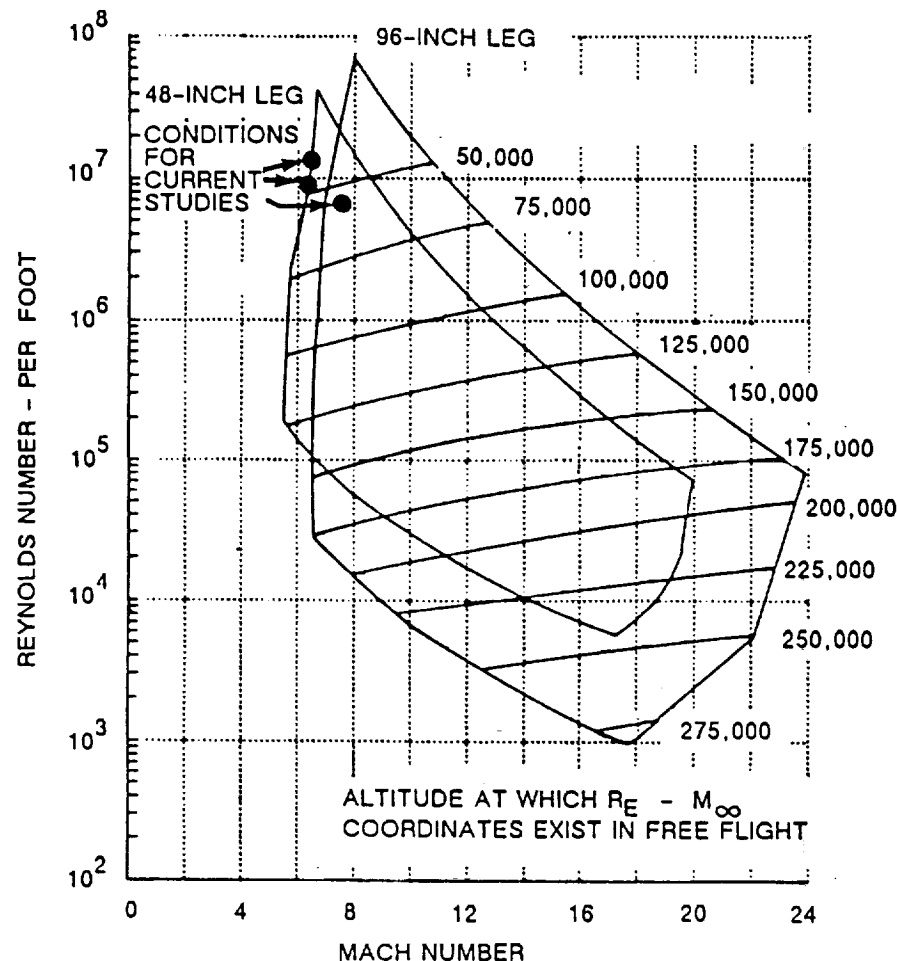


Figure 5 PERFORMANCE MAP OF CALSPAN'S SHOCK TUNNELS

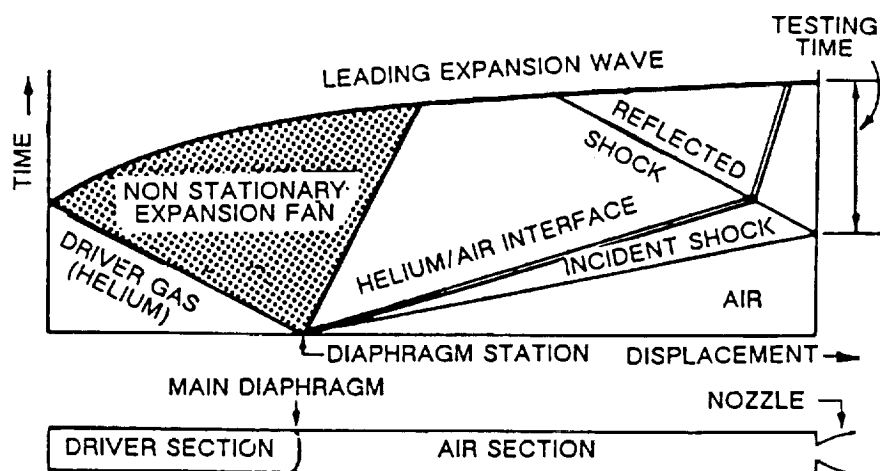


Figure 6 WAVE DIAGRAM FOR TAILORED-INTERFACE CONDITION

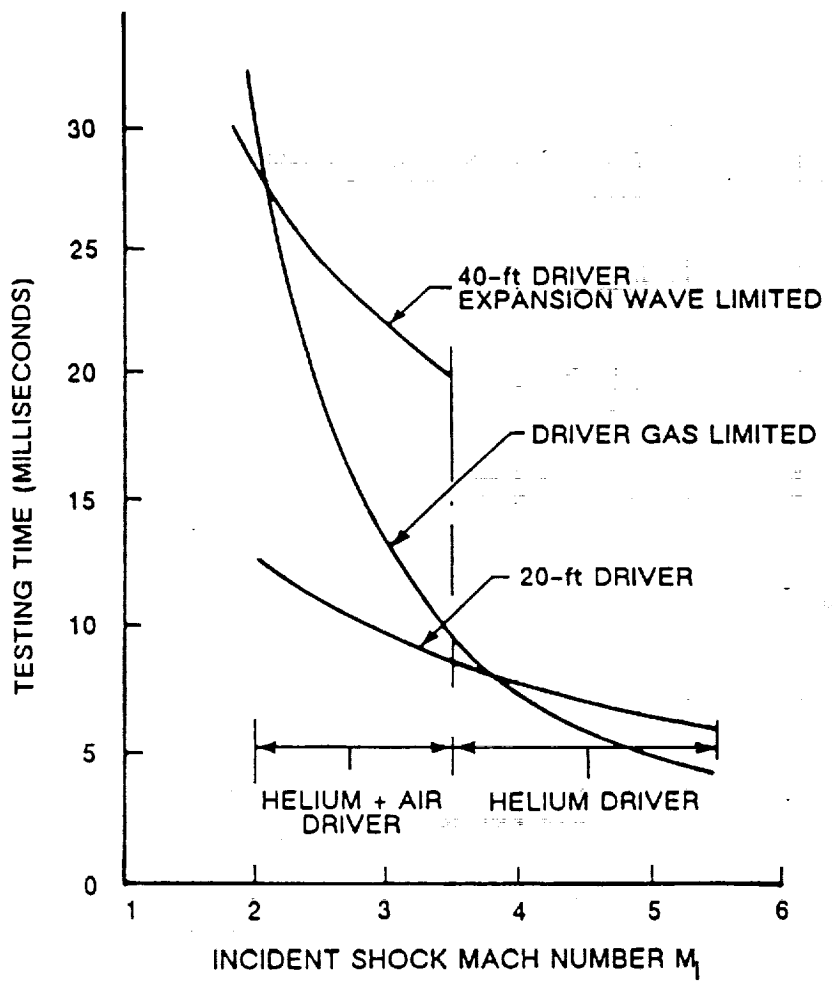


Figure 7 TEST TIME AVAILABLE FOR TAILORED-INTERFACE OPERATIONS OF SHOCK TUNNEL

2.2.2 Evaluation Of Test Conditions

The stagnation and freestream test conditions were determined from measurements of the incident-shock-wave speed, U_i , the initial temperature of the test gas (in the driven tube), T_1 , the initial pressure of the test gas, p_1 , and the pressure behind the reflected shock wave, p_0 . We calculated the incident-shock-wave Mach number, $M_i = U_i/a_1$, where the speed of sound, a_1 , is a function of p_1 and T_1 . The freestream Mach number, M_∞ , was determined from correlations of M_∞ with M_i and p_0 . These correlations were based on airflow calibrations of the "A" nozzle and are discussed in Section 2.2.4.

Freestream test conditions of pressure, temperature, Reynolds number, etc., were computed based on isentropic expansion of the test gas from the conditions behind the reflected shock wave to the freestream Mach number. Real gas effects were taken into account for this expansion under the justified assumption that the gas was in thermochemical equilibrium. In the freestream, the static temperature, T_∞ , was sufficiently low that the ideal gas equation of state, $p_\infty = \rho RT_\infty$, was applicable, where R is the gas constant for the test gas.

The stagnation enthalpy, H_0 , and temperature, T_0 , of the gas behind the reflected shock wave were calculated from:

$$H_0 = (H_4/H_1)H_1 \text{ and } T_0 = (T_4/T_1)T_1 \quad (1)$$

where (H_4/H_1) and (T_4/T_1) are functions of U_i (or M_i) and p_1 and are given in Reference 14 for air. H_1 was obtained from Reference 15 for air, knowing p_1 and T_1 .

The freestream static temperature was found from the energy equation, knowing H_0 and M_∞ ,

$$T_\infty = \frac{H_0}{c_p} \left(\frac{1}{1 + \frac{(\gamma-1)}{2} M_\infty^2} \right) \quad (2)$$

where $c_p = 6006 \text{ ft-lb/slug-}^\circ\text{R}$ and $\gamma = 1.40$.

The freestream static pressure was calculated from

$$p_{\infty} = \frac{p}{p_p} p_0 \left(1 + \frac{(\gamma-1)}{2} M_{\infty}^2 \right)^{\frac{-\gamma}{\gamma-1}} \quad (3)$$

where

$$\frac{p}{p_p} = \frac{(p_{\infty}/p_0)\text{REAL}}{(p_{\infty}/p_0)\text{IDEAL}} \quad (4)$$

is the real gas correction to the ideal gas static-to-total pressure ratio as described in Reference 16. The sources for the real gas data used in this technique are References 17 and 18.

The freestream velocity was determined from

$$U_{\infty} = M_{\infty} a_{\infty} \quad (5)$$

where

$$a_{\infty} = \sqrt{\gamma R T_{\infty}} \quad (6)$$

the speed of sound.

The freestream dynamic pressure was found from

$$q_{\infty} = \frac{1}{2} \gamma p_{\infty} M_{\infty}^2 \quad (7)$$

and the freestream density then was calculated from the ideal gas equation of state

$$\rho_{\infty} = p_{\infty} / (\bar{R} T_{\infty}) \quad (8)$$

where $R = 1717.91 \text{ ft-lb/slug-}^{\circ}\text{R}$ for air. Values of the absolute viscosity, μ , used to compute the freestream Reynolds number per foot were obtained using the technique described in Reference 14.

The test-section pitot pressure, p_0' , was determined from q_{∞} and the ratio (p_0'/q_{∞}) . This ratio has been correlated as a function of M_{∞} and H_0 for normal-shock waves in air in thermodynamic equilibrium.

2.2.3 Accuracy of Test Conditions

The test conditions at which these studies were conducted are listed in Table 1. At these conditions, where real gas effects are negligible, the uncertainty in the pitot pressure measurement from errors in calibration and recording is $\pm 2.5\%$. The reservoir pressure can be measured with an uncertainty of $\pm 2\%$, and the total enthalpy (H_0) can be determined from the driven-tube pressure and the incident-shock Mach number with an uncertainty of $\pm 2\%$. These measurements combine to yield an uncertainty in the Mach number and dynamic pressure measurements of $\pm 0.8\%$ and $\pm 3.5\%$, respectively.

2.2.4 Airflow Calibrations of the "A" Nozzle

Detailed flowfield surveys were made across the exit plane of the "A" nozzle to determine flow uniformity and core size at the Mach 6 conditions at which the experimental studies were conducted. Additional data were provided from measurements of the axial static pressure distribution along the flat plate. From the flowfield measurements of pitot pressure and total temperature, and the static pressure, we can determine the flow properties across the test section. Figure 8 shows the Mach number distribution across the exit plane of the nozzle for the Mach 6 conditions. It can be seen that the core size for this condition was 20 inches and the variation in Mach number across the test core was less than 2%.

2.3 MODEL AND INSTRUMENTATION

2.3.1 Film-Cooling/Shock-Interaction Model

The film-cooling/shock-interaction model used in these experimental studies is shown in Figure 10. The model is 18 inches wide and incorporates a 28-inch-long leading-edge plate instrumented with heat transfer and pressure gages. For the conditions studied, a well-developed turbulent boundary layer is formed well upstream of the injector station. A 4.343-inch-long injector section contains 40 two-dimensional nozzles as shown in Figure 11, and is attached to the 17-inch-long, two-piece trailing-edge plate. Figure 12 shows the model installed in the "A" nozzle in the 48-inch shock tunnel. The nozzle block, shown schematically in Figure 13, was fabricated in two heights, giving slot heights of 0.080 inch and 0.120 inch above the trailing edge of the plate. Coordinates of the nozzle contour are presented in Figure 13. This system is fed from five high-pressure reservoirs

Table 1 TEST CONDITIONS

Run#	Po (PSIA)	Ho (Ft/s) ²	To (°R)	M (-)	U (Ft/s)	T (°R)	P (PSIA)	p (Slug/Ft3)
4	2.766E+03	1.436E+07	2234.6	6.423	5.063E+03	258.4	1.131E+00	3.672E-04
5	4.083E+03	1.441E+07	2233.7	7.867	5.166E+03	179.3	4.694E-01	2.197E-04
6	4.155E+03	1.409E+07	2190.5	6.471	5.020E+03	250.3	1.666E+00	5.587E-04
8	2.556E+03	1.387E+07	2167.5	6.430	4.977E+03	249.1	1.043E+00	3.515E-04
14	2.662E+03	1.443E+07	2244.7	6.420	5.075E+03	259.8	1.088E+00	3.513E-04
15	2.475E+03	1.349E+07	2114.5	6.434	4.910E+03	242.1	1.013E+00	3.512E-04
21	2.324E+03	1.315E+07	2066.4	6.437	4.846E+03	235.7	9.514E-01	3.388E-04
23	2.317E+03	1.310E+07	2060.3	6.438	4.838E+03	234.9	9.488E-01	3.390E-04
24	2.319E+03	1.331E+07	2089.3	6.434	4.875E+03	238.8	9.489E-01	3.335E-04
25	2.370E+03	1.331E+07	2090.1	6.436	4.877E+03	238.7	9.690E-01	3.407E-04
26	2.380E+03	1.326E+07	2082.6	6.437	4.867E+03	237.8	9.735E-01	3.436E-04
27	2.323E+03	1.322E+07	2077.7	6.437	4.860E+03	237.0	9.494E-01	3.362E-04
28	2.386E+03	1.328E+07	2086.6	6.441	4.871E+03	237.8	9.714E-01	3.428E-04
29	2.444E+03	1.356E+07	2126.4	6.439	4.922E+03	243.0	9.935E-01	3.431E-04
30	2.377E+03	1.329E+07	2086.1	6.436	4.872E+03	238.3	9.724E-01	3.425E-04
31	2.298E+03	1.320E+07	2074.6	6.437	4.856E+03	236.6	9.394E-01	3.331E-04
32	2.225E+03	1.304E+07	2053.1	6.440	4.827E+03	233.6	9.030E-01	3.262E-04
33	2.359E+03	1.325E+07	2082.3	6.439	4.866E+03	237.4	9.626E-01	3.402E-04
34	2.365E+03	1.336E+07	2098.3	6.438	4.886E+03	239.5	9.643E-01	3.379E-04
35	2.416E+03	1.352E+07	2120.0	6.438	4.914E+03	242.2	9.825E-01	3.404E-04
36	2.372E+03	1.326E+07	2082.6	6.437	4.867E+03	237.8	9.705E-01	3.425E-04
37	2.400E+03	1.335E+07	2096.3	6.438	4.884E+03	239.3	9.791E-01	3.433E-04
38	2.396E+03	1.351E+07	2118.5	6.436	4.912E+03	242.2	9.761E-01	3.382E-04
39	2.324E+03	1.307E+07	2056.2	6.440	4.832E+03	234.1	9.501E-01	3.406E-04
40	2.354E+03	1.330E+07	2088.9	6.437	4.875E+03	238.4	9.613E-01	3.383E-04
41	2.377E+03	1.342E+07	2106.2	6.438	4.896E+03	240.5	9.685E-01	3.379E-04
43	2.671E+03	1.397E+07	2181.3	6.433	4.995E+03	250.7	1.088E+00	3.642E-04
44	2.623E+03	1.402E+07	2188.4	6.430	5.004E+03	251.8	1.070E+00	3.565E-04
45	2.487E+03	1.379E+07	2157.0	6.432	4.962E+03	247.5	1.014E+00	3.437E-04
46	2.640E+03	1.408E+07	2198.3	6.431	5.016E+03	252.9	1.074E+00	3.564E-04
47	2.590E+03	1.397E+07	2182.1	6.429	4.996E+03	251.1	1.057E+00	3.534E-04
50	2.613E+03	1.416E+07	2207.9	6.426	5.028E+03	254.6	1.066E+00	3.513E-04
51	2.547E+03	1.378E+07	2156.1	6.436	4.961E+03	247.1	1.036E+00	3.517E-04
52	2.639E+03	1.389E+07	2169.8	6.431	4.981E+03	249.4	1.079E+00	3.628E-04
53	2.560E+03	1.381E+07	2159.6	6.432	4.967E+03	247.9	1.045E+00	3.536E-04
55	2.432E+03	1.347E+07	2112.1	6.437	4.905E+03	241.4	9.915E-01	3.447E-04
56	2.454E+03	1.366E+07	2139.3	6.436	4.939E+03	244.9	9.982E-01	3.421E-04
57	2.382E+03	1.360E+07	2132.0	6.436	4.929E+03	243.9	9.692E-01	3.335E-04
58	2.381E+03	1.323E+07	2078.5	6.441	4.861E+03	236.9	9.711E-01	3.440E-04
59	2.481E+03	1.333E+07	2093.2	6.445	4.880E+03	238.4	1.008E+00	3.547E-04
60	2.377E+03	1.345E+07	2110.1	6.437	4.901E+03	241.1	9.687E-01	3.372E-04
61	2.325E+03	1.346E+07	2111.7	6.436	4.903E+03	241.3	9.475E-01	3.295E-04
62	2.431E+03	1.357E+07	2127.2	6.439	4.923E+03	243.1	9.877E-01	3.410E-04
63	2.312E+03	1.316E+07	2068.4	6.437	4.848E+03	235.9	9.459E-01	3.365E-04
65	2.453E+03	1.360E+07	2131.7	6.436	4.930E+03	243.9	9.986E-01	3.436E-04
66	2.423E+03	1.347E+07	2112.9	6.439	4.905E+03	241.3	9.860E-01	3.429E-04
67	2.426E+03	1.347E+07	2111.3	6.434	4.905E+03	241.6	9.922E-01	3.446E-04

AIRFLOW MACH NUMBER PROFILE
RUN 1161 D 2.570 P6 4000. P1 55.10 %He 68.0 MI 2.78

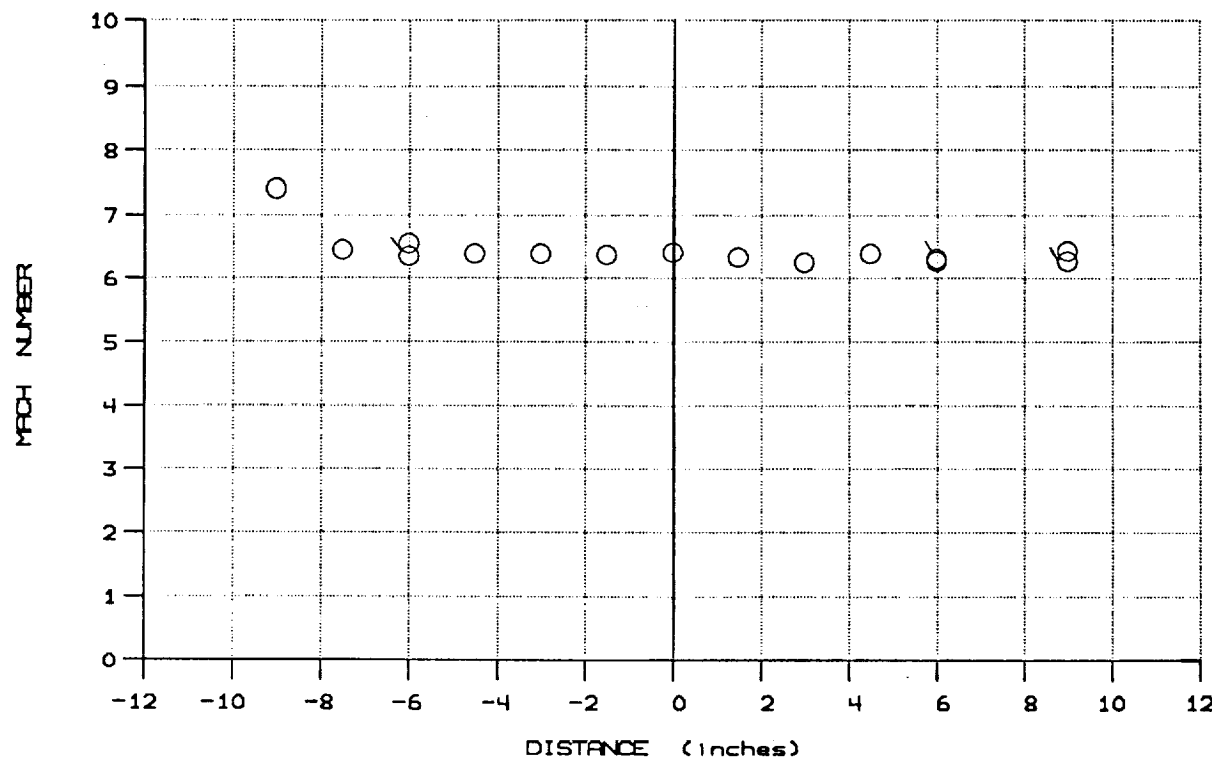


Figure 8 MACH NUMBER DISTRIBUTION FOR "A" NOZZLE, $M_{\infty}=6.4$

AIRFLOW MACH NUMBER PROFILE
RUN 1164 D 1.600 P6 5200. P1 72.00 %He 68.0 MI 2.90

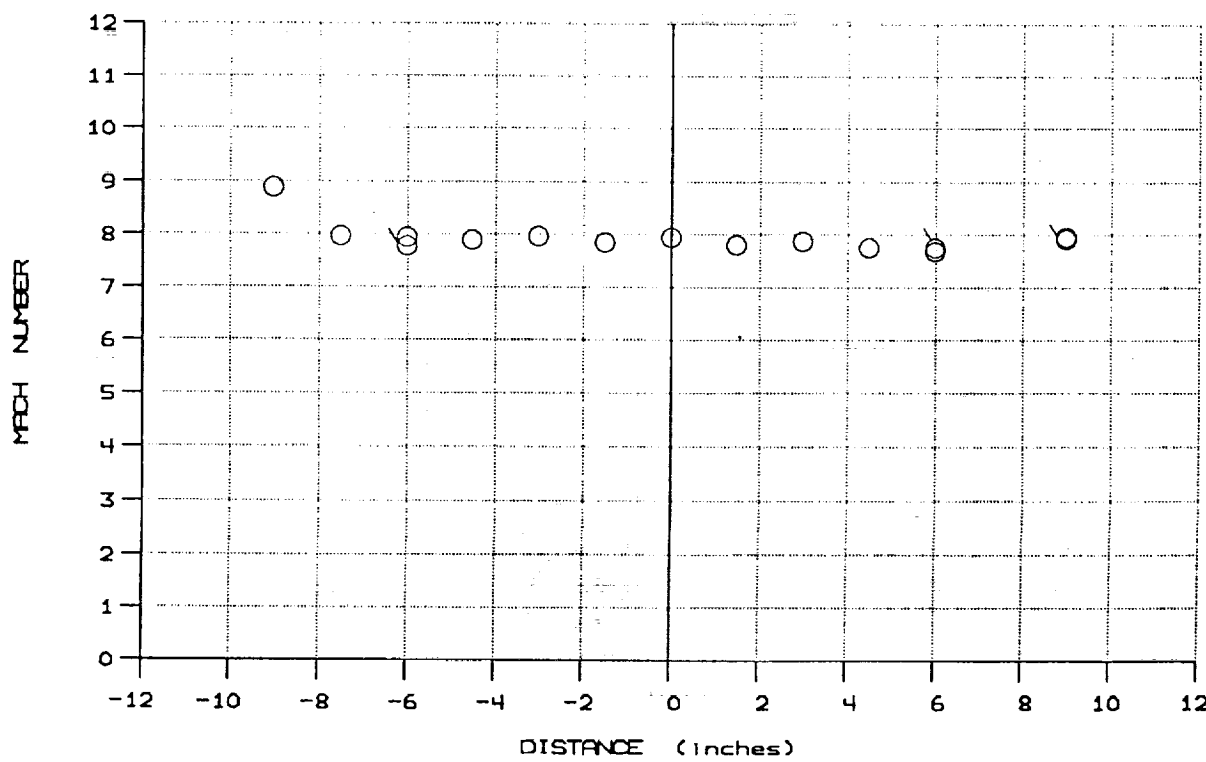


Figure 9 MACH NUMBER DISTRIBUTION FOR "A" NOZZLE, $M_{\infty}=7.9$

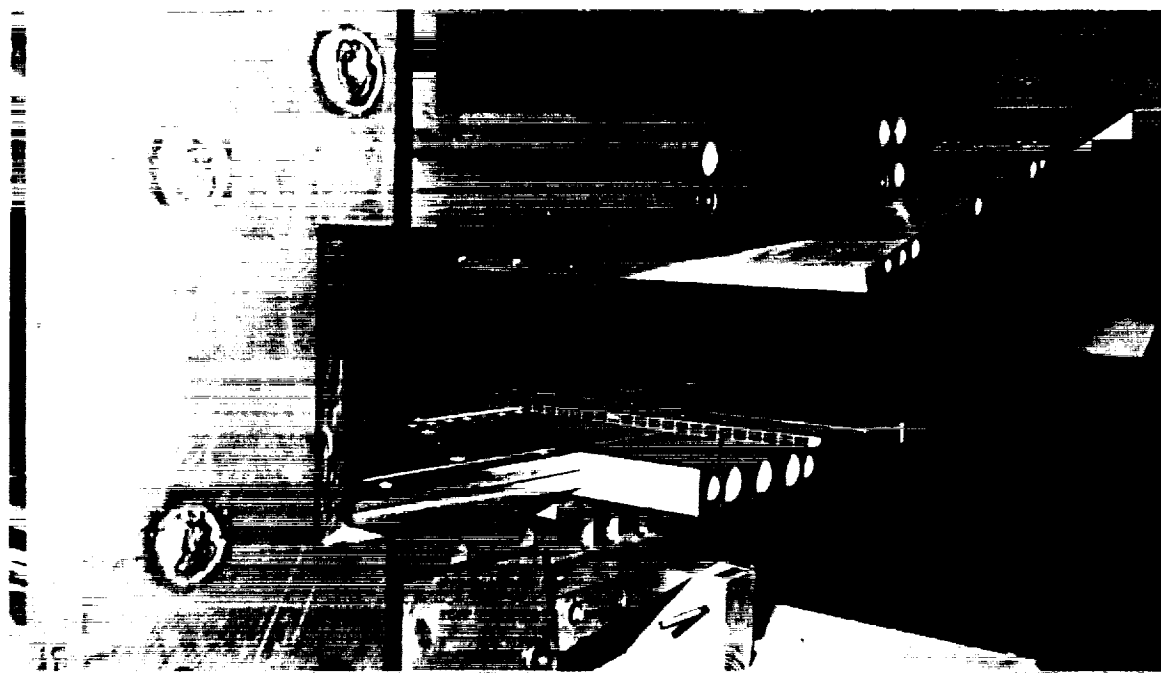


Figure 10 MODEL ASSEMBLY SHOWING GENERATOR AND INJECTOR NOZZLES

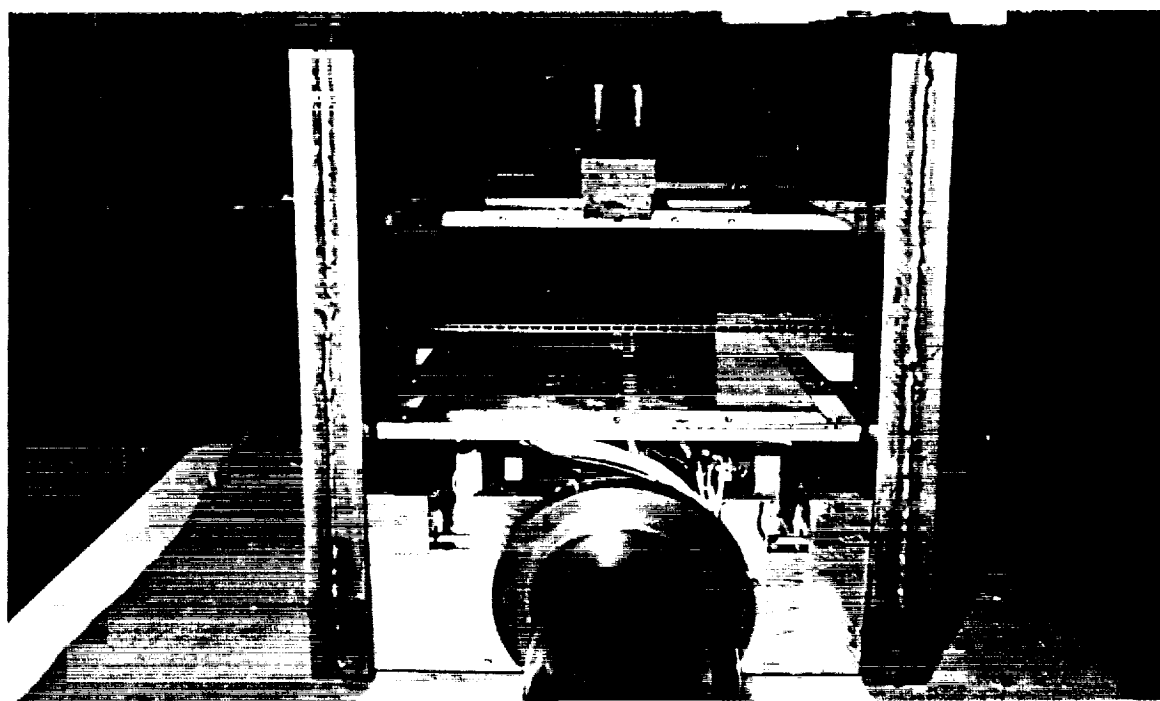


Figure 11 VIEW OF MODEL SHOWING NOZZLE SLOTS AND HIGHLY INSTRUMENTED FLAT PLATE

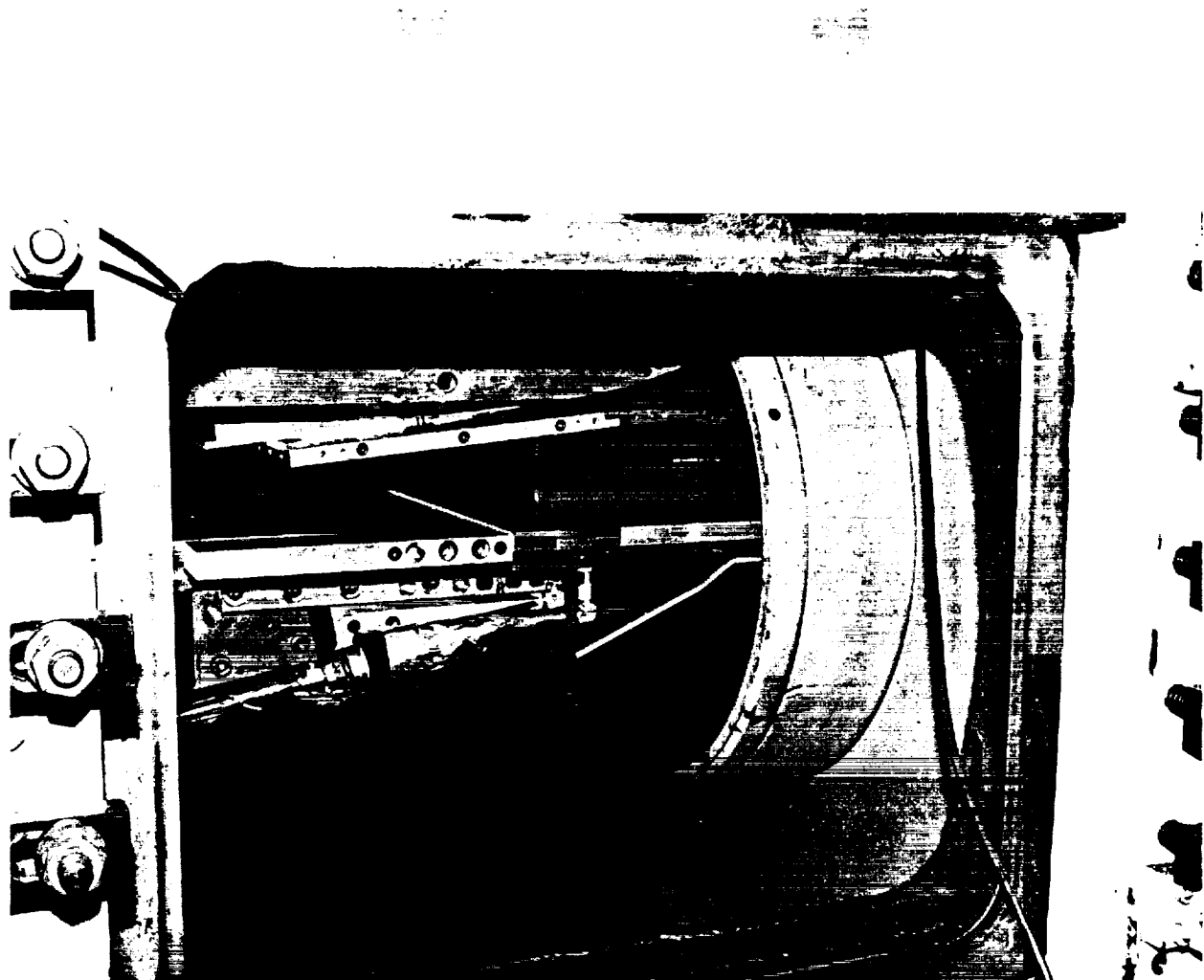


Figure 12 FILM-COOLING/SHOCK-INTERACTION MODEL INSTALLED IN CALSPAN'S 48-INCH SHOCK TUNNEL

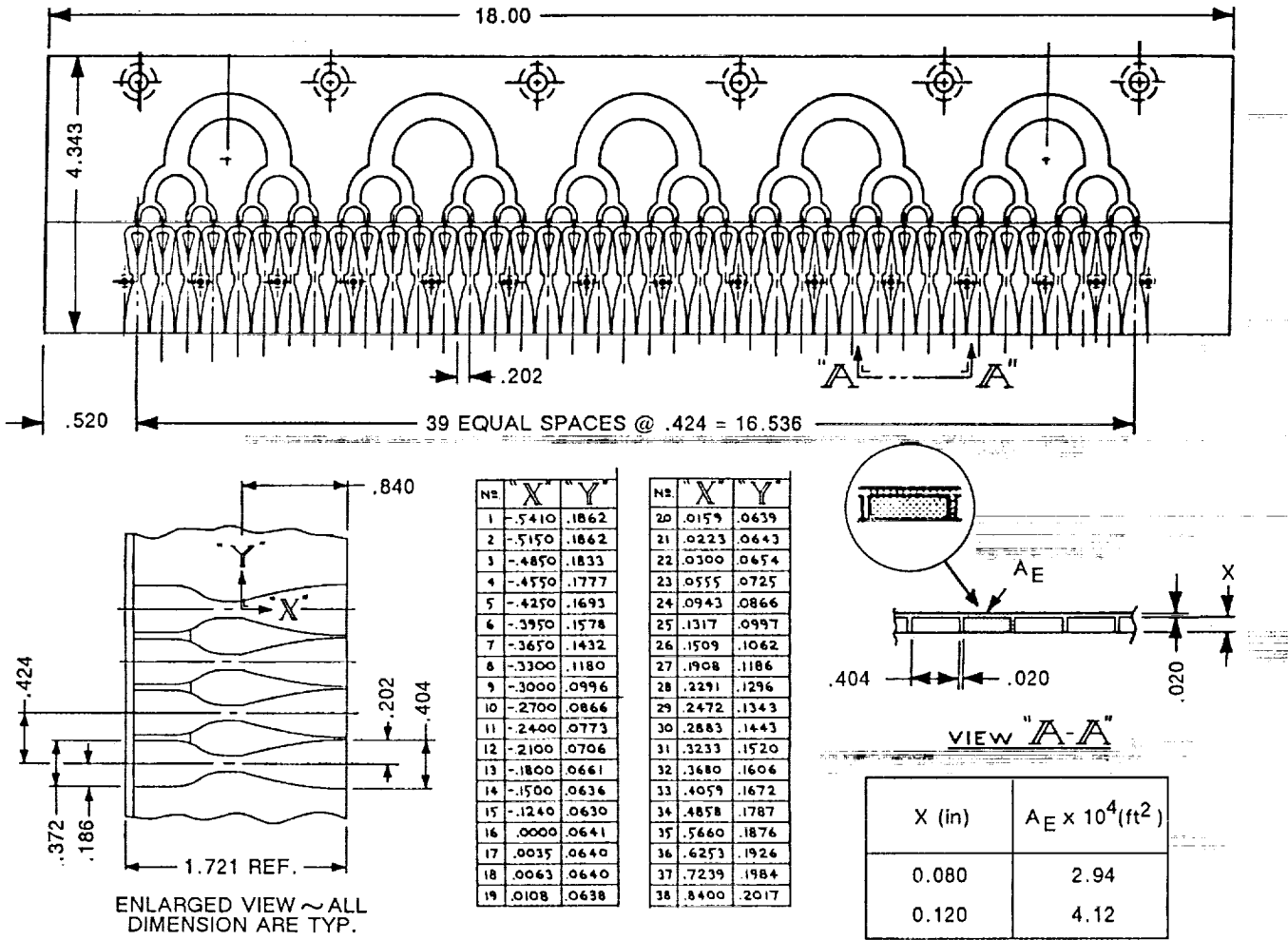


Figure 13 SCHEMATIC DIAGRAM OF INJECTOR SECTION OF MODEL

through five fast-acting valves and is designed so that flow is established within 5 milliseconds from valve actuation. Pressure instrumentation was placed in the passages ahead of the nozzles to monitor flow establishment and the flow rates through the nozzles. The two trailing-edge flat plates, mounted downstream of the slots, contained extensive heat transfer and pressure instrumentation covering the distance of 17 inches downstream of the injection station. A schematic diagram of the film cooling model showing the layout of the instrumentation is shown in Figure 14. The instrumentation density on each plate was graduated to achieve a high resolution in the shock-interaction region. During the studies without incident shocks, the plates were oriented to place a high density of instrumentation close to the nozzle exits. For the studies with shock impingement, the 5-inch plate was rotated 180° to obtain detailed measurements in the shock-interaction region. A sharp shock-generator plate was mounted above the film-cooling plate from support arms attached to the sting well downstream of the injection slots. The angle of the shock generator and its vertical and streamwise positions above the flat plate were adjustable to place a shock of the required strength at any prescribed streamwise location. The shock generator was designed to be of a length sufficient to prevent the trailing-edge expansion from decreasing the pressure in the interaction region.

2.3.2 Calculation of Coolant Rates

The mass flow rates of the coolant have been calculated under the assumptions of isentropic flow issuing from the coolant reservoirs through a choked orifice. Calibrations at various reservoir pressures were conducted, and an orifice calibration coefficient was experimentally determined from a comparison of experimental and theoretical reservoir change in mass, which occurred during a short-duration blowdown of the coolant reservoirs. The experimental change in mass measures the difference between the initial state of the reservoir pressure at room temperature and the final state reached once the valves have closed after blowdown and heat transfer from the surroundings has returned the reservoir gas to room temperature. The theoretical change in mass of the reservoir was calculated as the difference between the initial reservoir mass at the initial pressure and at room temperature and the final mass achieved by an isentropic blowdown through a known choked throat area. Since the isentropic relation is a function of time, the mass of the reservoir was calculated at the end of the calibration blowdown and was compared to the experimental results to obtain the orifice discharge coefficient, as shown in Equation 9. Once the discharge coefficient has been calculated, the isentropic blowdown equations may

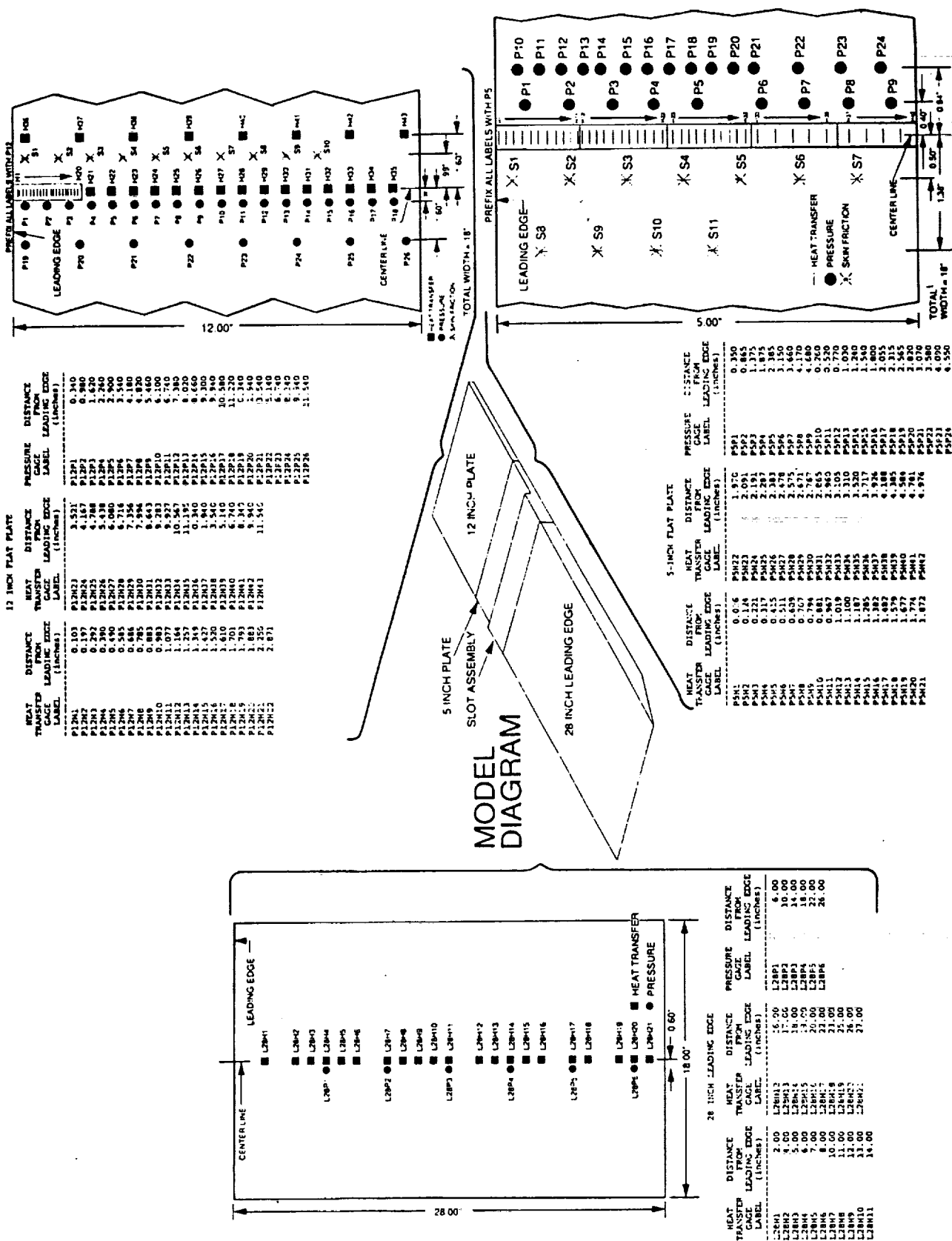


Figure 14 INSTRUMENTATION POSITIONS ON FILM-COOLING/SHOCK-INTERACTION MODEL

be utilized to determine the mass flow rate at any time t . In both methods, real gas effects can be neglected, since the pressure drops are relatively small.

$$C_D \int_0^{t_f} \dot{m}_{\text{theor.}} d\tau = m_{\text{final}} - m_{\text{initial}} \quad (9)$$

Hence,

$$C_D = \frac{\Delta P \left(\frac{V}{RT_{\text{room}}} \right)}{\frac{m(0)}{\gamma} \left[1 - \left(1 + \frac{\gamma-1}{2} \tau_{\text{final}} \right)^{\frac{2\gamma}{\gamma-1}} \right]}$$

Using the isentropic blowdown through a choked orifice of known discharge coefficient, the mass flow rates experienced during the tunnel run time can be calculated from Equation 10. These results are recorded in Table 2. As a check, the theoretical change in mass of the reservoirs was compared to that of the actual change, and the difference was typically within 5%.

$$\frac{\dot{m}(\tau)}{\dot{m}(0)} = \left[1 + \frac{\gamma-1}{2} \tau \right]^{\frac{\gamma+1}{\gamma-1}} \quad (10)$$

where

$$\tau = \frac{t}{\beta}$$

V = Volume of Reservoir

C_D = Discharge Coefficient

A^* = Area of Orifice

$a(0) = \sqrt{\gamma RT(0)}$ of Reservoir at $t=0$

$$\beta = \frac{V}{C_D A^* a(0)} \left(\frac{2}{\gamma+1} \right)^{\frac{\gamma+1}{2(\gamma-1)}}$$

$$\dot{m}(0) = \frac{p(0)}{\sqrt{T(0)}} A^* C_D K(\gamma)$$

2.3.3 Heat Transfer Instrumentation

The large heat transfer rates and gradients generated in the reattachment regions of hypersonic shock-wave/turbulent boundary interaction, coupled with the intrinsically unsteady characteristics of these flows, makes it essential that accurate time-resolved heat transfer measurements be obtained in experimental studies of these flows. In our earlier

studies¹⁶, we demonstrated that heat transfer measurements can also be used as an accurate indication of the occurrence of flow separation, and of the scales of the separated region. Because of the severe heat transfer gradients developed in these flows, it is essential to obtain finely spatially resolved measurements on models constructed with surfaces of low thermal conductivity to avoid distortion resulting from longitudinal heat conduction. The use of miniature thin-film heat transfer instrumentation based on a Pyrex substrate, coupled with the relatively small rise in surface temperatures inherent in shock tunnel studies of these flows, makes the thin-film heat transfer instrumentation we employed almost ideal for these types of studies. The high-frequency resolution of this instrumentation also provides the opportunity to obtain definitive information on the unsteady characteristics of turbulent interaction regions. In the current studies, we employed platinum thin-film gages mounted on Pyrex strips such that spatial resolutions of 0.050 inch were obtained in key areas of the flow. Because the thermal capacity of each of the gages is negligible, the instantaneous surface temperature of the backing material is related to the heat transfer rate by semi-infinite slab theory. A description of the data reduction procedure used for the thin-film heat transfer gages is given in Reference 19. Drawings of the model inserts and gage positions are shown in Figure 14.

For the thin-film heat transfer instrumentation, the uncertainties associated with the gage calibration and the recording equipment are estimated to be $\pm 5\%$ for the levels of heating obtained in the current studies.

2.3.4 Pressure Instrumentation

We employed two types of surface pressure transducers in these studies of shock-wave/wall-jet turbulent interaction. Calspan-designed and -constructed lead zirconium titanate piezoelectric pressure transducers were used to obtain essentially the mean pressure distribution through the interaction region, though the transducer and orifice combination could follow fluctuations up to 15 kHz. Extensive use was also made of Kulite flush-mounted pressure transducers in the model injector block and the instrumented flat plates. Miniature Kulite transducers were also used in the survey rake shown in Figure 15. This rake was used to survey the boundary layer characteristics ahead and downstream of the injection station. For the pressure instrumentation, the concentration is estimated to be $\pm 3\%$.

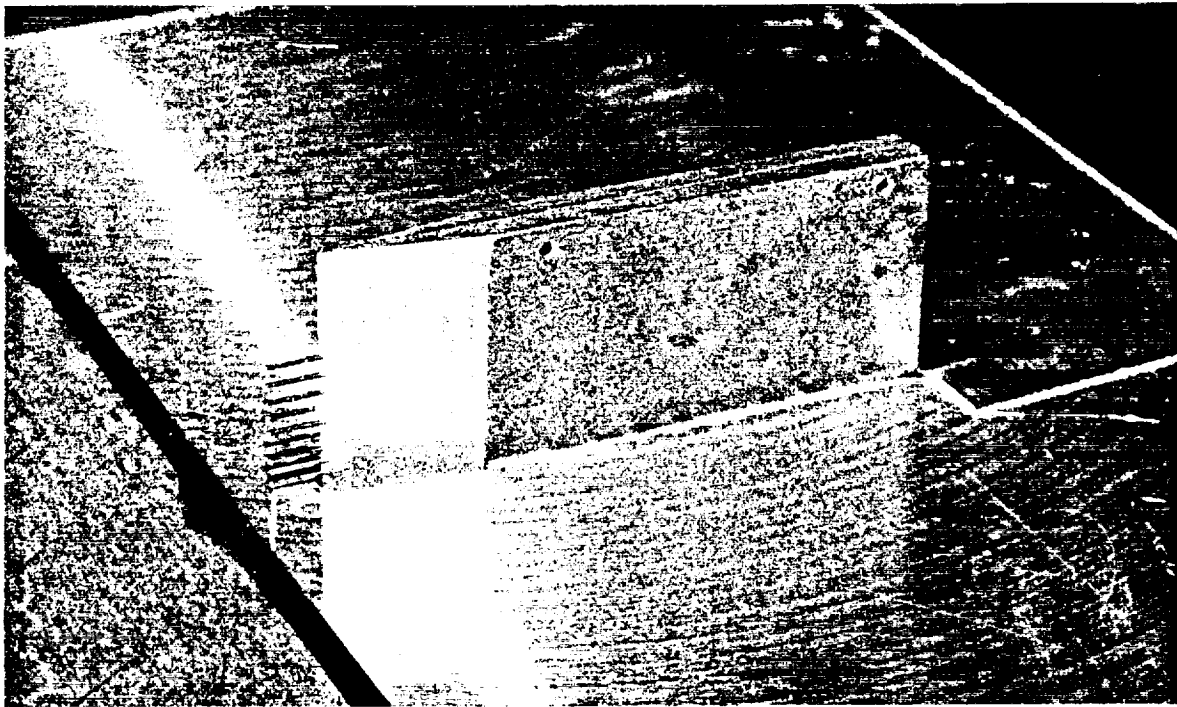


Figure 15a BOUNDARY LAYER SURVEY RAKE INSTALLED UPSTREAM OF NOZZLE EXIT

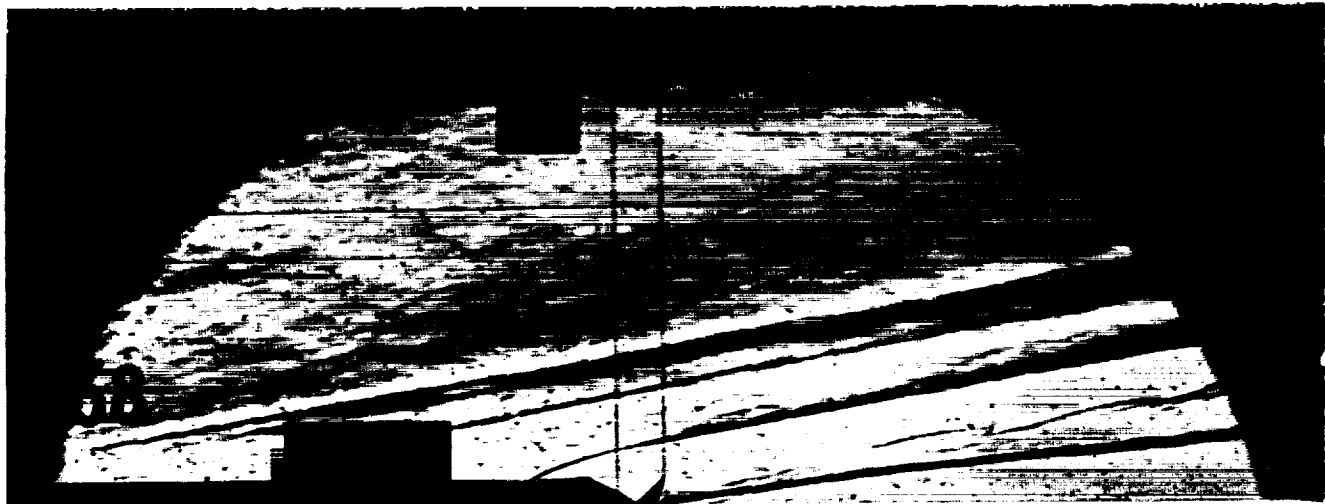


Figure 15b SCHLIEREN PHOTOGRAPH OF FLOW OVER SURVEY RAKE

2.3.5 Measurement Recording System

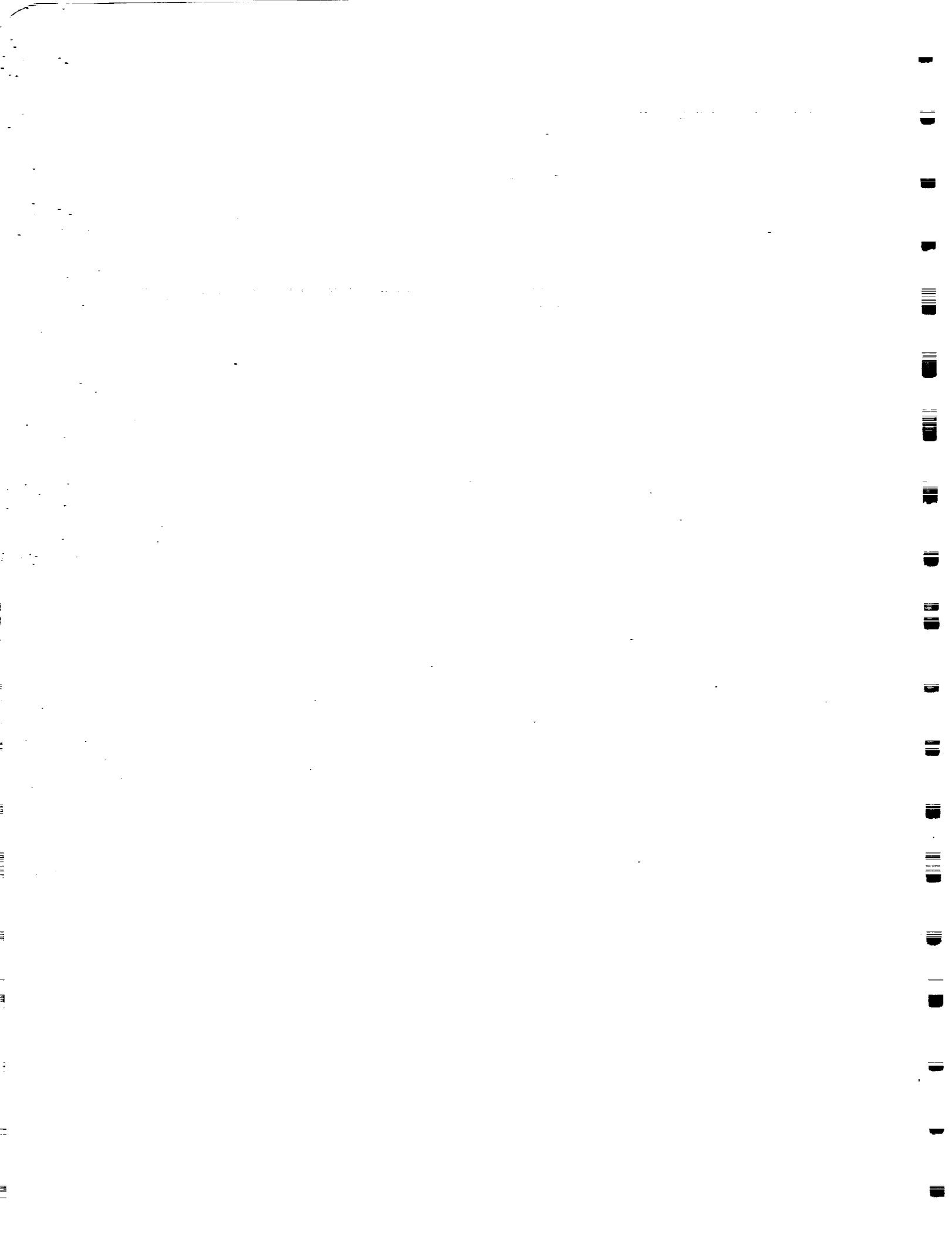
All data were recorded on the 128-channel Calspan Digital Data Acquisition System II (DDAS II). This system consists of 128 Marel Co. Model 117-22 amplifiers, an Analogic ANDS 5400 data acquisition and distribution system, and a DEC LSI-11/73 computer. The Analogic system functions as a transient-event recorder in that it acquires, digitizes, and stores the data in real time. Immediately after each test run, the data are transferred to the DEC computer for processing. The Marel amplifiers provide gains up to 1,000 for low-level signals, can be AC or DC coupled to the transducers, and have selectable low-pass filters with cutoff frequencies of 300, 1,000, or 3,000 Hz. The Analogic system contains a sample-and-hold amplifier, a 12-bit analog-to-digital converter, and a 4,096-sample memory for each channel. After the data are transferred to the DEC computer, plots of the analog voltage time histories are generated to determine the overall quality of the data and to select the steady-flow time interval. The data are then reduced to engineering units (psi or °F) and, in the case of pressures, averaged over the selected steady-flow time interval. An IBM-compatible computer program, CUBDAT, was constructed to provide the organization of raw voltage files for subsequent analysis of temporal and frequency-related phenomena. Additionally, the program was extended to include a major data-correlation function. The measurements made in this program are available in a database of measurements compiled on 3.5" diskettes together with CUBDAT, which provides access and presentation of these data. (See Appendix C for description.)

2.3.6 Holographic Interferometry

Holographic interferometry was used to make flowfield measurements. Interferograms of complex flowfields provide a good qualitative basis for evaluating some of the important phenomena that control the characteristics of these flows. CUBRC's holographic recording system¹⁹ was used for these studies. Both single-plate and dual-plate techniques are used to obtain holograms, which can be subsequently used in the playback step to obtain shadowgrams, schlieren photographs, and interferograms of the tests. Typical schlieren and holographic-interferometry photographs are presented in the following section. (See Figures 16a, 17, 18, 25, 26, 30, 35, 42, and 47.)

2.3.7 Flow Visualization

Flow visualization in these studies was accomplished via a standard off-axis, Z-type schlieren system, which uses 16-inch-diameter, f/7.5 schlieren-grade spherical mirrors as schlieren heads. A horizontal source-slit/knife-edge combination provides sensitivity in the vertical plane of 5 arc seconds, with test-section resolution better than 0.005 inch. A 1.5-microsecond FWHM (full-width, half-maximum) light pulse was generated from a high-voltage spark in air, triggered close to the end of the steady run time. The image was recorded on Kodak Tri-X panchromatic film.



Section 3 RESULTS AND DISCUSSION

3.1 INTRODUCTION

This program was conducted in a series of phases, and the results of the first phase were employed to select the model configurations and test conditions employed in the subsequent experimental phases. During the initial phase of the work, measurements were made on flat plates and in regions of shock/boundary layer interaction without coolant injection to select the freestream conditions and model configurations that would be suitable for the studies with combined film cooling and shock interaction. Measurements were then made for shock-wave/boundary layer interaction in the absence of cooling, using the film cooling configuration. Then, to establish the baseline conditions for the subsequent shock-interaction studies, measurements were made for a range of film cooling rates for both the 0.080-inch and 0.120-inch slot height configurations without shock impingement. The major body of research was conducted to investigate incident-shock/wall-jet interaction for a range of incident shock strengths and cooling-film conditions. Here, we were interested in establishing the occurrence and characteristics of the separated regions induced by shock-wave/wall-jet interaction. We also sought to understand the mechanism of the dispersion of the wall layer by the incident shock and the resultant loss in cooling in the recompression region of the flow. As part of this investigation, measurements were also made for lip thicknesses of 0.020 inch, 0.145 inch and 0.205 inch. The model configurations, injection pressures, and flow rates for each run in this experimental program are presented in Table 2.

3.2 MEASUREMENTS TO SELECT FREESTREAM CONDITIONS

During the first phase of the investigation, we made measurements to determine the heat transfer and pressure distributions along a flat-plate configuration at three different freestream conditions to select the flowfield configuration to be used in the experimental program. The heat transfer and pressure measurements on the flat-plate configuration, constructed by elevating the 5- and 12-inch instrumented plates to the level of the top of the injectors, are shown in Figures 16a and 16b. For the test conditions that we selected for the program ($M=6.4$, $Re/ft = 8.8 \times 10^6$), we show good agreement between the measured heat transfer rates and a prediction based on a modified Van Driest method²⁰.

Table 2
MODEL AND BLOWING CONFIGURATION

Run	Mach	Reynolds Number ($10^6/\text{ft}$)	Slot Height (in.)	λ $\rho_{\text{cuc}}/\rho_{\text{ue}}$	Schock Gen. Angle (deg)	Exit Pressure Ratio	Lip Thickness (in.)
4	6.423	8.81	FLAT PLATE	0.000	-	-	-
5	7.867	7.59	FLAT PLATE	0.000	-	-	-
6	6.471	13.70	FLAT PLATE	0.000	-	-	-
8	6.430	8.57	0.080	0.000	-	-	0.020
14	6.420	8.40	0.080	0.186	-	1.782	0.020
15	6.434	8.67	0.080	0.217	-	1.954	0.020
** 5 INCH FLAT PLATE ROTATED 180 DEGREES **							
21	6.437	8.46	0.080	0.301	-	2.609	0.020
23	6.438	8.48	0.080	0.148	-	1.666	0.020
24	6.434	8.28	0.080	0.094	-	1.109	0.020
25	6.436	8.46	0.080	0.000	10.5	-	0.020
26	6.437	8.55	0.080	0.000	8.0	-	0.020
27	6.437	8.39	0.080	0.107	8.0	1.131	0.020
28	6.441	8.54	0.080	0.202	8.0	1.707	0.020
29	6.439	8.46	0.080	0.224	8.0	2.049	0.020
30	6.436	8.52	0.080	0.000	5.5	-	0.020
31	6.437	8.31	0.080	0.105	5.5	1.198	0.020
32	6.440	8.19	0.080	0.261	5.5	2.405	0.020
33	6.439	8.48	0.080	0.109	10.5	1.172	0.020
34	6.438	8.38	0.080	0.243	10.5	2.118	0.020
35	6.438	8.41	0.080	0.000	10.5	-	0.020
36	6.437	8.52	0.080	0.237	10.5	2.112	0.020
37	6.438	8.52	0.080	0.000	10.5	-	0.020
38	6.436	8.35	0.080	0.240	10.5	2.121	0.020
39	6.440	8.54	0.080	0.000	10.5	-	0.145
40	6.437	8.41	0.080	0.104	10.5	1.169	0.145
41	6.438	8.37	0.080	0.252	10.5	2.131	0.145
43	6.433	8.86	0.120	0.000	-	-	0.020
44	6.430	8.65	0.120	0.069	-	0.766	0.020
45	6.432	8.40	0.120	0.106	-	1.028	0.020
46	6.431	8.63	0.120	0.155	-	1.395	0.020
47	6.429	8.58	0.120	0.217	-	1.839	0.020
50	6.426	8.48	0.120	0.102	8.0	1.019	0.020
51	6.436	8.61	0.120	0.237	8.0	1.890	0.020
52	6.431	8.84	0.120	0.000	8.0	-	0.020
53	6.432	8.14	0.120	0.000	8.0	-	0.020
55	6.437	8.52	0.120	0.105	8.0	1.319	0.020
56	6.436	8.41	0.120	0.249	8.0	1.901	0.020
57	6.436	8.21	0.120	0.000	5.5	-	0.020
58	6.441	8.58	0.120	0.102	5.5	1.077	0.020
59	6.445	8.83	0.120	0.236	5.5	1.891	0.020
60	6.437	8.34	0.120	0.246	5.5	2.003	0.020
61	6.436	8.15	0.120	0.000	5.5	-	0.020
62	6.439	8.41	0.120	0.237	10.5	1.932	0.020
63	6.437	8.41	0.120	0.000	10.5	-	0.020
65	6.436	8.46	0.120	0.099	-	1.031	0.205
66	6.439	8.48	0.120	0.000	-	-	0.205
67	6.434	8.51	0.120	0.237	-	1.948	0.205

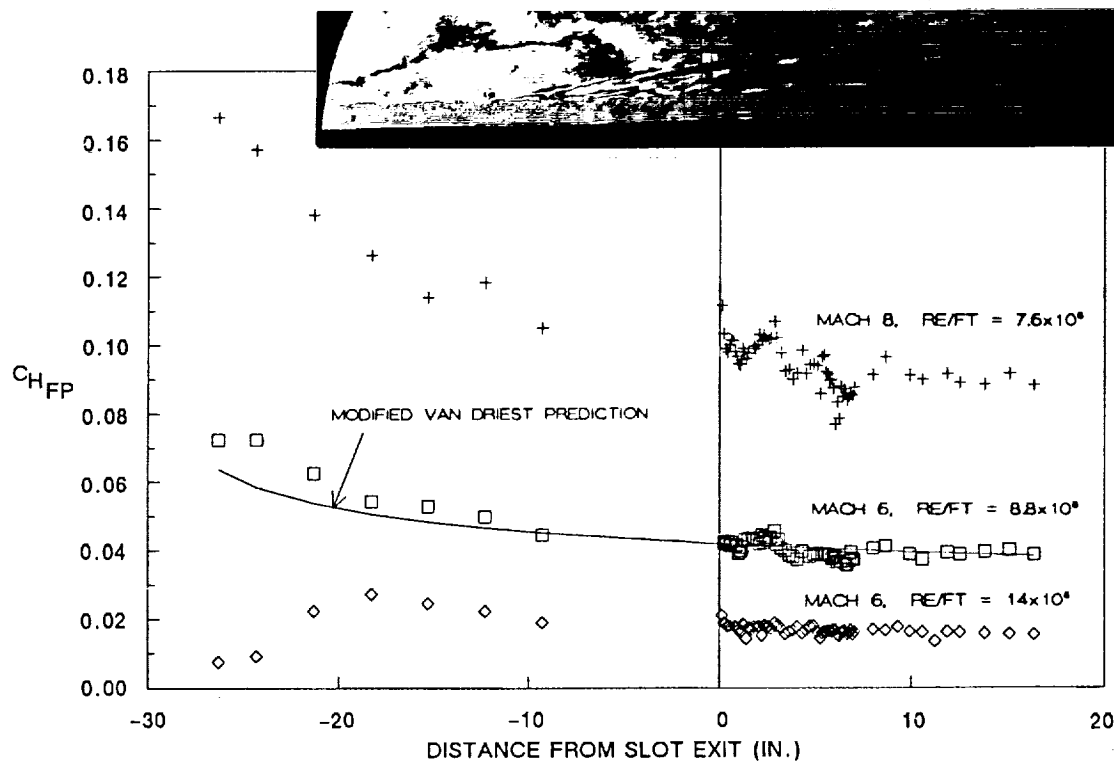


Figure 16a COMPARISON BETWEEN FLAT-PLATE HEAT TRANSFER MEASUREMENTS AND SIMPLE PREDICTIONS

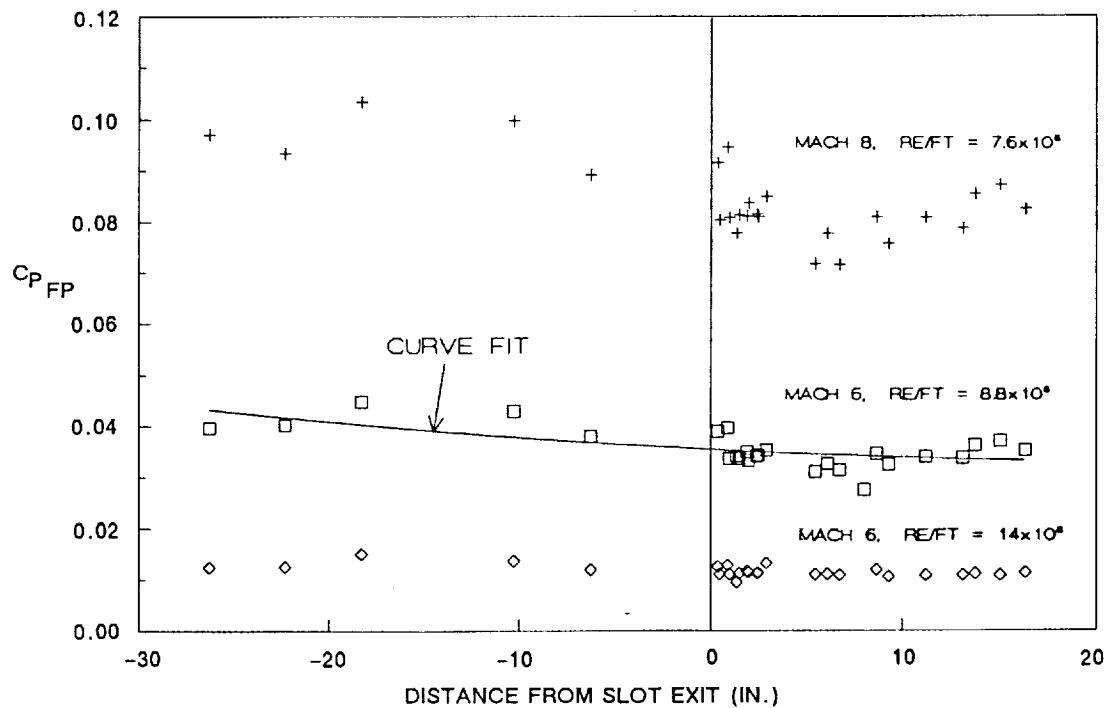


Figure 16b PRESSURE MEASUREMENTS ON FLAT PLATE

3.3 BOUNDARY LAYER PROFILE MEASUREMENTS UPSTREAM OF SLOT INJECTION

Flowfield surveys across the boundary layer just upstream of the exit plane of the slot were made to provide information both for experimental correlations and for CFD validation. To make these measurements, we employed two specially constructed boundary layer rakes containing pitot pressure and total temperature instrumentation. The measurements made with this instrumentation, combined with the static pressure measurements on the plate, provided a set of information to define the mean structure of the boundary layer just upstream of the lip. The pitot pressure and total temperature rakes used in this study are shown in Figure 13. We employed 0.062-inch-diameter Kulite strain gage transducers to obtain the pitot pressure measurements and shielded total temperature probes of the same diameter with thin-wire platinum-rhodium thermocouple sensing elements. Each rake contained eight probes, spaced 0.1-inch between centers. The velocity distribution and Mach number distribution across the flow can be determined by combining these two sets of measurements with the measurement of static pressure on the plate:

$$\frac{\rho_{\text{rake}}}{\rho_{\text{plate}}} = \left[\frac{(\gamma+1) M_b^2}{2} \right]^{\frac{\gamma}{\gamma-1}} * \left[\frac{\gamma+1}{2\gamma M_b^2 (\gamma-1)} \right]^{\frac{1}{\gamma-1}} \quad (11)$$

$$\frac{u_b}{u_e} = \left(\frac{M_b}{M_e} \right) \left(\frac{T_{o_b}}{T_{o_e}} \right)^{1/2} \left(\frac{1+m_e}{1+m_b} \right)^{1/2} \quad (12)$$

where

$$m_b = \frac{\gamma-1}{2} M_b^2$$

$$m_e = \frac{\gamma-1}{2} M_e^2$$

Tabulations of the measurements and the derived velocity distributions obtained in this set of studies are shown in Appendix B.

3.4 MEASUREMENTS IN REGIONS OF SHOCK-WAVE/BOUNDARY LAYER INTERACTION ON FLAT-PLATE CONFIGURATION WITHOUT FILM COOLING

In this segment of the program, we examined the effects of the step upstream of shock impingement on the characteristics of the region of shock-wave/boundary layer interaction without film cooling. The incident-shock strengths at which these studies were

conducted were selected such that they gave a range of the freestream pressure rises that may occur for shock propagated through scramjet combustors. For the model and flowfield configurations and freestream conditions used, our earlier studies indicated that the interacting flows would remain completely attached in the absence of film cooling. However, because the interactions were induced downstream of injector steps, we first sought to investigate whether the flow-relaxation process influenced the characteristics of the regions of shock-wave/boundary layer interaction. The heat transfer and pressure records from the interactions behind the 0.080- and 0.120-inch steps without film cooling are shown for the three interaction strengths in Figure 23a and Figure 23b, respectively. There is no evidence of flow separation in the heat transfer and pressure measurements or in the schlieren photographs in the region close to shock impingement. Plotting the conditions used in these studies, together with those for earlier measurements of incipient separation, as shown in Figure 24a, it can be seen that the total turning angles in the present studies are less than those found to induce incipient separation for flows with constant-pressure boundary layers upstream of the interaction. The maximum values of heat transfer and pressure at the end of the interaction region are correlated with those from earlier studies in Figure 24b. We see good agreement between the data sets and the power-law relationship $q/q_0 = (P/P_0)^{0.85}$ found in Reference 22. We conclude from these measurements that the disturbances to the turbulent boundary layer introduced by the step did not result in distortion to the flow structure that altered the scale or properties of the regions of shock-wave/boundary layer interactions.

3.5 BASELINE MEASUREMENTS WITH FILM COOLING IN THE ABSENCE OF SHOCK INTERACTION

3.5.1 Measurements of Film-Cooling Effectiveness

In preparation for the shock-interaction studies, measurements of heat transfer and pressure were made downstream of the 0.080- and 0.120-inch cooling slots for non-

dimensional blowing rates $\lambda_c = \frac{\rho_e U_c}{\rho_e U_e}$ from 0.0 to 0.28. Schlieren photographs of flow from the 0.120-inch slot for a range of blowing rates are shown in Figure 17. Figure 17a shows the case without film cooling, where a recompression shock is generated downstream of the step. As shown in Figure 18a, this induces a local peak in the heating rates at the end of the recompression process, followed by a local dip below, and a gradual return to the flat-plate level. The shocks seen ahead of the step, and halfway down the flat plate, are introduced by discontinuities at the spanwise extremities of the models. For film-cooling

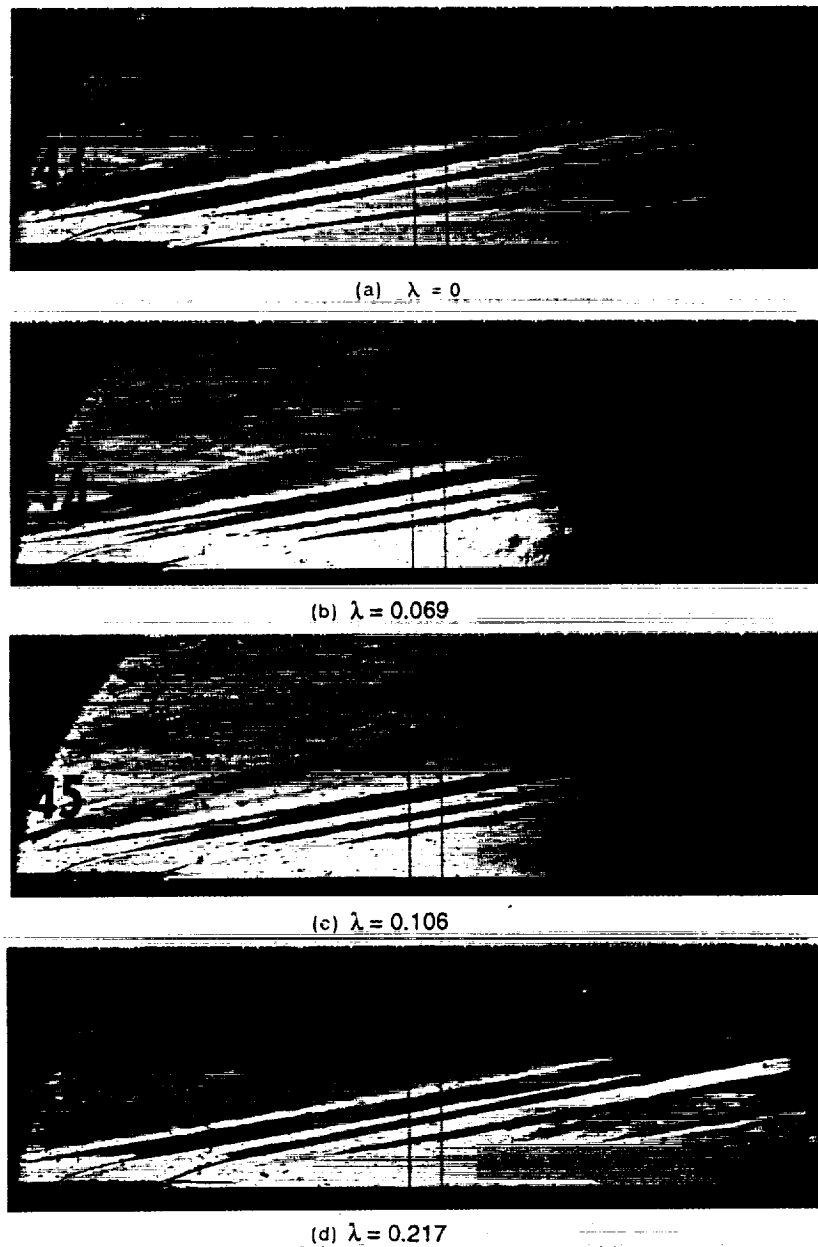


Figure 17 SCHLIEREN PHOTOGRAPHS OF SLOT-COOLING RUNS FOR 0.120-INCH SLOT WITH A RANGE OF INJECTION RATIOS

rates where the pressure at the exit plane of the nozzle equals the static pressure of the freestream, (the "matched-pressure" condition as shown in Figure 17c), there is a very weak wave at the top of the nozzle, and the initial boundary layer moves smoothly from the step. In contrast, for the highest blowing rates (Figure 17d), where the flow at the exit of the nozzle is underexpanded, strong shocks are generated above and behind the nozzle exit that may lead to enhanced mixing. It is clear from Figures 18a and 18b that the greatest rate of heating reduction occurs for the lower cooling rates, and that successive increases in coolant mass flow result in relatively little change in the heat transfer rates to the plate. Close to the matched-blown condition, the measurements from the two slot heights scale relatively well in terms of non-dimensional slot height. This can be seen by plotting the measurements in terms of cooling effectiveness (as shown in Figures 19a and 19b). Cooling effectiveness (η) is defined as

$$\eta = \frac{T_{awc} - T_{t\infty}}{T_{tc} - T_{t\infty}}$$

taking the reference value from the no-cooling run, we have

$$h_r = q_{nc}/(T_{aw} - T_w);$$

for coolant flow,

$$T_{awc} = \frac{q}{h_r} + T_w$$

thus,

$$\eta = (q/h_r + T_w - T_{t\infty})/(T_{tc} - T_{t\infty})$$

therefore,

$$\eta = \left[1 - \frac{q}{q_{nc}} \frac{(T_{aw} - T_w)}{(T_{0\infty} - T_{0c})} \right]$$

Our two sets of measurements correlate well, plotting η in terms of the scaled slot height $(X/S)/\lambda^{0.8}$ (derived in Reference 2), as shown in Figure 20a. Here, we follow the accepted convention of plotting measurements for η of 1 or less. Also shown in Figure 20a are the high Mach number data presented in Reference 10, in terms of this simple scaling parameter; clearly, the correlation is poor both for the breakpoint and for the subsequent rate of decay. Our measurements, in fact, scale better in terms of λ^{-1} , as shown in Figure 20b. For completeness, we have also compared our measurements (in Figure 21) with those compiled by Majeski and Weatherford¹⁰ in terms of the principal sets of non-dimensional parameters employed in their paper. It can be seen that, despite the inclusion of the constant Mach number, as suggested by Trolier, we still observe a larger

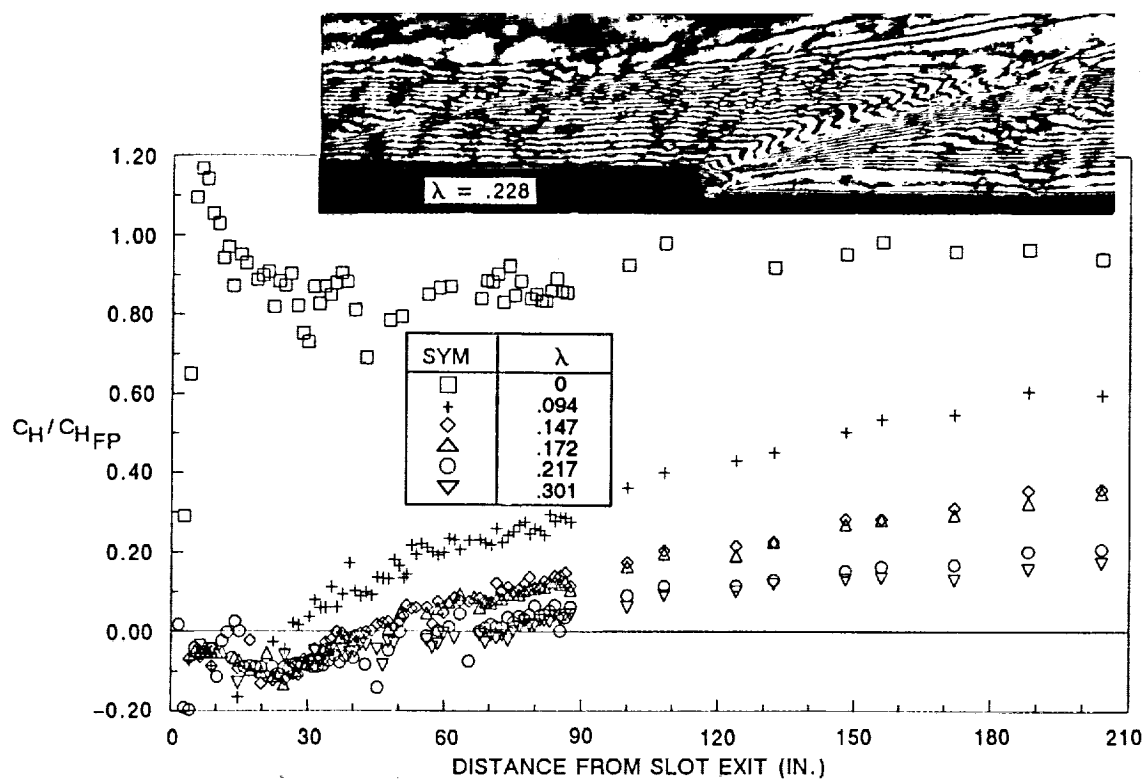


Figure 18a HEAT TRANSFER VARIATION WITH MASS ADDITION FOR 0.080-INCH SLOT

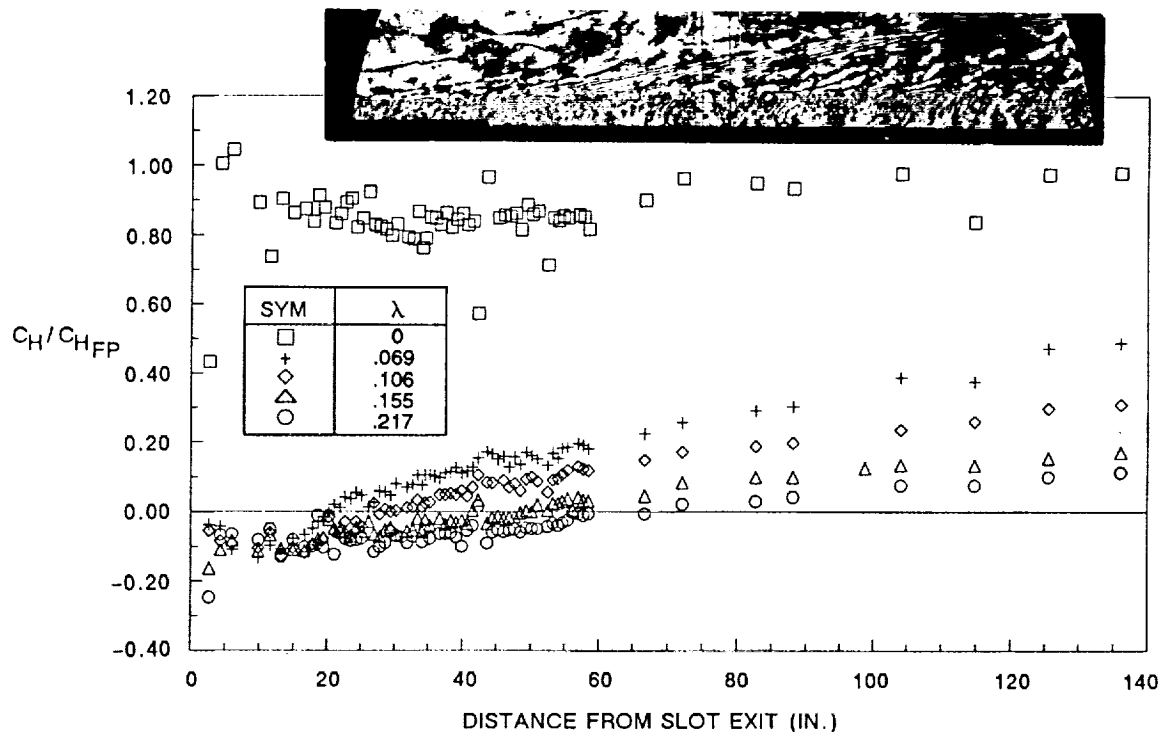


Figure 18b HEAT TRANSFER VARIATION WITH MASS ADDITION FOR 0.120-INCH SLOT

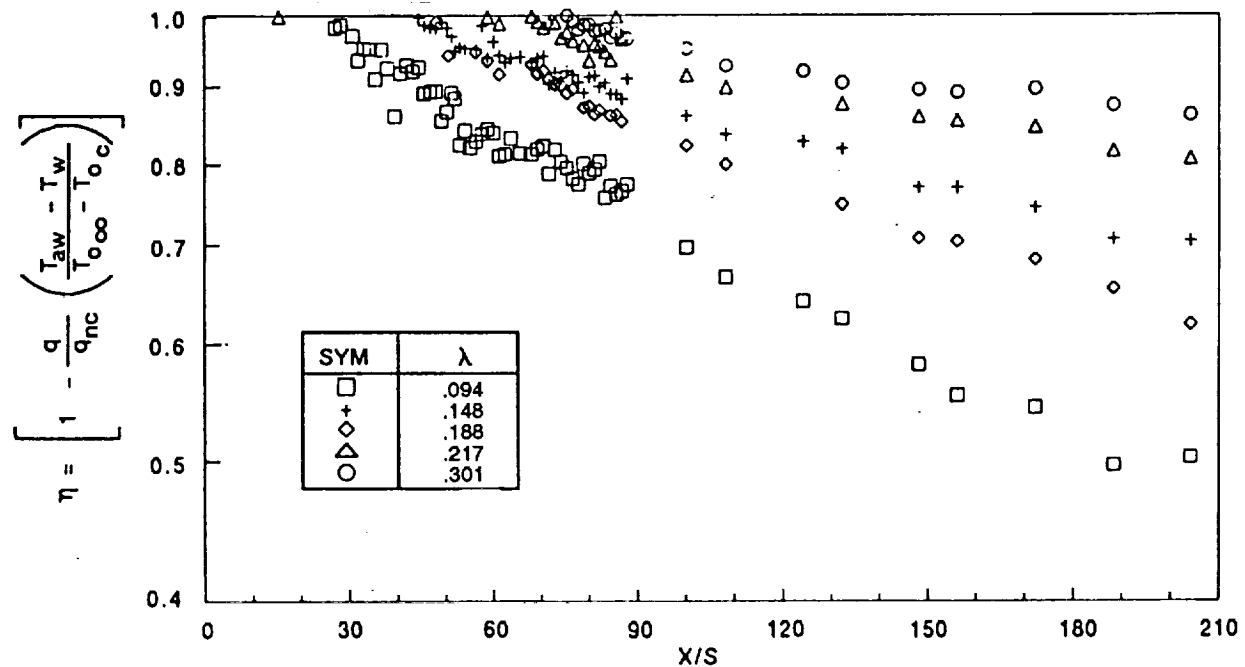


Figure 19a "EFFECTIVE EFFICIENCY" OF FILM COOLING FOR 0.080-INCH SLOT

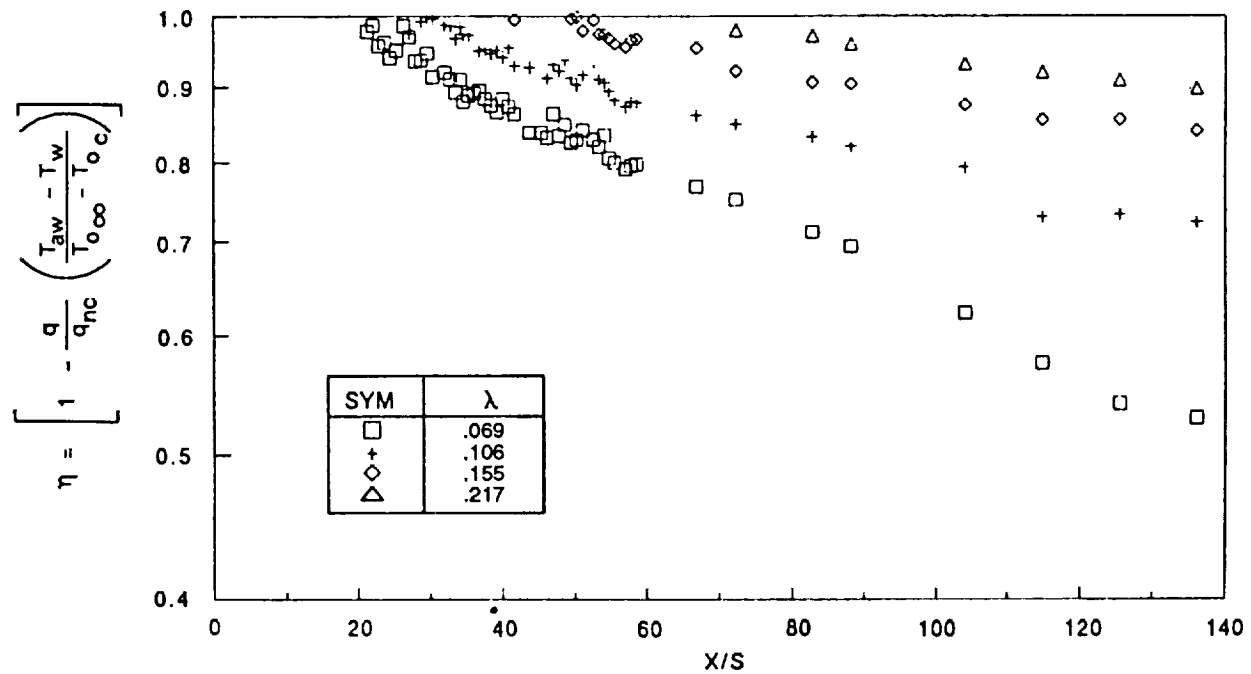


Figure 19b "EFFECTIVE EFFICIENCY" OF FILM COOLING FOR 0.120-INCH SLOT

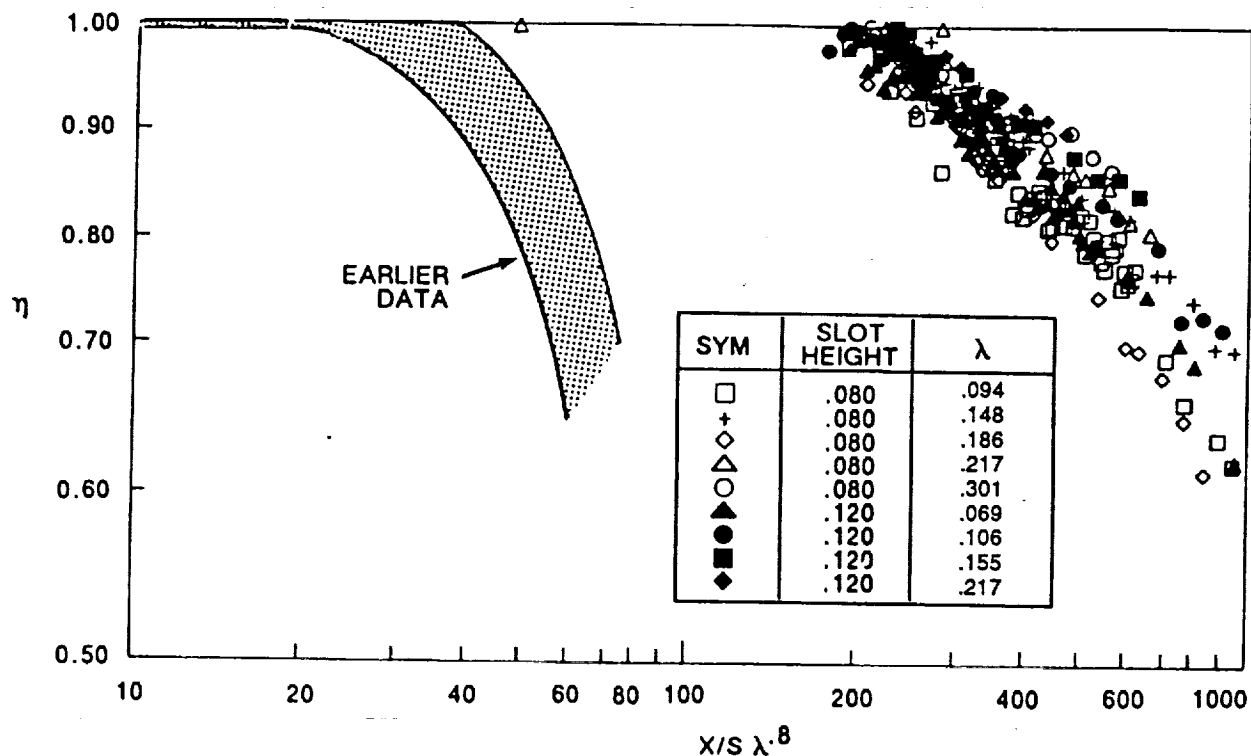


Figure 20a CORRELATION OF FILM-COOLING EFFECTIVE EFFICIENCY WITH SIMPLE SCALING PARAMETERS

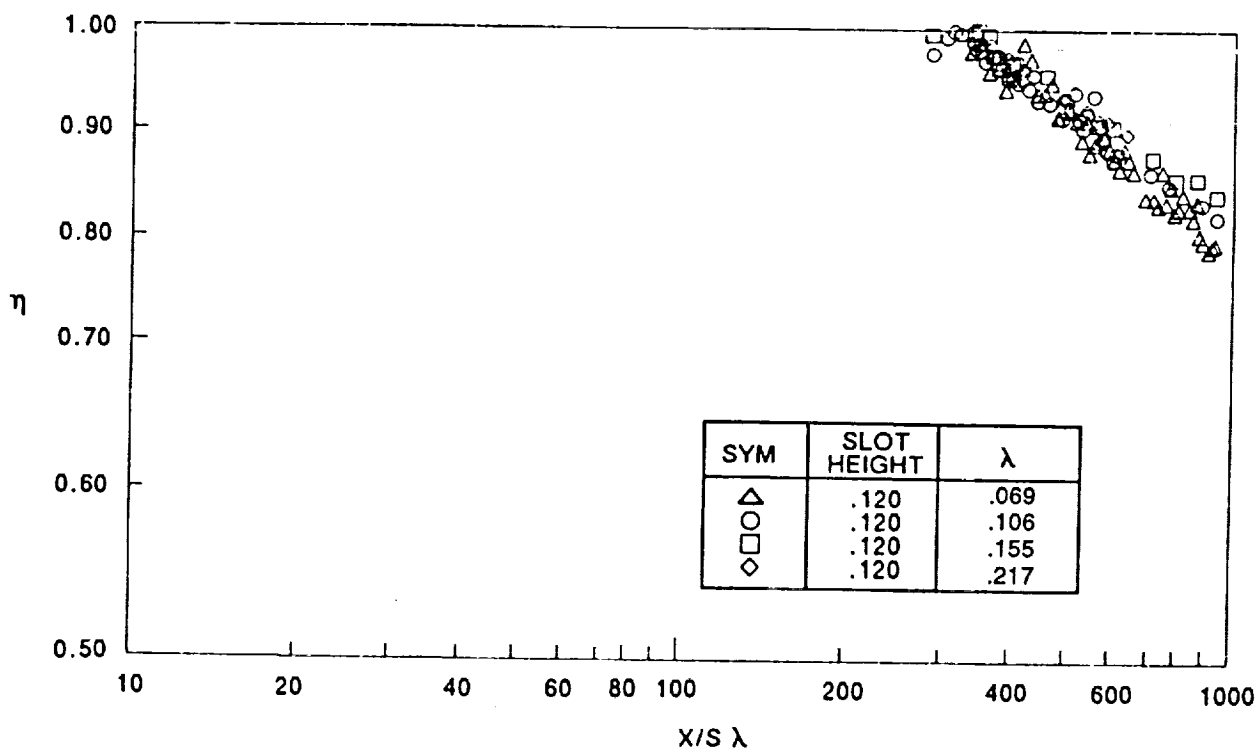


Figure 20b CORRELATION OF FILM-COOLING EFFECTIVE EFFICIENCY WITH SIMPLE SCALING PARAMETERS

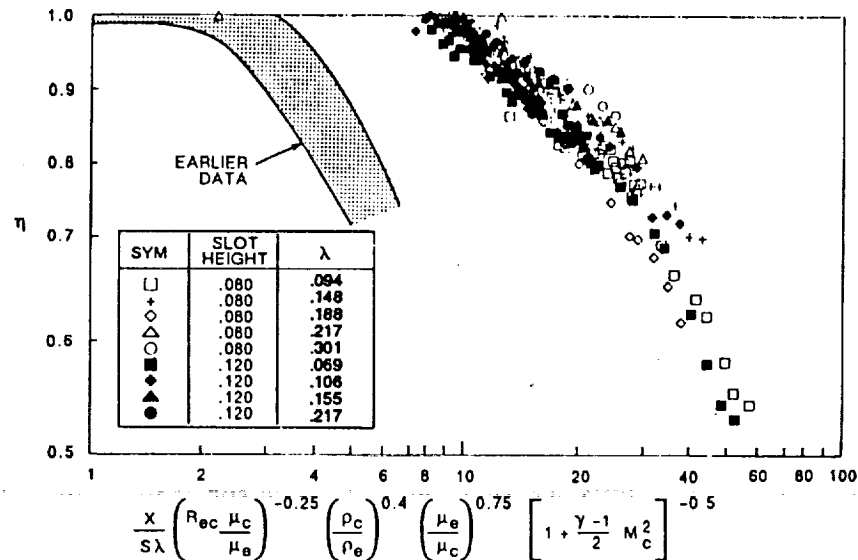


Figure 21a CORRELATIONS OF EFFECTIVE EFFICIENCY OF FILM COOLING

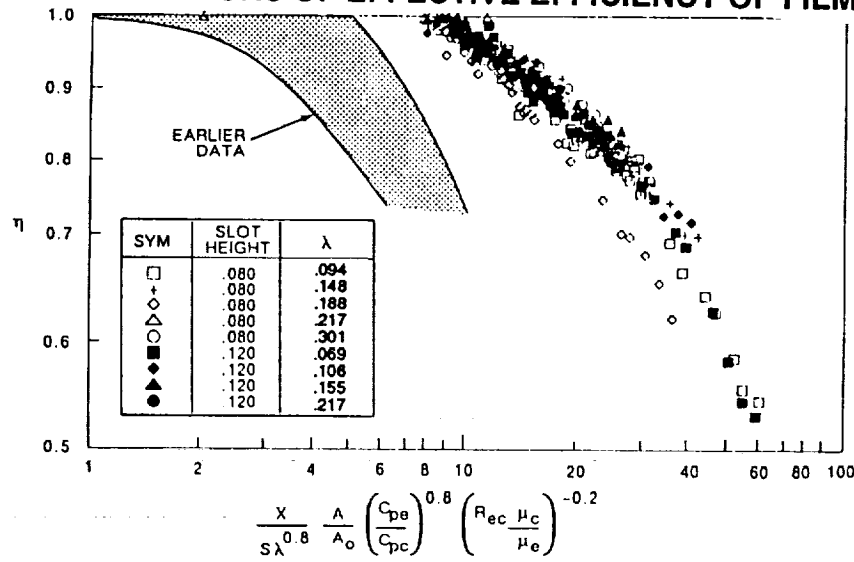


Figure 21b CORRELATIONS OF EFFECTIVE EFFICIENCY OF FILM COOLING

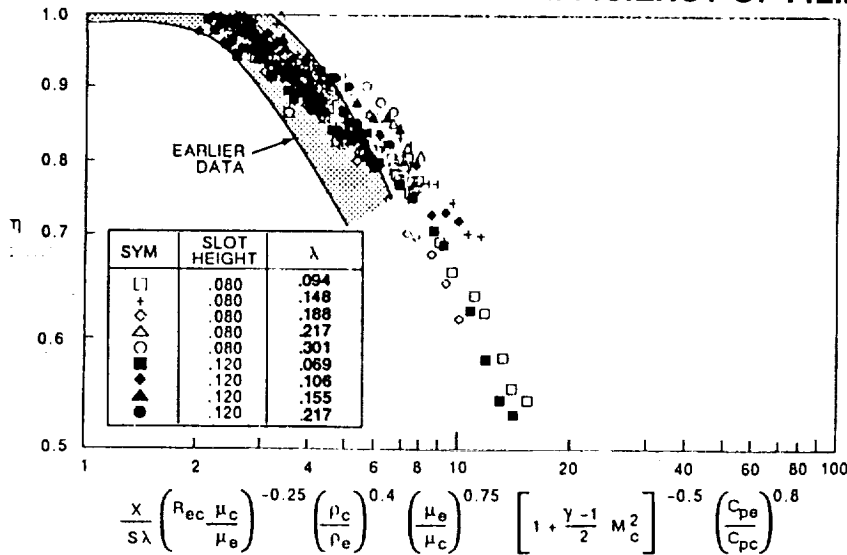


Figure 21c CORRELATIONS OF EFFECTIVE EFFICIENCY OF FILM COOLING

value for the breakpoint, and a slower decay in efficiency, in our studies. Including the specific heat ratios in the correlation (as shown in Figure 21b), as anticipated, improves the correlation. Combining the specific-heat term with the parameter shown in Figure 21a does improve the correlation, as shown in Figure 21c.

3.5.2 Lip Thickness Effect on Slot-Cooling Effectiveness

Although calculations with the "SHIP" code (Reference 8) indicate that increased lip thickness has a positive effect on slot-cooling effectiveness well downstream of the exit plane of the slot, there has been little experimental evidence to substantiate this calculation. Conceptually, it is difficult to rationalize that a small modification in the lip area of the flow could have a substantial effect on cooling effectiveness well downstream of the exit plane of the slot. In this limited experimental study, we selected a slot height of 0.120 inch and two lip thicknesses, one of 0.020 inch which was the thickness for which the basic studies were conducted, and a thicker lip, 0.205 inch in thickness, which represented an extremely thick lip configuration. We ran these two lip thicknesses for blowing rates equivalent to matched-pressure conditions ($\lambda = 0.094$) and a much higher blowing level ($\lambda = 0.222$). The principal objective was to determine how the heat transfer in the immediate vicinity of the slot, and well downstream of the slot, was influenced by the base flow behind the lip. Figure 22a shows a comparison between the heat transfer downstream of a slot operated under matched-pressure conditions for the two lip thicknesses. It can be seen that the strong interaction that occurred in the base region of the 0.205-inch lip influenced the heat transfer in the immediate vicinity of the slot, first increasing it, and then decreasing it relative to the thin slot configuration. However, well downstream of the immediate exit region, the effect of slot thickness is to very slightly decrease the effectiveness of slot cooling, rather than increasing it as predicted in the theoretical studies. The same trend is observed in the measurements for the larger blowing rates where there is a slightly greater variation in the cooling in the immediate vicinity of the slot, as shown in Figure 22b. But again, downstream of this region, the increase of lip thickness tends to degrade the cooling performance by a very small amount. We conclude that the effects of lip thickness for these flows without shocks are not strong enough to go to extreme measures to minimize lip thickness at the expense of complex construction techniques to obtain structural integrity.

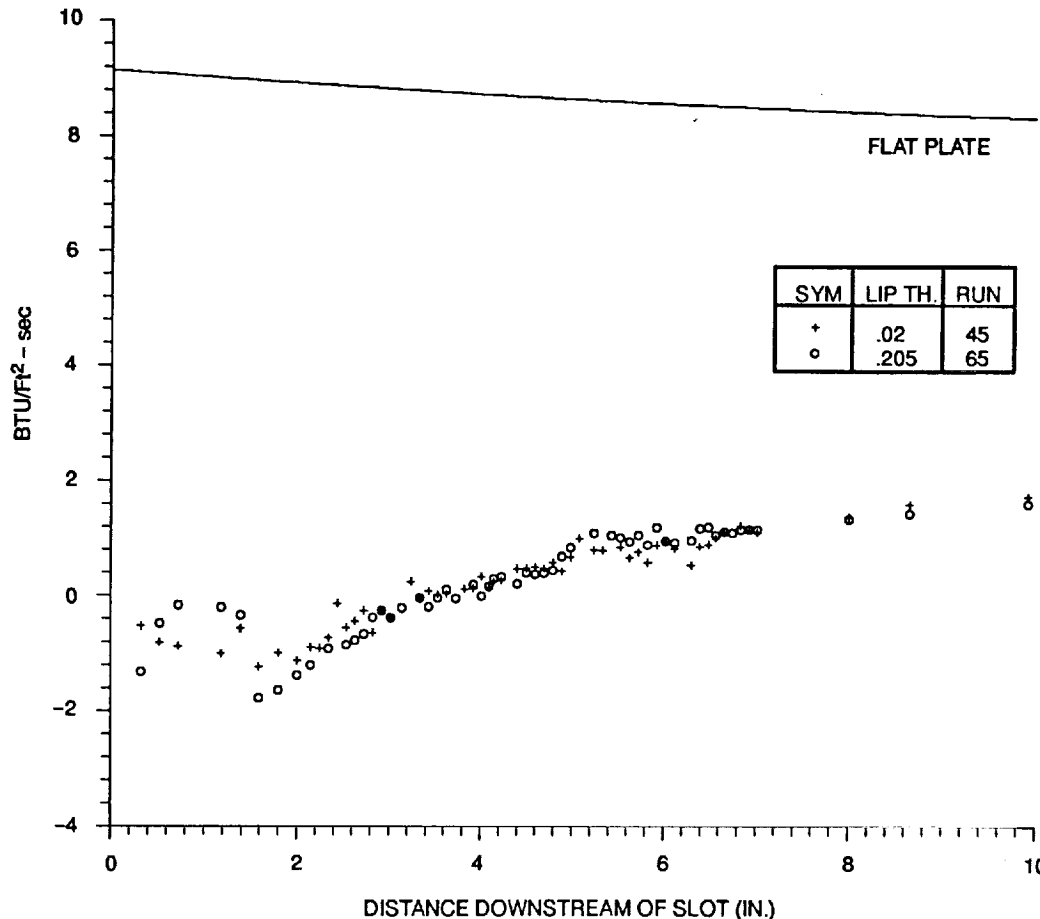


Figure 22a HEAT TRANSFER VARIATION WITH LIP THICKNESS FOR 0.120-INCH SLOT , MATCHED PRESSURE CONDITION ($\lambda=0.094$)

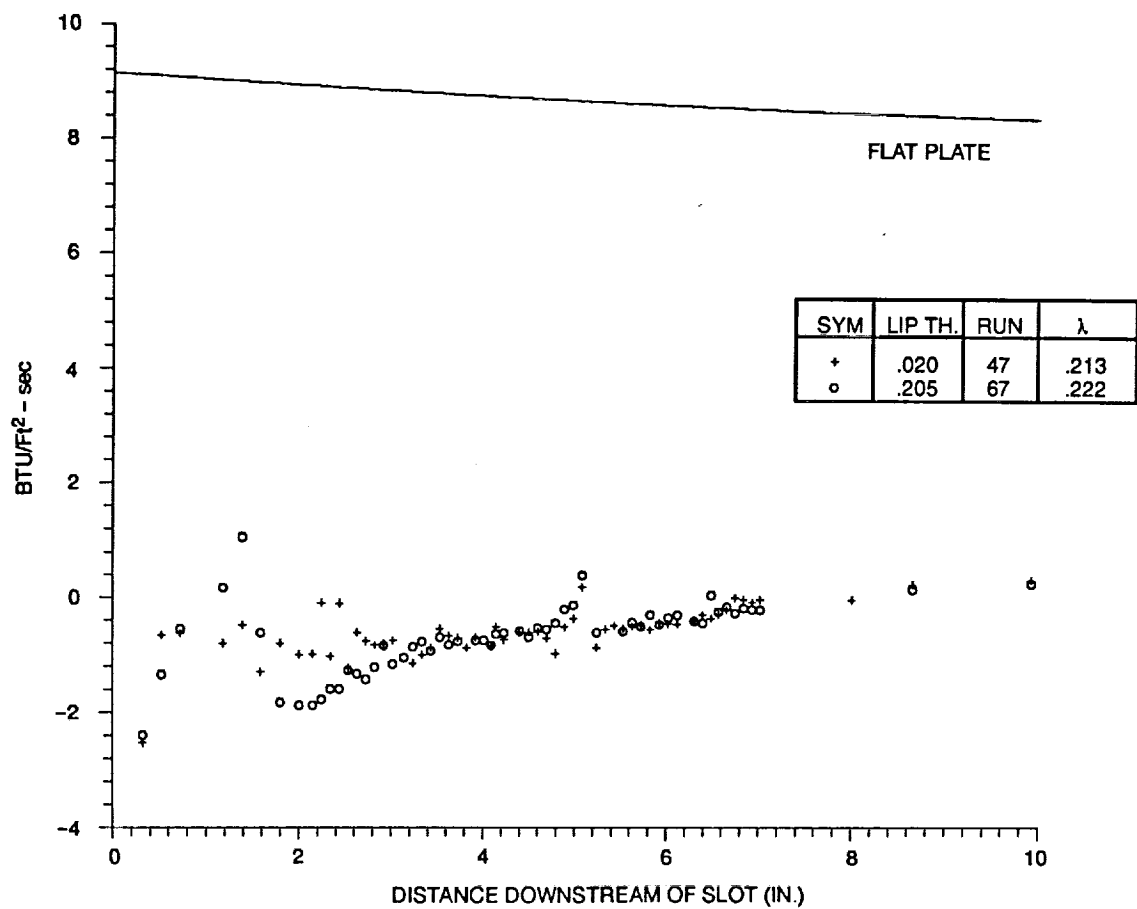


Figure 22b HEAT TRANSFER VARIATION WITH LIP THICKNESS FOR 0.120-INCH SLOT, "OVER-MATCHED" PRESSURE CONDITION ($\lambda=0.222$)

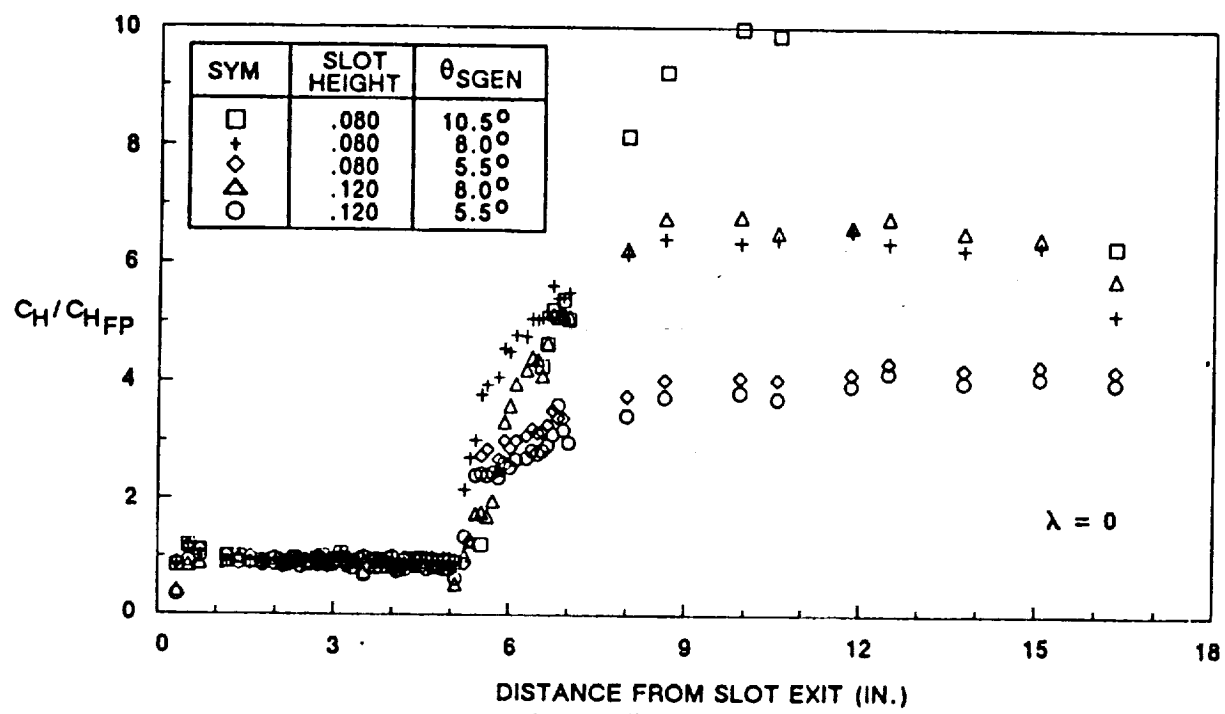


Figure 23a HEAT TRANSFER MEASUREMENTS IN SHOCK-INTERACTION REGION, WITHOUT FILM COOLING

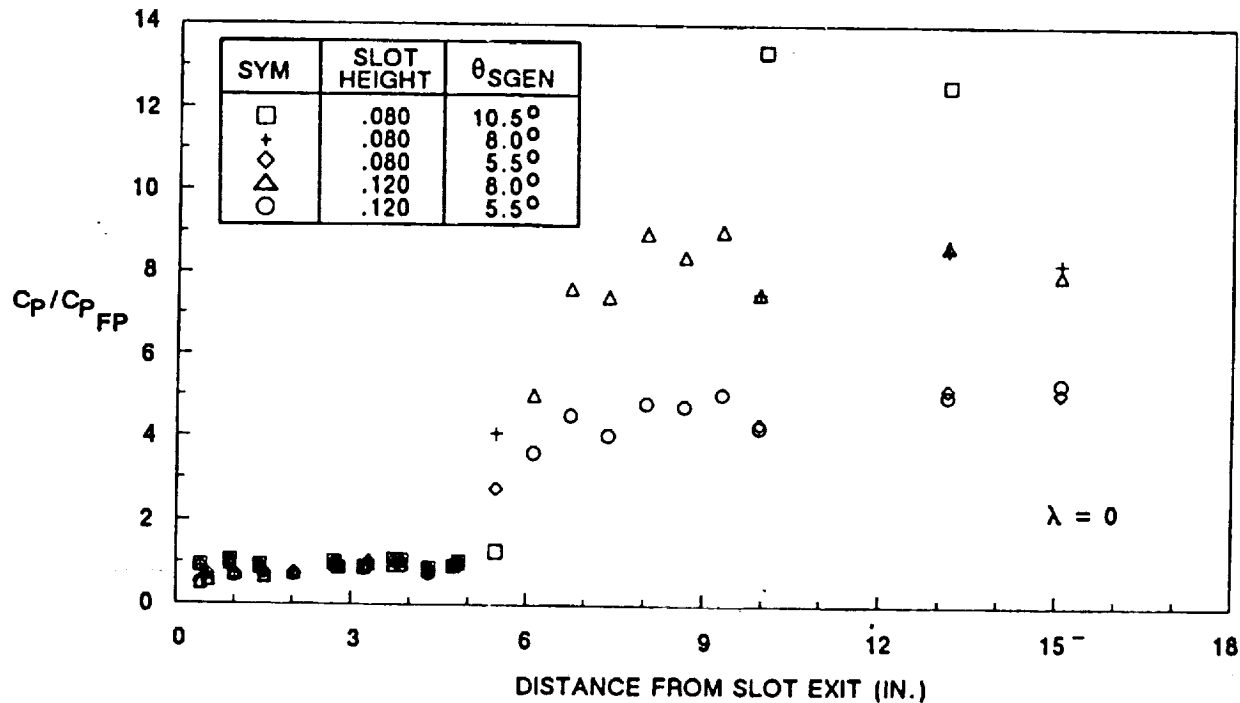


Figure 23b PRESSURE MEASUREMENTS IN SHOCK-INTERACTION REGION, WITHOUT FILM COOLING

3.6 STUDIES OF SHOCK-WAVE/WALL-JET INTERACTION

3.6.1 Purpose and Scope of Studies

The objective of this phase of the program was to determine the effectiveness of film cooling in regions of shock impingement. This segment of the studies was conducted in two parts: the first with the 0.080-inch slot, and the second with the 0.120-inch slot. In these studies, we were interested in the characteristics of, and in the changes in the structure of, the shock-impingement region, as well as in the distribution of wall properties with changes in film-cooling conditions, for a range of shock-interaction strengths. For each of the three interaction strengths ($\theta_{sgen} = 5.5^\circ, 8^\circ$, and 10.5°), measurements of the heat transfer and pressure distributions together with schlieren photographs of the flow were obtained for each blowing rate.

The major features of regions of shock-wave/wall-jet interaction are illustrated schematically, together with schlieren photographs, in Figures 24a and 24b. Figure 24a shows a flow with a large film-cooling rate and an incident-shock strength of 5.5° . Above and just downstream of the nozzles, the shocks generated by the underexpanded nozzle flow interacting with the freestream are clearly visible in the schlieren photography. Both of these shocks are weak and do not significantly alter the strength of the incident shock.

3.6.2 Studies With 0.080-Inch Slot Configuration

The three sets of measurements made with 0.080-inch slot are shown in Figures 25 through 29. For the 10.5° shock generator, it is readily apparent from the heat transfer and pressure distributions shown in Figures 26a and 26b (respectively), together with the schlieren photographs of Figure 26a, that well-separated regions are formed for the two blowing rates employed. Boundary layer separation is clearly indicated by a separation shock that traverses the boundary layer, and this flow feature is easily identified in the schlieren photographs in Figure 27. A well-defined plateau region is evident in the heat transfer and pressure distributions downstream of separation. These are shown more clearly in Figures 28 and 29, where we have replotted the measurements in the separated region on an expanded scale. For the lower blowing rate, the heat transfer rate in the separated region returns to approximately the non-cooling values. Downstream of reattachment, there is little difference between the heat transfer distributions with and

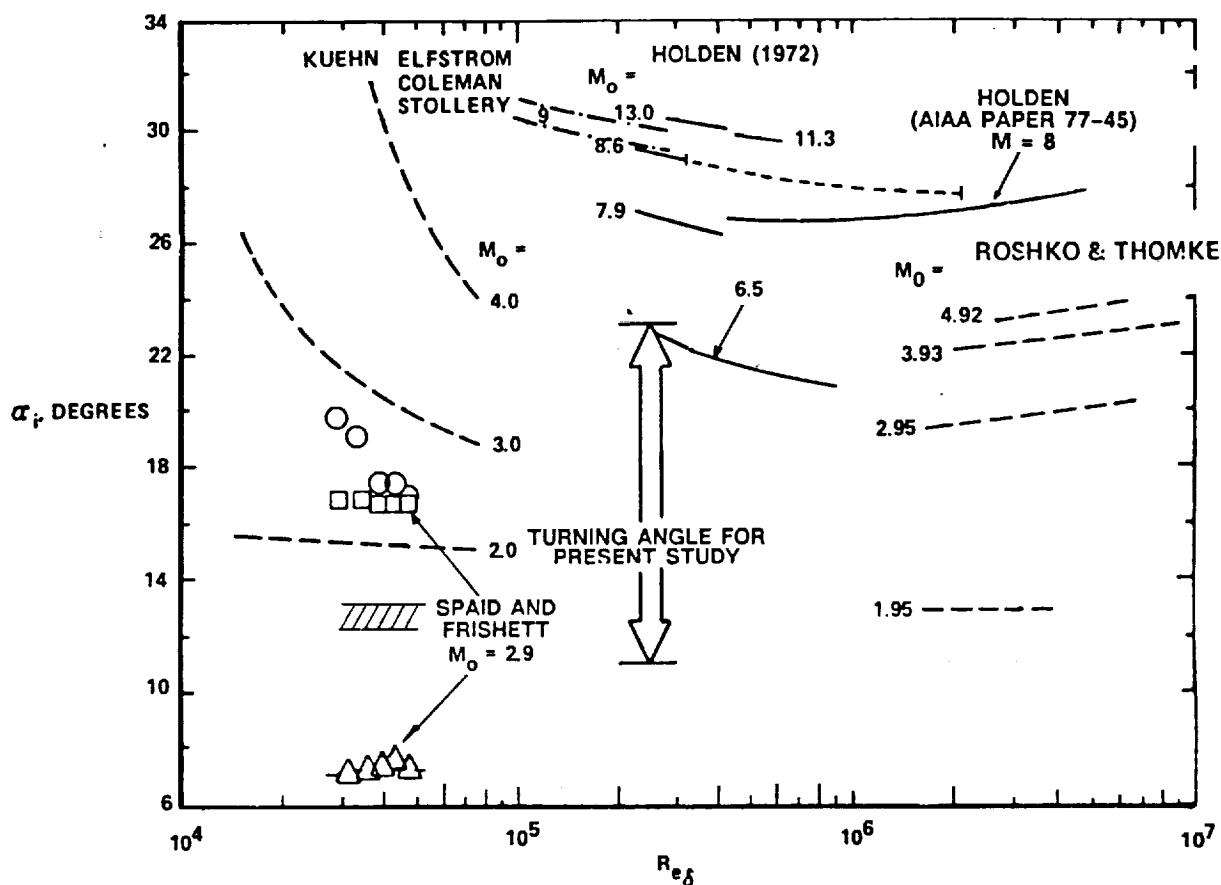


Figure 24a RANGE OF COMPRESSION ANGLES FOR PRESENT STUDY COMPARED WITH THOSE TO INDUCE INCIPIENT SEPARATION (HOLDEN AIAA PAPER 77-45)

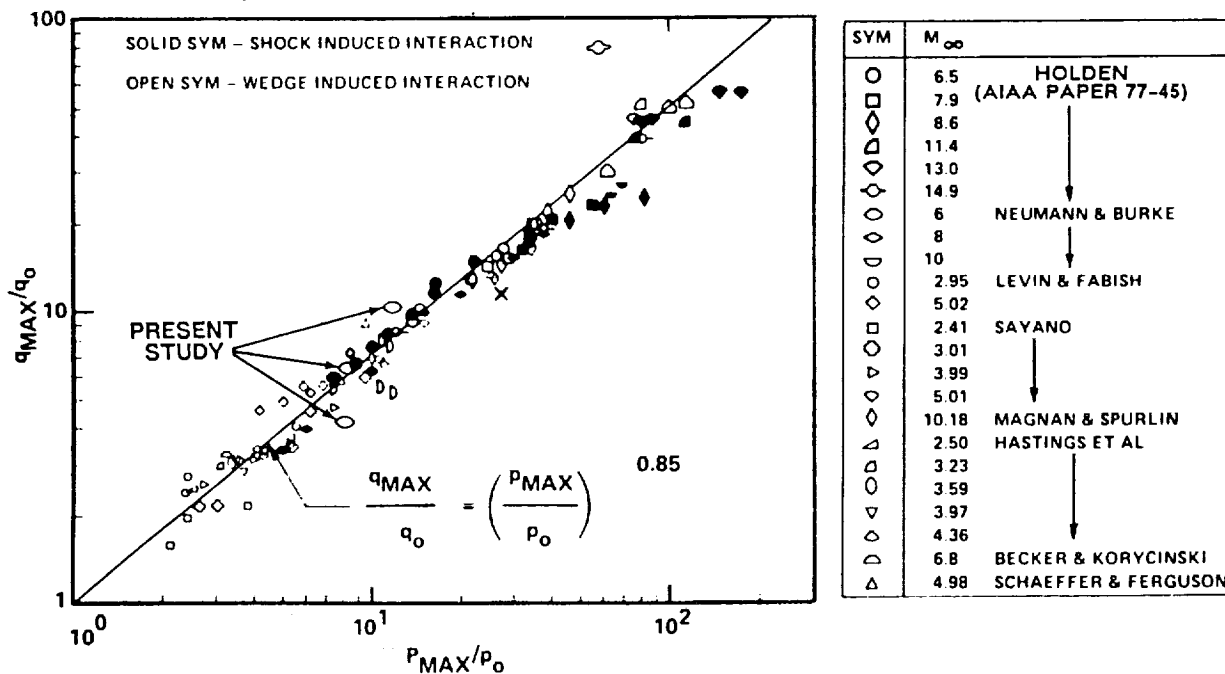


Figure 24b CORRELATION OF MAXIMUM HEATING RATE IN WEDGE- AND EXTERNALLY GENERATED SHOCK-INDUCED TURBULENT SEPARATED FLOWS (HOLDEN AIAA PAPER 77-45)

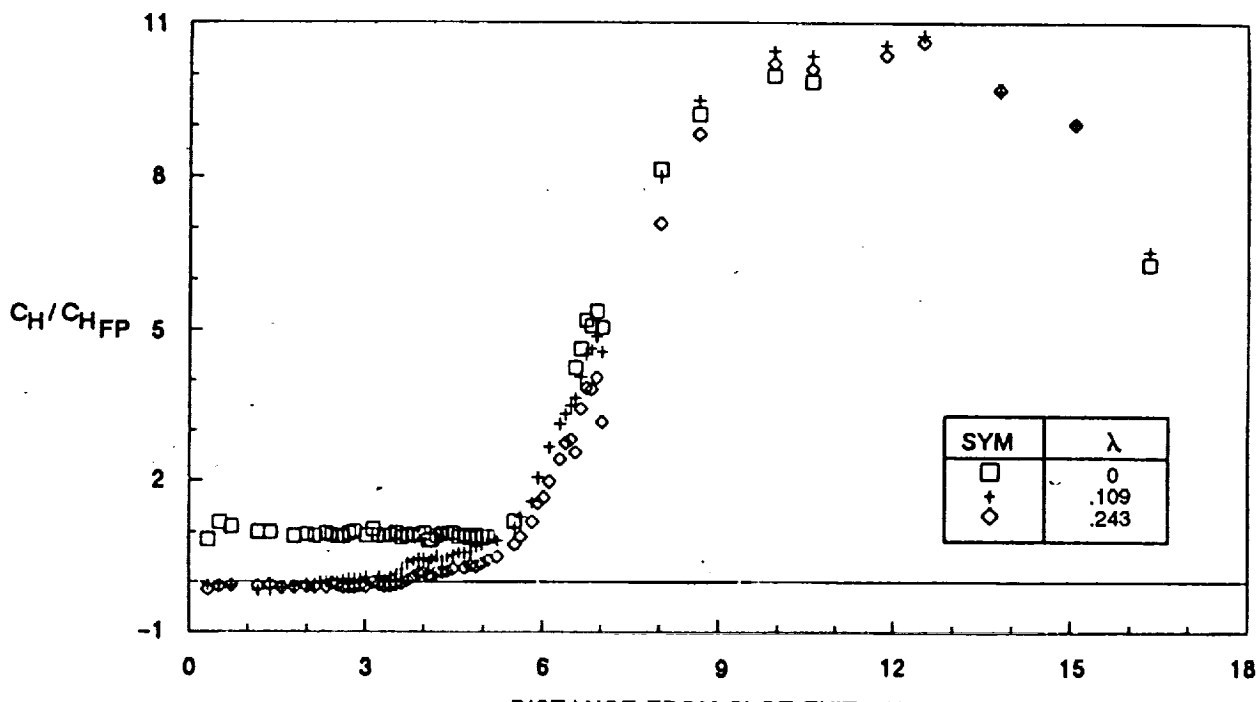


Figure 25a HEAT TRANSFER DISTRIBUTION IN REGIONS OF INCIDENT-SHOCK/WALL-JET INTERACTION ($\Theta_{sg} = 10.5$ DEGREES, SLOT HEIGHT = 0.080 INCH)

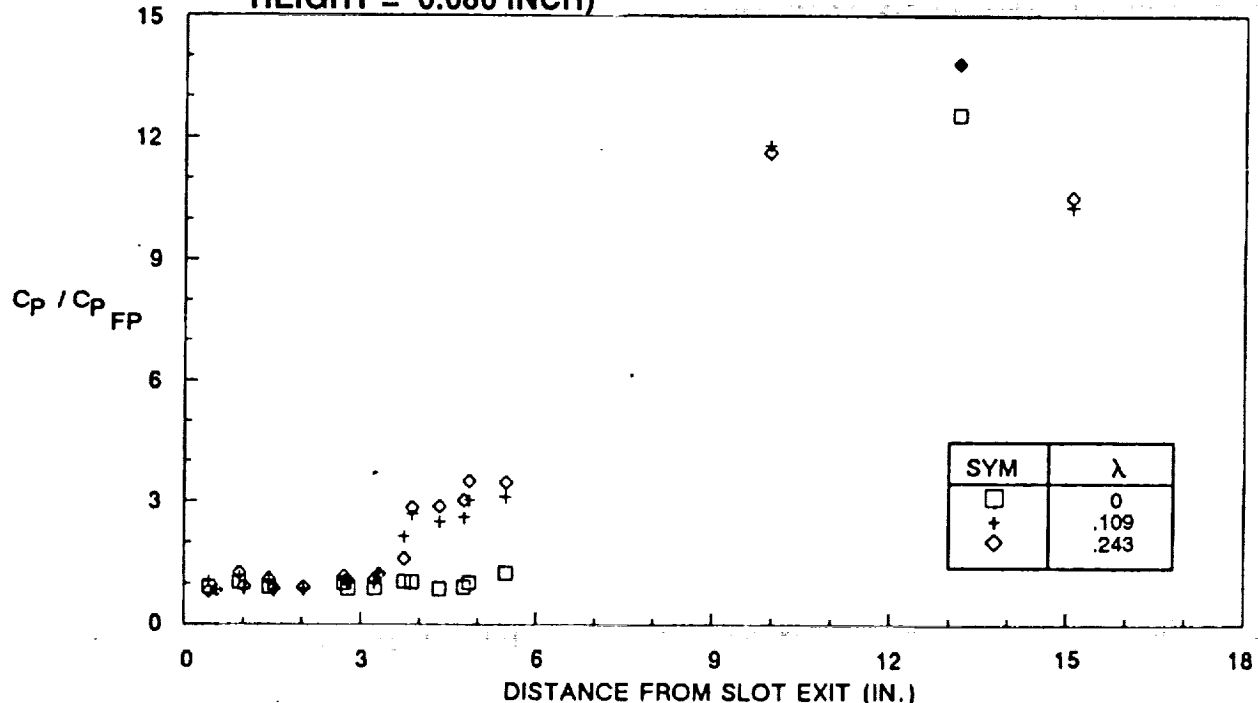


Figure 25b PRESSURE DISTRIBUTION IN REGIONS OF INCIDENT-SHOCK/WALL-JET INTERACTION ($\Theta_{sg} = 10.5$ DEGREES, SLOT HEIGHT = 0.080 INCH)

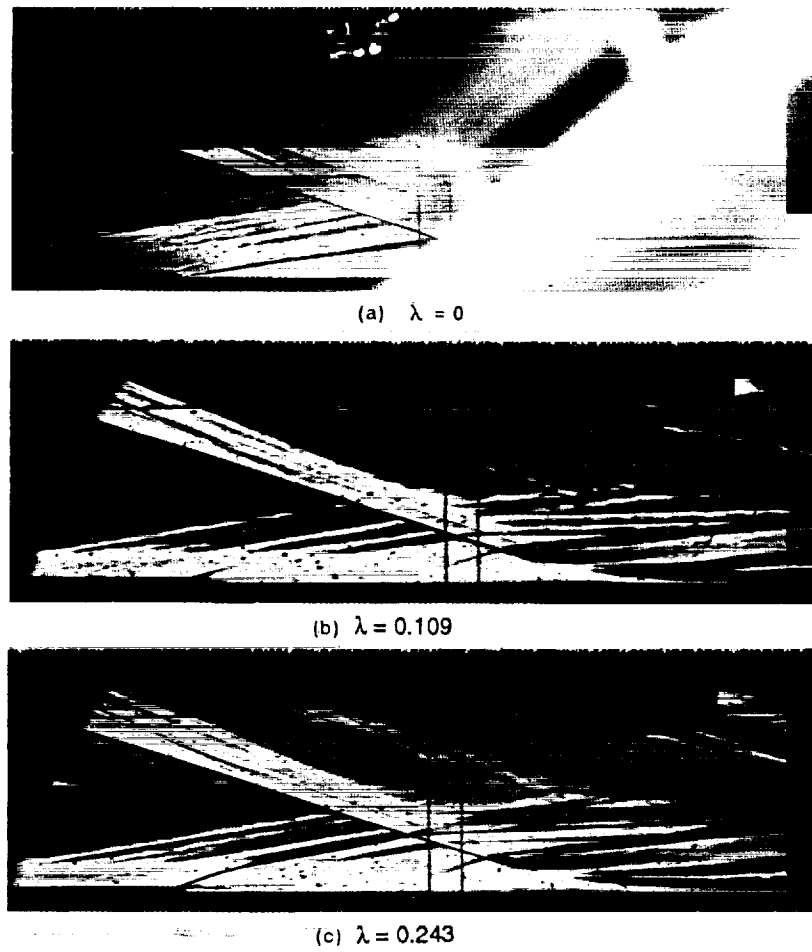


Figure 26 SCHLIEREN PHOTOGRAPHS FOR INCIDENT-SHOCK/WALL-JET INTERACTIONS ($\Theta_{Sg} = 10.5$ DEGREES, SLOT HEIGHT = 0.080 INCH)

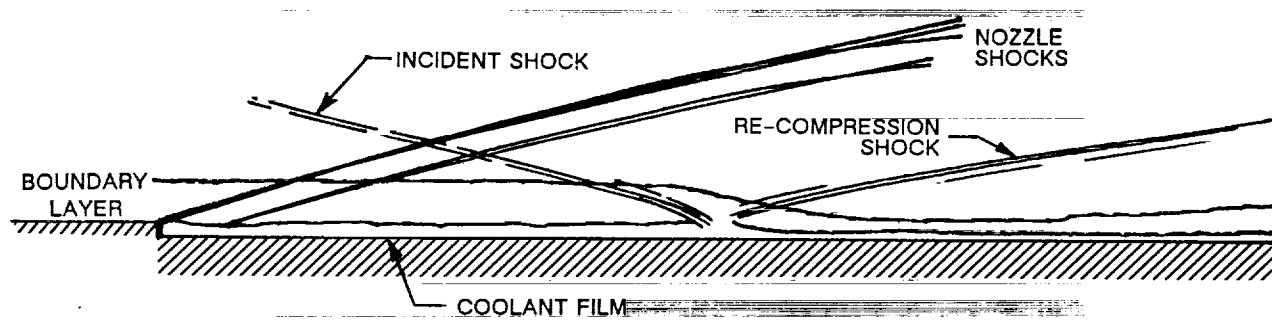


Figure 27a UNSEPARATED SHOCK-WAVE/COOLING-FILM INTERACTION

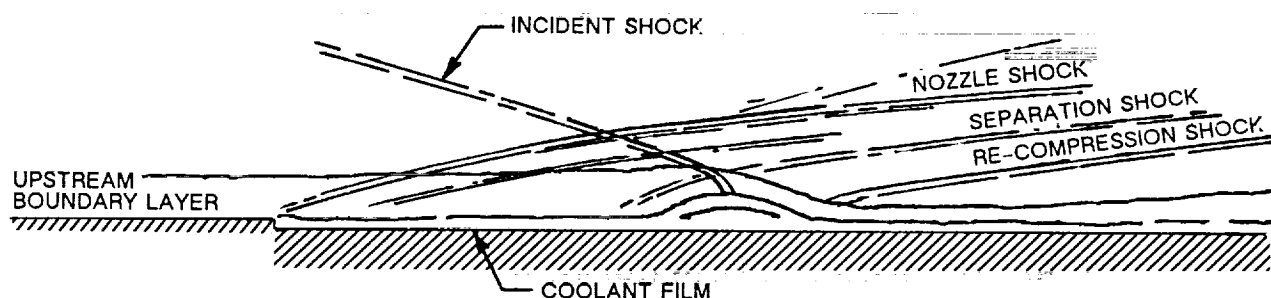


Figure 27b SEPARATED SHOCK-WAVE/COOLING-FILM INTERACTION

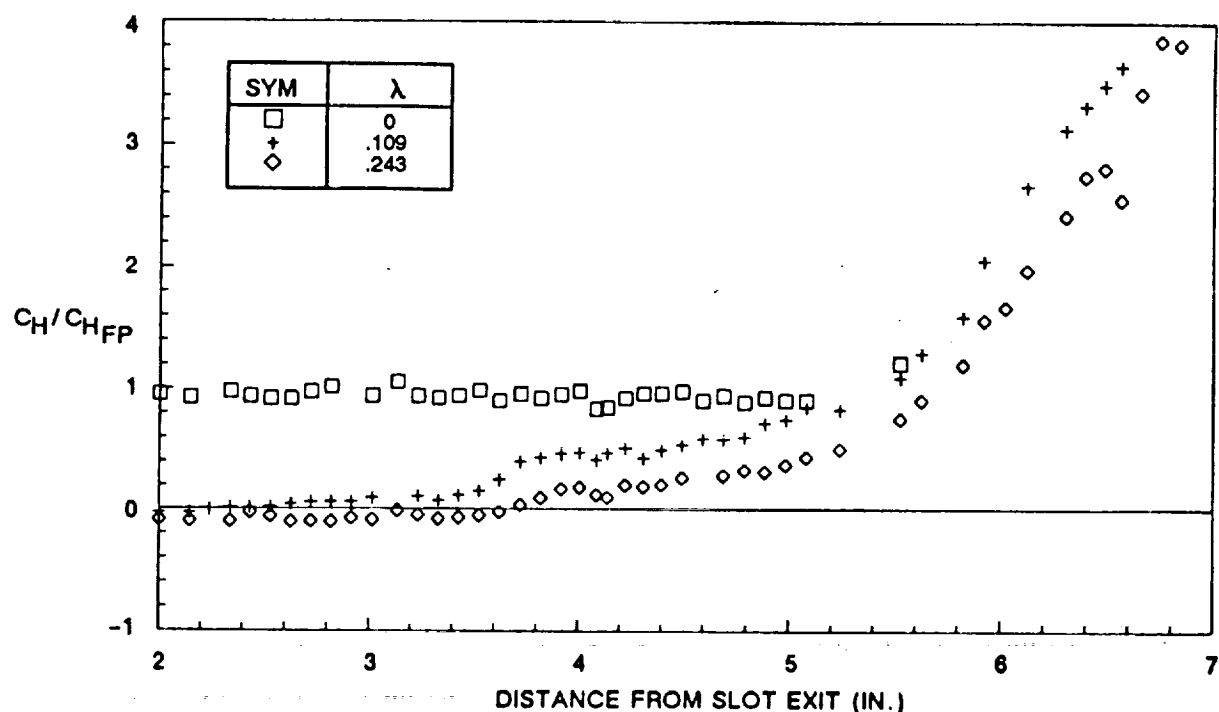


Figure 28 HEAT TRANSFER DISTRIBUTION IN SEPARATION REGION ($\Theta_{Sg} = 10.5$ DEGREES, SLOT HEIGHT = 0.080 INCH)

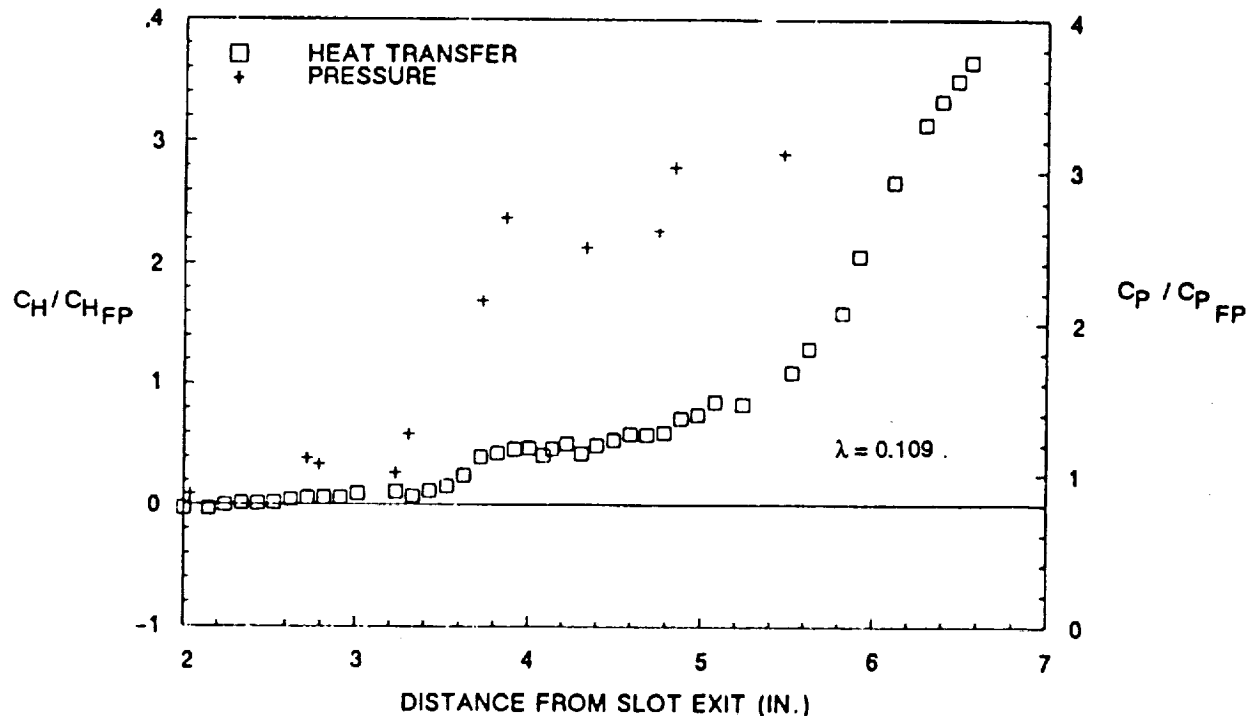


Figure 29 TYPICAL DISTRIBUTIONS OF HEAT TRANSFER AND PRESSURE IN INTERACTION REGION ($\Theta_{Sg} = 10.5$ DEGREES, SLOT HEIGHT = 0.080 INCH)

without film cooling. The coolant layer may be lifted from the surface in the separated region and dispersed by rapid mixing in the shear layer.

As the incident shock enters the boundary layer/coolant film, the flow is turned toward the flat plate, as can be seen in the schlieren photographs of the flow just downstream of the point where the incident shock enters the boundary layer. As the flow again turns parallel to the flat plate, a recompression shock is formed, and the boundary/coolant layer thins in this region. For this flow, the pressure gradient in the coolant layer, where the incident shock terminates and the recompression shock originates, is insufficient to locally reverse the flow; thus, the flow remains attached. The coolant layer is not dispersed by the interaction, and the heating in the recompression region is reduced by the coolant. This is not the case for the flow shown in Figure 27b. Again, the flow is for a large cooling rate; however, here, an incident shock from a 10.5° shock generator impinges on the boundary layer. The two nozzles' shocks are again clearly evident; however, just upstream of the incident shock, a third shock is observed that originates in the coolant layer. This "separation shock" is induced at the upstream boundary of the separated region, and, at that point, there is a sudden increase in the pressure and the heat transfer. For a separated region, these rapid gradients are followed by a region of approximately constant heat transfer and pressure in the plateau region. The separated shear layer reattaches after the outer boundary layer flow is turned toward the surface by the incident shock and then turned back again by the recompression shock. For turbulent flows, the separated region extends from the beginning of the heat transfer rise to the end of the plateau region. The coolant layer remained intact for the flow in Figure 27a, and the heating was reduced by film cooling. However, the separated interaction shown in Figure 27b resulted in the dispersion of the coolant layer in the separated and reattachment compression region, and film cooling was destroyed in the recompression region of the flow, as discussed next.

Reducing the interaction strength by employing an 8° shock generator reduces the length of the separated regions to approximately four boundary layer thicknesses as well as reducing the overall heat transfer and pressure rises, as illustrated in Figures 30a and 30b. Boundary layer separation is still clearly indicated in the schlieren photographs by separation shocks for all of the film-cooling runs, as shown in Figures 31b, 31c, and 31d. The penetration of the incident shock into the boundary layer and its reflection at the sonic line as the recompression shock is shown clearly for the unseparated interaction without blowing in Figure 31a. Here, the thinning of the boundary layer in the recompression

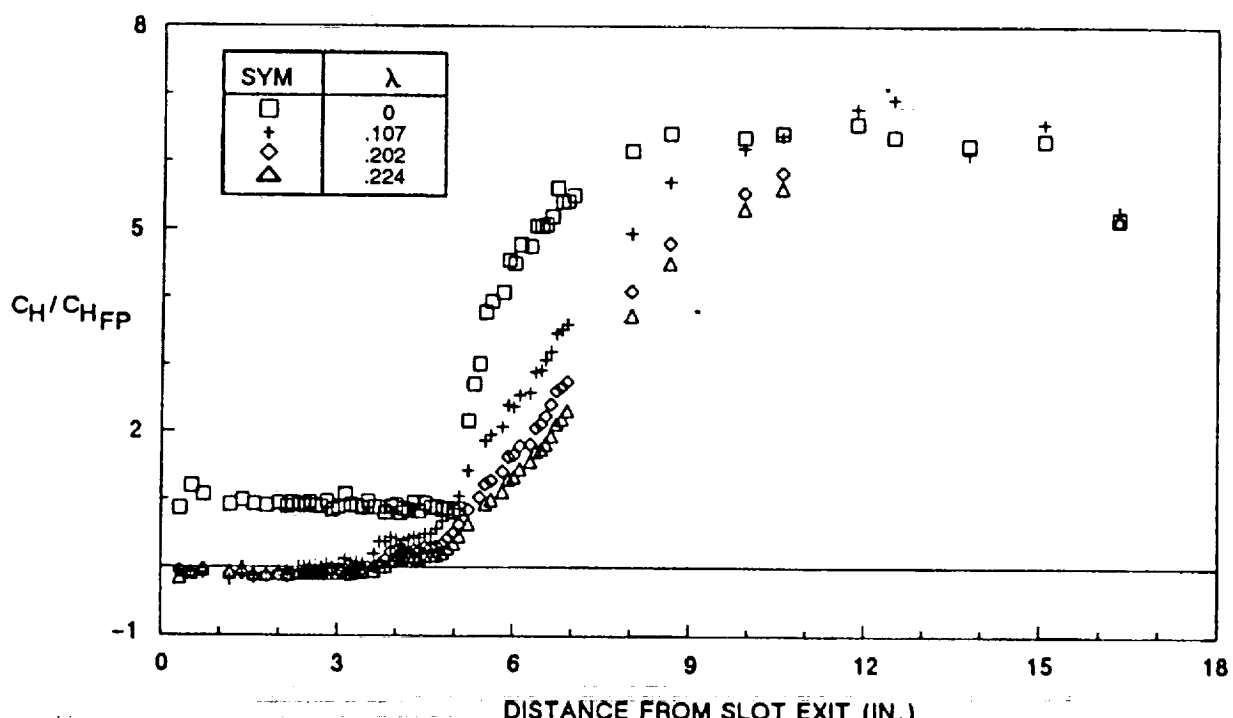


Figure 30a HEAT TRANSFER DISTRIBUTION IN REGIONS OF INCIDENT-SHOCK/WALL-JET INTERACTION ($\Theta_{sg} = 8.0$ DEGREES, SLOT HEIGHT = 0.080 INCH)

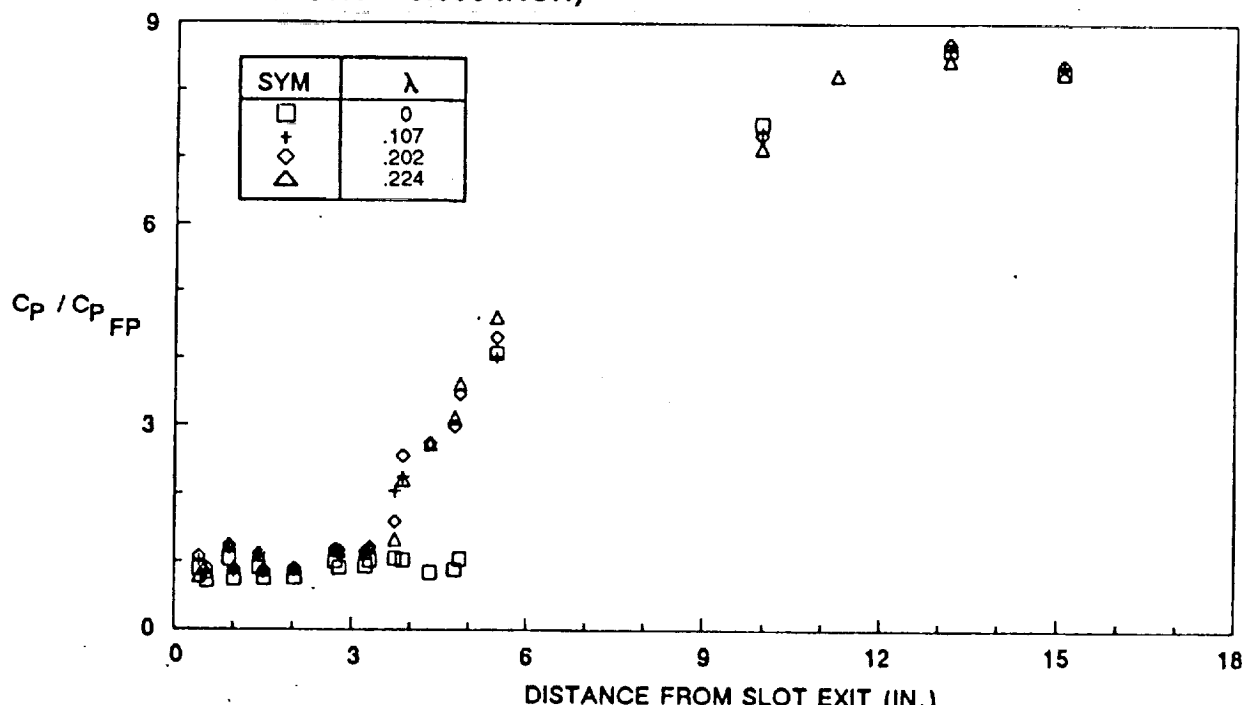


Figure 30b PRESSURE DISTRIBUTION IN REGIONS OF INCIDENT-SHOCK/WALL-JET INTERACTION ($\Theta_{sg} = 8.0$ DEGREES, SLOT HEIGHT = 0.080 INCH)

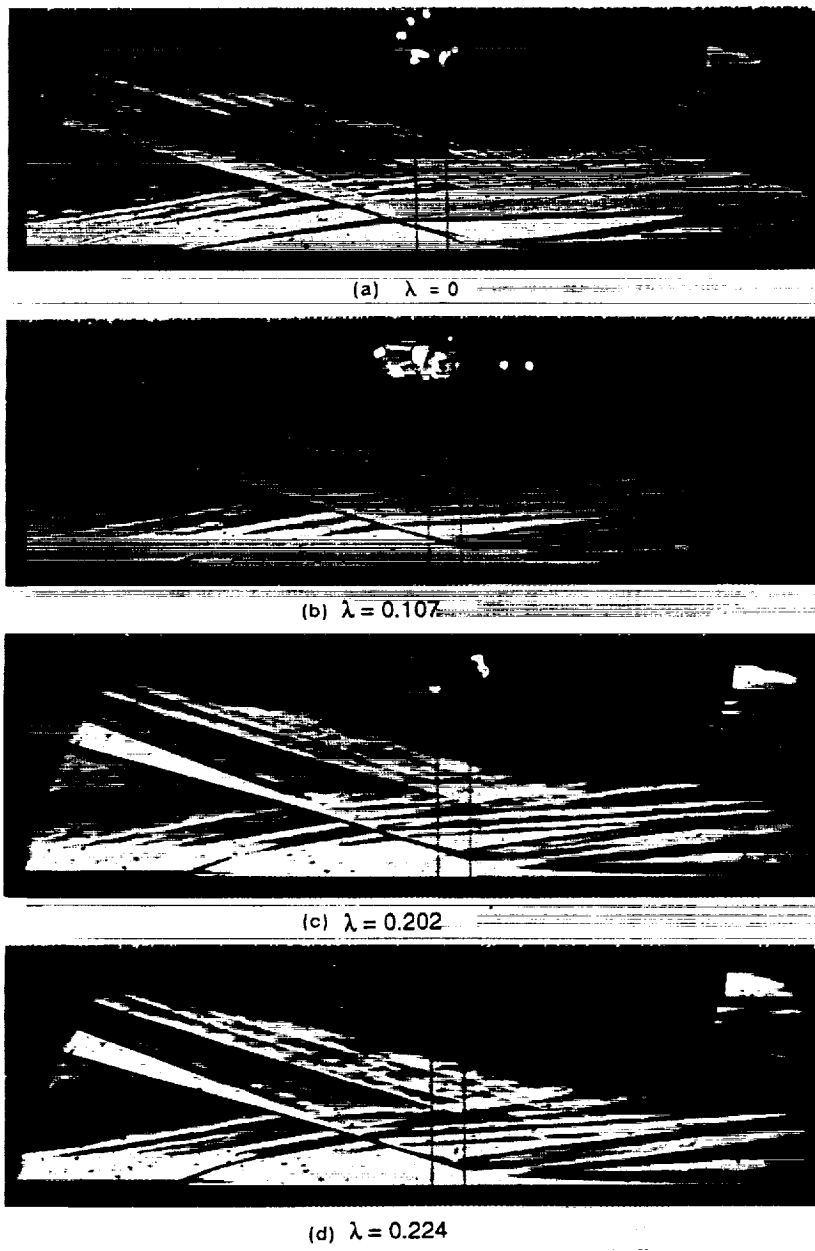


Figure 31 SCHLIEREN PHOTOGRAPHS FOR INCIDENT-SHOCK/WALL-JET INTERACTIONS ($\Theta_{sg} = 8.0$ DEGREES, SLOT HEIGHT = 0.080 INCH)

region can be clearly seen. Again, we have plotted the separated regions to a larger scale in Figures 32 and 33, showing a decreasing separation length with increased blowing. For this shock strength, the dispersion of the coolant films takes longer; for the largest blowing rates, it takes the entire length of the recompression process. At the end of the reattachment compression rise, there is little difference between the heat transfer with and without film cooling.

Reducing the shock-generator angle to 5.5° causes an interacting flow with little or no separation in the interaction region. The heat transfer distributions shown in Figures 34 and 37, together with the schlieren photograph for the lowest (matched) blowing rate in Figure 36, indicate that the flow is slightly separated for this blowing rate. However, the separated region is eliminated with increased blowing. For this interaction strength, Figures 34 and 35 illustrate that the cooling film has not been dispersed by the end of the compression rise, and that the heat transfer is reduced by approximately 25% by film cooling for maximum blowing--not a great deal, considering that the cooling mass flux is 25% of that of the freestream.

Figure 39 shows a correlation of the separation lengths determined from the measured distributions and schlieren photographs, plotted as a function of λ for the three incident-shock configurations. Because the experiment was designed so that the velocity of the coolant at the exit plane was equal to that of the freestream, λ is also equal to the momentum ratio, which we believe to be the more relevant parameter. For the largest incident-shock strengths, separated regions of the order of 10 initial boundary layer thicknesses are generated; surprisingly, the separation lengths are decreased only slightly by increased blowing. However, for the weakest interactions, where the initial separation lengths were only several boundary layer thicknesses, increased blowing eventually eliminated the separated regions. Figure 40 summarizes our results discussed earlier, which indicate that film cooling has little or no effect on reducing heat rate in the recompression region of the flow in all but the weakest interactions, and that, for the latter case, the cooling was not substantial.

3.6.3 Studies With 0.120-Inch Slot Configuration

To determine how the size of the separated interaction and the cooling-film effectiveness in the recompression region are influenced by the thickness of the cooling film, a set of measurements was made with a 0.120-inch slot height, an increase of 50% in

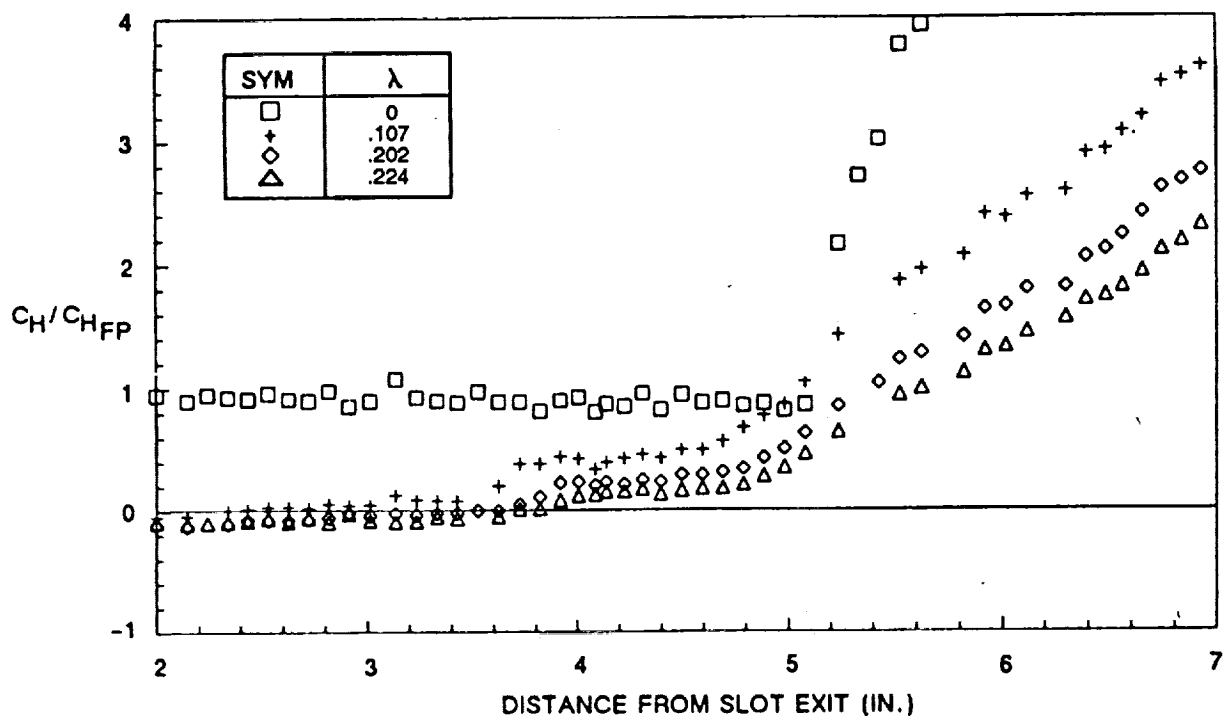


Figure 32 HEAT TRANSFER DISTRIBUTION IN SEPARATION REGION ($\Theta_{sg} = 8.0$ DEGREES, SLOT HEIGHT = 0.080 INCH)

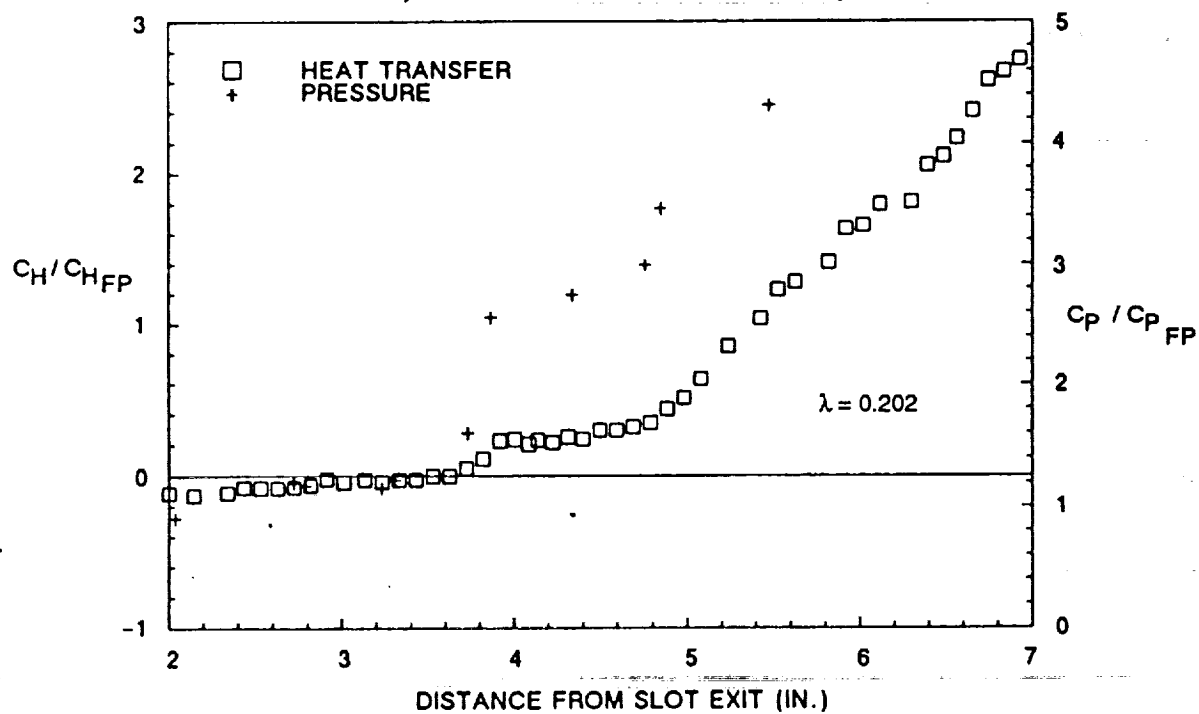


Figure 33 TYPICAL DISTRIBUTIONS OF HEAT TRANSFER AND PRESSURE IN SEPARATED INTERACTION REGION ($\Theta_{sg} = 8.0$ DEGREES, SLOT HEIGHT = 0.080 INCH)

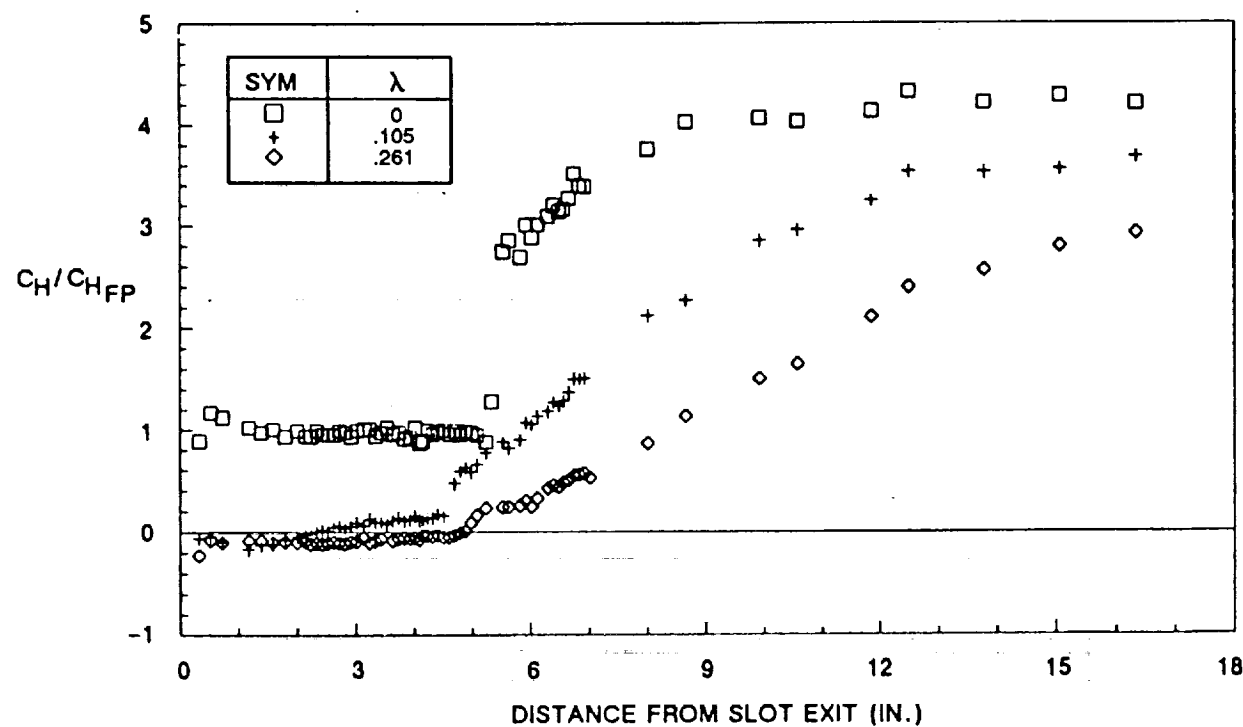


Figure 34 HEAT TRANSFER DISTRIBUTION IN REGIONS OF INCIDENT-SHOCK/WALL-JET INTERACTION ($\Theta_{sg} = 5.5$ DEGREES, SLOT HEIGHT = 0.080 INCH)

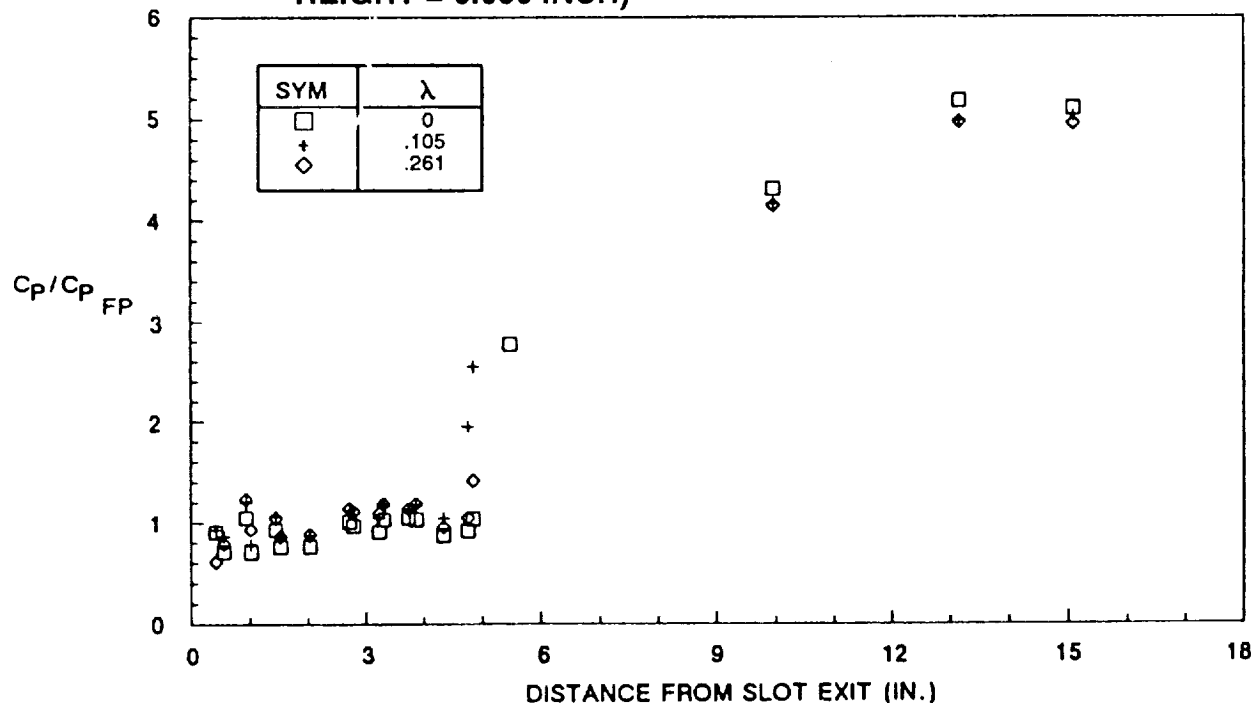


Figure 35 PRESSURE DISTRIBUTION IN REGIONS OF INCIDENT-SHOCK/WALL-JET INTERACTION ($\Theta_{sg} = 5.5$ DEGREES, SLOT HEIGHT = 0.080 INCH)

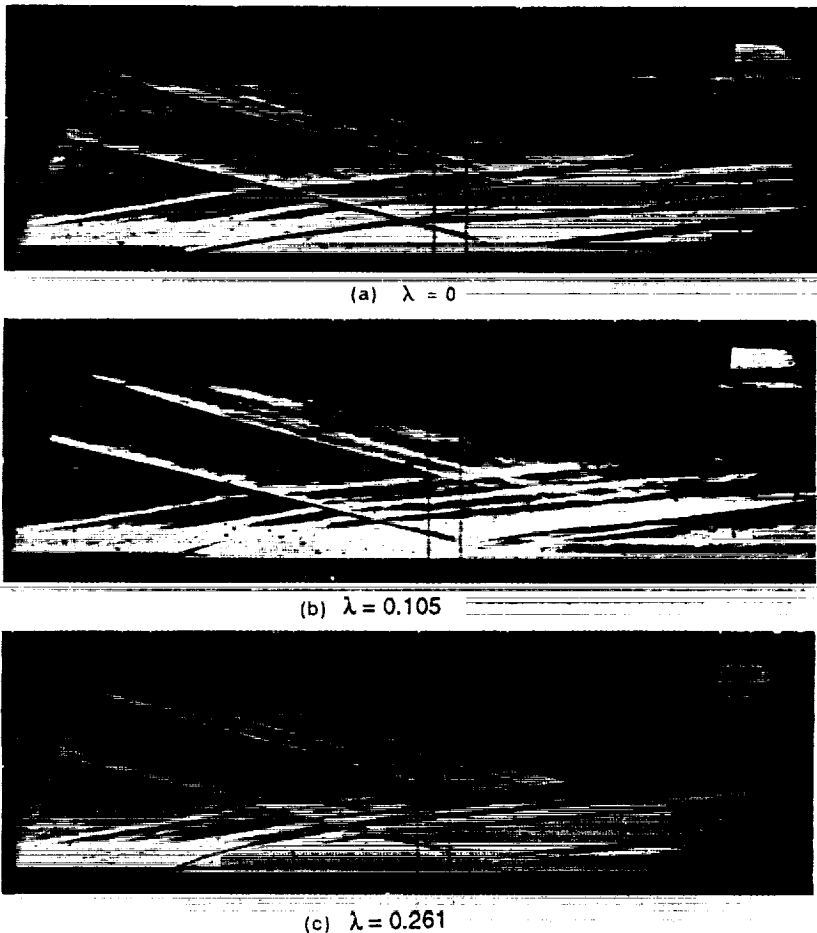


Figure 36 SCHLIEREN PHOTOGRAPHS FOR INCIDENT-SHOCK/WALL-JET INTERACTIONS ($\Theta_{sg} = 5.5$ DEGREES, SLOT HEIGHT = 0.080 INCH)

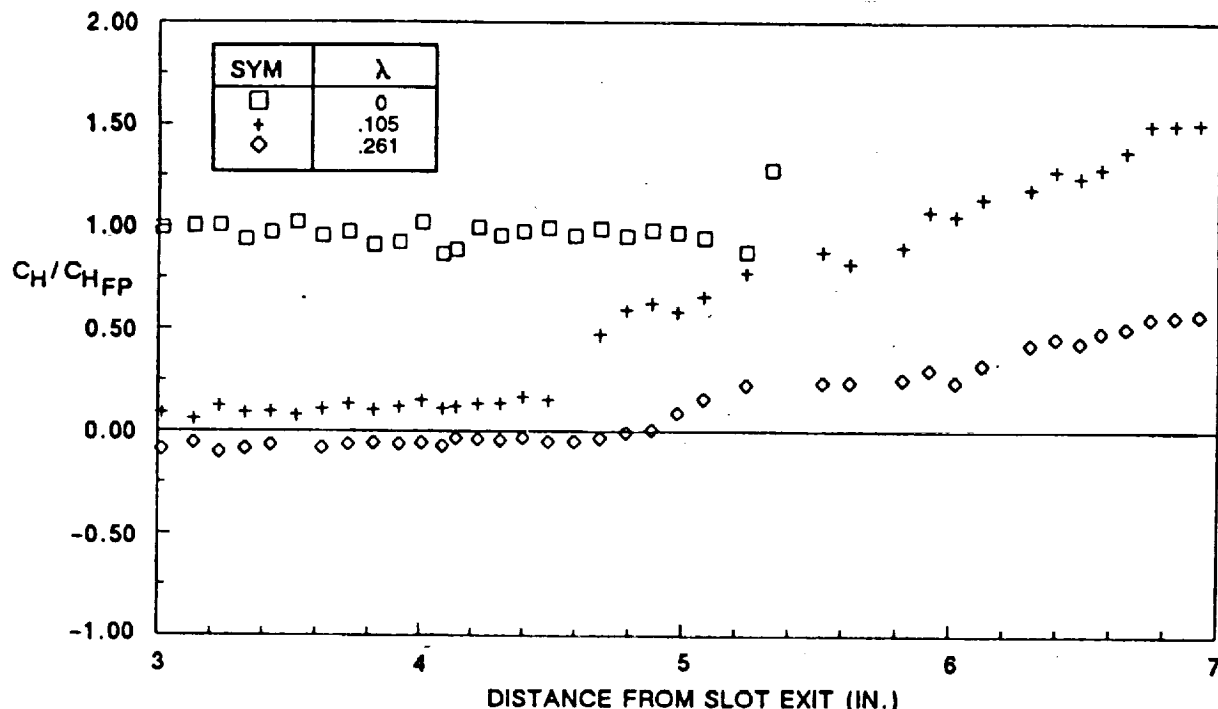


Figure 37 HEAT TRANSFER DISTRIBUTION IN SEPARATION REGION ($\Theta_{Sg} = 5.5$ DEGREES, SLOT HEIGHT = 0.080 INCH)

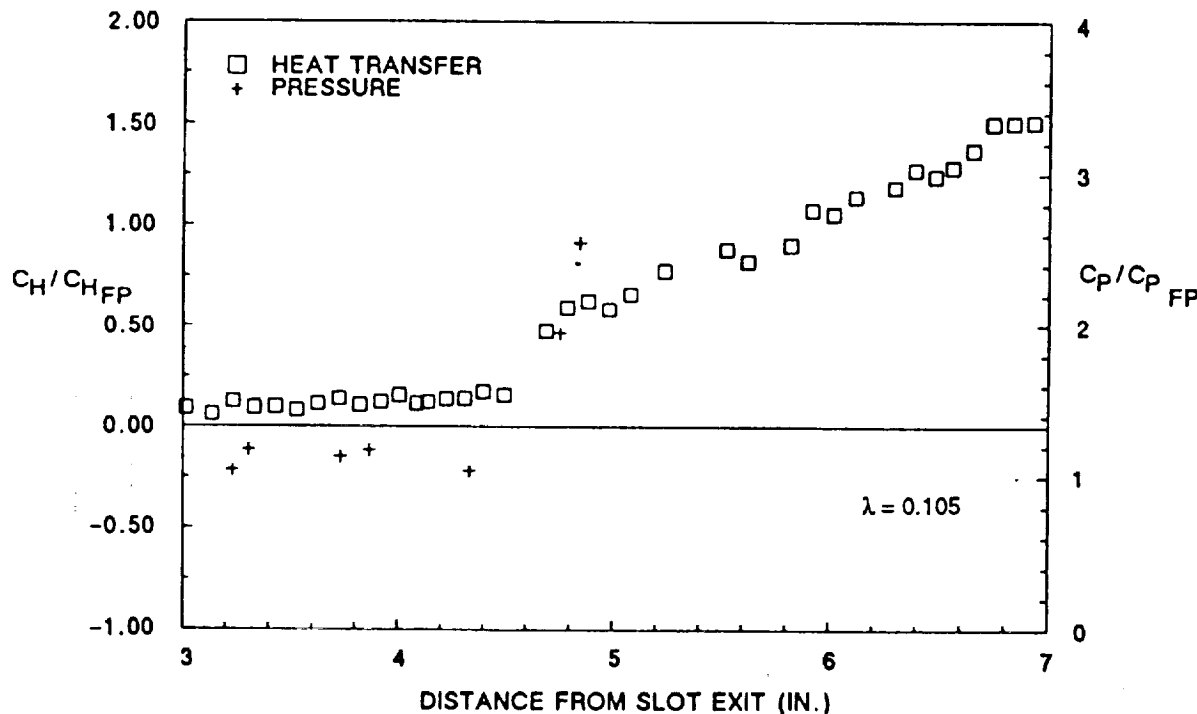


Figure 38 TYPICAL DISTRIBUTIONS OF HEAT TRANSFER AND PRESSURE IN SEPARATED INTERACTION REGION ($\Theta_{Sg} = 5.5$ DEGREES, SLOT HEIGHT = 0.080 INCH)

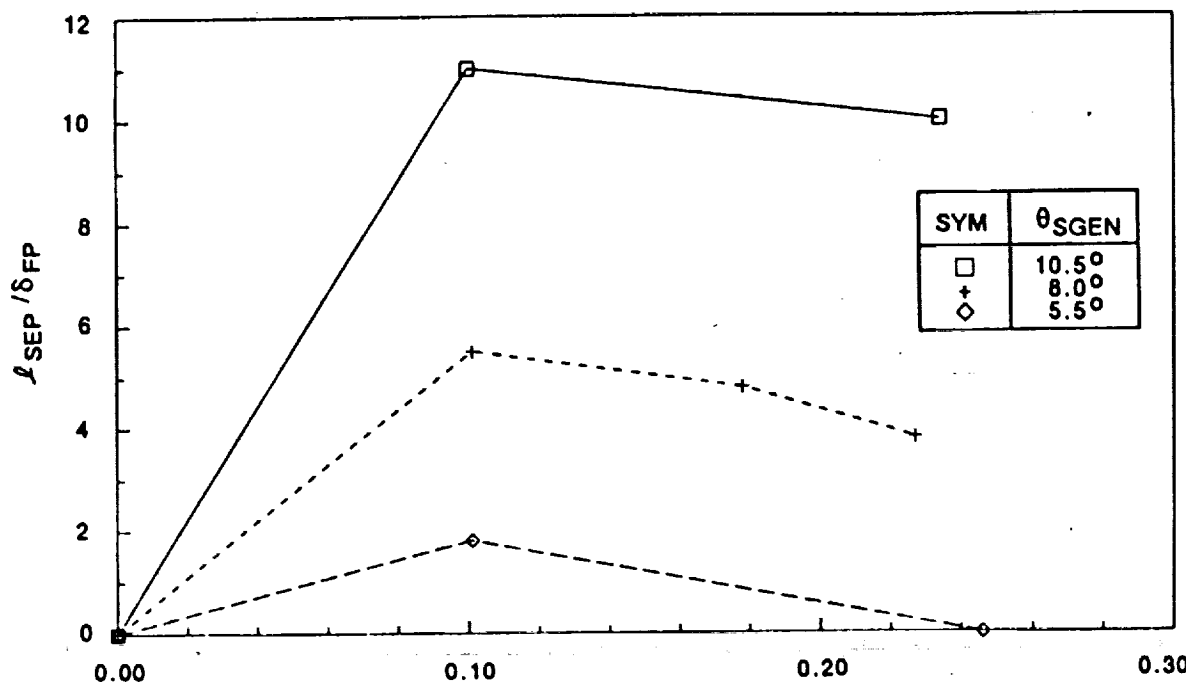


Figure 39 VARIATION OF SEPARATED FLOW LENGTH WITH BLOWING RATE
FOR VARIOUS INCIDENT-SHOCK STRENGTHS (SLOT HEIGHT =
0.080 INCH)

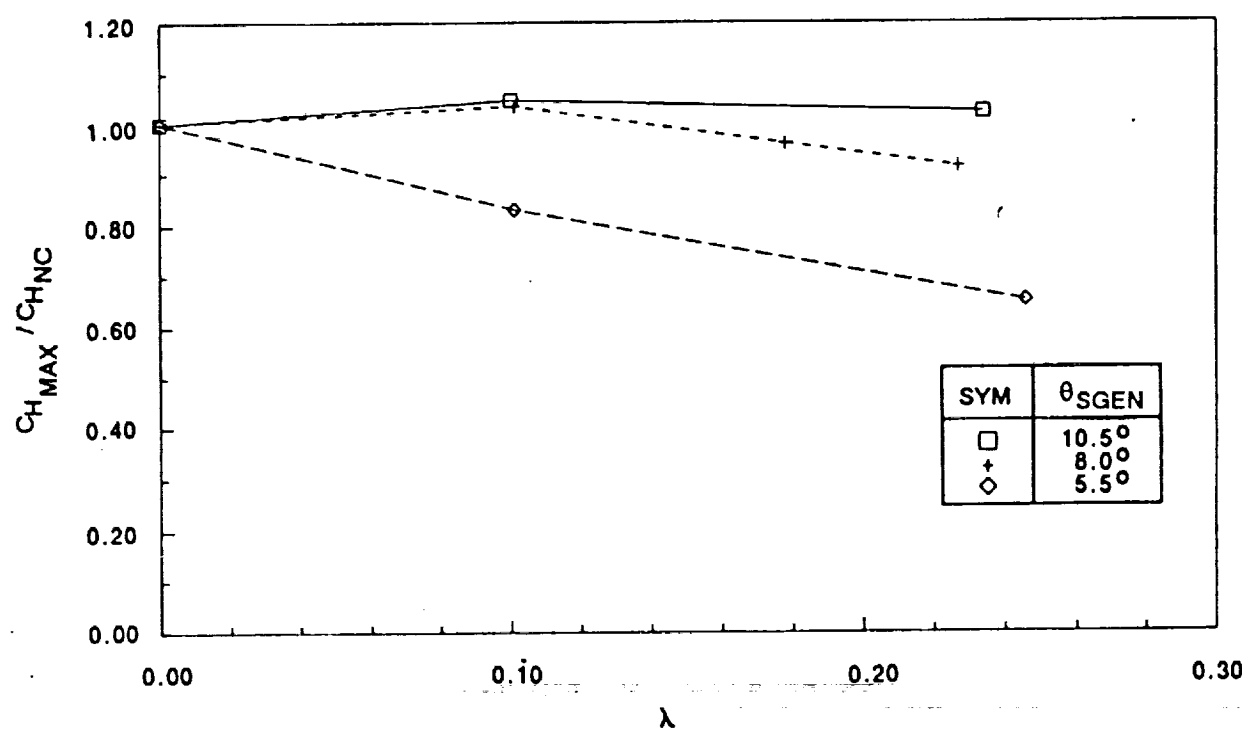


Figure 40 VARIATION OF MAXIMUM HEATING RATE WITH FILM-COOLANT
FLOW RATE (SLOT HEIGHT = 0.080 INCH)

wall-jet thickness. The initial measurements were made with an 8° shock generator for two film-cooling rates. From the heat transfer and pressure distributions for these conditions shown (respectively) in Figures 41 and 42, and the schlieren photographs of Figure 43, it can be seen that the flow is separated for both blowing conditions. Referring to Figures 44 and 45, we observe separation regions of five boundary layer thicknesses in length, only slightly less than observed for the 0.080-inch film measurements. As in the studies with the smaller slot height, the heating at the end of the recompression process was not reduced by film cooling; surprisingly, the thicker cooling film did not appear to persist to a greater downstream distance. Also, the measurements shown in Figure 41 suggest that a twofold increase in the blowing rate greater than matched blowing does not significantly reduce the heating across the recompression region.

For the 5.5° shock generator, the measurements shown in Figures 46 through 50 indicate that, while the flow was separated for the matched-blown condition, increased blowing removed the separated region. Here, film cooling produced a sizable reduction in recompression heating, with the reduction increasing with increased mass addition. The length of the separated region for the matched-pressure condition was slightly less than observed for the 0.080-inch slot case. Surprisingly, boundary layer separation in these flows was not strongly influenced by cooling-film thickness. In Figure 51, for the studies with the 0.120-inch slot height, we show the variation of the separated-flow length plotted against the blowing parameter λ for the different blowing and incident-shock configurations. As discussed earlier, since we were running with matched velocities, this is equal to the momentum ratio between the coolant and the freestream, which we believe to be the more important parameter controlling separation. As observed earlier for the 0.080-inch cases for the 8° shock generator, the large separated region ($l_{sep}/\delta_{fp} = 5$) is formed for matched-blown cases, and this region decreases slightly in size when the blowing rate is doubled. For the 5.5° shock generator, a small separated region formed for the matched-blown case is swept away when the blowing rate is doubled. Thus, the observations from the two data sets is that the size of the separated region is not strongly influenced by cooling-layer thickness. However, as illustrated in Figures 40 and 52, increased cooling-film thickness does result in a greater reduction in the heat transfer in the recompression region for the weakest incident shocks.

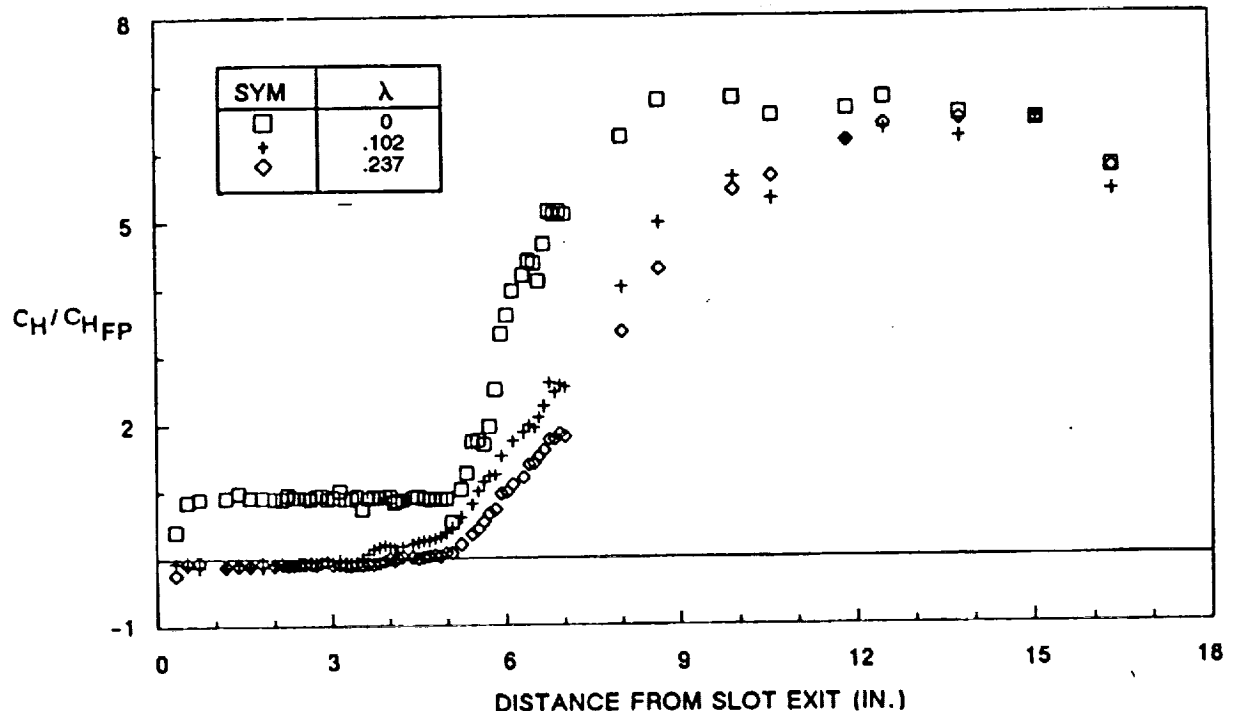


Figure 41 HEAT TRANSFER DISTRIBUTION IN REGIONS OF INCIDENT-SHOCK/WALL-JET INTERACTION ($= 8.0$ DEGREES, SLOT HEIGHT = 0.120 INCH)

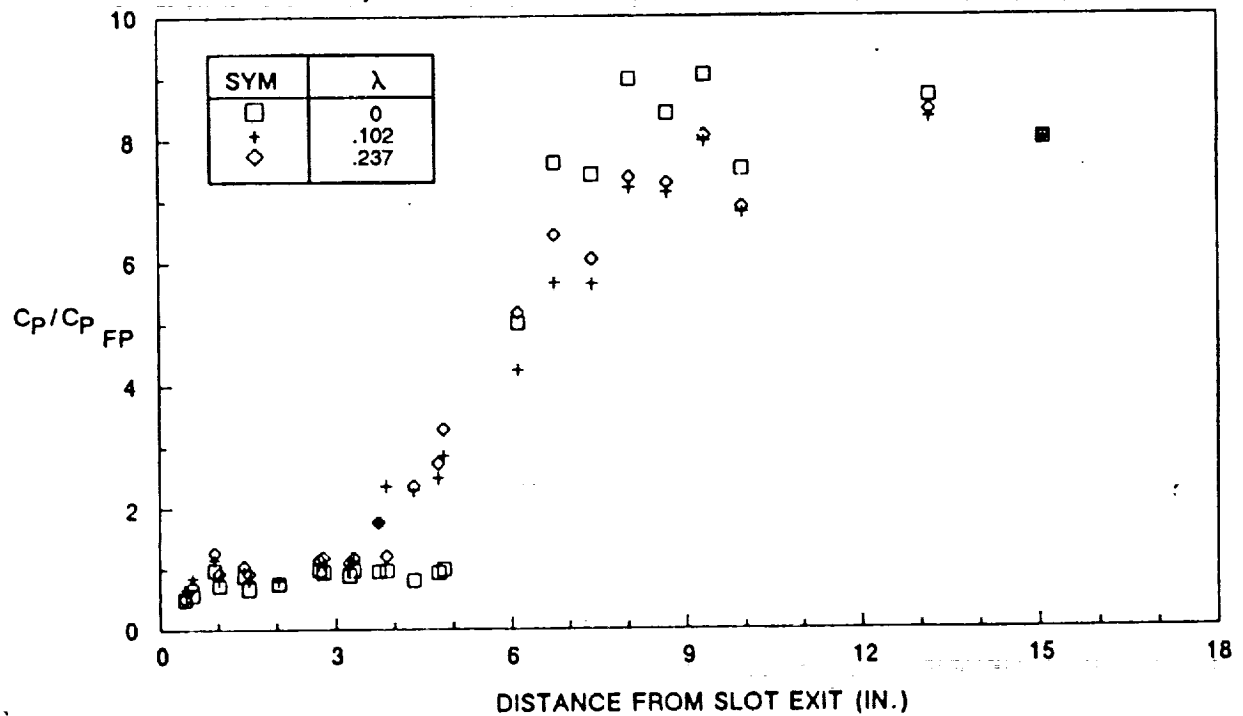


Figure 42 PRESSURE DISTRIBUTION IN REGIONS OF INCIDENT-SHOCK/WALL-JET INTERACTION ($\Theta_{sg} = 8.0$ DEGREES, SLOT HEIGHT = 0.120 INCH)

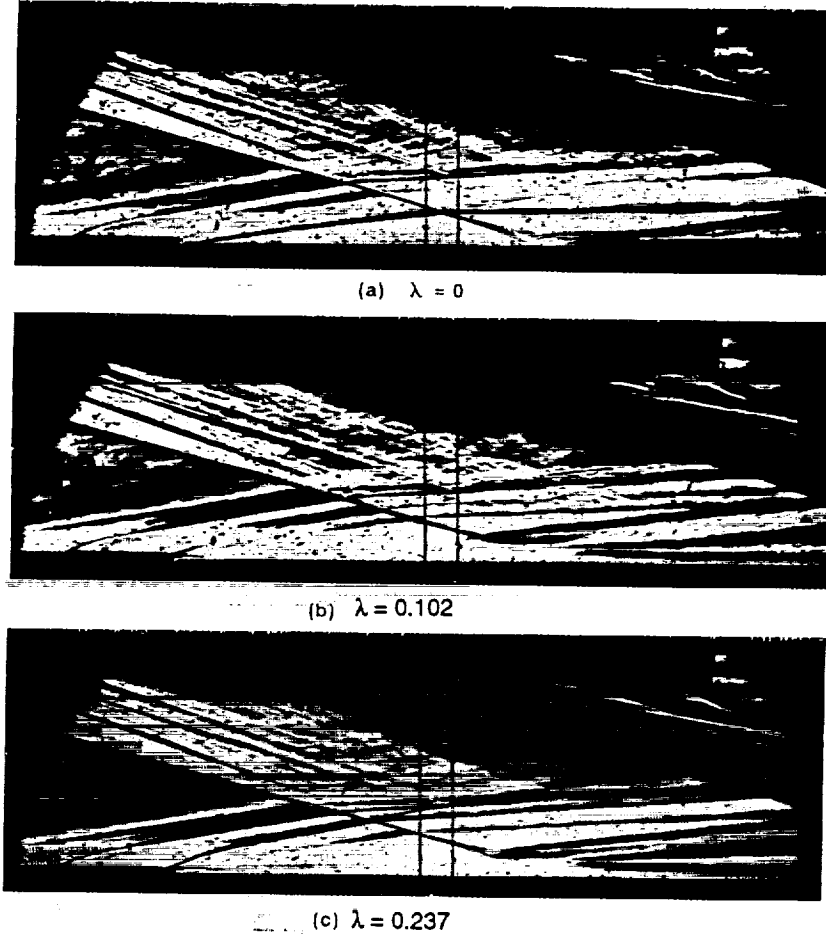


Figure 43 SCHLIEREN PHOTOGRAPHS FOR INCIDENT-SHOCK/WALL-JET INTERACTIONS ($\Theta_{Sg} = 8.0$ DEGREES, SLOT HEIGHT = 0.120 INCH)

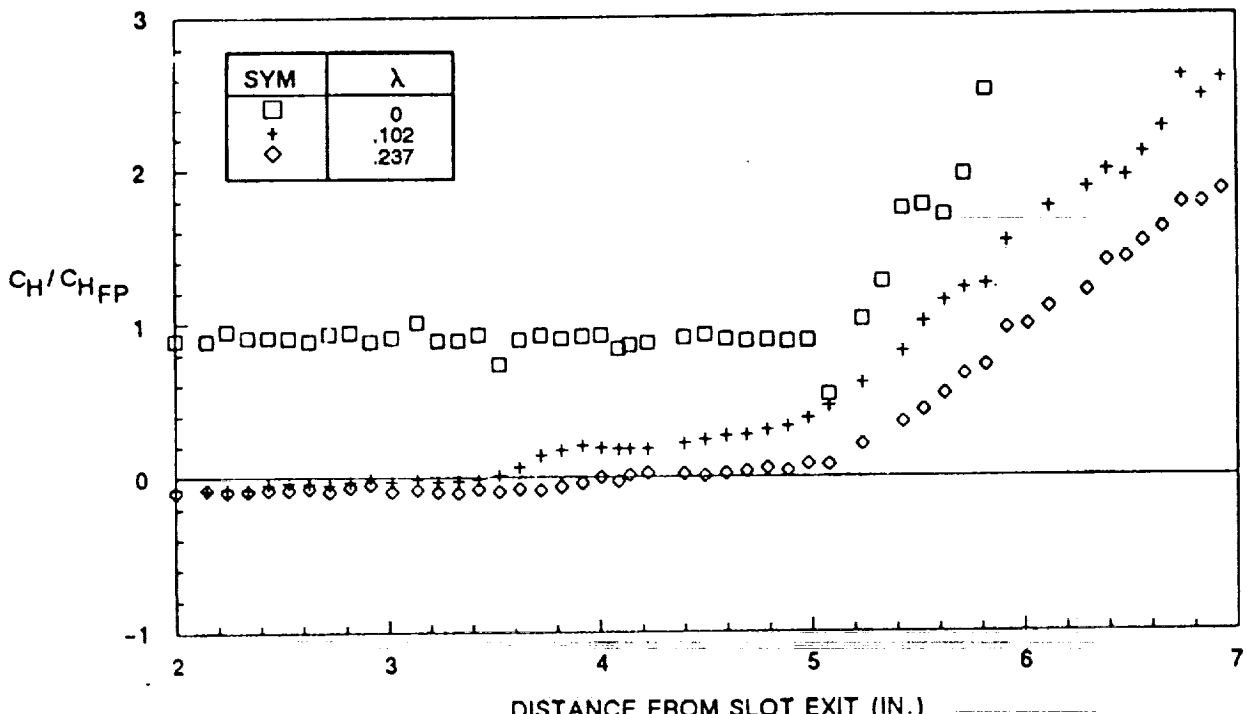


Figure 44 HEAT TRANSFER DISTRIBUTION IN SEPARATION REGION ($\Theta_{sg} = 8.0$ DEGREES, SLOT HEIGHT = 0.120 INCH)

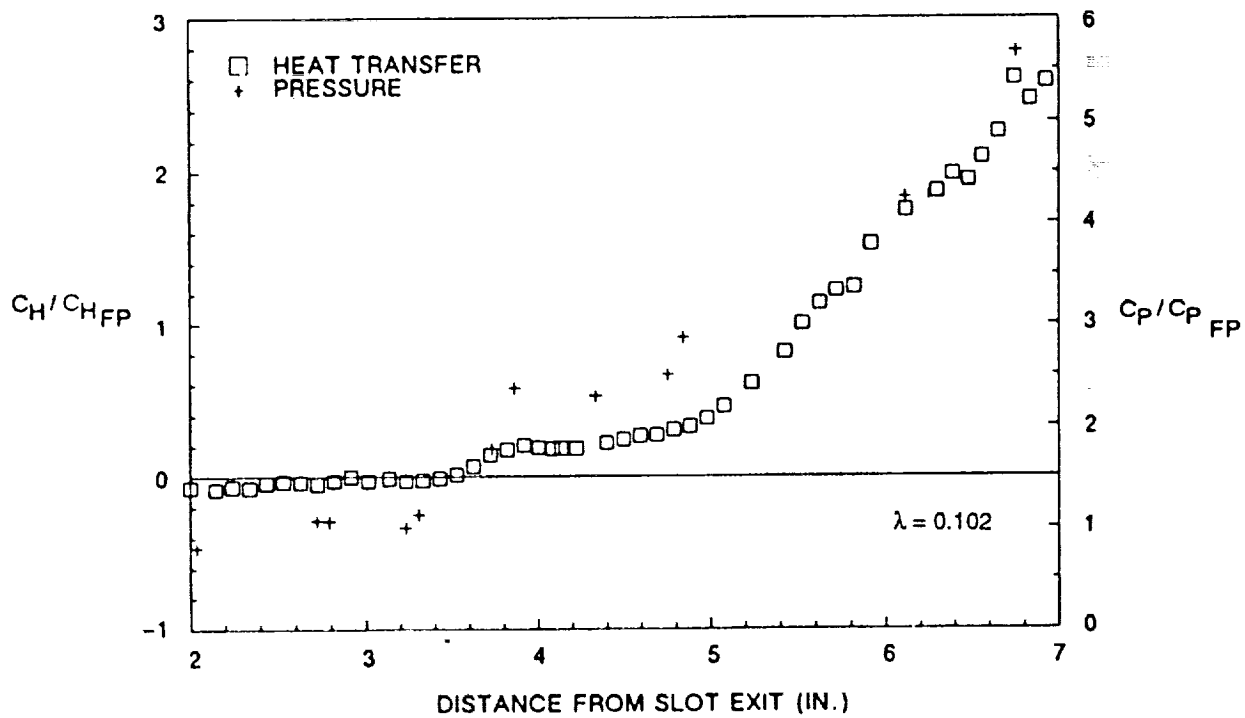


Figure 45 TYPICAL DISTRIBUTIONS OF HEAT TRANSFER AND PRESSURE IN SEPARATED INTERACTION REGION ($\Theta_{sg} = 8.0$ DEGREES, SLOT HEIGHT = 0.120 INCH)

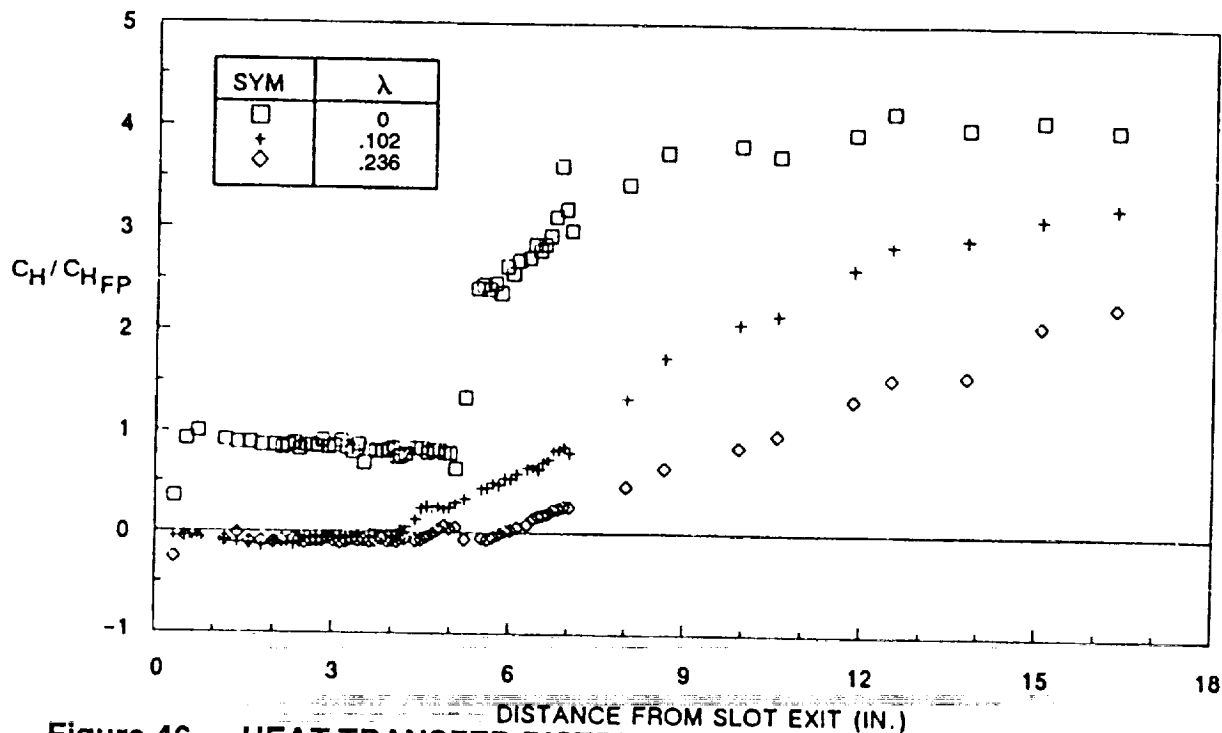


Figure 46 HEAT TRANSFER DISTRIBUTION IN REGIONS OF INCIDENT-SHOCK/WALL-JET INTERACTION ($\theta_{sg} = 5.5$ DEGREES, SLOT HEIGHT = 0.120 INCH)

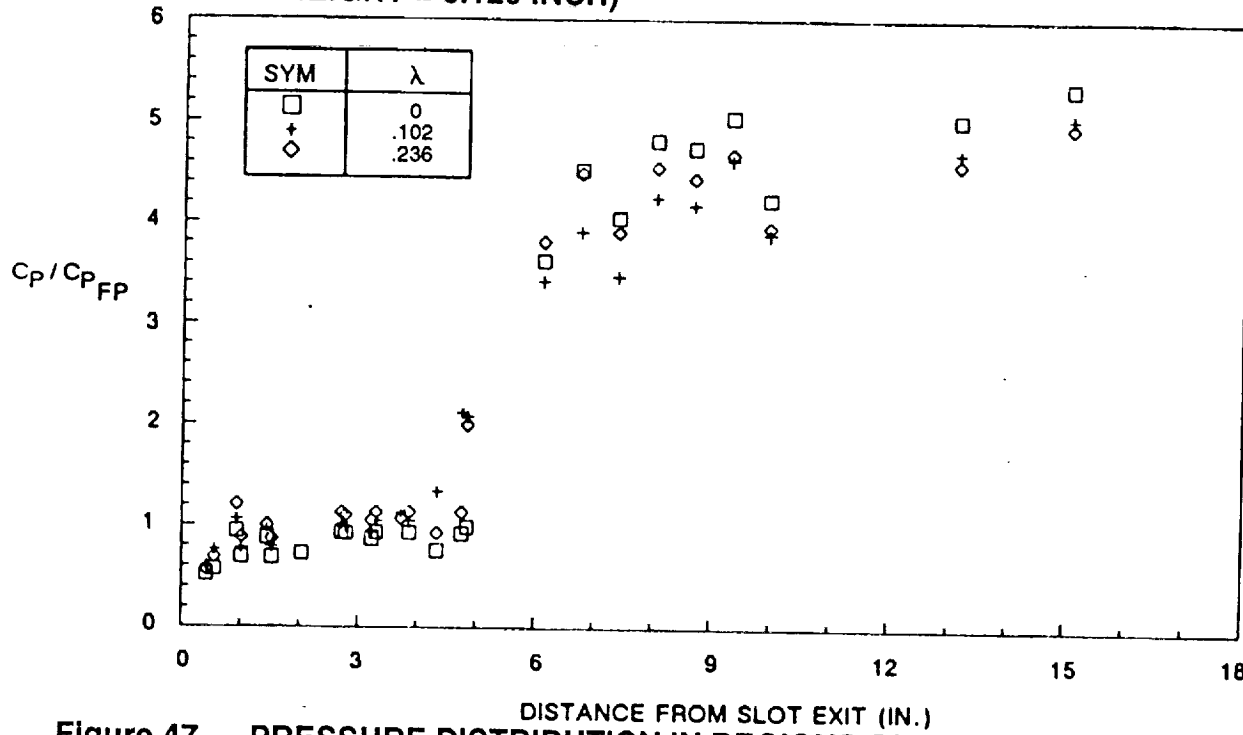


Figure 47 PRESSURE DISTRIBUTION IN REGIONS OF INCIDENT-SHOCK/WALL-JET INTERACTION ($\theta_{sg} = 5.5$ DEGREES, SLOT HEIGHT = 0.120 INCH)

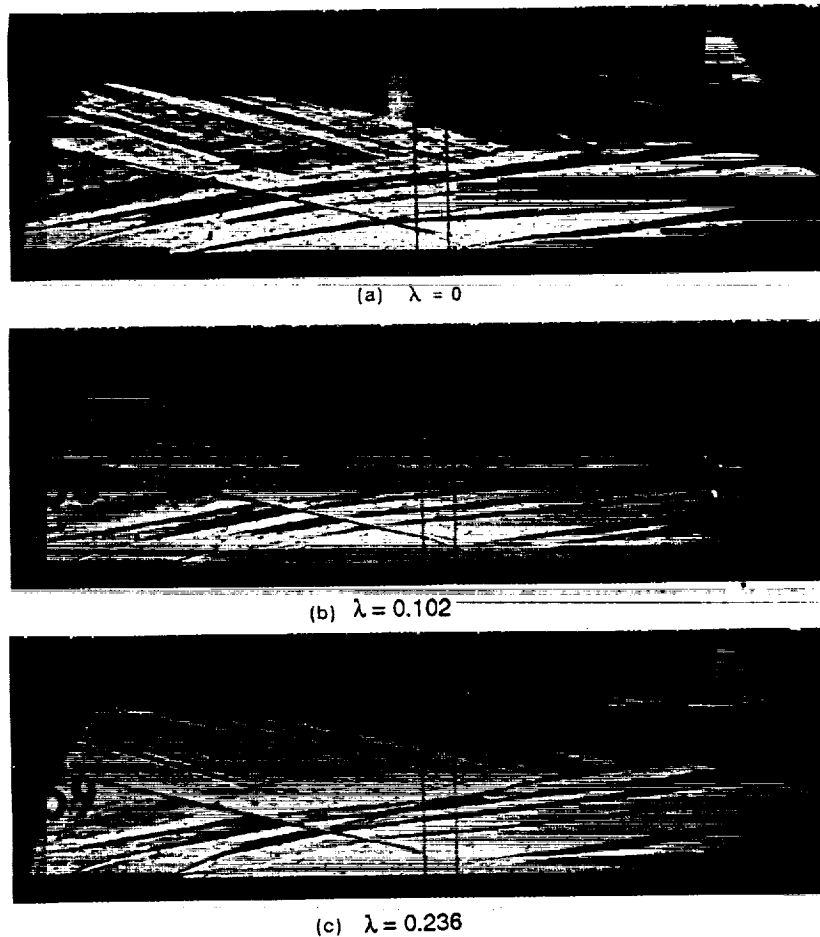


Figure 48 SCHLIEREN PHOTOGRAPHS FOR INCIDENT-SHOCK/WALL-JET INTERACTIONS ($\Theta_{sg} = 5.5$ DEGREES, SLOT HEIGHT = 0.120 INCH)

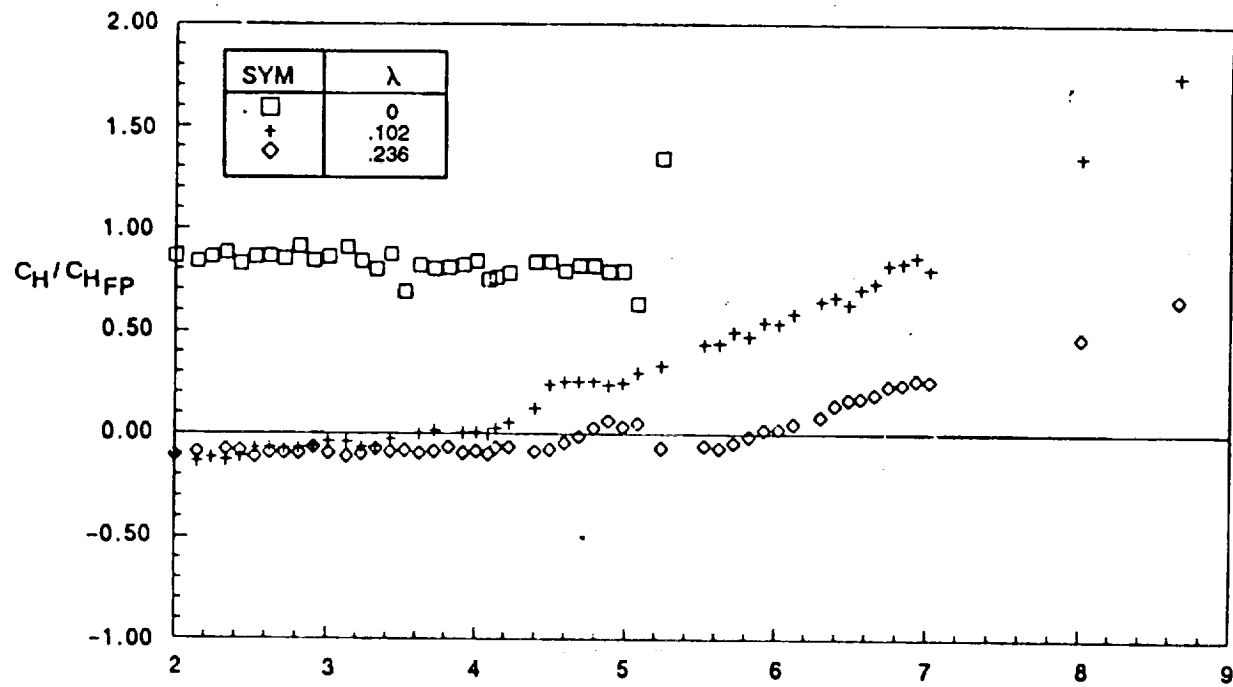


Figure 49 HEAT TRANSFER DISTRIBUTION IN SEPARATION REGION ($\Theta_{sg} = 5.5$ DEGREES, SLOT HEIGHT = 0.120 INCH)

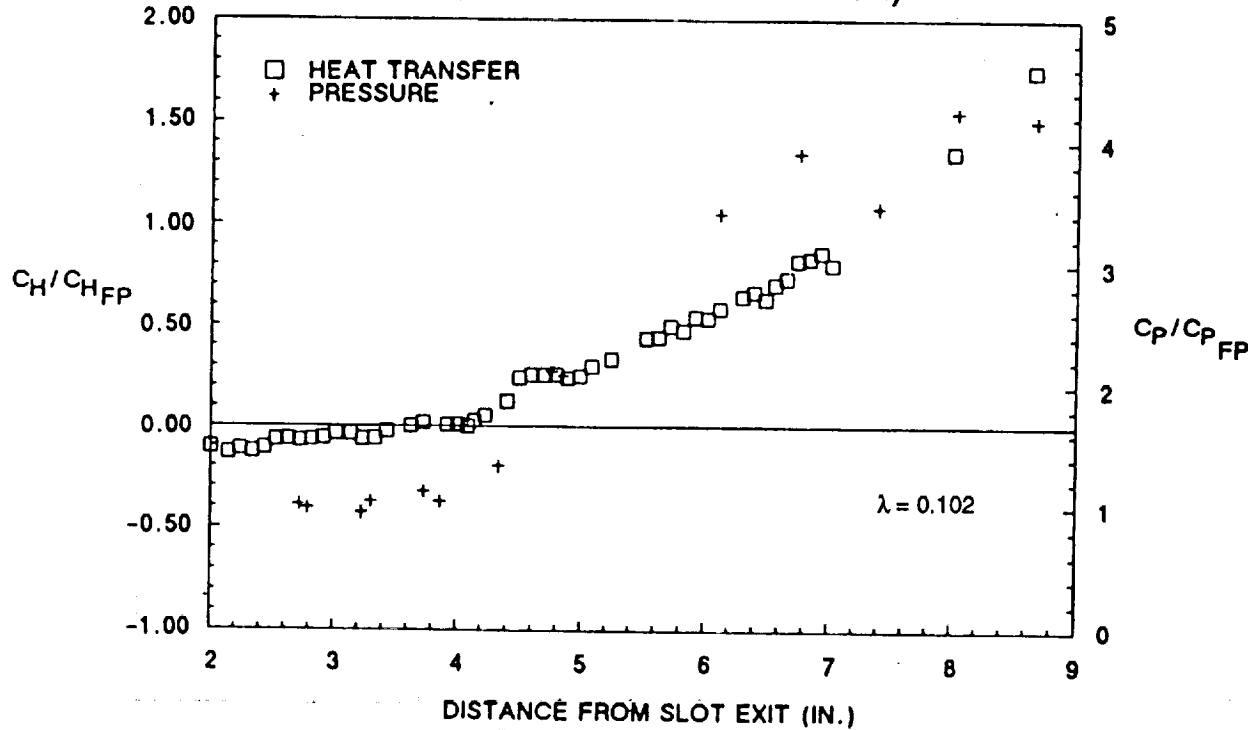


Figure 50 TYPICAL DISTRIBUTION OF HEAT TRANSFER AND PRESSURE IN SEPARATED INTERACTION REGION ($\Theta_{sg} = 5.5$ DEGREES, SLOT HEIGHT = 0.120 INCH)

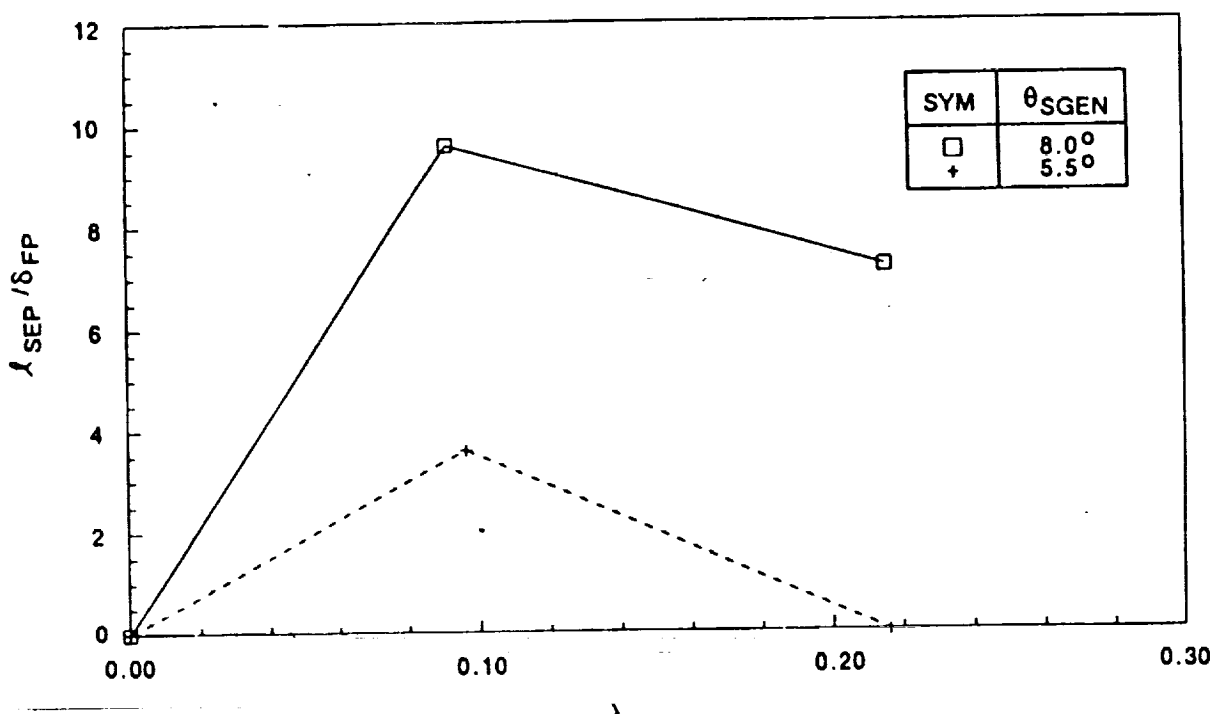


Figure 51 VARIATION OF SEPARATED FLOW LENGTH WITH BLOWING RATE FOR VARIOUS INCIDENT-SHOCK STRENGTHS (SLOT HEIGHT = 0.120 INCH)

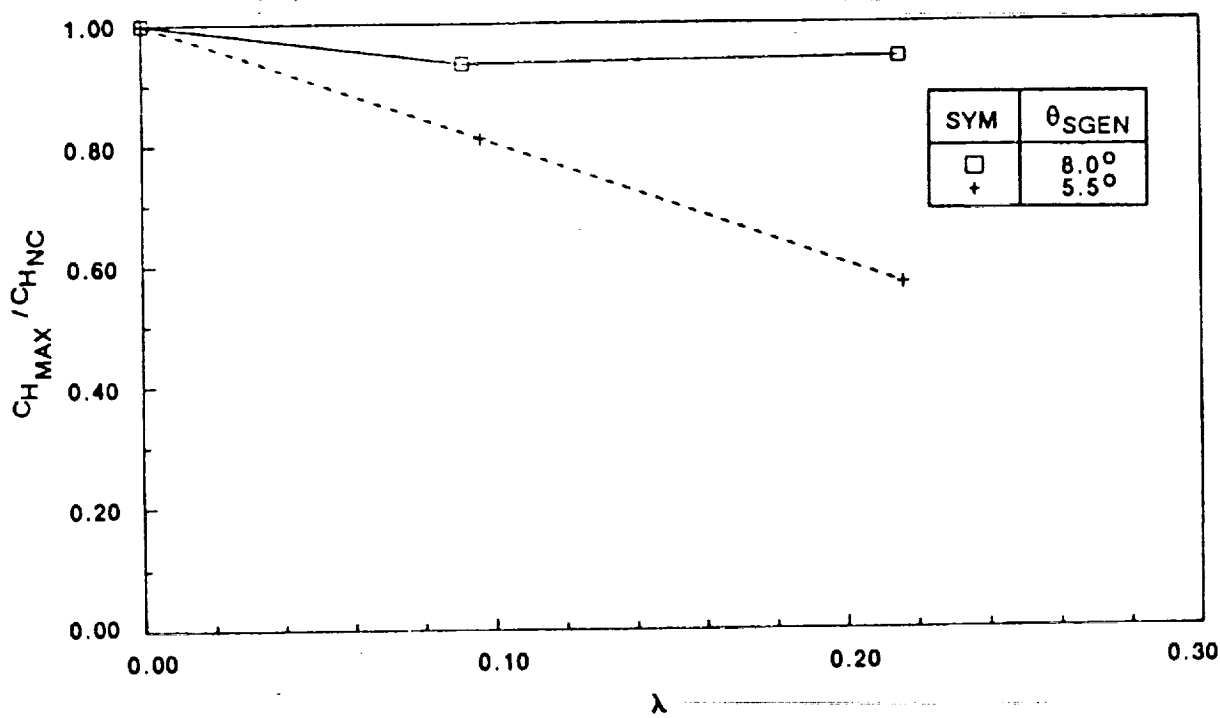


Figure 52 VARIATION OF MAXIMUM HEATING RATE WITH FILM-COOLANT FLOW RATE (SLOT HEIGHT= 0.120 INCH)

3.6.4 Lip Thickness Effects on Slot Cooling in Regions of Shock-wave/Boundary Layer Interaction

In the final segment of this program, we performed several sets of measurements to investigate the effects of lip thickness on slot-cooling effectiveness in regions of shock-wave/boundary layer interaction. In this limited study, we employed a shock-generator angle of 10.25° , at a single blowing rate for which the pressure at the exit to the slot was matched from the external flow. Two lip thicknesses, 0.020 inch and 0.145 inch were employed in this investigation. Figure 53 shows the two sets of measurements obtained in a shock-induced interaction region where only the thickness of the lip was varied. It can be seen that the effect of lip thickness was to introduce into the lower-momentum region ahead of the point of shock impingement a momentum deficit associated with the wake of the lip, which, in turn, caused an increase in the size of the separated interaction region. This is manifested by an increase in heat transfer and pressure in regions upstream of shock impingement. Thus, although we observed little effect of lip thickness on transpiration cooling in the absence of shock-interaction regions, if a shock-interaction region is present close to the exit of a slot-cooling system, the flow distortion generated by such interaction will be enhanced by the wake of the slot lip.

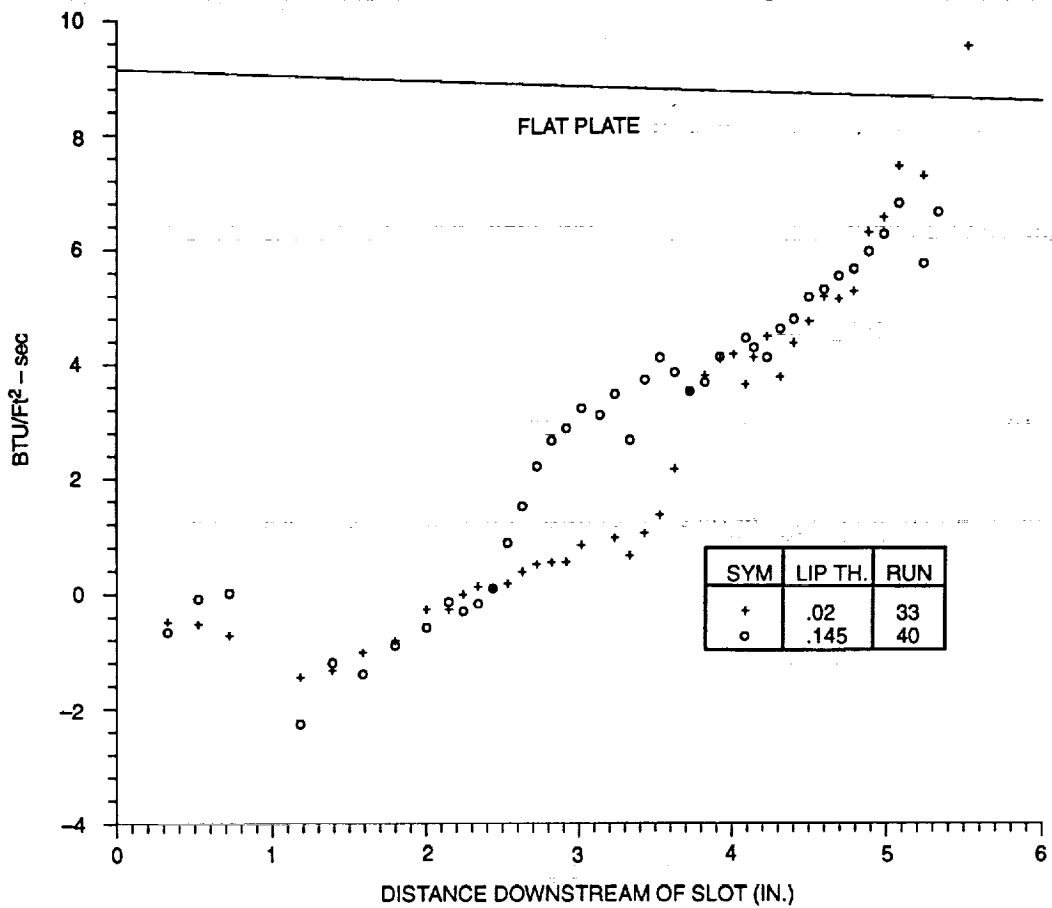


Figure 53 HEAT TRANSFER VARIATION WITH LIP THICKNESS IN REGIONS OF INCIDENT-SHOCK/WALL JET INTERACTION ($\Theta_{sg} = 10.5$ DEGREES, SLOT HEIGHT = 0.080 INCH, $\lambda=0.100$)

Section 4 CONCLUSIONS

Experimental studies have been conducted to examine the interaction between a planar shock wave and a wall jet produced by slot cooling in turbulent hypersonic flow to determine the effectiveness of a film-cooled surface disturbed by planar oblique shocks. This investigation was conducted in the 48-inch shock tunnel at a Calspan at freestream Mach numbers of 6 for Reynolds numbers up to 35×10^6 just upstream of the interaction region. The Mach 3 planar wall jet was generated from 40 small transverse nozzles producing a single film that extended the full 18-inch width of the model. Two slot heights, 0.08 inch and 0.120 inch, were employed in this study and operated at conditions where the exit pressures and the velocities matched the freestream values. Measurements were also made at "off-design" conditions, where the nozzle flows were operated in over- and under-expanded modes. A two-dimensional shock generator was used to generate shocks, causing flow deflection angles of 5°, 8°, and 10.5°. During these studies, the shock generators were translated to place the incident shock at a number of stations downstream from the nozzle exits. Detailed measurements of heat transfer and pressure were made both well ahead and downstream of the injection station, with the greatest concentration of measurements in the regions of shock-wave/wall-jet interaction.

The measurements of the effectiveness of film cooling in the absence of shock impingement showed that, for a common coolant Mach number, the measurements could be correlated in terms of a simple $(X/S)/\lambda^{0.8}$ parameter. Our measurements demonstrated greater cooling effectiveness of the helium coolant than the nitrogen coolant employed in earlier studies; however, the measurements with both nitrogen and helium coolants could be correlated when these data were plotted in terms of the more complex parameters that include the Mach number, specific heat, and molecular weight of the coolant. Our investigation of nozzle lip thickness effects on film-cooling performance showed a weak effect, suggesting that sophisticated nozzle structures to achieve thin nozzle lips are unnecessary.

Detailed distributions of heat transfer and pressure were obtained in the incident-shock/wall-jet interaction region for a range of coolant flow rates, shock strengths, and impingement positions for the two nozzle heights. The major conclusion from these studies is that the cooling film could be readily dispersed by relatively weak incident shocks such that the peak heating in the recompression region was not significantly reduced by even the

largest levels of film cooling. While, in the absence of film cooling, the interaction regions were unseparated, regions of boundary layer separation were induced in the film-cooling layer, with the size of these separated regions increasing with shock strength and decreased film cooling rate. Surprisingly, the size of the separated regions and magnitude of the recompression heating were not strongly influenced by the thickness of the cooling film or the point of shock impingement relative to the exit plane of the nozzles. The effects of nozzle lip thickness on the characteristics of the interaction region were found to be small and do not warrant the construction of sophisticated and expensive structures to achieve thin nozzle lips. The disparity between these results and those generated earlier by Alzner and Zakkay has yet to be explained.

Section 5 REFERENCES

1. Bushnell, D.M.; Cary, A.M., Jr.; and Harris, J.E., "Calculation Methods for Compressible Turbulent Boundary Layers 1976," NASA SP-422, 1977.
2. Goldstein, Richard J., "Film Cooling," Advances in Heat Transfer, Irving, Thomas F. and Hartnett, James (ed), Vol. 7, 1971, Academic Press, pp. 321-379.
3. Parthasarathy, K.; and Zakkay, V., "An Experimental Investigation of Turbulent Slot Injection at Mach 6," AIAA Journal, Vol. 8, No. 7, July 1970, pp. 1302-1307.
4. Cary, Aubrey M.; and Hefner, Jerry N., "An Investigation of Film-Cooling Effectiveness and Skin Friction in Hypersonic Turbulent Flow," AIAA 71-599, June 21-23, 1971.
5. Cary, Aubrey, M. Jr.; and Hefner, Jerry N., "Film Cooling Effectiveness in Hypersonic Turbulent Flow," AIAA Journal, Vol. 8, No. 11, Nov. 1970, pp. 2090-2091.
6. Richards, B.E.; and Stollery, J.L., "An Experimental Study of the Cooling Effectiveness of a Laminar Two-Dimensional Tangential Film in Hypersonic Flow," AIAA 77-703, June 27-29, 1977.
7. Cary, A.M. Jr.; Bushnell, D.M.; and Hefner, J.N., "Predicted Effects of Tangential Slot Injection on Turbulent Boundary Layer Flow over a Wide Speed Range," Journal of Heat Transfer, Nov. 1979, Vol. 101, pp. 699-704.
8. Baker, N.R.; Kamath, Pradeep S.; McClinton, Charles R.; and Olsen, George, C., "A Film Cooling Parametric Study for NASP Engine Applications Using the 'SHIP' Code," Paper No. 40, Presented at the Fifth National AeroSpace Plane Technology Symposium, Oct. 1988.
9. Swigart, R.J.; Shih, W.C.L.; Wang, J.H.; Snow, R.; Trolier, J.W.; Leone, S.A., Martellucci, A.; and Langanelli, A.L., "Hypersonic Film Cooling Effectiveness and Aero-Optical Effects," AIAA 88-3824-CP, 1988.
10. Majeski, J.A.; and Weatherford, R.H., "Development of an Empirical Correlation for Film-Cooling Effectiveness," AIAA 88-2624, June 1988.
11. Alzner, E.; and Zakkay, V., "Turbulent Boundary Layer Shock Interaction With and Without Injection," AIAA 70-91, Jan. 1970.
12. Ledford, O.C.; and Stollery, J.L., "Film Cooling of Hypersonic Inserts," Imperial College Aero Report 72-15, July 1972, Presented at the 1st International Symposium on Air Breathing Engines, Marseille, France, June 10-23, 1972.
13. Baryshev, Y.V.; Leontyev, A.I.; and Rozhdestvenskiy, V.I., "Heat Transfer in the Zone of Interaction Between a Shock and the Boundary Layer," Heat Transfer Soviet Research, Vol. 7, No. 6, Dec. 1975, pp. 19-39.

14. Lewis, C.H. and Burgess, E.G., III, Charts of Normal Shock Wave Properties in Imperfect Air (Supplement: M = 1 to 10)," AEDC-TR-196, September 1965.
15. Hilsenrath, J., et al., Tables of Thermal Properties of Gases," NBS Circular 565, 1955.
16. Reece, J.W., Test Section Conditions Generated in the Supersonic Expansion of Real Air," Journal of Aeronautical Sciences, Vol. 29, No. 5, May 1962, pp. 617 and 618.
17. Hilsenrath, J., et al., Tables of Thermodynamic Properties of Air Including Dissociation and Ionization from 1500°K to 15,000°K," AEDC-TR-59-20, December 1959.
18. Neil, C.A., and Lewis, C.H., Interpolations of Imperfect Air Thermodynamic Data II at Constant Pressure," AEDC-TDR-64-184, September 1964.
19. Cook, W.J., Determination of Heat Transfer Rates from Transient Surface Temperature Measurements," AIAA Journal, Vol. 8, No. 7, July 1970, pp. 1366-1368.
20. Havener, G.; Holden, M.S.; and Azevedo, D., "Preliminary Applications of Holographic Interferometry to Study Hypersonic Regions of Shock Wave/Boundary Layer Interaction," AIAA 87-1194, 1987.
21. Van Driest, E.R., "Problem of Aerodynamic Heating," Aeronautical Engineering Review, Vol. 15, No. 10, October 1956.
22. Olsen, G.C.; Nowak, R.J.; Holden, M.S.; and Baker, N.R., "Experimental Results for Film Cooling in 2-D Supersonic Flow Including Coolant Delivery Pressure, Geometry, and Incident Shock Effects," AIAA 90-0605, 1990.
23. Holden, M.S., "Shock Wave - Turbulent Boundary Layer Interaction in Hypersonic Flow," AIAA 15th Aerospace Sciences Meeting, 77-45, 1977.

Appendix A

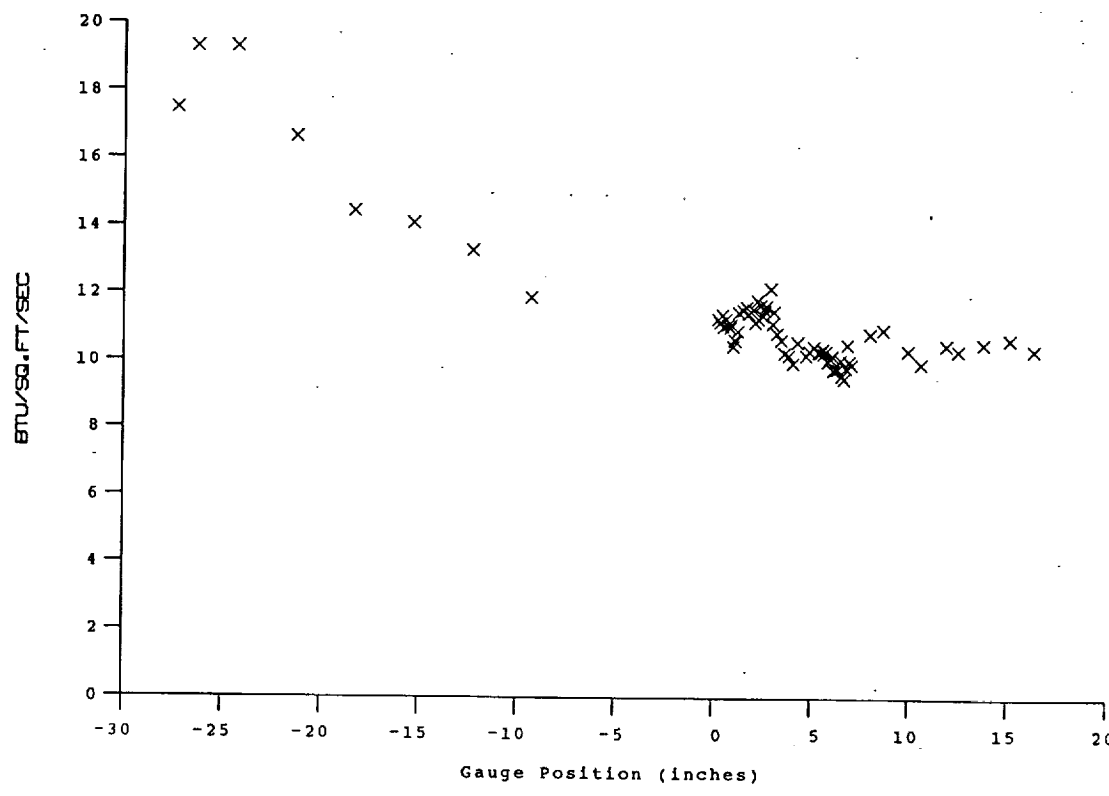
**SHOCK-WAVE/WALL-JET
STUDY DATA**

Test Conditions

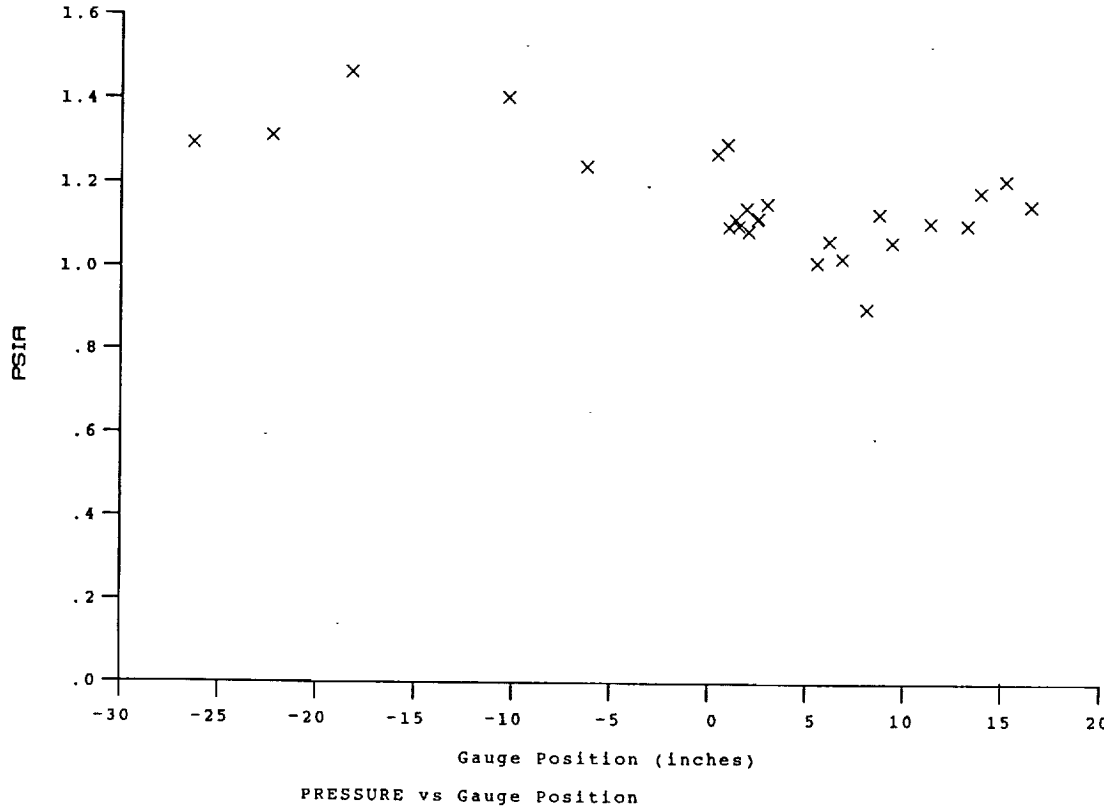
M_i = 2.9511
P_o = 2.7661X10+3 PSIA
H_o = 1.4360X10+7 (Ft/sec)²
T_o = 2.2346X10+3 Degrees R
M = 6.4231
U = 5.0637X10+3 Ft/sec
T = 2.5844X10+2 Degrees R
P = 1.1309 PSIA
Q = 3.2695X10+1 PSIA
Rho = 3.6722X10-4 Slugs/Ft³
Mu = 2.1117X10-7 Slugs/Ft-sec
Re = 8.8059X10+6 1/Ft
P_{o'} = 6.0992X10+1 PSIA

Model Configuration Parameter Value**Flat Plate**

Run 4



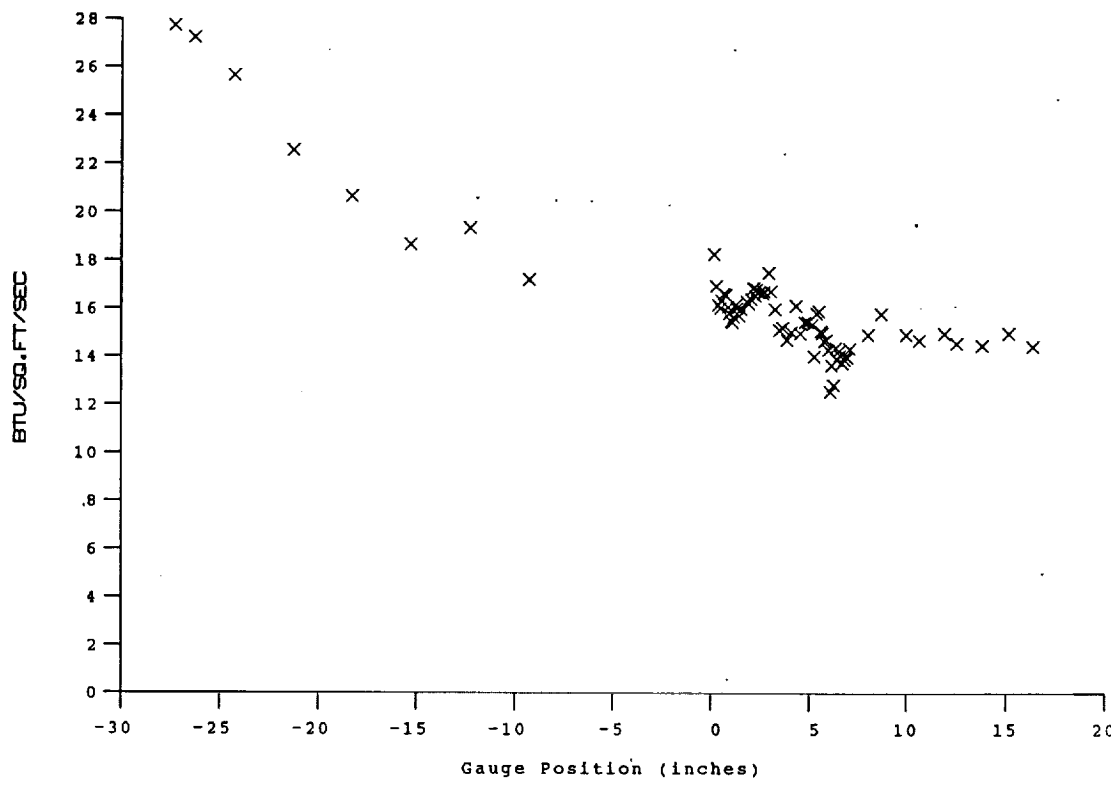
HEAT TRANSFER vs Gauge Position
Run 4



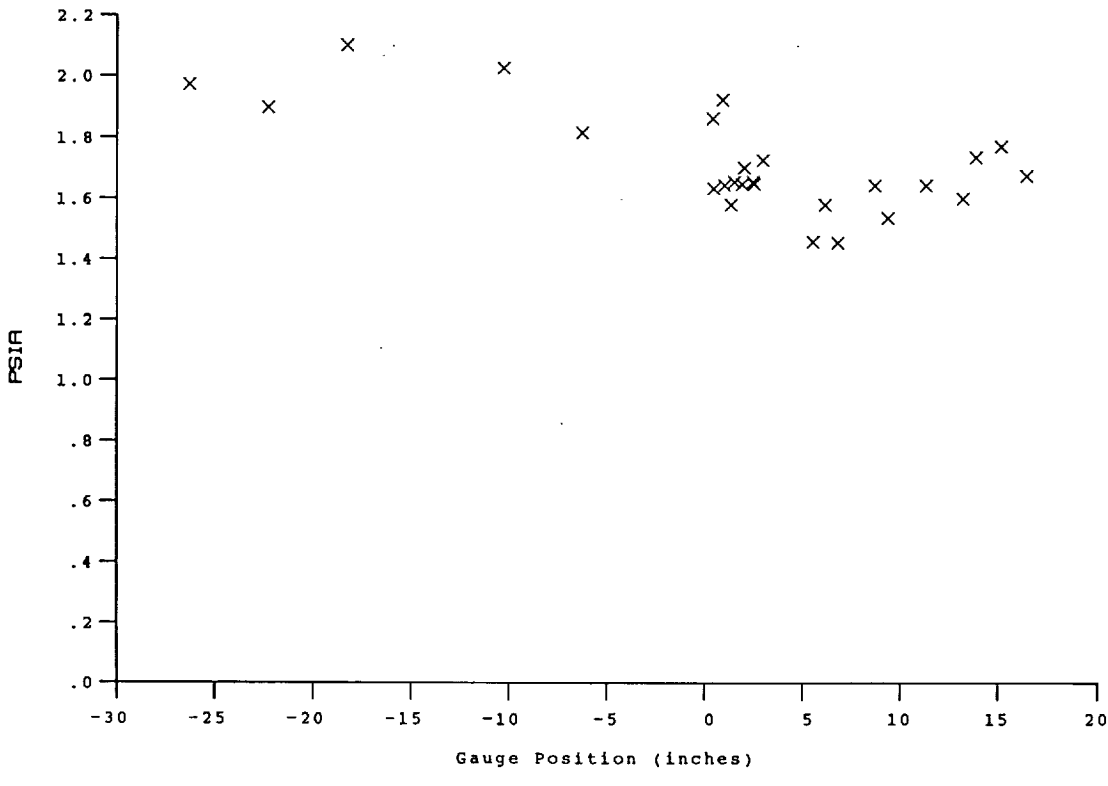
PRESSURE vs Gauge Position
Run 4

Test Conditions	Model Configuration Parameter	Value
		Flat Plate
M _i = 2.9469		
P _o = 4.0826x10+3	PSIA	
H _o = 1.4407x10+7	(Ft/sec) ²	
T _o = 2.2337x10+3	Degrees R	
M = 7.8675		
U = 5.1660x10+3	Ft/sec	
T = 1.7929x10+2	Degrees R	
P = 4.6940x10-1	PSIA	
Q = 2.0360x10+1	PSIA	
Rho = 2.1971x10-4	Slugs/Ft ³	
Mu = 1.4962x10-7	Slugs/Ft-sec	
Re = 7.5860x10+6	1/Ft	
P _{o'} = 3.7605x10+1	PSIA	

Run 5



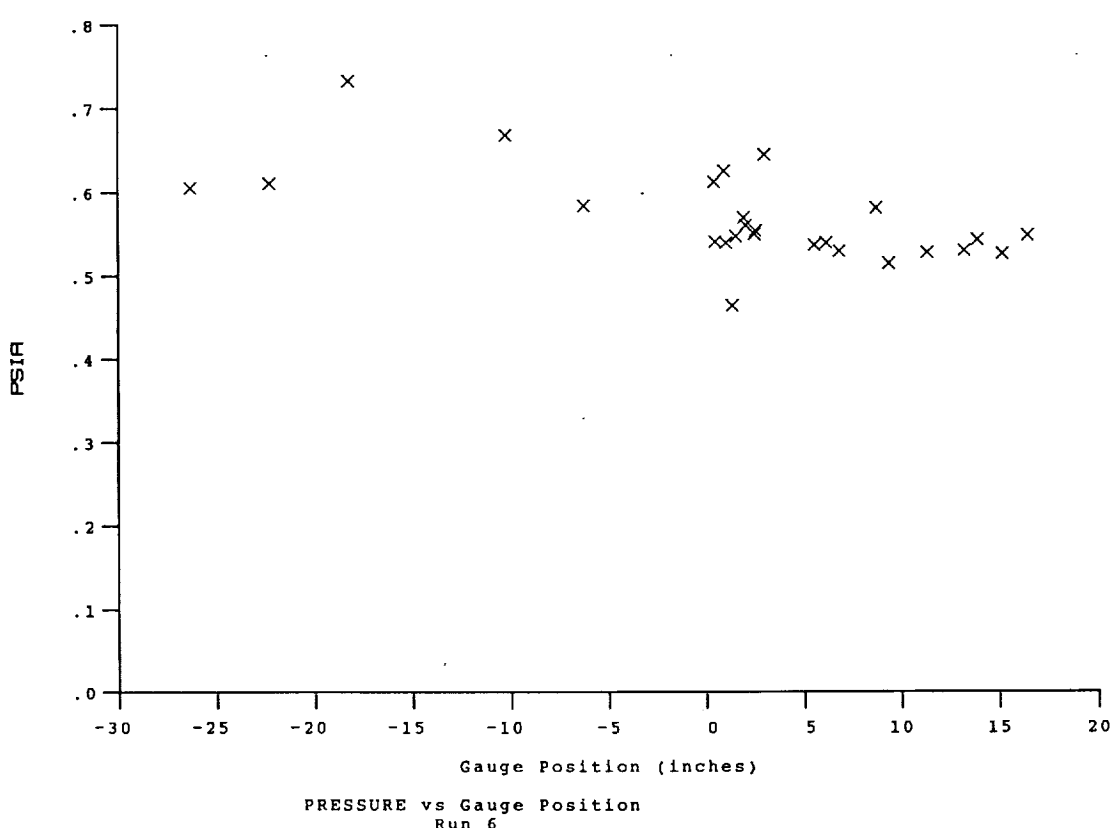
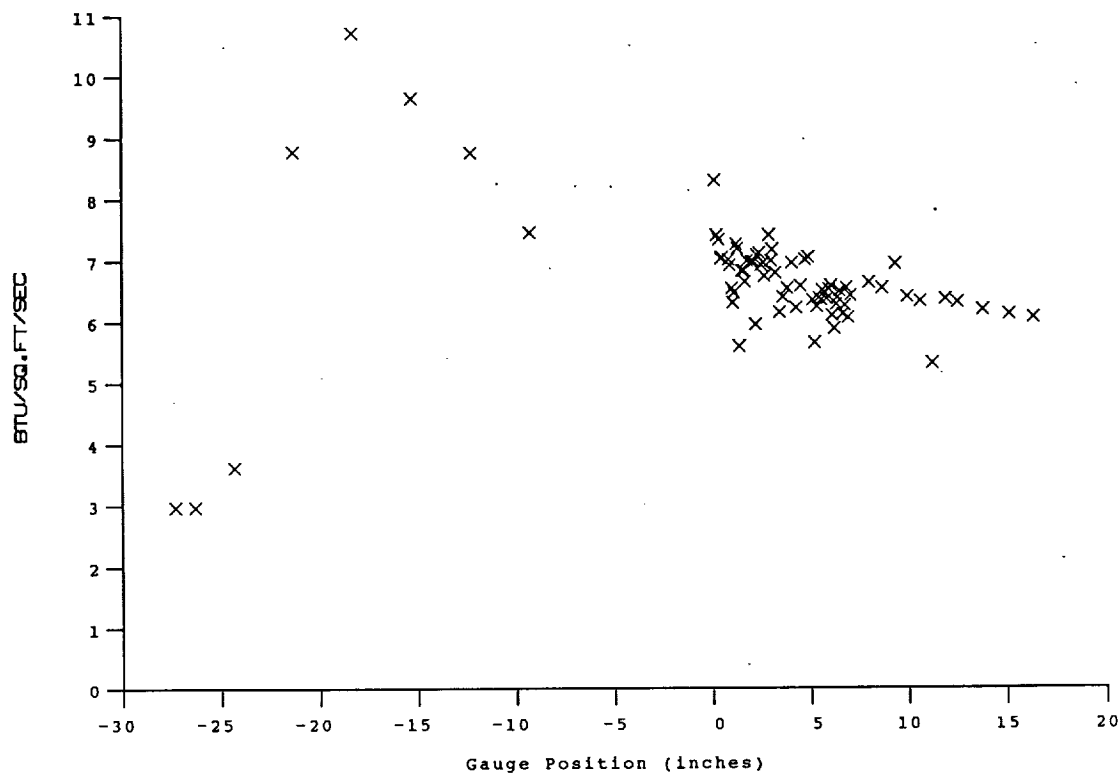
HEAT TRANSFER vs Gauge Position
Run 5



PRESSURE vs Gauge Position
Run 5

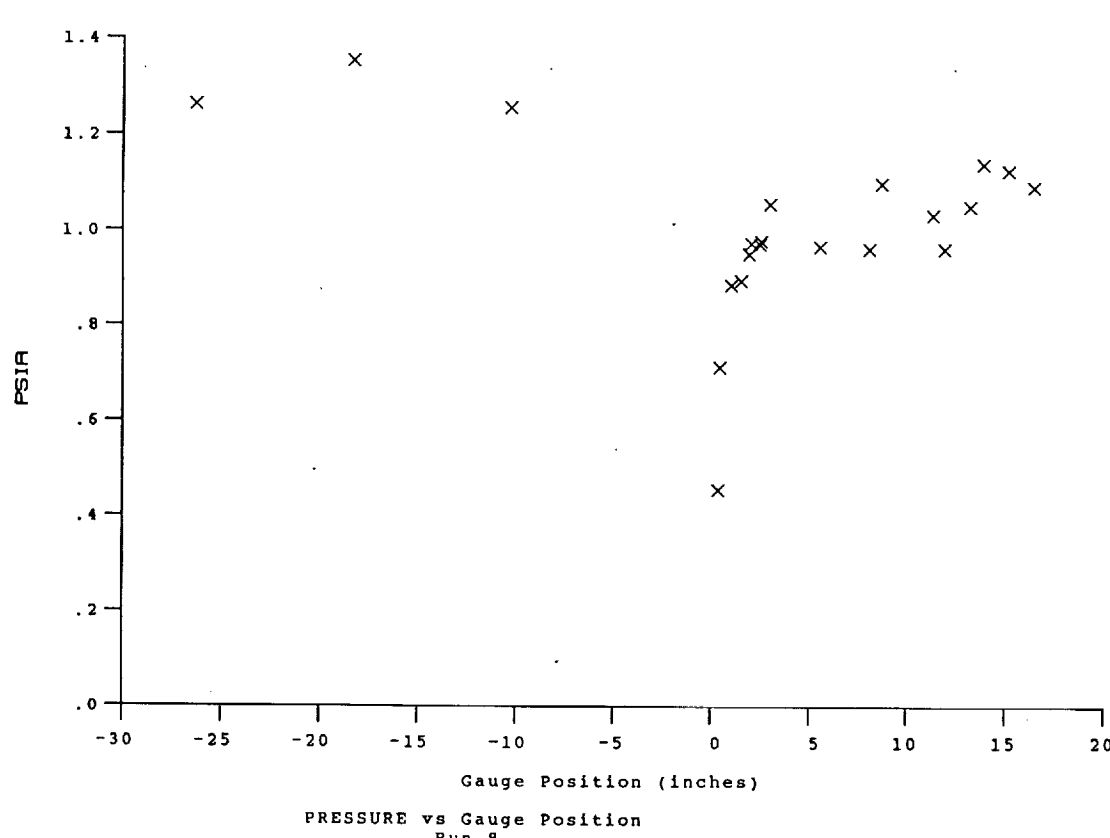
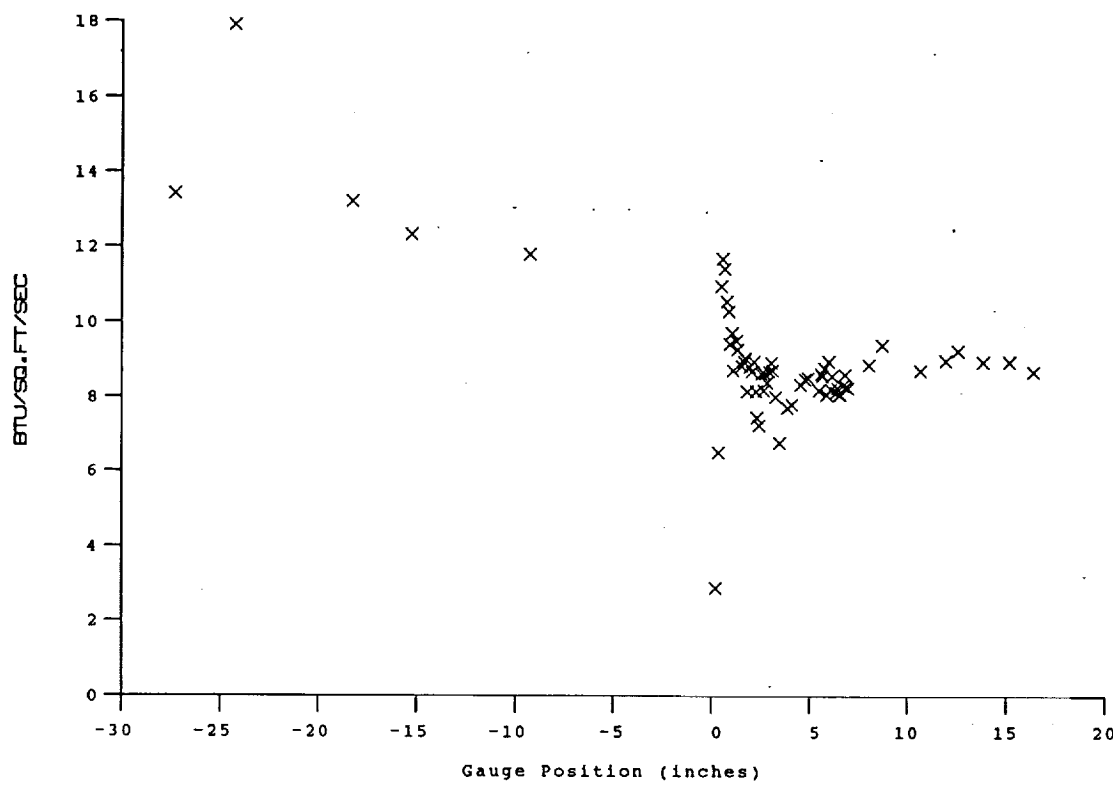
Test Conditions	Model Configuration Parameter	Value
M _i = 2.9081		
P _o = 4.1550x10+3	PSIA	Flat Plate
H _o = 1.4092x10+7	(Ft/sec) ²	
T _o = 2.1905x10+3	Degrees R	
M = 6.4708		
U = 5.0202x10+3	Ft/sec	
T = 2.5029x10+2	Degrees R	
P = 1.6663	PSIA	
Q = 4.8890x10+1	PSIA	
Rho = 5.5868x10-4	Slugs/Ft ³	
Mu = 2.0506x10-7	Slugs/Ft-sec	
Re = 1.3678x10+7	1/Ft	
Po' = 9.1179x10+1	PSIA	

Run 6



Test Conditions		Model Configuration Parameter	Value
$M_i = 2.8786$		Slot Height (inches)	0.080
$P_0 = 2.5555 \times 10^3$	PSIA	Lip Thickness (inches)	0.020
$H_0 = 1.3868 \times 10^7$	$(\text{Ft/sec})^2$	Lambda	0
$T_0 = 2.1675 \times 10^3$	Degrees R	Nozzle Exits Taped	
$M = 6.4303$			
$U = 4.9769 \times 10^3$	Ft/sec		
$T = 2.4909 \times 10^2$	Degrees R		
$P = 1.0434$	PSIA		
$Q = 3.0232 \times 10^1$	PSIA		
$\rho = 3.5152 \times 10^{-4}$	Slugs/Ft ³		
$\mu = 2.0415 \times 10^{-7}$	Slugs/Ft-sec		
$Re = 8.5694 \times 10^6$	1/Ft		
$P_0' = 5.6371 \times 10^1$	PSIA		

Run 8



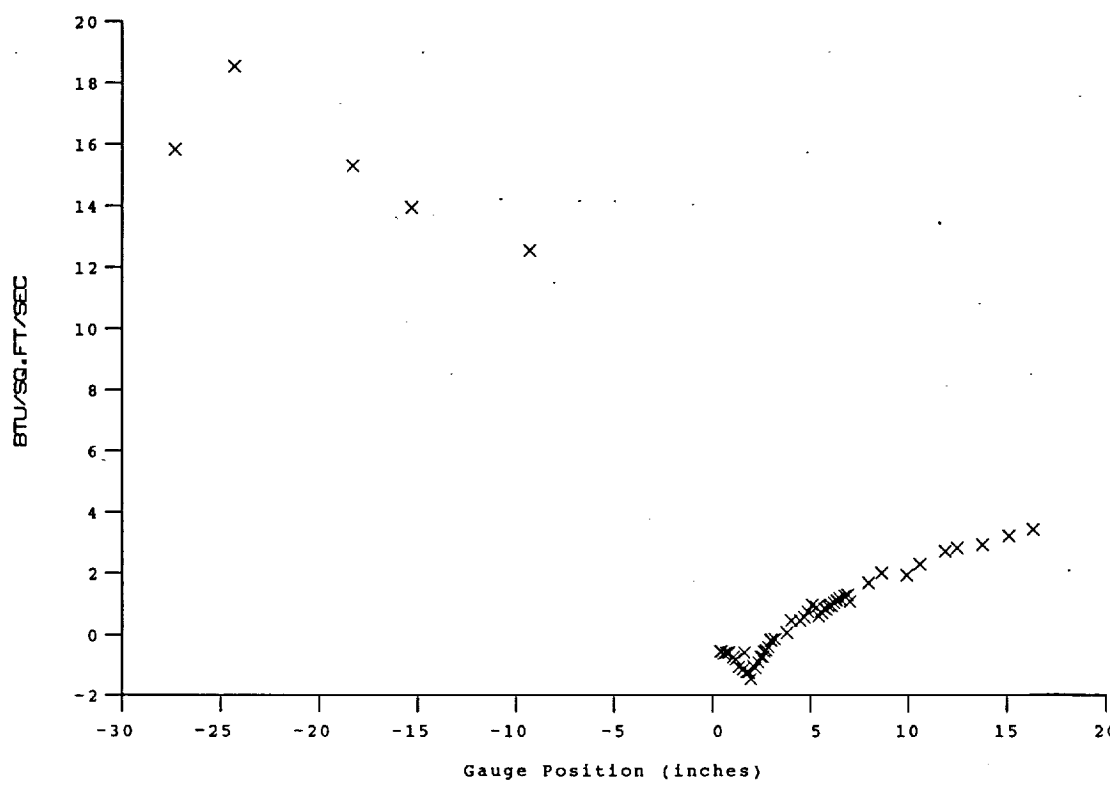
Test Conditions

M_i = 2.9444
P_o = 2.6621X10+3 PSIA
H_o = 1.4426X10+7 (Ft/sec)²
T_o = 2.2447X10+3 Degrees R
M = 6.4203
U = 5.0751X10+3 Ft/sec
T = 2.5984X10+2 Degrees R
P = 1.0877
Q = 3.1418X10+1 PSIA
Rho = 3.5130X10-4 Slugs/Ft³
Mu = 2.1220X10-7 Slugs/Ft-sec
Re = 8.4018X10+6 1/Ft
Po' = 5.8614X10+1 PSIA

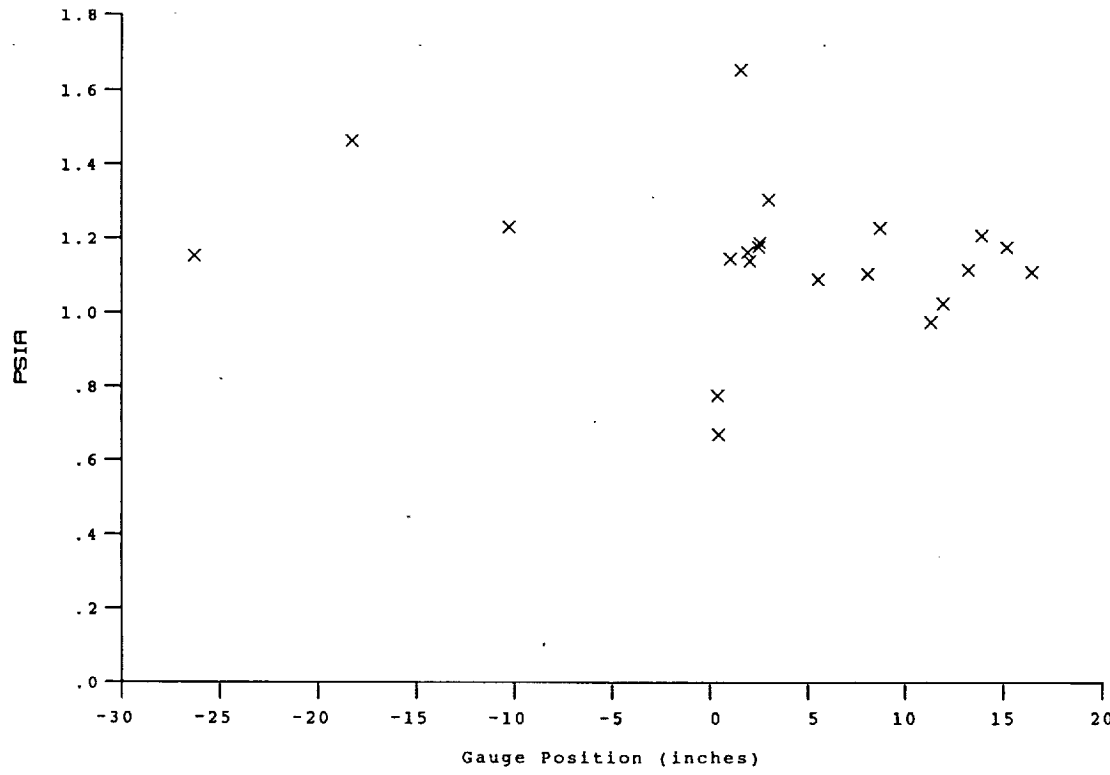
Model Configuration Parameter**Value**

Slot Height (inches)	0.080
Lip Thickness (inches)	0.020
Mass Flow Rate per Nozzle (slugs/sec)	9.783E-05
Non-dimensional Blowing Rate, Lambda	0.1864
Exit Plane Pressure (psia)	-
Coolant Total Temperature (Rankine)	530

Run 14



HEAT TRANSFER vs Gauge Position
Run 14



PRESSURE vs Gauge Position
Run 14

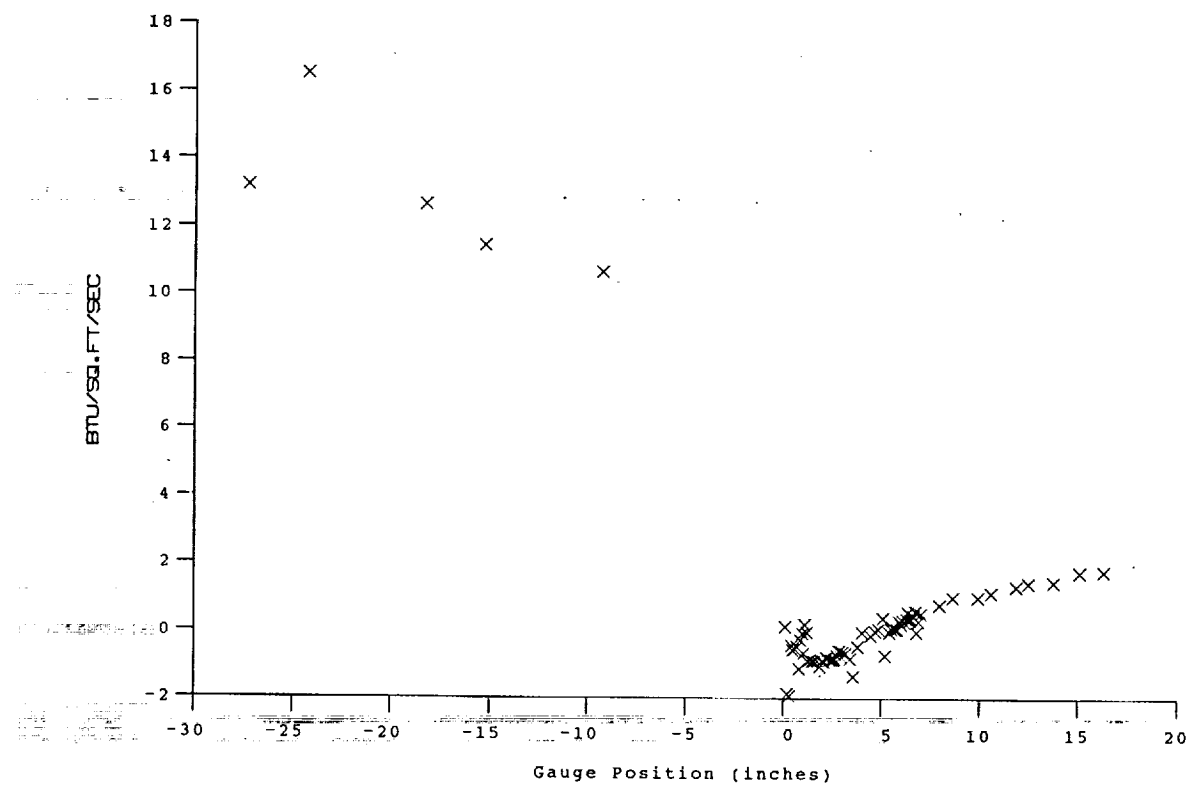
Test Conditions

M_i = 2.8464
P_o = 2.4754X10+3 PSIA
H_o = 1.3494X10+7 (Ft/sec)²
T_o = 2.1145X10+3 Degrees R
M = 6.4336
U = 4.9095X10+3 Ft/sec
T = 2.4215X10+2 Degrees R
P = 1.0133 PSIA
Q = 2.9391X10+1 PSIA
Rho = 3.5117X10-4 Slugs/Ft³
Mu = 1.9890X10-7 Slugs/Ft-sec
Re = 8.6680X10+6 1/Ft
P_{o'} = 5.4780X10+1 PSIA

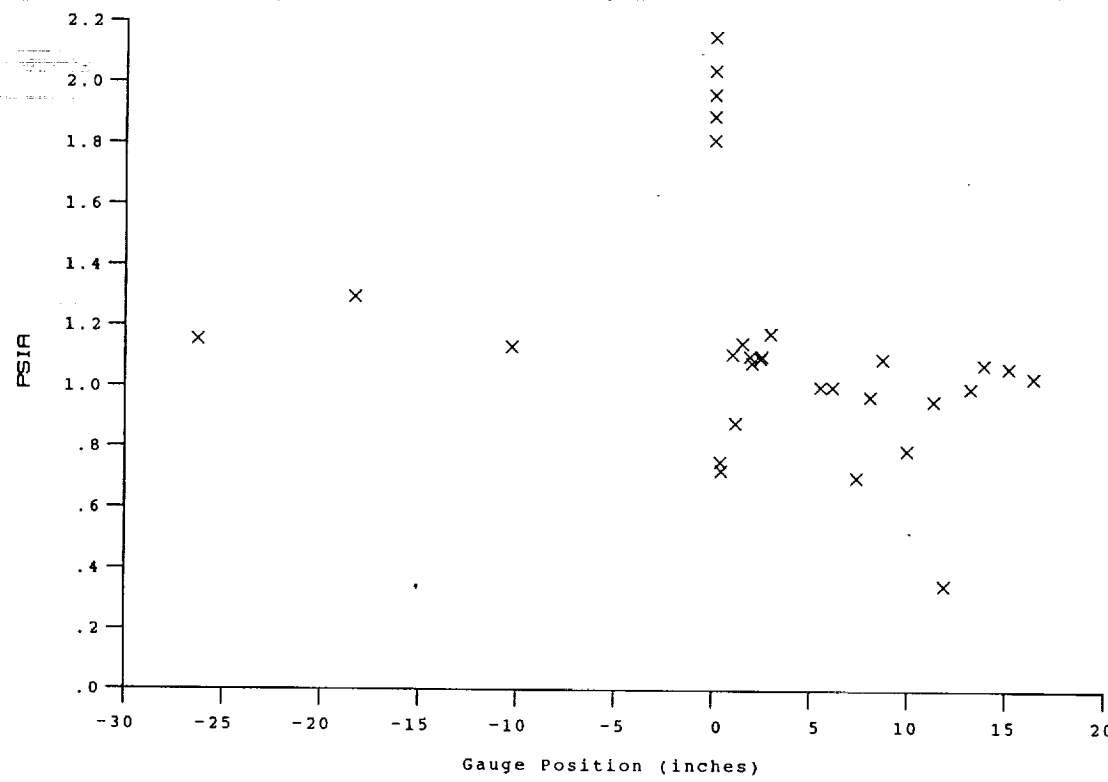
Model Configuration Parameter**Value**

Slot Height (inches)	0.080
Lip Thickness (inches)	0.020
Mass Flow Rate per Nozzle (slugs/sec)	1.104E-04
Non-dimensional Blowing Rate, Lambda	0.2174
Nozzle Reservoir Pressure (psia)	35.34
Exit Plane Pressure (psia)	1.979
Coolant Total Temperature (Rankine)	530

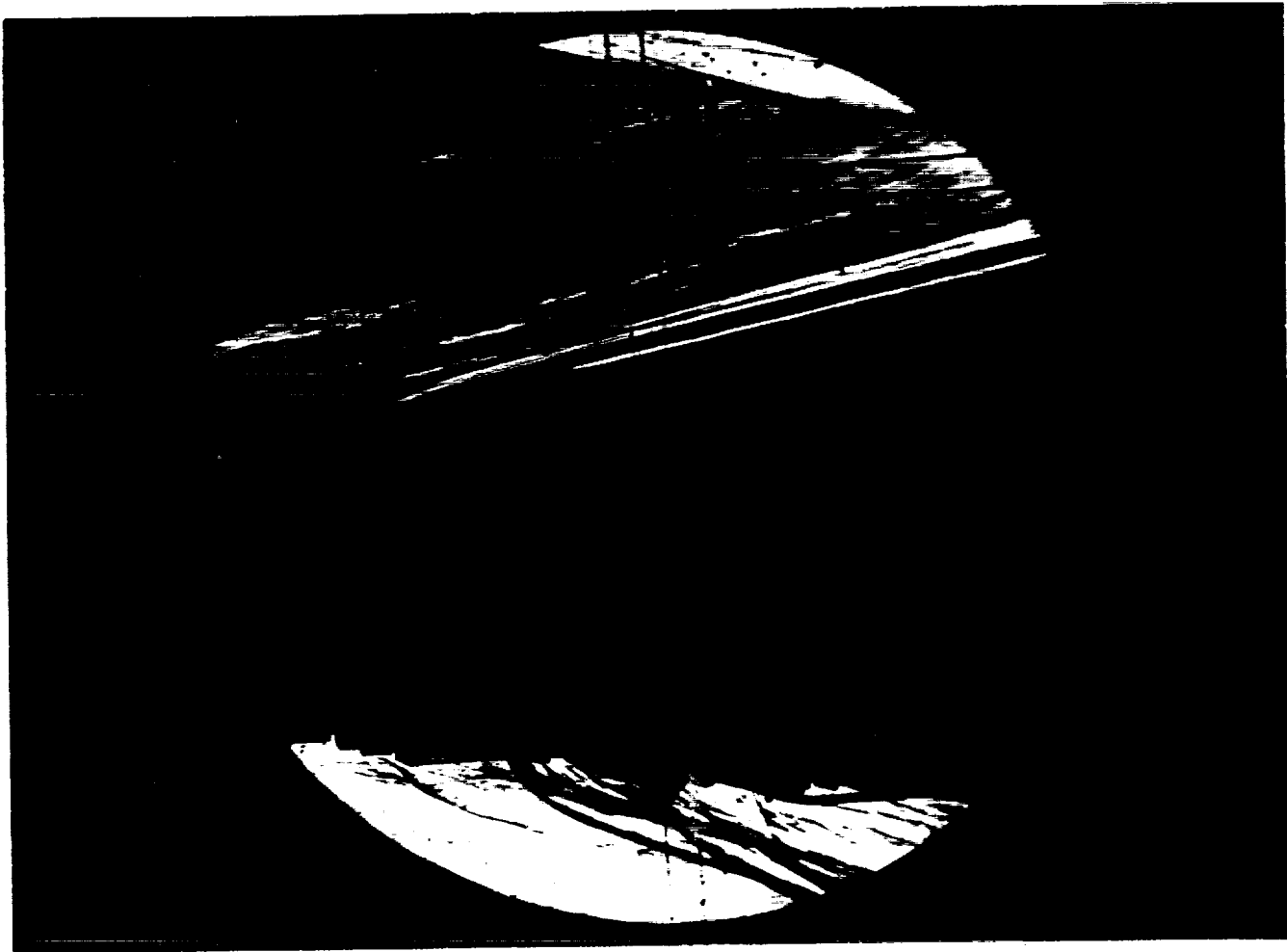
Run 15



HEAT TRANSFER vs Gauge Position
Run 15



PRESSURE vs Gauge Position
Run 15



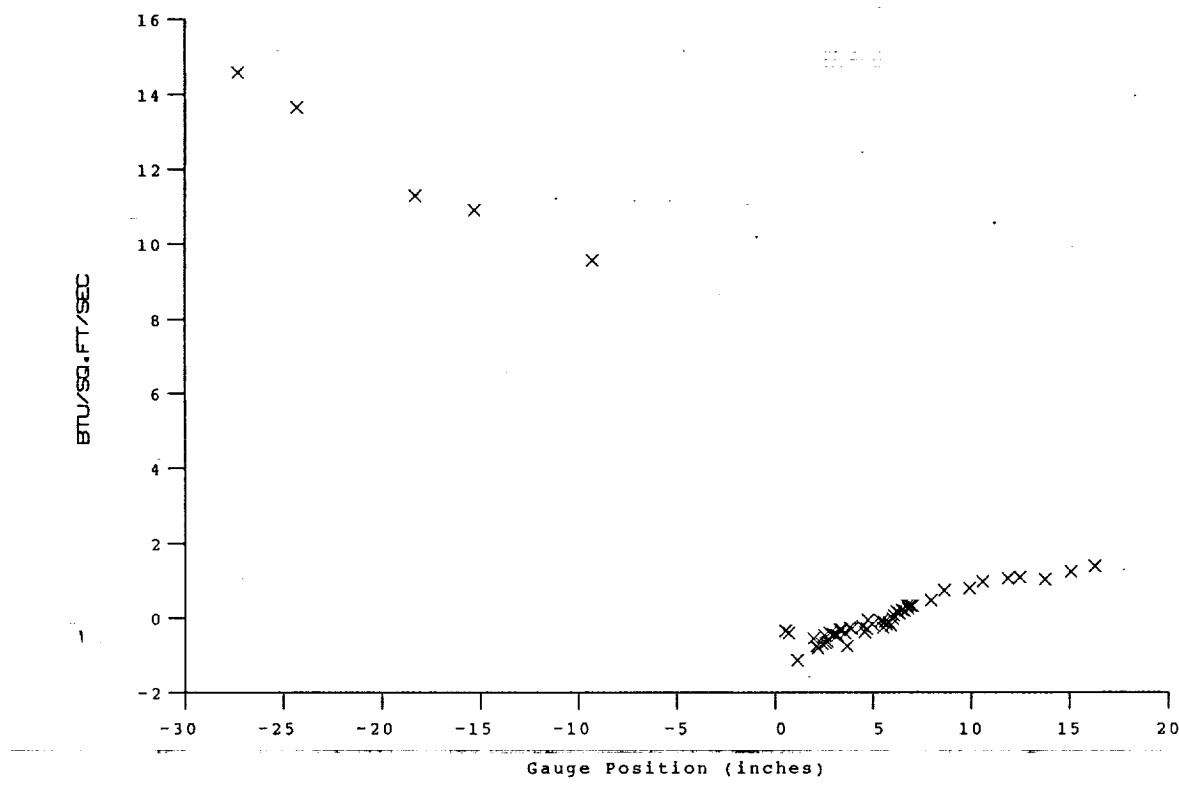
Test Conditions

M_i = 2.7947
P_o = 2.3237x10+3 PSIA
H_o = 1.3146X10+7 (Ft/sec)²
T_o = 2.0664x10+3 Degrees R
M = 6.4369
U = 4.8461X10+3 Ft/sec
T = 2.3569X10+2 Degrees R
P = 9.5141X10-1 PSIA
Q = 2.7624X10+1 PSIA
Rho = 3.3877X10-4 Slugs/Ft³
Mu = 1.9397X10-7 Slugs/Ft-sec
Re = 8.4635X10+6 1/Ft
P_{o'} = 5.1470X10+1 PSIA

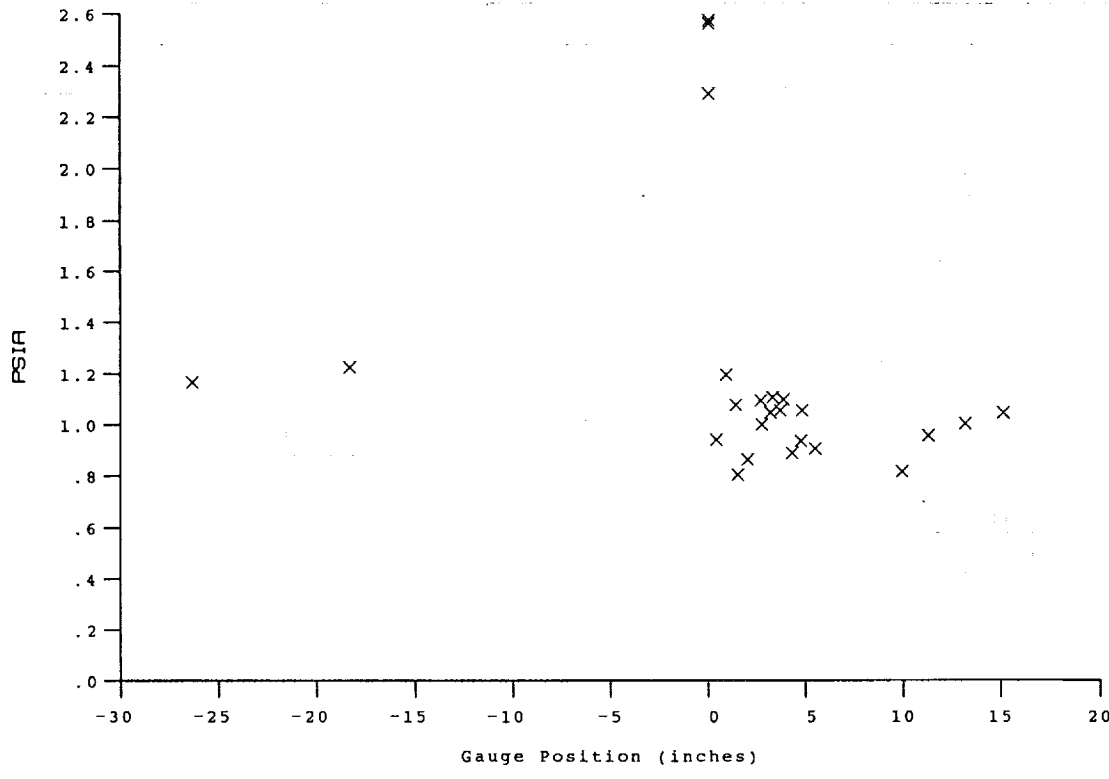
Model Configuration Parameter Value

Slot Height (inches)	0.080
Lip Thickness (inches)	0.020
Mass Flow Rate per Nozzle (slugs/sec)	1.460E-04
Non-dimensional Blowing Rate, Lambda	0.3011
Nozzle Reservoir Pressure (psia)	40.78
Exit Plane Pressure (psia)	2.482
Coolant Total Temperature (Rankine)	530

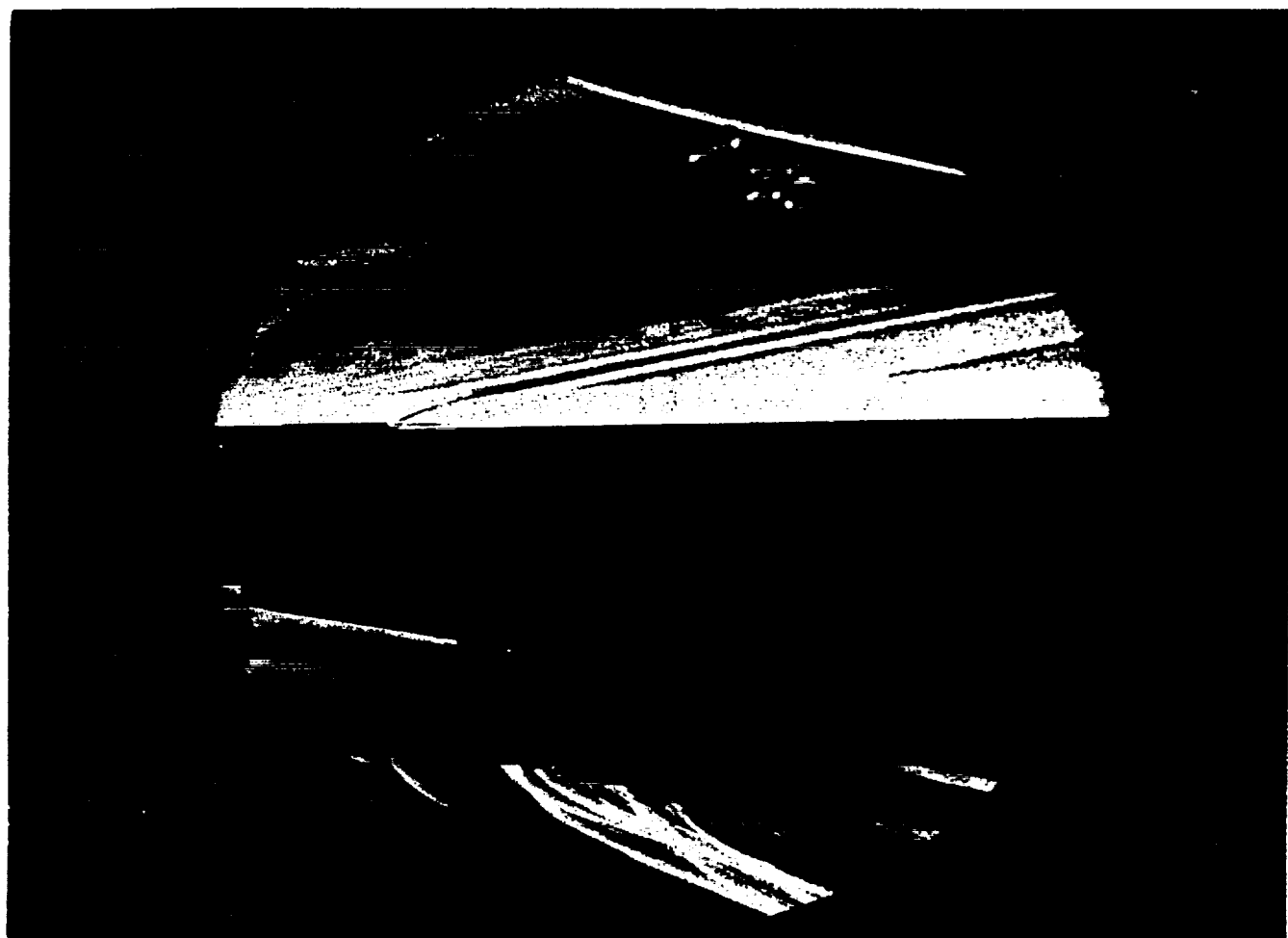
Run 21



HEAT TRANSFER vs Gauge Position
Run 21



PRESSURE vs Gauge Position
Run 21

**Test Conditions**

M_i = 2.7897
P_o = 2.3173X10+3 PSIA
H_o = 1.3102X10+7 (Ft/sec)²
T_o = 2.0603X10+3 Degrees R
M = 6.4377
U = 4.8381X10+3 Ft/sec
T = 2.3486X10+2 Degrees R
P = 9.4878X10-1 PSIA
Q = 2.7554X10+1 PSIA
Rho = 3.3902X10-4 Slugs/Ft³
Mu = 1.9334X10-7 Slugs/Ft-sec
Re = 8.4836X10+6 1/Ft
P_{o'} = 5.1337X10+1 PSIA

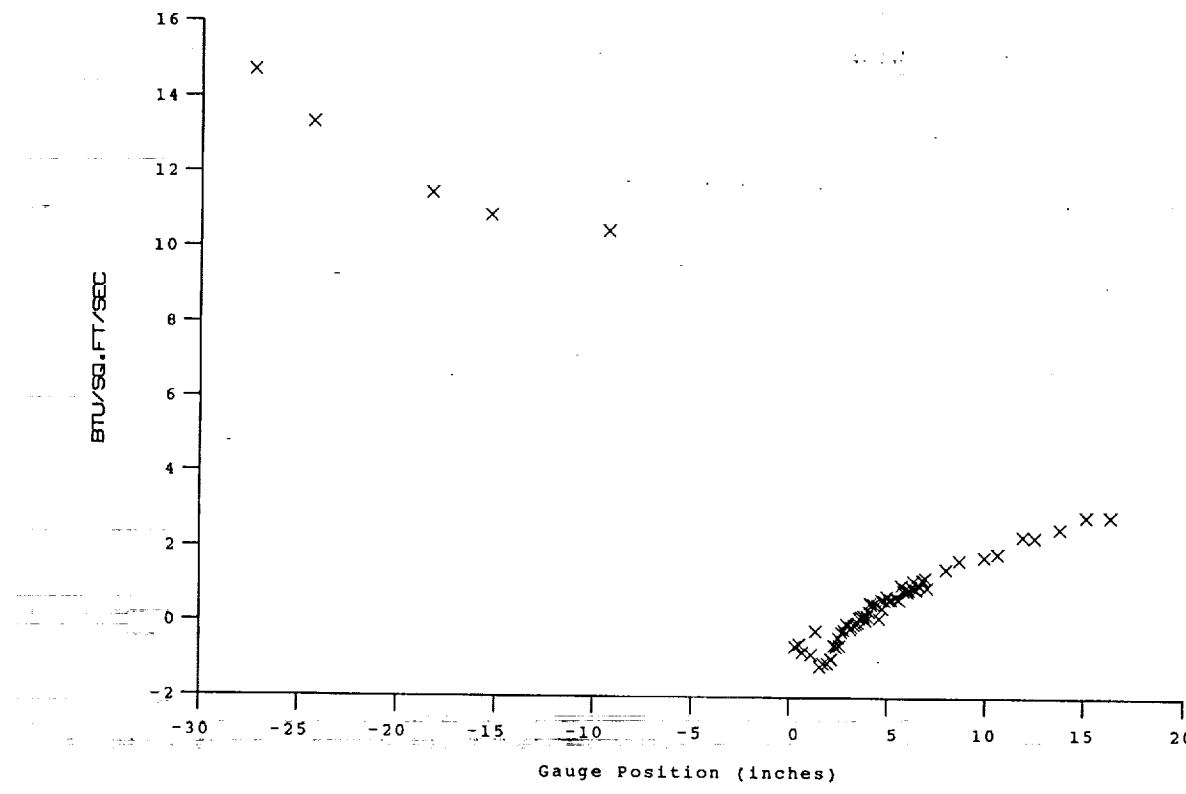
Model Configuration Parameter

	Value
Slot Height (inches)	0.080
Lip Thickness (inches)	0.020
Mass Flow Rate per Nozzle (slugs/sec)	7.167E-05
Non-dimensional Blowing Rate, Lambda	0.1484
Nozzle Reservoir Pressure (psia)	25.50
Exit Plane Pressure (psia)	1.581
Coolant Total Temperature (Rankine)	530

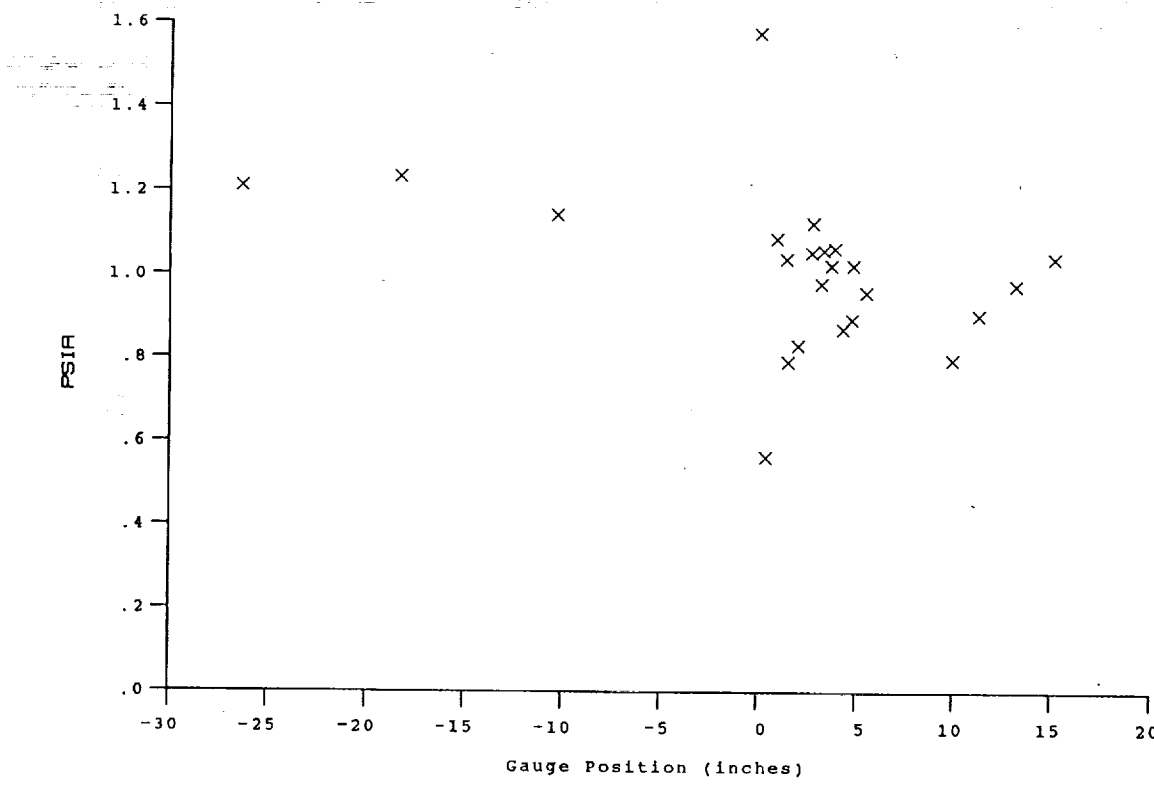
Run 23

A-16

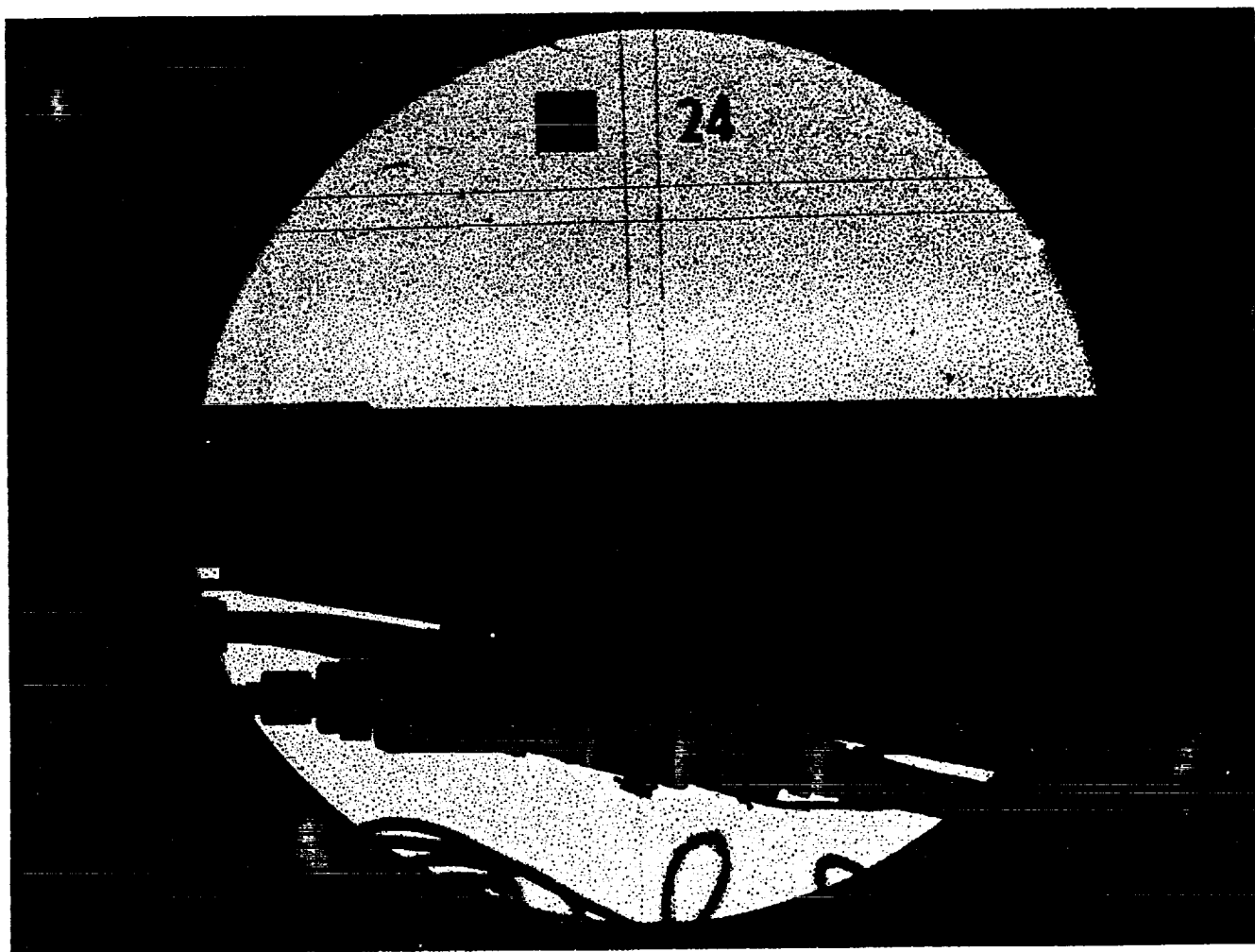
0.2.



HEAT TRANSFER vs Gauge Position
Run 23



PRESSURE vs Gauge Position
Run 23

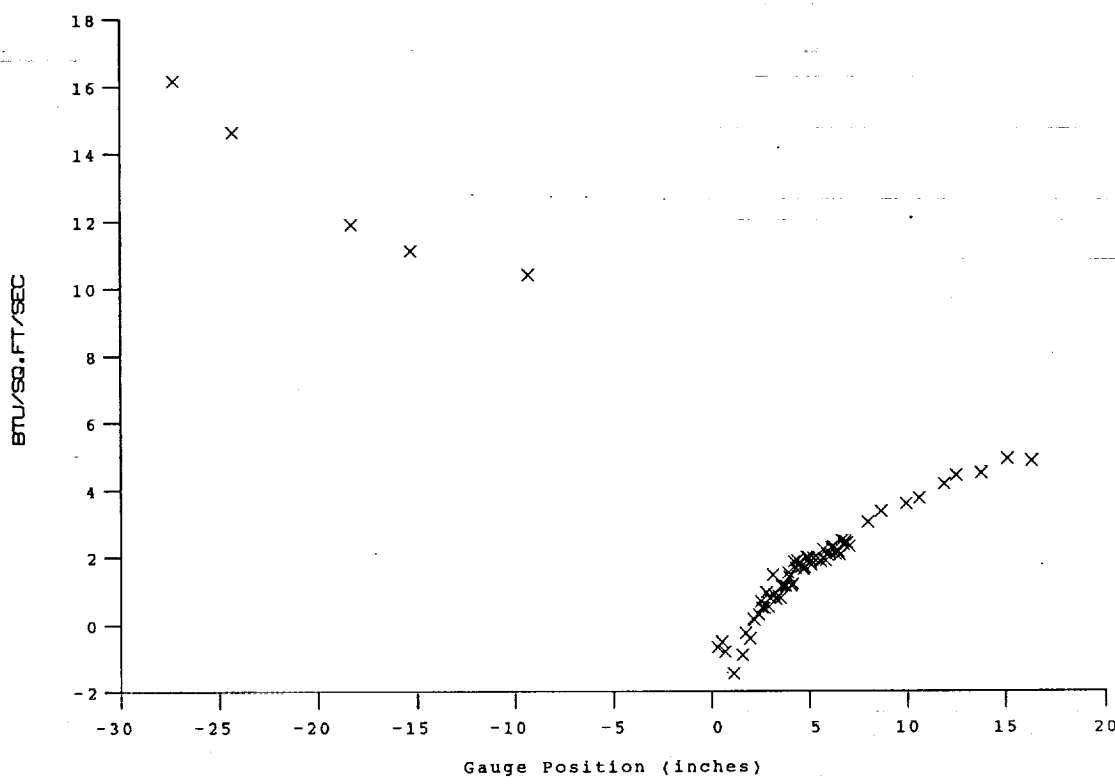
**Test Conditions**

M_i = 2.8070
P_o = 2.3185x10⁺³ PSIA
H_o = 1.3306x10⁺⁷ (Ft/sec)²
T_o = 2.0893x10⁺³ Degrees R
M = 6.4339
U = 4.8752x10⁺³ Ft/sec
T = 2.3875x10⁺² Degrees R
P = 9.4893x10⁻¹ PSIA
Q = 2.7526x10⁺¹ PSIA
Rho = 3.3354x10⁻⁴ Slugs/Ft³
Mu = 1.9632x10⁻⁷ Slugs/Ft-sec
Re = 8.2831x10⁺⁶ 1/Ft
P_{o'} = 5.1296x10⁺¹ PSIA

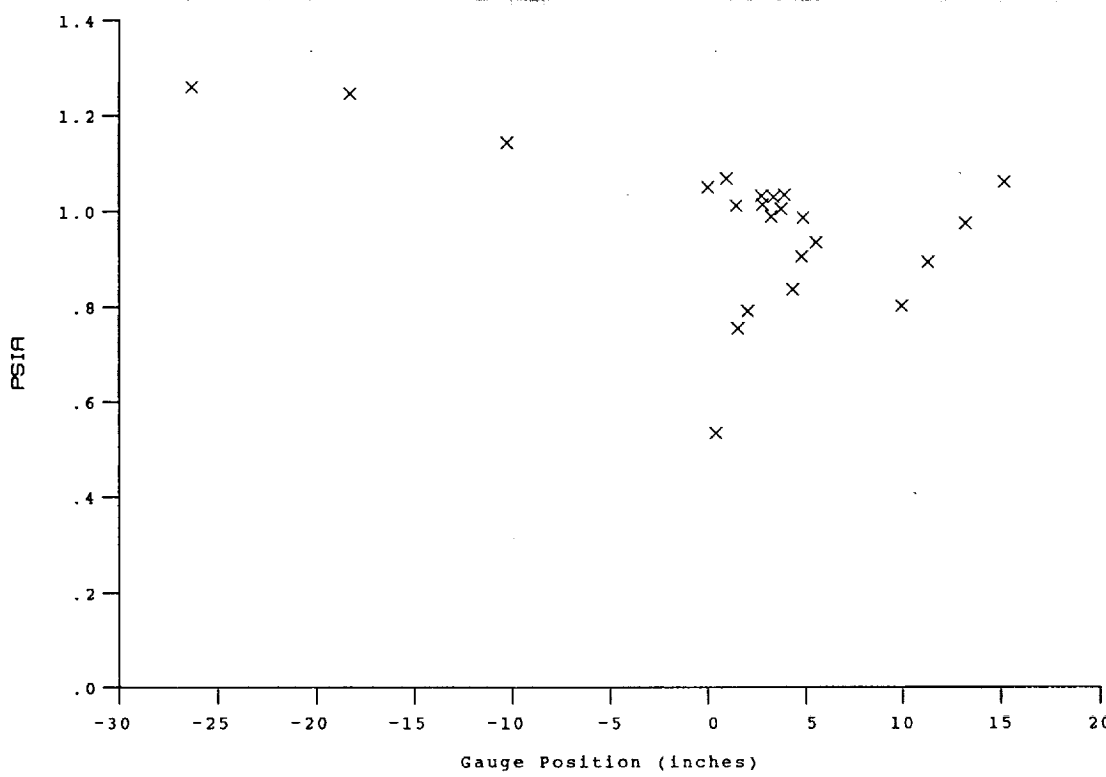
Model Configuration Parameter

Slot Height (inches)	0.080
Lip Thickness (inches)	0.020
Mass Flow Rate per Nozzle (slugs/sec)	4.519E-05
Non-dimensional Blowing Rate, Lambda	0.0944
Nozzle Reservoir Pressure (psia)	15.63
Exit Plane Pressure (psia)	1.052
Coolant Total Temperature (Rankine)	530

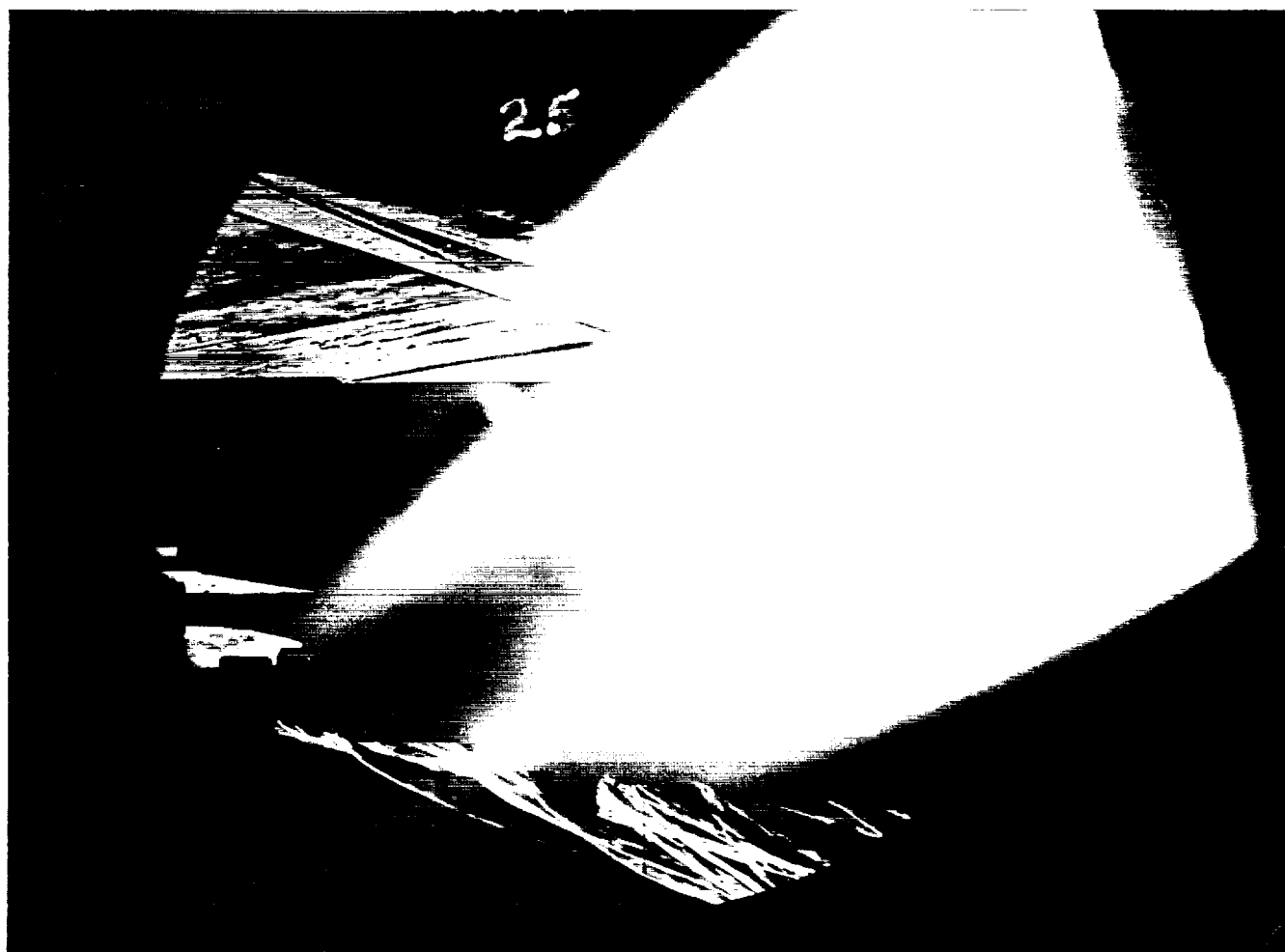
Run 24



HEAT TRANSFER vs Gauge Position
Run 24



PRESSURE vs Gauge Position
Run 24



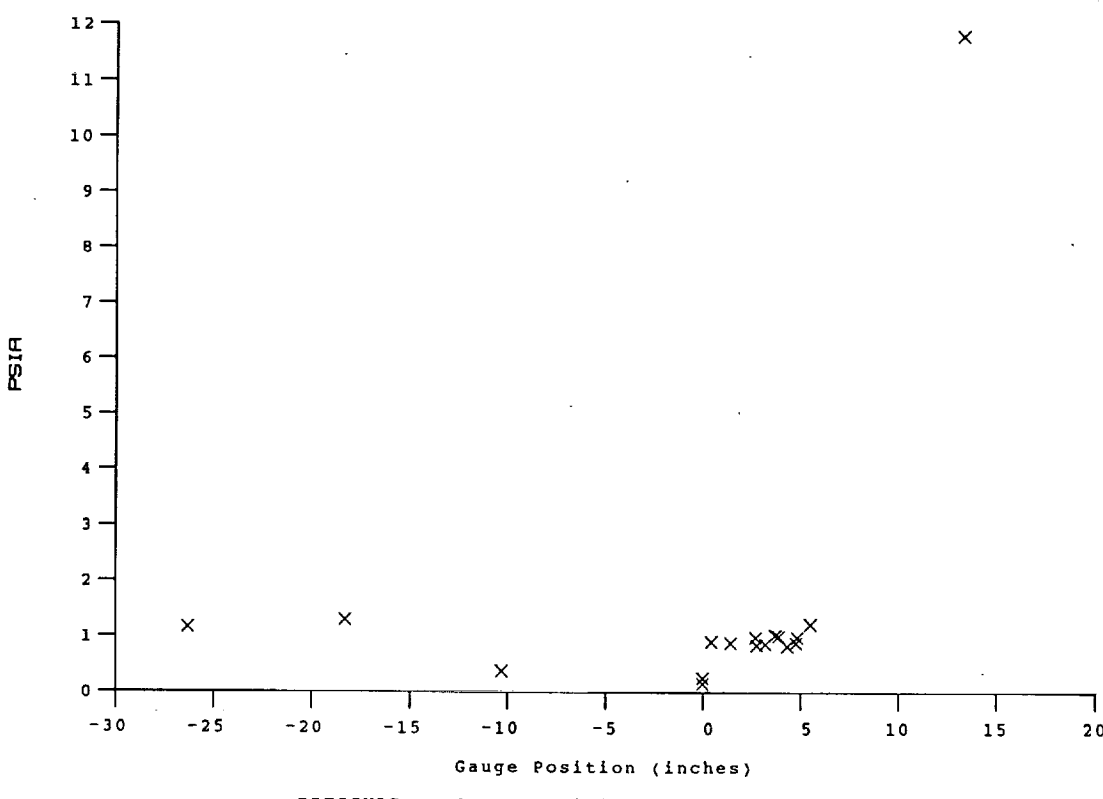
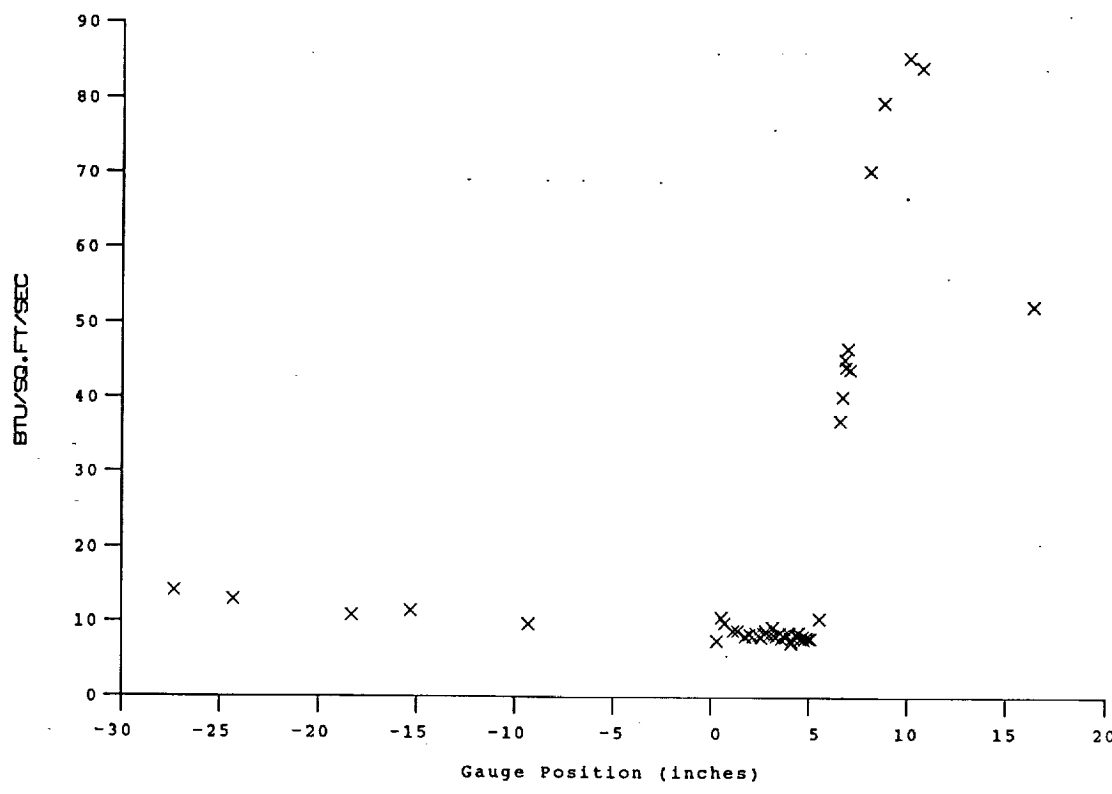
Test Conditions

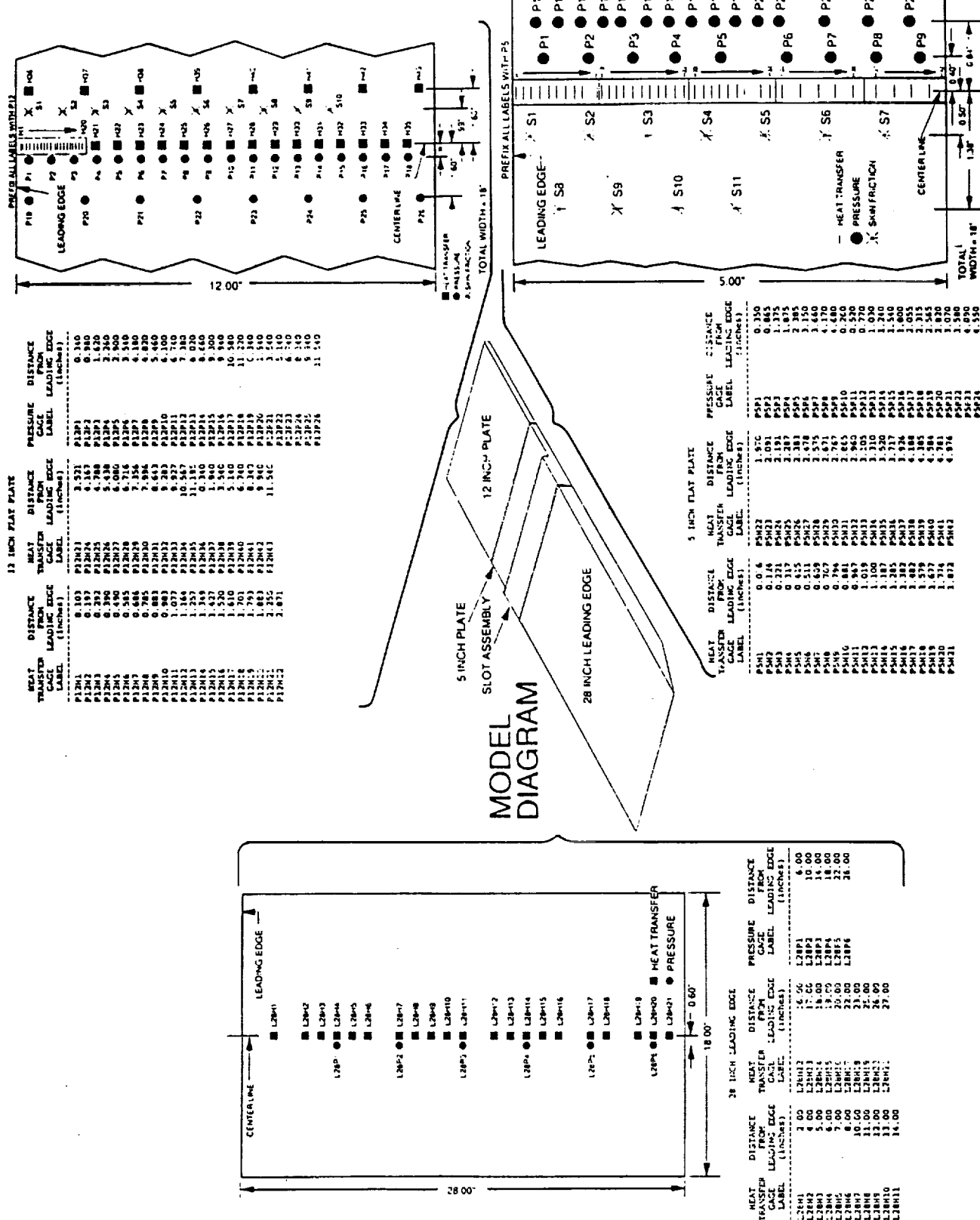
M_i = 2.8095
P_o = 2.3703X10+3 PSIA
H_o = 1.3312X10+7 (Ft/sec)²
T_o = 2.0901X10+3 Degrees R
M = 6.4363
U = 4.8766X10+3 Ft/sec
T = 2.3871X10+2 Degrees R
P = 9.6900X10-1 PSIA
Q = 2.8129X10+1 PSIA
Rho = 3.4066X10-4 Slugs/Ft³
Mu = 1.9628X10-7 Slugs/Ft-sec
Re = 8.4633X10+6 1/ft
P_{o'} = 5.2419X10+1 PSIA

Model Configuration Parameter	Value
Horizontal Shock Generator Angle (degrees)	10.5
X * (inches)	7.940
Y * (inches)	2.942
Slot Height (inches)	0.080
Lip Thickness (inches)	0.020
Lambda	0

* see shock generator diagram at page A-23

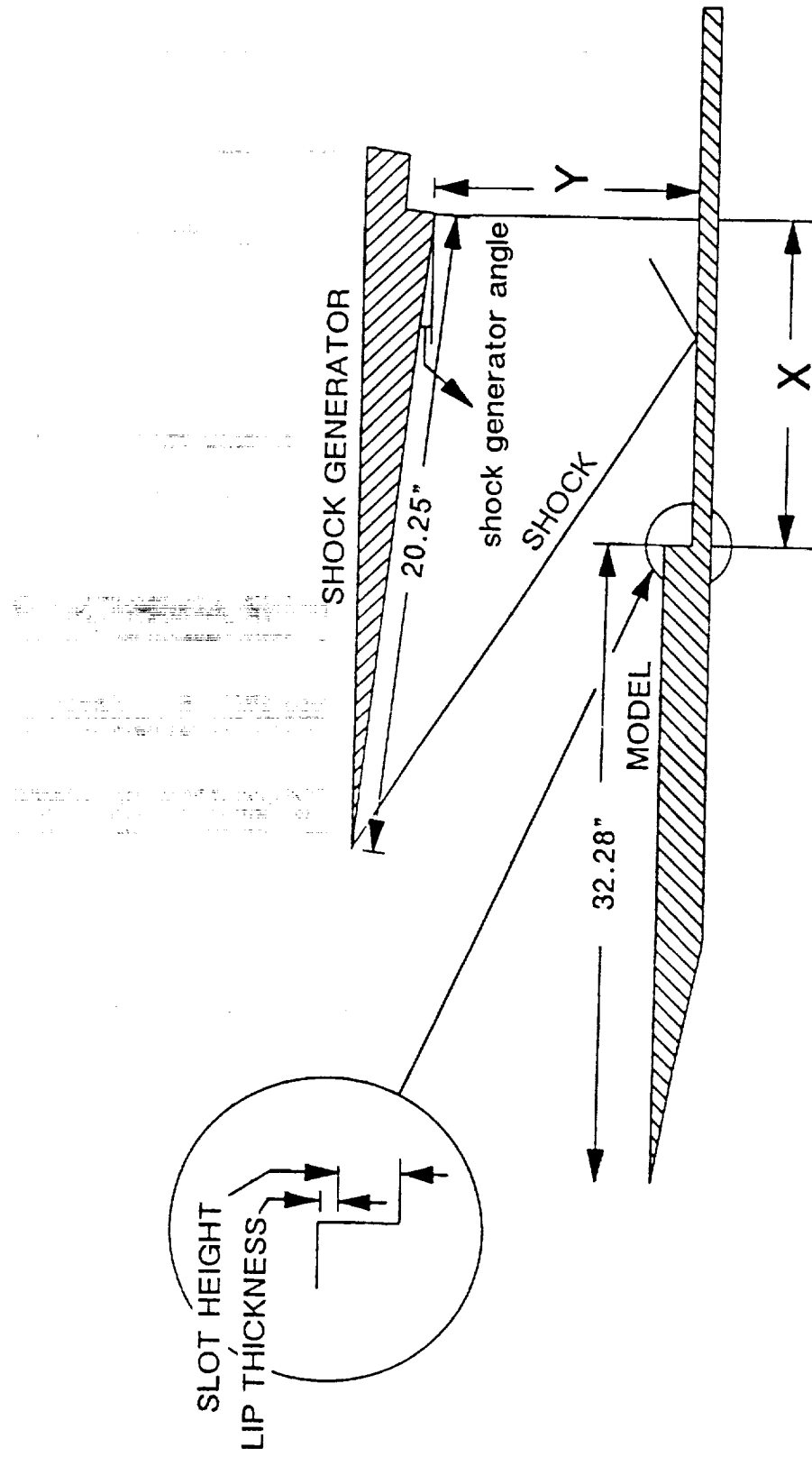
Run 25

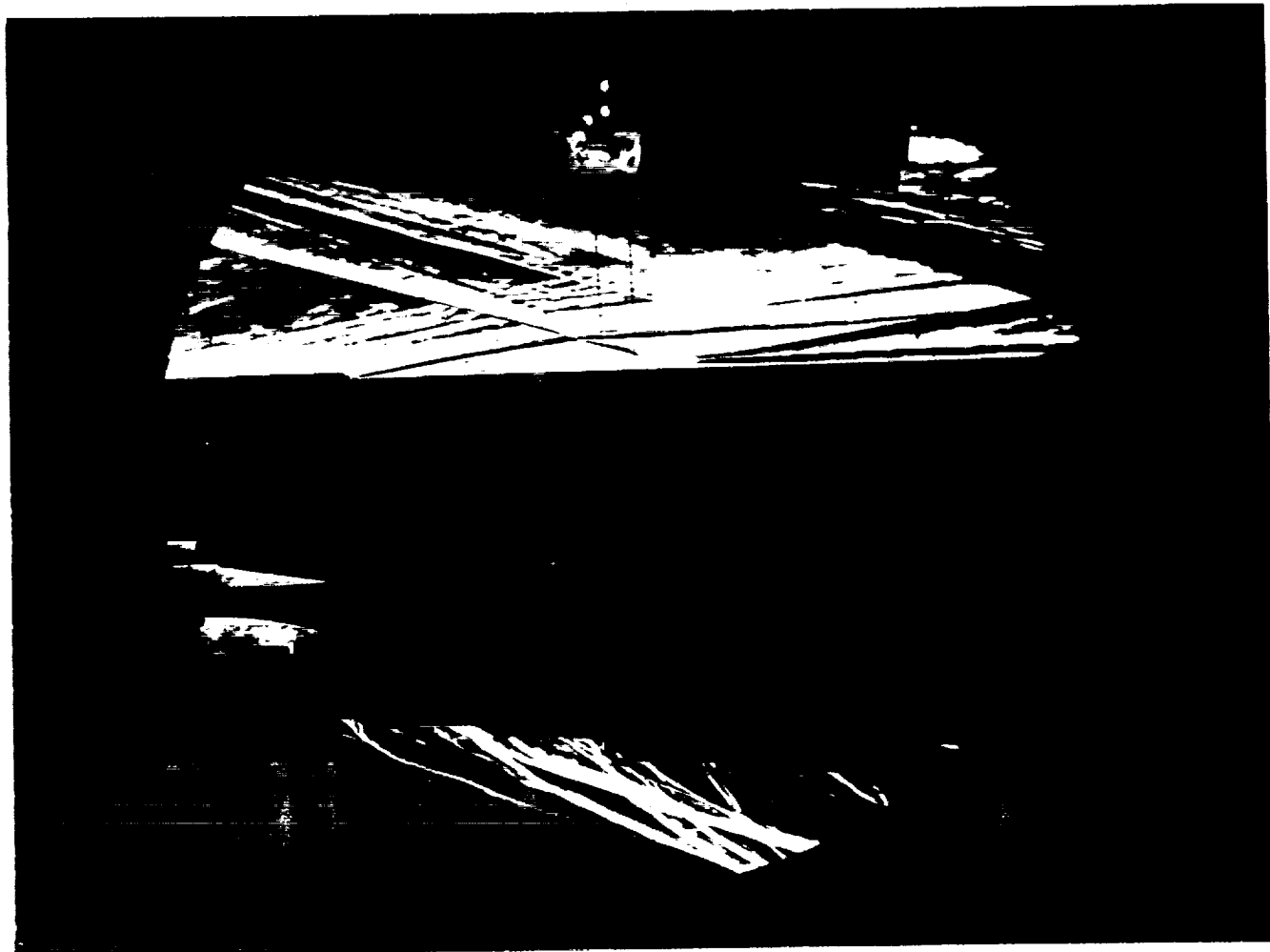




INSTRUMENTATION POSITIONS ON FILM-COOLING/SHOCK-INTERACTION MODEL

SHOCK GENERATOR DIAGRAM





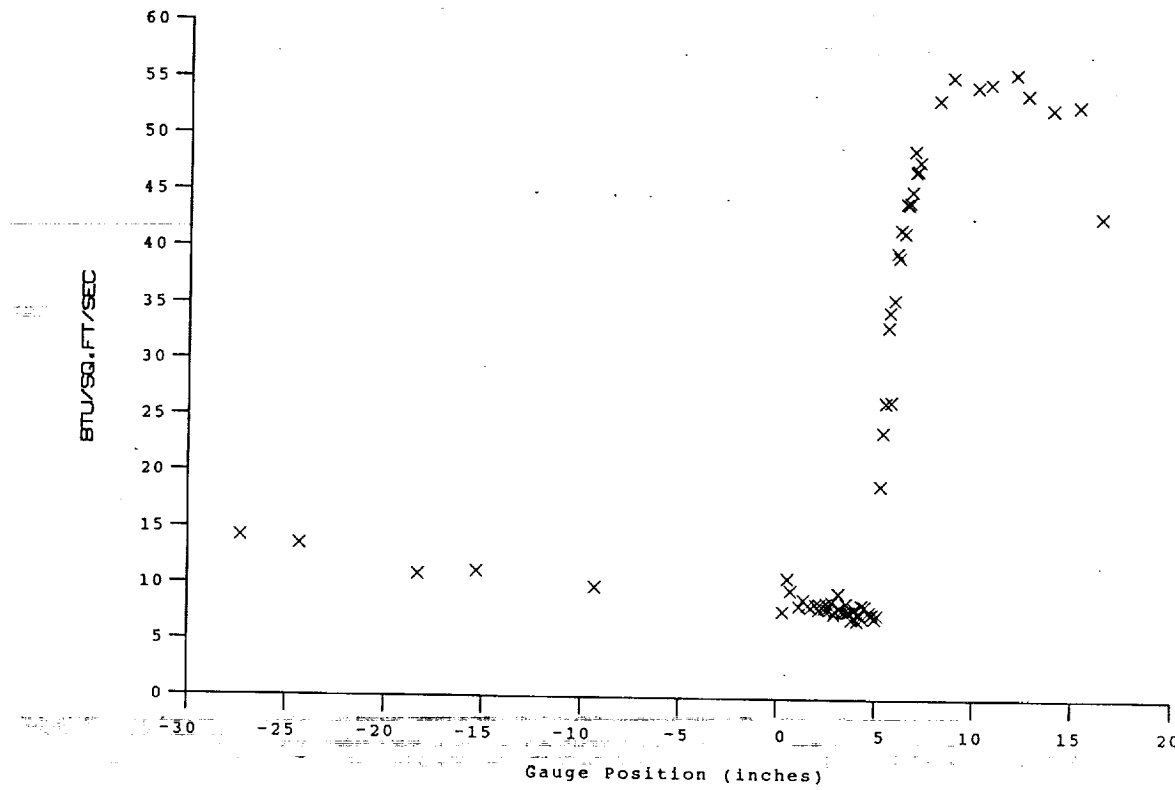
Test Conditions

M_i = 2.8084
P_o = 2.3801X10+3 PSIA
H_o = 1.3261X10+7 (Ft/sec)²
T_o = 2.0826X10+3 Degrees R
M = 6.4371
U = 4.8673X10+3 Ft/sec
T = 2.3775X10+2 Degrees R
P = 9.7345X10-1 PSIA
Q = 2.8265X10+1 PSIA
Rho = 3.4361X10-4 Slugs/Ft³
Mu = 1.9555X10-7 Slugs/Ft-sec
Re = 8.5525X10+6 1/Ft
P_{o'} = 5.2670X10+1 PSIA

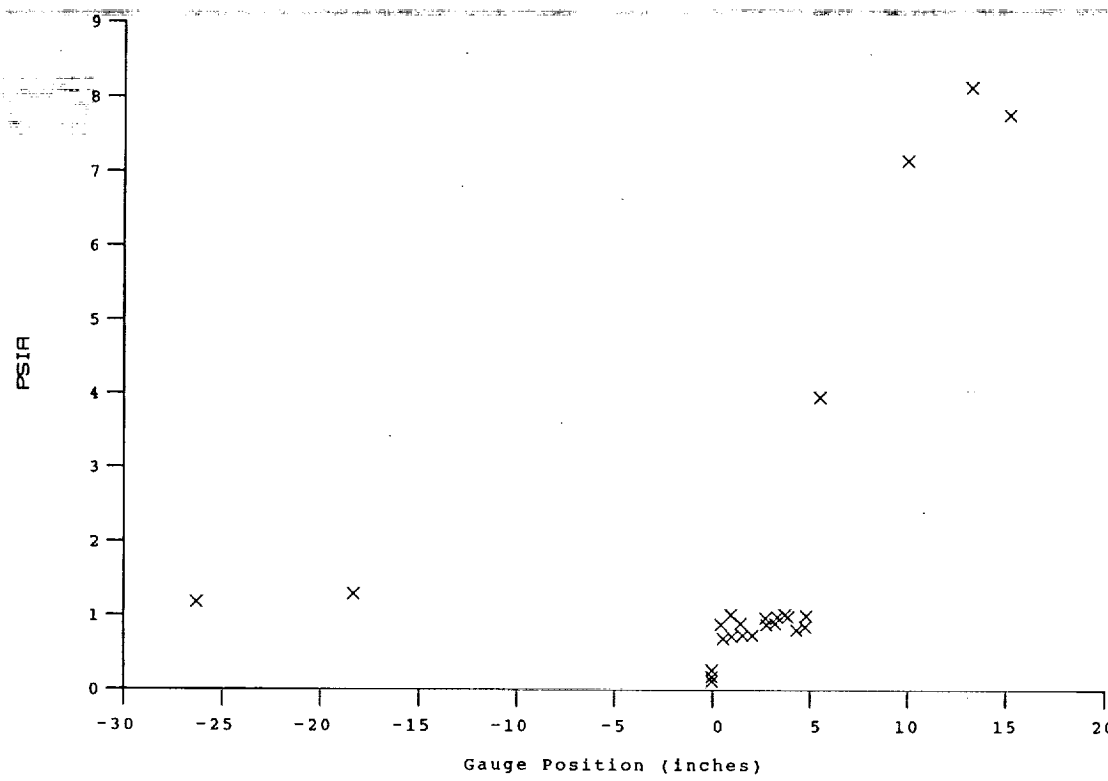
Model Configuration Parameter	Value
Horizontal Shock Generator Angle (degrees)	8.0
X * (inches)	7.745
Y * (inches)	2.609
Slot Height (inches)	0.080
Lip Thickness (inches)	0.020
Lambda	0

* see shock generator diagram at page A-23

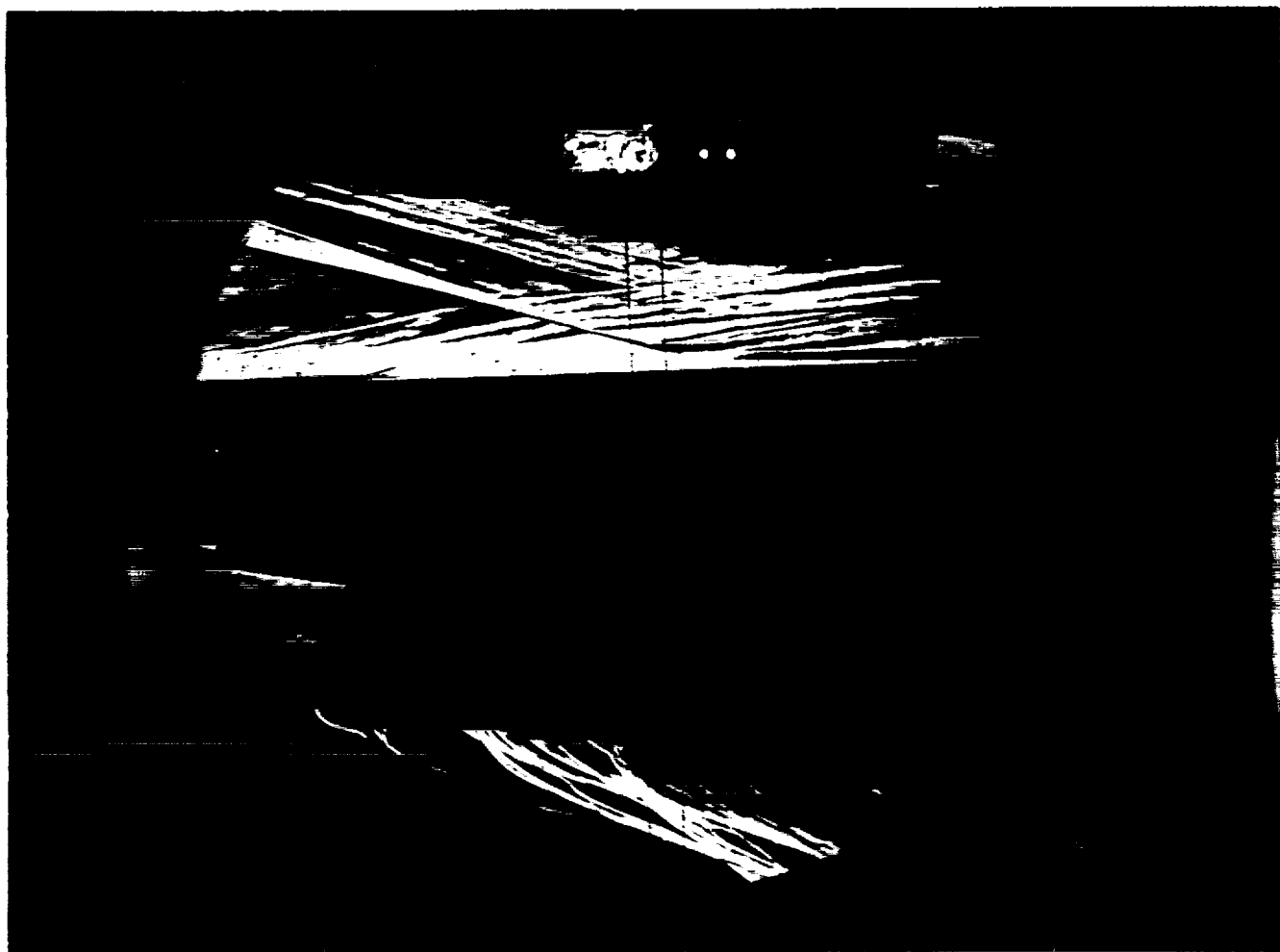
Run 26



HEAT TRANSFER vs Gauge Position
Run 26



PRESSURE vs Gauge Position
Run 26

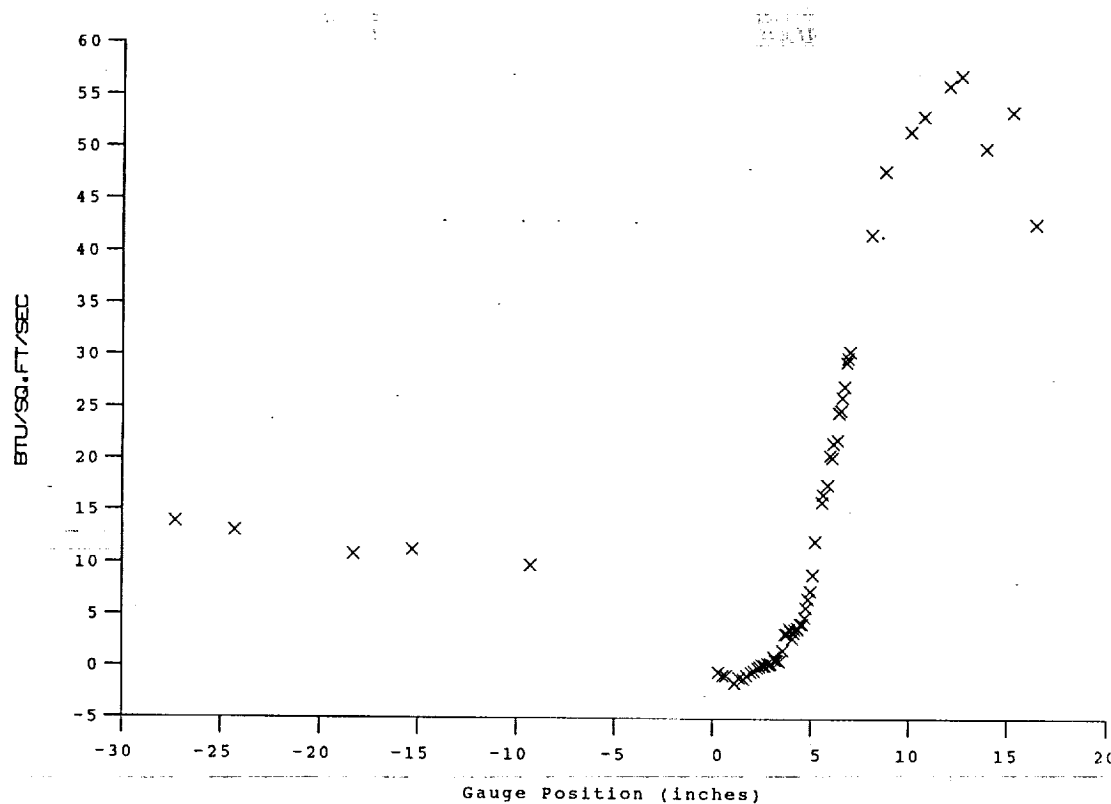


Test Conditions

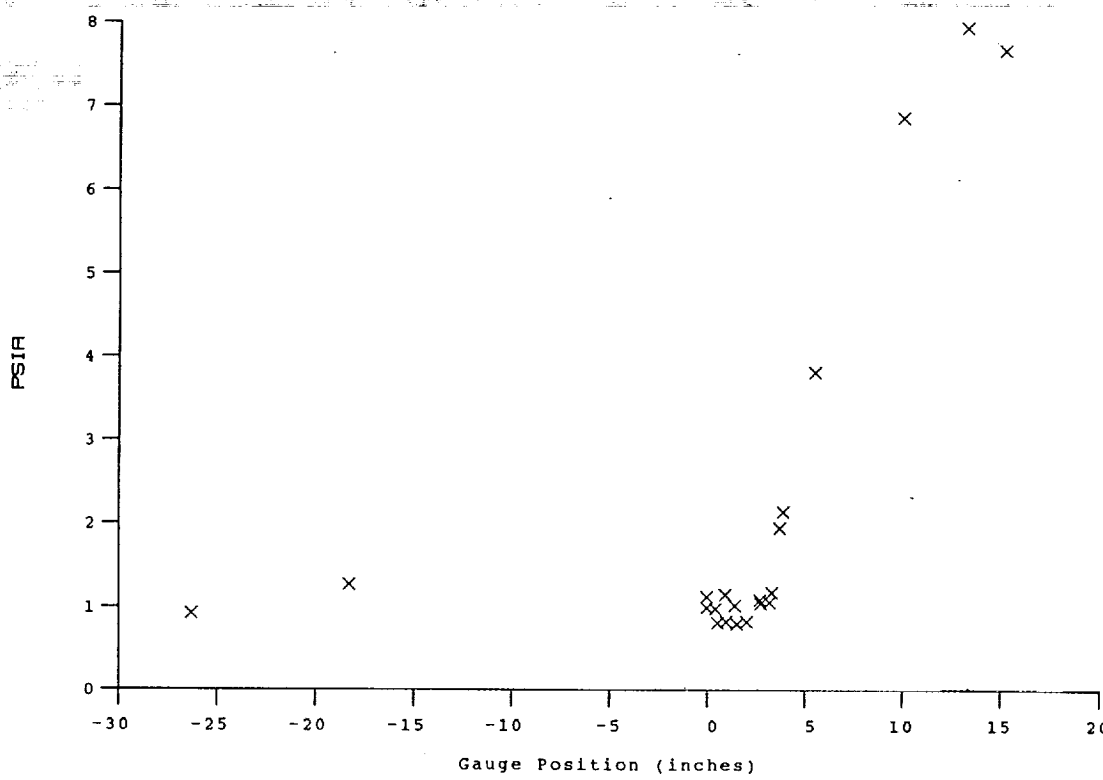
$M_i = 2.7932$
 $P_{o_1} = 2.3230 \times 10^3$ PSIA
 $H_{o_1} = 1.3221 \times 10^{+7}$ (Ft/sec)²
 $T_{o_1} = 2.0777 \times 10^{+3}$ Degrees R
 $M = 6.4372$
 $U = 4.8600 \times 10^{+3}$ Ft/sec
 $T = 2.3702 \times 10^{+2}$ Degrees R
 $P = 9.4943 \times 10^{-1}$ PSIA
 $Q = 2.7569 \times 10^{+1}$ PSIA
 $\rho_{o_1} = 3.3616 \times 10^{-4}$ Slugs/Ft³
 $\mu = 1.9499 \times 10^{-7}$ Slugs/Ft-sec
 $Re = 8.3784 \times 10^{+6}$ 1/Ft
 $P_{o_1}' = 5.1371 \times 10^{+1}$ PSIA

Model Configuration Parameter	Value
Horizontal Shock Generator Angle (degrees)	8.0
X * (inches)	7.745
Y * (inches)	2.609
Slot Height (inches)	0.080
Lip Thickness (inches)	0.020
Mass Flow Rate per Nozzle (slugs/sec)	5.188E-05
Non-dimensional Blowing Rate, Lambda	0.1078
Nozzle Reservoir Pressure (psia)	17.87
Exit Plane Pressure (psia)	1.074
Coolant Total Temperature (Rankine)	530
See Shock Generator Diagram (Page A23)	

Run 27

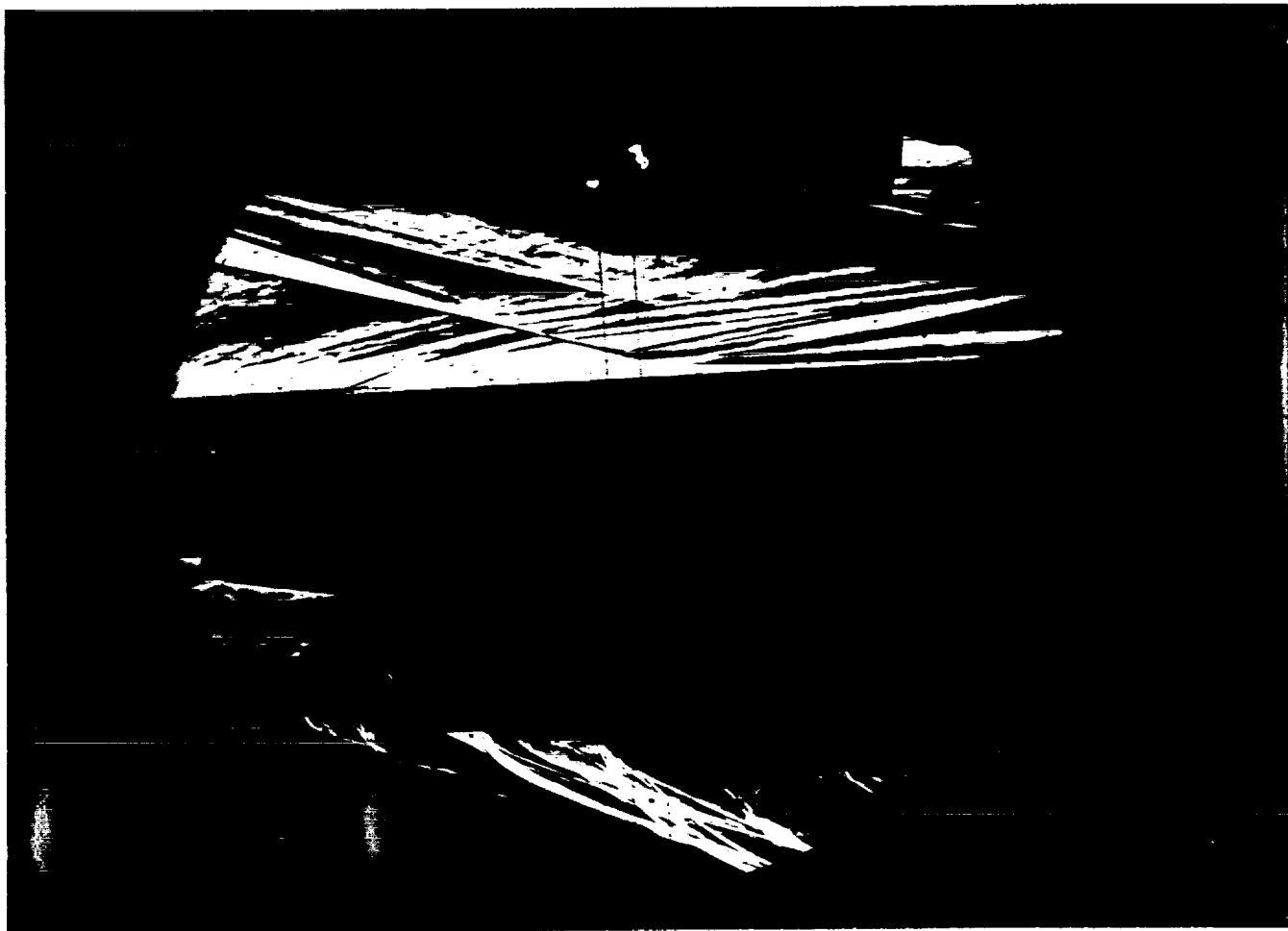


HEAT TRANSFER vs. Gauge Position
Run 27



PRESSURE vs Gauge Position
Run 27

A-27

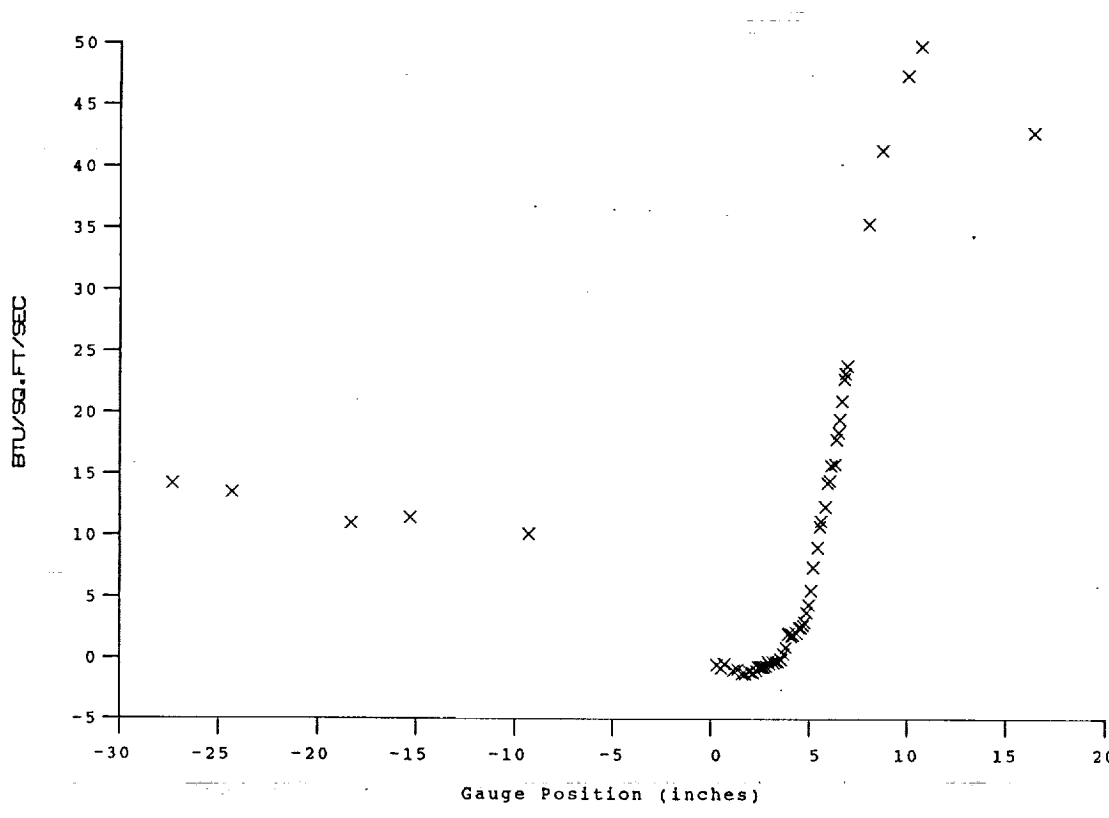


Test Conditions

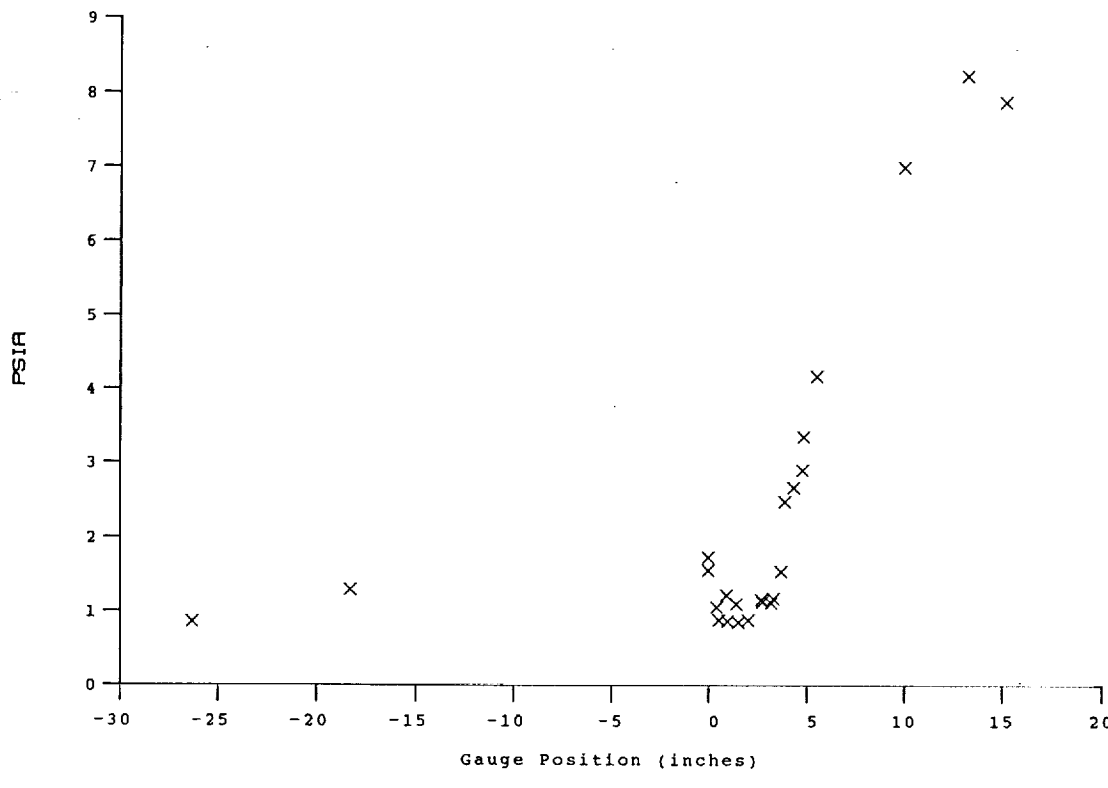
$M_i = 2.7902$
 $P_0 = 2.3857 \times 10^3$ PSIA
 $H_0 = 1.3281 \times 10^{-7}$ (Ft/sec)²
 $T_0 = 2.0866 \times 10^{-3}$ Degrees R
 $M = 6.4414$
 $U = 4.8712 \times 10^{-3}$ Ft/sec
 $T = 2.3781 \times 10^{-2}$ Degrees R
 $P = 9.7142 \times 10^{-1}$ PSIA
 $Q = 2.8244 \times 10^{-1}$ PSIA
 $\rho = 3.4280 \times 10^{-4}$ Slugs/Ft³
 $M_u = 1.9560 \times 10^{-7}$ Slugs/Ft-sec
 $R_e = 8.5374 \times 10^{+6}$ 1/Ft
 $P_{0'} = 5.2632 \times 10^{-1}$ PSIA

Model Configuration Parameter	Value
Horizontal Shock Generator Angle (degrees)	8.0
X * (inches)	7.745
Y * (inches)	2.609
Slot Height (inches)	0.080
Lip Thickness (inches)	0.020
Mass Flow Rate per Nozzle (slugs/sec)	1.007E-04
Non-dimensional Blowing Rate, Lambda	0.2028
Nozzle Reservoir Pressure (psia)	29.57
Exit Plane Pressure (psia)	1.658
Coolant Total Temperature (Rankine)	530

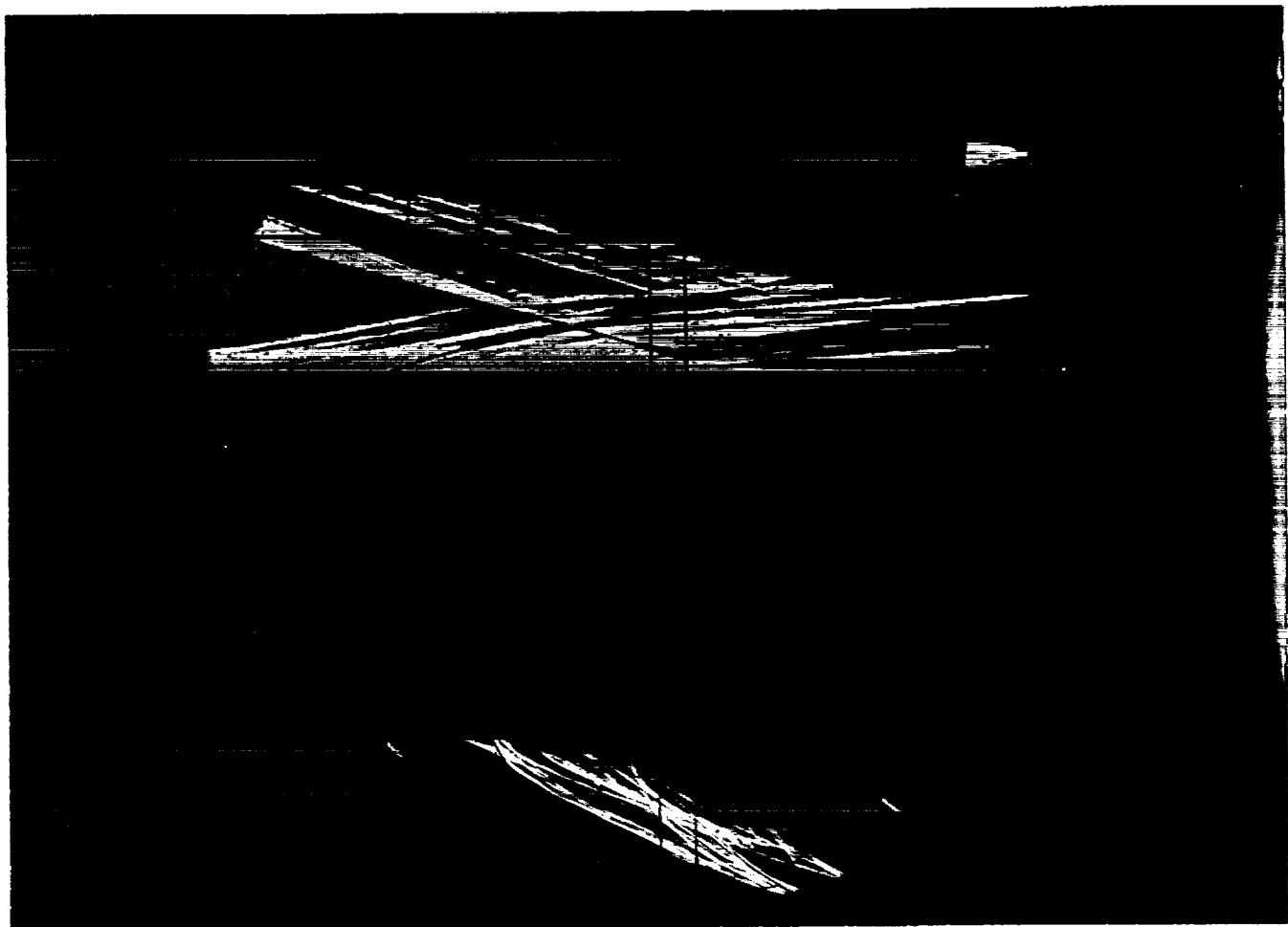
* See Shock Generator Diagram (Page A23)



HEAT TRANSFER vs Gauge Position
Run 28



PRESSURE vs Gauge Position
Run 28



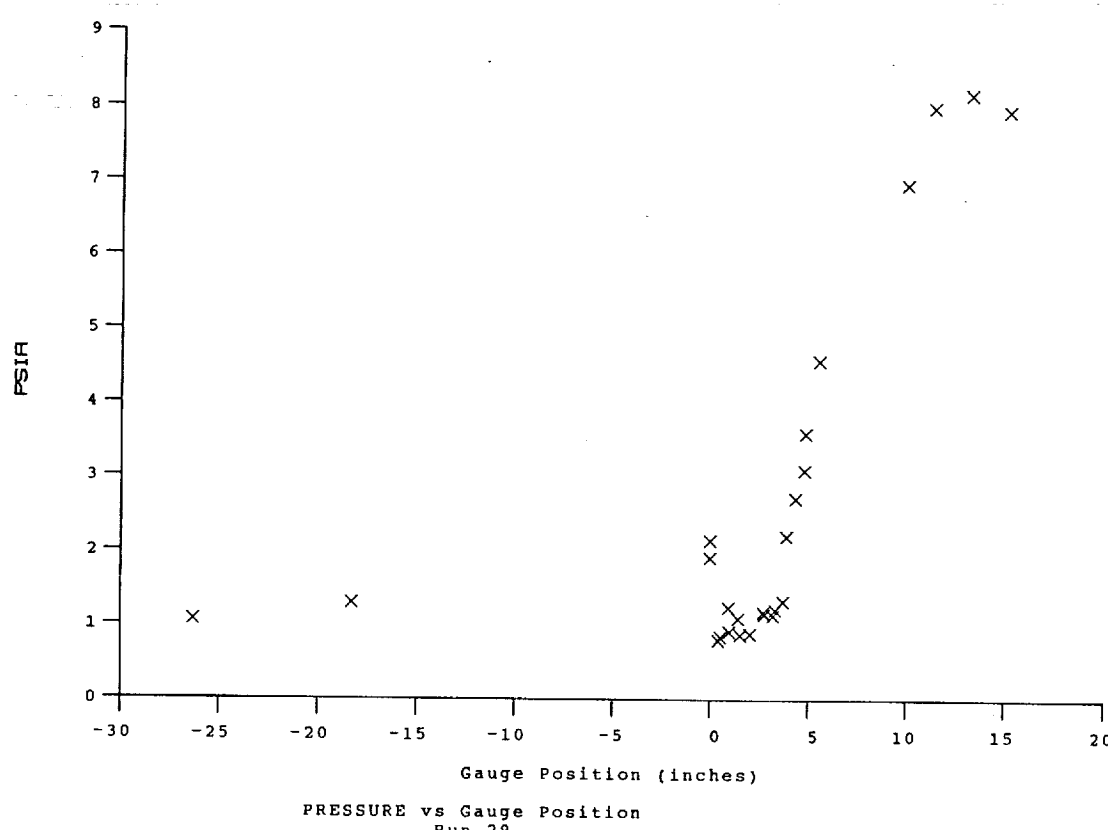
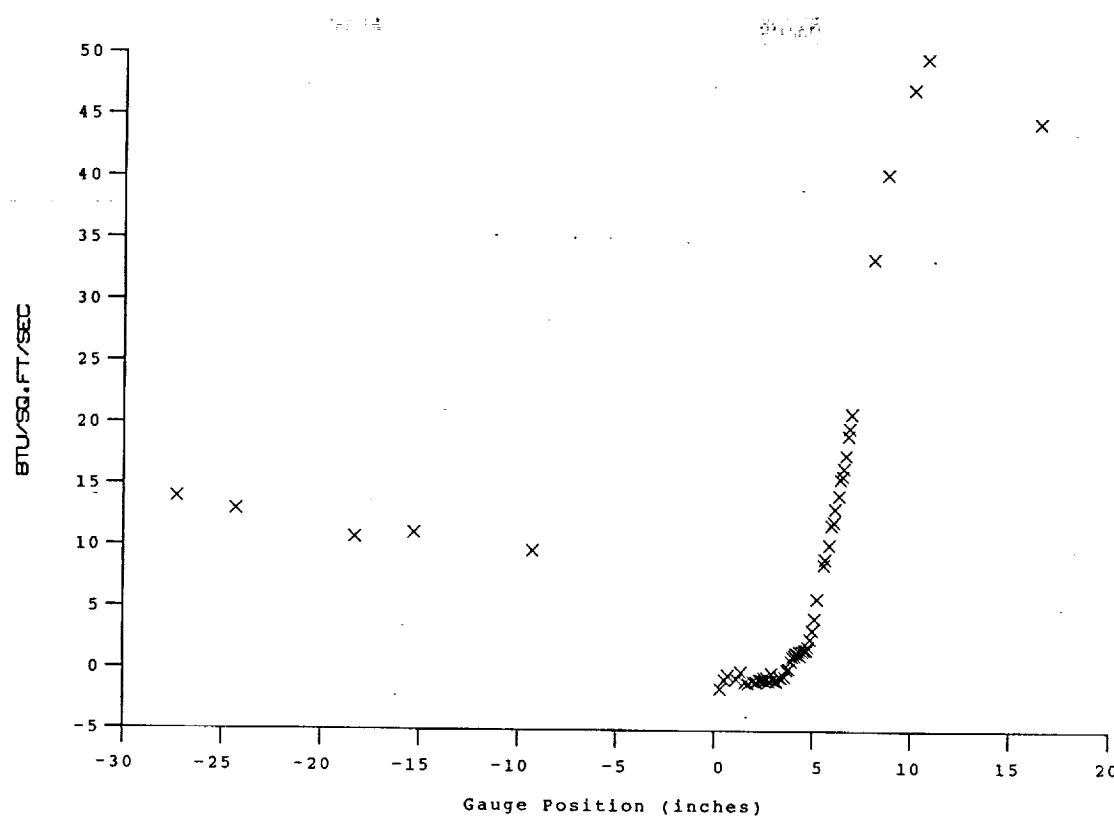
Test Conditions

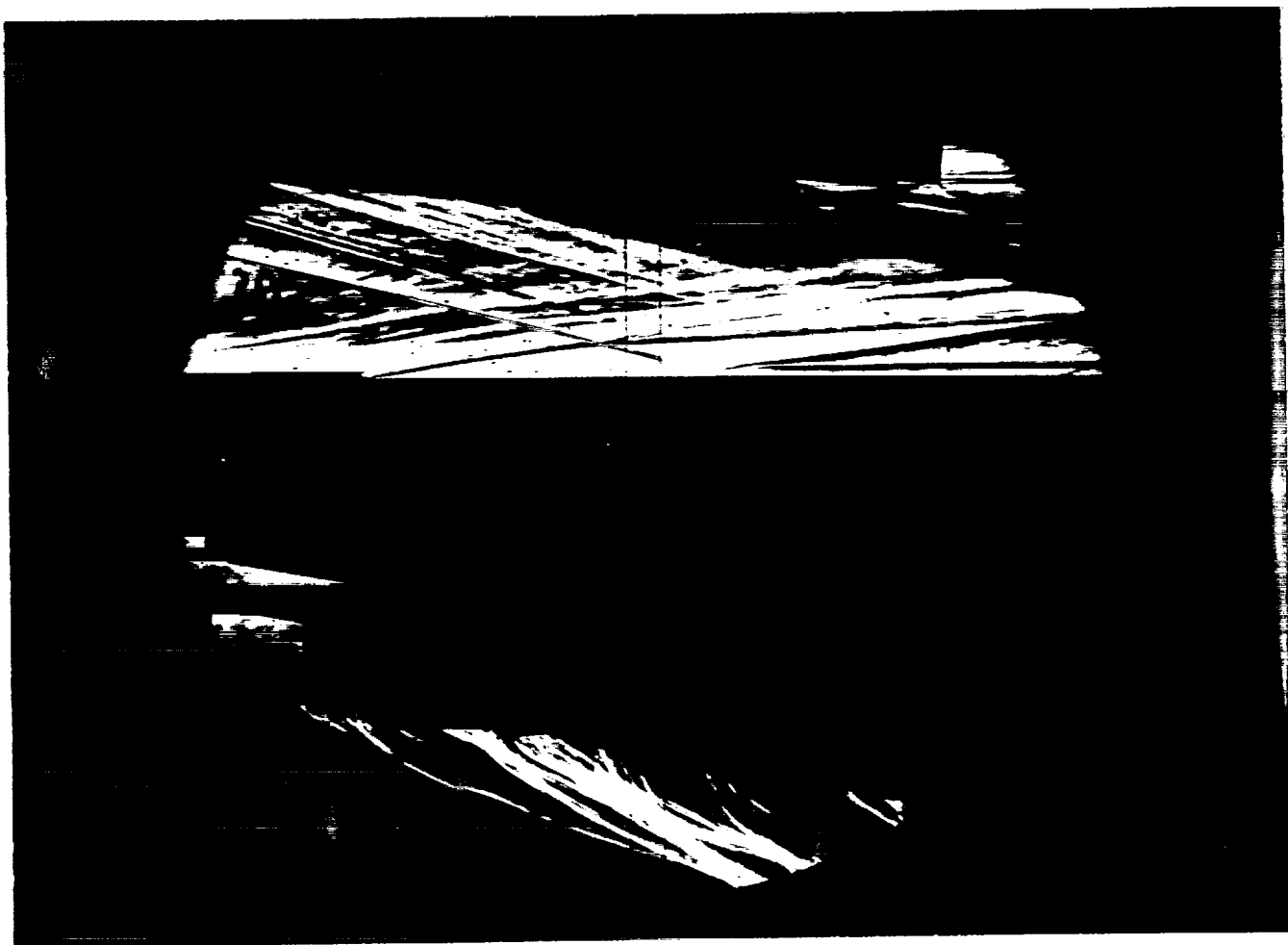
$M_i = 2.8164$
 $P_0 = 2.4439 \times 10^3$ PSIA
 $H_0 = 1.3561 \times 10^7$ (Ft/sec)²
 $T_0 = 2.1264 \times 10^3$ Degrees R
 $M = 6.4387$
 $U = 4.9222 \times 10^3$ Ft/sec
 $T = 2.4302 \times 10^2$ Degrees R
 $P = 9.9347 \times 10^{-1}$ PSIA
 $Q = 2.8861 \times 10^1$ PSIA
 $\rho = 3.4307 \times 10^{-4}$ Slugs/Ft³
 $\mu = 1.9956 \times 10^{-7}$ Slugs/Ft-sec
 $Re = 8.4619 \times 10^6$ 1/ft
 $P_{0'} = 5.3797 \times 10^1$ PSIA

Model Configuration Parameter Value

Horizontal Shock Generator Angle (degrees)	8.0
X * (inches)	7.745
Y * (inches)	2.609
Slot Height (inches)	0.080
Lip Thickness (inches)	0.020
Mass Flow Rate per Nozzle (slugs/sec)	1.118E-04
Non-dimensional Blowing Rate, Lambda	0.2248
Nozzle Reservoir Pressure (psia)	36.56
Exit Plane Pressure (psia)	2.036
Coolant Total Temperature (Rankine)	530
* See Shock Generator Diagram (Page A23)	

Run 29



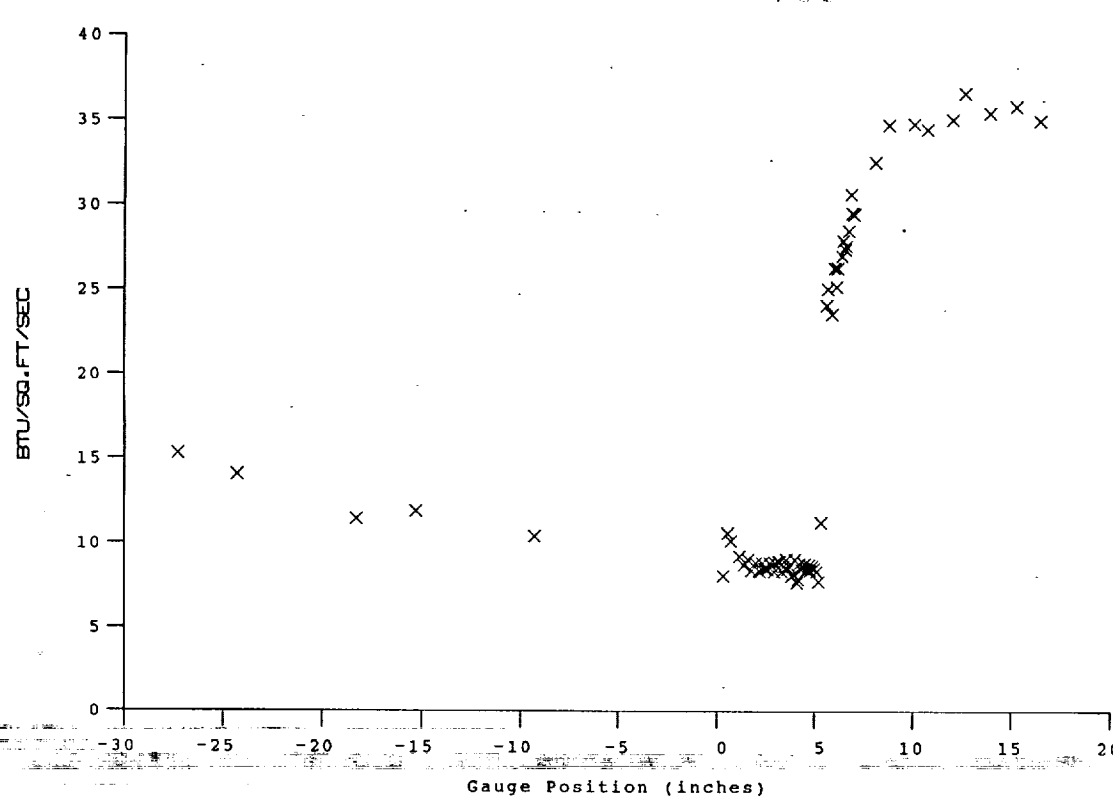
**Test Conditions**

M_i = 2.8122
P_o = 2.3766X10+3 PSIA
H_o = 1.3287X10+7 (Ft/sec)⁻²
T_o = 2.0861X10+3 Degrees R
M = 6.4360
U = 4.8719X10+3 Ft/sec
T = 2.3827X10+2 Degrees R
P = 9.7244X10-1 PSIA
Q = 2.8226X10+1 PSIA
Rho = 3.4250X10-4 Slugs/Ft³
Mu = 1.9595X10-7 Slugs/Ft-sec
Re = 8.5155X10+6 1/Ft
P_{o'} = 5.2599X10+1 PSIA

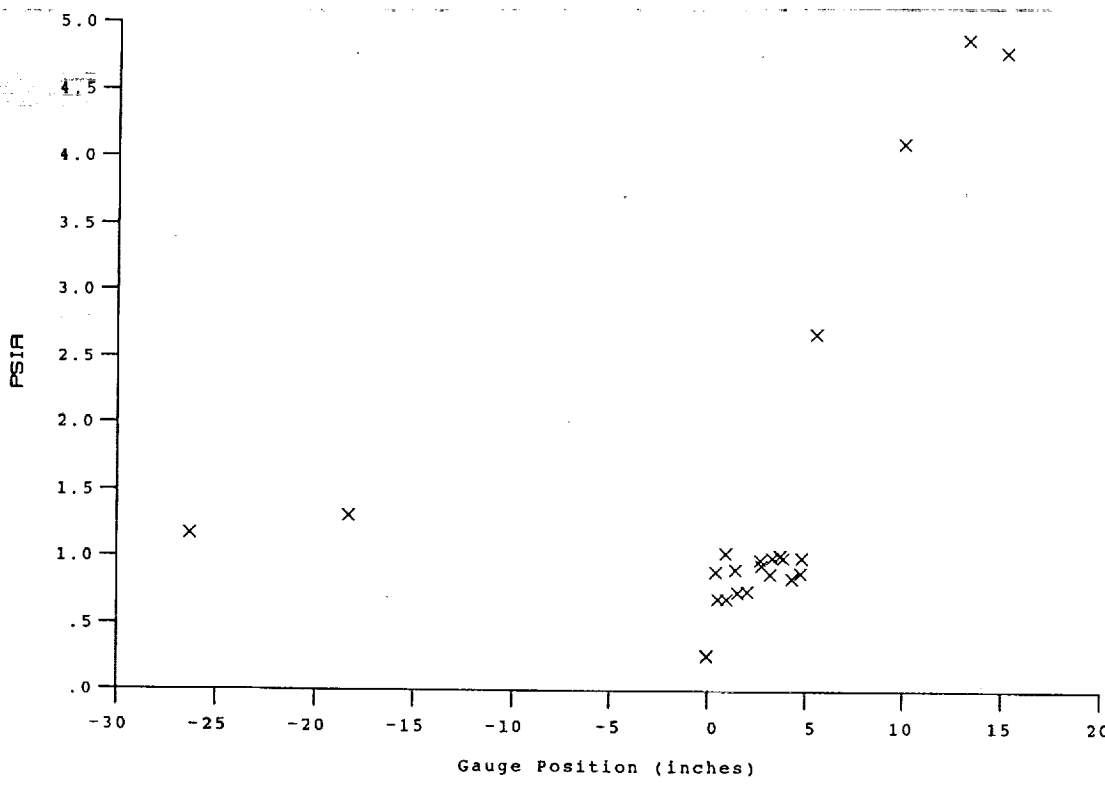
Model Configuration Parameter	Value
Horizontal Shock Generator Angle (degrees)	5.5
X * (inches)	7.349
Y * (inches)	2.840
Slot Height (inches)	0.080
Lip Thickness (inches)	0.020
Lambda	0

* see shock generator diagram at page A-23

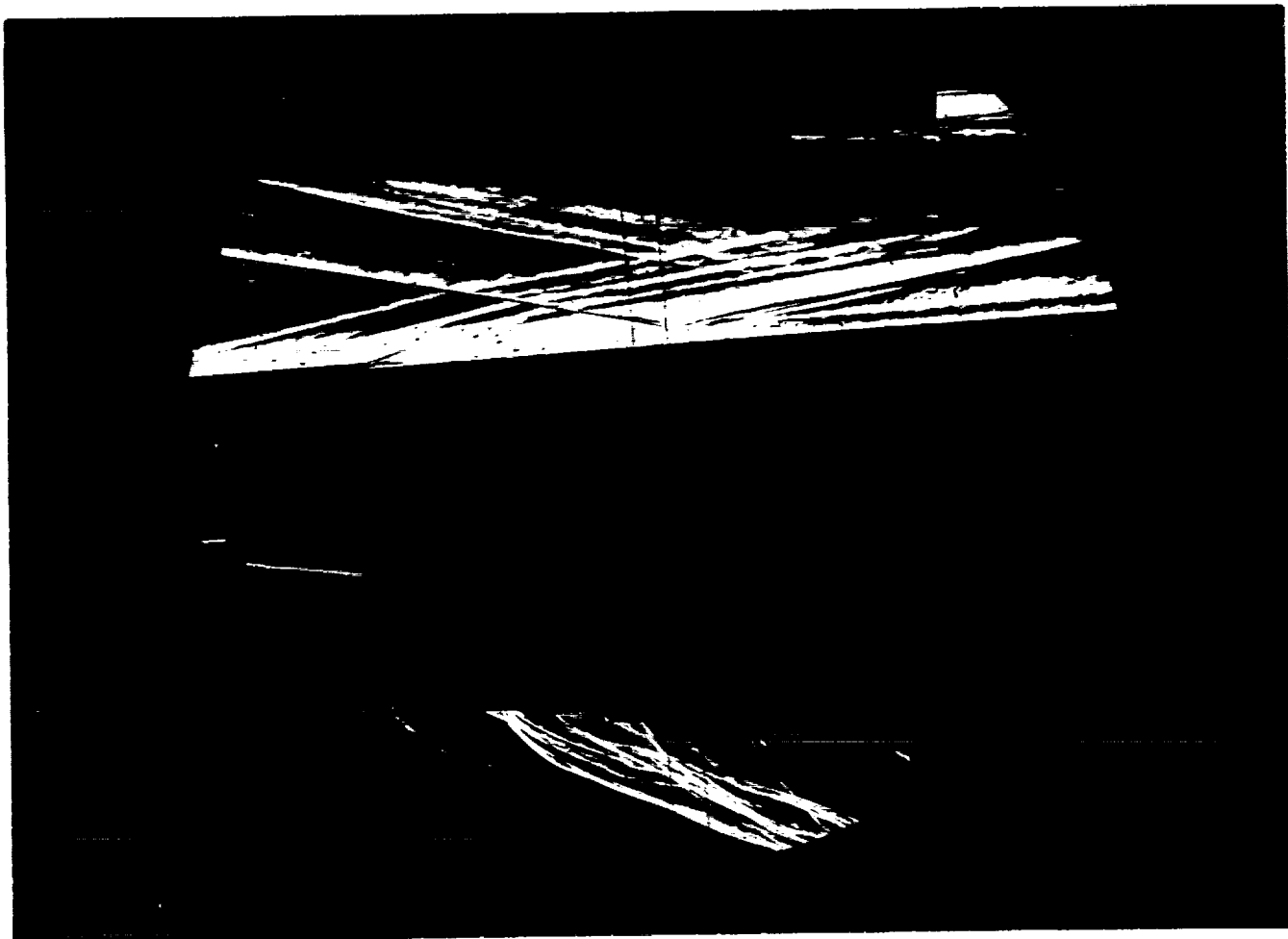
Run 30



HEAT TRANSFER vs Gauge Position
Run 30



PRESSURE vs Gauge Position
Run 30

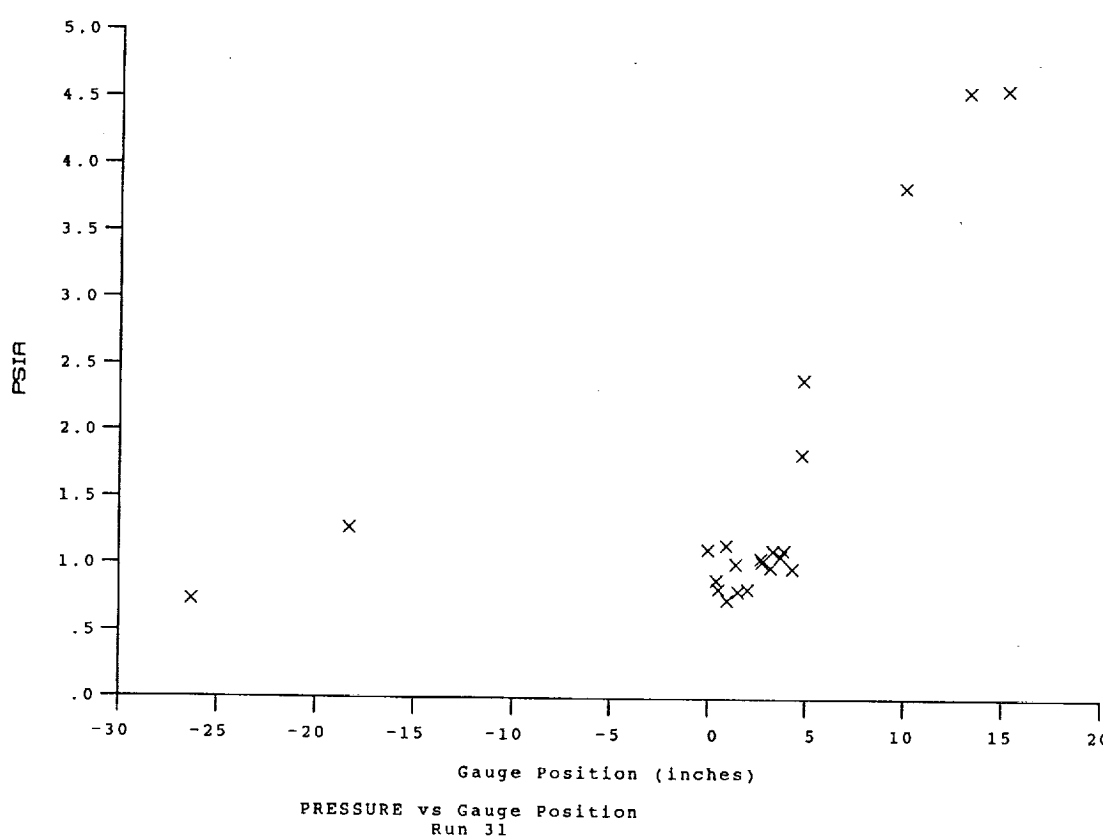
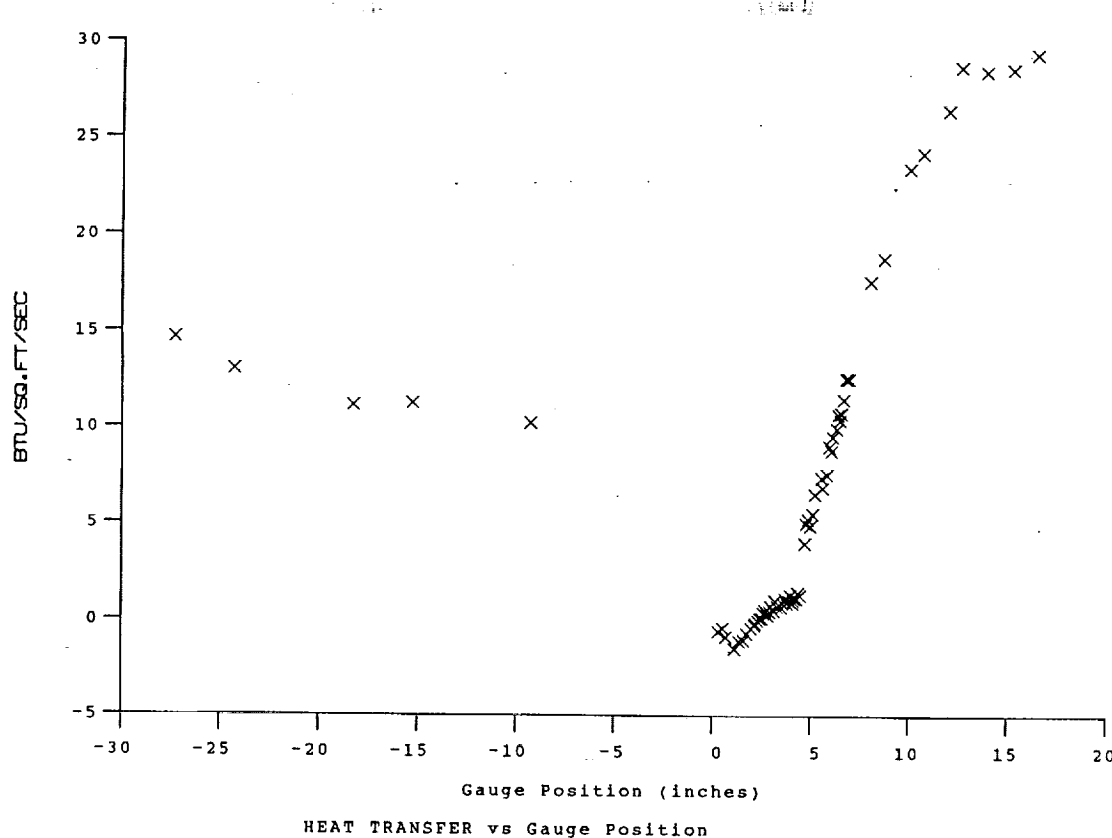
**Test Conditions**

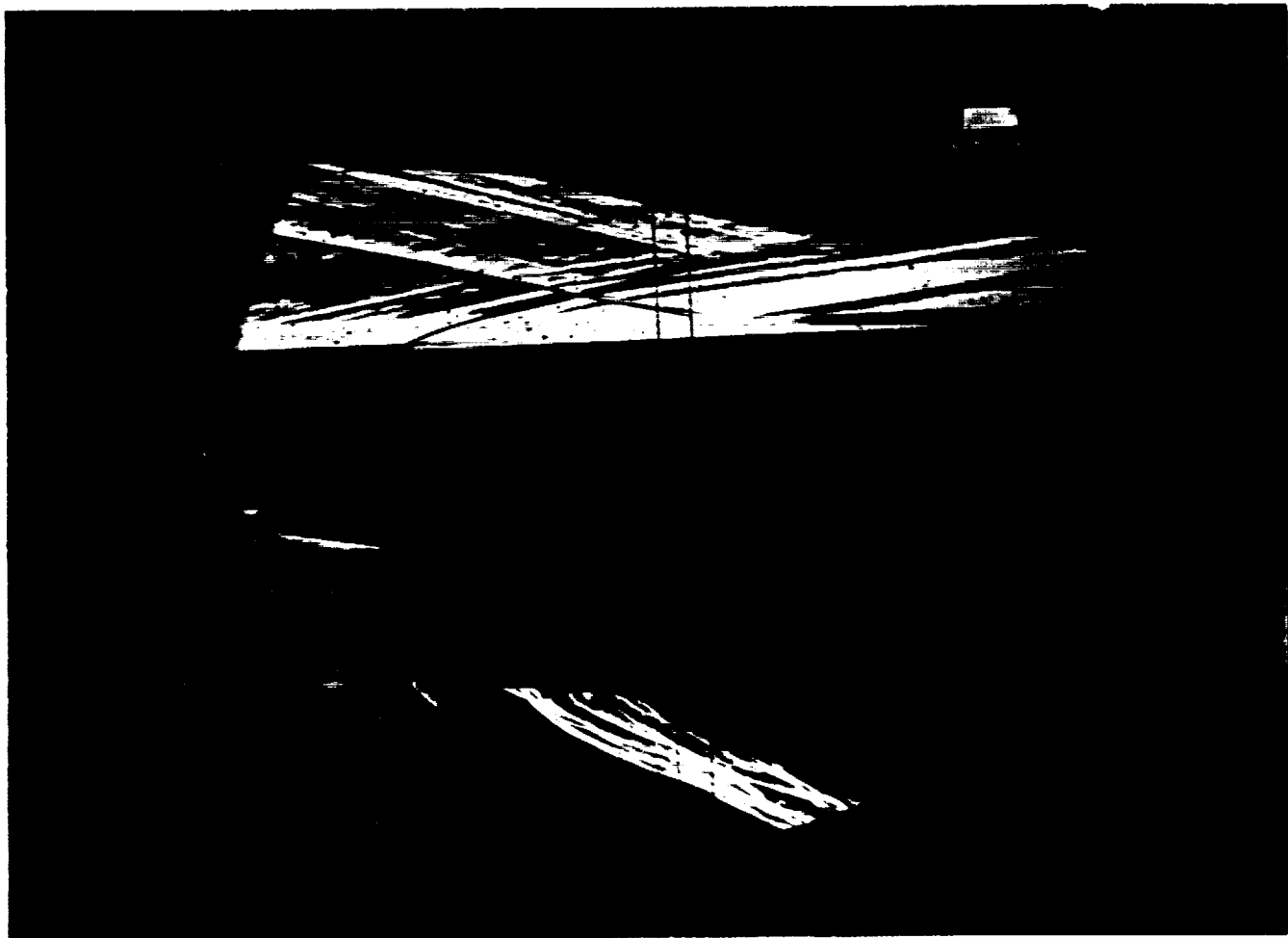
M_i = 2.7891
P_o = 2.2975X10+3 PSIA
H_o = 1.3199X10+7 (Ft/sec)²
T_o = 2.0746X10+3 Degrees R
M = 6.4367
U = 4.8558X10+3 Ft/sec
T = 2.3665X10+2 Degrees R
P = 9.3937X10-1 PSIA
Q = 2.7272X10+1 PSIA
Rho = 3.3311X10-4 Slugs/Ft³
Mu = 1.9471X10-7 Slugs/Ft-sec
Re = 8.3072X10+6 1/Ft
P_{o'} = 5.0816X10+1 PSIA

Model Configuration Parameter	Value
Horizontal Shock Generator Angle (degrees)	5.5
X * (inches)	7.349
Y * (inches)	2.840
Slot Height (inches)	0.080
Lip Thickness (inches)	0.020
Mass Flow Rate per Nozzle (slugs/sec)	5.065E-05
Non-dimensional Blowing Rate, Lambda	0.1052
Nozzle Reservoir Pressure (psia)	17.96
Exit Plane Pressure (psia)	1.125
Coolant Total Temperature (Rankine)	530

* See Shock Generator Diagram (Page A23)

Run 31



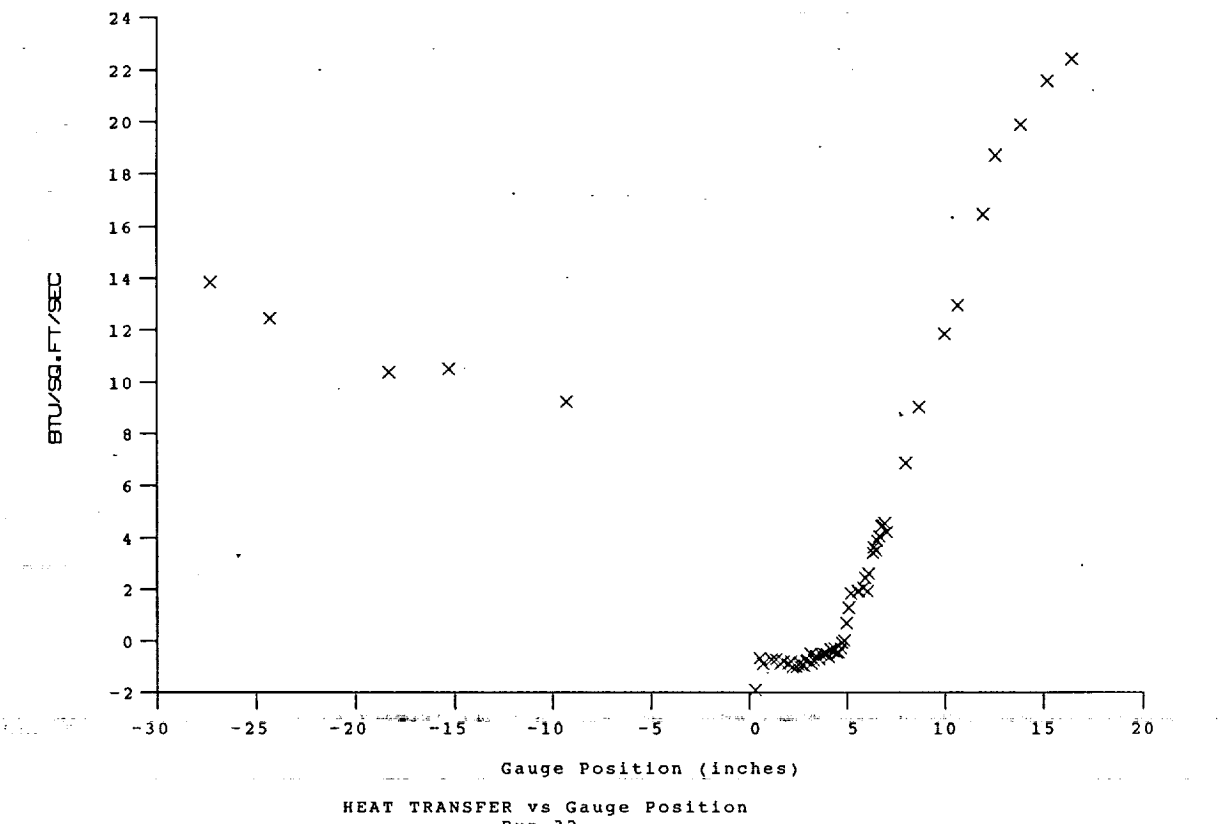


Test Conditions

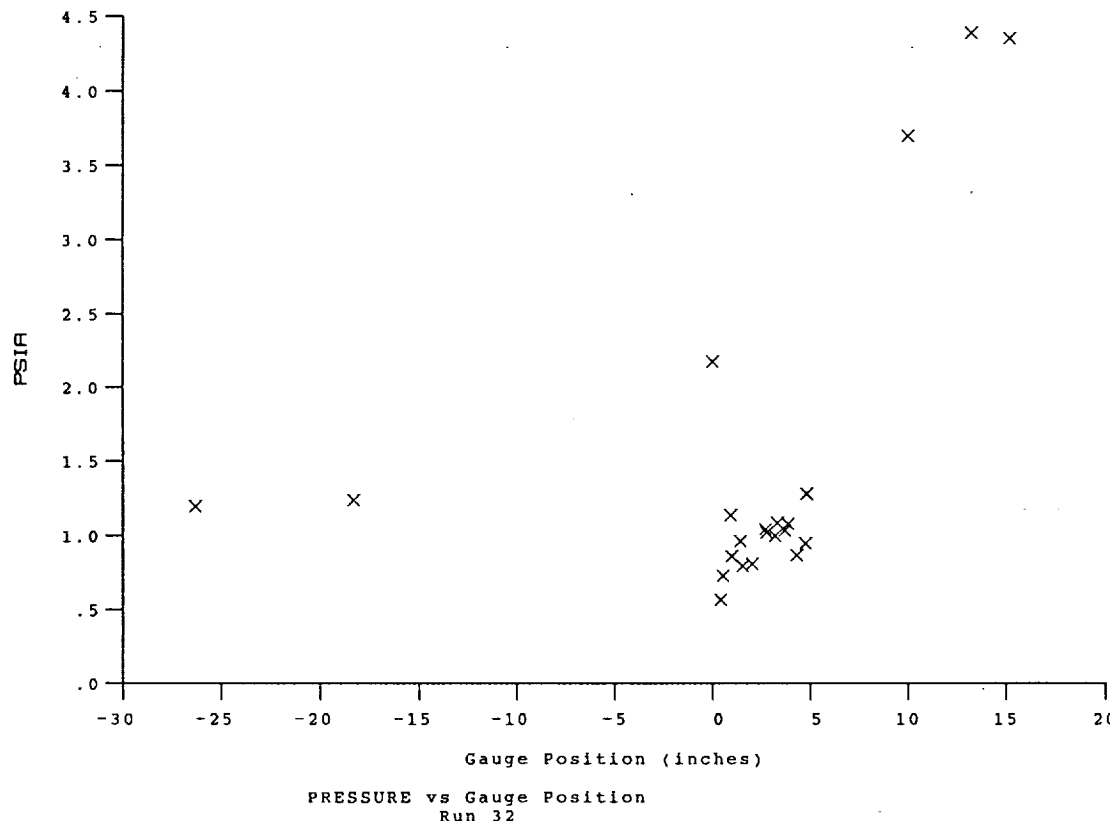
$M_i = 2.7553$
 $P_o = 2.2245 \times 10^3$ PSIA
 $H_o = 1.3039 \times 10^{-7}$ (Ft/sec)²
 $T_o = 2.0531 \times 10^{-3}$ Degrees R
 $M = 6.4398$
 $U = 4.8266 \times 10^3$ Ft/sec
 $T = 2.3358 \times 10^{-2}$ Degrees R
 $P = 9.0800 \times 10^{-1}$ PSIA
 $Q = 2.6387 \times 10^{-1}$ PSIA
 $\rho_o = 3.2622 \times 10^{-4}$ Slugs/Ft³
 $\mu_o = 1.9236 \times 10^{-7}$ Slugs/Ft-sec
 $Re = 8.1851 \times 10^6$ 1/Ft
 $P_o' = 4.9160 \times 10^{-1}$ PSIA

Model Configuration Parameter	Value
Horizontal Shock Generator Angle (degrees)	5.5
X * (inches)	7.349
Y * (inches)	2.840
Slot Height (inches)	0.080
Lip Thickness (inches)	0.020
Mass Flow Rate per Nozzle (slugs/sec)	1.213E-04
Non-dimensional Blowing Rate, Lambda	0.2616
Nozzle Reservoir Pressure (psia)	36.86
Exit Plane Pressure (psia)	2.184
Coolant Total Temperature (Rankine)	530
* See Shock Generator Diagram (Page A23)	

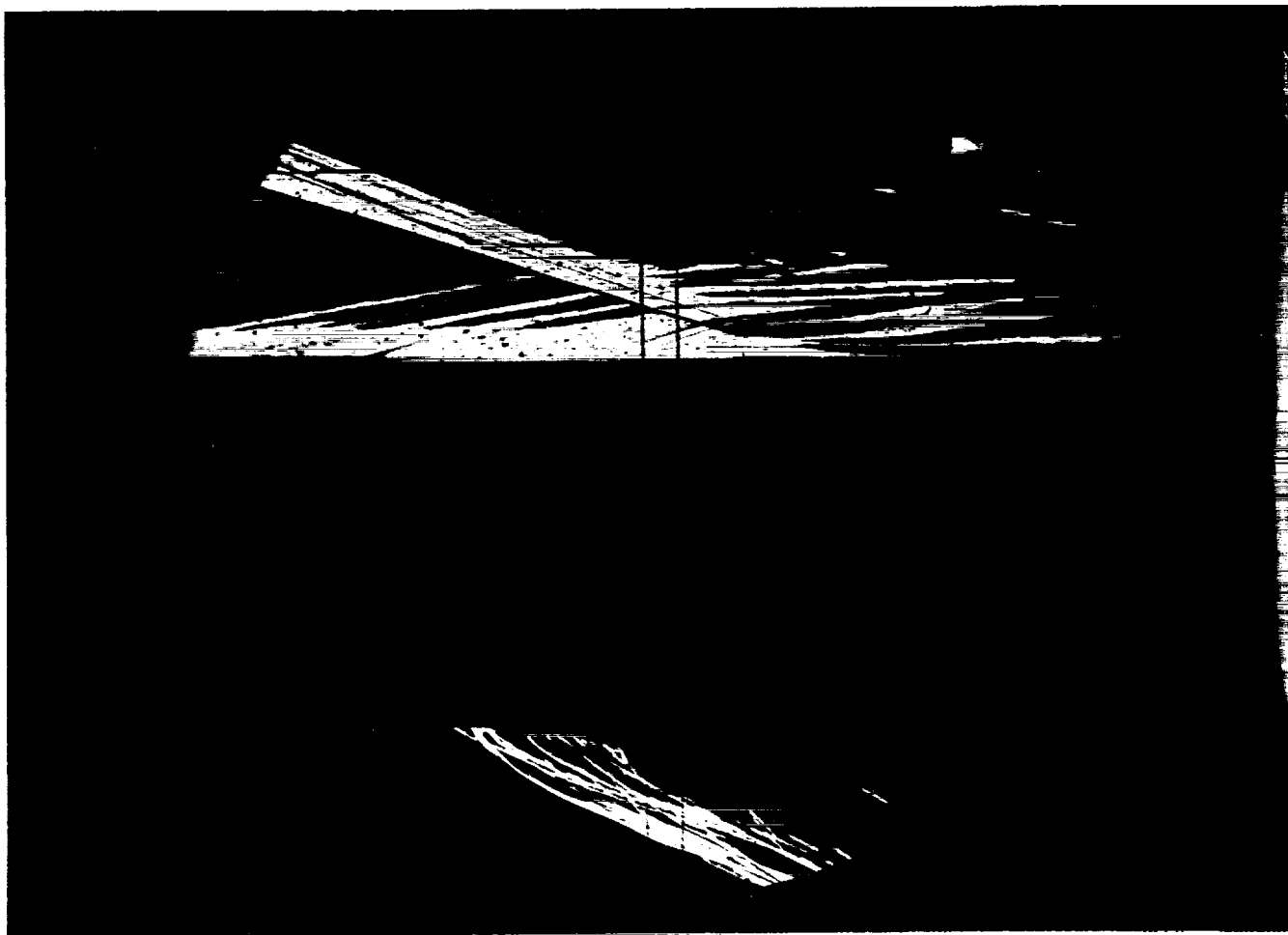
Run 32



HEAT TRANSFER vs Gauge Position
Run 32



PRESSURE vs Gauge Position
Run 32



Test Conditions

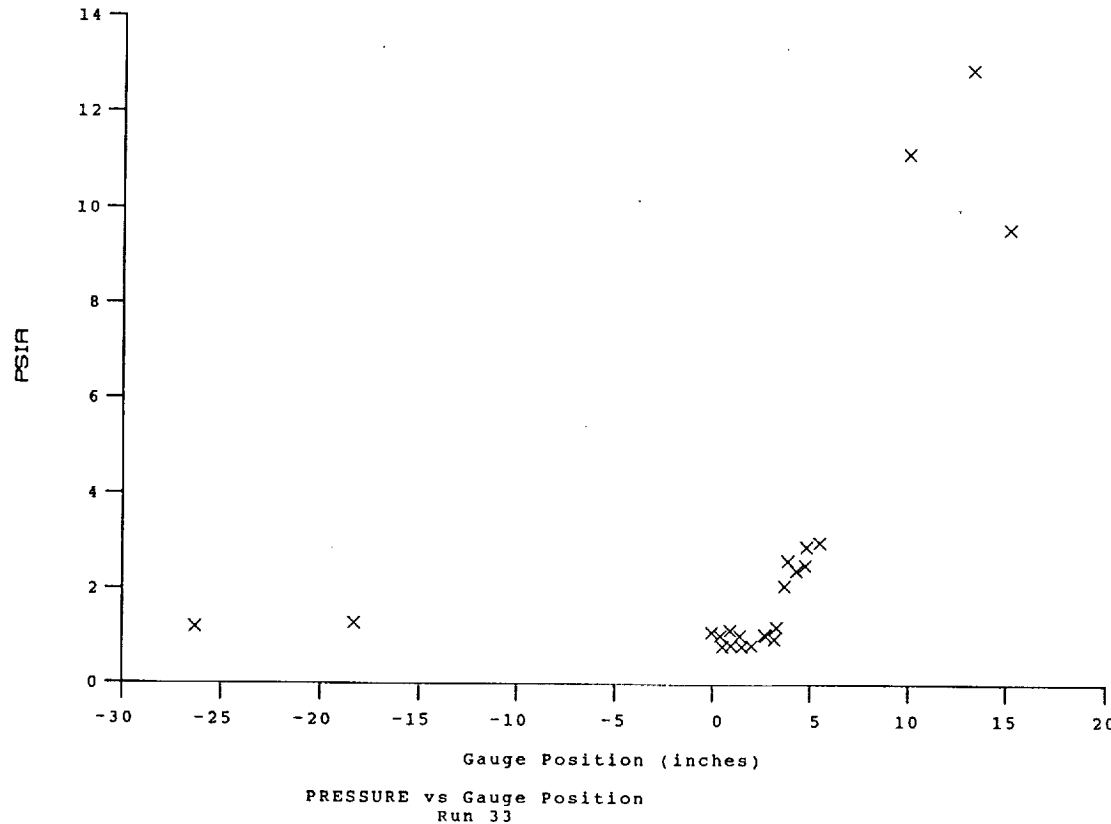
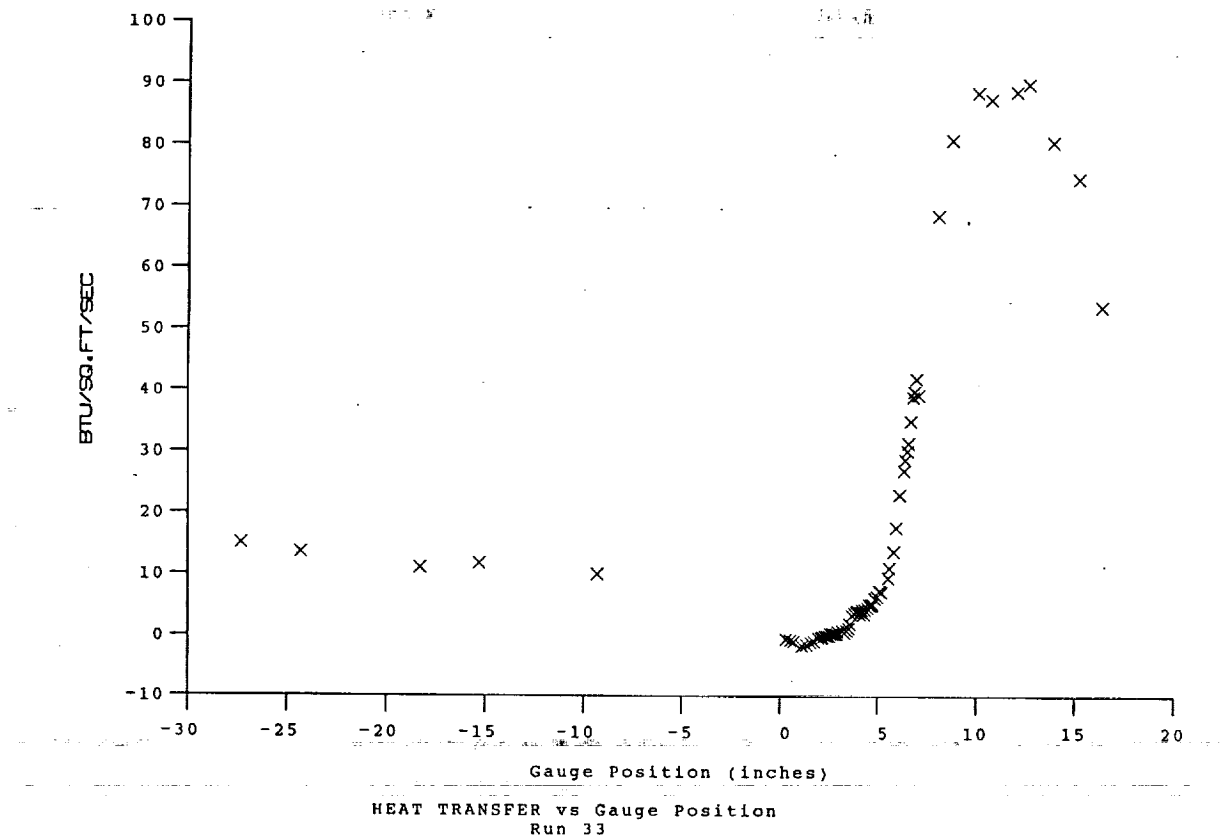
$M_i = 2.7931$
 $P_{o_1} = 2.3594 \times 10^3$ PSIA
 $H_{o_1} = 1.3253 \times 10^{+7}$ $(\text{Ft/sec})^2$
 $T_{o_1} = 2.0823 \times 10^{+3}$ Degrees R
 $M = 6.4393$
 $U = 4.8659 \times 10^{+3}$ Ft/sec
 $T = 2.3745 \times 10^{+2}$ Degrees R
 $P = 9.6260 \times 10^{-1}$ PSIA
 $\Omega = 2.7969 \times 10^{+1}$ PSIA
 $Rho = 3.4021 \times 10^{-4}$ Slugs/Ft 3
 $Mu = 1.9532 \times 10^{-7}$ Slugs/Ft-sec
 $Re = 8.4754 \times 10^{+6}$ 1/Ft
 $P_{o_1}' = 5.2119 \times 10^{+1}$ PSIA

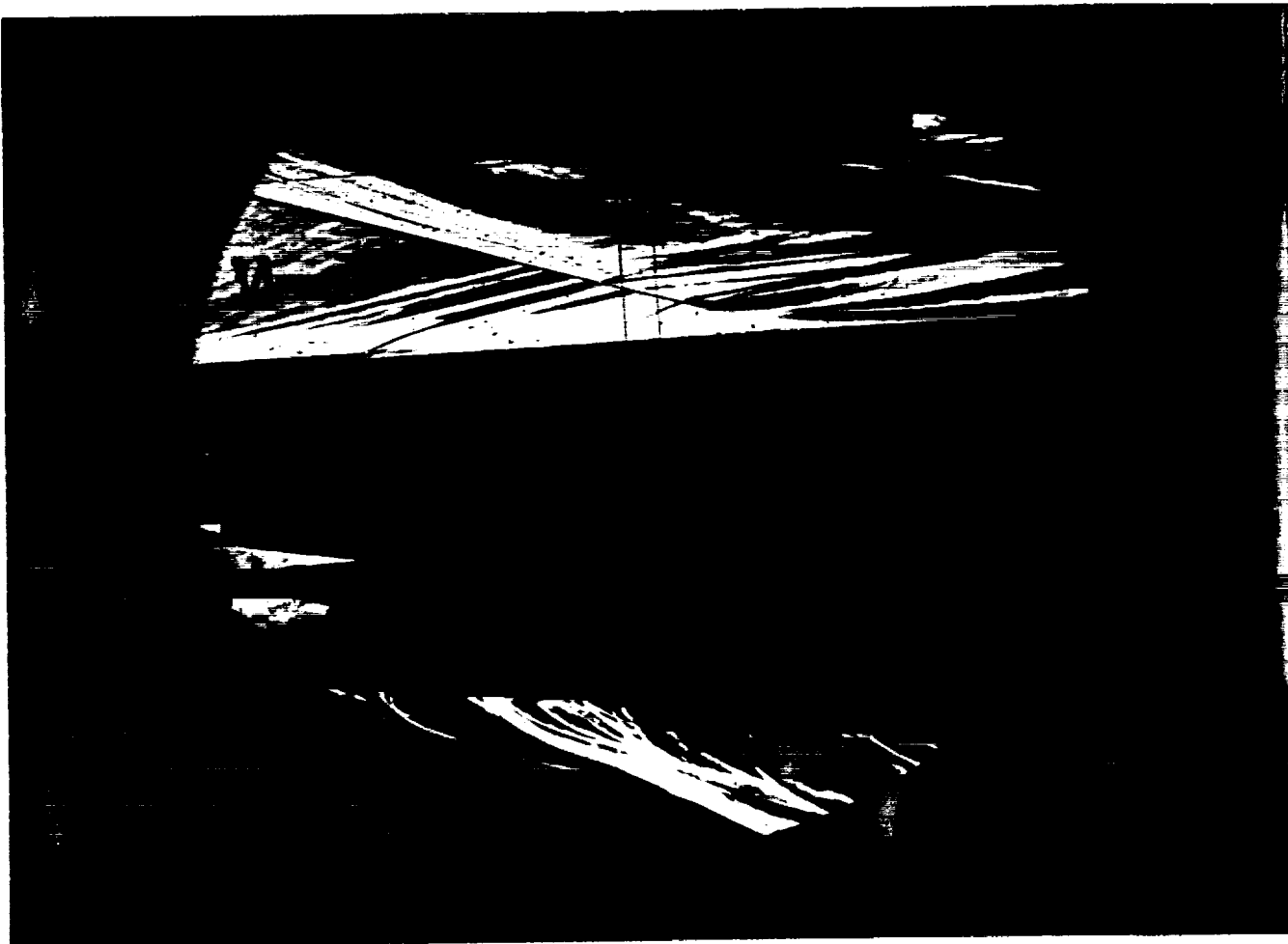
Model Configuration Parameter Value

Horizontal Shock Generator Angle (degrees)	10.5
X * (inches)	7.989
Y * (inches)	2.875
Slot Height (inches)	0.080
Lip Thickness (inches)	0.020
Mass Flow Rate per Nozzle (slugs/sec)	5.313E-05
Non-dimensional Blowing Rate, Lambda	0.1090
Nozzle Reservoir Pressure (psia)	17.97
Exit Plane Pressure (psia)	1.128
Coolant Total Temperature (Rankine)	530

* See Shock Generator Diagram (Page A23)

Run 33



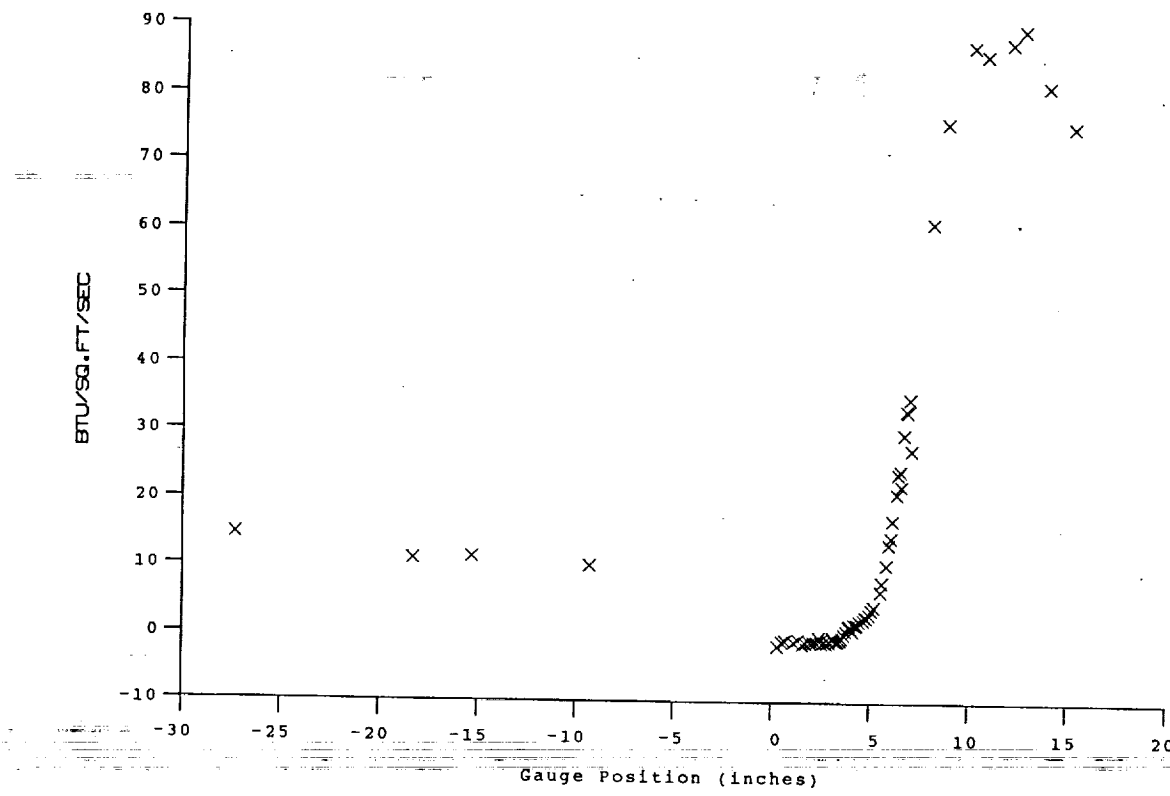


Test Conditions

$M_i = 2.8009$
 $P_{o_1} = 2.3654 \times 10^{+3}$ PSIA
 $H_o = 1.3364 \times 10^{+7}$ (Ft/sec) 2
 $T_o = 2.0983 \times 10^{+3}$ Degrees R
 $M = 6.4379$
 $U = 4.8862 \times 10^{+3}$ Ft/sec
 $T = 2.3954 \times 10^{-2}$ Degrees R
 $P = 9.6434 \times 10^{-1}$ PSIA
 $Q = 2.8008 \times 10^{+1}$ PSIA
 $\rho_o = 3.3785 \times 10^{-4}$ Slugs/Ft 3
 $M_u = 1.9691 \times 10^{-7}$ Slugs/Ft-sec
 $Re = 8.3834 \times 10^{+6}$ 1/Ft
 $P_{o'} = 5.2196 \times 10^{+1}$ PSIA

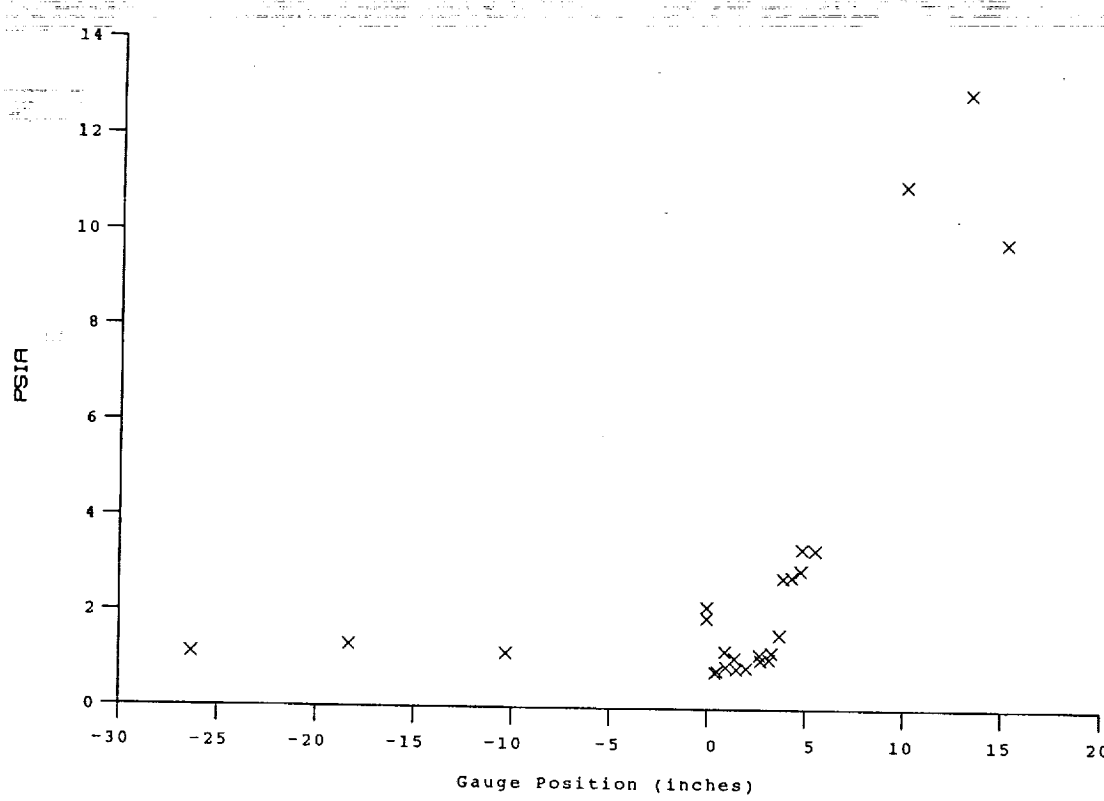
Model Configuration Parameter	Value
Horizontal Shock Generator Angle (degrees)	10.5
X * (inches)	7.989
Y * (inches)	2.875
Slot Height (inches)	0.080
Lip Thickness (inches)	0.020
Mass Flow Rate per Nozzle (slugs/sec)	1.183E-04
Non-dimensional Blowing Rate, Lambda	0.2434
Nozzle Reservoir Pressure (psia)	36.66
Exit Plane Pressure (psia)	2.042
Coolant Total Temperature (Rankine)	530
* See Shock Generator Diagram (Page A23)	

Run 34



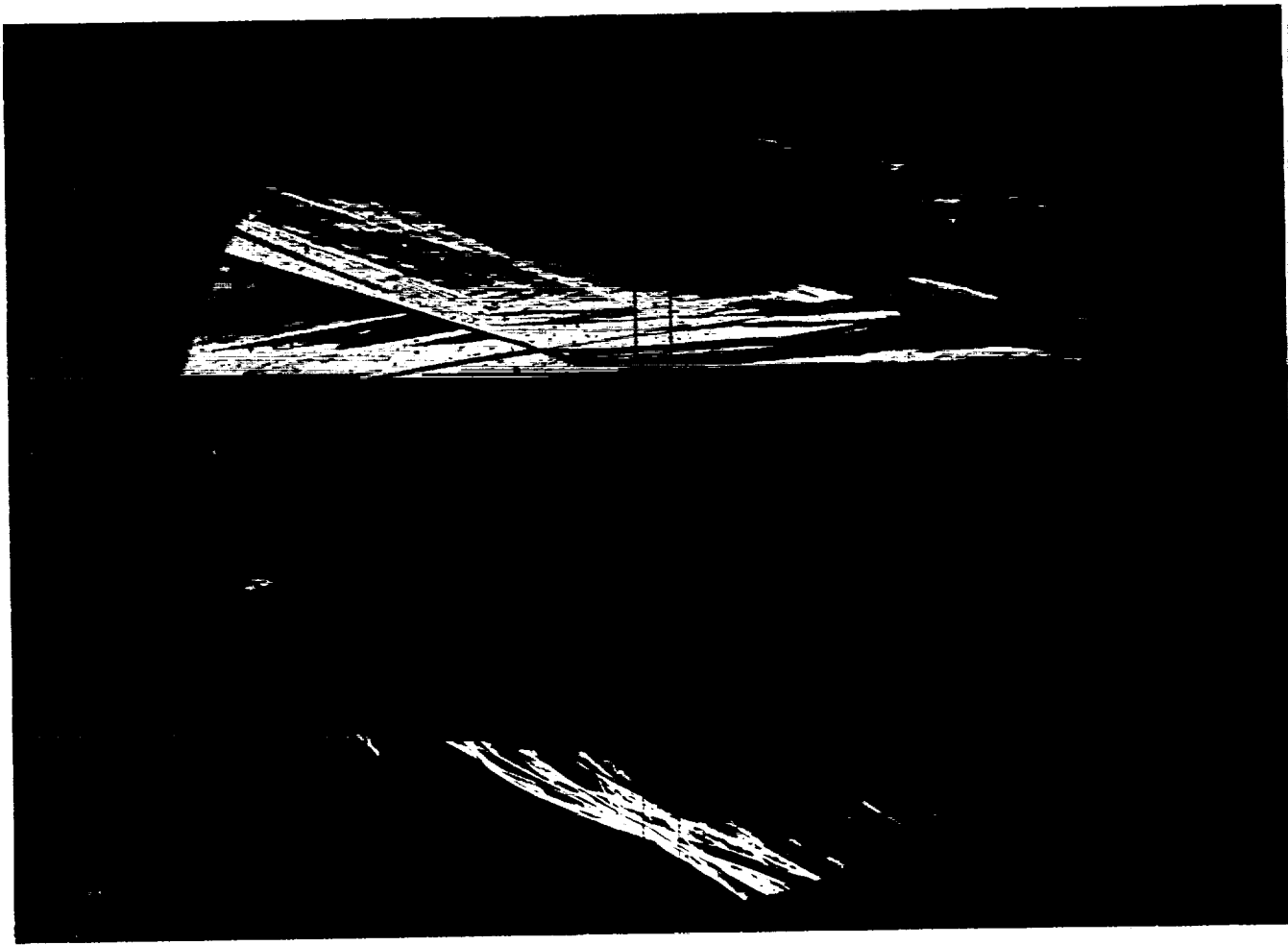
HEAT TRANSFER vs Gauge Position

Run 34



PRESSURE vs Gauge Position

Run 34



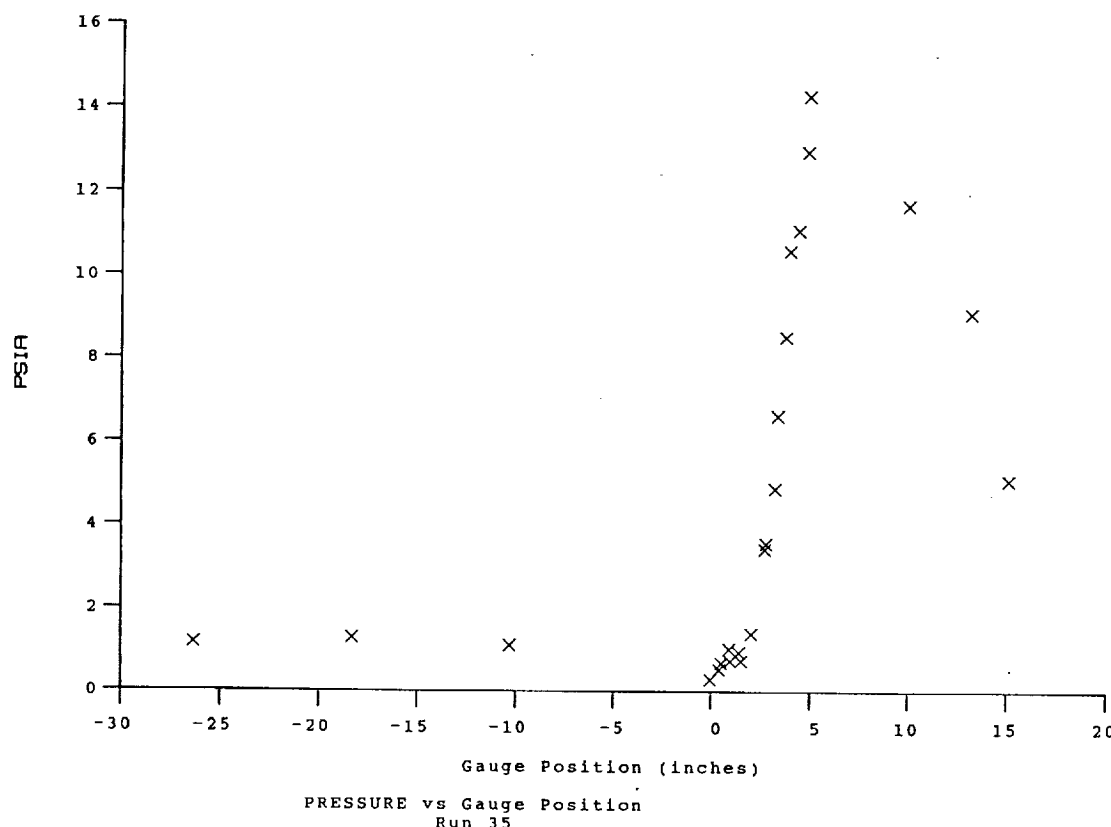
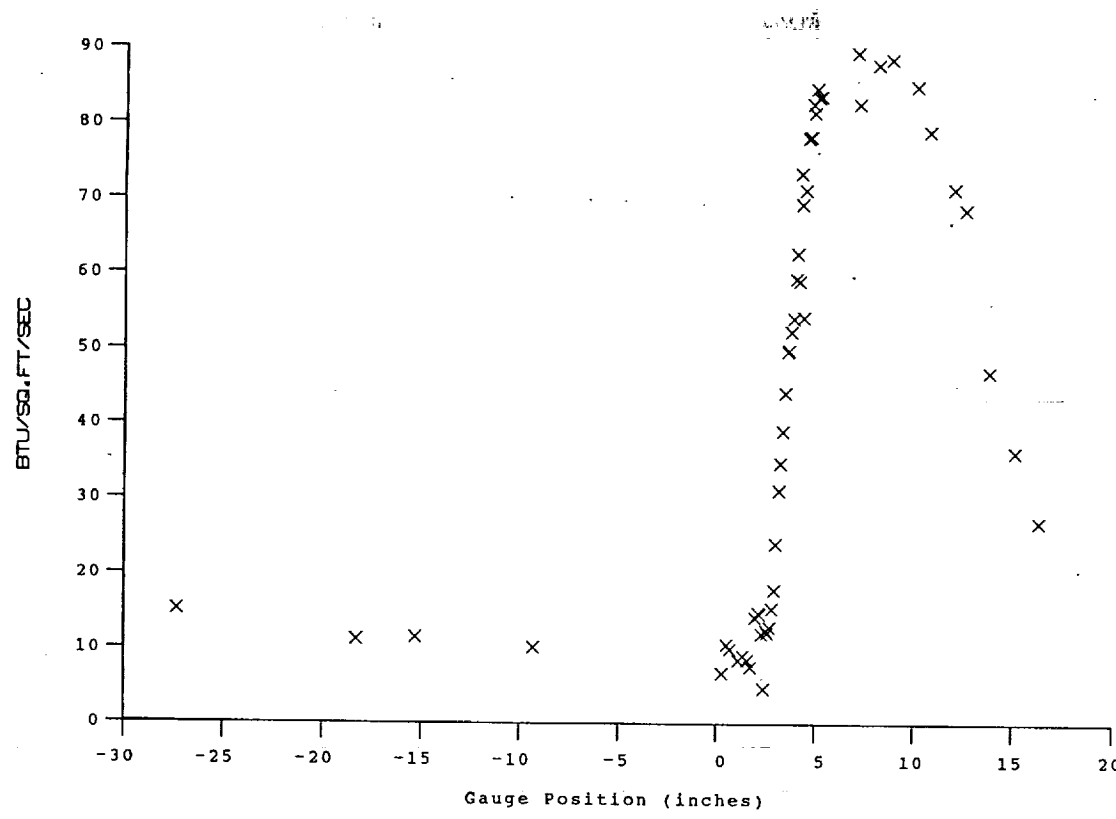
Test Conditions

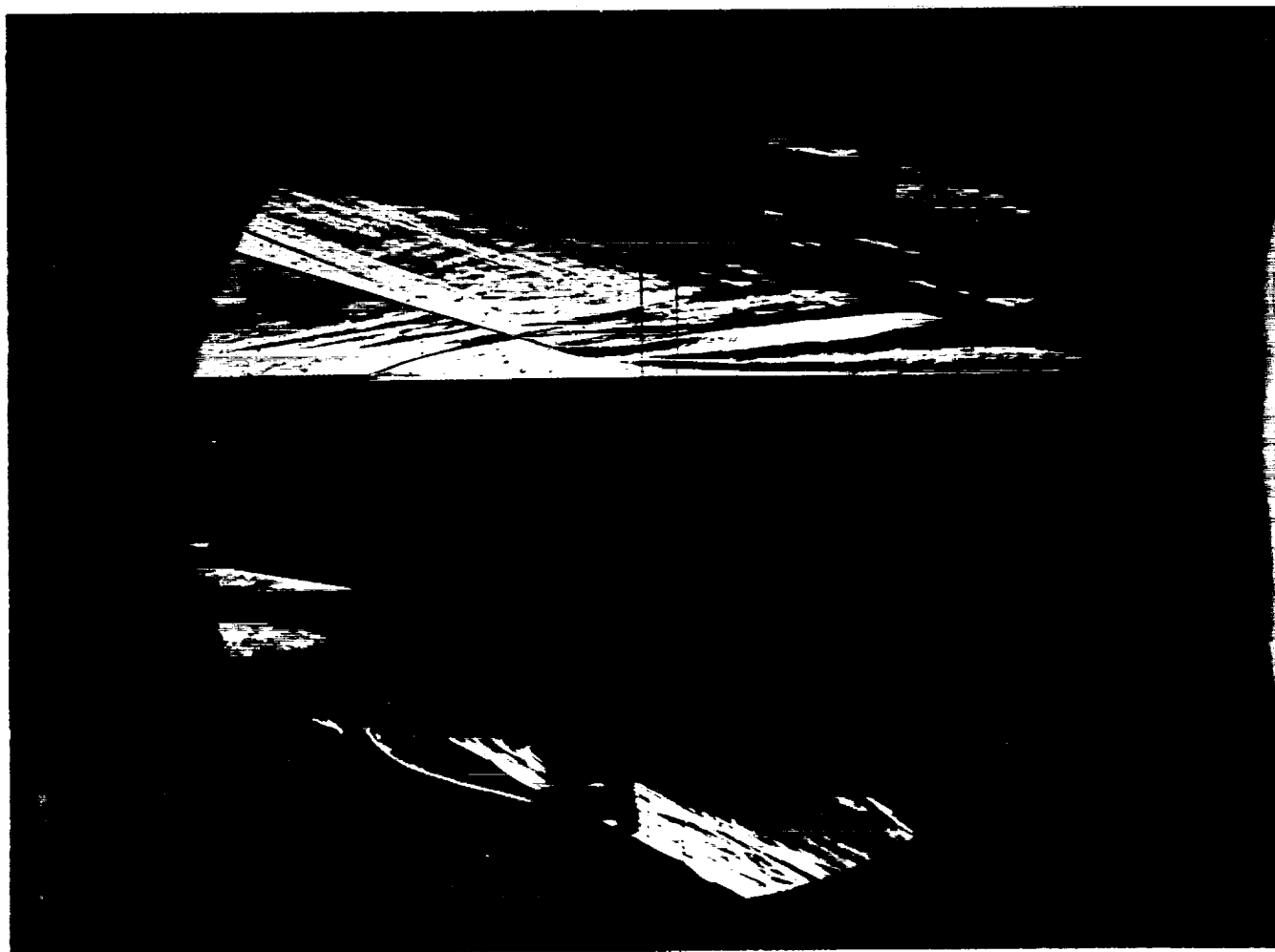
M_i = 2.8112
P_o = 2.4155X10+3 PSIA
H_o = 1.3516X10+7 (Ft/sec)²
T_o = 2.1200X10+3 Degrees R
M = 6.4383
U = 4.9139X10+3 Ft/sec
T = 2.4223X10+2 Degrees R
P = 9.8253X10-1 PSIA
Q = 2.8540X10+1 PSIA
Rho = 3.4040X10-4 Slugs/Ft³
Mu = 1.9896X10-7 Slugs/Ft-sec
Re = 8.4073X10+6 1/Ft
P_{o'} = 5.3196X10+1 PSIA

Model Configuration Parameter	Value
Horizontal Shock Generator Angle (degrees)	10.5
X * (inches)	6.458
Y * (inches)	2.272
Slot Height (inches)	0.080
Lip Thickness (inches)	0.020
Lambda	0

* see shock generator diagram at page A-23

Run 35





Test Conditions

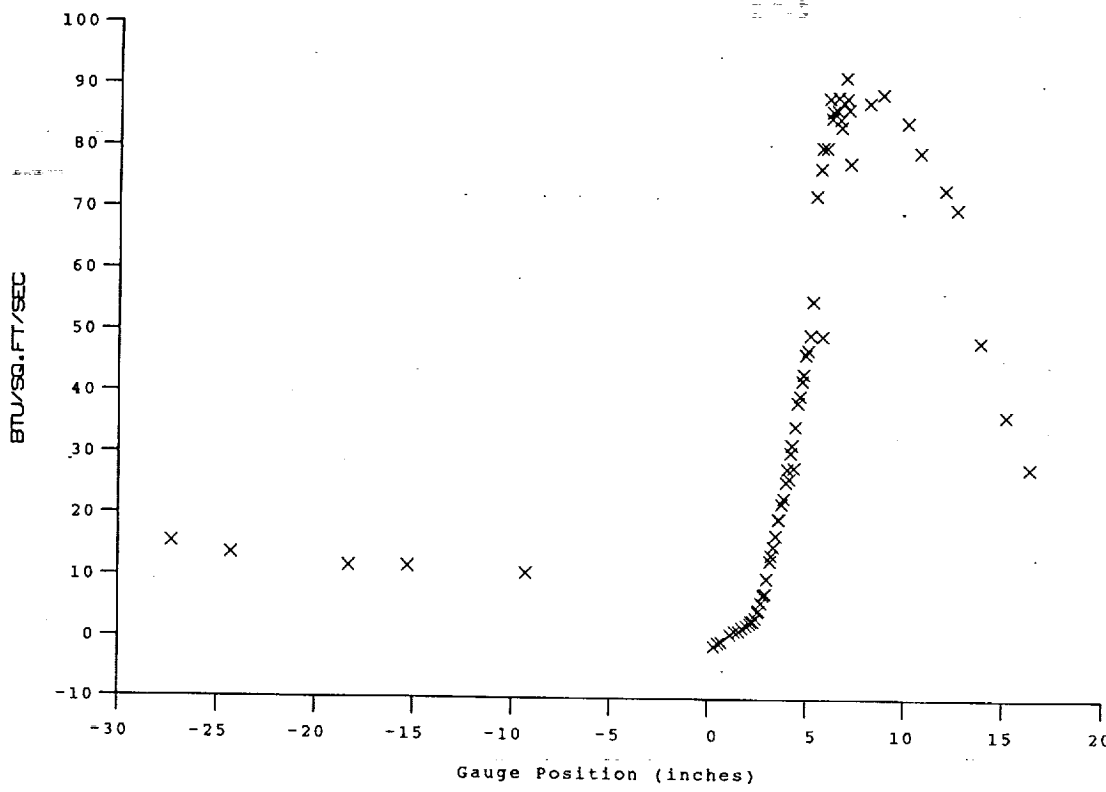
$M_i = 2.8084$
 $P_o = 2.3723 \times 10^3$ PSIA
 $H_o = 1.3261 \times 10^7$ (Ft/sec)²
 $T_o = 2.0826 \times 10^3$ Degrees R
 $M = 6.4366$
 $U = 4.8673 \times 10^3$ Ft/sec
 $T = 2.3778 \times 10^2$ Degrees R
 $P = 9.7049 \times 10^{-1}$ PSIA
 $Q = 2.8175 \times 10^{+1}$ PSIA
 $\rho_o = 3.4252 \times 10^{-4}$ Slugs/Ft³
 $\mu_o = 1.9557 \times 10^{-7}$ Slugs/Ft-sec
 $Re = 8.5245 \times 10^{+6}$ 1/Ft
 $P_o' = 5.2503 \times 10^{+1}$ PSIA

Model Configuration Parameter

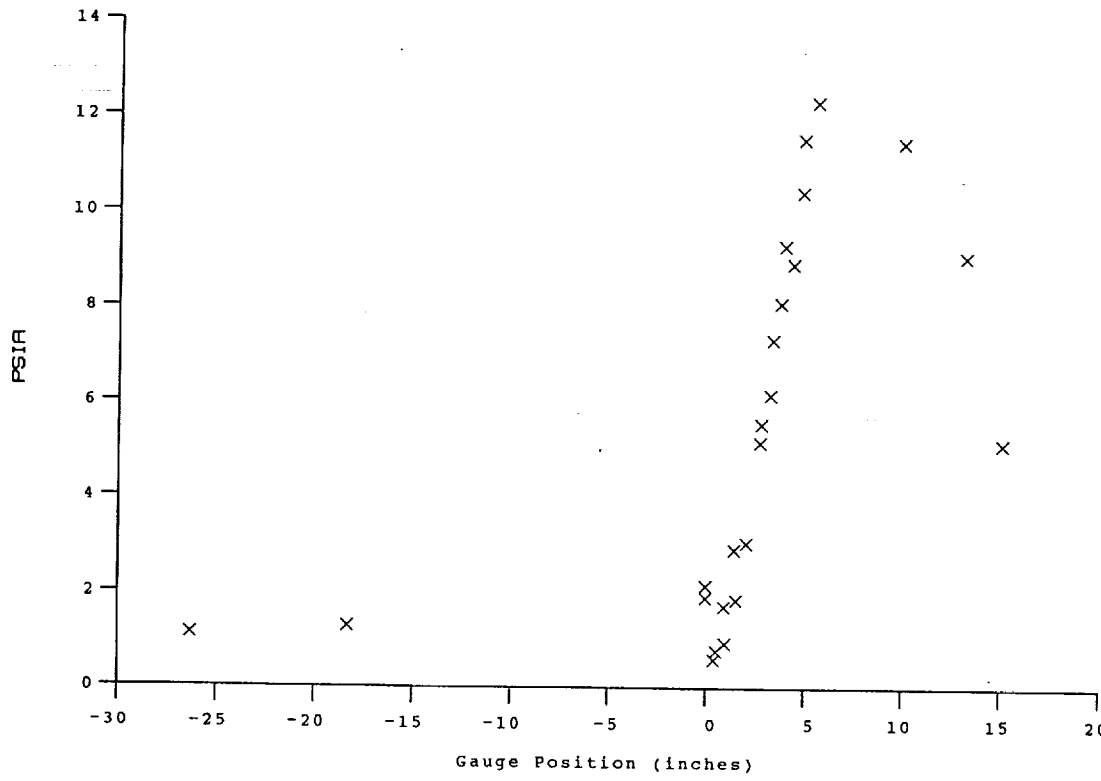
	Value
Horizontal Shock Generator Angle (degrees)	10.5
X * (inches)	6.458
Y * (inches)	2.272
Slot Height (inches)	0.080
Lip Thickness (inches)	0.020
Mass Flow Rate per Nozzle (slugs/sec)	1.166E-04
Non-dimensional Blowing Rate, Lambda	0.2375
Nozzle Reservoir Pressure (psia)	36.83
Exit Plane Pressure (psia)	2.050
Coolant Total Temperature (Rankine)	530

* See Shock Generator Diagram (Page A23)

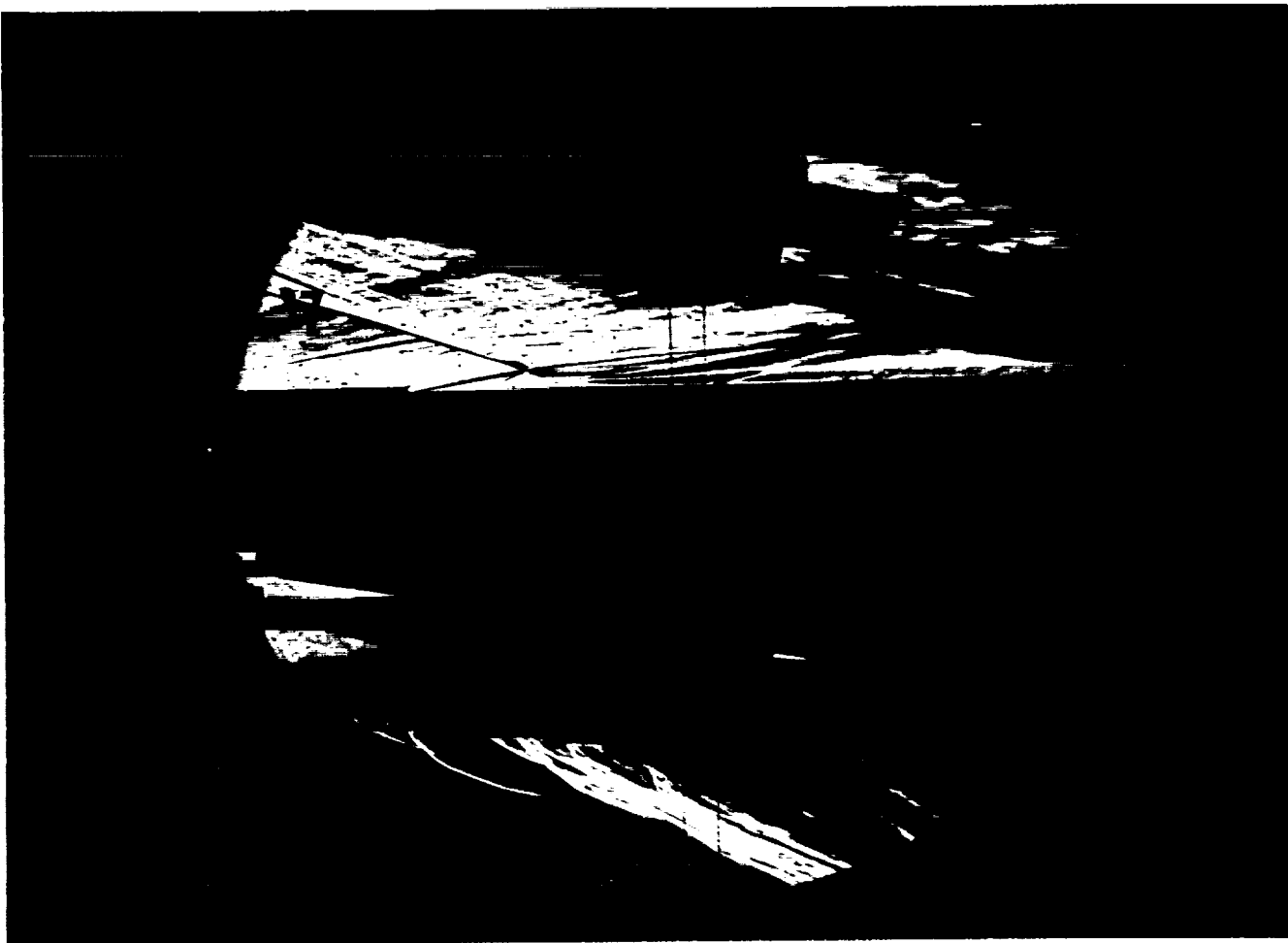
Run 36



HEAT TRANSFER vs Gauge Position
Run 36



PRESSURE vs Gauge Position
Run 36

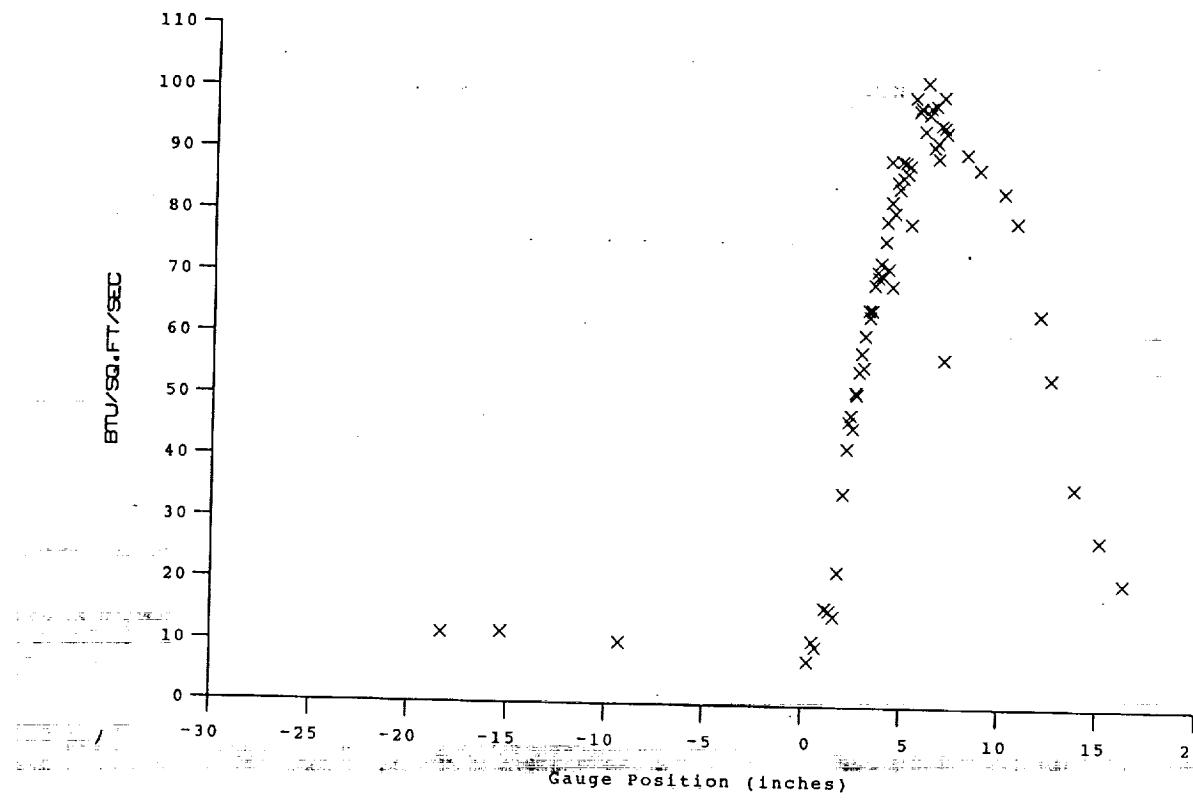
**Test Conditions**

M_i = 2.8084
P_o = 2.3997x10+3 PSIA
H_o = 1.3354x10+7 (Ft/sec)²
T_o = 2.0963x10+3 Degrees R
M = 6.4381
U = 4.8844x10+3 Ft/sec
T = 2.3934x10+2 Degrees R
P = 9.7910x10-1 PSIA
Q = 2.8438x10+1 PSIA
Rho = 3.4330x10-4 Slugs/Ft³
Mu = 1.9677x10-7 Slugs/Ft-sec
Re = 8.5219x10+6 1/Ft
P_{o'} = 5.2998x10+1 PSIA

Model Configuration Parameter	Value
Horizontal Shock Generator Angle (degrees)	10.5
X * (inches)	6.458
Y * (inches)	1.884
Slot Height (inches)	0.080
Lip Thickness (inches)	0.020
Lambda	0

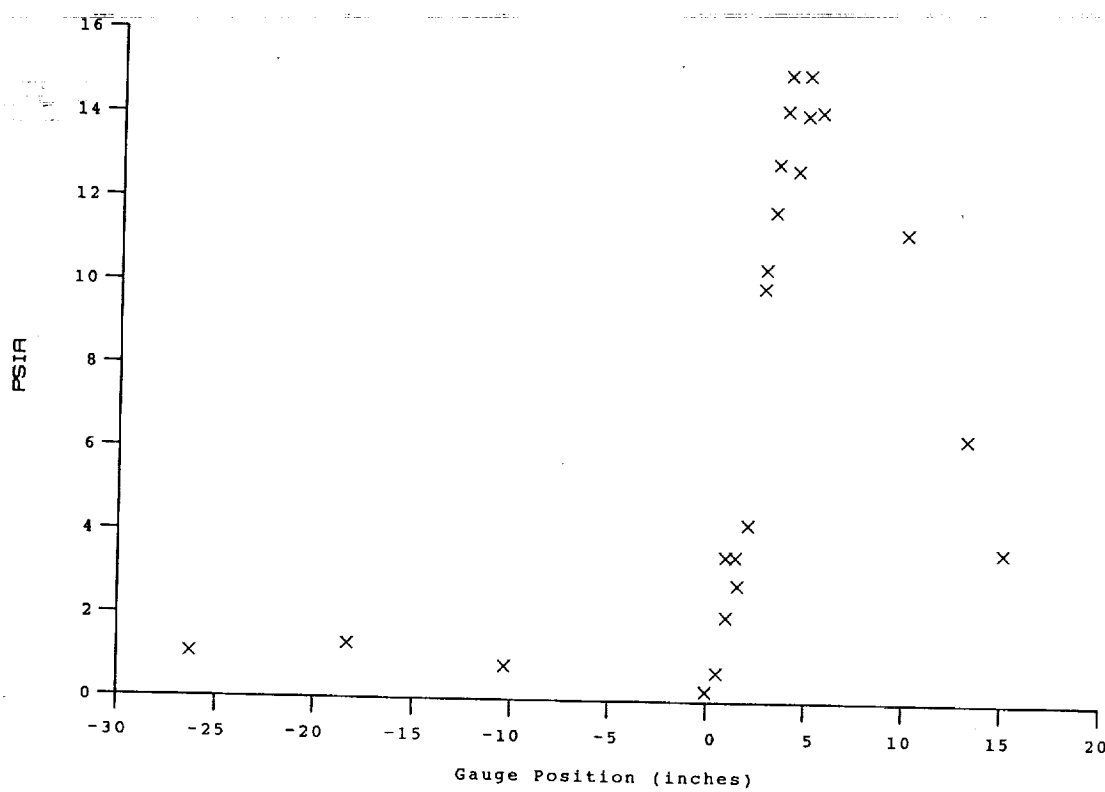
* see shock generator diagram at page A-23

Run 37



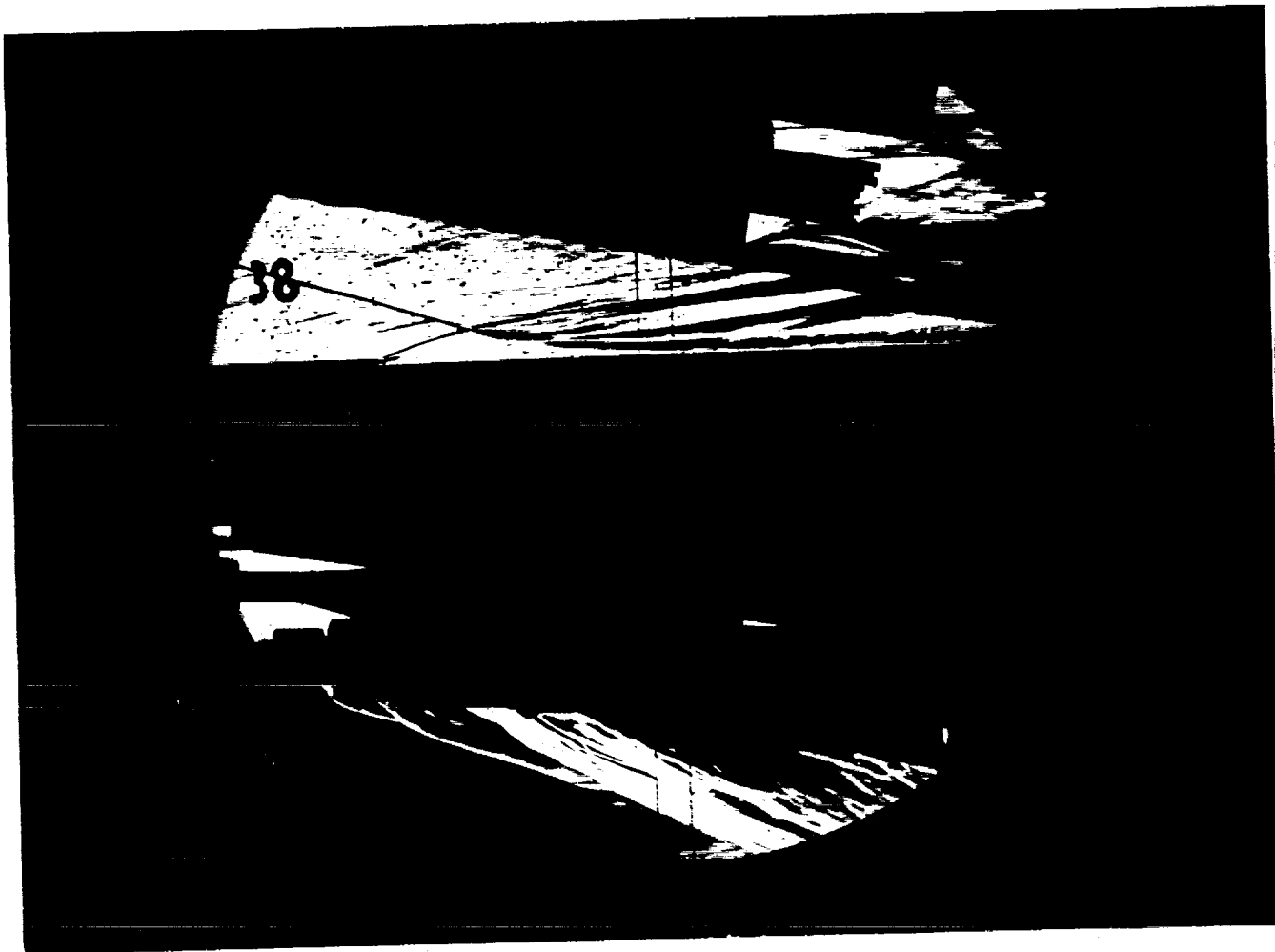
HEAT TRANSFER vs Gauge Position

Run 37



PRESSURE vs Gauge Position

Run 37



Test Conditions

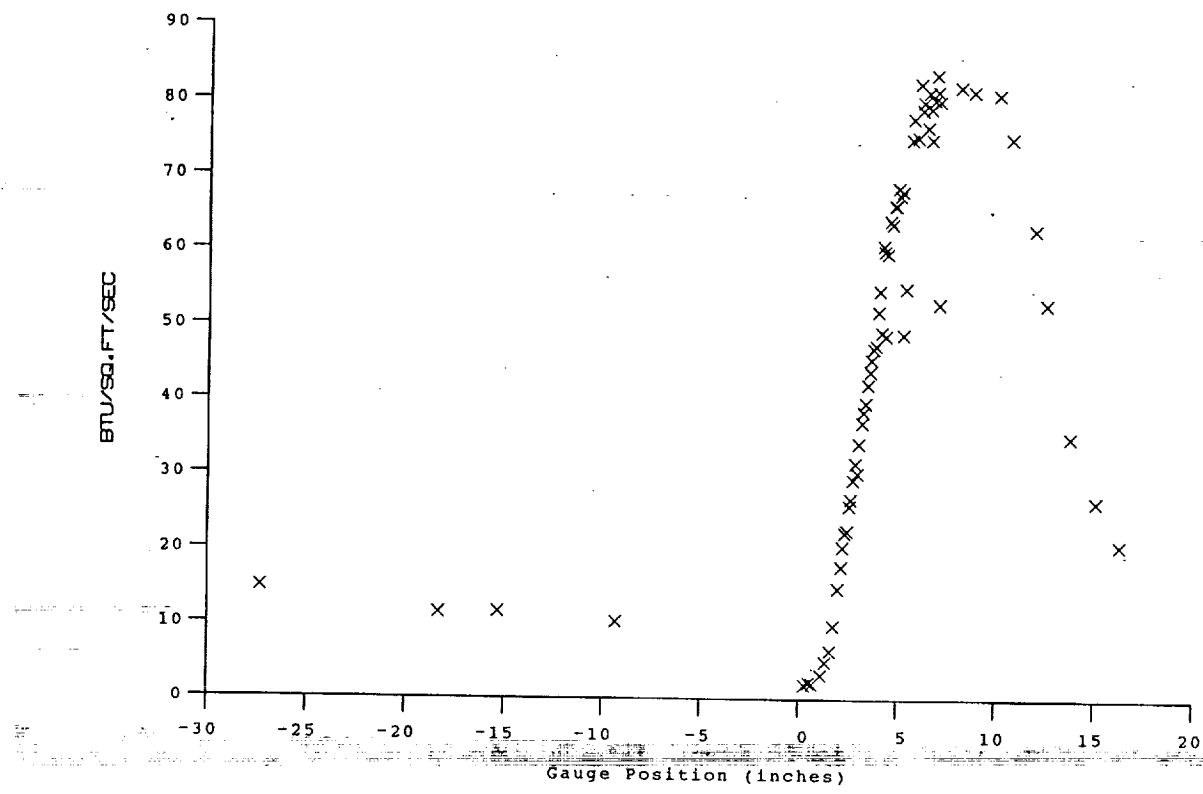
$M_i = 2.8154$
 $P_0 = 2.3958 \times 10^3$ PSIA
 $H_0 = 1.3507 \times 10^7$ (Ft/sec)²
 $T_0 = 2.1185 \times 10^3$ Degrees R
 $M = 6.4363$
 $U = 4.9121 \times 10^3$ Ft/sec
 $T = 2.4220 \times 10^2$ Degrees R
 $P = 9.7613 \times 10^{-1}$ PSIA
 $Q = 2.8336 \times 10^1$ PSIA
 $\rho_0 = 3.3822 \times 10^{-4}$ Slugs/Ft³
 $M_u = 1.9894 \times 10^{-7}$ Slugs/Ft-sec
 $R_e = 8.3511 \times 10^6$ 1/Ft
 $P_{0'} = 5.2816 \times 10^1$ PSIA

Model Configuration Parameter Value

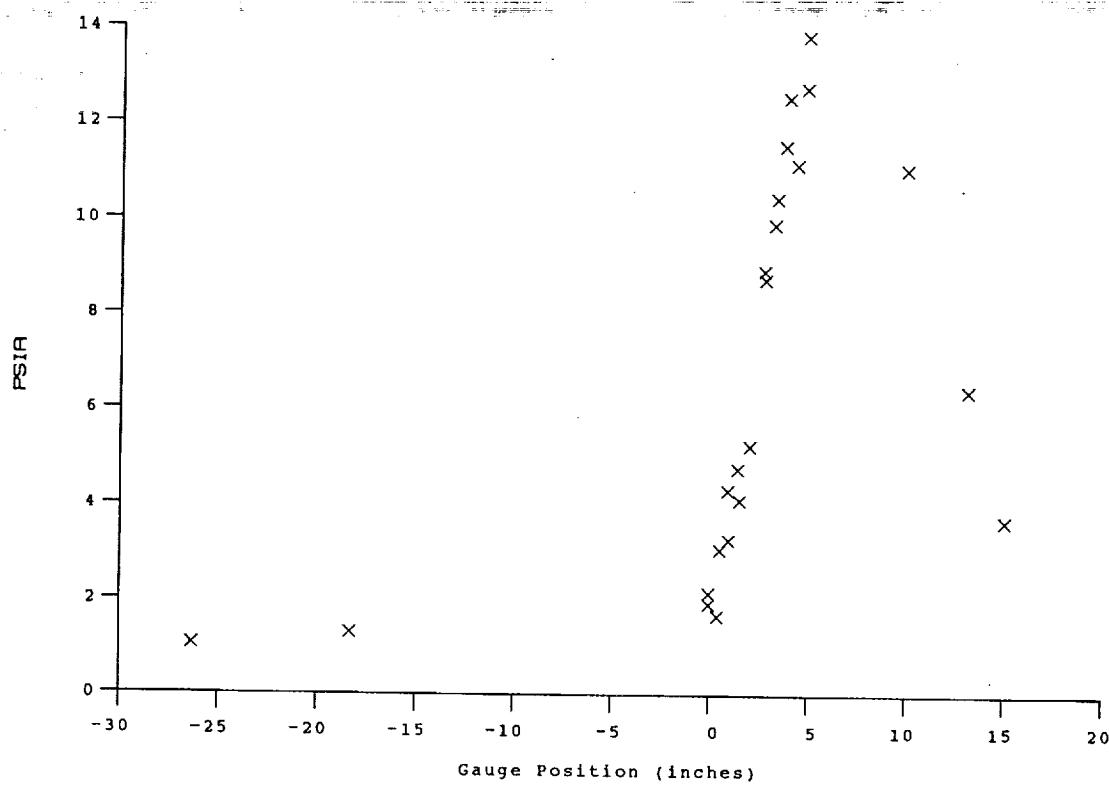
Horizontal Shock Generator Angle (degrees)	10.5
X * (inches)	6.458
Y * (inches)	1.884
Slot Height (inches)	0.080
Lip Thickness (inches)	0.020
Mass Flow Rate per Nozzle (slugs/sec)	1.176E-04
Non-dimensional Blowing Rate, Lambda	0.2404
Nozzle Reservoir Pressure (psia)	37.13
Exit Plane Pressure (psia)	2.070
Coolant Total Temperature (Rankine)	530

* See Shock Generator Diagram (Page A23)

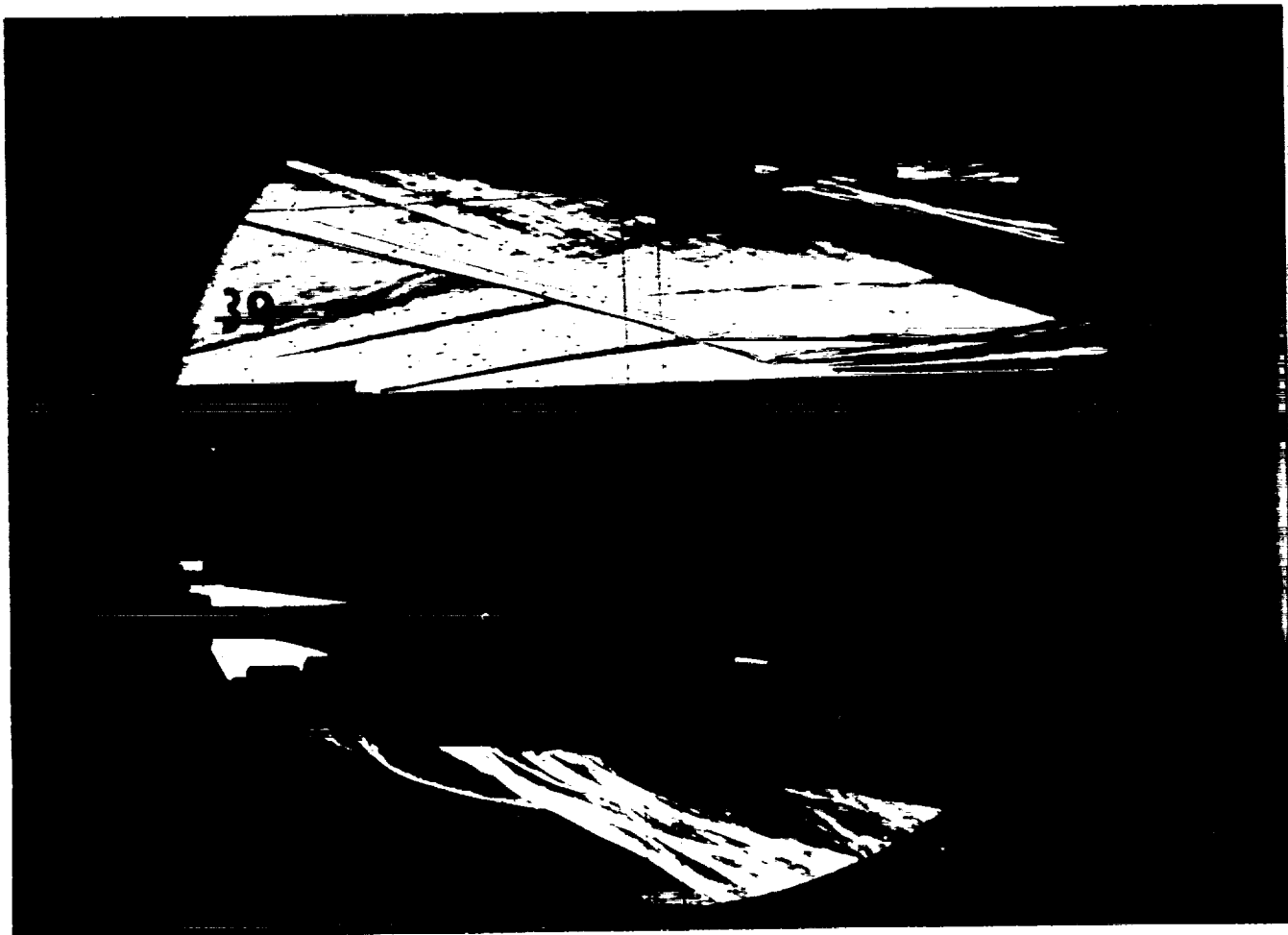
Run 38



HEAT TRANSFER vs Gauge Position
Run 38



PRESSURE vs Gauge Position
Run 38



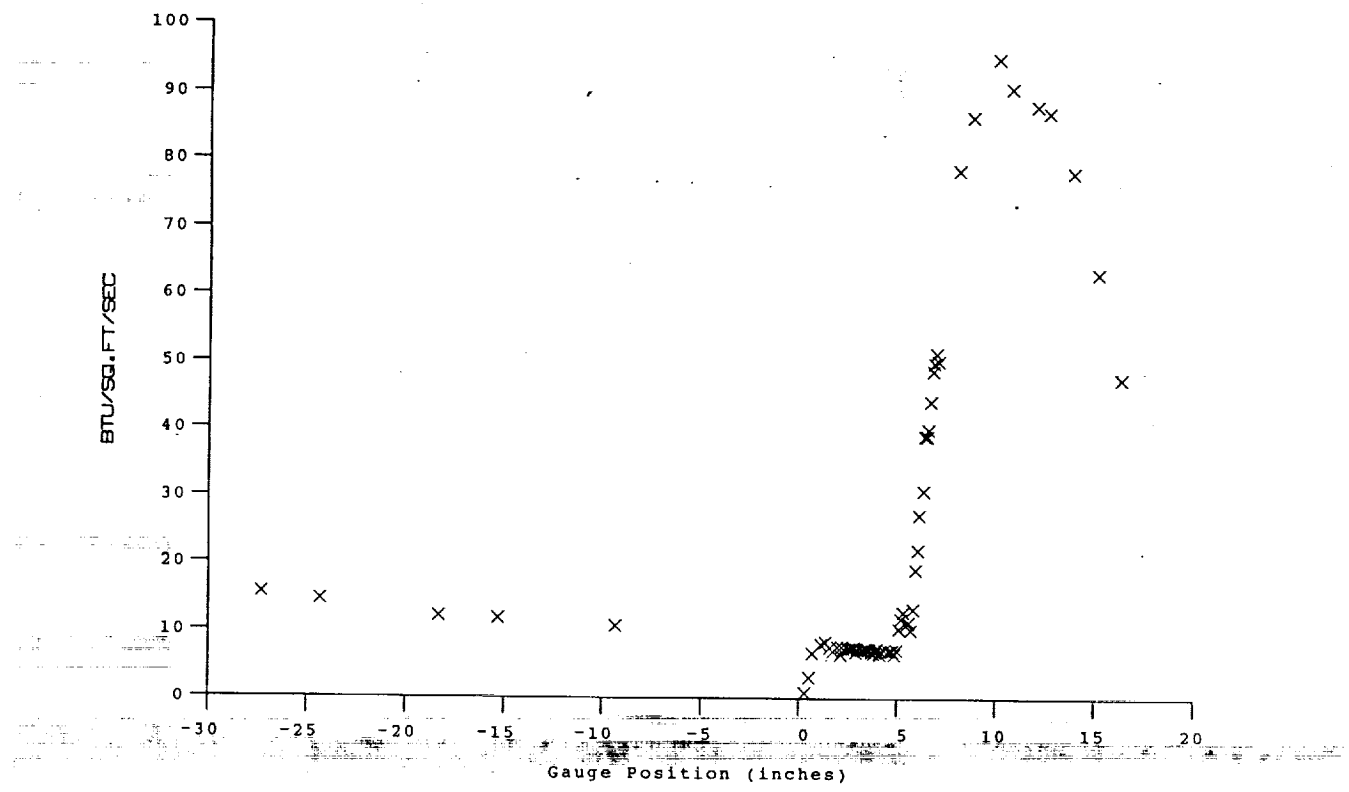
Test Conditions

M_i = 2.7803
P_o = 2.3243X10+3 PSIA
H_o = 1.3071X10+7 (Ft/sec)²
T_o = 2.0562X10+3 Degrees R
M = 6.4402
U = 4.8324X10+3 Ft/sec
T = 2.3413X10+2 Degrees R
P = 9.5012X10-1 PSIA
Q = 2.7614X10+1 PSIA
Rho = 3.4056X10-4 Slugs/Ft³
Mu = 1.9278X10-7 Slugs/Ft-sec
Re = 8.5369X10+6 1/Ft
P_{o'} = 5.1447X10+1 PSIA

Model Configuration Parameter	Value
Horizontal Shock Generator Angle (degrees)	10.5
X * (inches)	6.702
Y * (inches)	3.159
Slot Height (inches)	0.080
Lip Thickness (inches)	0.145
Lambda	0

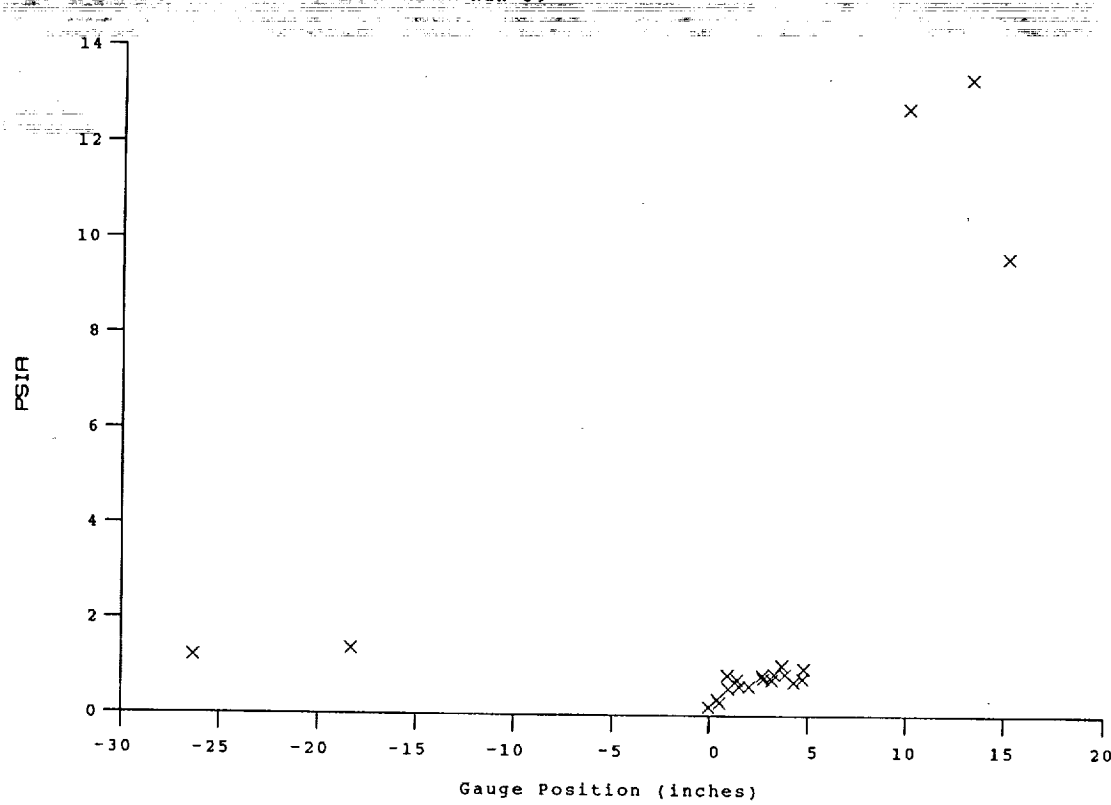
* see shock generator diagram at page A-23

Run 39



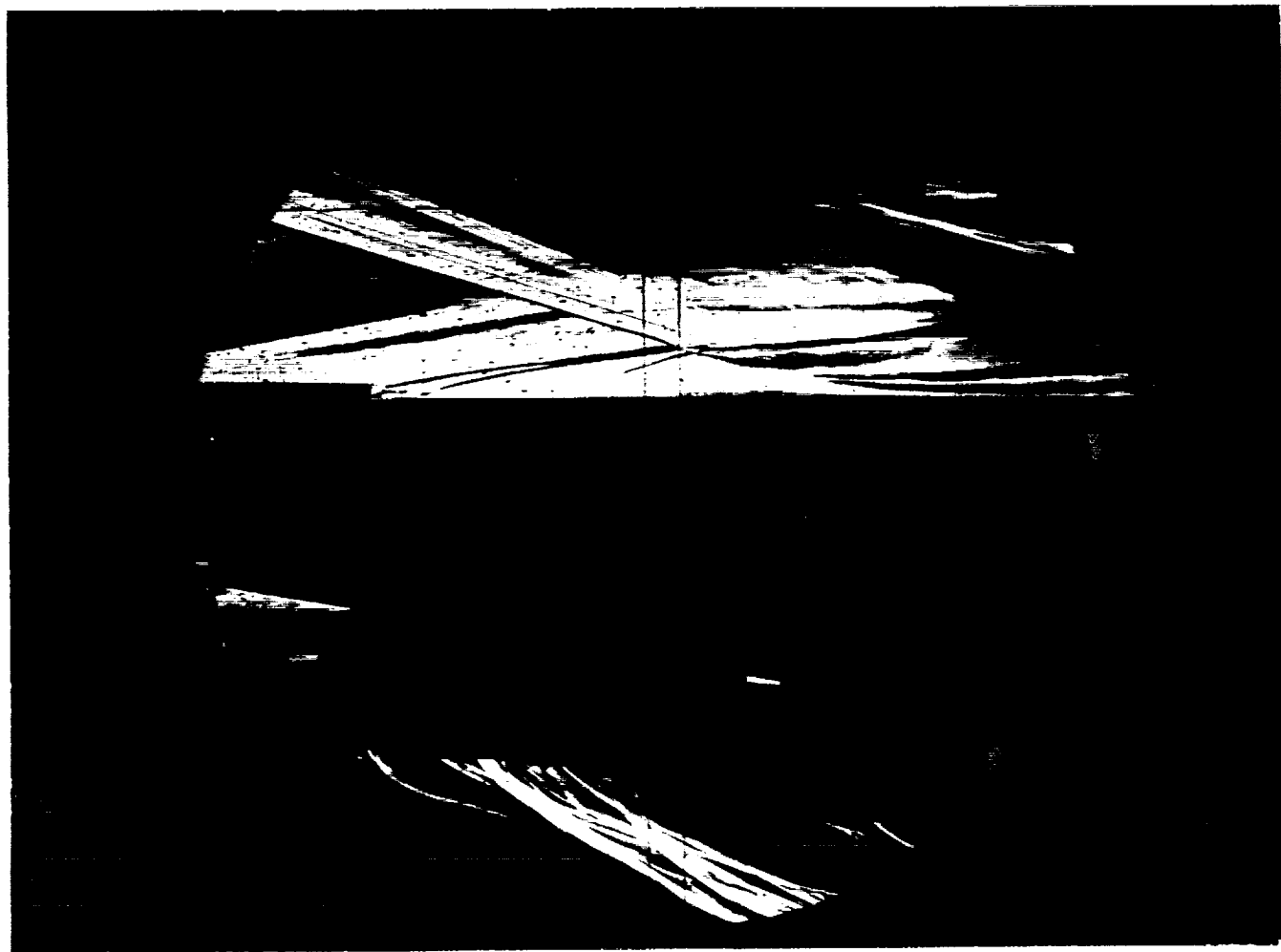
HEAT TRANSFER vs Gauge Position

Run 39



PRESSURE vs Gauge Position

Run 39



Test Conditions

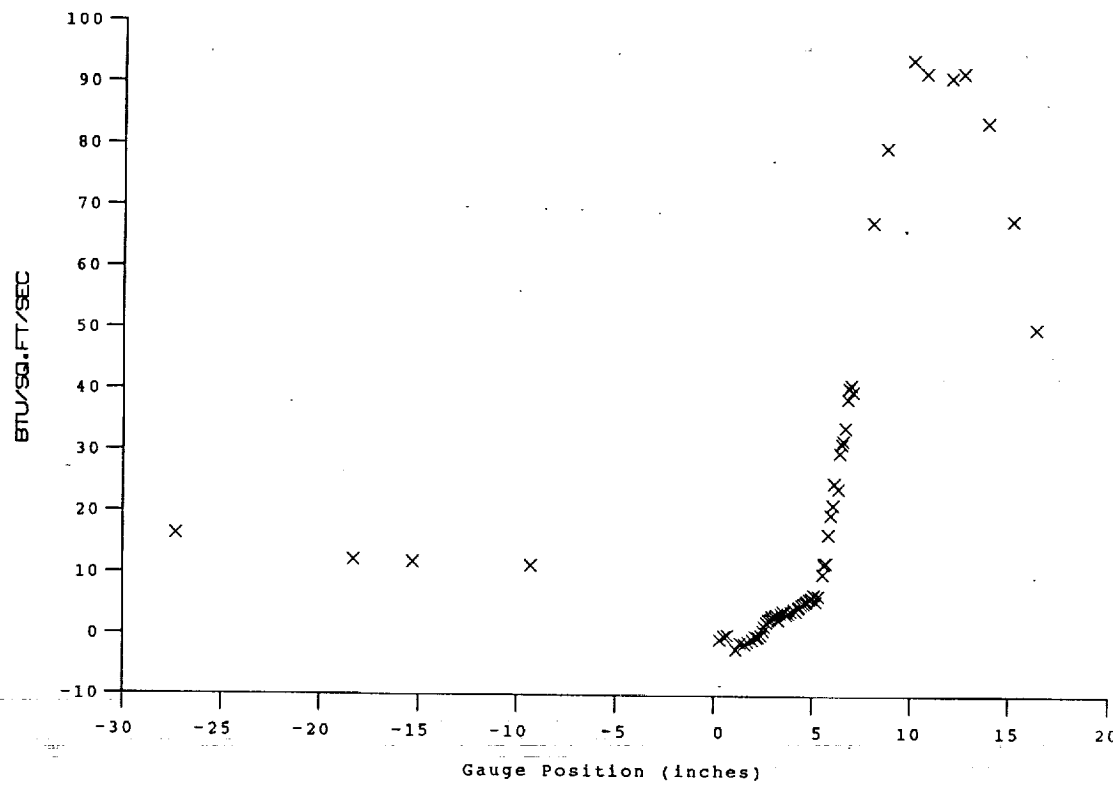
$M_i = 2.8010$
 $P_{o_1} = 2.3542 \times 10^3$ PSIA
 $H_o = 1.3301 \times 10^7$ (Ft/sec)²
 $T_o = 2.0889 \times 10^3$ Degrees R
 $M = 6.4373$
 $U = 4.8746 \times 10^3$ Ft/sec
 $T = 2.3844 \times 10^2$ Degrees R
 $P = 9.6134 \times 10^{-1}$ PSIA
 $Q = 2.7915 \times 10^1$ PSIA
 $\rho_o = 3.3835 \times 10^{-4}$ Slugs/Ft³
 $\mu_o = 1.9608 \times 10^{-7}$ Slugs/Ft-sec
 $Re = 8.4114 \times 10^6$ 1/Ft
 $P_{o_1}' = 5.2020 \times 10^1$ PSIA

Model Configuration Parameter Value

Horizontal Shock Generator Angle (degrees)	10.5
X * (inches)	6.702
Y * (inches)	3.159
Slot Height (inches)	0.080
Lip Thickness (inches)	0.145
Mass Flow Rate per Nozzle (slugs/sec)	5.059E-05
Non-dimensional Blowing Rate, Lambda	0.1042
Nozzle Reservoir Pressure (psia)	18.16
Exit Plane Pressure (psia)	1.124
Coolant Total Temperature (Rankine)	530

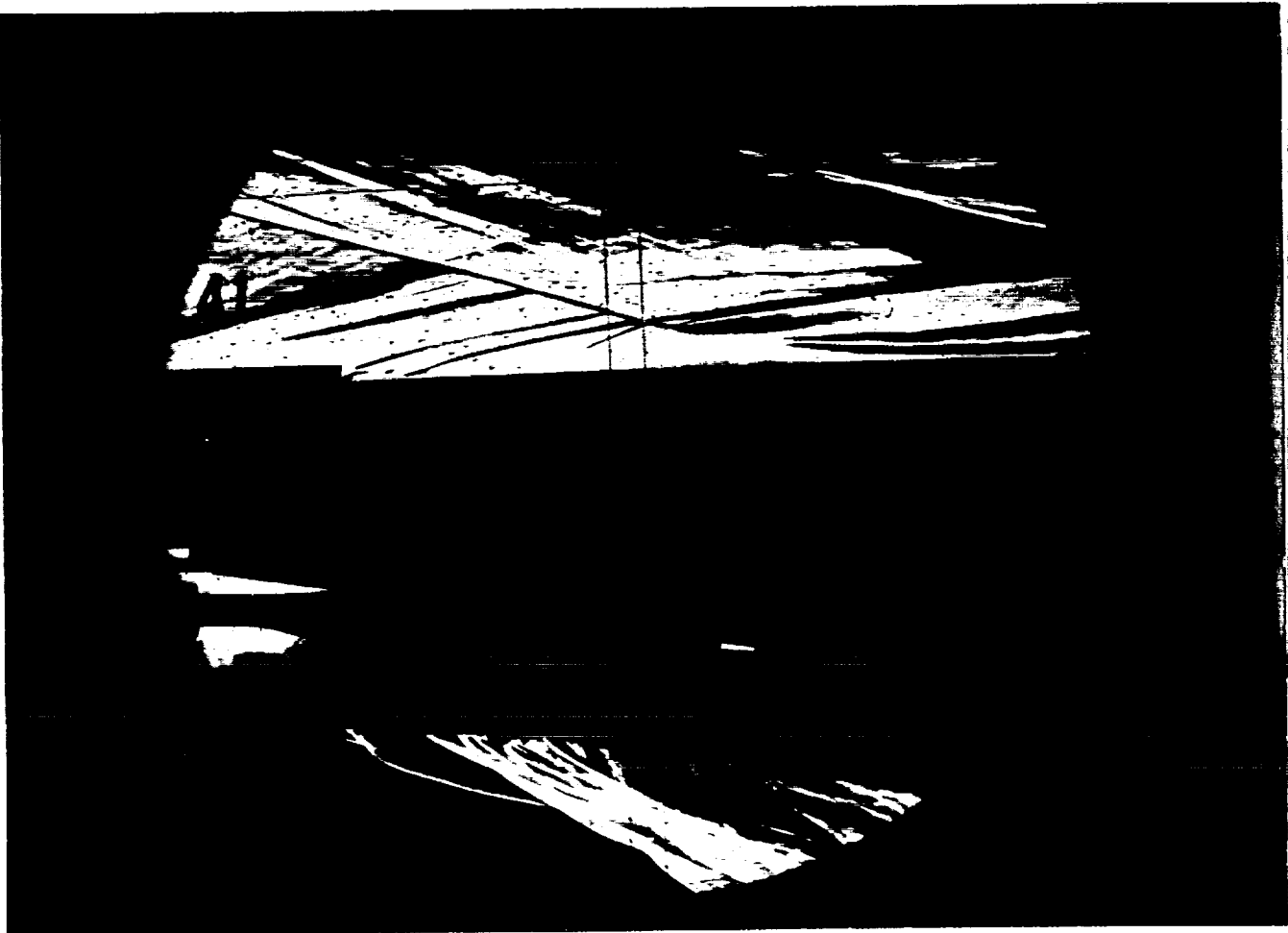
* See Shock Generator Diagram (Page A23)

Run 40



PRESSURE vs Gauge Position
Run 40

A-53



Test Conditions

$M_i = 2.8049$
 $P_{o_1} = 2.3769 \times 10^3$ PSIA
 $H_o = 1.3419 \times 10^7$ (Ft/sec)²
 $T_o = 2.1062 \times 10^3$ Degrees R
 $M = 6.4376$
 $U = 4.8963 \times 10^3$ Ft/sec
 $T = 2.4054 \times 10^2$ Degrees R
 $P = 9.6847 \times 10^{-1}$ PSIA
 $Q = 2.8126 \times 10^1$ PSIA
 $\rho_o = 3.3788 \times 10^{-4}$ Slugs/Ft³
 $\mu_o = 1.9768 \times 10^{-7}$ Slugs/Ft-sec
 $Re = 8.3690 \times 10^6$ 1/Ft
 $P_{o_1}' = 5.2419 \times 10^1$ PSIA

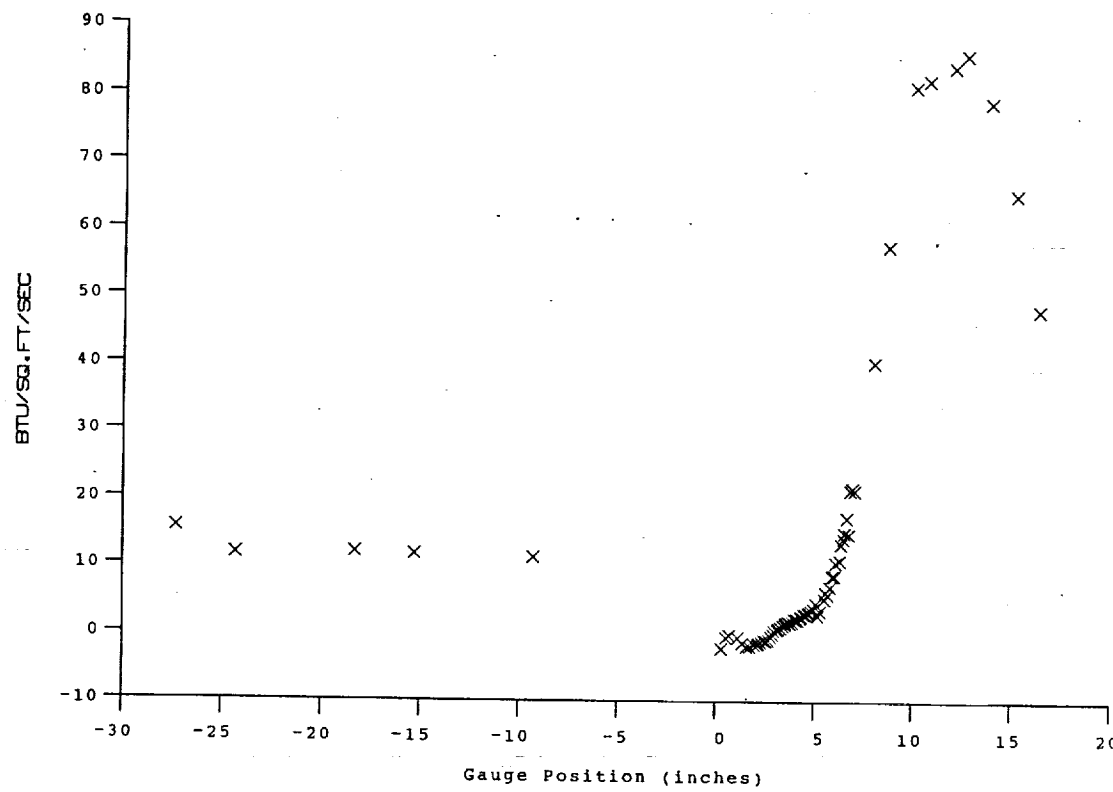
Model Configuration Parameter

Value

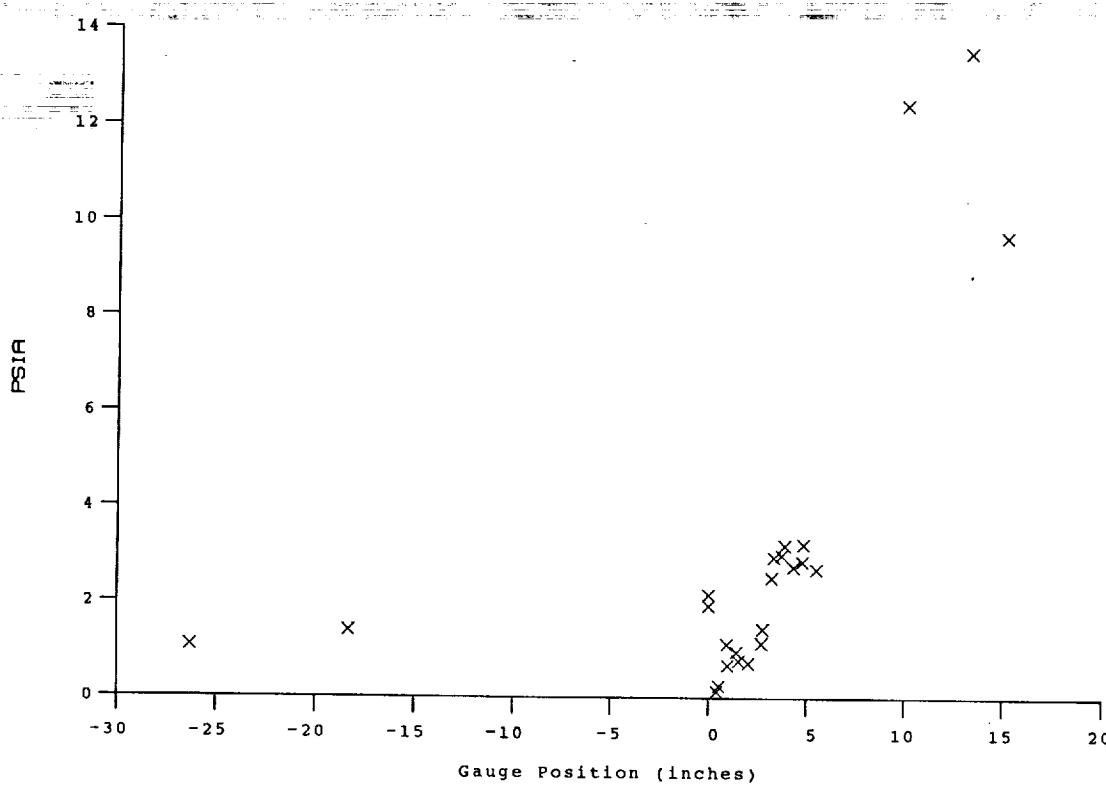
Horizontal Shock Generator Angle (degrees)	10.5
X * (inches)	6.702
Y * (inches)	3.159
Slot Height (inches)	0.080
Lip Thickness (inches)	0.145
Mass Flow Rate per Nozzle (slugs/sec)	1.228E-04
Non-dimensional Blowing Rate, Lambda	0.2521
Nozzle Reservoir Pressure (psia)	37.01
Exit Plane Pressure (psia)	2.064
Coolant Total Temperature (Rankine)	530

* See Shock Generator Diagram (Page A23)

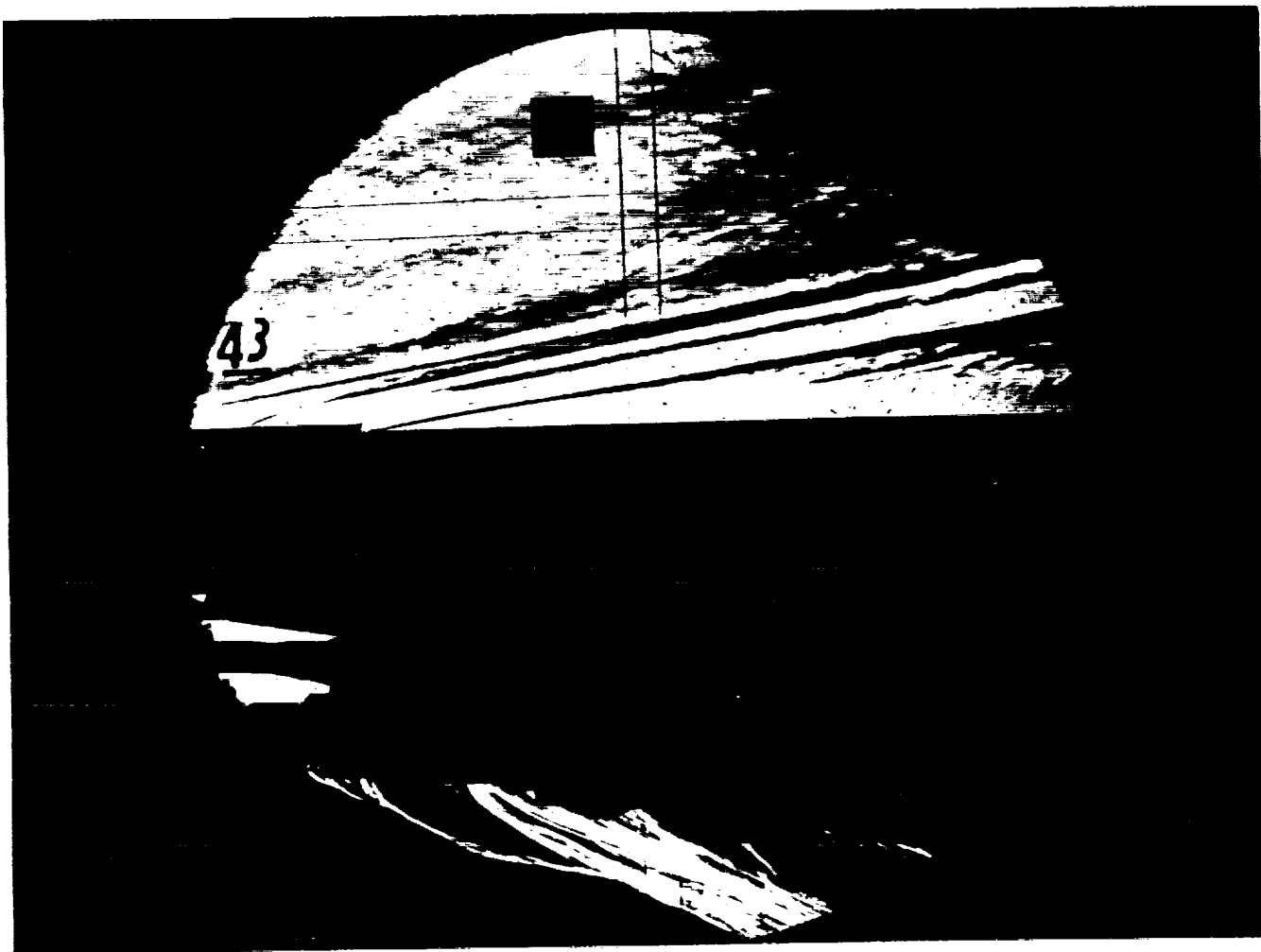
Run 41



HEAT TRANSFER vs Gauge Position
Run 41



PRESSURE vs Gauge Position
Run 41

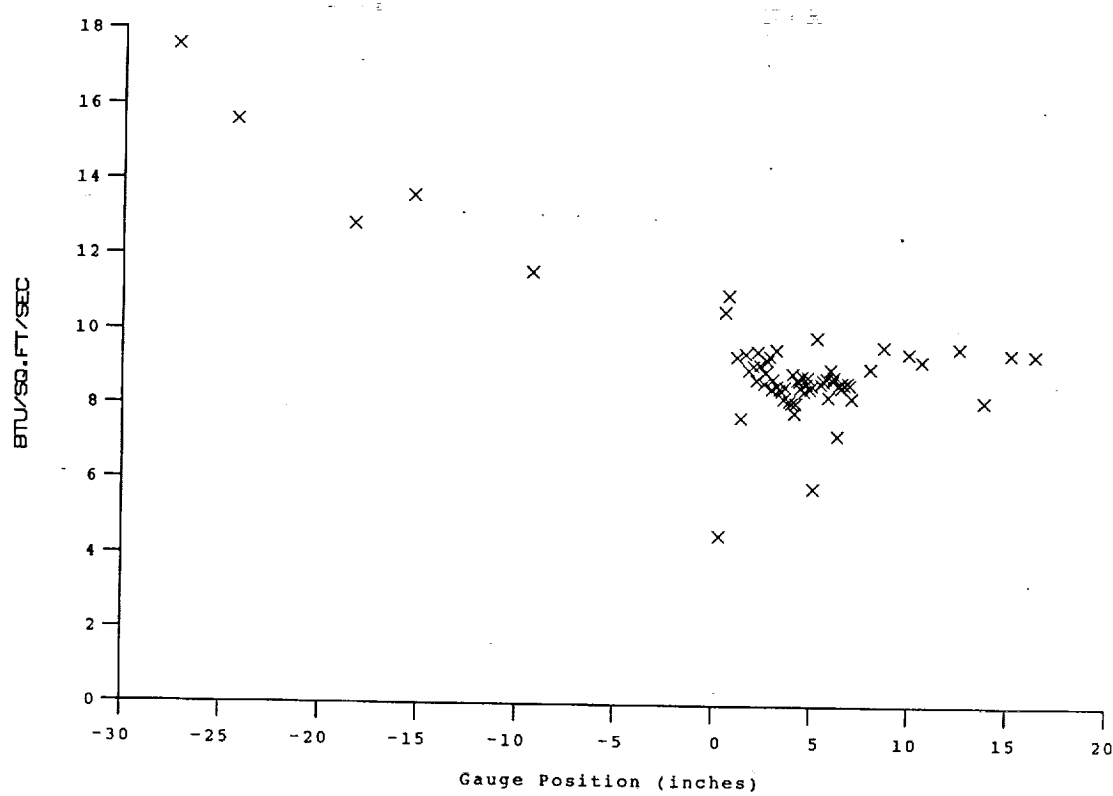


Test Conditions

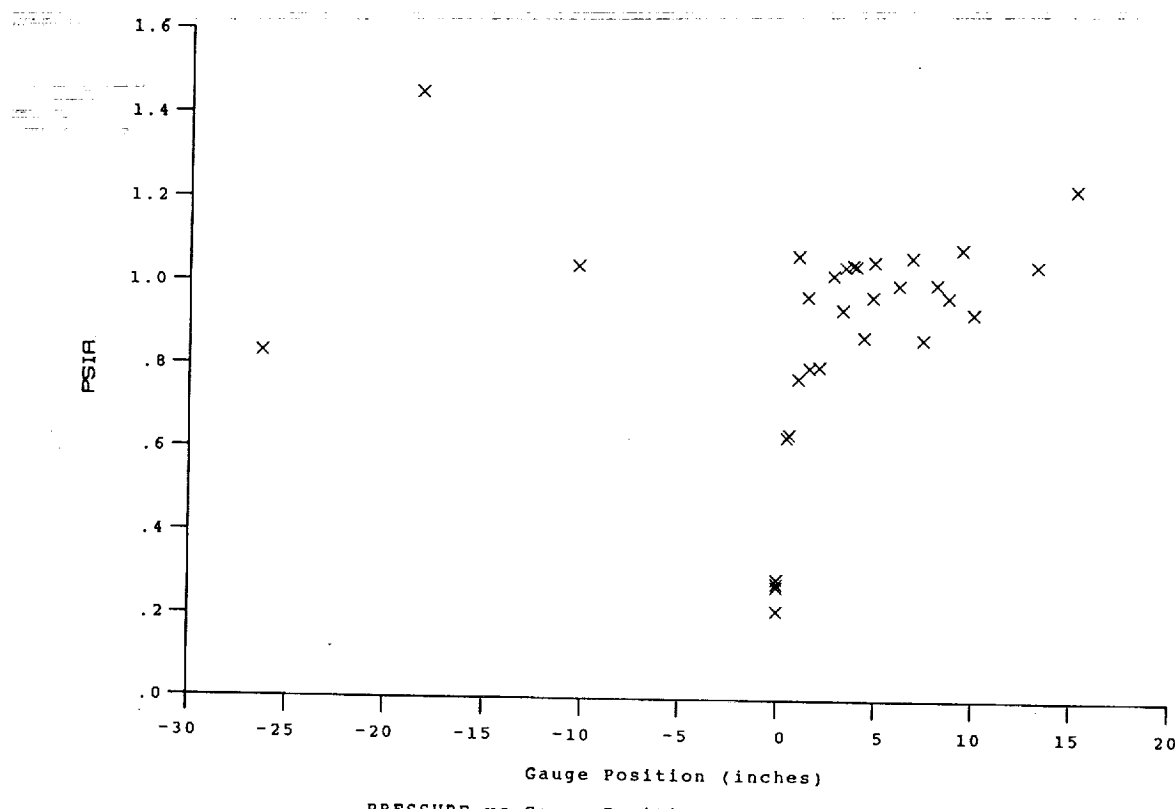
P_0 = 2.6710X10+3 PSIA	Reservoir Total Pressure
H_0 = 1.3967X10+7 (Ft/sec) ²	Reservoir Total Enthalpy
T_0 = 2.1813X10+3 degR	Reservoir Total Temperature
M = 6.4332	Freestream Mach Number
U = 4.9948X10+3 Ft/sec	Freestream Velocity
T = 2.5066X10+2 degR	Freestream Temperature
P = 1.0879 PSIA	Freestream Static Pressure
ρ_0 = 3.6423X10-4 Slugs/Ft ³	Freestream Density
μ = 2.0534X10-7 Slugs/Ft·sec	Freestream Viscosity
Re = 8.8597X10+6 1/Ft	Freestream Reynolds Number
P_{01} = 5.8836X10+1 PSIA	Pitot Pressure
Q = 3.1551X10+1 PSIA	Dynamic Pressure ($\rho_0 U^2/288$)
M_1 = 2.8891	Shock Tube Incident Shock Mach Number
H_w = 3.1832X10+6 (Ft/sec) ²	Wall Enthalpy [$C_p T_w$]
C_{Pf} = 3.1694X10-2 1/PSIA	Pressure to CP factor (1/Q)
CH_f = 3.9656X10-5 Ft ² -s/BTU	Heat Rate to CH factor (778/($\rho_0 U (H_0 - H_w)$))
$QoFR$ = 6.6273X10+1 BTU/Ft ² -s	Fay-Riddell Heat Transfer (.25' Diam Cylin.)

Model Parameter	Value
Slot Height (inches)	0.120
Lip Thickness (inches)	0.020
Non-dimensional Blowing Rate, Lambda **	0
** See Nozzle Geometry Diagram (Figure 9)	

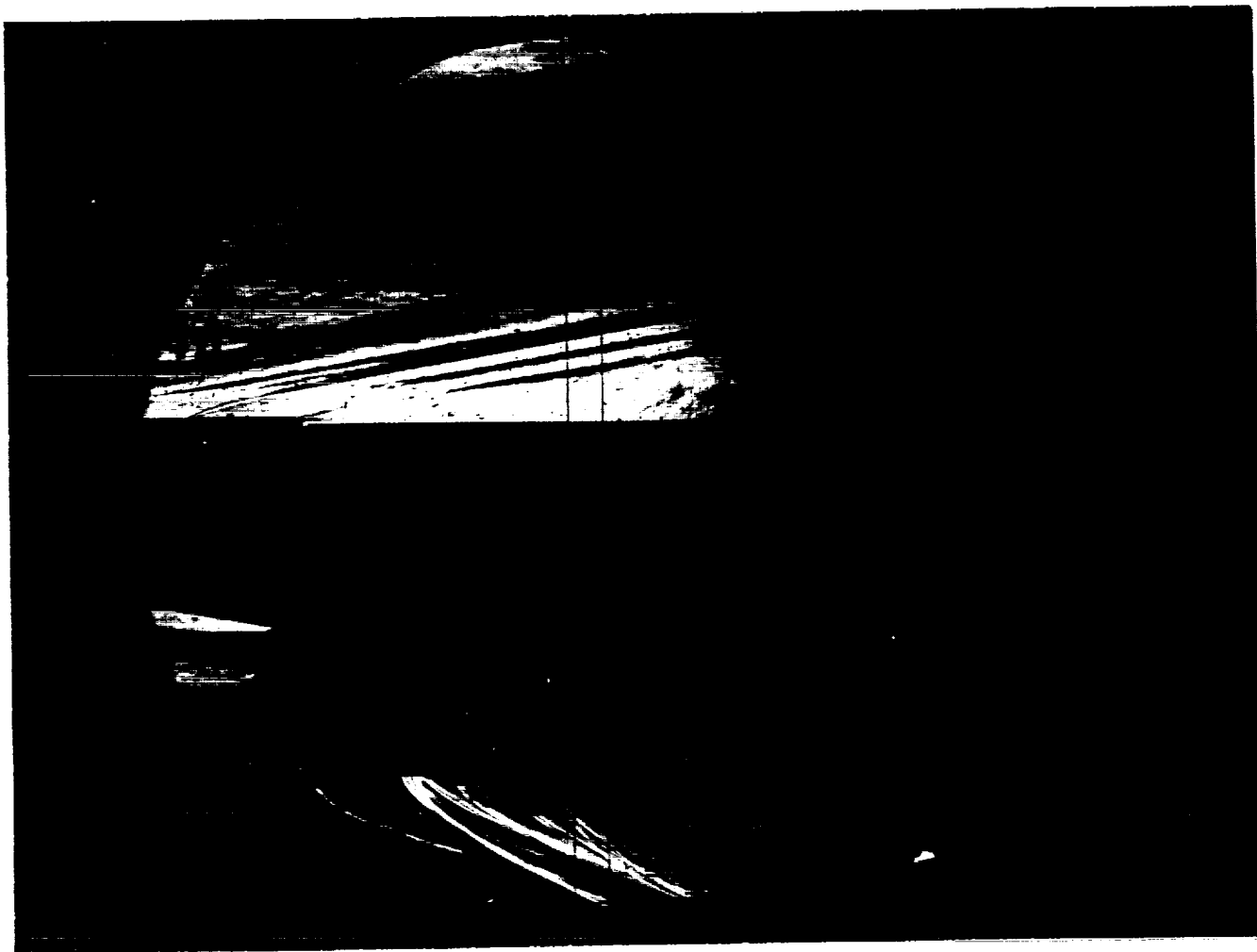
Run 43



HEAT TRANSFER vs Gauge Position
Run 43



PRESSURE vs Gauge Position
Run 43

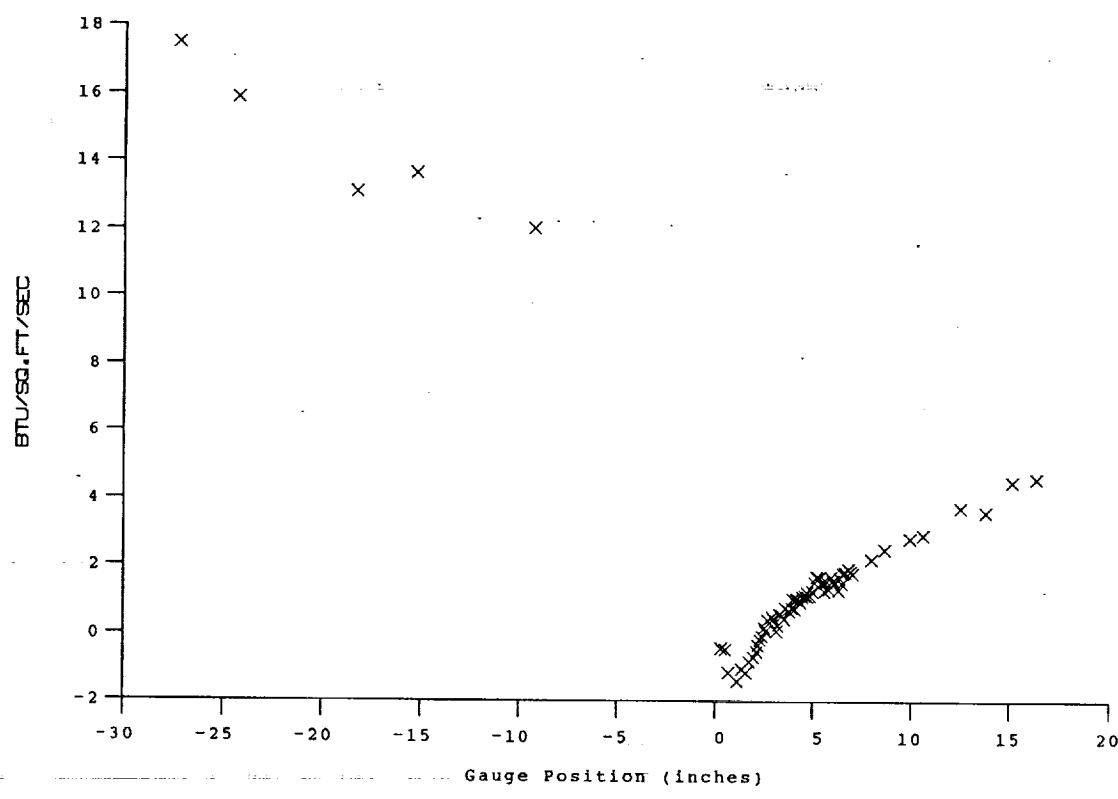


Test Conditions

$P_0 = 2.6232 \times 10^3$ PSIA Reservoir Total Pressure
 $H_0 = 1.4018 \times 10^7$ (Ft/sec)² Reservoir Total Enthalpy
 $T_0 = 2.1884 \times 10^3$ degR Reservoir Total Temperature
 $M = 6.4300$ Freestream Mach Number
 $U = 5.0037 \times 10^3$ Ft/sec Freestream Velocity
 $T = 2.5181 \times 10^2$ degR Freestream Temperature
 $P = 1.0697$ PSIA Freestream Static Pressure
 $\rho_0 = 3.5650 \times 10^{-4}$ Slugs/Ft³ Freestream Density
 $\mu = 2.0620 \times 10^{-7}$ Slugs/Ft-sec Freestream Viscosity
 $Re = 8.6508 \times 10^6$ 1/Ft Freestream Reynolds Number
 $P_0' = 5.7795 \times 10^1$ PSIA Pitot Pressure
 $Q = 3.0992 \times 10^1$ PSIA Dynamic Pressure ($\rho_0 U^2 / 288$)
 $M_1 = 2.8942$ Shock Tube Incident Shock Mach Number
 $H_w = 3.1832 \times 10^6$ (Ft/sec)² Wall Enthalpy ($C_p T_w$)
 $CP_F = 3.2266 \times 10^{-2}$ 1/PSIA Pressure to CP factor (1/Q)
 $CH_F = 4.0254 \times 10^{-5}$ Ft²-s/BTU Heat Rate to CH factor (778/($\rho_0 U (H_0 - H_w)$))
 $Q_{FR} = 6.6013 \times 10^1$ BTU/Ft²-s Fay-Riddell Heat Transfer (.25' Diam Cylin.)

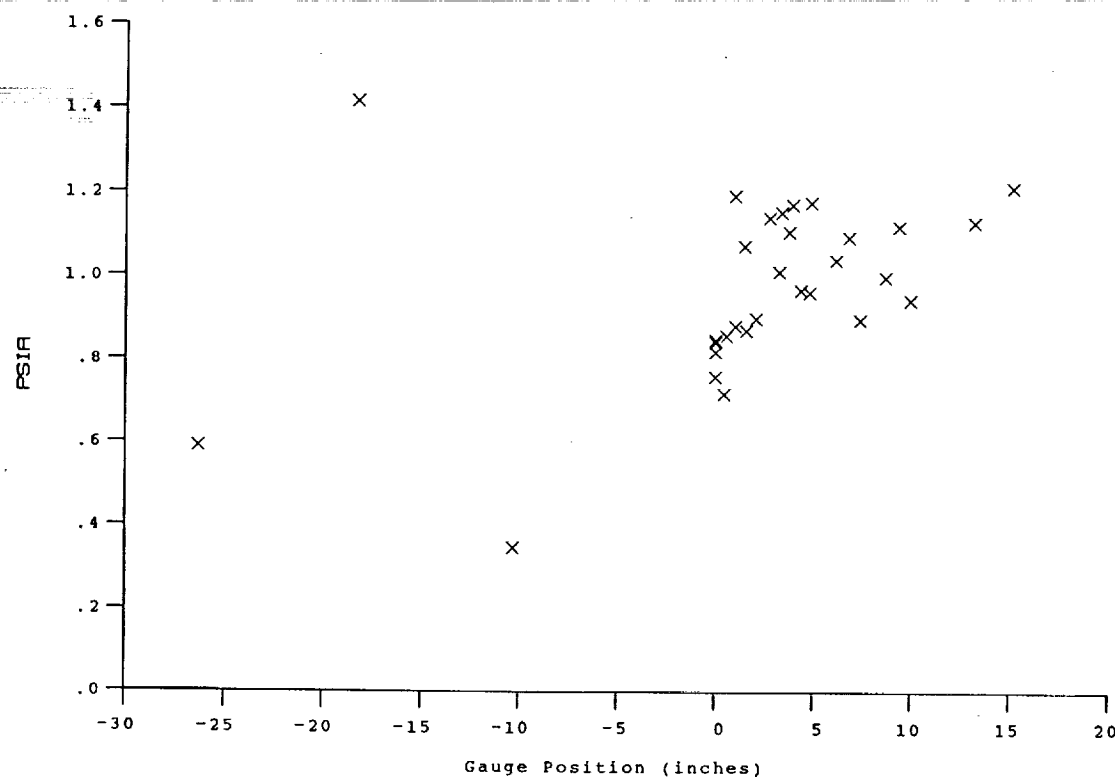
Model Parameter	Value
Slot Height (inches)	0.120
Lip Thickness (inches)	0.020
Mass Flow Rate per Nozzle (slugs/sec)	5.063E-05
Non-dimensional Blowing Rate, Lambda	0.0688
Nozzle Reservoir Pressure (psia)	13.38
Exit Plane Pressure (psia)	0.8191
Coolant Total Temperature (Rankine)	530

Run 44



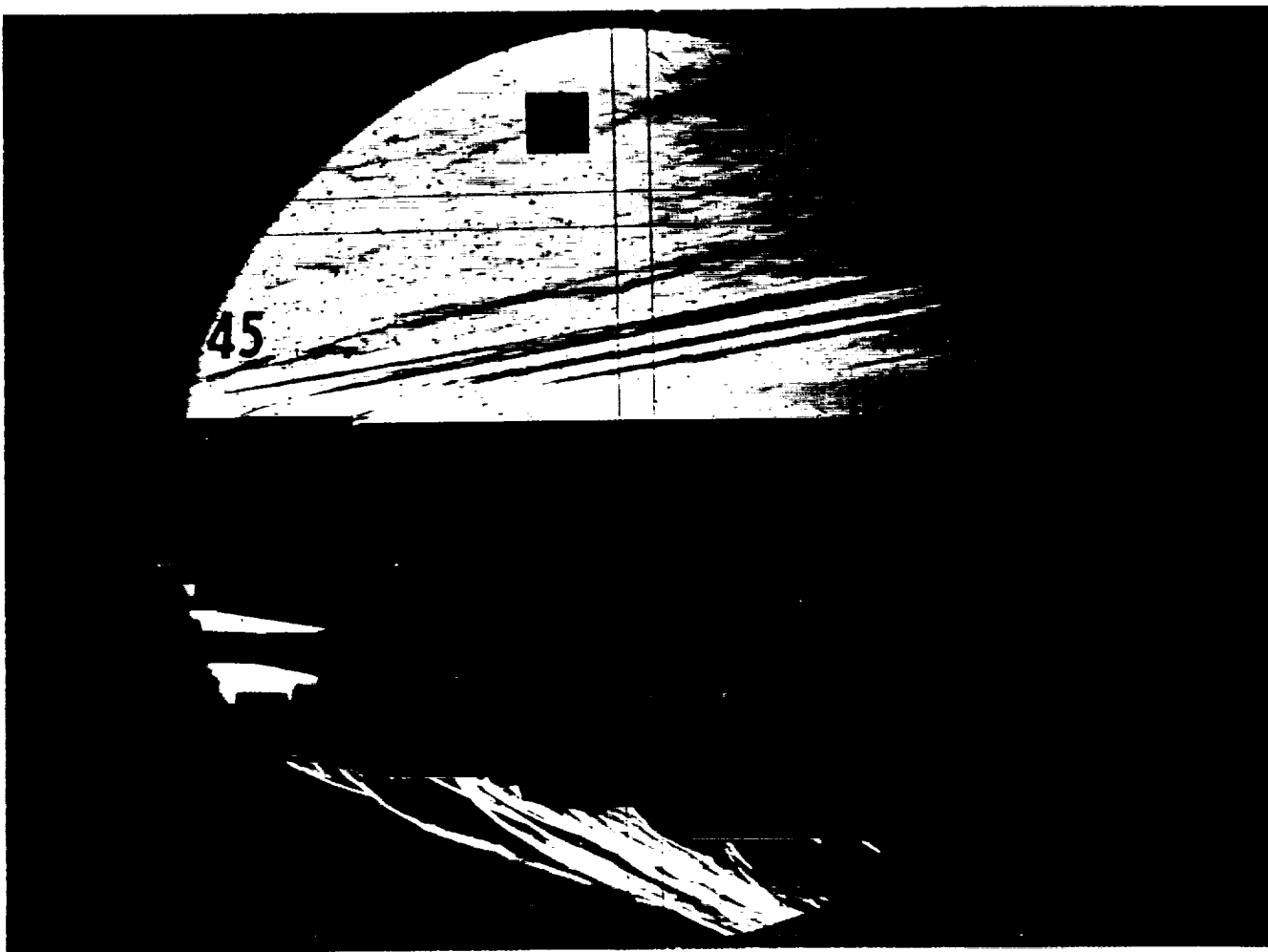
HEAT TRANSFER vs Gauge Position

Run 44



PRESSURE vs Gauge Position

Run 44

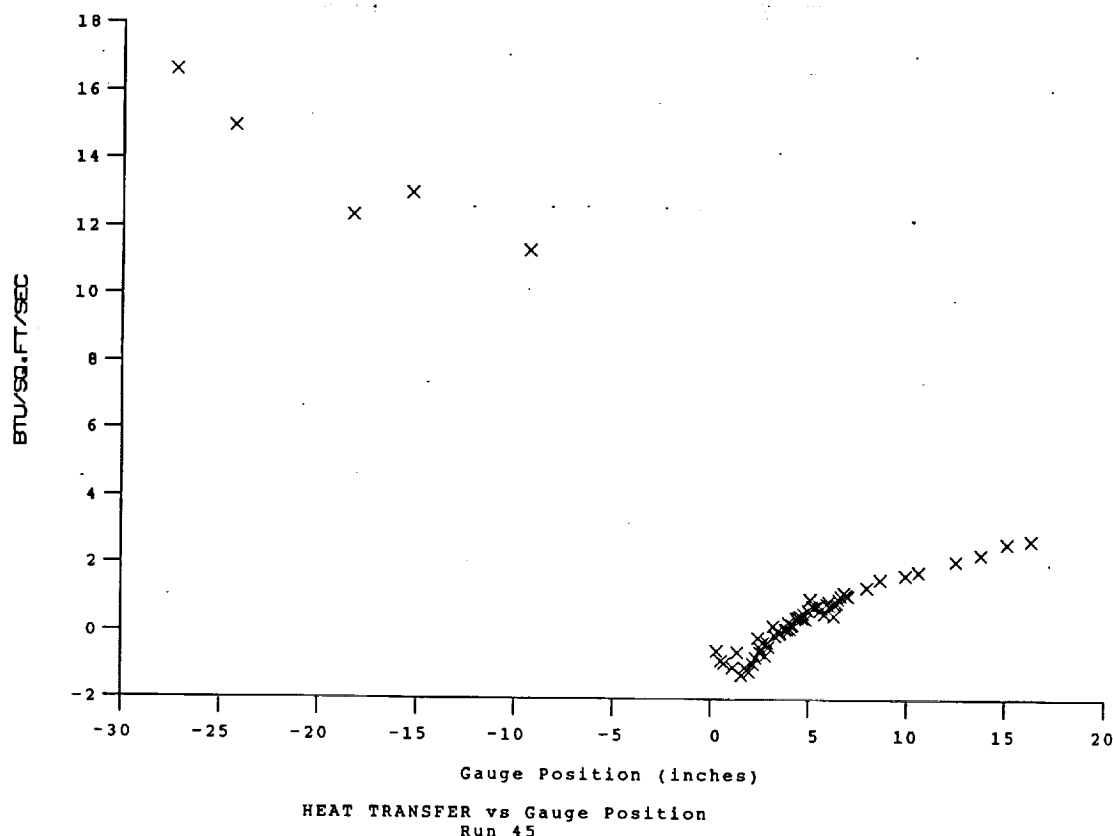


Test Conditions

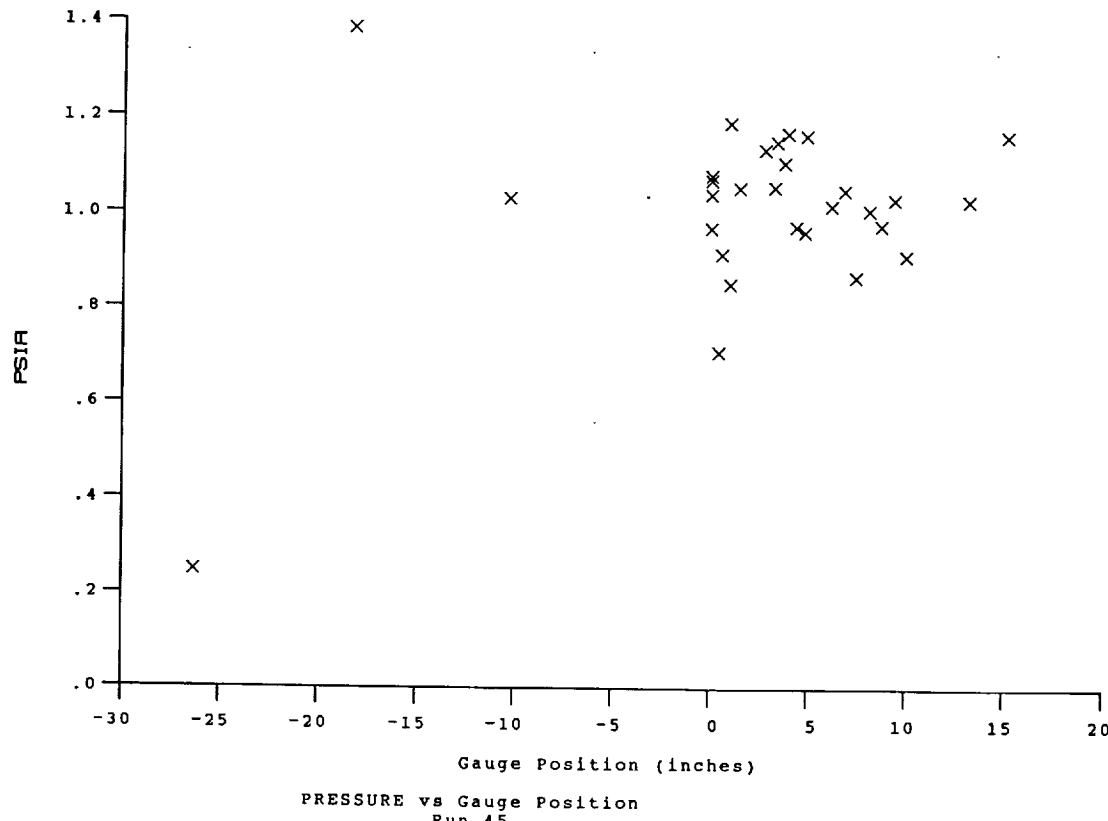
P _o = 2.4866X10+3 PSIA	Reservoir Total Pressure
H _o = 1.3787X10+7 (Ft/sec) ²	Reservoir Total Enthalpy
T _o = 2.1570X10+3 degR	Reservoir Total Temperature
M = 6.4319	Freestream Mach Number
U = 4.9624X10+3 Ft/sec	Freestream Velocity
T = 2.4752X10+2 degR	Freestream Temperature
P = 1.0138 PSIA	Freestream Static Pressure
Rho = 3.4374X10-4 Slugs/Ft ³	Freestream Density
Mu = 2.0297X10-7 Slugs/Ft-sec	Freestream Viscosity
Re = 8.4342X10-6 1/Ft	Freestream Reynolds Number
P _{o'} = 5.4798X10+1 PSIA	Pitot Pressure
Q = 2.9391X10+1 PSIA	Dynamic Pressure (Rho U ² /288)
M ₁ = 2.8564	Shock Tube Incident Shock Mach Number
H _w = 3.1832X10-6 (Ft/sec) ²	Wall Enthalpy (Cp Tw)
C _{PF} = 3.4023X10-2 1/PSIA	Pressure to CP factor (1/Q)
C _{HF} = 4.3013X10-5 Ft ² -s/BTU	Heat Rate to CH factor (778/(Rho U (H _o -H _w)))
CoFR = 6.2832X10+1 BTU/Ft ² -s	Fay-Riddell Heat Transfer (.25' Diam Cylin.)

Model Parameter	Value
Slot Height (inches)	0.120
Lip Thickness (inches)	0.020
Mass Flow Rate per Nozzle (slugs/sec)	7.454E-05
Non-dimensional Blowing Rate, Lambda	0.1060
Nozzle Reservoir Pressure (psia)	18.32
Exit Plane Pressure (psia)	1.042
Coolant Total Temperature (Rankine)	530

Run 45



HEAT TRANSFER vs Gauge Position
Run 45



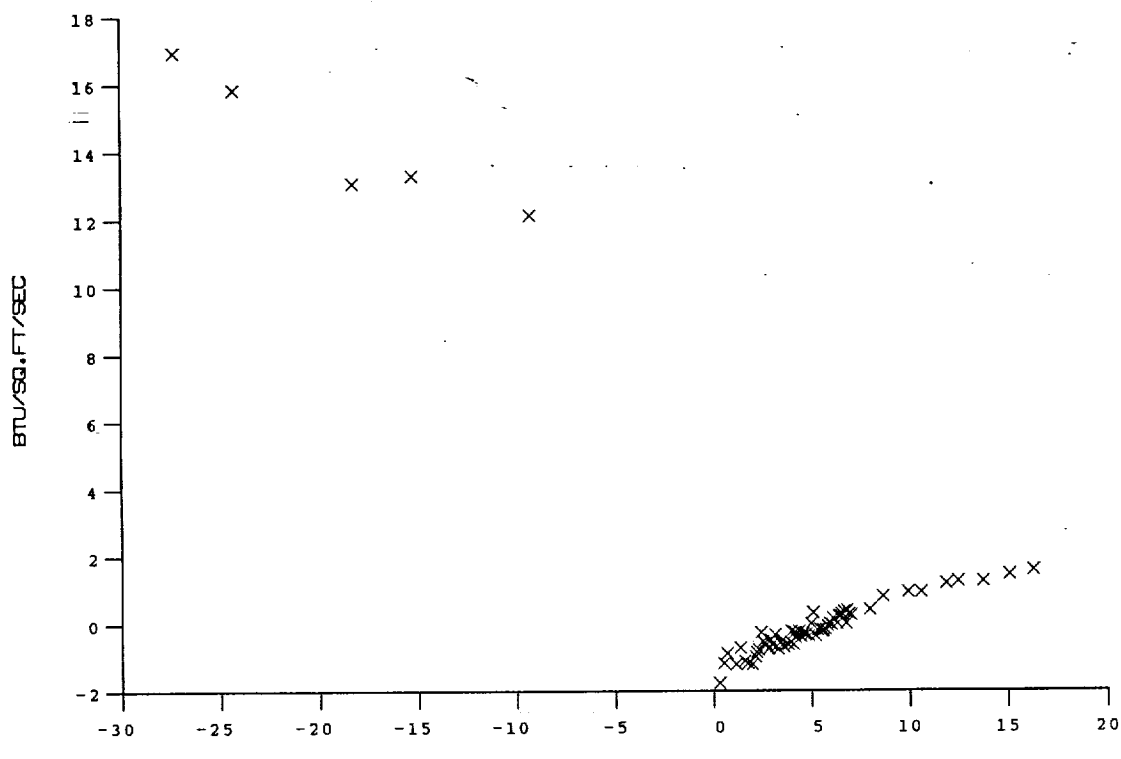
PRESSURE vs Gauge Position
Run 45

Test Conditions

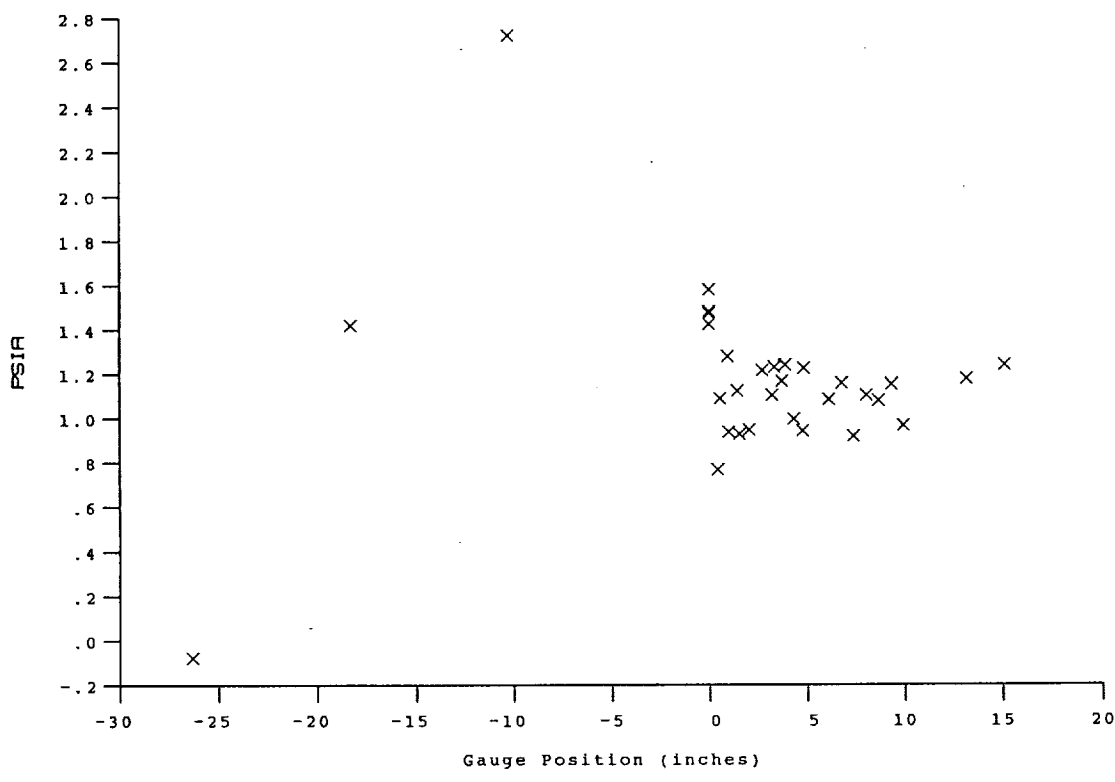
M_i = 2.8909
P_o = 2.6399X10+3 PSIA
H_o = 1.4084X10+7 (Ft/sec)²
T_o = 2.1983X10+3 Degrees R
M = 6.4314
U = 5.0156X10+3 Ft/sec
T = 2.5290X10+2 Degrees R
P = 1.0739
Q = 3.1127X10+1 PSIA
Rho = 3.5636X10-4 Slugs/Ft³
Mu = 2.0702X10-7 Slugs/Ft²-sec
Re = 8.6340X10+6 1/Ft
P_{o'} = 5.8052X10+1 PSIA

Model Parameter	Value
Slot Height (inches)	0.120
Lip Thickness (inches)	0.020
Mass Flow Rate per Nozzle (slugs/sec)	1.139E-04
Non-dimensional Blowing Rate, Lambda	0.1546
Nozzle Reservoir Pressure (psia)	28.12
Exit Plane Pressure (psia)	1.498
Coolant Total Temperature (Rankine)	530

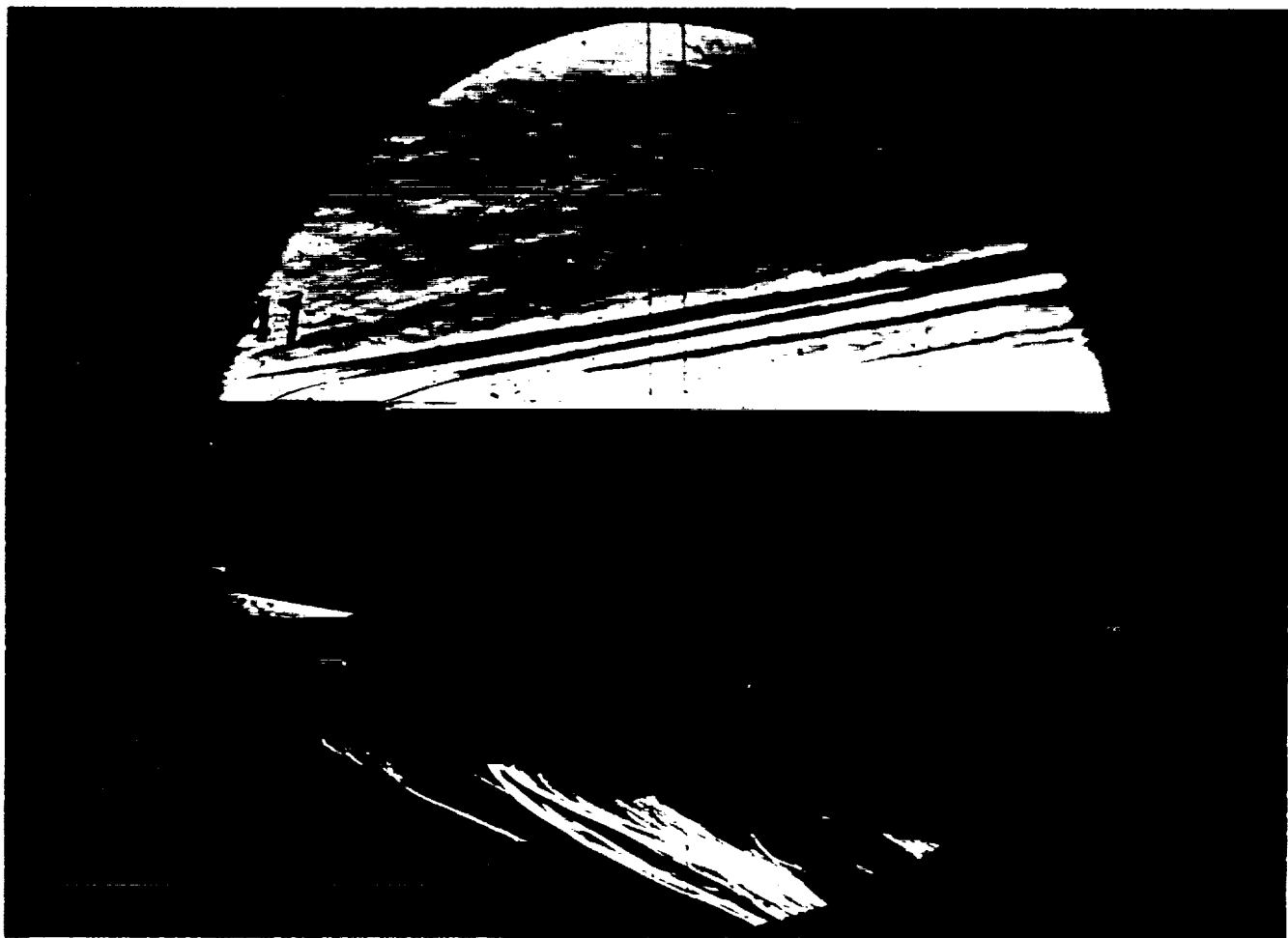
Run 46



HEAT TRANSFER vs Gauge Position
Run 46



PRESSURE vs Gauge Position
Run 46

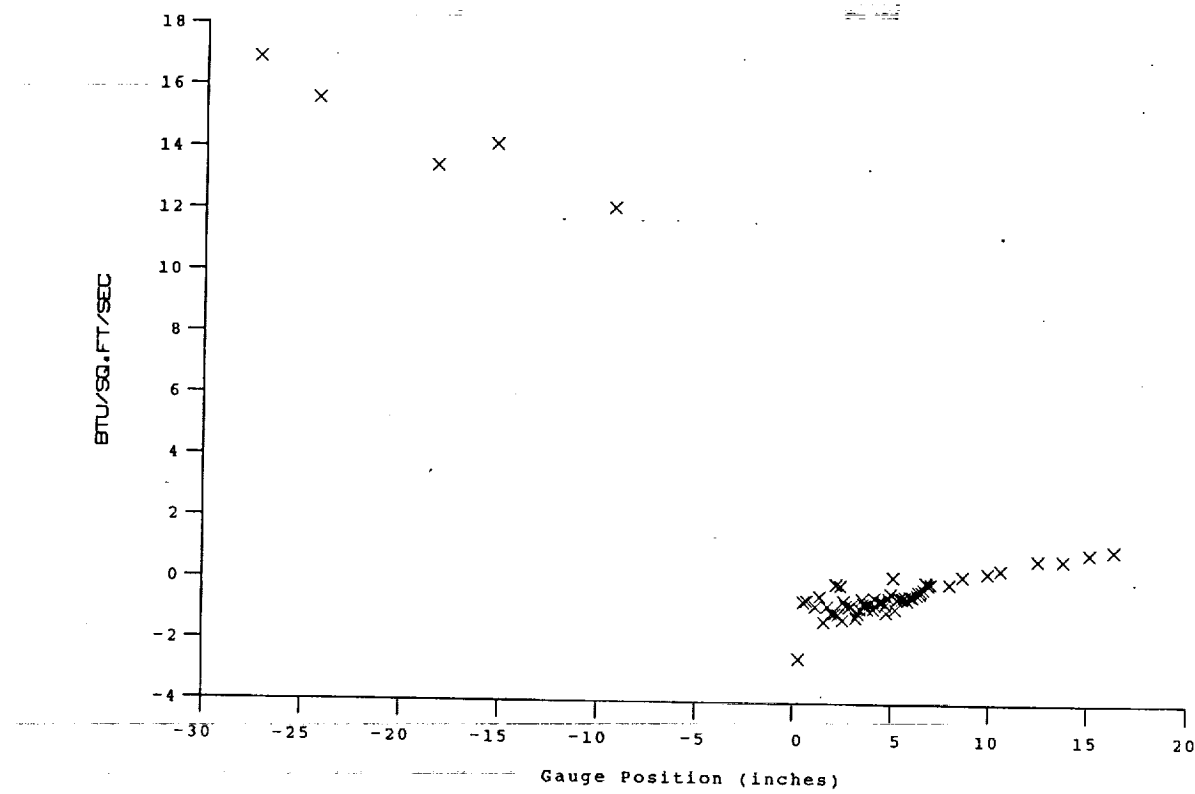


Test Conditions

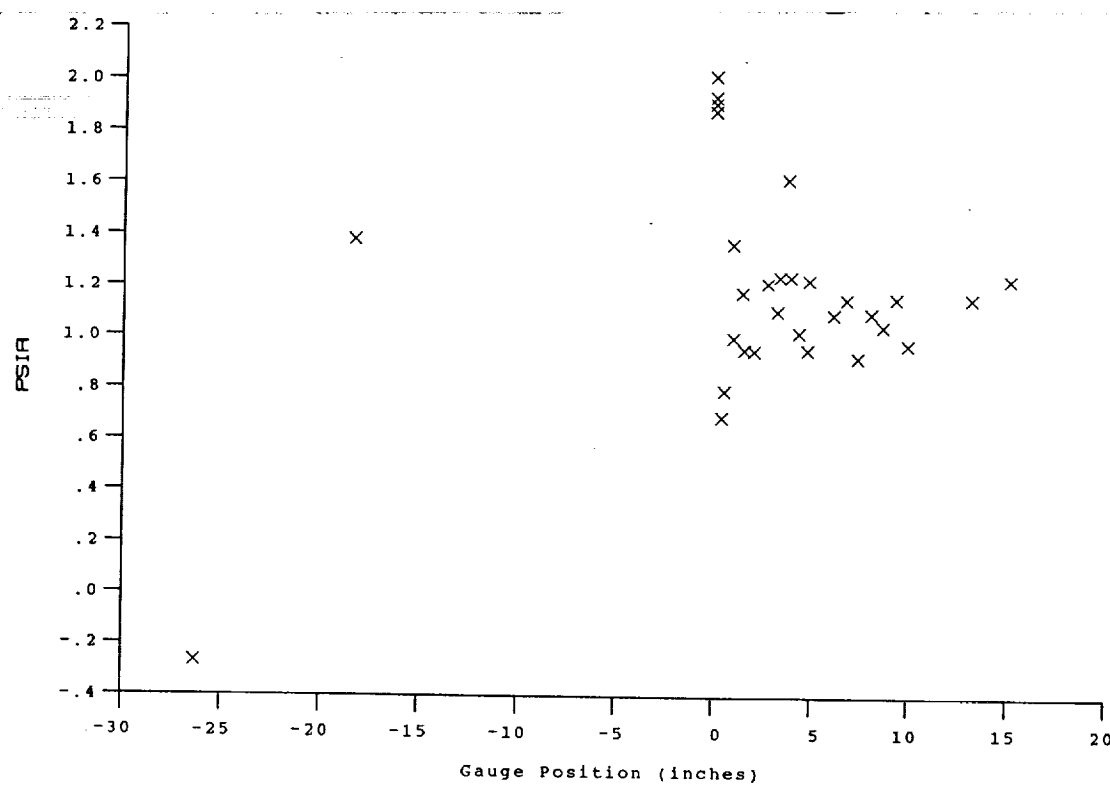
P_0 = 2.5898X10+3 PSIA	Reservoir Total Pressure
H_0 = 1.3974X10+7 (Ft/sec) ²	Reservoir Total Enthalpy
T_0 = 2.1821X10+3 degR	Reservoir Total Temperature
M = 6.4290	Freestream Mach Number
U = 4.9957X10+3 Ft/sec	Freestream Velocity
T = 2.5109X10+2 degR	Freestream Temperature
P = 1.0573 PSIA	Freestream Static Pressure
ρ_0 = 3.5337X10-4 Slugs/Ft ³	Freestream Density
μ_0 = 2.0566X10-7 Slugs/Ft-sec	Freestream Viscosity
Re = 8.5840X10+6 1/Ft	Freestream Reynolds Number
P_{0f} = 5.7104X10+1 PSIA	Pitot Pressure
Q = 3.0623X10+1 PSIA	Dynamic Pressure ($\rho_0 U^2/288$)
M_1 = 2.8918	Shock Tube Incident Shock Mach Number
H_w = 3.1832X10+6 (Ft/sec) ²	Wall Enthalpy (Cp Tw)
Cp_f = 3.2657X10-2 1/PSIA	Pressure to CP factor (1/Q)
CH_f = 4.0841X10-5 Ft ² -s/BTU	Heat Rate to CH factor (778/($\rho_0 U (H_0 - H_w)$))
Q_{FR} = 6.5335X10+1 BTU/Ft ² -s	Fay-Riddell Heat Transfer (.25' Diam Cylin.)

Model Parameter	Value
Slot Height (inches)	0.120
Lip Thickness (inches)	0.020
Mass Flow Rate per Nozzle (slugs/sec)	1.576E-04
Non-dimensional Blowing Rate, Lambda	0.2165
Nozzle Reservoir Pressure (psia)	38.24
Exit Plane Pressure (psia)	1.944
Coolant Total Temperature (Rankine)	530

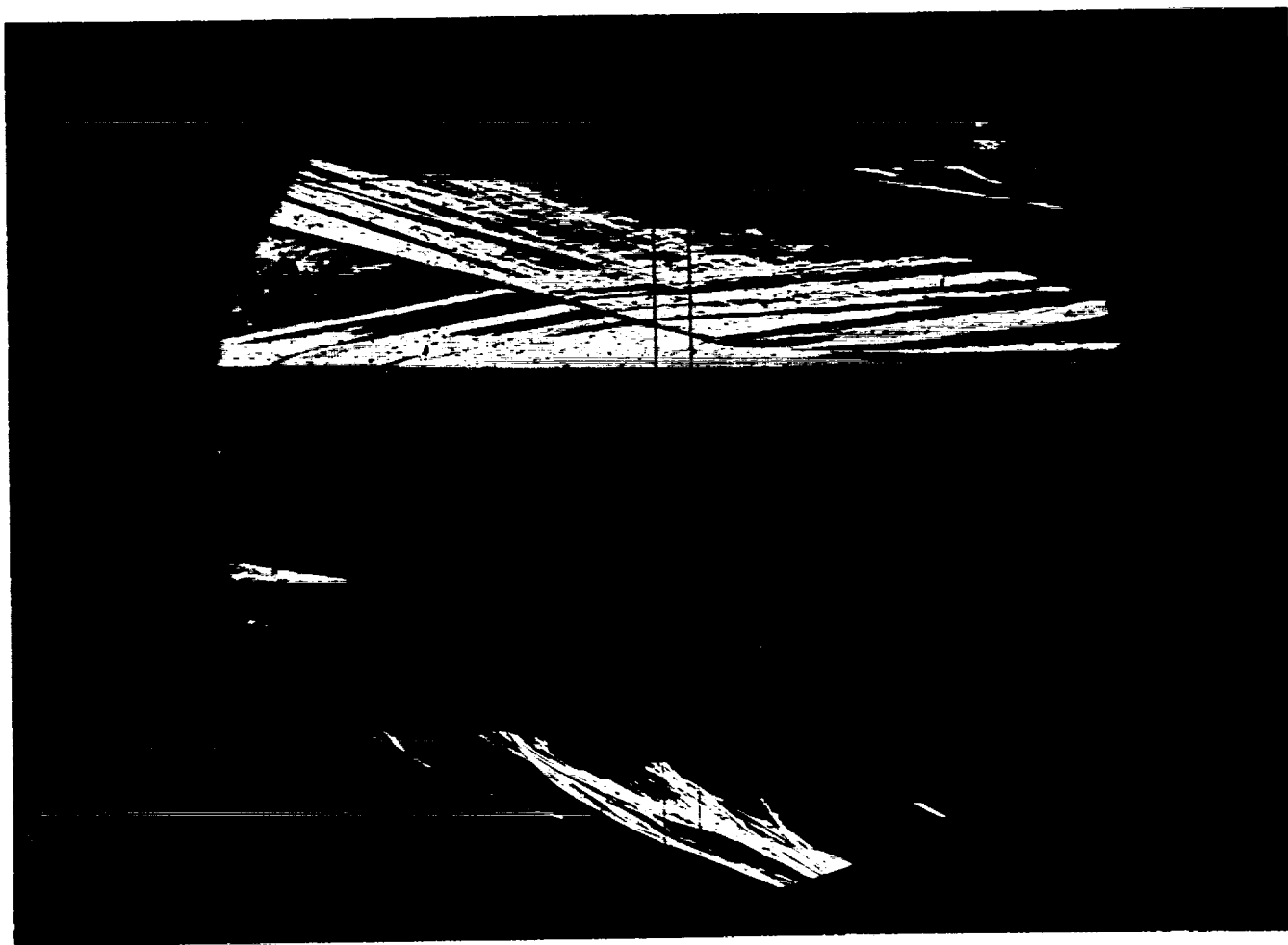
Run 47



HEAT TRANSFER vs Gauge Position
Run 47



PRESSURE vs Gauge Position
Run 47

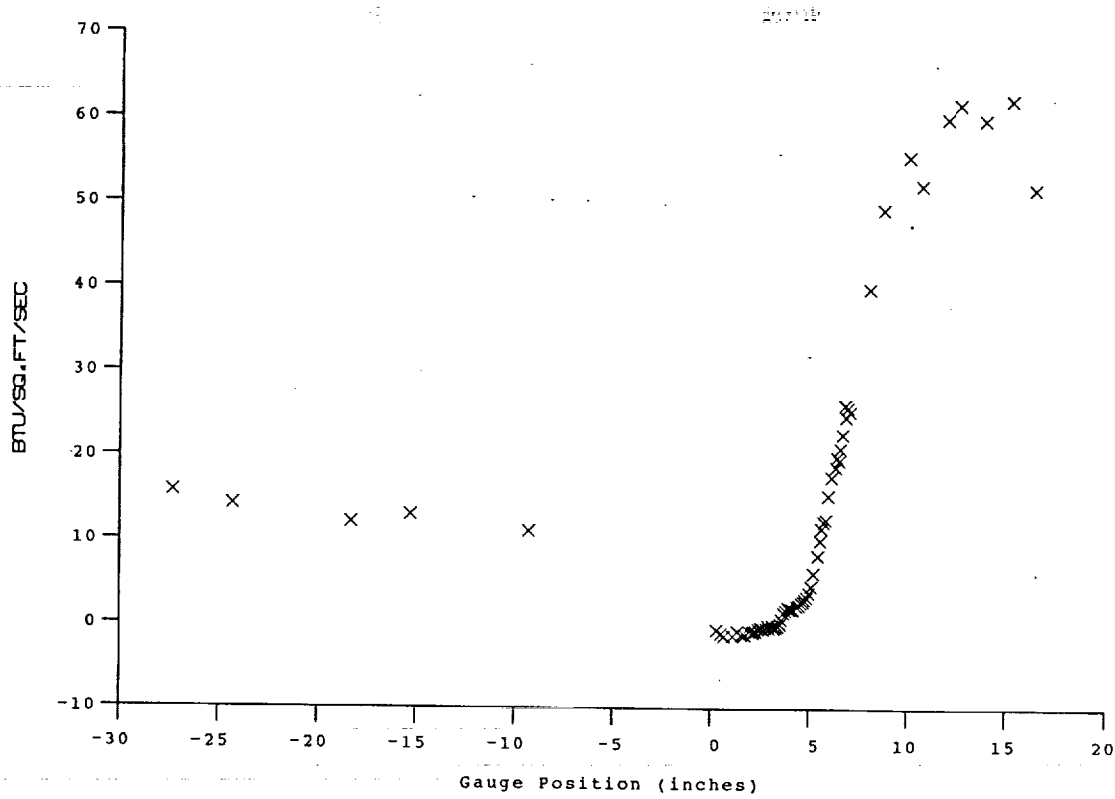


Test Conditions

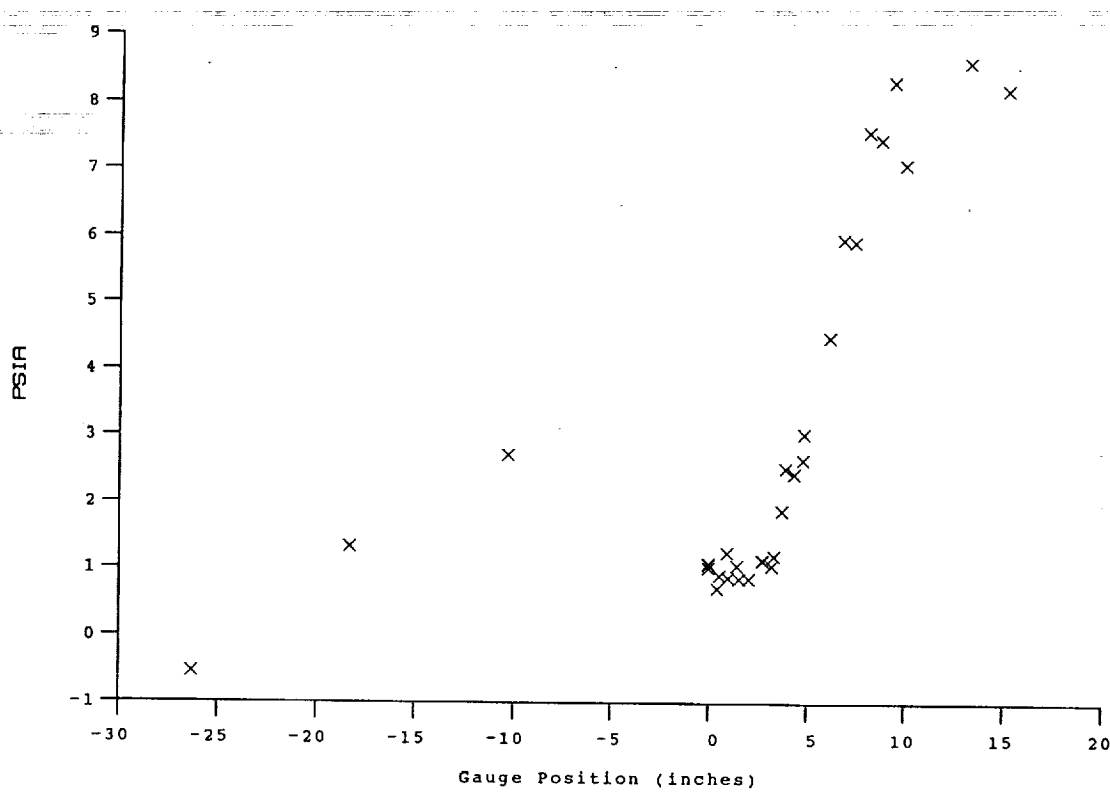
$P_0 = 2.6125 \times 10^3$ PSIA Reservoir Total Pressure
 $H_0 = 1.4158 \times 10^7$ (Ft/sec)² Reservoir Total Enthalpy
 $T_0 = 2.2079 \times 10^3$ degR Reservoir Total Temperature
 $M = 6.4264$ Freestream Mach Number
 $U = 5.0282 \times 10^3$ Ft/sec Freestream Velocity
 $T = 2.5457 \times 10^2$ degR Freestream Temperature
 $P = 1.0658$ PSIA Freestream Static Pressure
 $\rho_0 = 3.5135 \times 10^{-4}$ Slugs/Ft³ Freestream Density
 $\mu = 2.0827 \times 10^{-7}$ Slugs/Ft·sec Freestream Viscosity
 $Re = 8.4826 \times 10^6$ 1/ft Freestream Reynolds Number
 $P_{0'} = 5.7528 \times 10^1$ PSIA Pitot Pressure
 $Q = 3.0844 \times 10^1$ PSIA Dynamic Pressure ($\rho_0 U^2 / 288$)
 $M_1 = 2.9078$ Shock Tube Incident Shock Mach Number
 $H_w = 3.1832 \times 10^{-6}$ (Ft/sec)² Wall Enthalpy ($C_p T_w$)
 $CP_f = 3.2421 \times 10^{-2}$ 1/PSIA Pressure to CP factor (1/Q)
 $CH_f = 4.0126 \times 10^{-5}$ Ft²·s/BTU Heat Rate to CH factor ($778 / (\rho_0 U (H_0 - H_w))$)
 $QoFR = 6.6760 \times 10^1$ BTU/Ft²·s Fay-Riddell Heat Transfer (.25' Diam Cylin.)

Model Parameter	Value
Horizontal Shock Generator Angle (degrees)	8.0
X * (inches)	6.880
Y * (inches)	3.167
Slot Height (inches)	0.120
Lip Thickness (inches)	0.020
Mass Flow Rate per Nozzle (slugs/sec)	7.414E-05
Non-dimensional Blowing Rate, Lambda	0.1018
Nozzle Reservoir Pressure (psia)	18.38
Exit Plane Pressure (psia)	1.086
Coolant Total Temperature (Rankine)	530
* See Shock Generator Diagram (Page A23)	

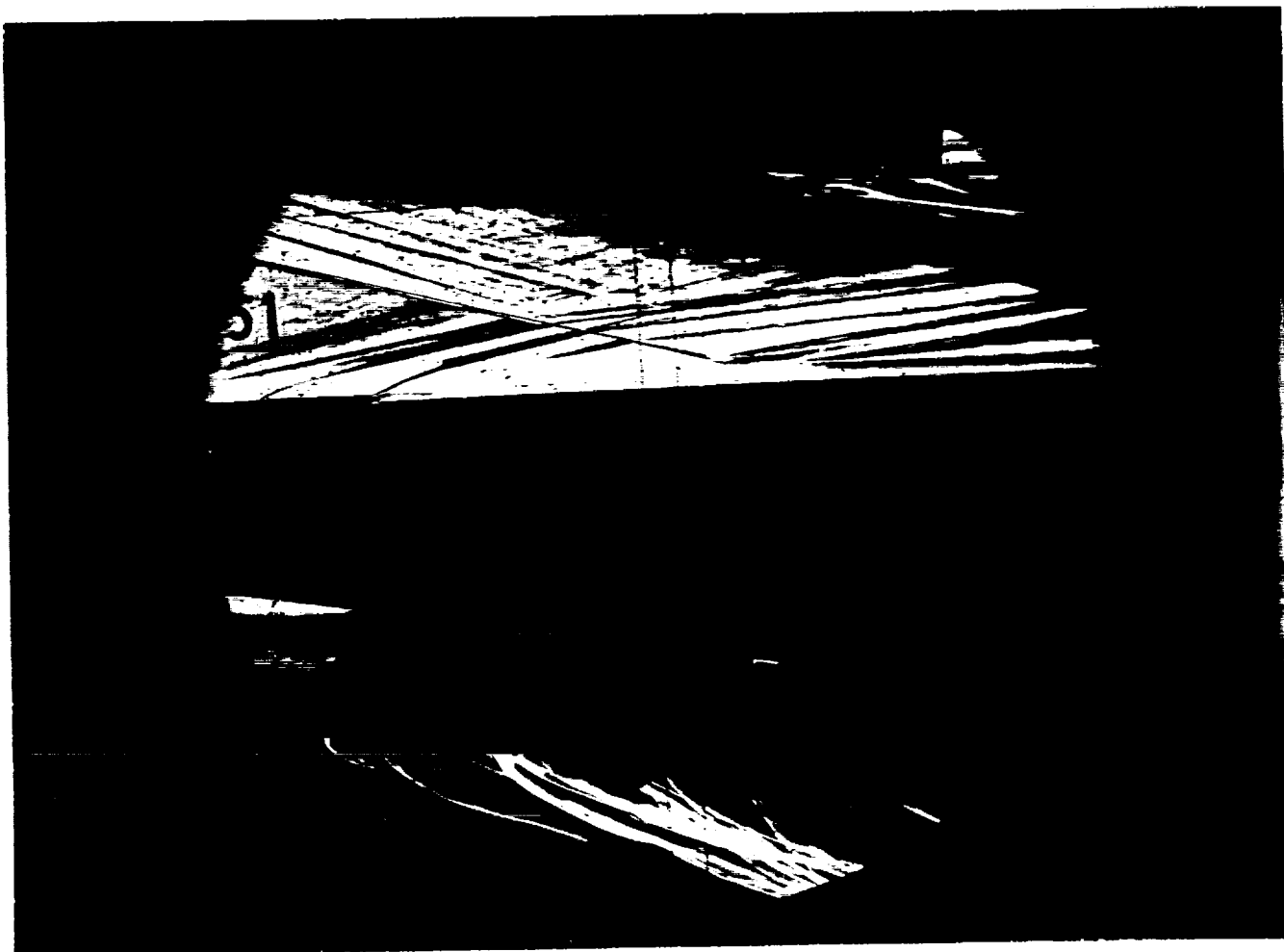
Run 50



HEAT TRANSFER vs Gauge Position
Run 50



PRESSURE vs Gauge Position
Run 50

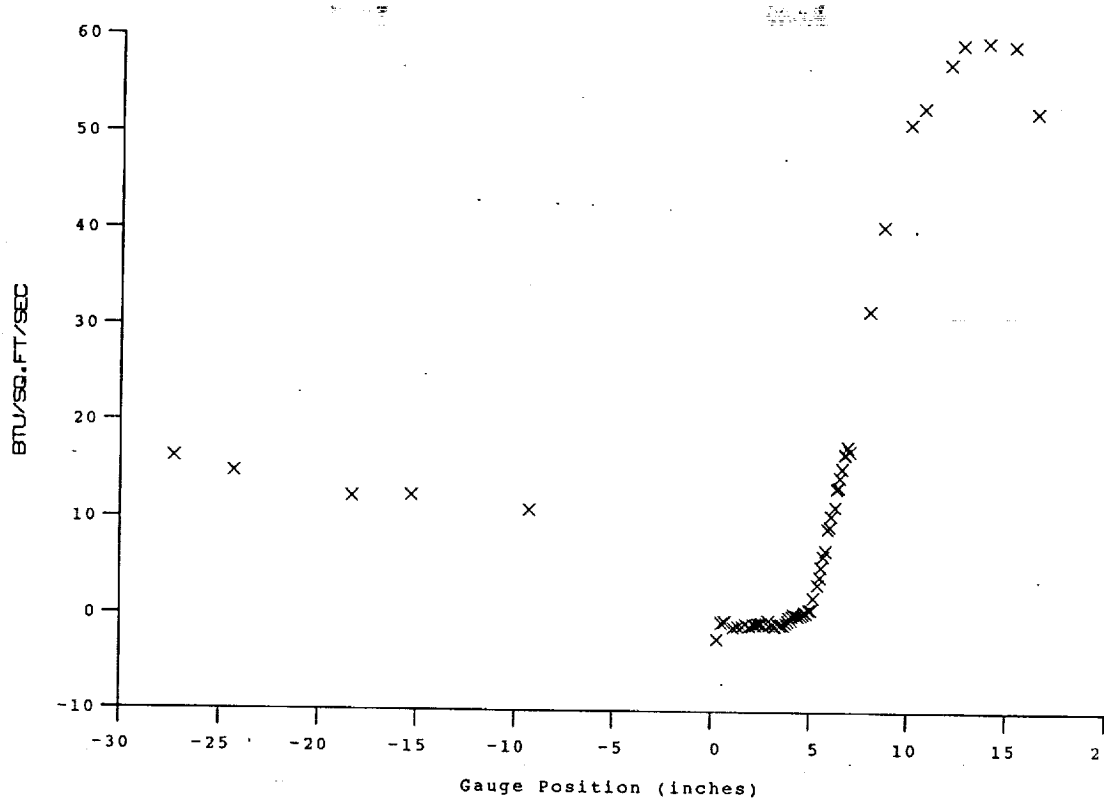


Test Conditions

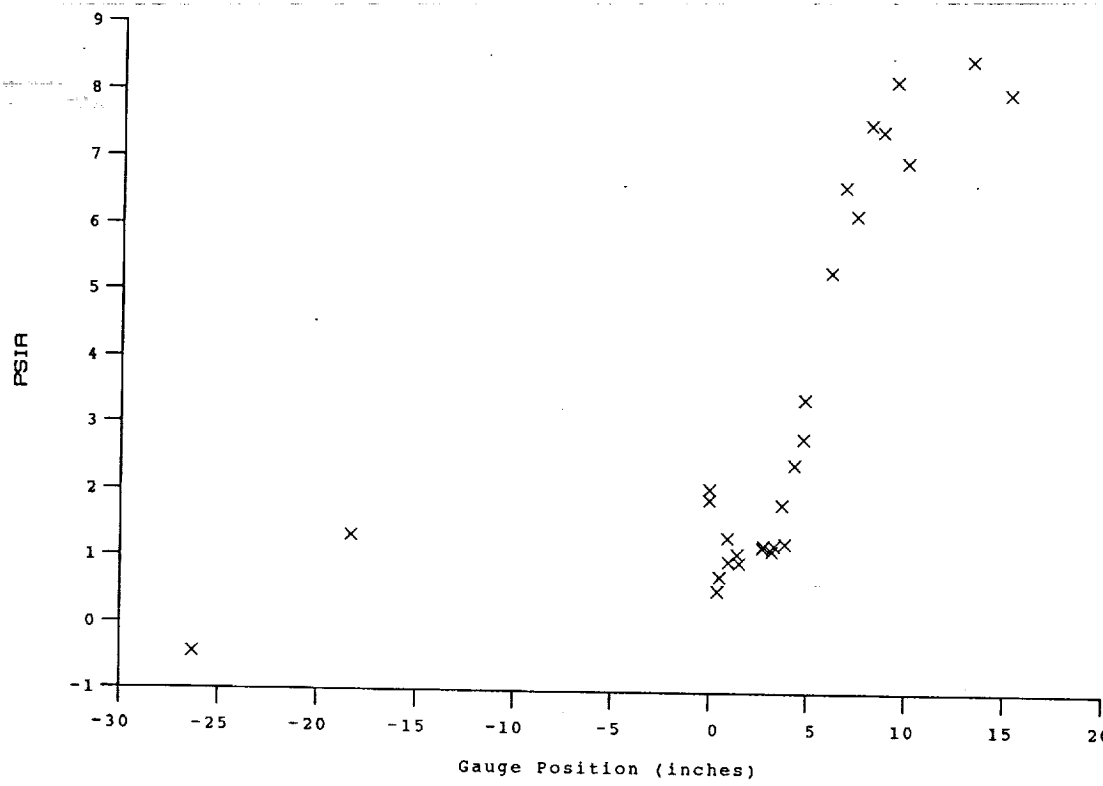
P ₀ = 2.5466X10+3 PSIA	Reservoir Total Pressure
H ₀ = 1.3778X10+7 (Ft/sec) ²	Reservoir Total Enthalpy
T ₀ = 2.1561X10+3 degR	Reservoir Total Temperature
M = 6.4362	Freestream Mach Number
U = 4.9612X10+3 Ft/sec	Freestream Velocity
T = 2.4707X10+2 degR	Freestream Temperature
P = 1.0355 PSIA	Freestream Static Pressure
Rho = 3.5173X10-4 Slugs/Ft ³	Freestream Density
Mu = 2.0263X10-7 Slugs/Ft·sec	Freestream Viscosity
Re = 8.6118X10+6 1/Ft	Freestream Reynolds Number
Po' = 5.6044X10+1 PSIA	Pitot Pressure
Q = 3.0060X10+1 PSIA	Dynamic Pressure (Rho U ² /288)
MI = 2.8506	Shock Tube Incident Shock Mach Number
Hw = 3.1832X10+6 (Ft/sec) ²	Wall Enthalpy (Cp Tw)
CPf = 3.3267X10-2 1/PSIA	Pressure to CP factor (1/Q)
CHf = 4.2081X10-5 Ft ² -s/BTU	Heat Rate to CH factor (778/(Rho U (H ₀ -Hw)))
QoFR = 6.3487X10+1 BTU/Ft ² -s	Fay-Riddell Heat Transfer (.25' Diam Cylin.)

Model Parameter	Value
Horizontal Shock Generator Angle (degrees)	8.0
X * (inches)	6.880
Y * (inches)	3.167
Slot Height (inches)	0.120
Lip Thickness (inches)	0.020
Mass Flow Rate per Nozzle (slugs/sec)	1.710E-04
Non-dimensional Blowing Rate, Lambda	0.2377
Nozzle Reservoir Pressure (psia)	37.61
Exit Plane Pressure (psia)	1.958
Coolant Total Temperature (Rankine)	530
* See Shock Generator Diagram (Page A23)	

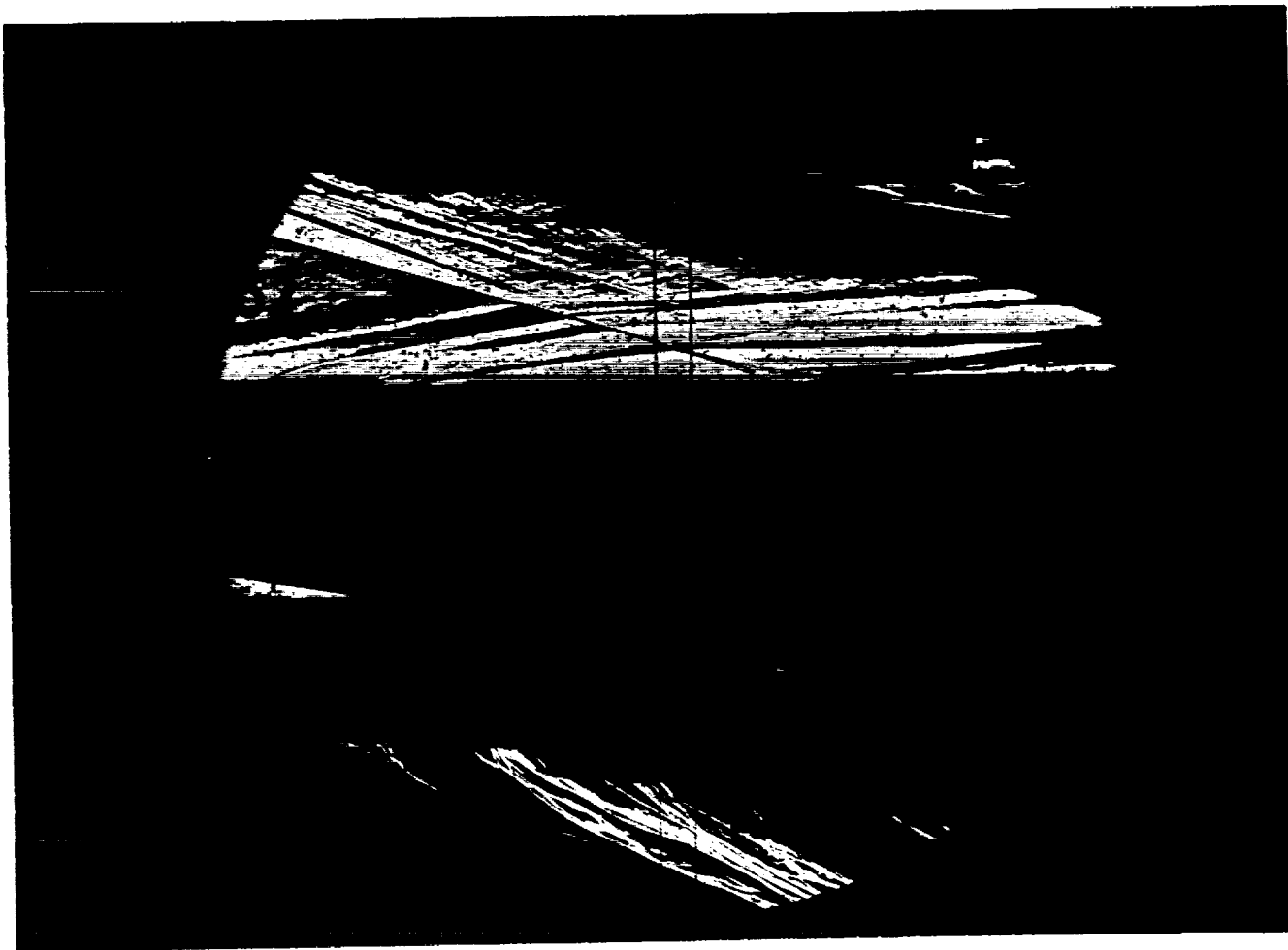
Run 51



HEAT TRANSFER vs Gauge Position
Run 51



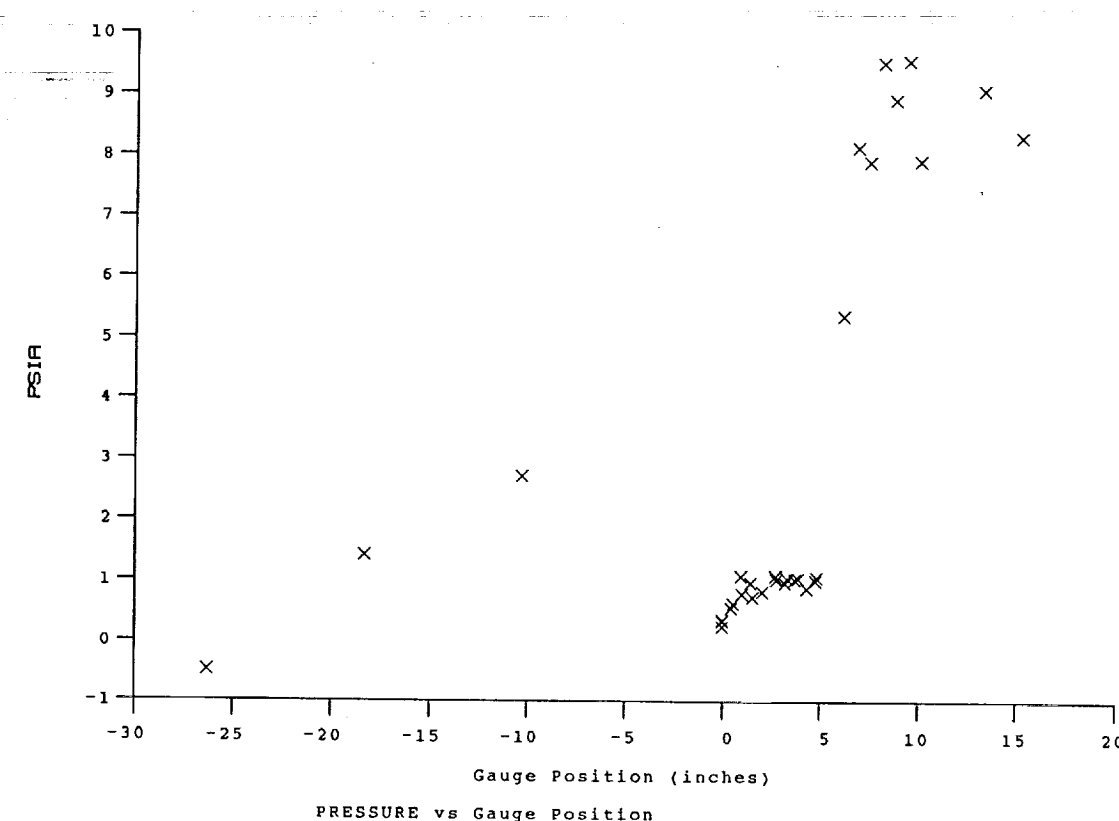
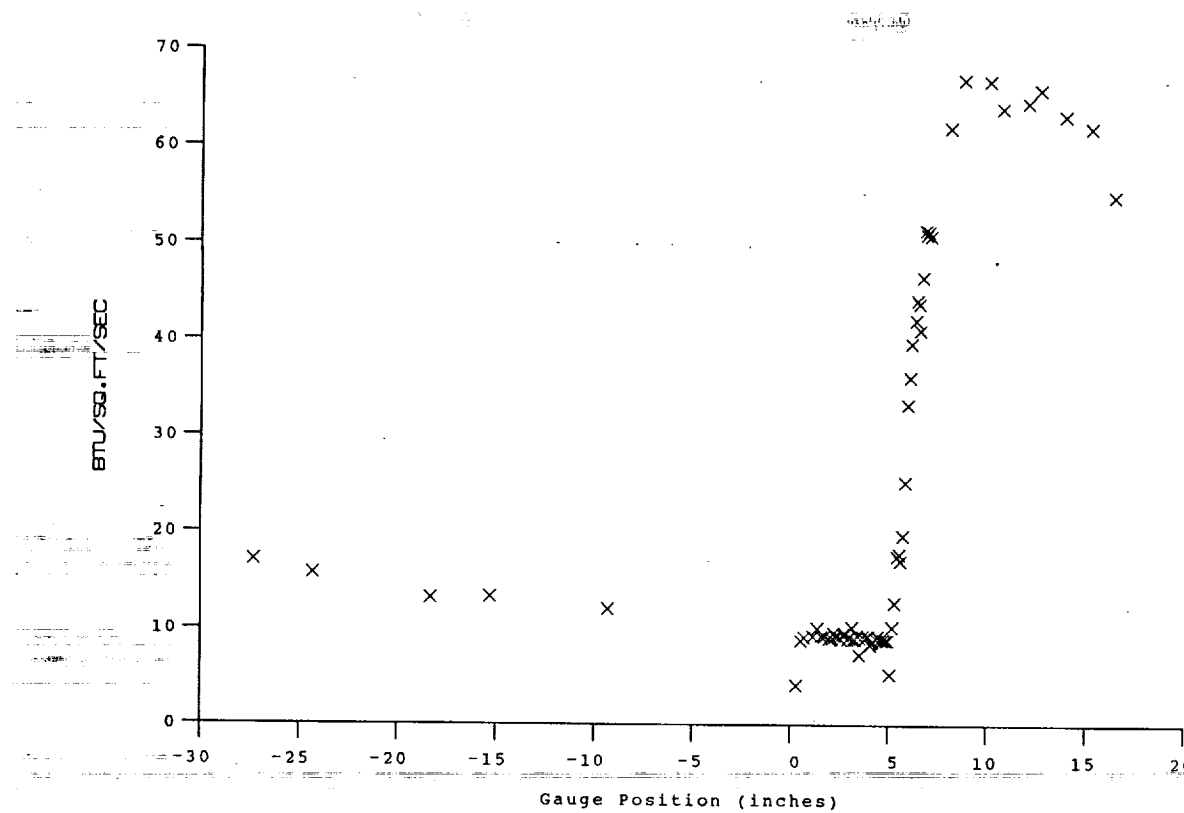
PRESSURE vs Gauge Position
Run 51

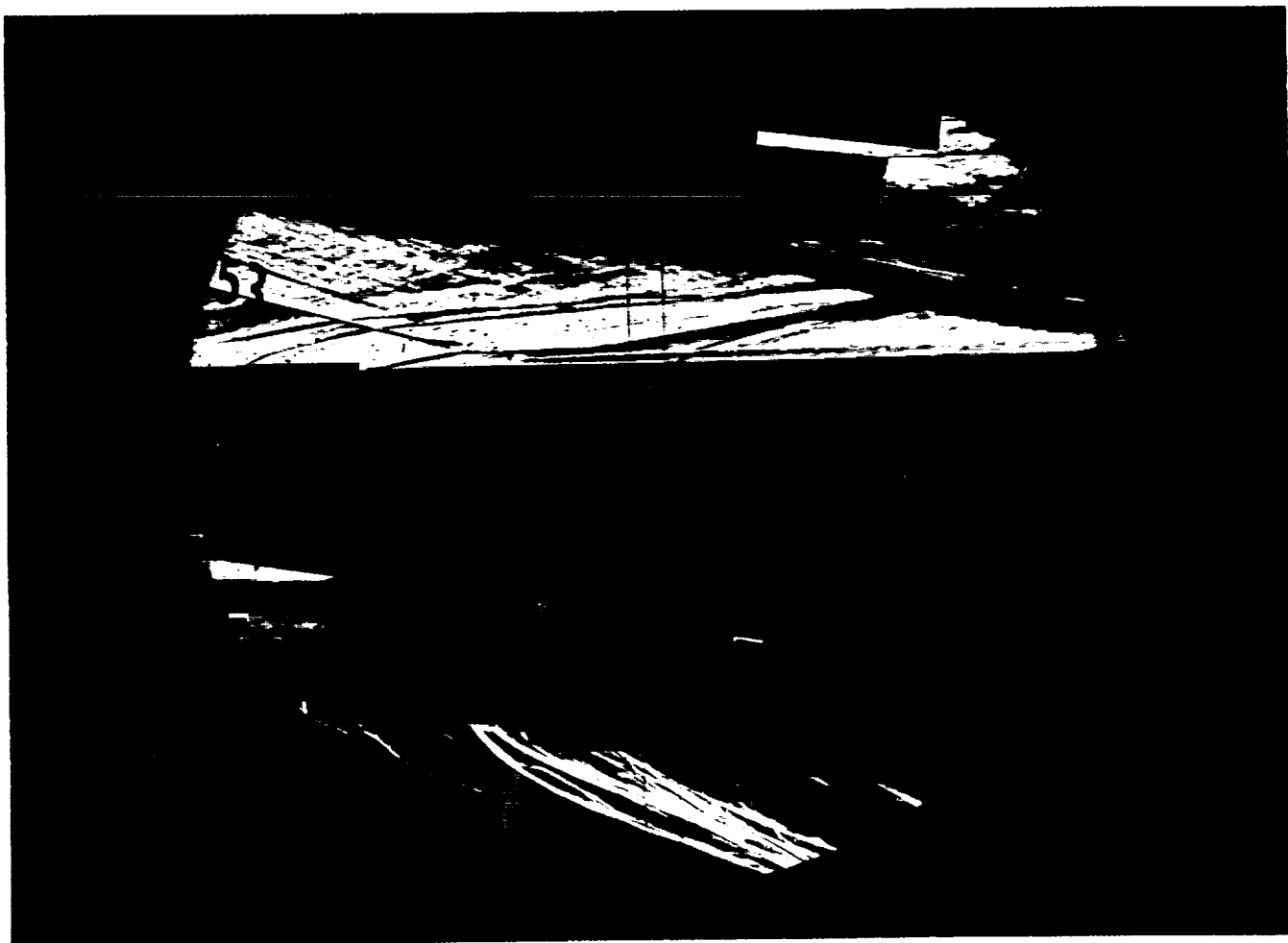


Test Conditions

P_0 = 2.6393X10+3 PSIA	Reservoir Total Pressure
H_0 = 1.3890X10+7 (FT/sec) ²	Reservoir Total Enthalpy
T_0 = 2.1698X10+3 degR	Reservoir Total Temperature
M = 6.4309	Freestream Mach Number
U = 4.9809X10+3 Ft/sec	Freestream Velocity
T = 2.4945X10+2 degR	Freestream Temperature
P = 1.0785	Freestream Static Pressure
ρ_0 = 3.6281X10-4 Slugs/Ft ³	Freestream Density
μ = 2.0443X10-7 Slugs/ft-sec	Freestream Viscosity
Re = 8.8398X10+6 1/Ft	Freestream Reynolds Number
P_0' = 5.8276X10+1 PSIA	Pitot Pressure
Q = 3.1254X10+1 PSIA	Dynamic Pressure ($\rho_0 U^2/288$)
M_1 = 2.8935	Shock Tube Incident Shock Mach Number
H_w = 3.1832X10+6 (Ft/sec) ²	Wall Enthalpy ($C_p T_w$)
C_{Pf} = 3.1996X10-2 1/PSIA	Pressure to CP factor ($1/Q$)
CH_f = 4.0210X10-5 Ft ² -s/BTU	Heat Rate to CH factor (778/($\rho_0 U (H_0 - H_w)$))
Q_{oFF} = 6.5458X10+1 BTU/Ft ² -s	Fay-Riddell Heat Transfer (.25' Diam Cylin.)

Model Parameter	Value
Horizontal Shock Generator Angle (degrees)	8.0
X * (inches)	6.880
Y * (inches)	3.167
Slot Height (inches)	0.120
Lip Thickness (inches)	0.020
Non-dimensional Blowing Rate, Lambda	0
* See Shock Generator Diagram (page A-23)	



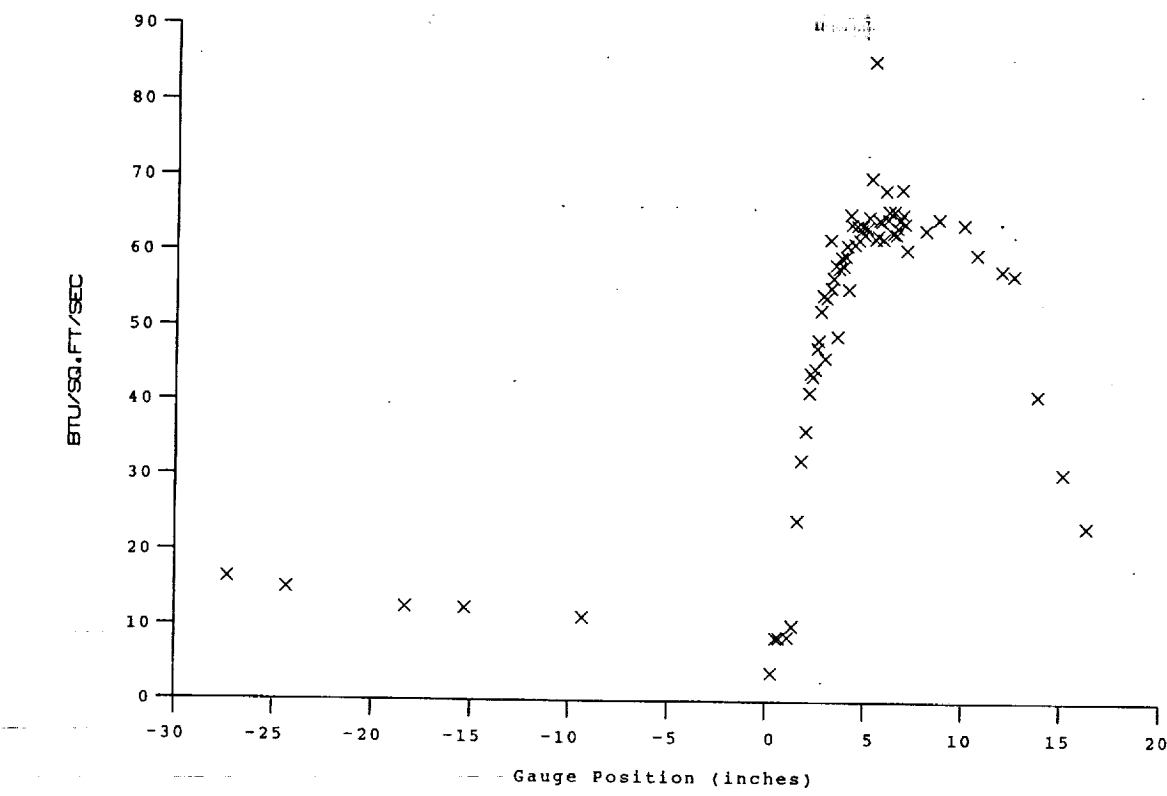


Test Conditions

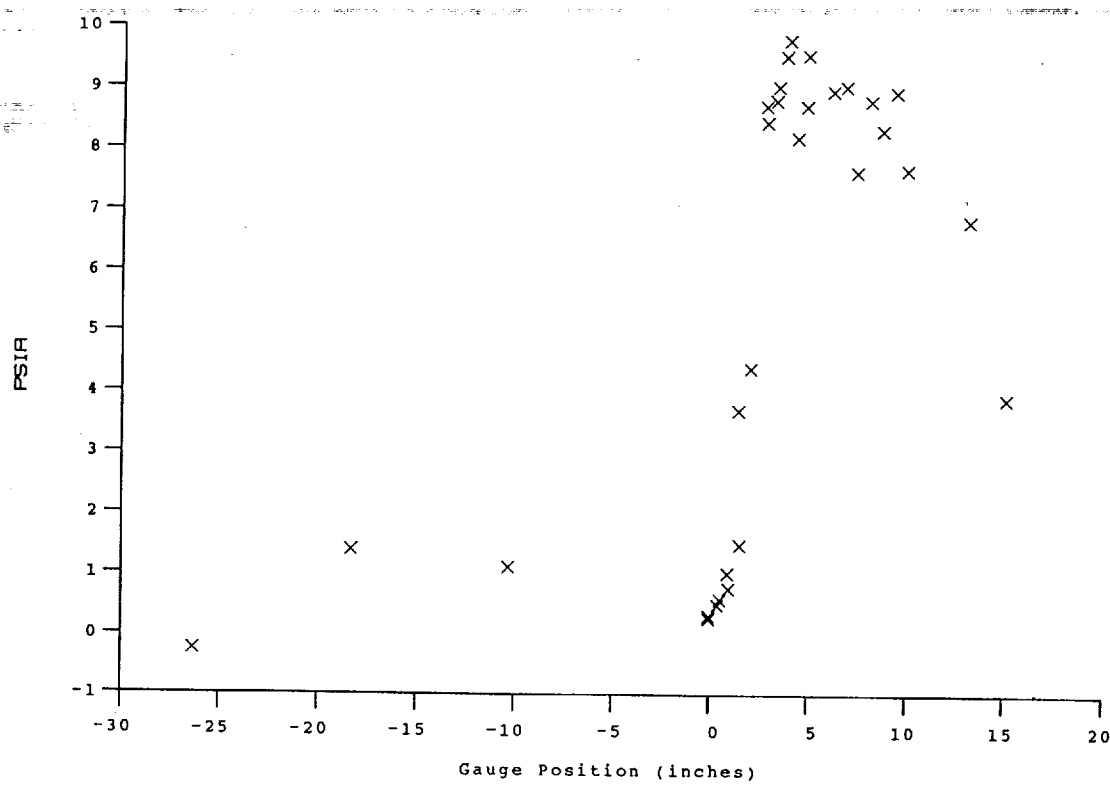
P_0 = 2.5604X10⁺³ PSIA Reservoir Total Pressure
 H_0 = 1.3811X10⁺⁷ (Ft/sec)² Reservoir Total Enthalpy
 T_0 = 2.1596X10⁺³ degR Reservoir Total Temperature
 M = 6.4323 Freestream Mach Number
 U = 4.9668X10⁻³ Ft/sec Freestream Velocity
 T = 2.4793X10⁺² degR Freestream Temperature
 P = 1.0447 PSIA Freestream Static Pressure
 ρ_0 = 3.5361X10⁻⁴ Slugs/Ft³ Freestream Density
 μ = 2.0328X10⁻⁷ Slugs/Ft-sec Freestream Viscosity
 Re = 8.6400X10⁺⁶ 1/Ft Freestream Reynolds Number
 P_0' = 5.6473X10⁺¹ PSIA Pitot Pressure
 Q = 3.0289X10⁺¹ PSIA Dynamic Pressure ($\rho_0 U^2 / 288$)
 M_1 = 2.8708 Shock Tube Incident Shock Mach Number
 H_w = 3.1832X10⁺⁶ (Ft/sec)² Wall Enthalpy ($C_p T_w$)
 $C_P f$ = 3.3015X10⁻² 1/PSIA Pressure to CP factor (1/Q)
 CH_f = 4.1681X10⁻⁵ Ft²-s/BTU Heat Rate to CH factor (778/($\rho_0 U (H_0 - H_w)$))
 Q_{FR} = 6.3936X10⁺¹ BTU/Ft²-s Fay-Riddell Heat Transfer (.25' Diam Cylin.)

Model Parameter	Value
Horizontal Shock Generator Angle (degrees)	8.0
X * (inches)	6.798
Y * (inches)	1.959
Slot Height (inches)	0.120
Lip Thickness (inches)	0.020
Non-dimensional Blowing Rate, Lambda	0
* See Shock Generator Diagram (page A-23)	

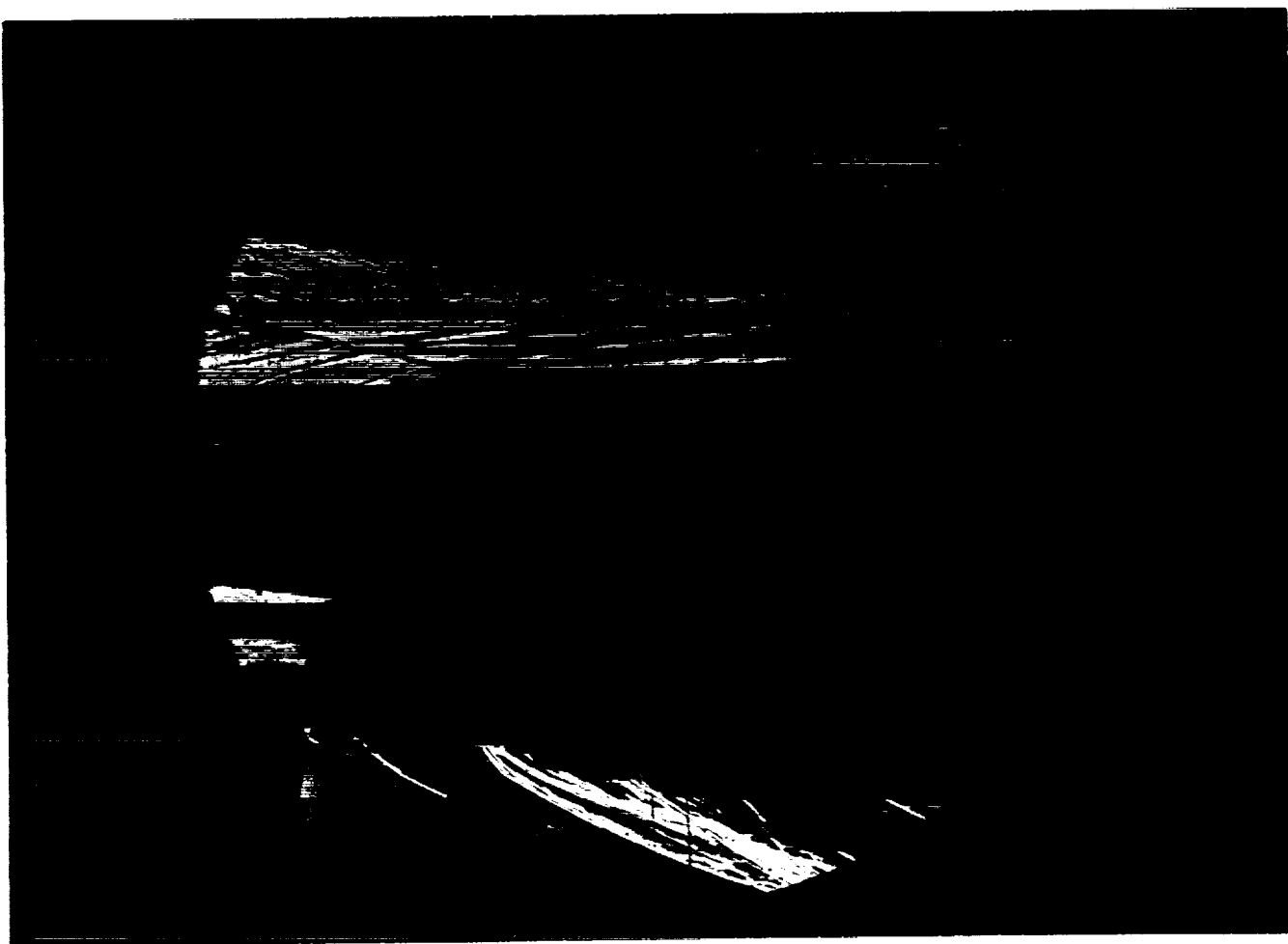
Run 53



HEAT TRANSFER vs Gauge Position
Run 53



PRESSURE vs Gauge Position
Run 53



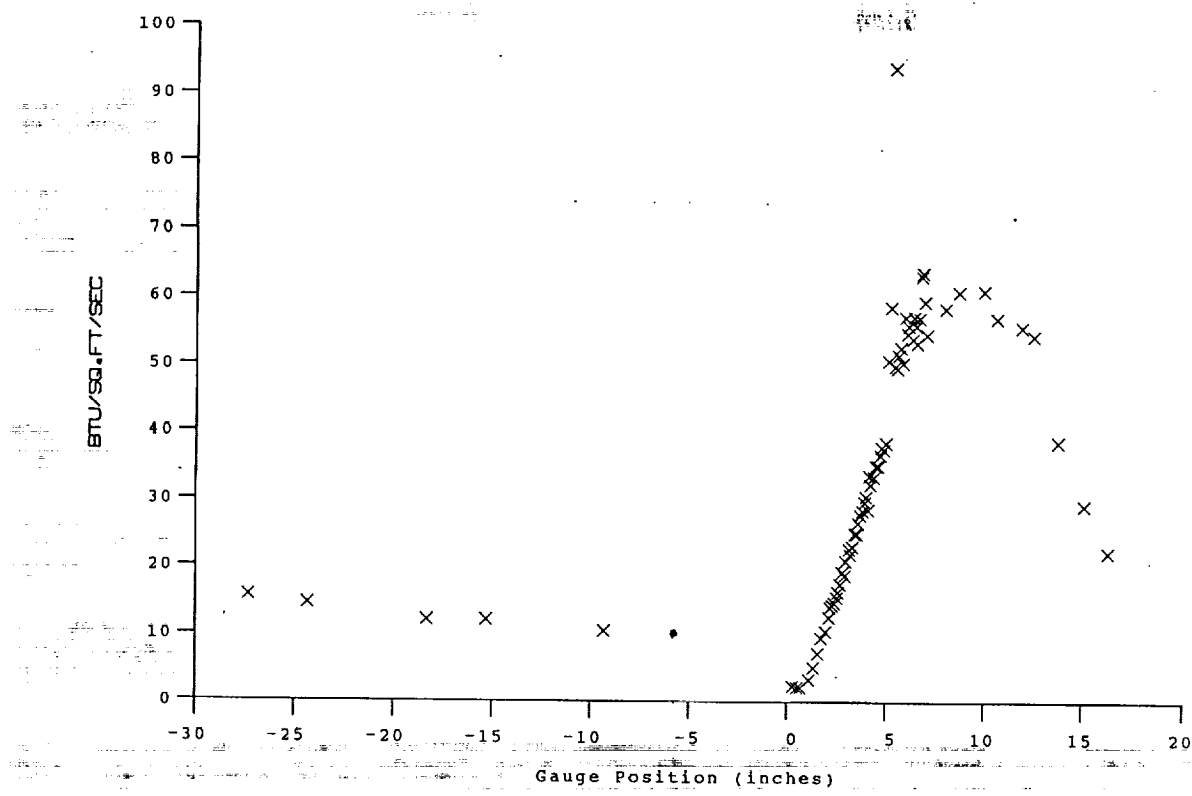
Test Conditions

$P_0 = 2.4319 \times 10^3$ PSIA
 $H_0 = 1.3466 \times 10^7$ (Ft/sec) 2
 $T_0 = 2.1121 \times 10^{-3}$ degR
 $M = 6.4373$
 $U = 4.9047 \times 10^{-3}$ Ft/sec
 $T = 2.4140 \times 10^{-2}$ degR
 $P = 9.9151 \times 10^{-1}$ PSIA
 $\rho_0 = 3.4469 \times 10^{-4}$ Slugs/Ft 3
 $\mu = 1.9833 \times 10^{-7}$ Slugs/Ft-sec
 $Re = 8.5243 \times 10^{-6}$ 1/Ft
 $P_0' = 5.3663 \times 10^{-1}$ PSIA
 $Q = 2.8792 \times 10^{-1}$ PSIA
 $M_1 = 2.8197$
 $H_w = 3.1832 \times 10^{-6}$ (Ft/sec) 2
 $C_P F = 3.4733 \times 10^{-2}$ 1/PSIA
 $CH_f = 4.4753 \times 10^{-5}$ Ft 2 -s/BTU
 $Q_{FR} = 6.0190 \times 10^{-1}$ BTU/Ft 2 -s

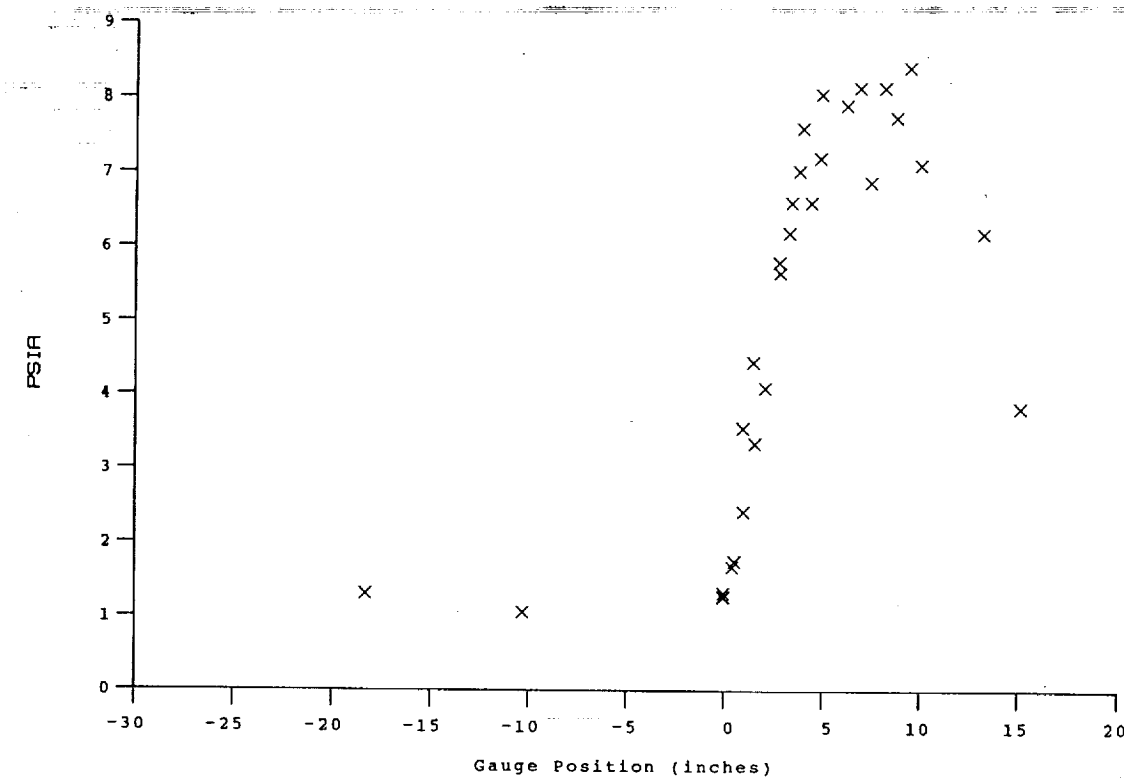
Model Parameter	Value
Horizontal Shock Generator Angle (degrees)	8.0
X * (inches)	6.798
Y * (inches)	1.959
Slot Height (inches)	0.120
Lip Thickness (inches)	0.020
Mass Flow Rate per Nozzle (slugs/sec)	7.324E-05
Non-dimensional Blowing Rate, Lambda	0.1051
Nozzle Reservoir Pressure (psia)	17.36
Exit Plane Pressure (psia)	1.308
Coolant Total Temperature (Rankine)	530

* See Shock Generator Diagram (Page A23)

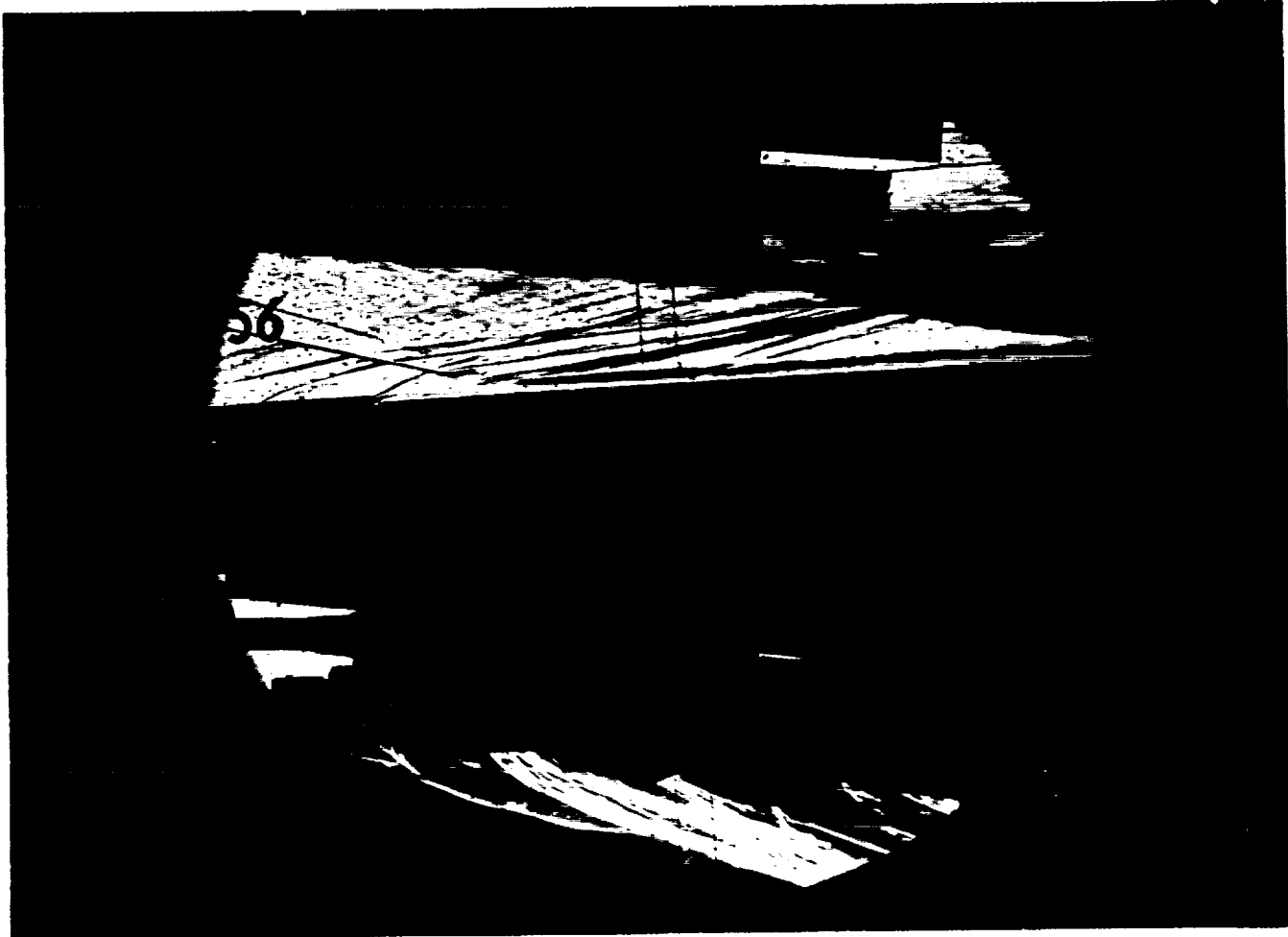
Run 55



HEAT TRANSFER vs Gauge Position
Run 55



PRESSURE vs Gauge Position
Run 55

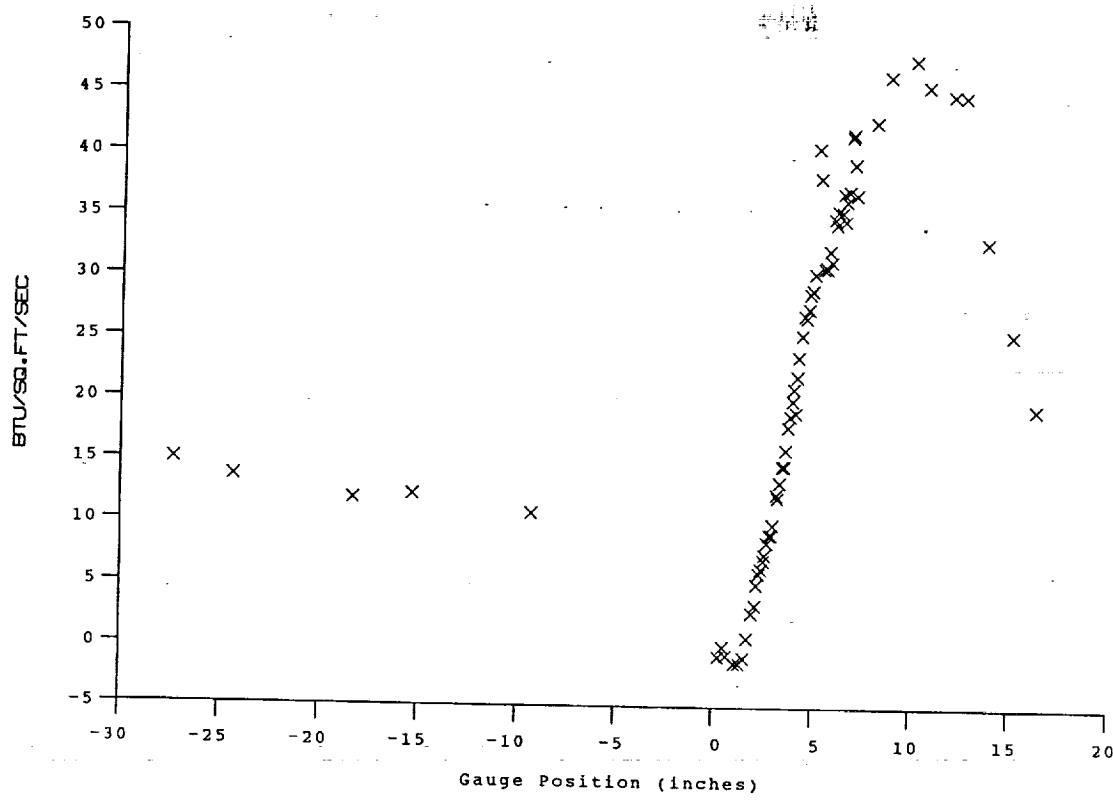


Test Conditions

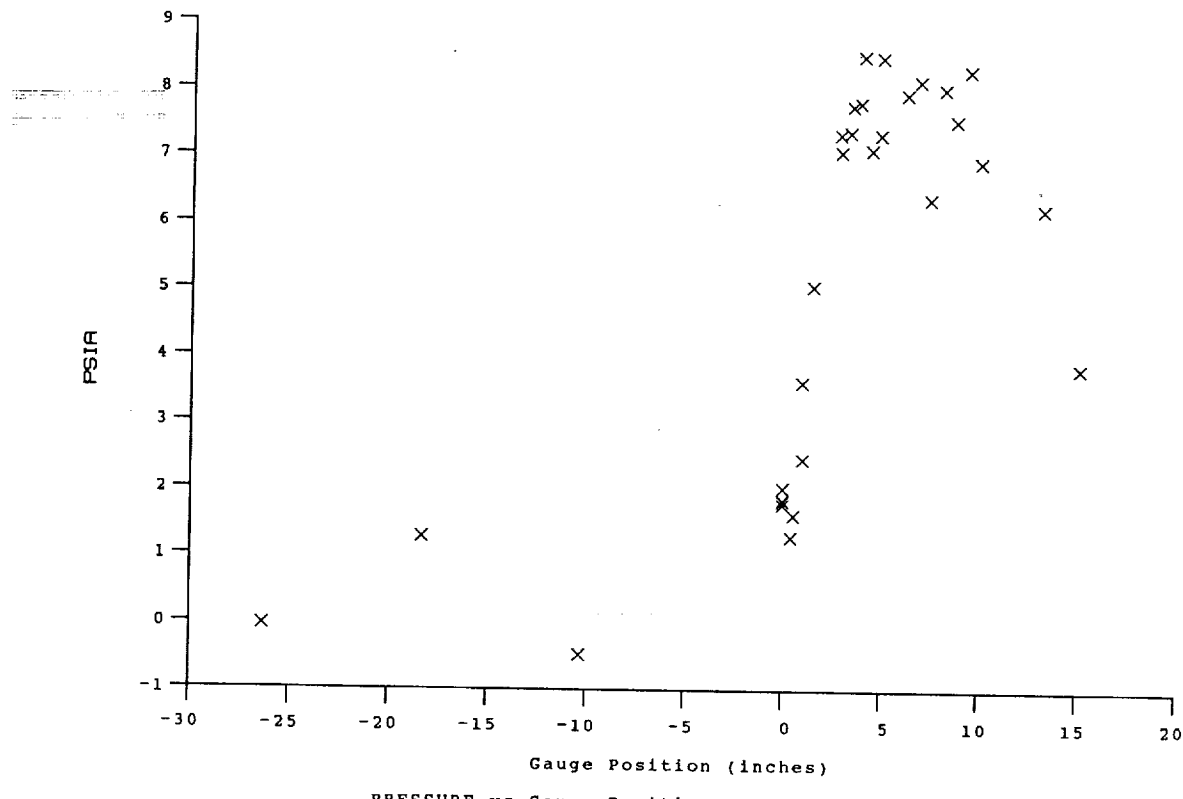
P _o = 2.4537X10+3 PSIA	Reservoir Total Pressure
H _o = 1.3655X10+7 (Ft/sec) ²	Reservoir Total Enthalpy
T _o = 2.1393X10+3 degR	Reservoir Total Temperature
M = 6.4362	Freestream Mach Number
U = 4.9389X10+3 Ft/sec	Freestream Velocity
T = 2.4486X10+2 degR	Freestream Temperature
P = 9.9822X10-1 PSIA	Freestream Static Pressure
Rho = 3.4212X10-4 Slugs/Ft ³	Freestream Density
Mu = 2.0096X10-7 Slugs/Ft·sec	Freestream Viscosity
Re = 8.4082X10+6 1/Ft	Freestream Reynolds Number
Po' = 5.4017X10+1 PSIA	Pitot Pressure
Q = 2.8976X10+1 PSIA	Dynamic Pressure (Rho U ² /288)
M1 = 2.8299	Shock Tube Incident Shock Mach Number
Hw = 3.1832X10+6 (Ft/sec) ²	Wall Enthalpy (Cp Tw)
CPr = 3.4511X10-2 1/PSIA	Pressure to CP factor (1/Q)
CHf = 4.1969X10-5 Ft ² ·s/BTU	Heat Rate to CH factor (778/(Rho U (Ho-Hw)))
QoFR = 6.1564X10+1 BTU/Ft ² s	Fay-Riddell Heat Transfer (.25' Diam Cylin.)

Model Parameter	Value
Horizontal Shock Generator Angle (degrees)	8.0
X * (inches)	6.798
Y * (inches)	1.959
Slot Height (inches)	0.120
Lip Thickness (inches)	0.020
Mass Flow Rate per Nozzle (slugs/sec)	1.733E-04
Non-dimensional Blowing Rate, Lambda	0.2488
Nozzle Reservoir Pressure (psia)	37.38
Exit Plane Pressure (psia)	1.898
Coolant Total Temperature (Rankine)	530
* See Shock Generator Diagram (Page A23)	

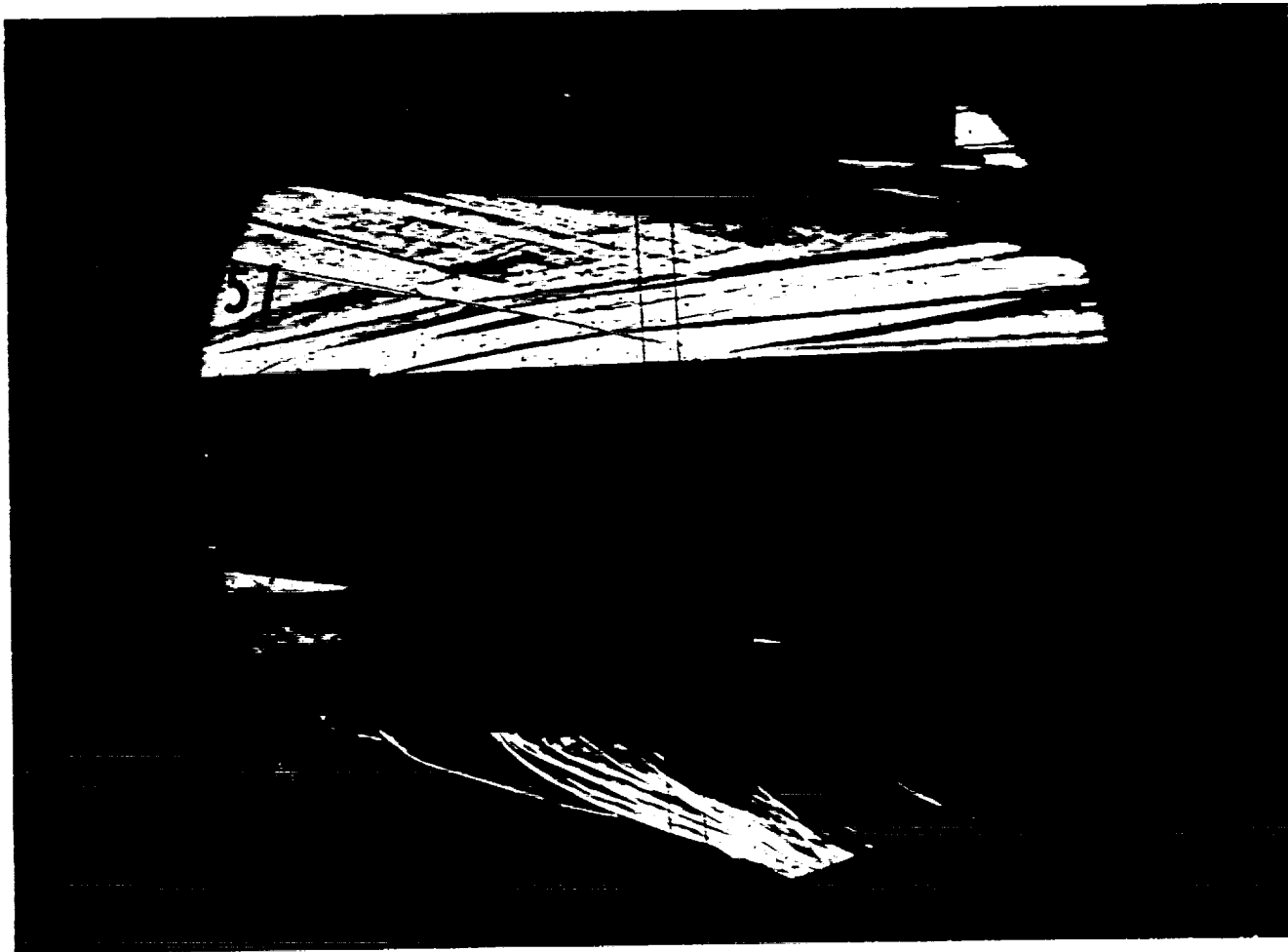
Run 56



HEAT TRANSFER vs Gauge Position
Run 56



PRESSURE vs Gauge Position
Run 56

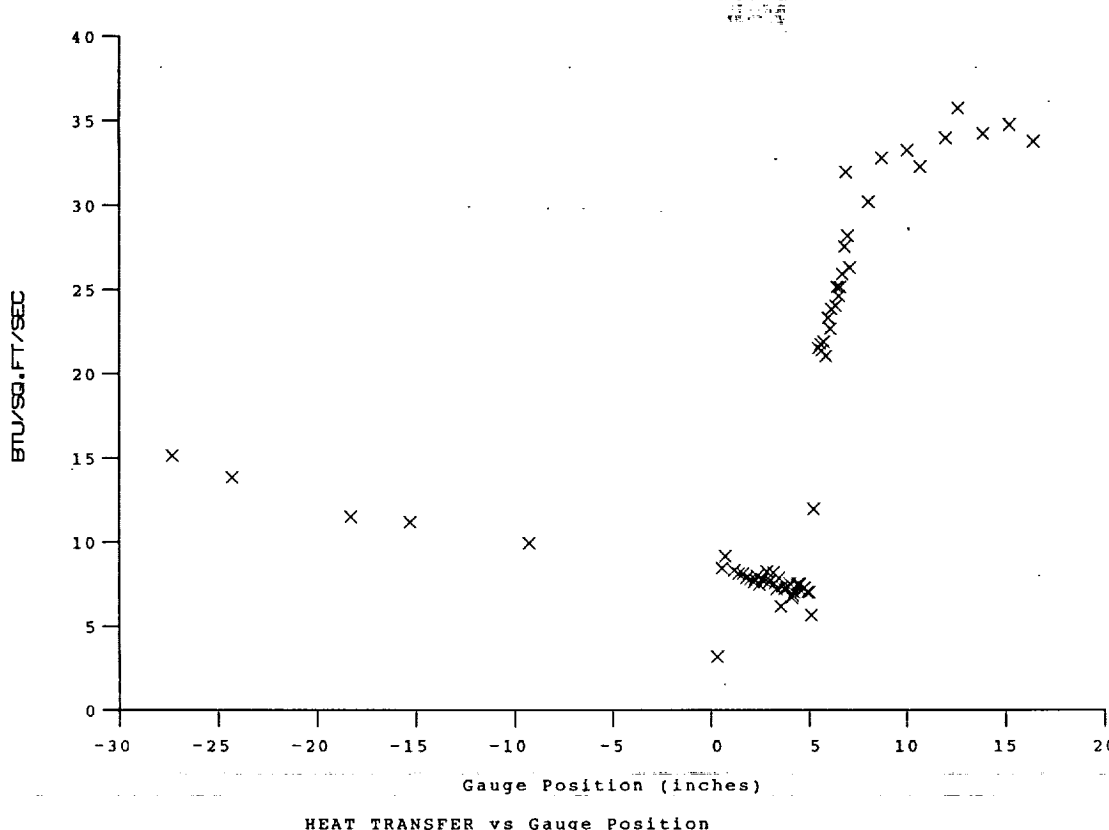


Test Conditions

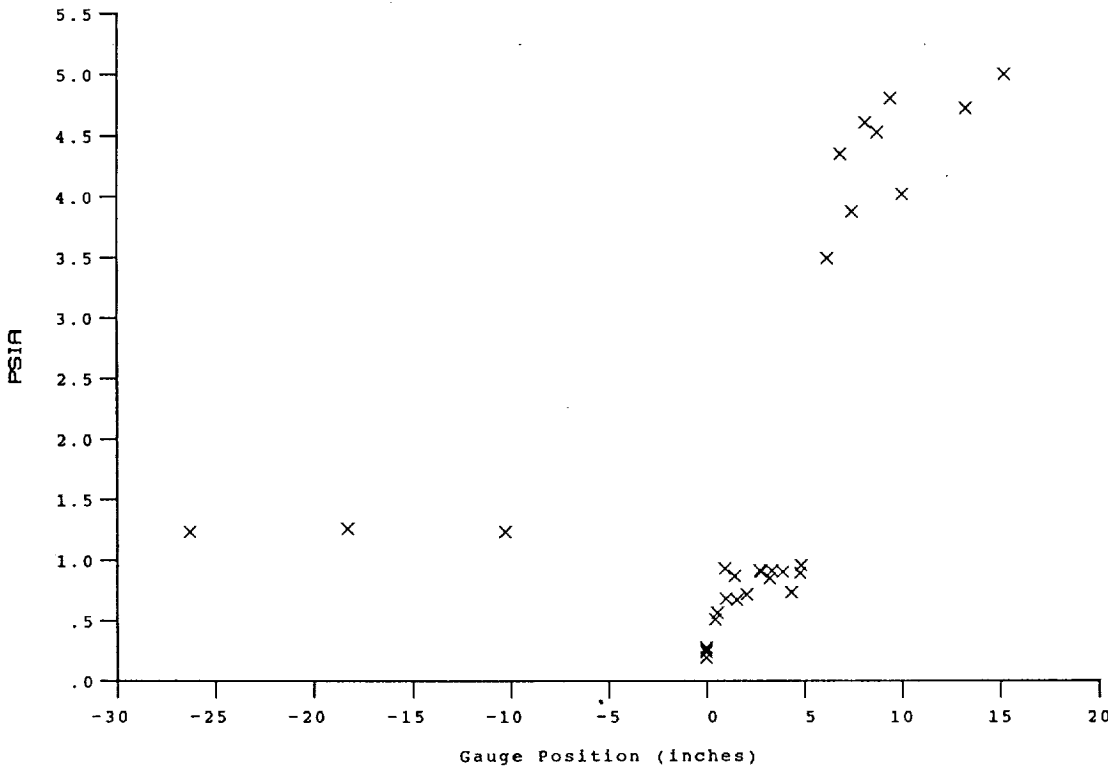
P_0 = 2.3820X10 ⁺³ PSIA	Reservoir Total Pressure
H_0 = 1.3599X10 ⁺⁷ (Ft/sec) ²	Reservoir Total Enthalpy
T_0 = 2.1320X10 ⁺³ degR	Reservoir Total Temperature
M = 6.4355	Freestream Mach Number
U = 4.9287X10 ⁺³ Ft/sec	Freestream Velocity
T = 2.4391X10 ⁺² degR	Freestream Temperature
P = 9.6921X10 ⁻¹ PSIA	Freestream Static Pressure
ρ_0 = 3.3348X10 ⁻⁴ Slugs/Ft ³	Freestream Density
μ = 2.0023X10 ⁻⁷ Slugs/FT-sec	Freestream Viscosity
Re = 8.2085X10 ⁺⁶ 1/ft	Freestream Reynolds Number
P_0' = 5.2433X10 ⁺¹ PSIA	pitot Pressure
Q = 2.8128X10 ⁺¹ PSIA	Dynamic Pressure ($\rho_0 U^2/288$)
M_1 = 2.8158	Shock Tube Incident Shock Mach Number
H_w = 3.1832X10 ⁺⁶ (Ft/sec) ²	Wall Enthalpy ($C_p T_w$)
CP_f = 3.5551X10 ⁻² 1/PSIA	Pressure to CP factor (1/Q)
CH_f = 4.5445X10 ⁻⁵ Ft ² -s/BTU	Heat Rate to CH factor (778/($\rho_0 U (H_0 - H_w)$))
Q_{FR} = 6.0313X10 ⁺¹ BTU/Ft ² -s	Fay-Riddell Heat Transfer (.25' Diam Cylin.)

Model Parameter	Value
Horizontal Shock Generator Angle (degrees)	5.5
X * (inches)	8.050
Y * (inches)	2.794
Slot Height (inches)	0.120
Lip Thickness (inches)	0.020
Non-dimensional Blowing Rate, Lambda **	0
* See Shock Generator Diagram (Figure 8)	
** See Nozzle Geometry Diagram (Figure 9)	

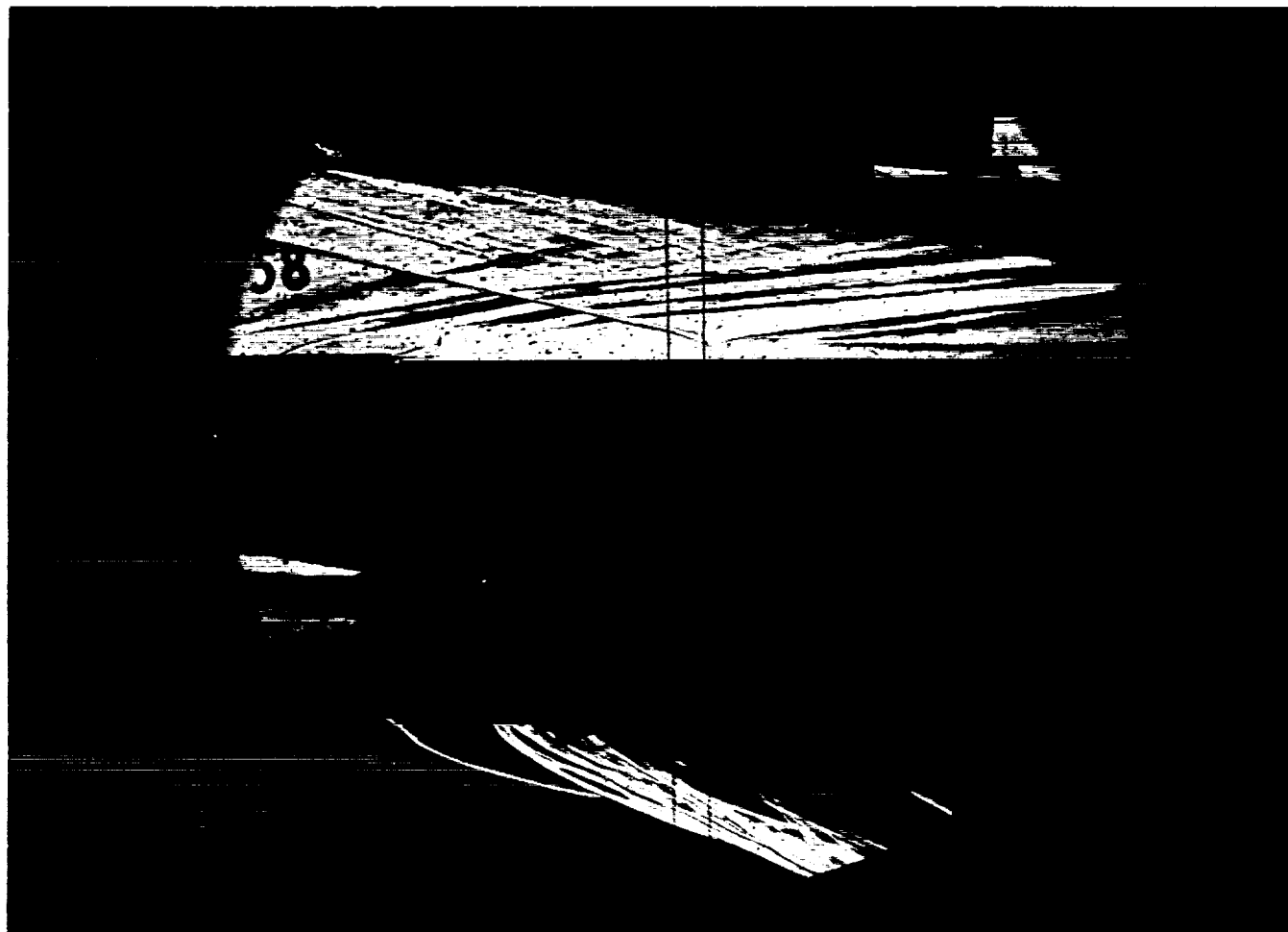
Run 57



HEAT TRANSFER vs Gauge Position
Run 57



PRESSURE vs Gauge Position
Run 57

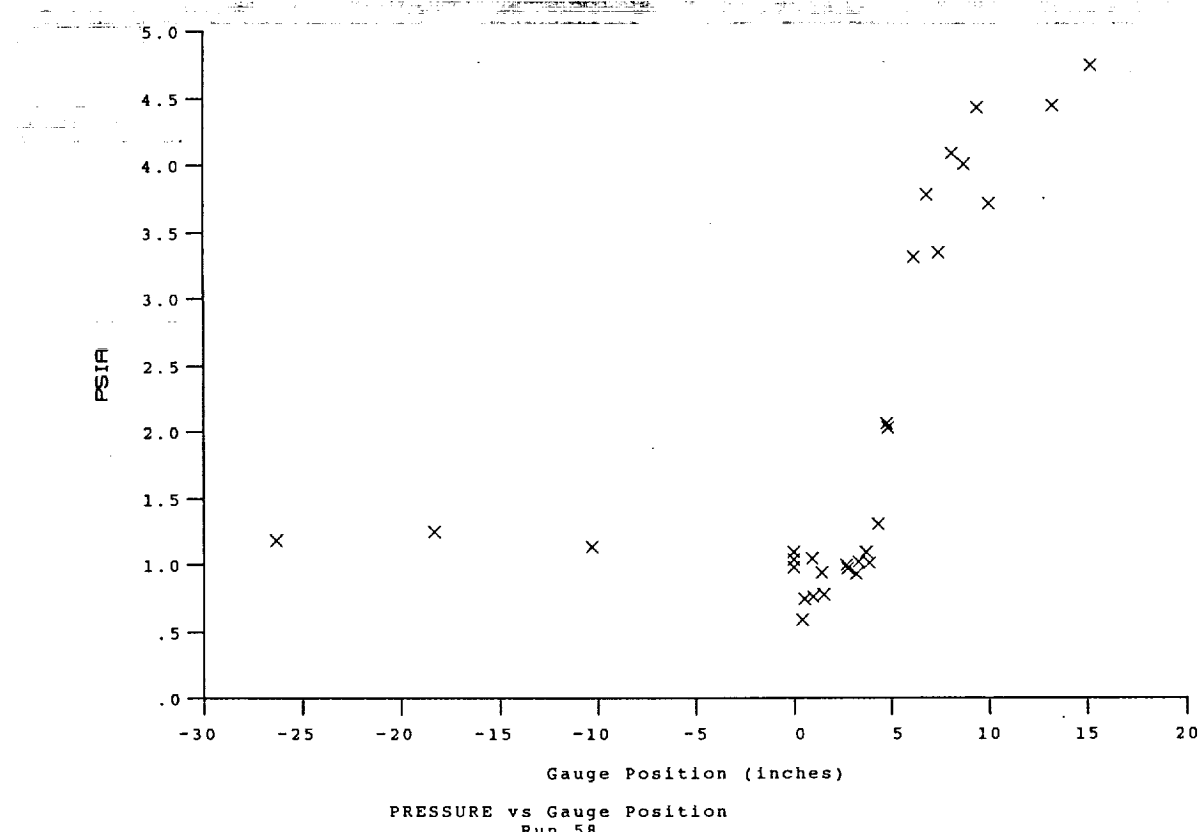
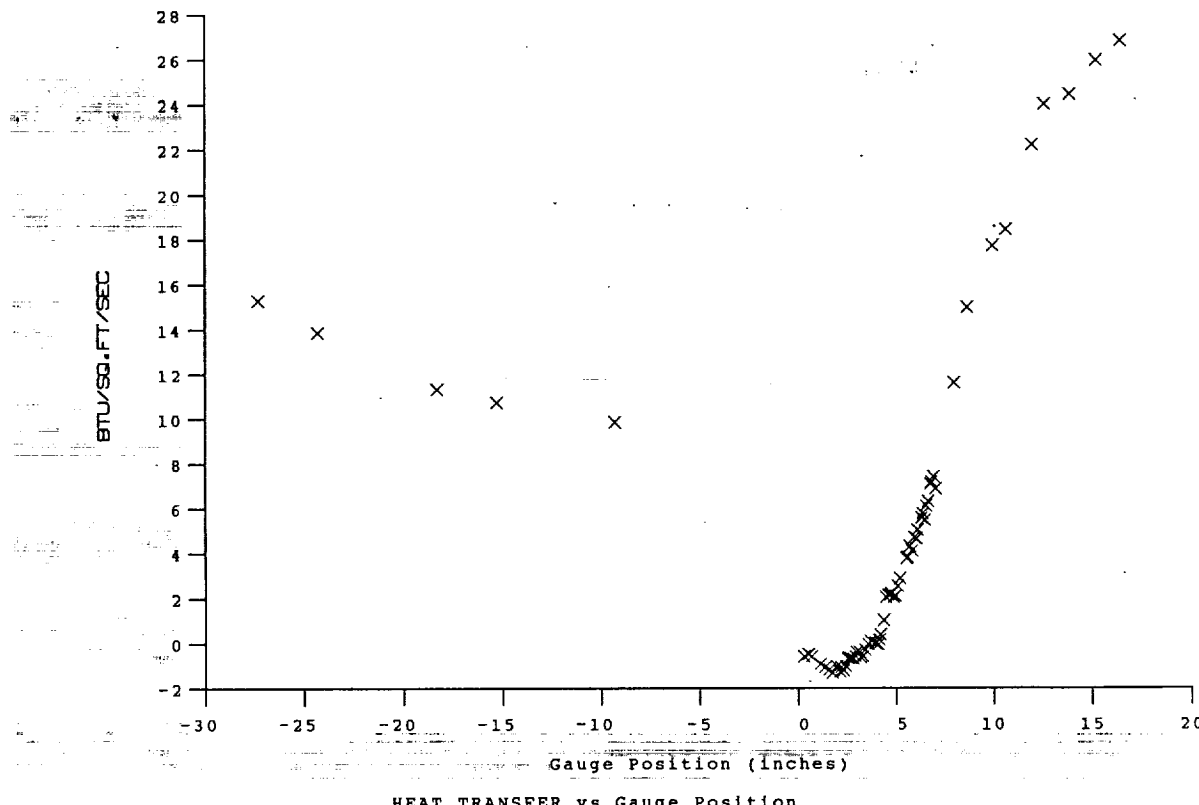


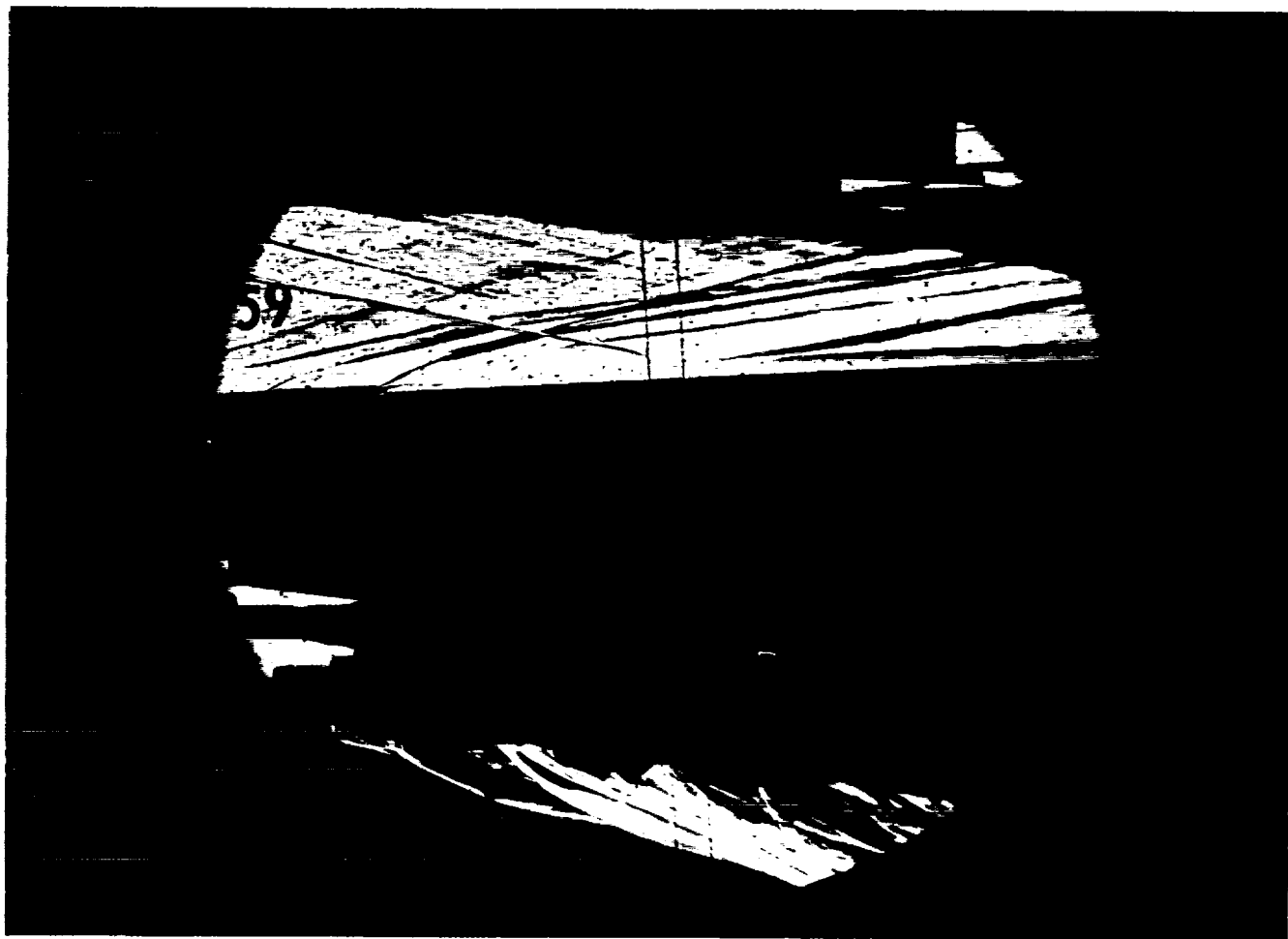
Test Conditions

P_0	= 2.3808X10 ⁻³ PSIA	Reservoir Total Pressure
H_0	= 1.3226X10 ⁻⁷ (Ft/sec) ²	Reservoir Total Enthalpy
T_0	= 2.0785X10 ⁻³ degR	Reservoir Total Temperature
M	= 6.4406	Freestream Mach Number
U	= 4.8612X10 ⁻³ Ft/sec	Freestream Velocity
T	= 2.3689X10 ⁻² degR	Freestream Temperature
P	= 9.7112X10 ⁻¹ PSIA	Freestream Static Pressure
ρ_0	= 3.4403X10 ⁻⁴ Slugs/Ft ³	Freestream Density
μ	= 1.9489X10 ⁻⁷ Slugs/Ft ^{-sec}	Freestream Viscosity
Re	= 8.5810X10 ⁻⁶ 1/Ft	Freestream Reynolds Number
$P_{0'}$	= 5.2599X10 ⁻¹ PSIA	Pitot Pressure
Q	= 2.8228X10 ⁻¹ PSIA	Dynamic Pressure ($\rho_0 U^2 / 288$)
M_1	= 2.7927	Shock Tube Incident Shock Mach Number
H_w	= 3.1832X10 ⁻⁶ (Ft/sec) ²	Wall Enthalpy ($C_p T_w$)
$C_P F$	= 3.5425X10 ⁻² 1/PSIA	Pressure to CP factor (1/Q)
CH_F	= 4.6322X10 ⁻⁵ Ft ² -s/BTU	Heat Rate to CH factor (778/($\rho_0 U (H_0 - H_w)$))
Q_{FR}	= 5.8120X10 ⁻¹ BTU/Ft ² -s	Fay-Riddell Heat Transfer (.25' Diam Cylin.)

Model Parameter	Value
Horizontal Shock Generator Angle (degrees)	5.5
X * (inches)	8.050
Y * (inches)	2.794
Slot Height (inches)	0.120
Lip Thickness (inches)	0.020
Mass Flow Rate per Nozzle (slugs/sec)	7.043E-05
Non-dimensional Blowing Rate, Lambda	0.1022
Nozzle Reservoir Pressure (psia)	18.24
Exit Plane Pressure (psia)	1.046
Coolant Total Temperature (Rankine)	530
* See Shock Generator Diagram (Page A23)	

* Run 58





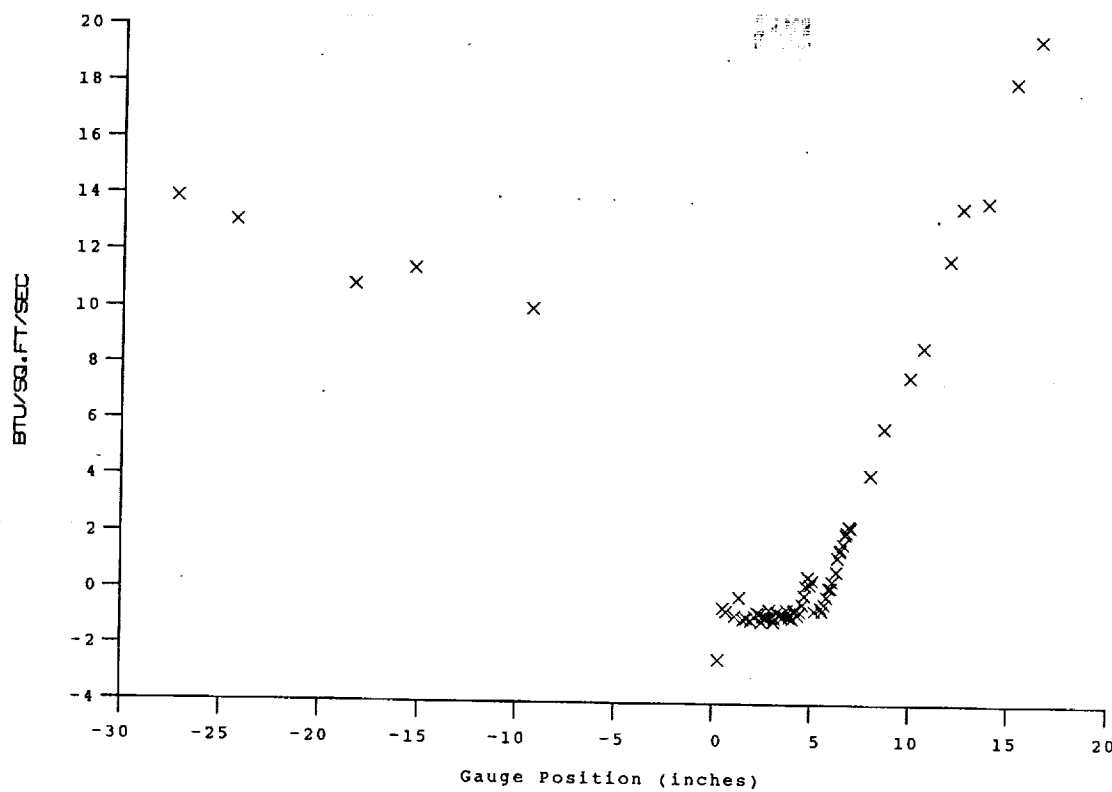
Test Conditions

P _o = 2.4810X10 ⁻³ PSIA	Reservoir Total Pressure
H _o = 1.3327X10 ⁻⁷ (Ft/sec) ²	Reservoir Total Enthalpy
T _o = 2.0932X10 ⁻³ degR	Reservoir Total Temperature
M = 6.4453	Freestream Mach Number
U = 4.8801X10 ⁻³ Ft/sec	Freestream Velocity
T = 2.3838X10 ⁻² degR	Freestream Temperature
P = 1.0076 PSIA	Freestream Static Pressure
Rho = 3.5471X10 ⁻⁴ Slugs/Ft ³	Freestream Density
Mu = 1.9604X10 ⁻⁷ Slugs/Ft ² sec	Freestream Viscosity
Re = 8.8301X10 ⁻⁶ 1/Ft	Freestream Reynolds Number
P _{o'} = 5.4662X10 ⁻¹ PSIA	Pitot Pressure
Q = 2.9332X10 ⁻¹ PSIA	Dynamic Pressure (Rho U ² /288)
M ₁ = 2.7950	Shock Tube Incident Shock Mach Number
H _w = 3.1832X10 ⁻⁶ (Ft/sec) ²	Wall Enthalpy (Cp T _w)
CPf = 3.4093X10 ⁻² 1/PSIA	Pressure to CP factor (1/Q)
CHf = 4.4307X10 ⁻⁵ Ft ² s/BTU	Heat Rate to CH factor (778/(Rho U (H _o -H _w)))
QoFR = 5.9881X10 ⁻¹ BTU/Ft ² s	Fay-Riddell Heat Transfer (.25' Diam Cylin.)

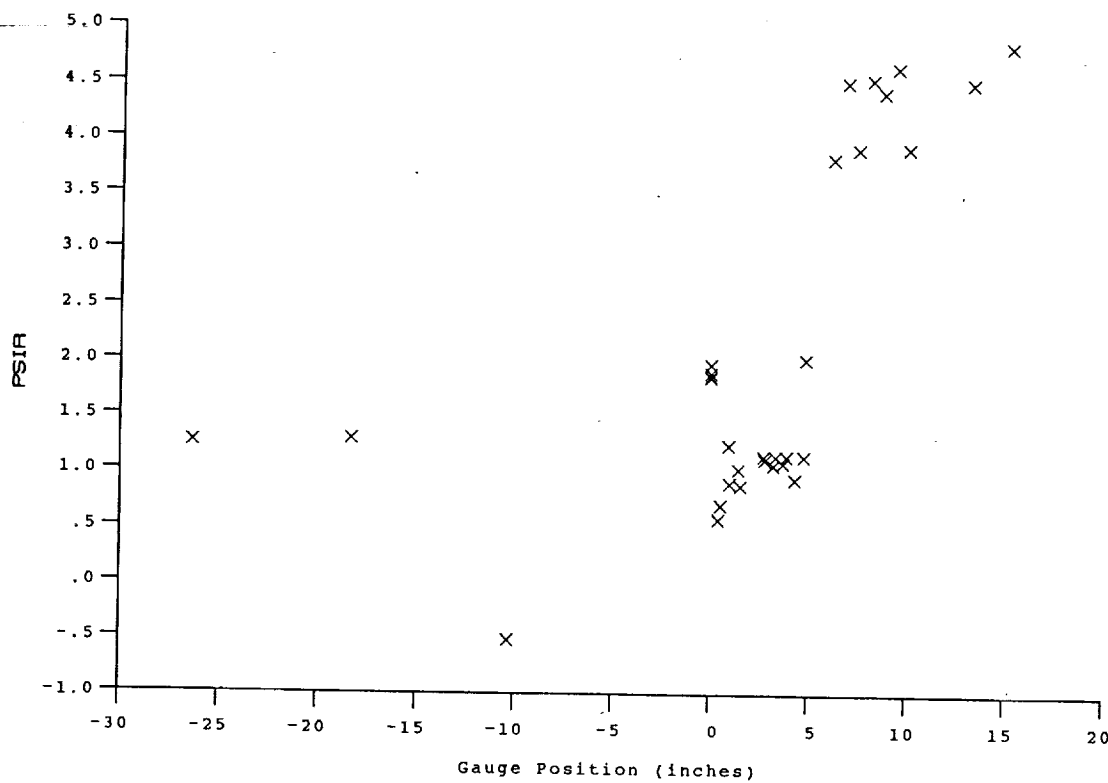
Model Parameter	Value
Horizontal Shock Generator Angle (degrees)	5.5
X * (inches)	8.050
Y * (inches)	2.794
Slot Height (inches)	0.120
Lip Thickness (inches)	0.020
Mass Flow Rate per Nozzle (slugs/sec)	1.683E-04
Non-dimensional Blowing Rate, Lambda	0.2359
Nozzle Reservoir Pressure (psia)	36.81
Exit Plane Pressure (psia)	1.906
Coolant Total Temperature (Rankine)	530

* See Shock Generator Diagram (Page A23)

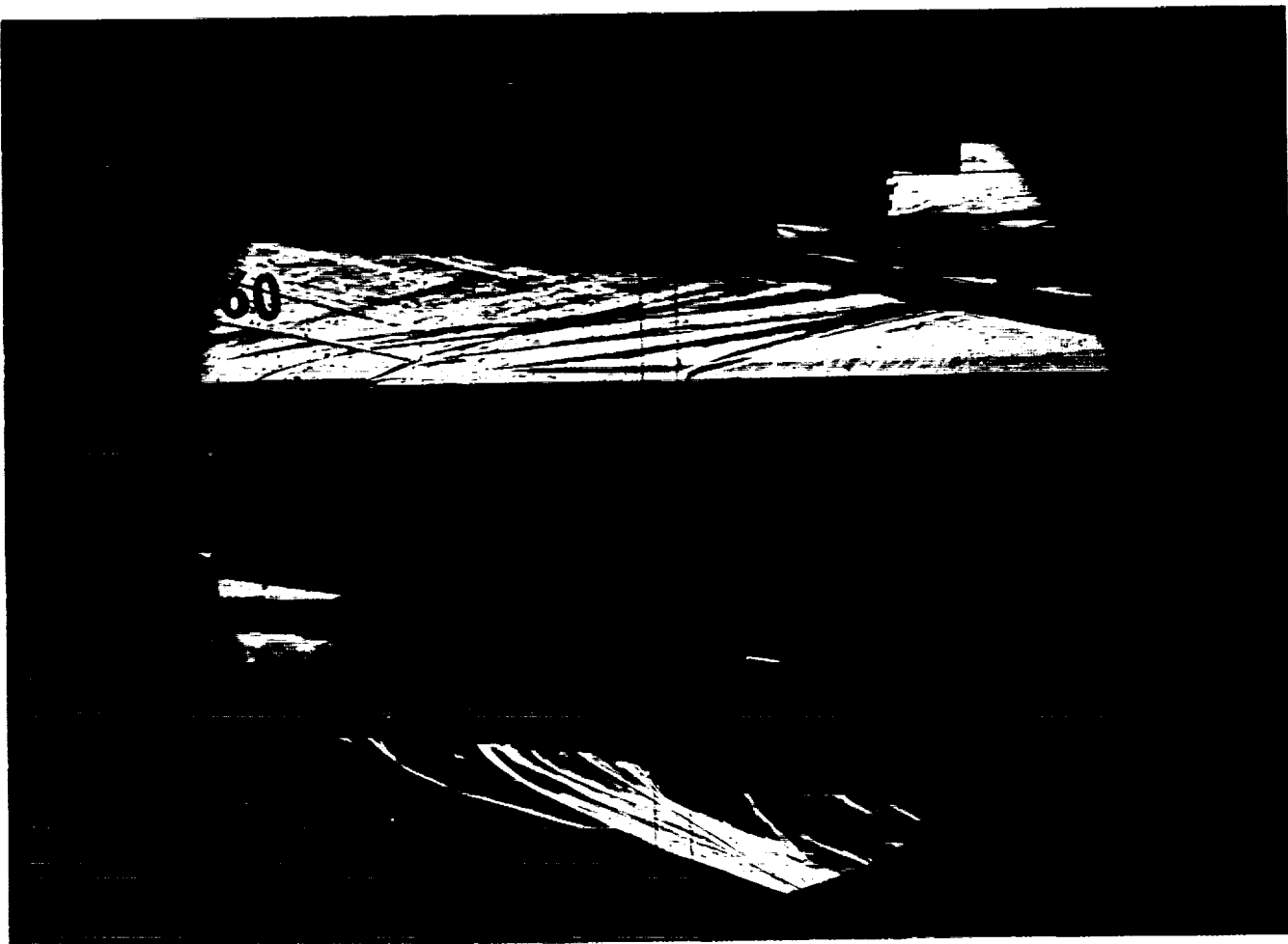
Run 59



HEAT TRANSFER vs Gauge Position
Run 59



PRESSURE vs Gauge Position
Run 59



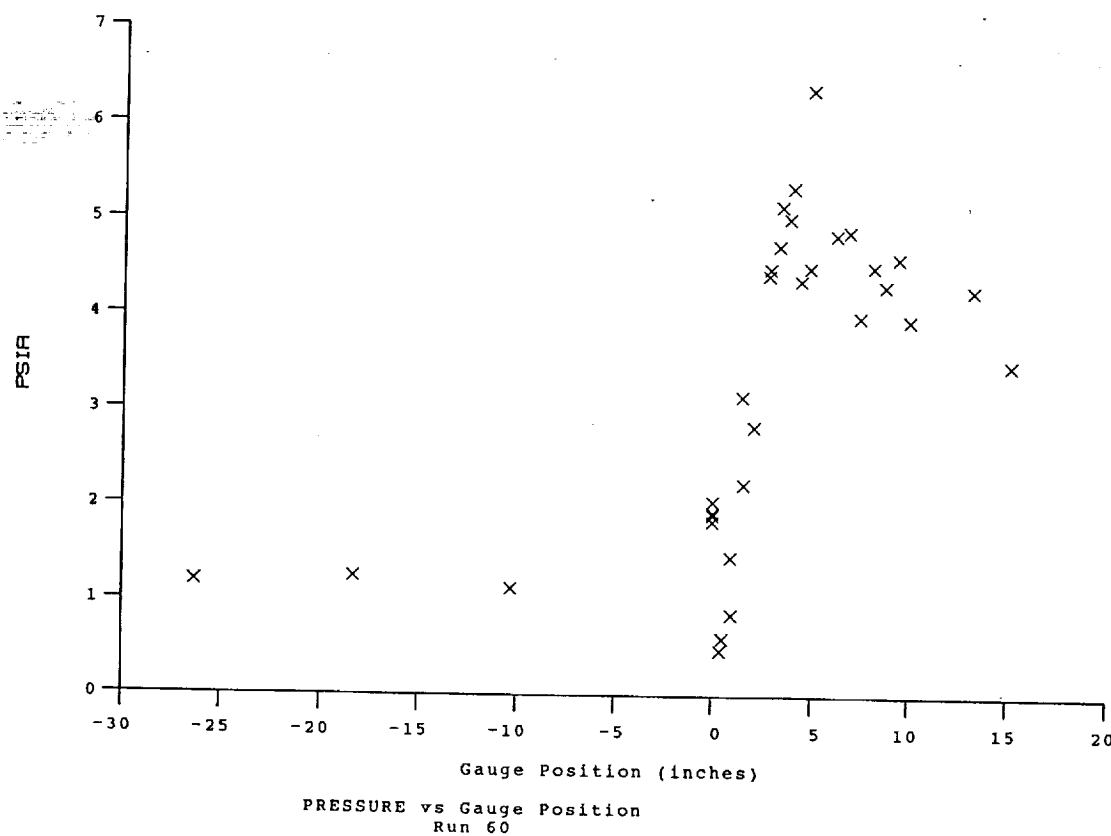
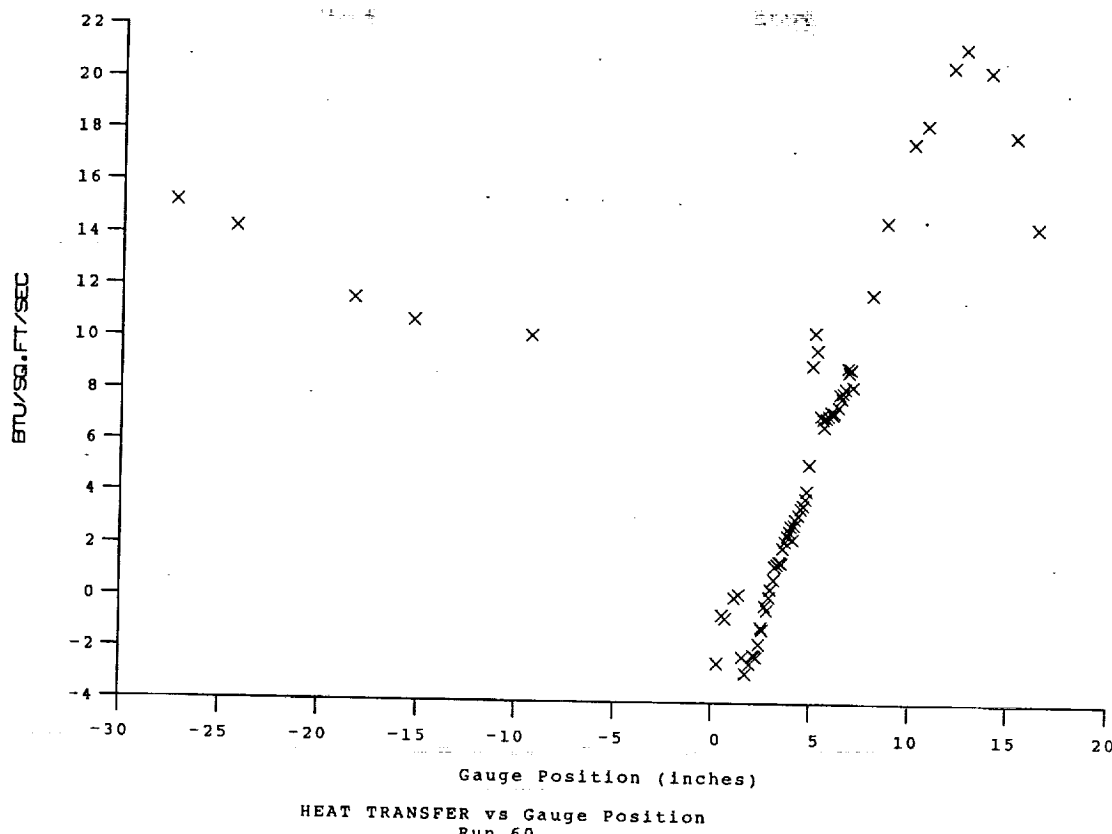
Test Conditions

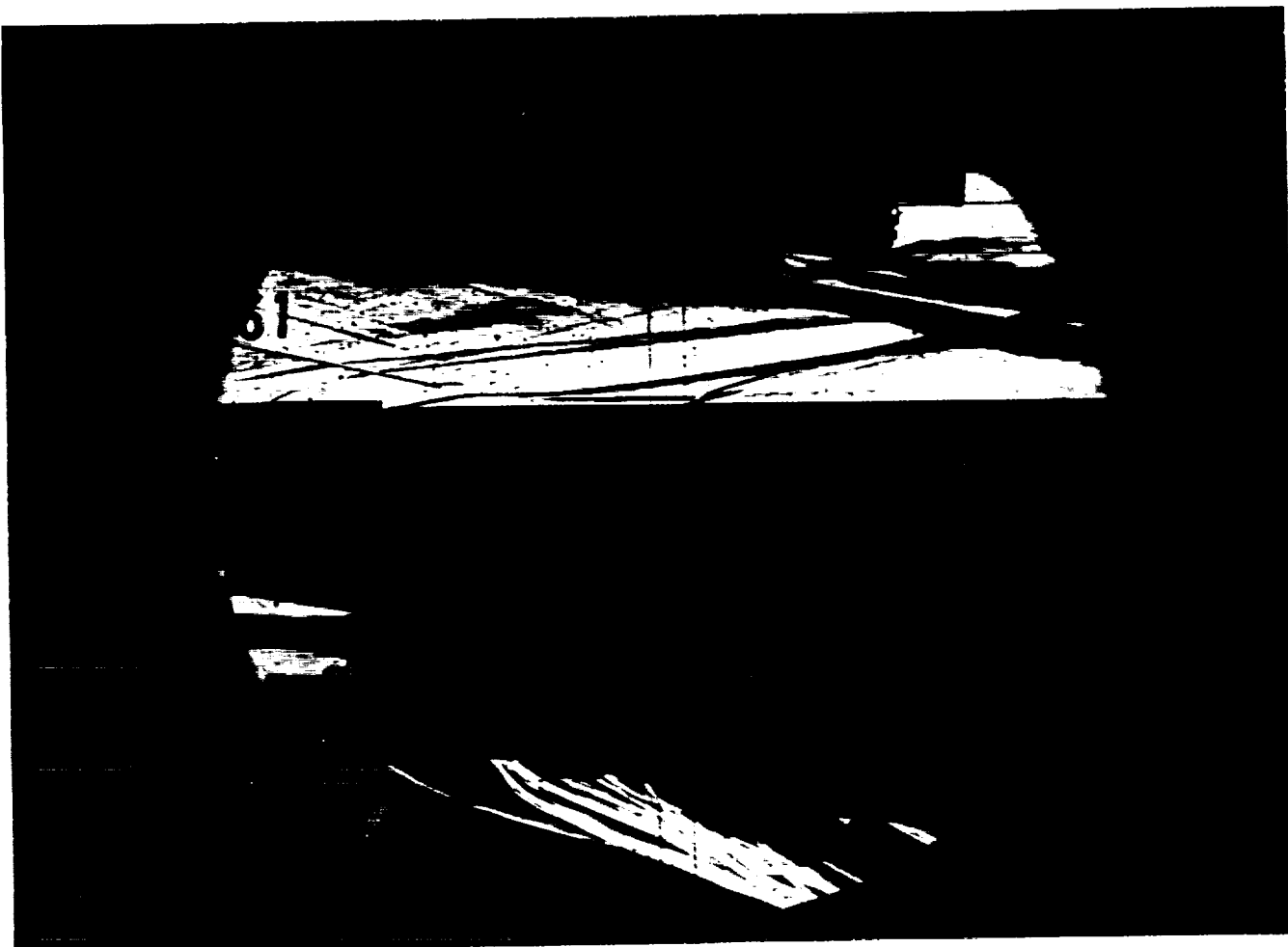
$M_i = 2.8085$
 $P_{o_1} = 2.3769 \times 10^3$ PSIA
 $H_{o_1} = 1.3447 \times 10^7$ $(\text{Ft/sec})^2$
 $T_{o_1} = 2.1101 \times 10^{-3}$ Degrees R
 $M = 6.4369$
 $U = 4.9014 \times 10^3$ Ft/sec
 $T = 2.4110 \times 10^{-2}$ Degrees R
 $P = 9.6868 \times 10^{-1}$ PSIA
 $Q = 2.8125 \times 10^{-1}$ PSIA
 $\rho_{noz} = 3.3717 \times 10^{-4}$ Slugs/ Ft^3
 $M_u = 1.9810 \times 10^{-7}$ Slugs/ $\text{Ft}\cdot\text{sec}$
 $Re = 8.3420 \times 10^6$ 1/Ft
 $P_{o_1}' = 5.2418 \times 10^{-1}$ PSIA

Model Parameter	Value
Horizontal Shock Generator Angle (degrees)	5.5
X * (inches)	6.916
Y * (inches)	2.104
Slot Height (inches)	0.120
Lip Thickness (inches)	0.020
Mass Flow Rate per Nozzle (slugs/sec)	1.679E-04
Non-dimensional Blowing Rate, Lambda	0.2460
Nozzle Reservoir Pressure (psia)	37.77
Exit Plane Pressure (psia)	1.940
Coolant Total Temperature (Rankine)	530

* See Shock Generator Diagram (Page A23)

Run 60





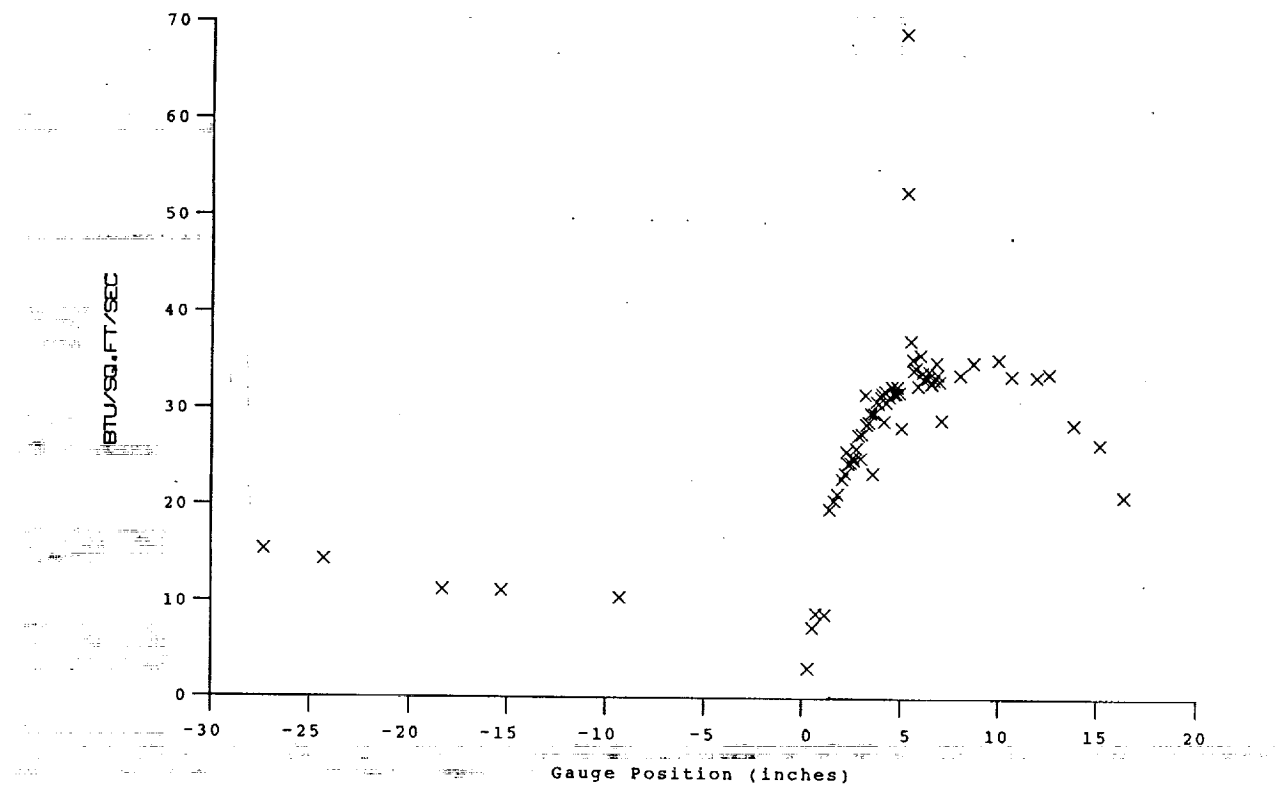
Test Conditions

M_i = 2.8012
P_o = 2.3253X10+3 PSIA
H_o = 1.3455X10+7 (Ft/sec)²
T_o = 2.1117X10+3 Degrees R
M = 6.4356
U = 4.9026X10+3 Ft/sec
T = 2.4132X10+2 Degrees R
P = 9.4754X10-1 PSIA
Q = 2.7500X10+1 PSIA
Rho = 3.2951X10-4 Slugs/Ft³
Mu = 1.9827X10-7 Slugs/Ft-sec
Re = 8.1478X10+6 1/Ft
P_{o'} = 5.1254X10+1 PSIA

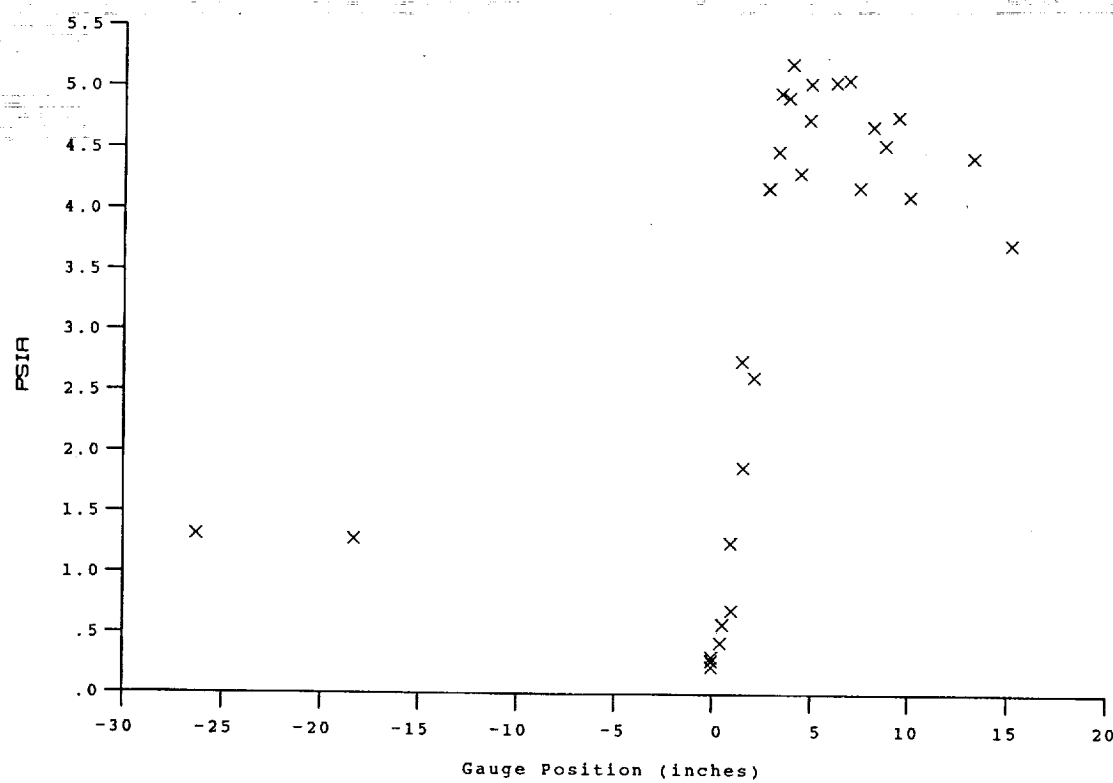
Model Configuration Parameter	Value
Horizontal Shock Generator Angle (degrees)	5.5
X * (inches)	6.916
Y * (inches)	2.104
Slot Height (inches)	0.120
Lip Thickness (inches)	0.020
Lambda	0

* see shock generator diagram at page A-23

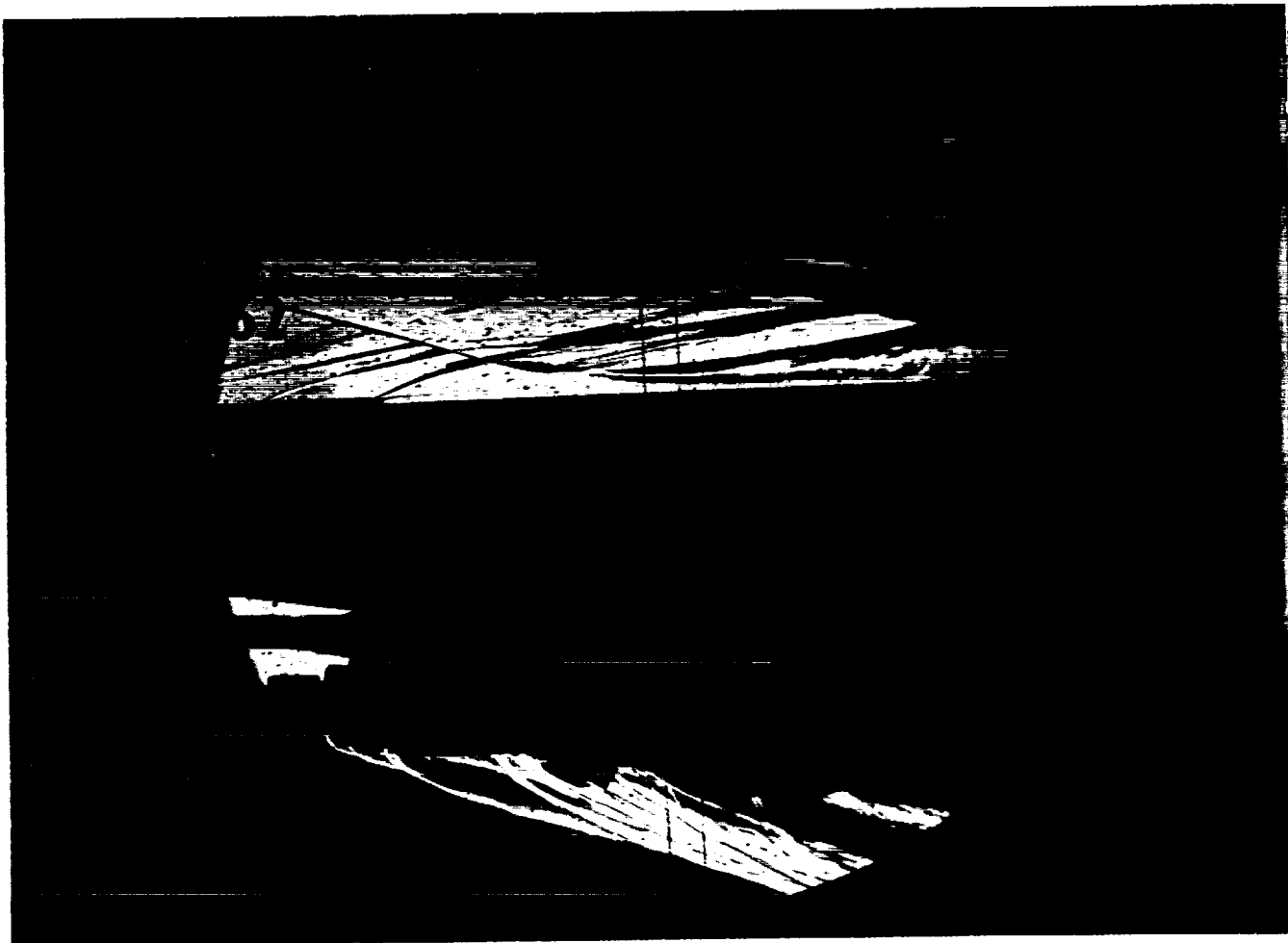
Run 61



HEAT TRANSFER vs Gauge Position
Run 61



PRESSURE vs Gauge Position
Run 61



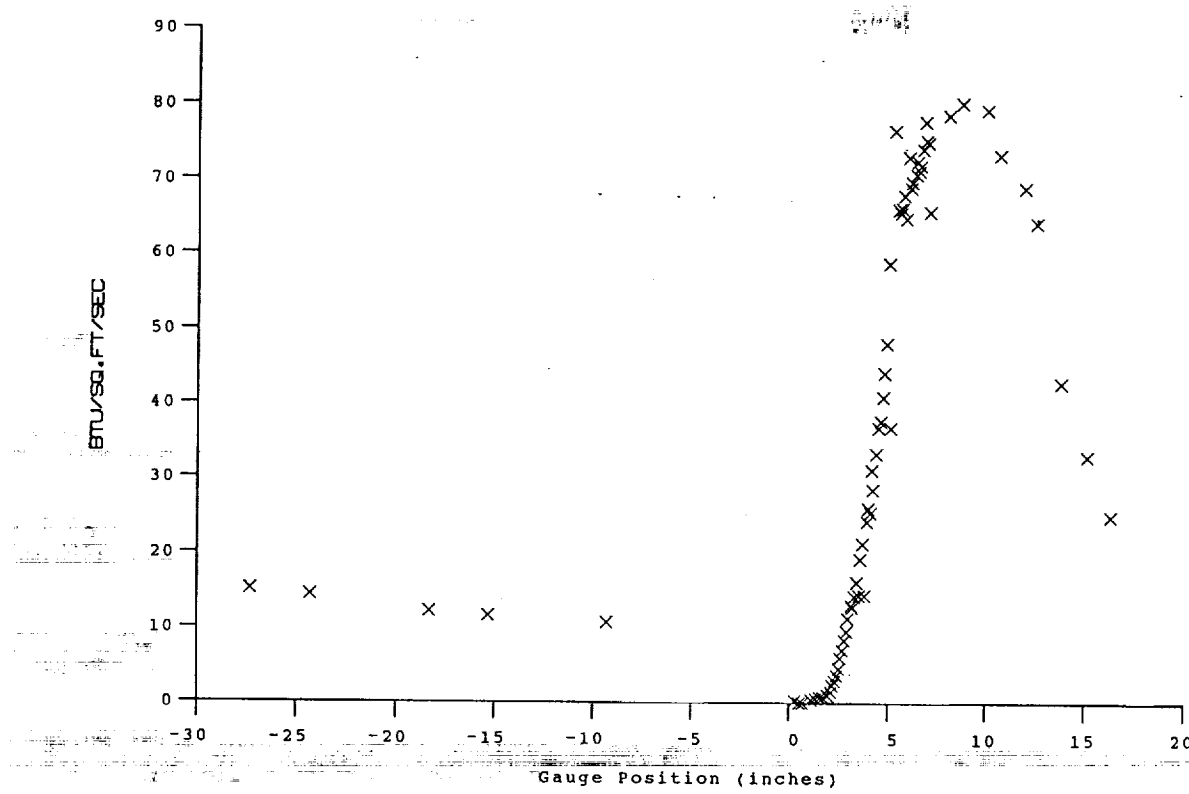
Test Conditions

M_i = 2.8127
P_o = 2.4308x10⁺³ PSIA
H_o = 1.3565x10⁺⁷ (Ft/sec)²
T_o = 2.1272x10⁺³ Degrees R
M = 6.4388
U = 4.9229x10⁺³ Ft/sec
T = 2.4307x10⁺² Degrees R
P = 9.8767x10⁻¹ PSIA
Q = 2.8693x10⁺¹ PSIA
Rho = 3.4099x10⁻⁴ Slugs/Ft³
Mu = 1.9960x10⁻⁷ Slugs/Ft-sec
Re = 8.4098x10⁺⁶ 1/Ft
P_{o'} = 5.3485x10⁺¹ PSIA

Model Parameter	Value
Horizontal Shock Generator Angle (degrees)	10.5
X * (inches)	6.678
Y * (inches)	2.278
Slot Height (inches)	0.120
Lip Thickness (inches)	0.020
Mass Flow Rate per Nozzle (slugs/sec)	1.638E-04
Non-dimensional Blowing Rate, Lambda	0.2367
Nozzle Reservoir Pressure (psia)	36.84
Exit Plane Pressure (psia)	1.908
Coolant Total Temperature (Rankine)	530

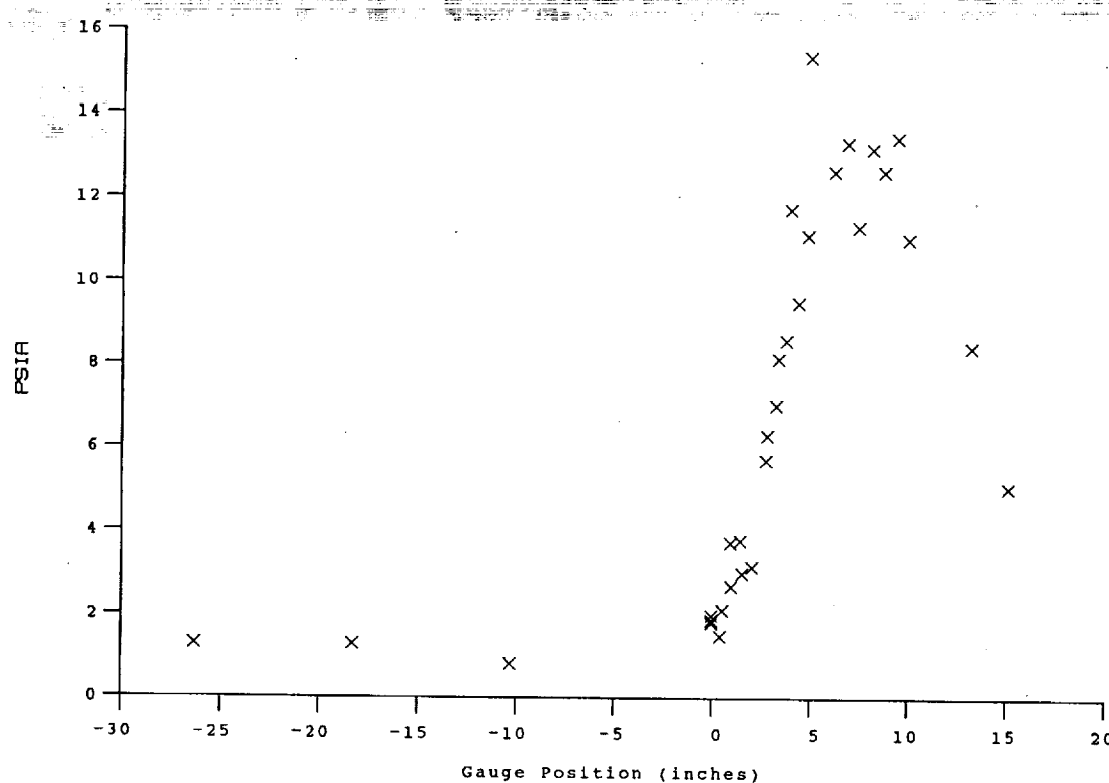
* See Shock Generator Diagram (Page A23)

Run 62



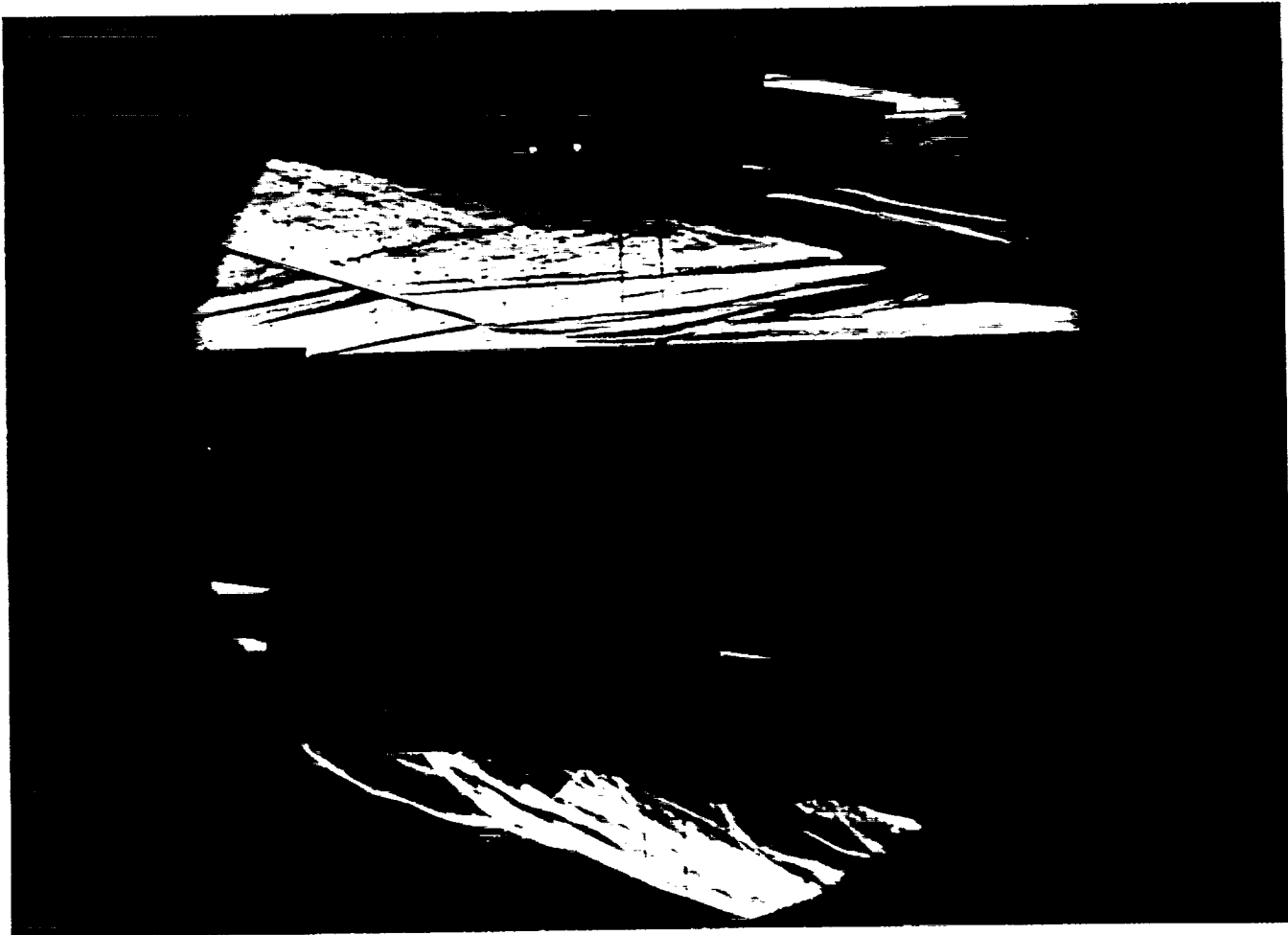
HEAT TRANSFER vs Gauge Position

Run 62



PRESSURE vs Gauge Position

Run 62



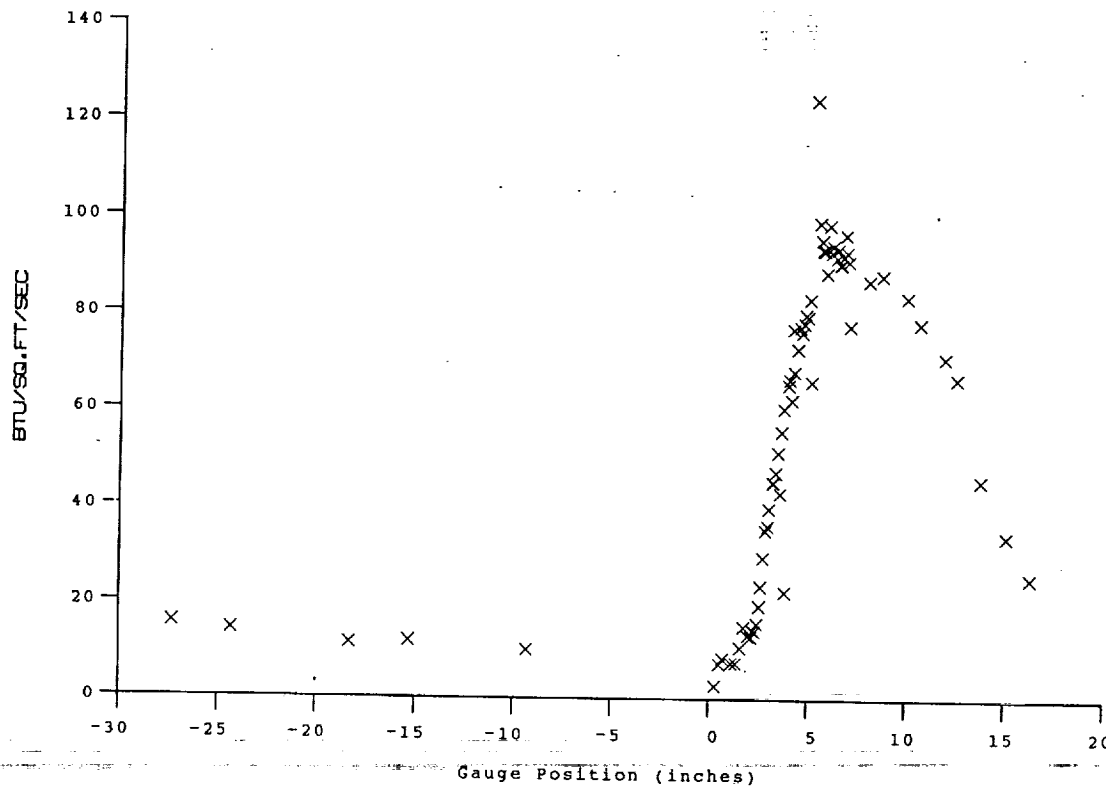
Test Conditions

$M_i = 2.7903$
 $P_{o1} = 2.3121 \times 10^3$ PSIA
 $H_o = 1.3157 \times 10^7$ (Ft/sec)²
 $T_o = 2.0684 \times 10^{-3}$ Degrees R
 $M = 6.4373$
 $U = 4.8482 \times 10^3$ Ft/sec
 $T = 2.3587 \times 10^{-2}$ Degrees R
 $P = 9.4590 \times 10^{-1}$ PSIA
 $Q = 2.7467 \times 10^{-1}$ PSIA
 $\rho_o = 3.3654 \times 10^{-4}$ Slugs/Ft³
 $\mu = 1.9412 \times 10^{-7}$ Slugs/Ft-sec
 $Re = 8.4054 \times 10^6$ 1/ft
 $P_{o1}' = 5.1177 \times 10^{-1}$ PSIA

Model Configuration Parameter	Value
Horizontal Shock Generator Angle (degrees)	10.5
X * (inches)	6.678
Y * (inches)	2.278
Slot Height (inches)	0.120
Lip Thickness (inches)	0.020
Lambda	0

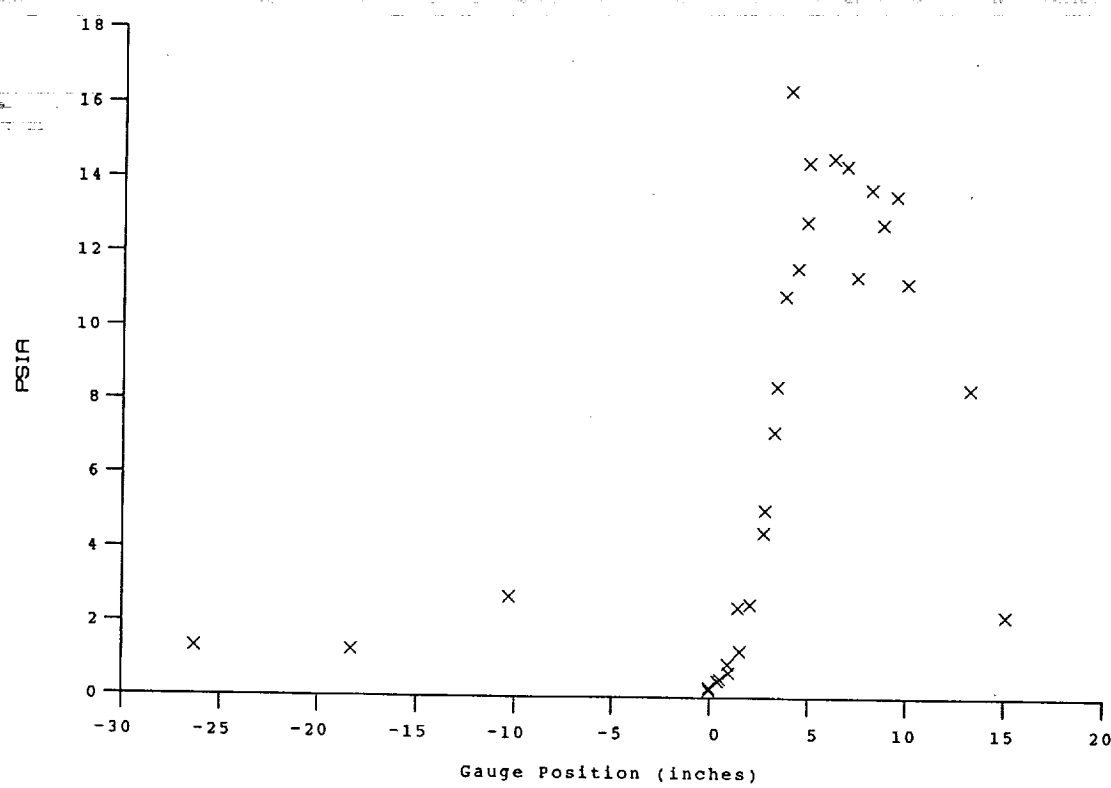
* see shock generator diagram at page A-23

Run 63



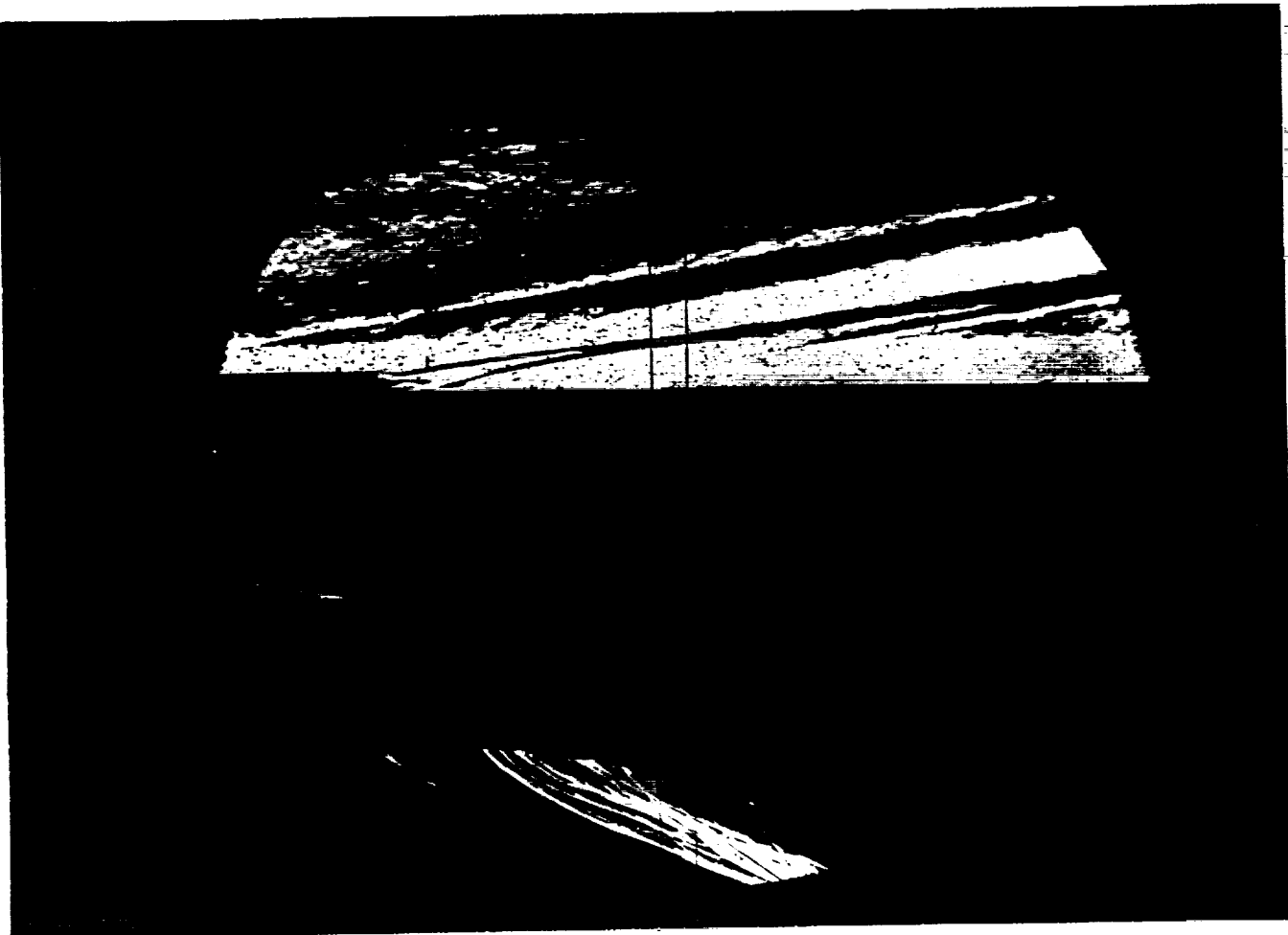
HEAT TRANSFER vs Gauge Position

Run 63



PRESSURE vs Gauge Position

Run 63



Test Conditions

M_i = 2.8286
P_o = 2.4527X10+3 PSIA
H_o = 1.3602X10+7 (Ft/sec)²
T_o = 2.1317X10+3 Degrees R
M = 6.4364
U = 4.9295X10+3 Ft/sec
T = 2.4391X10+2 Degrees R
P = 9.9861X10-1 PSIA
Q = 2.8990X10+1 PSIA
Rho = 3.4359X10-4 Slugs/Ft³
Mu = 2.0024X10-7 Slugs/Ft-sec
Re = 8.4586X10+6 1/Ft
P_{o'} = 5.4039X10+1 PSIA

Model Parameter	Value
Slot Height (inches)	0.120
Lip Thickness (inches)	0.205
Mass Flow Rate per Nozzle (slugs/sec)	6.894E-05
Non-dimensional Blowing Rate, Lambda	0.0988
Nozzle Reservoir Pressure (psia)	18.00
Exit Plane Pressure (psia)	1.030
Coolant Total Temperature (Rankine)	530

Run 65

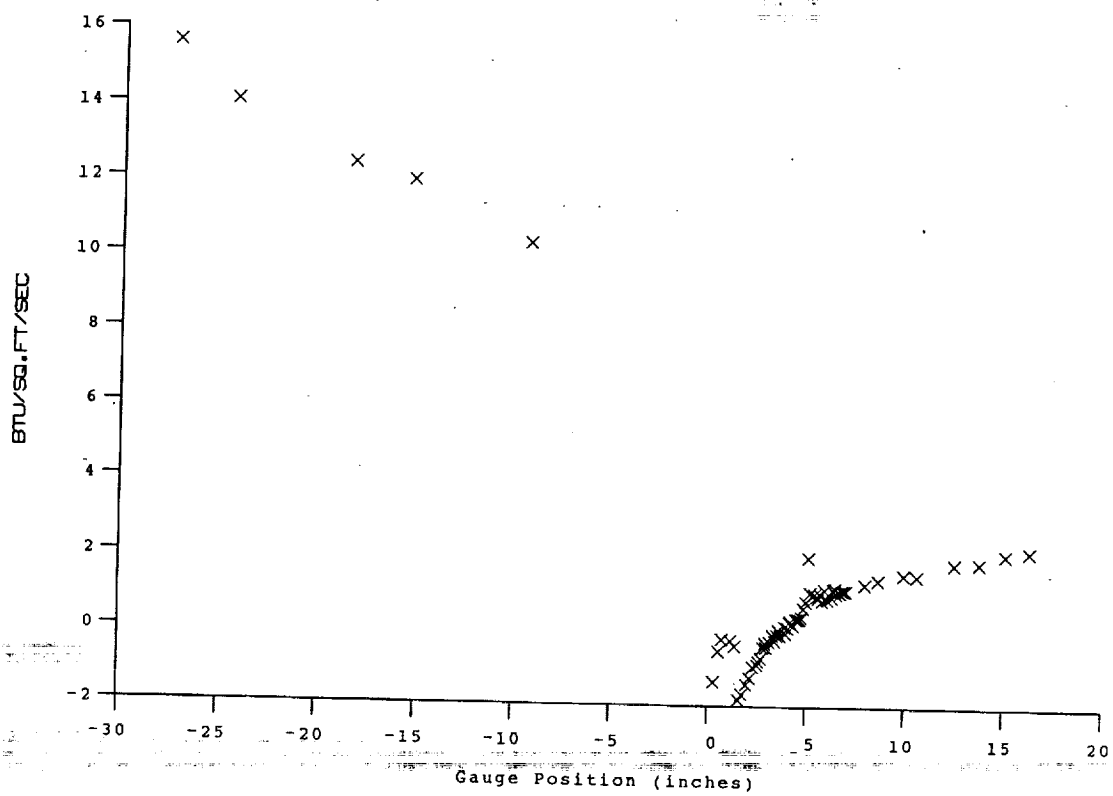


Figure HEAT TRANSFER vs Gauge Position
Run 65

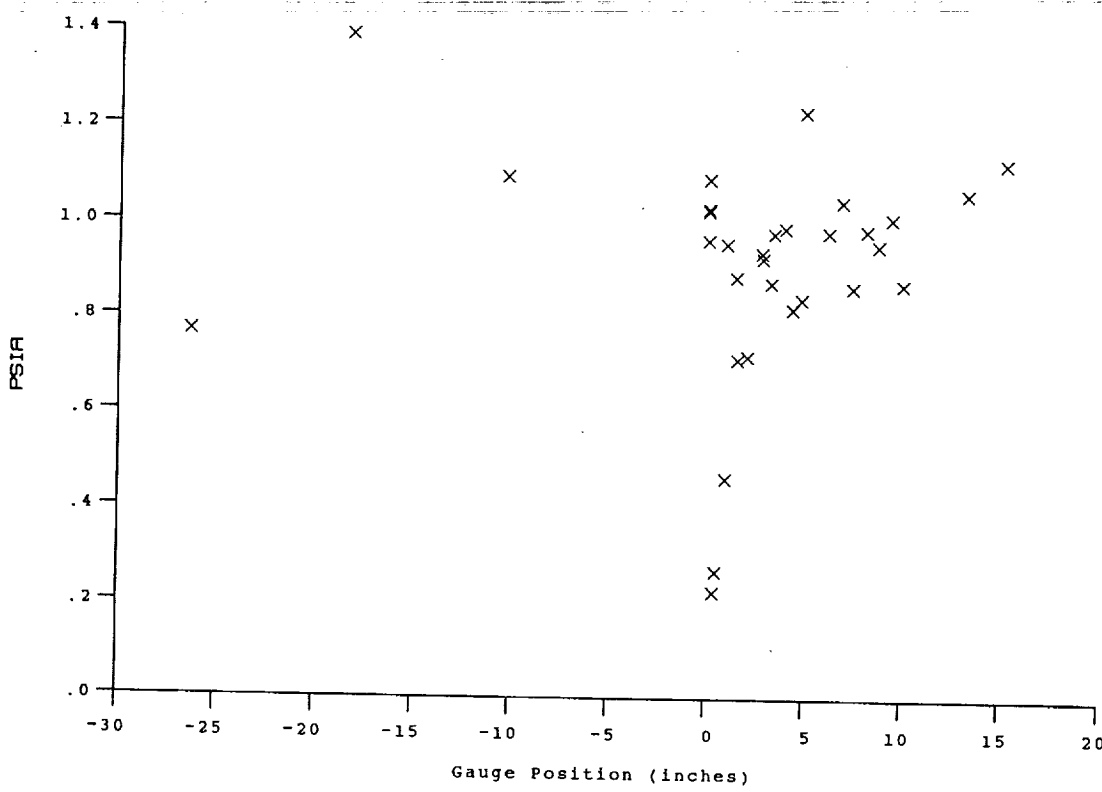
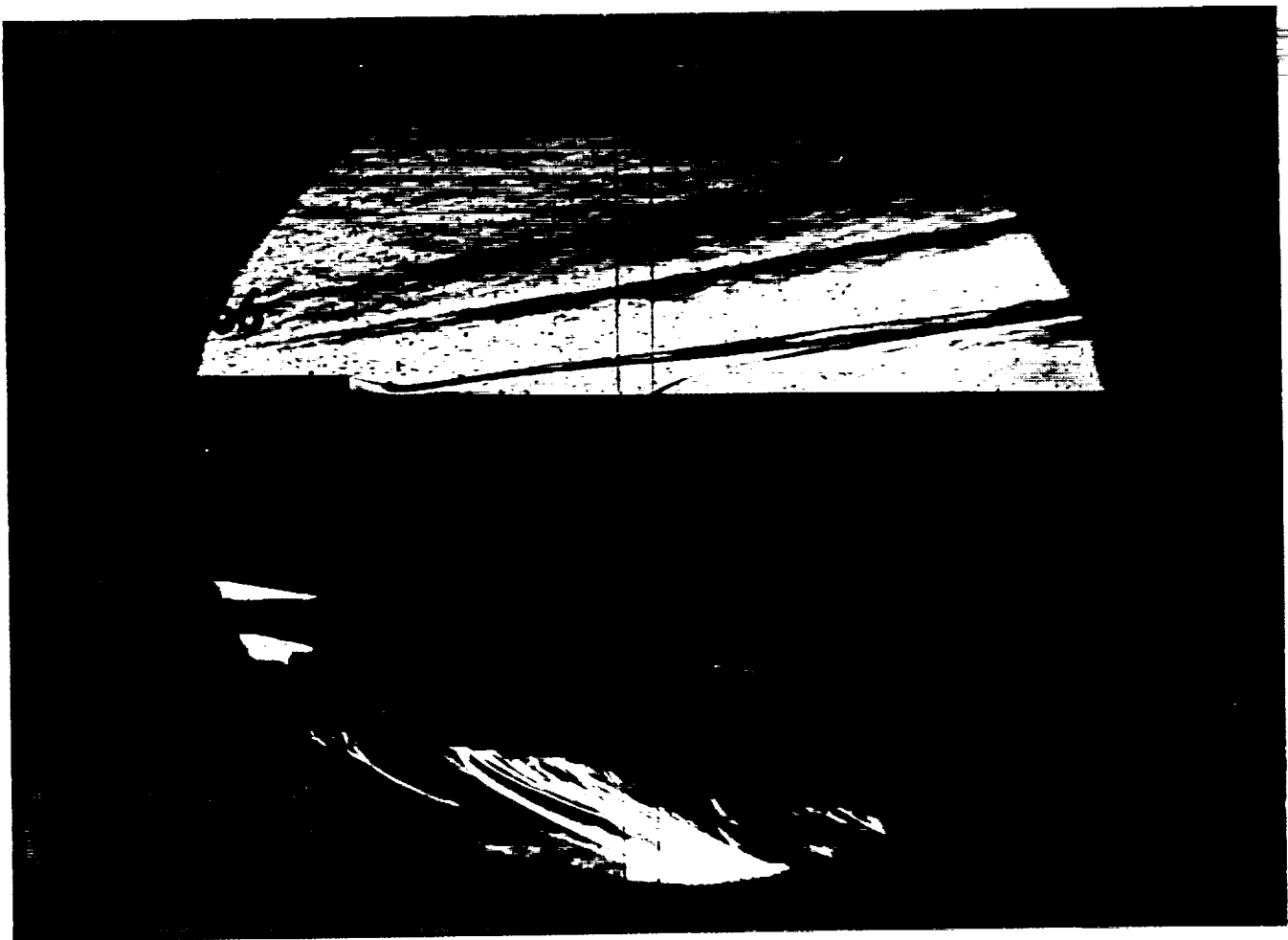


Figure PRESSURE vs Gauge Position
Run 65



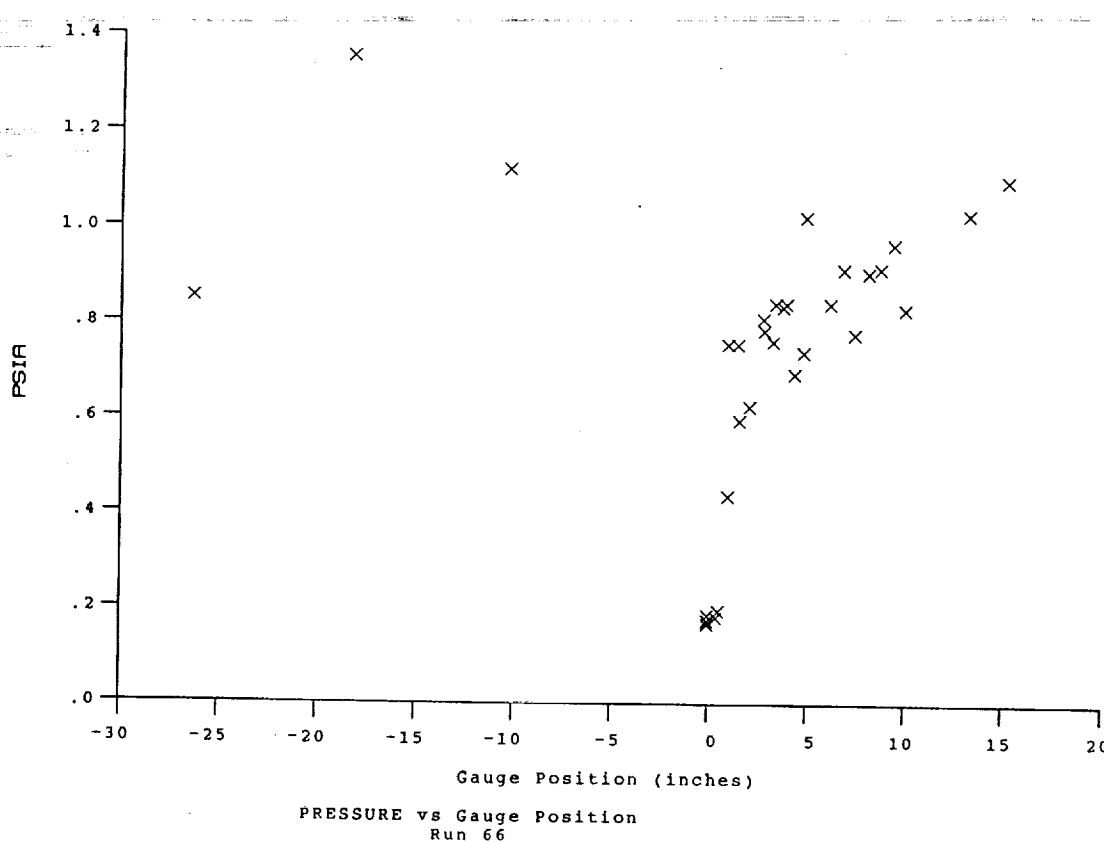
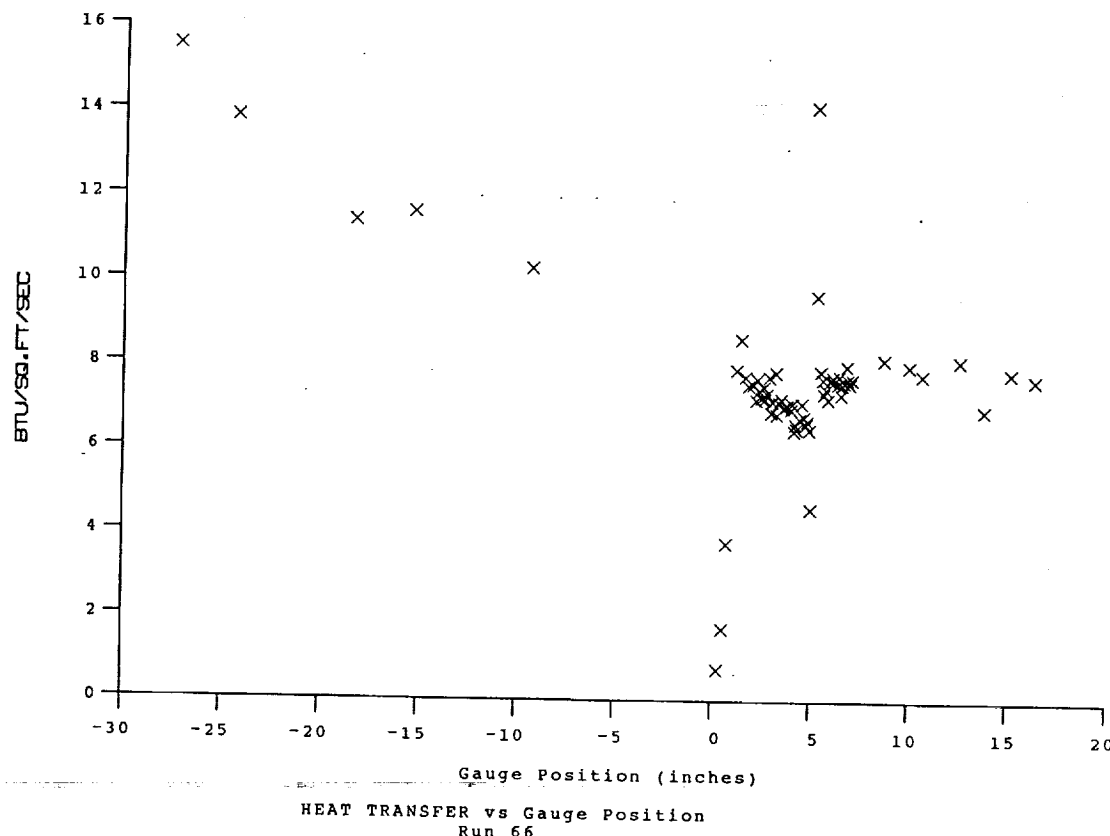
Test Conditions

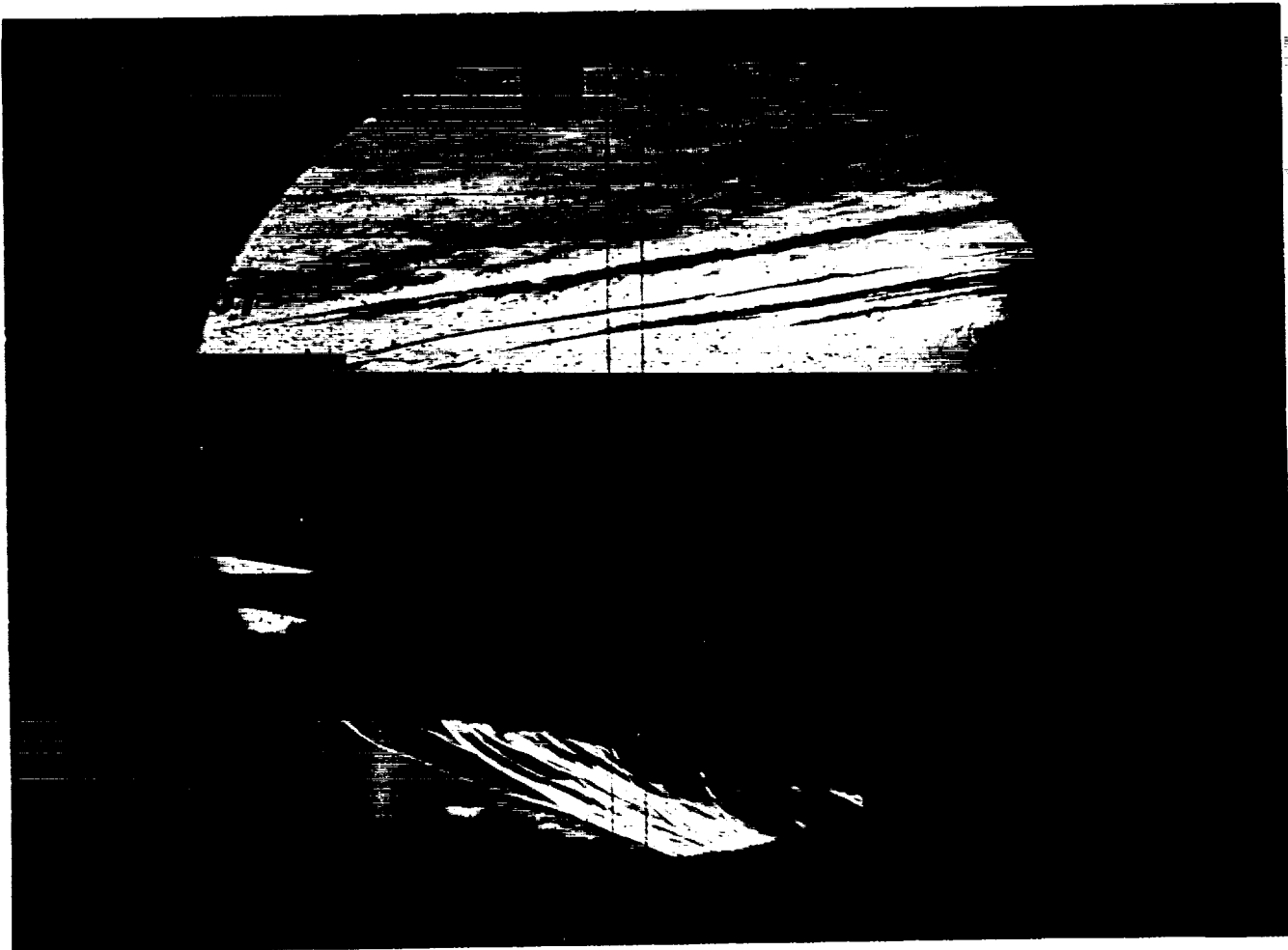
M_i = 2.8098
P_o = 2.4230X10+3 PSIA
H_o = 1.3467X10+7 (Ft/sec)²
T_o = 2.1129X10+3 Degrees R
M = 6.4391
U = 4.9050X10+3 Ft/sec
T = 2.4130X10+2 Degrees R
P = 9.8601X10-1 PSIA
Q = 2.8648X10+1 PSIA
Rho = 3.4292X10-4 Slugs/Ft³
Mu = 1.9825X10-7 Slugs/Ft-sec
Re = 8.4842X10+6 1/Ft
P_{o'} = 5.3394X10+1 PSIA

Model Configuration Parameter

	Value
Slot Height (inches)	0.120
Lip Thickness (inches)	0.205
Lambda	0

Run 66



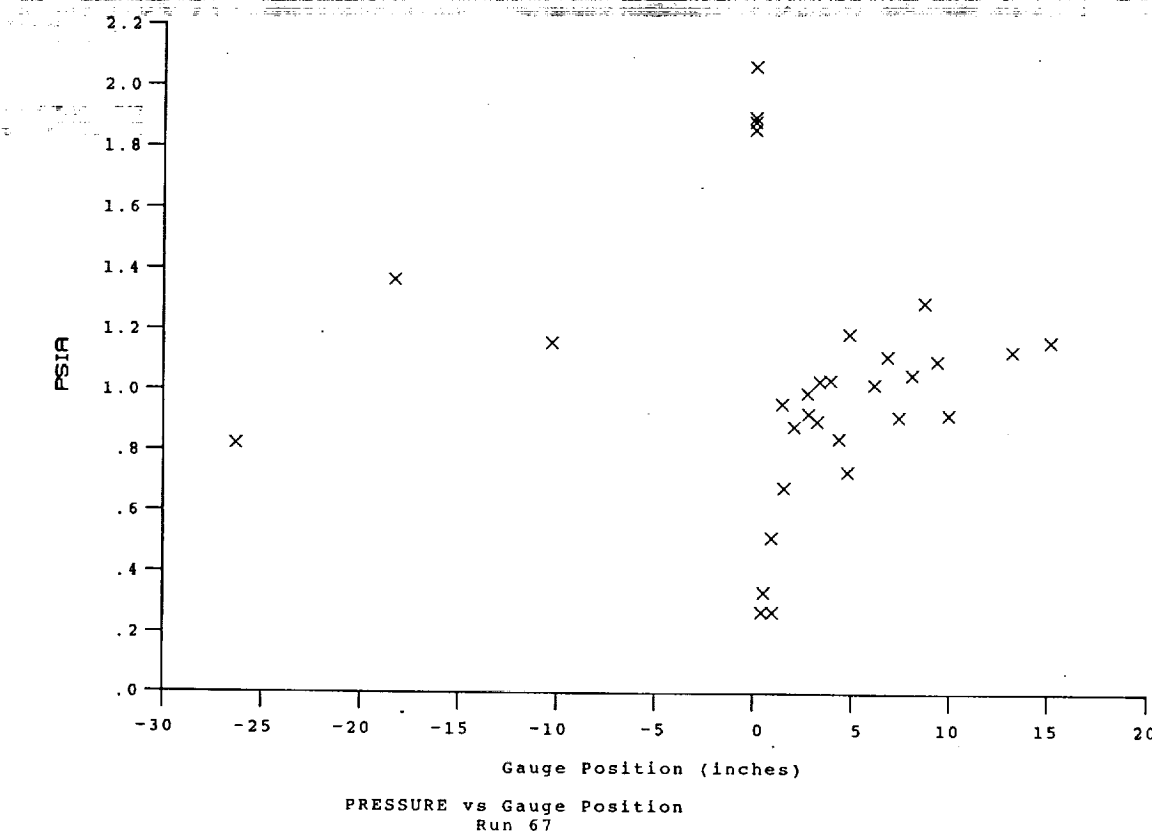
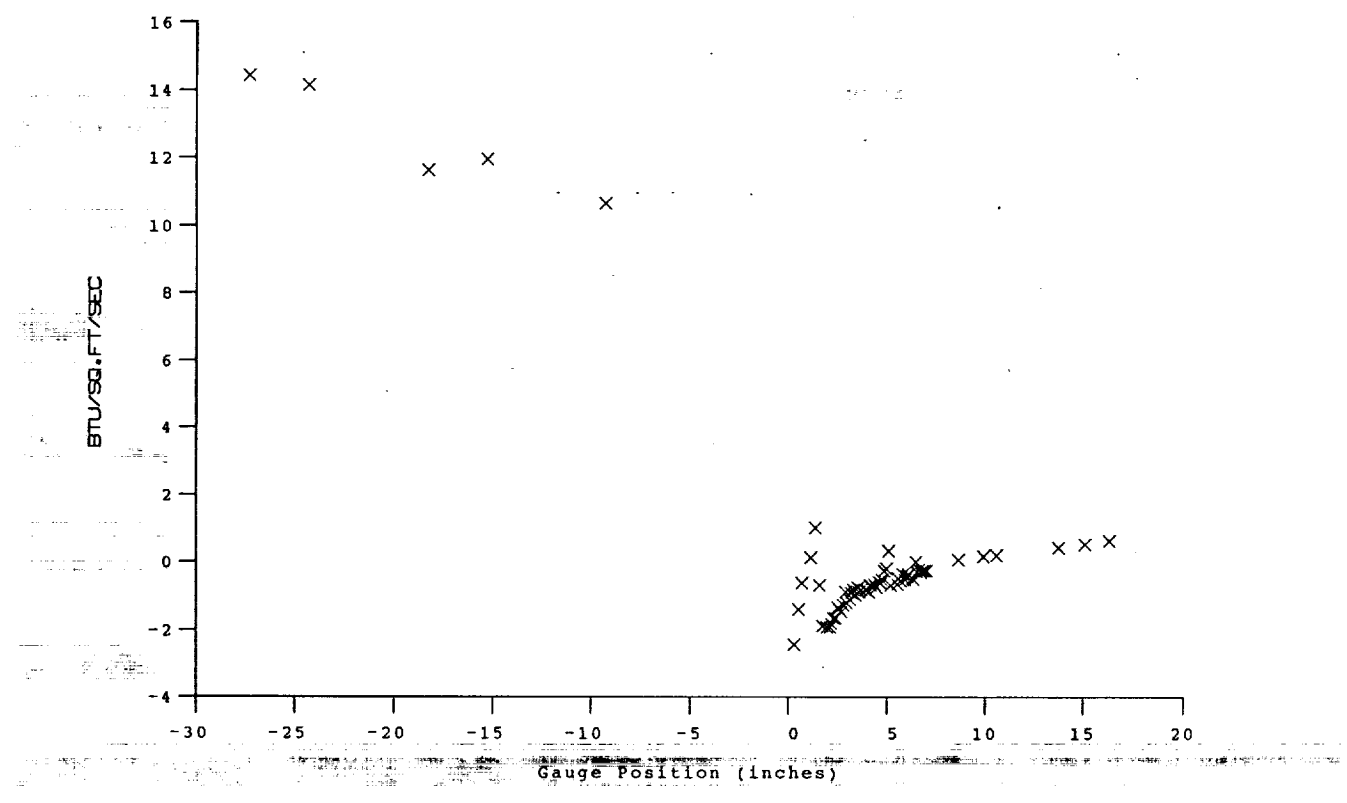


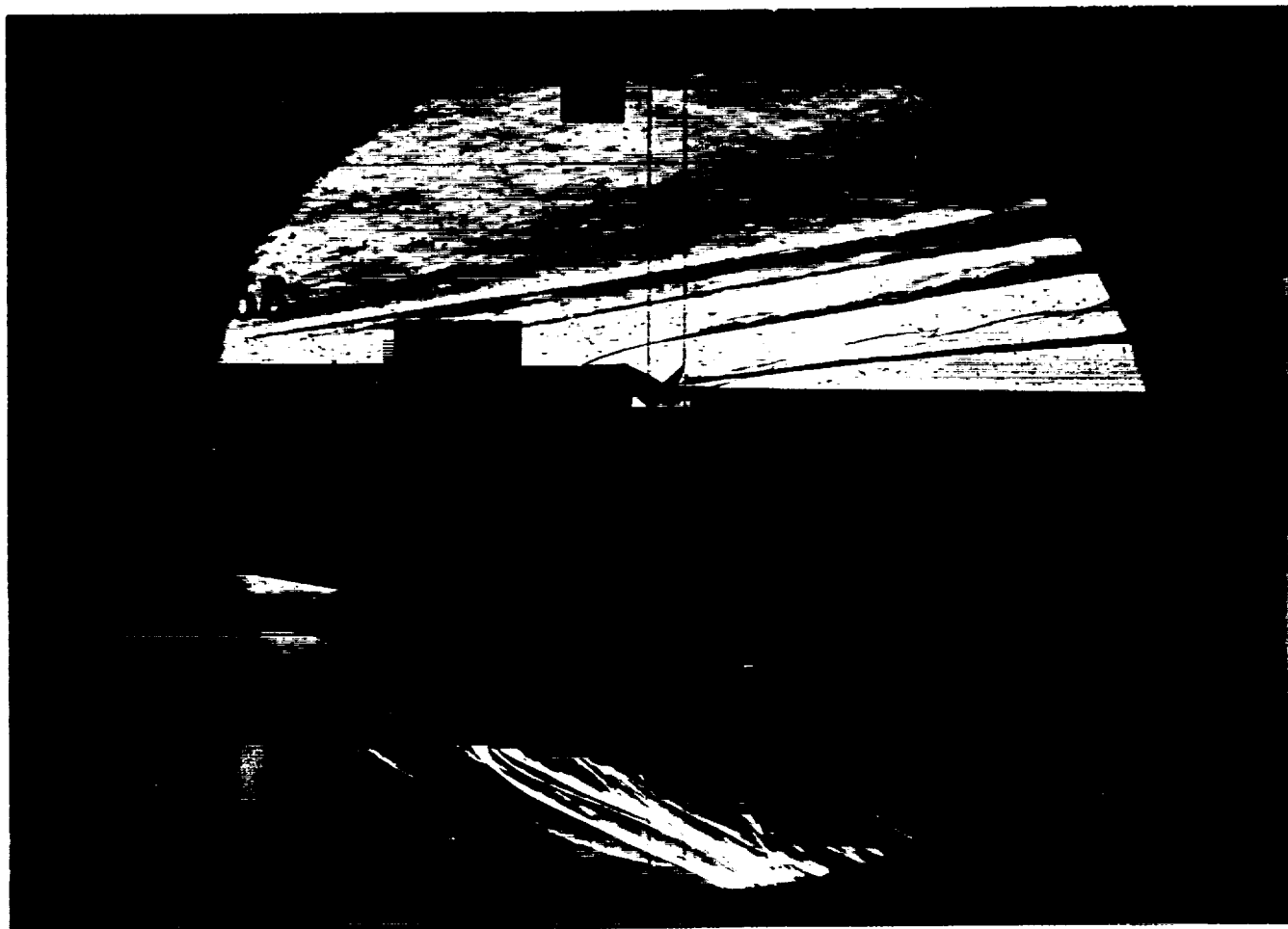
Test Conditions

$M_i = 2.8328$
 $P_o = 2.4263 \times 10+3$ PSIA
 $H_o = 1.3466 \times 10+7$ (Ft/sec)²
 $T_o = 2.1113 \times 10+3$ Degrees R
 $M = 6.4341$
 $U = 4.9045 \times 10+3$ Ft/sec
 $T = 2.4162 \times 10+2$ Degrees R
 $P = 9.9218 \times 10-1$ PSIA
 $Q = 2.8782 \times 10+1$ PSIA
 $Rho = 3.4461 \times 10-4$ Slugs/Ft³
 $Mu = 1.9850 \times 10-7$ Slugs/Ft-sec
 $Re = 8.5145 \times 10+6$ 1/Ft
 $Po' = 5.3645 \times 10+1$ PSIA

Model Parameter	Value
Slot Height (inches)	0.120
Lip Thickness (inches)	0.205
Mass Flow Rate per Nozzle (slugs/sec)	1.650E-04
Non-dimensional Blowing Rate, Lambda	0.2368
Nozzle Reservoir Pressure (psia)	37.85
Exit Plane Pressure (psia)	1.933
Coolant Total Temperature (Rankine)	530

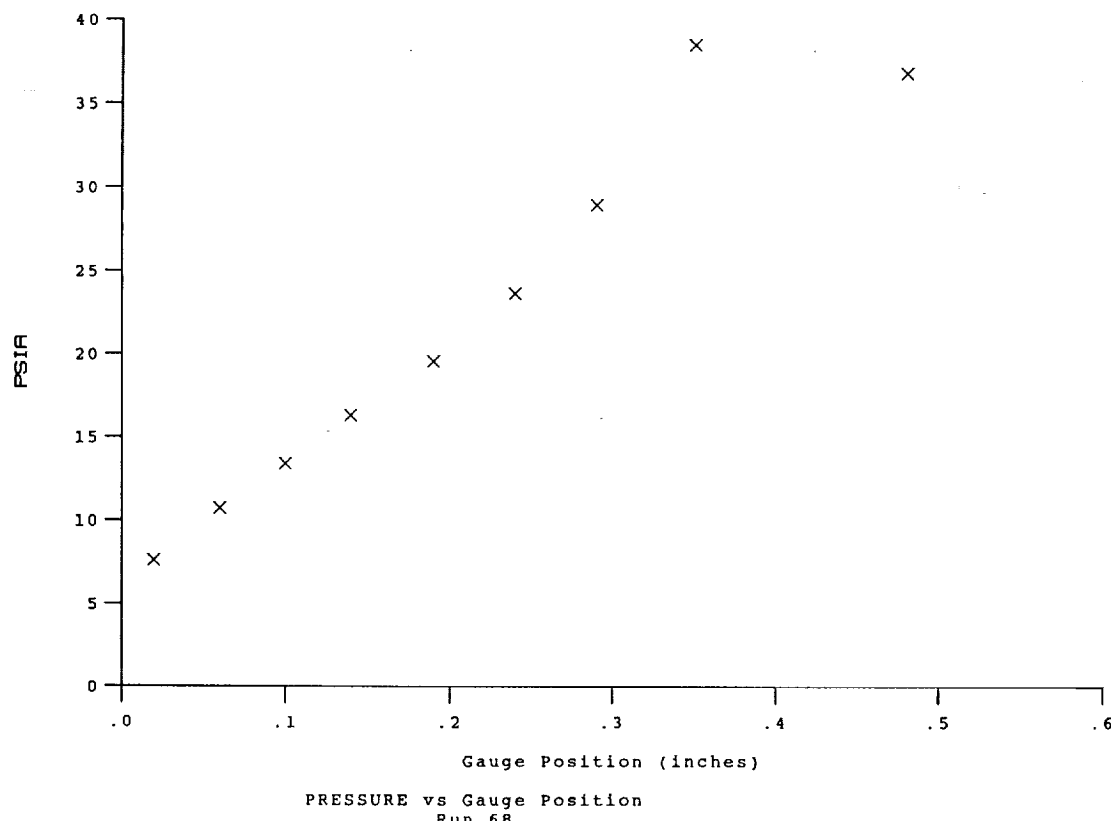
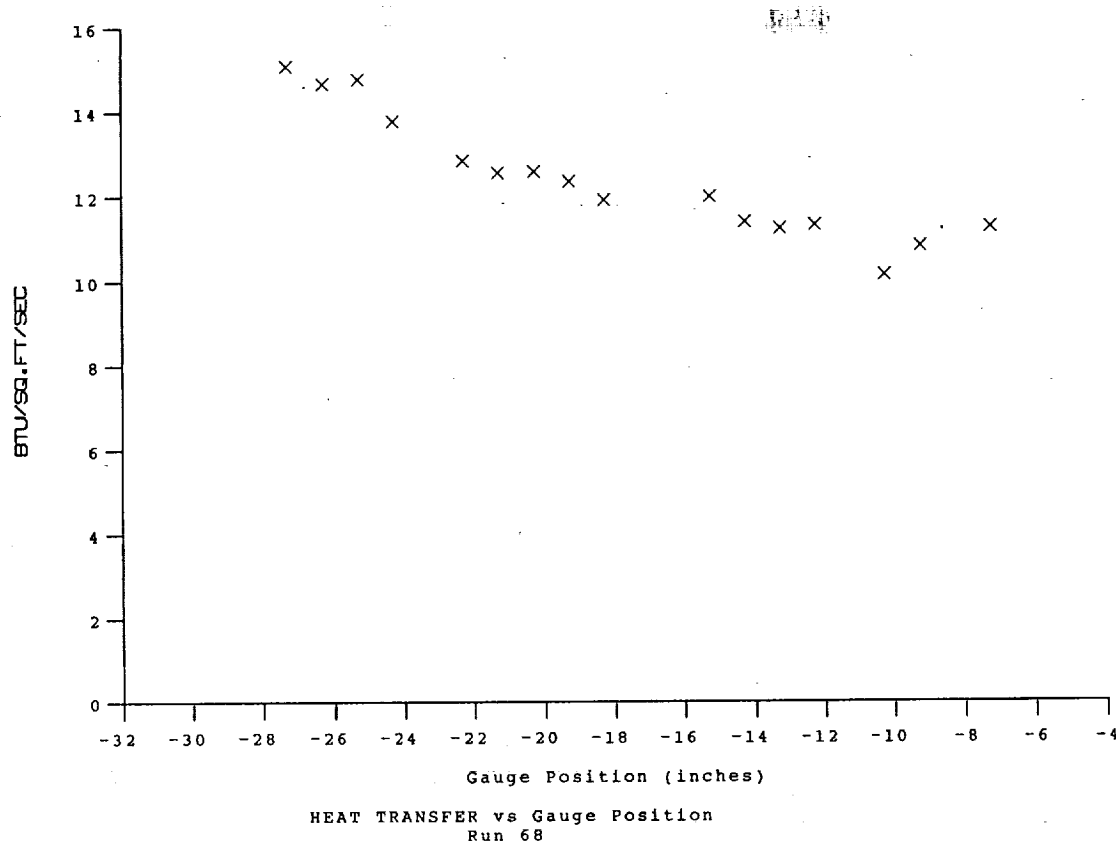
Run 67

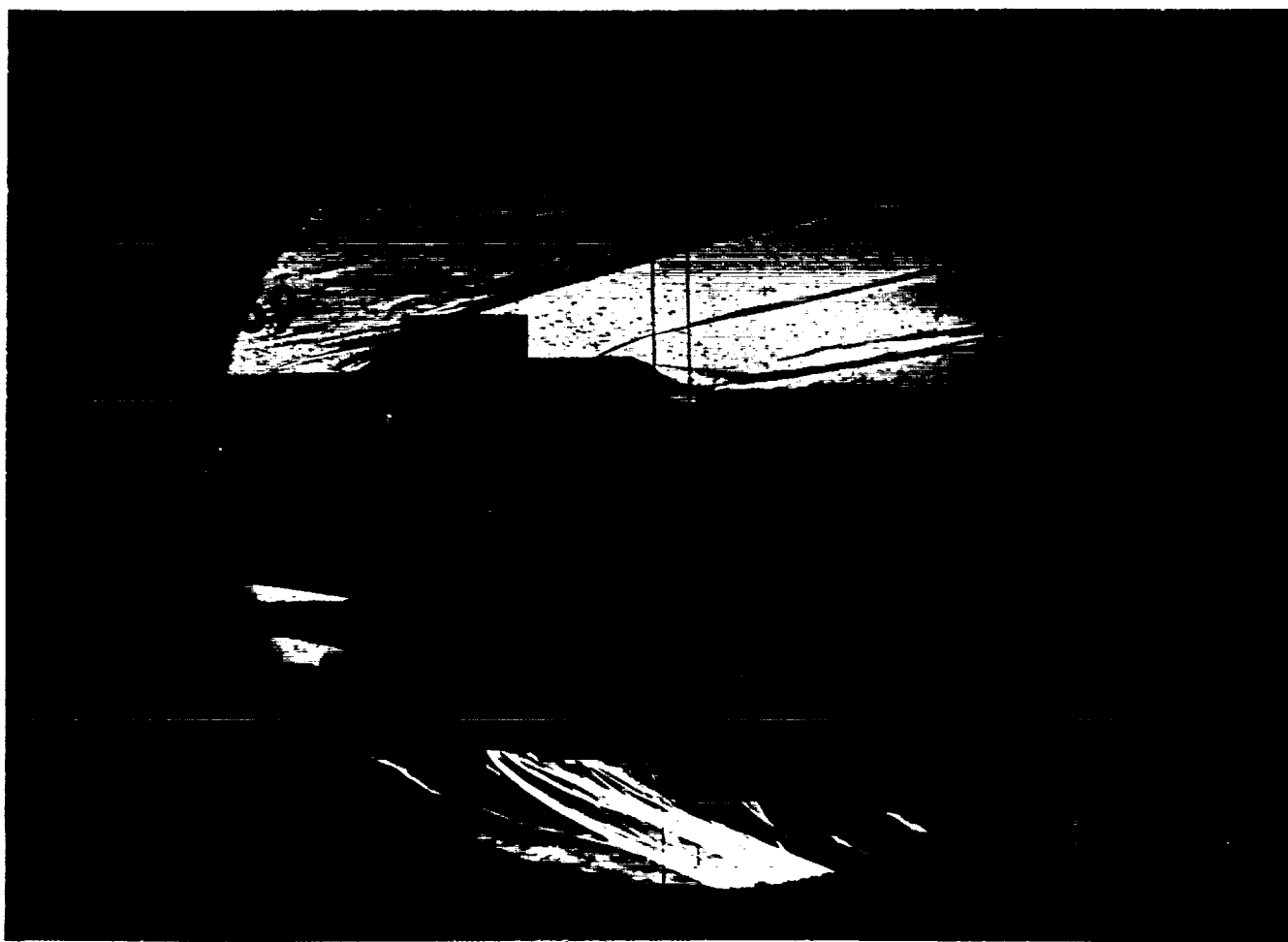




Test Conditions	Model Configuration Parameter	Value
$M_i = 2.8142$	Boundary Layer Rake	
$P_0 = 2.3163 \times 10^3$ PSIA		
$H_0 = 1.3298 \times 10^7$ $(\text{Ft/sec})^2$		
$T_0 = 2.0877 \times 10^{-3}$ Degrees R		
$M = 6.4322$		
$U = 4.8737 \times 10^3$ Ft/sec		
$T = 2.3873 \times 10^{-2}$ Degrees R		
$P = 9.4973 \times 10^{-1}$ PSIA		
$Q = 2.7535 \times 10^1$ PSIA		
$\rho = 3.3386 \times 10^{-4}$ Slugs/ Ft^3		
$\mu = 1.9630 \times 10^{-7}$ Slugs/ Ft-sec		
$Re = 8.2889 \times 10^6$ 1/Ft		
$P_0' = 5.1311 \times 10^1$ PSIA		

Run 68



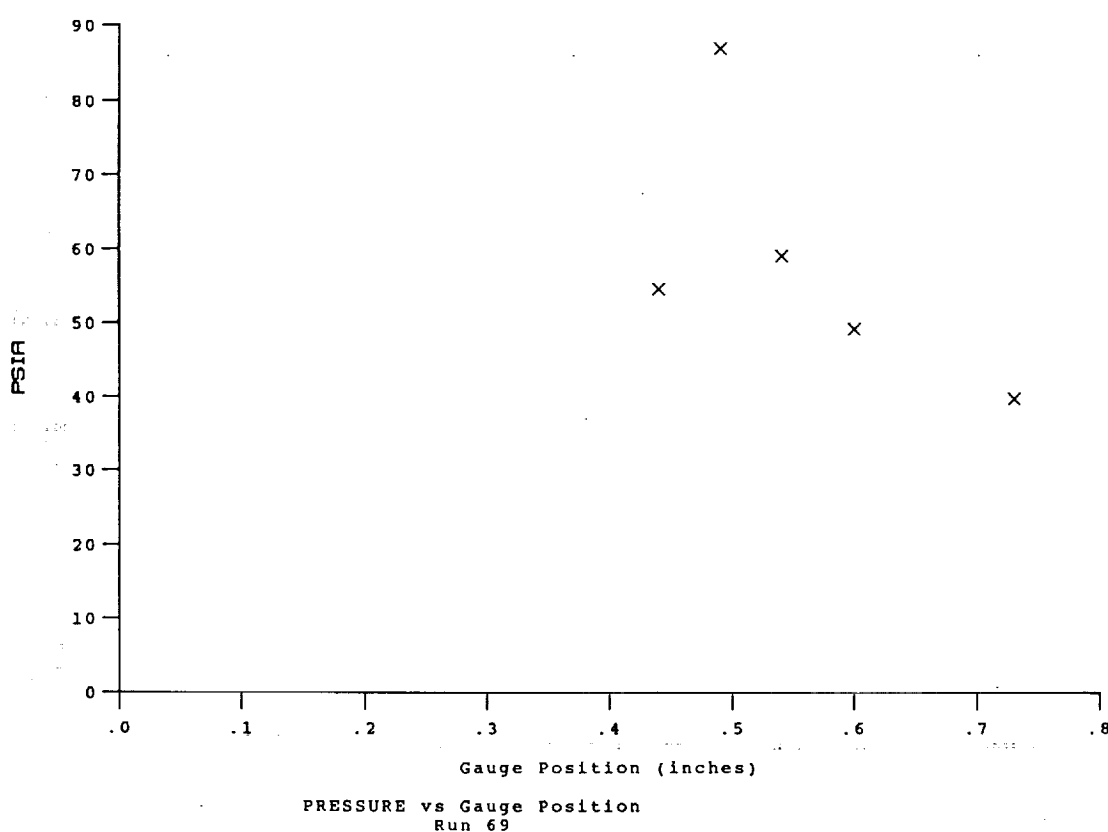
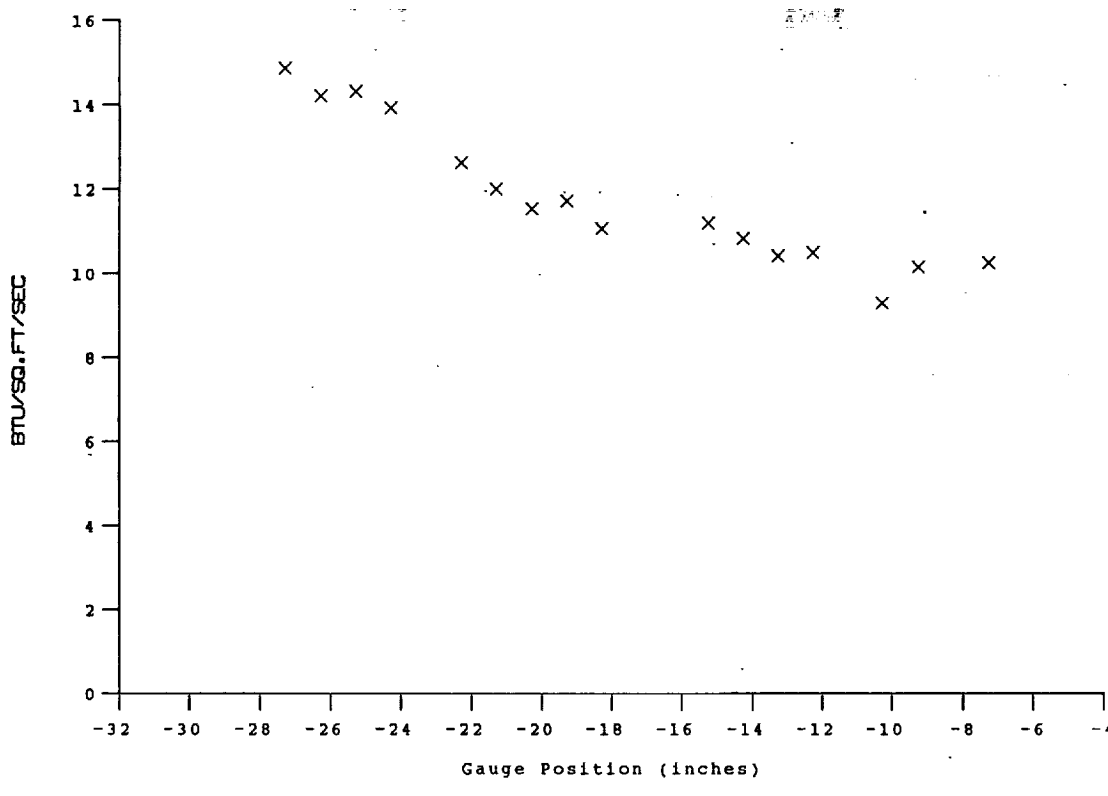
**Test Conditions**

M_i = 2.7925
P_o = 2.2760X10+3 PSIA
H_o = 1.3197X10+7 (Ft/sec)²
T_o = 2.0742X10+3 Degrees R
M = 6.4347
U = 4.8554X10+3 Ft/sec
T = 2.3676X10+2 Degrees R
P = 9.3192X10-1 PSIA
Q = 2.7039X10+1 PSIA
Rho = 3.3032X10-4 Slugs/Ft³
Mu = 1.9479X10-7 Slugs/Ft-sec
Re = 8.2334X10+6 1/Ft
P_{o'} = 5.0382X10+1 PSIA

Model Configuration Parameter Value

Boundary Layer Rake

Run 69



A-101

Gauge Label	Loc. (in)	Value (PSIA) or (BTU/Ft ² -Sec)	T Surf (DegR)	Gauge Label	Loc. (in)	Value (PSIA) or (BTU/Ft ² -Sec)	T Surf (DegR)	Gauge Label	Loc. (in)	Value (PSIA) or (BTU/Ft ² -Sec)	T Surf (DegR)
L28P1	-26.28	1.296(0)	L28H8	-21.28	1.671(1)	546.12	P5H36	3.82	1.022(1)	539.54	
L28P2	-22.28	1.316(0)	L28H11	-18.28	1.450(1)	544.35	P5H37	4.03	9.998(0)	539.73	
L28P3	-18.28	1.466(0)	L28H13	-15.28	1.413(1)	543.52	P5H38	4.29	1.062(1)	540.30	
L28P4	-14.28	Null	L28H16	-12.28	1.332(1)	543.05	P5H39	4.49	Null	Null	
L28P5	-10.28	1.406(0)	L28H18	-9.28	1.191(1)	541.60	P5H40	4.69	1.023(1)	539.85	
L28P6	-6.28	1.243(0)	PSH1	.13	Null	Null	P5H41	4.89	1.037(1)	540.03	
P5P10	.37	1.274(0)	PSH2	.23	1.131(1)	540.99	P5H42	5.08	1.048(1)	540.06	
P5P1	.46	Null	PSH3	.33	1.119(1)	540.77	P12H1	5.24	Null	Null	
P5P12	.88	1.297(0)	PSH4	.42	1.142(1)	540.75	P12H2	5.33	1.034(1)	539.93	
P5P2	.97	1.100(0)	PSH5	.52	1.108(1)	540.56	P12H3	5.43	1.033(1)	539.98	
P5P14	1.35	1.116(0)	PSH6	.62	1.131(1)	540.81	P12H4	5.53	1.042(1)	539.93	
P5P3	1.48	1.100(0)	PSH7	.71	1.114(1)	540.60	P12H5	5.63	1.029(1)	539.82	
P5P16	1.91	1.143(0)	PSH8	.81	1.104(1)	540.35	P12H6	5.72	1.035(1)	539.84	
P5P4	1.98	1.088(0)	PSH9	.90	1.114(1)	540.55	P12H7	5.82	1.007(1)	539.50	
P5P18	2.42	1.116(0)	PSH10	.99	1.049(1)	540.14	P12H8	5.92	1.015(1)	539.70	
P5P5	2.49	1.121(0)	PSH11	1.07	1.068(1)	540.10	P12H9	6.02	1.023(1)	539.58	
P5P20	2.93	1.153(0)	PSH12	1.13	1.064(1)	539.98	P12H10	6.12	9.790(0)	539.41	
P12P1	5.47	1.014(0)	PSH13	1.21	1.096(1)	540.54	P12H11	6.21	Null	Null	
P12P2	6.11	1.065(0)	PSH14	1.29	1.150(1)	540.74	P12H12	6.30	9.830(0)	539.82	
P12P3	6.76	1.025(0)	PSH15	1.39	Null	Null	P12H13	6.39	Null	Null	
P12P5	8.03	9.003(-1)	PSH16	1.49	1.157(1)	540.49	P12H14	6.48	1.011(1)	539.55	
P12P6	8.68	1.130(0)	PSH17	1.59	Null	Null	P12H15	6.56	9.644(0)	539.56	
P12P7	9.31	1.062(0)	PSH18	1.68	1.165(1)	540.66	P12H16	6.66	9.553(0)	539.50	
P12P9	10.60	Null	PSH19	1.78	1.148(1)	540.74	P12H17	6.74	9.860(0)	539.52	
P12P10	11.23	1.110(0)	PSH20	1.88	Null	Null	P12H18	6.84	1.056(1)	539.70	
P12P11	11.88	Null	PSH21	1.98	1.160(1)	540.79	P12H19	6.93	1.007(1)	539.52	
P12P13	13.15	1.104(0)	PSH22	2.08	1.119(1)	540.76	P12H20	7.02	9.978(0)	539.60	
P12P14	13.80	1.183(0)	PSH23	2.20	1.186(1)	540.93	P12H21	7.39	Null	Null	
P12P16	15.07	1.212(0)	PSH24	2.30	1.132(1)	540.82	P12H22	8.01	1.087(1)	540.21	
P12P18	16.35	1.151(0)	PSH25	2.39	1.173(1)	540.97	P12H23	8.66	1.102(1)	540.45	
P5S2	1.00	Null	PSH26	2.49	1.141(1)	540.79	P12H24	9.30	Null	Null	
P5S3	1.65	Null	PSH27	2.58	1.157(1)	540.89	P12H25	9.92	1.040(1)	539.96	
P5S4	2.33	Null	PSH28	2.68	1.170(1)	540.83	P12H26	10.57	9.986(0)	539.72	
P5S6	3.69	Null	PSH29	2.78	Null	Null	P12H27	11.22	Null	Null	
P12S1	5.47	Null	PSH30	2.87	1.221(1)	541.31	P12H28	11.85	1.054(1)	540.07	
P12S2	6.43	Null	PSH31	2.97	1.116(1)	540.52	P12H29	12.49	1.039(1)	539.87	
P12S3	7.39	Null	PSH32	3.07	1.154(1)	540.75	P12H31	13.78	1.058(1)	539.86	
L28H3	-27.28	1.752(1)	544.88	P5H33	3.21	1.087(1)	540.38	P12H33	15.06	1.072(1)	539.92
L28H4	-26.28	1.932(1)	547.49	P5H34	3.42	1.068(1)	539.86	P12H35	16.33	1.038(1)	539.71
L28H6	-24.28	1.934(1)	548.39	P5H35	3.63	1.030(1)	539.72				

Run 4 Reduced Data Tabulation

Gauge Label	Loc. (in)	Value (PSIA) or (BTU/Ft ² -Sec)	T Surf (DegR)	Gauge Label	Loc. (in)	Value (PSIA) or (BTU/Ft ² -Sec)	T Surf (DegR)	Gauge Label	Loc. (in)	Value (PSIA) or (BTU/Ft ² -Sec)	T Surf (DegR)
L28P1	-26.28	1.976(0)	L28H8	-21.28	2.261(1)	548.40	P5H36	3.82	1.474(1)	541.76	
L28P2	-22.28	1.902(0)	L28H11	-18.28	2.069(1)	546.83	P5H37	4.03	1.504(1)	541.79	
L28P3	-18.28	2.106(0)	L28H13	-15.28	1.869(1)	545.17	P5H38	4.29	1.612(1)	542.55	
L28P4	-14.28	Null	L28H16	-12.28	1.939(1)	545.37	P5H39	4.49	1.501(1)	541.83	
L28P5	-10.28	2.032(0)	L28H18	-9.28	1.722(1)	543.74	P5H40	4.69	1.545(1)	542.13	
L28P6	-6.28	1.817(0)	PSH1	.13	1.829(1)	544.58	P5H41	4.89	1.546(1)	542.38	
P5P10	.37	1.864(0)	PSH2	.23	1.694(1)	543.30	P5H42	5.08	1.539(1)	541.91	
P5P1	.46	1.638(0)	PSH3	.33	1.620(1)	543.00	P12H1	5.24	1.406(1)	541.41	
P5P12	.88	1.927(0)	PSH4	.42	1.605(1)	542.84	P12H2	5.33	1.582(1)	542.25	
P5P2	.97	1.646(0)	PSH5	.52	1.639(1)	542.97	P12H3	5.43	1.590(1)	542.28	
P5P14	1.35	1.583(0)	PSH6	.62	1.663(1)	543.13	P12H4	5.53	1.510(1)	541.90	
P5P3	1.48	1.657(0)	PSH7	.71	1.658(1)	542.97	P12H5	5.63	1.500(1)	541.80	
P5P16	1.91	1.653(0)	PSH8	.81	1.608(1)	542.79	P12H6	5.72	1.469(1)	541.58	
P5P4	1.98	1.705(0)	PSH9	.90	1.584(1)	542.52	P12H7	5.82	1.474(1)	541.63	
P5P18	2.42	1.660(0)	PSH10	.99	1.548(1)	542.26	P12H8	5.92	1.431(1)	541.53	
P5P5	2.49	1.650(0)	PSH11	1.07	1.544(1)	542.17	P12H9	6.02	1.260(1)	540.12	
P5P20	2.93	1.731(0)	PSH12	1.13	1.566(1)	542.37	P12H10	6.12	1.366(1)	541.14	
P12P1	5.47	1.460(0)	PSH13	1.21	1.621(1)	542.41	P12H11	6.21	1.287(1)	540.52	
P12P2	6.11	1.583(0)	PSH14	1.29	1.605(1)	542.64	P12H12	6.30	1.443(1)	541.47	
P12P3	6.76	1.456(0)	PSH15	1.39	1.572(1)	542.36	P12H13	6.39	1.392(1)	541.13	
P12P5	8.03	Null	PSH16	1.49	1.599(1)	542.58	P12H14	6.48	1.427(1)	541.28	
P12P6	8.68	1.649(0)	PSH17	1.59	Null	Null	P12H15	6.56	1.408(1)	541.15	
P12P7	9.31	1.540(0)	PSH18	1.68	Null	Null	P12H16	6.66	1.377(1)	541.01	
P12P9	10.60	Null	PSH19	1.78	1.633(1)	542.92	P12H17	6.74	1.390(1)	541.12	
P12P10	11.23	1.647(0)	PSH20	1.88	1.621(1)	542.73	P12H18	6.84	1.406(1)	541.13	
P12P11	11.88	Null	PSH21	1.98	1.639(1)	542.95	P12H19	6.93	1.398(1)	540.98	
P12P13	13.15	1.604(0)	PSH22	2.08	1.687(1)	543.01	P12H20	7.02	1.435(1)	541.39	
P12P14	13.80	1.740(0)	PSH23	2.20	1.657(1)	542.93	P12H21	7.39	Null	Null	
P12P16	15.07	1.775(0)	PSH24	2.30	1.683(1)	543.16	P12H22	8.01	1.496(1)	541.84	
P12P18	16.35	1.680(0)	PSH25	2.39	1.668(1)	543.10	P12H23	8.66	1.581(1)	542.34	
P5S2	1.00	Null	PSH26	2.49	Null	Null	P12H24	9.30	Null	Null	
P5S3	1.65	Null	PSH27	2.58	1.666(1)	543.29	P12H25	9.92	1.493(1)	541.76	
P5S4	2.33	Null	PSH28	2.68	1.672(1)	542.99	P12H26	10.57	1.474(1)	541.42	
P5S6	3.69	Null	PSH29	2.78	Null	Null	P12H27	11.22	Null	Null	
P12S1	5.47	Null	PSH30	2.87	1.752(1)	543.34	P12H28	11.85	1.500(1)	541.60	
P12S2	6.43	Null	PSH31	2.97	1.673(1)	543.03	P12H29	12.49	1.459(1)	541.51	
P12S3	7.39	Null	PSH32	3.07	Null	Null	P12H31	13.78	1.451(1)	541.38	
L28H3	-27.28	2.779(1)	550.98	P5H33	3.21	1.601(1)	542.52	P12H33	15.06	1.501(1)	541.49
L28H4	-26.28	2.728(1)	551.10	P5H34	3.42	1.515(1)	541.74	P12H35	16.33	1.446(1)	541.29
L28H6	-24.28	2.572(1)	550.39	P5H35	3.63	1.521(1)	541.94				

Run 5 Reduced Data Tabulation

Gauge Label	Loc. (in)	Value (PSIA) or (BTU/Ft ² -Sec)	T Surf (DegR)	Gauge Label	Loc. (in)	Value (PSIA) or (BTU/Ft ² -Sec)	T Surf (DegR)	Gauge Label	Loc. (in)	Value (PSIA) or (BTU/Ft ² -Sec)	T Surf (DegR)
L28P1	-26.28	6.069(-1)		L28H8	-21.28	8.784(0)	538.58	P5H36	3.82	6.559(0)	536.25
L28P2	-22.28	6.126(-1)		L28H11	-18.28	1.074(1)	540.09	P5H37	4.03	6.970(0)	536.34
L28P3	-18.28	7.346(-1)		L28H13	-15.28	9.671(0)	539.01	P5H38	4.29	6.241(0)	535.64
L28P4	-14.28	Null		L28H16	-12.28	8.782(0)	538.27	P5H39	4.49	6.591(0)	536.23
L28P5	-10.28	6.697(-1)		L28H18	-9.28	7.466(0)	537.22	P5H40	4.69	7.023(0)	536.54
L28P6	-6.28	5.851(-1)		PSH1	.13	8.300(0)	537.60	P5H41	4.89	7.058(0)	536.66
P5P10	.37	6.135(-1)		PSH2	.23	7.418(0)	536.98	P5H42	5.08	6.361(0)	535.88
P5P1	.46	5.421(-1)		PSH3	.33	7.337(0)	536.99	P12H1	5.24	5.664(0)	535.56
P5P12	.88	6.262(-1)		PSH4	.42	7.033(0)	536.63	P12H2	5.33	6.249(0)	535.91
P5P2	.97	5.402(-1)		PSH5	.52	7.058(0)	536.63	P12H3	5.43	6.393(0)	536.18
P5P14	1.35	4.654(-1)		PSH6	.62	Null	Null	P12H4	5.53	6.352(0)	536.05
P5P3	1.48	5.486(-1)		PSH7	.71	Null	Null	P12H5	5.63	6.517(0)	536.04
P5P16	1.91	5.698(-1)		PSH8	.81	7.014(0)	536.54	P12H6	5.72	6.486(0)	536.09
P5P4	1.98	5.614(-1)		PSH9	.90	6.931(0)	536.54	P12H7	5.82	6.381(0)	536.01
P5P18	2.42	5.513(-1)		PSH10	.99	6.558(0)	536.35	P12H8	5.92	6.539(0)	536.11
P5P5	2.49	5.545(-1)		PSH11	1.07	6.329(0)	536.24	P12H9	6.02	6.598(0)	536.15
P5P20	2.93	6.462(-1)		PSH12	1.13	6.487(0)	536.26	P12H10	6.12	6.103(0)	535.95
P12P1	5.47	5.380(-1)		PSH13	1.21	7.266(0)	536.79	P12H11	6.21	5.888(0)	535.67
P12P2	6.11	5.408(-1)		PSH14	1.29	7.200(0)	536.76	P12H12	6.30	6.295(0)	536.05
P12P3	6.76	5.307(-1)		PSH15	1.39	5.603(0)	535.52	P12H13	6.39	6.396(0)	535.96
P12P5	8.03	Null		PSH16	1.49	6.850(0)	536.48	P12H14	6.48	6.501(0)	536.05
P12P6	8.68	5.819(-1)		PSH17	1.59	6.837(0)	536.08	P12H15	6.56	Null	Null
P12P7	9.31	5.154(-1)		PSH18	1.68	6.661(0)	535.94	P12H16	6.66	6.135(0)	535.81
P12P9	10.60	Null		PSH19	1.78	6.994(0)	536.67	P12H17	6.74	6.266(0)	535.88
P12P10	11.23	5.288(-1)		PSH20	1.88	Null	Null	P12H18	6.84	6.560(0)	535.99
P12P11	11.88	Null		PSH21	1.98	6.993(0)	536.66	P12H19	6.93	6.071(0)	535.77
P12P13	13.15	5.313(-1)		PSH22	2.08	6.977(0)	536.60	P12H20	7.02	6.425(0)	536.00
P12P14	13.80	5.444(-1)		PSH23	2.20	5.963(0)	535.78	P12H21	7.39	Null	Null
P12P16	15.07	5.280(-1)		PSH24	2.30	7.088(0)	536.73	P12H22	8.01	6.647(0)	536.26
P12P18	16.35	5.499(-1)		PSH25	2.39	7.134(0)	536.76	P12H23	8.66	6.561(0)	536.21
P5S2	1.00	Null		PSH26	2.49	6.927(0)	536.62	P12H24	9.30	6.947(0)	536.52
P5S3	1.65	Null		PSH27	2.58	6.967(0)	536.73	P12H25	9.92	6.415(0)	536.06
P5S4	2.33	Null		PSH28	2.68	6.752(0)	536.64	P12H26	10.57	6.337(0)	535.94
P5S6	3.69	Null		PSH29	2.78	Null	Null	P12H27	11.22	5.326(0)	535.27
P12S1	5.47	Null		PSH30	2.87	7.407(0)	536.95	P12H28	11.85	6.384(0)	536.00
P12S2	6.43	Null		PSH31	2.97	6.995(0)	536.75	P12H29	12.49	6.319(0)	535.93
P12S3	7.39	Null		PSH32	3.07	7.188(0)	536.86	P12H31	13.78	6.196(0)	535.90
L28H3	-27.28	2.982(0)	533.99	PSH33	3.21	6.811(0)	536.53	P12H33	15.06	6.128(0)	535.77
L28H4	-26.28	2.974(0)	533.95	PSH34	3.42	6.154(0)	535.97	P12H35	16.33	6.078(0)	535.80
L28H6	-24.28	3.624(0)	534.72	PSH35	3.63	6.414(0)	536.27				

Run 6 Reduced Data Tabulation

Gauge Label	Loc. (in)	Value (PSIA) or (BTU/Ft ² -Sec)	T Surf (DegR)	Gauge Label	Loc. (in)	Value (PSIA) or (BTU/Ft ² -Sec)	T Surf (DegR)	Gauge Label	Loc. (in)	Value (PSIA) or (BTU/Ft ² -Sec)	T Surf (DegR)
L28P1	-26.28	1.265(0)		P5S2	1.00	Null	PSH33	3.21	8.020(0)	538.79	
L28P3	-18.28	1.356(0)		P5S4	2.33	Null	PSH34	3.42	6.818(0)	538.93	
L28P5	-10.28	1.258(0)		P12S2	6.43	Null	PSH35	3.63	Null	Null	
S8P2	-1.98	Null		L28H3	-27.28	1.346(1)	542.12	P5H36	3.82	7.728(0)	538.44
S8P3	-1.98	Null		L28H6	-24.28	1.794(1)	547.36	P5H37	4.03	7.815(0)	539.08
S8P4	-1.98	Null		L28H11	-18.28	1.324(1)	543.98	P5H39	4.49	8.347(0)	519.33
S8P6	-1.67	Null		L28H13	-15.28	1.236(1)	543.05	P5H40	4.69	8.498(0)	539.44
S8P7	-1.67	Null		L28H18	-9.28	1.183(1)	542.14	P5H41	4.89	8.522(0)	539.68
S8P8	-1.67	Null		PSH1	.13	Null	PSH42	5.08	Null	Null	
S8P9	-1.67	Null		PSH2	.23	2.926(0)	535.01	P12H1	5.24	Null	Null
S8P10	-1.67	Null		PSH3	.33	6.535(0)	537.69	P12H2	5.33	Null	Null
S8P13	-.98	Null		PSH4	.42	1.100(1)	541.49	P12H3	5.43	8.199(0)	539.16
S8P17	-.03	Null		PSH5	.52	1.172(1)	541.90	P12H4	5.53	8.638(0)	539.48
S8P19	-.03	Null		PSH6	.62	1.146(1)	541.70	P12H5	5.63	8.602(0)	539.53
S8P25	-.03	Null		PSH7	.71	1.058(1)	541.11	P12H6	5.72	8.792(0)	539.58
S8P26	-.03	Null		PSH8	.81	1.033(1)	540.87	P12H7	5.82	8.084(0)	539.21
S8P27	-.03	Null		PSH9	.90	9.452(0)	540.37	P12H8	5.92	8.972(0)	539.78
S8P28	-.03	Null		PSH10	.99	9.723(0)	540.32	P12H9	6.02	8.242(0)	539.38
P5P10	.37	4.563(-1)		PSH11	1.07	8.737(0)	539.73	P12H10	6.12	8.595(0)	539.62
P5P1	.46	7.146(-1)		PSH12	1.13	Null	PSH11	6.21	Null	Null	
P5P2	.97	8.877(-1)		PSH13	1.21	9.517(0)	540.03	P12H12	6.30	8.153(0)	539.20
P5P13	1.14	Null		PSH14	1.29	9.299(0)	540.11	P12H13	6.39	8.262(0)	539.41
P5P3	1.48	8.950(-1)		PSH15	1.39	Null	PSH14	6.48	8.098(0)	539.14	
P5P16	1.91	9.521(-1)		PSH16	1.49	8.868(0)	539.87	P12H15	6.56	8.082(0)	539.12
P5P4	1.98	9.746(-1)		PSH17	1.59	8.972(0)	539.81	P12H16	6.66	8.327(0)	539.32
P5P18	2.42	9.730(-1)		PSH18	1.68	9.066(0)	540.10	P12H17	6.74	8.627(0)	539.64
P5P5	2.49	9.800(-1)		PSH19	1.78	8.170(0)	539.30	P12H18	6.84	8.309(0)	539.31
P5P20	2.93	1.056(0)		PSH20	1.88	8.813(0)	539.66	P12H19	6.93	8.269(0)	539.25
P12P1	5.47	9.681(-1)		PSH21	1.98	8.695(0)	539.58	P12H20	7.02	Null	Null
P12P2	6.11	Null		PSH22	2.08	8.980(0)	539.80	P12H22	8.01	8.894(0)	539.74
P12P4	7.39	Null		PSH23	2.20	8.172(0)	539.48	P12H23	8.66	9.399(0)	539.93
P12P5	8.03	9.648(-1)		PSH24	2.30	7.474(0)	538.54	P12H25	9.92	Null	Null
P12P6	8.68	1.102(0)		PSH25	2.39	7.260(0)	538.41	P12H26	10.57	8.728(0)	539.58
P12P8	9.95	Null		PSH26	2.49	8.642(0)	539.52	P12H28	11.85	8.992(0)	539.80
P12P10	11.23	1.035(0)		PSH27	2.58	8.207(0)	539.24	P12H29	12.49	9.256(0)	539.95
P12P11	11.88	9.640(-1)		PSH28	2.68	8.635(0)	539.54	P12H31	13.78	8.974(0)	539.69
P12P13	13.15	1.053(0)		PSH29	2.78	8.421(0)	539.34	P12H33	15.06	8.970(0)	539.66
P12P14	13.80	1.141(0)		PSH30	2.87	8.712(0)	539.73	P12H35	16.33	8.703(0)	539.61
P12P16	15.07	1.127(0)		PSH31	2.97	8.952(0)	540.04				
P12P18	16.35	1.094(0)		PSH32	3.07	8.732(0)	539.69				

Run 8 Reduced Data Tabulation

Gauge Label	Loc. (in)	Value (PSIA) or (BTU/Ft ² -Sec)	T Surf (DegR)	Gauge Label	Loc. (in)	Value (PSIA) or (BTU/Ft ² -Sec)	T Surf (DegR)	Gauge Label	Loc. (in)	Value (PSIA) or (BTU/Ft ² -Sec)	T Surf (DegR)
L28P1	-26.28	1.156(0)	PSS2	1.00	Null	P5H33	3.21	-1.305(-1)	533.09		
L28P3	-18.28	1.464(0)	PSS4	2.33	Null	P5H34	3.42	Null	Null		
L28P5	-10.28	1.233(0)	P12S2	6.43	Null	P5H35	3.63	Null	Null		
S8P2	-1.98	Null	L28H3	-27.28	1.587(1)	544.92	P5H36	3.82	7.952(-2)	533.64	
S8P3	-1.98	Null	L28H6	-24.28	1.859(1)	547.38	P5H37	4.03	4.908(-1)	533.71	
S8P4	-1.98	Null	L28H11	-18.28	1.534(1)	545.18	P5H39	4.49	4.833(-1)	533.64	
S8P6	-1.67	Null	L28H13	-15.28	1.397(1)	544.53	P5H40	4.69	6.045(-1)	533.80	
S8P7	-1.67	Null	L28H18	-9.28	1.257(1)	543.21	P5H41	4.89	7.741(-1)	534.00	
S8P8	-1.67	Null	P5H1	.13	Null	P5H42	5.08	9.793(-1)	534.05		
S8P9	-1.67	Null	P5H2	.23	Null	P12H1	5.24	Null	Null		
S8P10	-1.67	Null	P5H3	.33	Null	P12H2	5.33	9.056(-1)	533.31		
S8P13	-.98	Null	P5H4	.42	-5.210(-1)	524.85	P12H3	5.43	6.270(-1)	533.96	
S8P17	-.03	Null	P5H5	.52	-5.282(-1)	526.98	P12H4	5.53	7.771(-1)	534.05	
S8P19	-.03	Null	P5H6	.62	-5.764(-1)	527.83	P12H5	5.63	7.406(-1)	534.02	
S8P25	-.03	Null	P5H7	.71	-5.360(-1)	528.59	P12H6	5.72	8.665(-1)	534.09	
S8P26	-.03	Null	P5H8	.81	-5.580(-1)	529.78	P12H7	5.82	8.545(-1)	534.11	
S8P27	-.03	Null	P5H9	.90	-5.490(-1)	529.62	P12H8	5.92	9.609(-1)	534.22	
S8P28	-.03	Null	P5H10	.99	Null	P12H9	6.02	9.744(-1)	534.22		
P5P10	.37	7.779(-1)	P5H11	1.07	Null	P12H10	6.12	9.684(-1)	534.29		
P5P1	.46	6.709(-1)	P5H12	1.13	-7.011(-1)	530.56	P12H11	6.21	1.070(0)	534.29	
P5P2	.97	1.145(0)	P5H13	1.21	-7.790(-1)	530.68	P12H12	6.30	1.131(0)	534.37	
P5P13	1.14	Null	P5H14	1.29	Null	P12H13	6.39	1.130(0)	534.36		
P5P3	1.48	1.656(0)	P5H15	1.39	-1.021(0)	531.11	P12H14	6.48	1.197(0)	534.40	
P5P16	1.91	1.164(0)	P5H16	1.49	Null	P12H15	6.56	1.155(0)	534.26		
P5P4	1.98	1.140(0)	P5H17	1.59	-1.076(0)	531.33	P12H16	6.66	Null	Null	
P5P18	2.42	1.177(0)	P5H18	1.68	-5.660(-1)	532.10	P12H17	6.74	1.290(0)	534.31	
P5P5	2.49	1.191(0)	P5H19	1.78	-1.192(0)	531.73	P12H18	6.84	1.234(0)	534.17	
P5P20	2.93	1.307(0)	P5H20	1.88	-1.192(0)	531.69	P12H19	6.93	1.306(0)	534.20	
P12P1	5.47	1.091(0)	P5H21	1.98	-1.408(0)	531.74	P12H20	7.02	1.078(0)	533.89	
P12P2	6.11	Null	P5H22	2.08	-9.963(-1)	531.95	P12H22	8.01	1.694(0)	533.87	
P12P4	7.39	Null	P5H23	2.20	-1.054(0)	532.08	P12H23	8.66	2.020(0)	533.91	
P12P5	8.03	1.104(0)	P5H24	2.30	Null	P12H25	9.92	1.960(0)	533.70		
P12P6	8.68	1.232(0)	P5H25	2.39	-8.644(-1)	532.27	P12H26	10.57	2.303(0)	533.96	
P12P8	9.95	Null	P5H26	2.49	-6.973(-1)	532.38	P12H28	11.85	2.735(0)	534.27	
P12P10	11.23	9.748(-1)	P5H27	2.58	-6.890(-1)	532.49	P12H29	12.49	2.849(0)	534.36	
P12P11	11.88	1.025(0)	P5H28	2.68	-5.025(-1)	532.57	P12H31	13.78	2.949(0)	534.49	
P12P13	13.15	1.115(0)	P5H29	2.78	-4.708(-1)	532.74	P12H33	15.06	3.234(0)	534.73	
P12P14	13.80	1.209(0)	P5H30	2.87	-3.738(-1)	532.73	P12H35	16.33	3.465(0)	534.88	
P12P16	15.07	1.177(0)	P5H31	2.97	-1.616(-1)	533.00					
P12P18	16.35	1.111(0)	P5H32	3.07	-1.481(-1)	533.04					

Run 14 Reduced Data Tabulation

Gauge Label	Loc. (in)	Value (PSIA) or (BTU/Ft ² -Sec)	T Surf (DegR)	Gauge Label	Loc. (in)	Value (PSIA) or (BTU/Ft ² -Sec)	T Surf (DegR)	Gauge Label	Loc. (in)	Value (PSIA) or (BTU/Ft ² -Sec)	T Surf (DegR)
L28P1	-26.28	1.156(0)	PSS2	1.00	Null	P5H32	3.07	-5.738(-1)	529.59		
L28P3	-18.28	1.300(0)	PSS4	2.33	Null	P5H33	3.21	-6.132(-1)	529.61		
L28P5	-10.28	1.135(0)	P12S2	6.43	Null	P5H34	3.42	-7.724(-1)	530.36		
S8P2	-1.98	Null	L28H3	-27.28	1.324(1)	539.18					
S8P3	-1.98	Null	L28H6	-24.28	1.656(1)	541.58					
S8P4	-1.98	Null	L28H11	-18.28	1.270(1)	539.76					
S8P6	-1.67	Null	L28H13	-15.28	1.146(1)	538.82					
S8P7	-1.67	Null	L28H18	-9.28	1.071(1)	538.23					
S8P8	-1.67	Null	P5H1	.13	1.693(-1)	523.62					
S8P9	-1.67	Null	P5H2	.23	-1.831(0)	519.16					
S8P10	-1.67	Null	P5H3	.33	-1.877(0)	520.63					
S8P13	-.98	Null	P5H4	.42	-3.994(-1)	523.73					
S8P17	-.03	2.047(0)	P5H5	.52	-5.339(-1)	525.33					
S8P25	-.03	1.259(0)	P5H6	.62	-4.915(-1)	525.97					
S8P26	-.03	1.970(0)	P5H7	.71	-4.290(-1)	526.66					
S8P27	-.03	1.898(0)	P5H8	.81	-1.078(0)	527.65					
S8P28	-.03	1.820(0)	P5H9	.90	-2.214(-1)	527.59					
P5P10	.37	7.573(-1)	P5H10	.99	-1.642(-2)	528.05					
P5P1	.46	7.276(-1)	P5H11	1.07	-6.237(-1)	528.24					
P5P2	.97	1.113(0)	P5H12	1.13	2.432(-1)	529.22					
P5P13	1.14	8.668(-1)	P5H13	1.21	1.457(-2)	529.09					
P5P3	1.48	1.151(0)	P5H14	1.29	-8.395(-1)	528.21					
P5P16	1.91	1.107(0)	P5H15	1.39	-8.131(-1)	528.45					
P5P4	1.98	1.086(0)	P5H16	1.49	-8.320(-1)	528.46					
P5P18	2.42	1.100(0)	P5H17	1.59	-8.442(-1)	528.52					
P5P5	2.49	1.108(0)	P5H18	1.68	Null	P12H11	6.21	2.946(-1)	530.37		
P5P20	2.93	1.183(0)	P5H19	1.78	-8.334(-1)	528.66					
P12P1	5.47	1.007(0)	P5H20	1.88	-1.001(0)	528.62					
P12P2	6.11	1.008(0)	P5H21	1.98	-8.546(-1)	528.97					
P12P4	7.39	7.055(-1)	P5H22	2.08	-8.738(-1)	528.78					
P12P5	8.03	9.758(-1)	P5H23	2.20	-7.450(-1)	528.96					
P12P6	8.68	1.100(0)	P5H24	2.30	-7.637(-1)	529.13					
P12P8	9.95	7.951(-1)	P5H25	2.39	-7.971(-1)	529.07					
P12P10	11.23	9.598(-1)	P5H26	2.49	-8.277(-1)	529.14					
P12P11	11.88	3.507(-1)	P5H27	2.58	-8.177(-1)	529.17					
P12P13	13.15	1.005(0)	P5H28	2.68	-7.870(-1)	529.27					
P12P14	13.80	1.083(0)	P5H29	2.78	-6.831(-1)	529.42					
P12P16	15.07	1.071(0)	P5H30	2.87	-5.606(-1)	529.43					
P12P18	16.35	1.041(0)	P5H31	2.97	-7.154(-1)	529.47					

Run 15 Reduced Data Tabulation

Gauge Label	Loc. (in)	Value (PSIA) or (BTU/Ft ² -Sec)	T Surf (DegR)	Gauge Label	Loc. (in)	Value (PSIA) or (BTU/Ft ² -Sec)	T Surf (DegR)	Gauge Label	Loc. (in)	Value (PSIA) or (BTU/Ft ² -Sec)	T Surf (DegR)
L28P1	-26.28	1.169(0)		P5S4	2.89	Null		P5H9	4.31	Null	
L28P3	-18.28	1.229(0)		P5S2	4.25	Null		P5H8	4.40	Null	
L28P5	-10.28	Null		L28H3	-27.28	1.460(1)	544.89	P5H7	4.50	-1.856(-1)	531.06
S8P2	-1.98	Null		L28H6	-24.28	1.368(1)	544.06	P5H6	4.59	-3.402(-1)	530.97
S8P3	-1.98	Null		L28H11	-18.28	1.132(1)	541.99	P5H5	4.69	-2.719(-1)	531.05
S8P6	-1.67	Null		L28H13	-15.28	1.096(1)	541.82	P5H4	4.79	-3.756(-2)	530.93
S8P7	-1.67	Null		L28H18	-9.28	9.605(0)	540.64	P5H3	4.89	Null	
S8P8	-1.67	Null		P5H42	.13	Null		P5H2	4.98	-1.324(-1)	531.08
S8P9	-1.67	Null		P5H41	.32	Null		P5H1	5.08	Null	
S8P10	-1.67	Null		P5H40	.52	-3.028(-1)	530.40	P12H1	5.24	Null	
S8P13	.98	Null		P5H39	.72	-3.827(-1)	530.49	P12H2	5.33	Null	
S8P17	-.03	2.295(0)		P5H37	1.18	-1.121(0)	530.51	P12H3	5.43	-6.729(-2)	531.04
S8P19	-.03	Null		P5H36	1.39	Null		P12H4	5.53	-2.361(-1)	530.98
S8P25	-.03	2.570(0)		P5H35	1.59	Null		P12H5	5.63	-7.996(-2)	531.04
S8P26	-.03	Null		P5H34	1.80	Null		P12H6	5.72	-1.406(-1)	531.10
S8P27	-.03	Null		P5H33	2.00	-5.263(-1)	530.58	P12H7	5.82	-7.817(-2)	531.11
S8P28	-.03	2.580(0)		P5H32	2.15	-7.406(-1)	530.65	P12H8	5.92	-1.803(-1)	531.11
P5P9	.43	9.465(-1)		P5H31	2.24	-7.853(-1)	530.56	P12H9	6.02	1.486(-3)	531.14
P5P24	.56	Null		P5H30	2.34	Null		P12H10	6.12	9.530(-2)	531.27
P5P8	.94	1.199(0)		P5H29	2.43	-6.732(-1)	530.52	P12H11	6.21	2.243(-1)	531.35
P5P23	1.02	Null		P5H28	2.53	-4.243(-1)	530.48	P12H12	6.30	1.509(-1)	531.36
P5P7	1.45	1.078(0)		P5H27	2.63	-6.401(-1)	530.50	P12H13	6.39	1.431(-1)	531.29
P5P22	1.53	8.104(-1)		P5H26	2.72	-6.046(-1)	530.53	P12H14	6.48	2.419(-1)	531.43
P5P21	2.04	8.708(-1)		P5H25	2.82	-3.898(-1)	530.59	P12H15	6.56	2.366(-1)	531.35
P5P5	2.72	1.097(0)		P5H24	2.91	Null		P12H16	6.66	2.084(-1)	531.35
P5P18	2.79	1.006(0)		P5H23	3.02	-4.042(-1)	530.77	P12H17	6.74	3.429(-1)	531.39
P5P4	3.23	1.049(0)		P5H22	3.14	-4.590(-1)	530.69	P12H18	6.84	2.790(-1)	531.38
P5P16	3.31	1.110(0)		P5H21	3.23	-4.330(-1)	530.52	P12H19	6.93	3.515(-1)	531.45
P5P3	3.73	1.061(0)		P5H20	3.33	-2.758(-1)	530.73	P12H20	7.02	3.621(-1)	531.44
P5P14	3.87	1.102(0)		P5H19	3.43	-2.866(-1)	530.78	P12H22	8.01	5.124(-1)	531.59
P5P2	4.24	Null		P5H18	3.53	Null		P12H23	8.66	7.630(-1)	531.74
P5P12	4.34	8.948(-1)		P5H17	3.62	-3.827(-1)	530.84	P12H25	9.92	8.356(-1)	531.87
P5P1	4.76	9.404(-1)		P5H16	3.72	-7.333(-1)	530.61	P12H26	10.57	9.928(-1)	532.03
P5P10	4.85	1.058(0)		P5H15	3.82	-2.232(-1)	530.89	P12H28	11.85	1.084(0)	532.12
P12P1	5.47	9.123(-1)		P5H14	3.92	-2.559(-1)	530.98	P12H29	12.49	1.117(0)	532.17
P12P8	9.95	8.209(-1)		P5H13	4.01	Null		P12H31	13.78	1.060(0)	532.08
P12P10	11.23	9.623(-1)		P5H12	4.09	Null		P12H33	15.06	1.276(0)	532.37
P12P13	13.15	1.008(0)		P5H11	4.14	Null		P12H35	16.33	1.398(0)	532.45
P12P16	15.07	1.049(0)		P5H10	4.22	Null					

Run 21 Reduced Data Tabulation

Gauge Label	Loc. (in)	Value (PSIA) or (BTU/Ft ² -Sec)	T Surf (DegR)	Gauge Label	Loc. (in)	Value (PSIA) or (BTU/Ft ² -Sec)	T Surf (DegR)	Gauge Label	Loc. (in)	Value (PSIA) or (BTU/Ft ² -Sec)	T Surf (DegR)
L28P1	-26.28	1.213(0)		P5S4	2.89	Null		P5H9	4.31	5.177(-1)	531.34
L28P3	-18.28	1.237(0)		P5S2	4.25	Null		P5H8	4.40	Null	
L28P5	-10.28	1.146(0)		L28H3	-27.28	1.472(1)	543.51	P5H7	4.50	5.242(-1)	531.33
S8P2	-1.98	Null		L28H6	-24.28	1.334(1)	542.74	P5H6	4.59	1.600(-1)	531.28
S8P3	-1.98	Null		L28H11	-18.28	1.147(1)	540.87	P5H5	4.69	6.524(-1)	531.39
S8P6	-1.67	Null		L28H13	-15.28	1.088(1)	540.36	P5H4	4.79	4.107(-1)	531.32
S8P7	-1.67	Null		L28H18	-9.28	1.049(1)	539.66	P5H3	4.89	6.158(-1)	531.43
S8P8	-1.67	Null		P5H42	.13	Null		P5H2	4.98	7.234(-1)	531.47
S8P9	-1.67	Null		P5H41	.32	-5.999(-1)	529.60	P5H1	5.08	6.628(-1)	531.52
S8P10	-1.67	Null		P5H40	.52	-5.638(-1)	529.98	P12H1	5.24	6.437(-1)	531.53
S8P13	.98	Null		P5H39	.72	-7.581(-1)	530.10	P12H2	5.33	Null	
S8P17	-.03	Null		P5H37	1.18	-8.001(-1)	530.13	P12H3	5.43	7.188(-1)	531.47
S8P19	-.03	Null		P5H36	1.39	-1.875(-1)	530.56	P12H4	5.53	6.637(-1)	531.52
S8P25	-.03	1.581(0)		P5H35	1.59	-1.128(0)	530.03	P12H5	5.63	6.389(-1)	531.52
S8P26	-.03	Null		P5H34	1.80	-1.056(0)	530.08	P12H6	5.72	1.038(0)	531.68
S8P27	-.03	Null		P5H33	2.00	-1.043(0)	530.08	P12H7	5.82	8.711(-1)	531.63
S8P28	-.03	Null		P5H32	2.15	-9.219(-1)	530.22	P12H8	5.92	9.519(-1)	531.68
P5P9	.43	5.650(-1)		P5H31	2.24	-9.375(-1)	530.30	P12H9	6.02	8.506(-1)	531.65
P5P24	.56	Null		P5H30	2.34	-5.925(-1)	530.40	P12H10	6.12	9.044(-1)	531.68
P5P8	.94	1.090(0)		P5H29	2.43	-6.083(-1)	530.45	P12H11	6.21	1.013(0)	531.68
P5P23	1.02	Null		P5H28	2.53	-3.748(-1)	530.50	P12H12	6.30	1.158(0)	531.80
P5P7	1.45	1.041(0)		P5H27	2.63	-5.716(-1)	530.49	P12H13	6.39	9.334(-1)	531.69
P5P22	1.53	7.941(-1)		P5H26	2.72	-2.277(-1)	530.65	P12H14	6.48	9.173(-1)	531.72
P5P21	2.04	8.338(-1)		P5H25	2.82	-1.742(-1)	530.66	P12H15	6.56	1.070(0)	531.74
P5P5	2.72	1.057(0)		P5H24	2.91	-1.448(-3)	530.75	P12H16	6.66	1.022(0)	531.76
P5P18	2.79	1.128(0)		P5H23	3.02	-3.856(-2)	530.77	P12H17	6.74	1.173(0)	531.86
P5P4	3.23	9.816(-1)		P5H22	3.14	-1.268(-1)	530.83	P12H18	6.84	1.173(0)	531.85
P5P16	3.31	1.062(0)		P5H21	3.23	-8.276(-2)	530.84	P12H19	6.93	1.242(0)	531.87
P5P3	3.73	1.027(0)		P5H20	3.33	-3.668(-2)	530.93	P12H20	7.02	9.581(-1)	531.64
P5P14	3.87	1.067(0)		P5H19	3.43	-3.085(-4)	530.93	P12H22	8.01	1.462(0)	532.11
P5P2	4.24	Null		P5H18	3.53	-2.685(-2)	530.95	P12H23	8.66	1.705(0)	532.27
P5P12	4.34	8.727(-1)		P5H17	3.62	1.576(-1)	531.01	P12H25	9.92	1.792(0)	532.38
P5P1	4.76	8.975(-1)		P5H16	3.72	1.895(-1)	531.06	P12H26	10.57	1.874(0)	532.40
P5P10	4.85	1.025(0)		P5H15	3.82	2.130(-1)	531.10	P12H28	11.85	2.333(0)	532.75
P12P1	5.47	9.621(-1)		P5H14	3.92	1.039(-1)	531.11	P12H29	12.49	2.329(0)	532.78
P12P8	9.95	8.006(-1)		P5H13	4.01	1.999(-1)	531.07	P12H31	13.78	2.540(0)	532.93
P12P10	11.23	9.075(-1)		P5H12	4.09	3.334(-1)	531.13	P12H33	15.06	2.876(0)	533.25
P12P13	13.15	9.807(-1)		P5H11	4.14	5.676(-1)	531.31	P12H35	16.33	2.885(0)	533.30
P12P16	15.07	1.045(0)		P5H10	4.22	4.991(-1)	531.26				

Run 23 Reduced Data Tabulation

Gauge	Loc.	Value	Gauge	Loc.	Value	Gauge	Loc.	Value
Label	(in)	(PSIA) or (BTU/Ft ² -Sec)	Label	(in)	(PSIA) or (BTU/Ft ² -Sec)	Label	(in)	(PSIA) or (BTU/Ft ² -Sec)
		(DegR)			(DegR)			(DegR)
L28P1	-26.28	1.262(0)	PSS4	2.89	Null	P5H9	4.31	1.694(0)
L28P3	-18.28	1.248(0)	PSS2	4.25	Null	P5H8	4.40	1.920(0)
L28P5	-10.28	1.146(0)	L28H3	-27.28	1.621(1)	P5H7	4.50	1.839(0)
S8P2	-1.98	Null	L28H6	-24.28	1.468(1)	P5H6	4.59	1.736(0)
S8P3	-1.98	Null	L28H11	-18.28	1.194(1)	P5H5	4.69	1.672(0)
S8P6	-1.67	Null	L28H13	-15.28	1.115(1)	P5H4	4.79	1.720(0)
S8P7	-1.67	Null	L28H18	-9.28	1.044(1)	P5H3	4.89	2.021(0)
S8P8	-1.67	Null	P5H42	.13	Null	P5H2	4.98	1.998(0)
S8P9	-1.67	Null	P5H41	.32	-6.420(-1)	P5H1	5.08	1.788(0)
S8P10	-1.67	Null	P5H40	.52	-4.719(-1)	P12H1	5.24	1.982(0)
S8P13	.98	Null	P5H39	.72	-7.672(-1)	P12H2	5.33	Null
S8P17	.03	Null	P5H37	1.18	-1.445(0)	P12H3	5.43	1.993(0)
S8P19	.03	Null	P5H36	1.39	Null	P12H4	5.53	1.926(0)
S8P25	.03	1.052(0)	P5H35	1.59	-8.763(-1)	P12H5	5.63	1.883(0)
S8P26	.03	Null	P5H34	1.80	-2.201(-1)	P12H6	5.72	2.237(0)
S8P27	.03	Null	P5H33	2.00	-3.777(-1)	P12H7	5.82	1.930(0)
S8P28	.03	Null	P5H32	2.15	1.970(-1)	P12H8	5.92	2.082(0)
P5P9	.43	5.362(-1)	P5H31	2.24	1.546(-1)	P12H9	6.02	2.161(0)
P5P24	.56	Null	P5H30	2.34	Null	P12H10	6.12	2.293(0)
P5P8	.94	1.072(0)	P5H29	2.43	3.235(-1)	P12H11	6.21	2.357(0)
P5P23	1.02	Null	P5H28	2.53	7.038(-1)	P12H12	6.30	2.103(0)
P5P7	1.45	1.014(0)	P5H27	2.63	5.218(-1)	P12H13	6.39	2.221(0)
P5P22	1.53	7.559(-1)	P5H26	2.72	5.289(-1)	P12H14	6.48	2.176(0)
P5P21	2.04	7.930(-1)	P5H25	2.82	9.815(-1)	P12H15	6.56	2.076(0)
P5P5	2.72	1.034(0)	P5H24	2.91	5.380(-1)	P12H16	6.66	2.513(0)
P5P18	2.79	1.017(0)	P5H23	3.02	8.237(-1)	P12H17	6.74	2.373(0)
P5P4	3.23	9.919(-1)	P5H22	3.14	1.510(0)	P12H18	6.84	2.470(0)
P5P16	3.31	1.033(0)	P5H21	3.23	8.981(-1)	P12H19	6.93	2.433(0)
P5P3	3.73	1.008(0)	P5H20	3.33	7.828(-1)	P12H20	7.02	2.354(0)
P5P14	3.87	1.036(0)	P5H19	3.43	8.650(-1)	P12H22	8.01	3.065(0)
P5P2	4.24	Null	P5H18	3.53	8.068(-1)	P12H23	8.66	3.381(0)
P5P12	4.34	8.384(-1)	P5H17	3.62	1.184(0)	P12H25	9.92	3.610(0)
P5P1	4.76	9.061(-1)	P5H16	3.72	1.162(0)	P12H26	10.57	3.773(0)
P5P10	4.85	9.888(-1)	P5H15	3.82	1.156(0)	P12H28	11.85	4.180(0)
P12P1	5.47	9.356(-1)	P5H14	3.92	1.566(0)	P12H29	12.49	4.439(0)
P12P8	9.95	8.044(-1)	P5H13	4.01	1.441(0)	P12H31	13.78	4.513(0)
P12P10	11.23	8.957(-1)	P5H12	4.09	1.172(0)	P12H33	15.06	4.955(0)
P12P13	13.15	9.771(-1)	P5H11	4.14	1.251(0)	P12H34	16.33	4.866(0)
P12P16	15.07	1.184(1)	P5H10	4.22	1.888(0)	P12H35	16.33	5.242(1)

Run 24 Reduced Data Tabulation

Gauge	Loc.	Value	Gauge	Loc.	Value	Gauge	Loc.	Value
Label	(in)	(PSIA) or (BTU/Ft ² -Sec)	Label	(in)	(PSIA) or (BTU/Ft ² -Sec)	Label	(in)	(PSIA) or (BTU/Ft ² -Sec)
		(DegR)			(DegR)			(DegR)
L28P1	-26.28	1.184(0)	PSS4	2.89	Null	P5H9	4.40	8.488(0)
L28P3	-18.28	1.317(0)	PSS2	4.25	Null	P5H8	4.50	8.499(0)
L28P5	-10.28	3.972(-1)	L28H3	-27.28	1.420(1)	P5H7	4.59	7.999(0)
S8P2	-1.98	Null	L28H6	-24.28	1.310(1)	P5H6	4.69	8.315(0)
S8P3	-1.98	Null	L28H11	-18.28	1.105(1)	P5H5	4.79	7.849(0)
S8P6	-1.67	Null	L28H13	-15.28	1.161(1)	P5H4	4.89	8.181(0)
S8P7	-1.67	Null	L28H18	-9.28	9.862(0)	P5H3	4.98	7.983(0)
S8P8	-1.67	Null	P5H42	.13	Null	P5H2	5.08	7.966(0)
S8P9	-1.67	Null	P5H41	.32	7.699(0)	P12H1	5.24	Null
S8P10	-1.67	Null	P5H40	.52	1.072(1)	P12H2	5.33	Null
S8P13	.98	Null	P5H39	.72	1.004(1)	P12H3	5.43	Null
S8P17	.03	1.904(-1)	P5H37	1.18	9.031(0)	P12H4	5.53	1.063(1)
S8P19	.03	Null	P5H36	1.39	8.966(0)	P12H5	5.63	Null
S8P25	.03	Null	P5H35	1.59	Null	P12H6	5.72	Null
S8P26	.03	2.912(-1)	P5H34	1.80	8.268(0)	P12H7	5.82	Null
S8P27	.03	Null	P5H33	2.00	8.519(0)	P12H8	5.92	Null
S8P28	.03	Null	P5H32	2.15	8.286(0)	P12H9	6.02	Null
P5P9	.43	9.198(-1)	P5H31	2.24	Null	P12H10	6.12	Null
P5P24	.56	Null	P5H30	2.34	8.719(0)	P12H11	6.21	Null
P5P8	.94	Null	P5H29	2.43	8.173(0)	P12H12	6.30	Null
P5P23	1.02	Null	P5H28	2.53	8.199(0)	P12H13	6.39	Null
P5P7	1.45	9.166(-1)	P5H27	2.63	8.168(0)	P12H14	6.48	Null
P5P22	1.53	Null	P5H26	2.72	8.696(0)	P12H15	6.56	3.712(1)
P5P21	2.04	Null	P5H25	2.82	9.039(0)	P12H16	6.66	4.036(1)
P5P5	2.72	1.004(0)	P5H24	2.91	Null	P12H17	6.74	4.527(1)
P5P18	2.79	8.755(-1)	P5H23	3.02	8.366(0)	P12H18	6.84	4.429(1)
P5P4	3.23	8.793(-1)	P5H22	3.14	9.399(0)	P12H19	6.93	4.675(1)
P5P3	3.73	1.041(0)	P5H21	3.23	8.355(0)	P12H20	7.02	4.392(1)
P5P14	3.87	1.028(0)	P5H20	3.33	8.199(0)	P12H21	7.01	7.049(1)
P5P2	4.24	Null	P5H19	3.43	8.368(0)	P12H22	7.01	608.02
P5P12	4.34	8.567(-1)	P5H17	3.62	7.990(0)	P12H23	8.66	7.958(1)
P5P1	4.76	8.999(-1)	P5H16	3.72	8.465(0)	P12H25	9.92	8.554(1)
P5P10	4.85	1.007(0)	P5H15	3.82	8.158(0)	P12H26	10.57	8.427(1)
P12P1	5.47	1.234(0)	P5H14	3.92	8.428(0)	P12H28	11.85	Null
P12P8	9.95	Null	P5H13	4.01	8.671(0)	P12H29	12.49	Null
P12P10	11.23	Null	P5H12	4.09	7.386(0)	P12H31	13.78	Null
P12P13	13.15	1.184(1)	P5H11	4.14	7.407(0)	P12H33	15.06	Null
P12P16	15.07	Null	P5H10	4.22	8.158(0)	P12H35	16.33	5.242(1)

Run 25 Reduced Data Tabulation

Gauge Label	Loc. (in)	Value (PSIA) or (BTU/Ft ² -Sec)	T Surf (DegR)	Gauge Label	Loc. (in)	Value (PSIA) or (BTU/Ft ² -Sec)	T Surf (DegR)	Gauge Label	Loc. (in)	Value (PSIA) or (BTU/Ft ² -Sec)	T Surf (DegR)
L28P1	-26.28	1.197(0)		P5S4	2.89	Null		P5H9	4.31	8.448(0)	541.06
L28P3	-18.28	1.310(0)		P5S2	4.25	Null		P5H8	4.40	7.282(0)	540.48
L28P5	-10.28	Null		L28H3	-27.28	1.430(1)	549.37	P5H7	4.50	8.348(0)	541.09
S8P2	-1.98	Null		L28H6	-24.28	1.363(1)	548.19	P5H6	4.59	Null	Null
S8P3	-1.98	Null		L28H11	-18.28	1.101(1)	545.22	P5H5	4.69	7.893(0)	540.82
S8P6	-1.67	Null		L28H13	-15.28	1.131(1)	544.82	P5H4	4.79	7.539(0)	540.77
S8P7	-1.67	Null		L28H18	-9.28	9.889(0)	543.34	P5H3	4.89	7.690(0)	540.69
S8P8	-1.67	Null		P5H42	.13	Null	Null	P5H2	4.98	7.232(0)	540.58
S8P9	-1.67	Null		P5H41	.32	7.889(0)	542.60	P5H1	5.08	7.584(0)	540.01
S8P10	-1.67	Null		P5H40	.52	1.082(1)	543.98	P12H1	5.24	1.905(1)	547.98
S8P13	.98	Null		P5H39	.72	9.665(0)	542.42	P12H2	5.33	2.388(1)	551.42
S8P17	.03	2.027(-1)		P5H37	1.18	8.318(0)	540.97	P12H3	5.43	2.651(1)	553.88
S8P19	.03	Null		P5H36	1.39	8.895(0)	541.25	P12H4	5.53	3.322(1)	559.56
S8P25	.03	2.818(-1)		P5H35	1.59	8.393(0)	541.26	P12H5	5.63	3.459(1)	562.12
S8P26	.03	2.892(-1)		P5H34	1.80	8.198(0)	540.74	P12H6	5.72	2.658(1)	556.27
S8P27	.03	Null		P5H33	2.00	8.499(0)	541.07	P12H7	5.82	3.569(1)	565.34
S8P28	.03	1.392(-1)		P5H32	2.15	8.067(0)	540.73	P12H8	5.92	3.990(1)	570.73
P5P9	.43	8.934(-1)		P5H31	2.24	8.514(0)	541.38	P12H9	6.02	3.944(1)	570.53
P5P24	.56	7.160(-1)		P5H30	2.34	8.296(0)	541.12	P12H10	6.12	4.186(1)	573.35
P5P8	.94	1.033(0)		P5H29	2.43	8.189(0)	540.82	P12H11	6.21	Null	Null
P5P23	1.02	7.447(-1)		P5H28	2.53	8.587(0)	541.00	P12H12	6.30	4.160(1)	573.17
P5P7	1.45	9.075(-1)		P5H27	2.63	8.143(0)	540.82	P12H13	6.39	4.420(1)	576.33
P5P22	1.53	7.537(-1)		P5H26	2.72	8.031(0)	541.05	P12H14	6.48	4.412(1)	576.49
P5P21	2.04	7.594(-1)		P5H25	2.82	8.713(0)	541.39	P12H15	6.56	4.431(1)	577.18
P5P5	2.72	9.950(-1)		P5H24	2.91	7.616(0)	540.33	P12H16	6.66	4.530(1)	578.03
P5P18	2.79	9.027(-1)		P5H23	3.02	7.972(0)	541.01	P12H17	6.74	4.895(1)	582.17
P5P4	3.23	9.212(-1)		P5H22	3.14	9.558(0)	541.98	P12H18	6.84	4.712(1)	580.64
P5P16	3.31	1.003(0)		P5H21	3.23	8.225(0)	540.95	P12H19	6.93	4.721(1)	581.17
P5P3	3.73	1.035(0)		P5H20	3.33	7.990(0)	540.79	P12H20	7.02	4.793(1)	582.30
P5P14	3.87	1.005(0)		P5H19	3.43	7.852(0)	540.89	P12H22	8.01	5.337(1)	590.62
P5P2	4.24	Null		P5H18	3.53	8.613(0)	541.66	P12H23	8.66	5.545(1)	594.06
P5P12	4.34	8.231(-1)		P5H17	3.62	7.883(0)	540.83	P12H25	9.92	5.456(1)	595.19
P5P1	4.76	8.666(-1)		P5H16	3.72	7.857(0)	540.91	P12H26	10.57	5.490(1)	596.96
P5P10	4.85	1.014(0)		P5H15	3.82	7.201(0)	540.00	P12H28	11.85	5.577(1)	599.12
P12P1	5.47	3.968(0)		P5H14	3.92	7.953(0)	540.72	P12H29	12.49	5.395(1)	596.63
P12P8	9.95	7.185(0)		P5H13	4.01	8.177(0)	541.07	P12H31	13.78	5.262(1)	594.72
P12P10	11.23	Null		P5H12	4.09	7.122(0)	540.16	P12H33	15.06	5.293(1)	595.78
P12P13	13.15	8.160(0)		P5H11	4.14	7.691(0)	540.33	P12H35	16.33	4.304(1)	583.88
P12P16	15.07	7.799(0)		P5H10	4.22	7.513(0)	540.45				

Run 26 Reduced Data Tabulation

Gauge Label	Loc. (in)	Value (PSIA) or (BTU/Ft ² -Sec)	T Surf (DegR)	Gauge Label	Loc. (in)	Value (PSIA) or (BTU/Ft ² -Sec)	T Surf (DegR)	Gauge Label	Loc. (in)	Value (PSIA) or (BTU/Ft ² -Sec)	T Surf (DegR)
L28P1	-26.28	9.278(-1)		P5S4	2.89	Null		P5H9	4.31	3.947(0)	537.14
L28P3	-18.28	1.285(0)		P5S2	4.25	Null		P5H8	4.40	3.724(0)	537.23
L28P5	-10.28	Null		L28H3	-27.28	1.395(1)	550.62	P5H7	4.50	4.271(0)	537.61
S8P2	-1.98	Null		L28H6	-24.28	1.310(1)	549.44	P5H6	4.59	4.271(0)	537.62
S8P3	-1.98	Null		L28H11	-18.28	1.093(1)	546.73	P5H5	4.69	4.878(0)	537.90
S8P6	-1.67	Null		L28H13	-15.28	1.135(1)	546.48	P5H4	4.79	5.834(0)	538.33
S8P7	-1.67	Null		L28H18	-9.28	9.899(0)	545.01	P5H3	4.89	6.660(0)	539.07
S8P8	-1.67	Null		P5H42	.13	Null	Null	P5H2	4.98	7.422(0)	540.01
S8P9	-1.67	Null		P5H41	.32	-4.499(-1)	531.59	P5H1	5.08	8.988(0)	541.31
S8P10	-1.67	Null		P5H40	.52	-6.698(-1)	531.78	P12H1	5.24	1.222(1)	543.83
S8P13	.98	Null		P5H39	.72	-7.474(-1)	531.80	P12H2	5.33	Null	Null
S8P17	.03	Null		P5H37	1.18	-1.434(0)	531.06	P12H3	5.43	Null	Null
S8P19	.03	Null		P5H36	1.39	-8.856(-1)	531.53	P12H4	5.53	1.598(1)	547.74
S8P25	.03	1.140(0)		P5H35	1.59	-1.084(0)	531.49	P12H5	5.63	1.672(1)	548.81
S8P26	.03	1.007(0)		P5H34	1.80	-6.881(-1)	531.97	P12H6	5.72	Null	Null
S8P27	.03	Null		P5H33	2.00	-4.203(-1)	532.27	P12H7	5.82	1.771(1)	550.30
S8P28	.03	Null		P5H32	2.15	-3.334(-1)	532.54	P12H8	5.92	2.052(1)	553.28
P5P9	.43	9.964(-1)		P5H31	2.24	Null	Null	P12H9	6.02	2.029(1)	553.35
P5P24	.56	8.221(-1)		P5H30	2.34	2.828(-2)	532.82	P12H10	6.12	2.173(1)	554.72
P5P8	.94	1.160(0)		P5H29	2.43	1.353(-1)	532.88	P12H11	6.21	Null	Null
P5P23	1.02	8.389(-1)		P5H28	2.53	2.900(-1)	533.02	P12H12	6.30	2.205(1)	555.06
P5P7	1.45	1.036(0)		P5H27	2.63	2.777(-1)	533.15	P12H13	6.39	2.469(1)	557.74
P5P22	1.53	8.151(-1)		P5H26	2.72	1.874(-1)	533.22	P12H14	6.48	2.490(1)	558.22
P5P21	2.04	8.455(-1)		P5H25	2.82	4.920(-1)	533.34	P12H15	6.56	2.615(1)	559.29
P5P5	2.72	1.102(0)		P5H24	2.91	3.757(-1)	533.33	P12H16	6.66	2.720(1)	560.28
P5P18	2.79	1.056(0)		P5H23	3.02	4.043(-1)	533.43	P12H17	6.74	2.947(1)	562.70
P5P4	3.23	1.069(0)		P5H22	3.14	1.089(0)	533.74	P12H18	6.84	2.993(1)	562.97
P5P16	3.31	1.188(0)		P5H21	3.23	7.577(-1)	533.65	P12H19	6.93	3.054(1)	564.02
P5P3	3.73	1.955(0)		P5H20	3.33	7.198(-1)	533.65	P12H20	7.02	Null	Null
P5P14	3.87	2.149(0)		P5H19	3.43	6.823(-1)	533.74	P12H22	8.01	4.172(1)	577.44
P5P2	4.24	Null		P5H18	3.53	Null	Null	P12H23	8.66	4.792(1)	584.60
P5P12	4.34	Null		P5H17	3.62	1.734(0)	534.29	P12H25	9.92	5.172(1)	590.14
P5P1	4.76	Null		P5H16	3.72	3.309(0)	535.23	P12H26	10.57	5.315(1)	592.38
P5P10	4.85	Null		P5H15	3.82	3.306(0)	535.60	P12H28	11.85	5.618(1)	596.90
P12P1	5.47	3.828(0)		P5H14	3.92	3.798(0)	536.31	P12H29	12.49	5.710(1)	598.02
P12P8	9.95	6.894(0)		P5H13	4.01	3.656(0)	536.40	P12H31	13.78	5.016(1)	590.55
P12P10	11.23	Null		P5H12	4.09	2.925(0)	536.15	P12H33	15.06	5.356(1)	595.19
P12P13	13.15	7.963(0)		P5H11	4.14	3.413(0)	536.48	P12H35	16.33	4.281(1)	584.06
P12P16	15.07	7.696(0)		P5H10	4.22	3.706(0)	536.91				

Run 27 Reduced Data Tabulation

Gauge Label	Loc. (in)	Value (PSIA) or (BTU/Ft ² -Sec)	T Surf (DegR)	Gauge Label	Loc. (in)	Value (PSIA) or (BTU/Ft ² -Sec)	T Surf (DegR)	Gauge Label	Loc. (in)	Value (PSIA) or (BTU/Ft ² -Sec)	T Surf (DegR)
L28P1	-26.28	8.663(-1)		P5S4	2.89	Null		P5H9	4.31	2.210(0)	536.81
L28P3	-18.28	1.307(0)		P5S2	4.25	Null		P5H8	4.40	2.084(0)	536.90
L28P5	-10.28	Null		L28H3	-27.28	1.431(1)	552.67	P5H7	4.50	2.590(0)	537.29
S8P2	-1.98	Null		L28H6	-24.28	1.352(1)	551.42	P5H6	4.59	2.590(0)	537.40
S8P3	-1.98	Null		L28H11	-18.28	1.109(1)	548.65	P5H5	4.69	2.776(0)	537.51
S8P6	-1.67	Null		L28H13	-15.28	1.151(1)	548.31	P5H4	4.79	3.014(0)	537.70
S8P7	-1.67	Null		L28H18	-9.28	1.015(1)	547.03	P5H3	4.89	3.796(0)	538.27
S8P8	-1.67	Null		P5H42	.13	Null		P5H2	4.98	4.446(0)	538.91
S8P9	-1.67	Null		P5H41	.32	-5.093(-1)	533.34	P5H1	5.08	5.571(0)	539.85
S8P10	-1.67	Null		P5H40	.52	-7.664(-1)	533.56	P12H1	5.24	7.493(0)	541.39
S8P13	-.98	Null		P5H39	.72	-3.931(-1)	534.02	P12H2	5.33	Null	Null
S8P17	-.03	Null		P5H37	1.18	-9.294(-1)	533.61	P12H3	5.43	9.111(0)	542.97
S8P19	-.03	Null		P5H36	1.39	-8.249(-1)	533.81	P12H4	5.53	1.081(1)	544.37
S8P25	-.03	1.747(0)		P5H35	1.59	-1.235(0)	533.42	P12H5	5.63	1.124(1)	545.14
S8P26	-.03	1.569(0)		P5H34	1.80	-1.155(0)	533.48	P12H6	5.72	Null	Null
S8P27	-.03	Null		P5H33	2.00	-1.005(0)	533.47	P12H7	5.82	1.239(1)	546.33
S8P28	-.03	Null		P5H32	2.15	-1.114(0)	533.54	P12H8	5.92	1.436(1)	548.27
P5P9	.43	1.074(0)		P5H31	2.24	Null		P12H9	6.02	1.454(1)	548.61
P5P24	.56	9.010(-1)		P5H30	2.34	-9.633(-1)	533.61	P12H10	6.12	1.576(1)	549.90
P5P8	.94	1.232(0)		P5H29	2.43	-6.737(-1)	533.76	P12H11	6.21	Null	Null
P5P23	1.02	8.891(-1)		P5H28	2.53	-6.801(-1)	533.78	P12H12	6.30	1.588(1)	549.84
P5P7	1.45	1.115(0)		P5H27	2.63	-7.006(-1)	533.93	P12H13	6.39	1.798(1)	551.90
P5P22	1.53	8.672(-1)		P5H26	2.72	-6.511(-1)	533.92	P12H14	6.48	1.950(1)	552.43
P5P21	2.04	8.949(-1)		P5H25	2.82	-5.383(-1)	533.97	P12H15	6.56	1.952(1)	553.30
P5P5	2.72	1.176(0)		P5H24	2.91	-1.871(-1)	534.39	P12H16	6.66	2.107(1)	554.57
P5P18	2.79	1.154(0)		P5H23	3.02	-3.782(-1)	534.15	P12H17	6.74	2.283(1)	556.43
P5P4	3.23	1.137(0)		P5H22	3.14	-2.115(-1)	534.22	P12H18	6.84	2.332(1)	556.93
P5P16	3.31	1.196(0)		P5H21	3.23	-3.401(-1)	534.28	P12H19	6.93	2.396(1)	557.54
P5P3	3.73	1.563(0)		P5H20	3.33	-2.140(-1)	534.36	P12H20	7.02	Null	Null
P5P14	3.87	2.502(0)		P5H19	3.43	-2.094(-1)	534.45	P12H22	8.01	3.546(1)	571.24
P5P2	4.24	Null		P5H18	3.53	-5.373(-3)	534.55	P12H23	8.66	4.148(1)	578.82
P5P12	4.34	2.683(0)		P5H17	3.62	-1.356(-2)	534.57	P12H25	9.92	4.755(1)	585.72
P5P1	4.76	2.922(0)		P5H16	3.72	4.286(-1)	534.85	P12H26	10.57	4.992(1)	589.47
P5P10	4.85	3.380(0)		P5H15	3.82	9.656(-1)	535.26	P12H28	11.85	Null	Null
P12P1	5.47	4.196(0)		P5H14	3.92	2.002(0)	536.07	P12H29	12.49	Null	Null
P12P8	9.95	7.011(0)		P5H13	4.01	2.073(0)	536.37	P12H31	13.78	Null	Null
P12P10	11.23	Null		P5H12	4.09	1.808(0)	536.33	P12H33	15.06	Null	Null
P12P13	13.15	8.241(0)		P5H11	4.14	2.042(0)	536.64	P12H35	16.33	4.289(1)	584.28
P12P16	15.07	7.962(0)		P5H10	4.22	1.903(0)	536.76				

Run 28 Reduced Data Tabulation

Gauge Label	Loc. (in)	Value (PSIA) or (BTU/Ft ² -Sec)	T Surf (DegR)	Gauge Label	Loc. (in)	Value (PSIA) or (BTU/Ft ² -Sec)	T Surf (DegR)	Gauge Label	Loc. (in)	Value (PSIA) or (BTU/Ft ² -Sec)	T Surf (DegR)
L28P1	-26.28	1.073(0)		P5S4	2.89	Null		P5H9	4.31	1.617(0)	537.91
L28P3	-18.28	1.306(0)		P5S2	4.25	Null		P5H8	4.40	1.251(0)	537.85
L28P5	-10.28	Null		L28H3	-27.28	1.400(1)	555.38	P5H7	4.50	1.535(0)	538.26
S8P2	-1.98	Null		L28H6	-24.28	1.304(1)	553.93	P5H6	4.59	1.663(0)	538.31
S8P3	-1.98	Null		L28H11	-18.28	1.074(1)	550.90	P5H5	4.69	1.677(0)	538.40
S8P6	-1.67	Null		L28H13	-15.28	1.112(1)	550.81	P5H4	4.79	1.967(0)	538.56
S8P7	-1.67	Null		L28H18	-9.28	9.726(0)	549.41	P5H3	4.89	2.599(0)	539.11
S8P8	-1.67	Null		P5H42	.13	Null		P5H2	4.98	3.262(0)	539.68
S8P9	-1.67	Null		P5H41	.32	-1.457(0)	534.01	P5H1	5.08	4.275(0)	540.57
S8P10	-1.67	Null		P5H40	.52	-7.806(-1)	535.20	P12H1	5.24	5.890(0)	541.90
S8P13	-.98	Null		P5H39	.72	-3.573(-1)	535.68	P12H2	5.33	Null	Null
S8P17	-.03	Null		P5H37	1.18	-7.016(-1)	535.30	P12H3	5.43	Null	Null
S8P19	-.03	Null		P5H36	1.39	-1.417(-1)	535.73	P12H4	5.53	8.619(0)	544.91
S8P25	-.03	2.153(0)		P5H35	1.59	-9.145(-1)	535.24	P12H5	5.63	9.101(0)	545.76
S8P26	-.03	1.919(0)		P5H34	1.80	-1.007(0)	535.29	P12H6	5.72	Null	Null
S8P27	-.03	Null		P5H33	2.00	-8.629(-1)	535.25	P12H7	5.82	1.022(1)	546.97
S8P28	-.03	Null		P5H32	2.15	-9.546(-1)	535.24	P12H8	5.92	1.189(1)	548.98
P5P9	.43	8.050(-1)		P5H31	2.24	-8.977(-1)	535.29	P12H9	6.02	1.217(1)	549.37
P5P24	.56	8.556(-1)		P5H30	2.34	-7.956(-1)	535.30	P12H10	6.12	1.323(1)	550.52
P5P8	.94	1.258(0)		P5H29	2.43	-7.401(-1)	535.33	P12H11	6.21	Null	Null
P5P23	1.02	9.230(-1)		P5H28	2.53	-5.731(-1)	535.40	P12H12	6.30	1.424(1)	551.60
P5P7	1.45	1.111(0)		P5H27	2.63	-8.471(-1)	535.34	P12H13	6.39	1.558(1)	553.02
P5P22	1.53	8.887(-1)		P5H26	2.72	-5.378(-1)	535.48	P12H14	6.48	1.585(1)	553.34
P5P21	2.04	9.042(-1)		P5H25	2.82	-8.818(-1)	535.40	P12H15	6.56	1.654(1)	554.39
P5P5	2.72	1.193(0)		P5H24	2.91	-2.359(-1)	536.06	P12H16	6.65	1.761(1)	555.50
P5P18	2.79	1.167(0)		P5H23	3.02	-7.531(-1)	535.49	P12H17	6.74	1.921(1)	557.28
P5P4	3.23	1.149(0)		P5H22	3.14	-8.633(-1)	535.46	P12H18	6.84	1.984(1)	557.68
P5P16	3.31	1.224(0)		P5H21	3.23	-8.213(-1)	535.64	P12H19	6.93	2.098(1)	558.72
P5P3	3.73	1.337(0)		P5H20	3.33	-4.869(-1)	535.66	P12H20	7.02	Null	Null
P5P14	3.87	2.214(0)		P5H19	3.43	-6.021(-1)	535.68	P12H22	8.01	3.363(1)	573.08
P5P2	4.24	Null		P5H18	3.53	Null		P12H23	8.66	4.049(1)	581.50
P5P12	4.34	2.730(0)		P5H17	3.62	-4.523(-1)	535.82	P12H25	9.92	4.734(1)	590.52
P5P1	4.76	3.109(0)		P5H16	3.72	9.606(-2)	536.05	P12H26	10.57	4.984(1)	593.98
P5P10	4.85	3.609(0)		P5H15	3.82	1.248(-1)	536.31	P12H28	11.85	Null	Null
P12P1	5.47	4.589(0)		P5H14	3.92	7.643(-1)	536.83	P12H29	12.49	Null	Null
P12P8	9.95	6.974(0)		P5H13	4.01	1.103(0)	537.31	P12H31	13.78	Null	Null
P12P10	11.23	8.006(0)		P5H12	4.09	1.178(0)	537.28	P12H33	15.06	Null	Null
P12P13	13.15	8.181(0)		P5H11	4.14	1.429(0)	537.64	P12H35	16.33	4.466(1)	589.07
P12P16	15.07	7.961(0)		P5H10	4.22	1.437(0)	537.76				

Run 29 Reduced Data Tabulation

Gauge Label	Loc. (in)	Value (PSIA) or (BTU/Ft ² -Sec)	T Surf (DegR)	Gauge Label	Loc. (in)	Value (PSIA) or (BTU/Ft ² -Sec)	T Surf (DegR)	Gauge Label	Loc. (in)	Value (PSIA) or (BTU/Ft ² -Sec)	T Surf (DegR)
L28P1	-26.28	1.181(0)		P5S4	2.89	Null		P5H9	4.31	8.478(0)	540.40
L28P3	-18.28	1.318(0)		P5S2	4.25	Null		P5H8	4.40	8.648(0)	540.66
L28P5	-10.28	Null		L28H3	-27.28	1.535(1)	548.94	P5H7	4.50	8.793(0)	540.93
S8P2	-1.98	Null		L28H6	-24.28	1.407(1)	547.79	P5H6	4.59	8.466(0)	540.62
S8P3	-1.98	Null		L28H11	-18.28	1.151(1)	544.96	P5H5	4.69	8.750(0)	540.77
S8P6	-1.67	Null		L28H13	-15.28	1.193(1)	544.64	P5H4	4.79	8.425(0)	540.54
S8P7	-1.67	Null		L28H18	-9.28	1.041(1)	543.40	P5H3	4.89	8.678(0)	540.82
S8P8	-1.67	Null		P5H42	.13	Null		P5H2	4.98	8.562(0)	540.56
S8P9	-1.67	Null		P5H41	.32	8.086(0)	542.19	P5H1	5.08	8.346(0)	540.30
S8P10	-1.67	Null		P5H40	.52	1.064(1)	542.85	P12H1	5.24	7.743(0)	540.65
S8P13	-.98	Null		P5H39	.72	1.020(1)	542.14	P12H2	5.33	1.126(1)	540.87
S8P17	-.03	Null		P5H37	1.18	9.240(0)	541.07	P12H3	5.43	Null	Null
S8P19	-.03	Null		P5H36	1.39	8.772(0)	540.80	P12H4	5.53	2.417(1)	548.39
S8P25	-.03	2.752(-1)		P5H35	1.59	9.051(0)	540.99	P12H5	5.63	2.511(1)	552.75
S8P26	-.03	2.837(-1)		P5H34	1.80	8.414(0)	540.26	P12H6	5.72	Null	Null
S8P27	-.03	Null		P5H33	2.00	8.904(0)	540.92	P12H7	5.82	2.364(1)	554.14
S8P28	-.03	Null		P5H32	2.15	8.407(0)	540.45	P12H8	5.92	2.639(1)	557.14
P5P9	.43	9.049(-1)		P5H31	2.24	8.375(0)	540.52	P12H9	6.02	2.529(1)	556.24
P5P24	.56	7.069(-1)		P5H30	2.34	8.881(0)	540.97	P12H10	6.12	2.636(1)	557.72
P5P8	.94	1.044(0)		P5H29	2.43	8.559(0)	540.62	P12H11	6.21	Null	Null
P5P23	1.02	7.016(-1)		P5H28	2.53	8.552(0)	540.68	P12H12	6.30	2.708(1)	558.11
P5P7	1.45	9.238(-1)		P5H27	2.63	8.498(0)	540.55	P12H13	6.39	2.802(1)	559.08
P5P22	1.53	7.516(-1)		P5H26	2.72	8.862(0)	540.81	P12H14	6.48	2.746(1)	558.47
P5P21	2.04	7.583(-1)		P5H25	2.82	8.695(0)	540.98	P12H15	6.56	2.765(1)	559.12
P5P5	2.72	9.964(-1)		P5H24	2.91	8.349(0)	540.34	P12H16	6.66	2.856(1)	560.01
P5P18	2.79	9.561(-1)		P5H23	3.02	8.864(0)	540.80	P12H17	6.74	3.072(1)	562.25
P5P4	3.23	8.930(-1)		P5H22	3.14	8.948(0)	541.08	P12H18	6.84	2.965(1)	561.36
P5P16	3.31	1.013(0)		P5H21	3.23	8.974(0)	540.76	P12H19	6.93	2.956(1)	561.40
P5P3	3.73	1.031(0)		P5H20	3.33	8.361(0)	540.54	P12H20	7.02	Null	Null
P5P14	3.87	1.014(0)		P5H19	3.43	8.663(0)	540.85	P12H22	8.01	3.262(1)	566.67
P5P2	4.24	Null		P5H18	3.53	9.098(0)	541.26	P12H23	8.66	3.483(1)	569.35
P5P12	4.34	8.564(-1)		P5H17	3.62	8.507(0)	540.67	P12H25	9.92	3.492(1)	570.53
P5P1	4.76	8.986(-1)		P5H16	3.72	8.676(0)	540.71	P12H26	10.57	3.454(1)	570.40
P5P10	4.85	1.012(0)		P5H15	3.82	8.104(0)	540.24	P12H28	11.85	3.518(1)	571.25
P12P1	5.47	2.699(0)		P5H14	3.92	8.210(0)	540.30	P12H29	12.49	3.669(1)	573.07
P12P8	9.95	4.124(0)		P5H13	4.01	9.068(0)	540.88	P12H31	13.78	3.553(1)	571.34
P12P10	11.23	Null		P5H12	4.09	7.707(0)	539.91	P12H33	15.06	3.591(1)	571.79
P12P13	13.15	4.904(0)		P5H11	4.14	7.881(0)	540.03	P12H35	16.33	3.509(1)	571.27
P12P16	15.07	4.806(0)		P5H10	4.22	8.826(0)	540.90				

Run 30 Reduced Data Tabulation

Gauge Label	Loc. (in)	Value (PSIA) or (BTU/Ft ² -Sec)	T Surf (DegR)	Gauge Label	Loc. (in)	Value (PSIA) or (BTU/Ft ² -Sec)	T Surf (DegR)	Gauge Label	Loc. (in)	Value (PSIA) or (BTU/Ft ² -Sec)	T Surf (DegR)
L28P1	-26.28	7.423(-1)		P5S4	2.89	Null		P5H9	4.31	1.185(0)	534.44
L28P3	-18.28	1.278(0)		P5S2	4.25	Null		P5H8	4.40	1.461(0)	534.56
L28P5	-10.28	Null		L28H3	-27.28	1.473(1)	550.24	P5H7	4.50	1.331(0)	534.62
S8P2	-1.98	Null		L28H6	-24.28	1.307(1)	548.82	P5H6	4.59	Null	Null
S8P3	-1.98	Null		L28H11	-18.28	1.119(1)	546.27	P5H5	4.69	4.020(0)	535.96
S8P6	-1.67	Null		L28H13	-15.28	1.131(1)	545.98	P5H4	4.79	5.029(0)	536.85
S8P7	-1.67	Null		L28H18	-9.28	1.027(1)	544.99	P5H3	4.89	5.295(0)	537.43
S8P8	-1.67	Null		P5H42	.13	Null		P5H2	4.98	4.945(0)	537.57
S8P9	-1.67	Null		P5H41	.32	-5.244(-1)	531.89	P5H1	5.08	5.576(0)	538.23
S8P10	-1.67	Null		P5H40	.52	-3.647(-1)	532.10	P12H1	5.24	6.559(0)	538.68
S8P13	-.98	Null		P5H39	.72	-8.014(-1)	532.02	P12H2	5.33	Null	Null
S8P17	-.03	Null		P5H37	1.18	-1.433(0)	531.35	P12H3	5.43	Null	Null
S8P19	-.03	Null		P5H36	1.39	-1.053(0)	531.85	P12H4	5.53	7.444(0)	540.11
S8P25	-.03	1.125(0)		P5H35	1.59	-9.999(-1)	531.78	P12H5	5.63	6.941(0)	539.36
S8P26	-.03	Null		P5H34	1.80	-6.437(-1)	532.22	P12H6	5.72	Null	Null
S8P27	-.03	Null		P5H33	2.00	-3.871(-1)	532.57	P12H7	5.82	7.609(0)	540.91
S8P28	-.03	Null		P5H32	2.15	-2.046(-1)	532.79	P12H8	5.92	9.063(0)	542.05
P5P9	.43	8.981(-1)		P5H31	2.24	-1.372(-1)	532.92	P12H9	6.02	8.883(0)	541.80
P5P24	.56	8.316(-1)		P5H30	2.34	4.133(-2)	533.11	P12H10	6.12	9.587(0)	542.63
P5P8	.94	1.157(0)		P5H29	2.43	1.746(-1)	533.16	P12H11	6.21	Null	Null
P5P23	1.02	7.553(-1)		P5H28	2.53	1.403(-1)	533.25	P12H12	6.30	9.978(0)	543.11
P5P7	1.45	1.020(0)		P5H27	2.63	4.263(-1)	533.43	P12H13	6.39	1.071(1)	543.63
P5P22	1.53	8.208(-1)		P5H26	2.72	5.354(-1)	533.46	P12H14	6.48	1.043(1)	543.71
P5P21	2.04	8.325(-1)		P5H25	2.82	3.343(-1)	533.50	P12H15	6.56	1.080(1)	543.98
P5P5	2.72	1.063(0)		P5H24	2.91	4.962(-1)	533.59	P12H16	6.66	1.151(1)	544.59
P5P18	2.79	1.035(0)		P5H23	3.02	7.853(-1)	533.74	P12H17	6.74	1.259(1)	545.77
P5P4	3.23	9.965(-1)		P5H22	3.14	5.237(-1)	533.81	P12H18	6.84	1.262(1)	545.57
P5P16	3.31	1.122(0)		P5H21	3.23	1.069(0)	533.96	P12H19	6.93	1.264(1)	545.80
P5P3	3.73	1.077(0)		P5H20	3.33	8.026(-1)	533.91	P12H20	7.02	Null	Null
P5P14	3.87	1.116(0)		P5H19	3.43	8.460(-1)	533.99	P12H22	8.01	1.768(1)	551.84
P5P2	4.24	Null		P5H18	3.53	6.955(-1)	533.86	P12H23	8.66	1.885(1)	553.38
P5P12	4.34	9.850(-1)		P5H17	3.62	9.610(-1)	534.05	P12H25	9.92	2.355(1)	559.21
P5P1	4.76	1.840(0)		P5H16	3.72	1.176(0)	534.19	P12H26	10.57	2.435(1)	560.36
P5P10	4.85	2.405(0)		P5H15	3.82	9.189(-1)	534.14	P12H28	11.85	2.658(1)	563.04
P12P1	5.47	Null		P5H14	3.92	1.041(0)	534.26	P12H29	12.49	2.882(1)	565.38
P12P8	9.95	3.050(0)		P5H13	4.01	1.319(0)	534.36	P12H31	13.78	2.860(1)	565.07
P12P10	11.23	Null		P5H12	4.09	9.705(-1)	534.13	P12H33	15.06	2.871(1)	565.91
P12P13	13.15	4.563(0)		P5H11	4.14	1.041(0)	534.29	P12H35	16.33	2.954(1)	566.79
P12P16	15.07	4.585(0)		P5H10	4.22	1.159(0)	534.45				

Run 31 Reduced Data Tabulation

Gauge Label	Loc. (in)	Value (PSIA) or (BTU/Ft ² -Sec)	T Surf (DegR)	Gauge Label	Loc. (in)	Value (PSIA) or (BTU/Ft ² -Sec)	T Surf (DegR)	Gauge Label	Loc. (in)	Value (PSIA) or (BTU/Ft ² -Sec)	T Surf (DegR)
L28P1	-26.28	1.204(0)		P5S4	2.89	Null		P5H9	4.31	-3.540(-1)	535.14
L28P3	-18.28	1.245(0)		P5S2	4.25	Null		P5H8	4.40	-2.480(-1)	535.10
L28P5	-10.28	Null		L28H3	-27.28	1.389(1)	551.01	P5H7	4.50	-3.983(-1)	535.10
S8P2	-1.98	Null		L28H6	-24.28	1.250(1)	549.61	P5H6	4.59	-3.937(-1)	535.14
S8P3	-1.98	Null		L28H11	-18.28	1.042(1)	547.23	P5H5	4.69	-2.566(-1)	535.21
S8P6	-1.67	Null		L28H13	-15.28	1.053(1)	546.71	P5H4	4.79	-3.604(-2)	535.30
S8P7	-1.67	Null		L28H18	-9.28	9.259(0)	545.88	P5H3	4.89	5.942(-2)	535.45
S8P8	-1.67	Null		PSH42	.13	Null	Null	P5H2	4.98	7.400(-1)	535.80
S8P9	-1.67	Null		PSH41	.32	-1.858(0)	532.82	P5H1	5.08	1.306(0)	536.29
S8P10	-1.67	Null		PSH40	.52	-6.373(-1)	534.32	P12H1	5.24	1.859(0)	536.78
S8P13	-.98	Null		PSH39	.72	-8.311(-1)	534.52	P12H2	5.33	Null	Null
S8P17	-.03	Null		PSH37	1.18	-6.757(-1)	534.47	P12H3	5.43	Null	Null
S8P19	-.03	Null		PSH36	1.39	-6.688(-1)	534.70	P12H4	5.53	1.947(0)	537.15
S8P25	-.03	2.184(0)		PSH35	1.59	-8.302(-1)	534.46	P12H5	5.63	1.962(0)	537.22
S8P26	-.03	Null		PSH34	1.80	-7.724(-1)	534.50	P12H6	5.72	Null	Null
S8P27	-.03	Null		PSH33	2.00	-8.213(-1)	534.51	P12H7	5.82	2.070(0)	537.47
S8P28	-.03	Null		PSH32	2.15	-7.503(-1)	534.60	P12H8	5.92	2.440(0)	537.75
P5P9	.43	5.723(-1)		PSH31	2.24	-9.609(-1)	534.47	P12H9	6.02	1.963(0)	537.19
P5P24	.56	7.369(-1)		PSH30	2.34	-8.903(-1)	534.55	P12H10	6.12	2.634(0)	537.77
P5P8	.94	1.148(0)		PSH29	2.43	-9.543(-1)	534.57	P12H11	6.21	Null	Null
P5P23	1.02	8.658(-1)		PSH28	2.53	-8.758(-1)	534.51	P12H12	6.30	3.416(0)	538.60
P5P7	1.45	9.703(-1)		PSH27	2.63	-7.985(-1)	534.62	P12H13	6.39	3.664(0)	538.81
P5P22	1.53	8.021(-1)		PSH26	2.72	-8.672(-1)	534.54	P12H14	6.48	3.498(0)	538.81
P5P21	2.04	8.189(-1)		PSH25	2.82	-9.112(-1)	534.57	P12H15	6.56	3.885(0)	539.07
P5P5	2.72	1.054(0)		PSH24	2.91	-7.631(-1)	534.67	P12H16	6.66	4.060(0)	539.35
P5P18	2.79	1.027(0)		PSH23	3.02	-7.263(-1)	534.66	P12H17	6.74	4.437(0)	539.84
P5P4	3.23	1.005(0)		PSH22	3.14	-4.621(-1)	534.74	P12H18	6.84	4.500(0)	539.81
P5P16	3.31	1.090(0)		PSH21	3.23	-8.351(-1)	534.67	P12H19	6.93	4.561(0)	540.01
P5P3	3.73	1.046(0)		PSH20	3.33	-6.934(-1)	534.74	P12H20	7.02	4.228(0)	539.54
P5P14	3.87	1.088(0)		PSH19	3.43	-5.428(-1)	534.76	P12H22	8.01	6.913(0)	542.54
P5P2	4.24	Null		PSH18	3.53	Null	Null	P12H23	8.66	9.058(0)	544.72
P5P12	4.34	8.756(-1)		PSH17	3.62	-6.524(-1)	534.85	P12H25	9.92	1.190(1)	547.73
P5P1	4.76	9.576(-1)		PSH16	3.72	-5.085(-1)	534.84	P12H26	10.57	1.297(1)	549.00
P5P10	4.85	1.293(0)		PSH15	3.82	-4.668(-1)	534.95	P12H28	11.85	1.650(1)	552.46
P12P1	5.47	Null		PSH14	3.92	-5.014(-1)	534.95	P12H29	12.49	1.874(1)	554.53
P12P8	9.95	3.706(0)		PSH13	4.01	-4.477(-1)	534.95	P12H31	13.78	1.992(1)	555.72
P12P10	11.23	Null		PSH12	4.09	-5.755(-1)	534.91	P12H33	15.06	2.160(1)	557.55
P12P13	13.15	4.400(0)		PSH11	4.14	-2.680(-1)	535.13	P12H35	16.33	2.246(1)	558.91
P12P16	15.07	4.363(0)		PSH10	4.22	-3.060(-1)	535.09				

Run 32 Reduced Data Tabulation

Gauge Label	Loc. (in)	Value (PSIA) or (BTU/Ft ² -Sec)	T Surf (DegR)	Gauge Label	Loc. (in)	Value (PSIA) or (BTU/Ft ² -Sec)	T Surf (DegR)	Gauge Label	Loc. (in)	Value (PSIA) or (BTU/Ft ² -Sec)	T Surf (DegR)
L28P1	-26.28	1.209(0)		P5S4	2.89	Null		P5H9	4.31	3.765(0)	537.28
L28P3	-18.28	1.312(0)		P5S2	4.25	Null		P5H8	4.40	4.352(0)	538.06
L28P5	-10.28	Null		L28H3	-27.28	1.514(1)	551.32	P5H7	4.50	4.735(0)	538.58
S8P2	-1.98	Null		L28H6	-24.28	1.363(1)	549.84	P5H6	4.59	5.164(0)	539.02
S8P3	-1.98	Null		L28H11	-18.28	1.120(1)	547.18	P5H5	4.69	5.127(0)	539.17
S8P6	-1.67	Null		L28H13	-15.28	1.183(1)	546.98	P5H4	4.79	5.256(0)	539.44
S8P7	-1.67	Null		L28H18	-9.28	1.011(1)	545.67	P5H3	4.89	6.269(0)	540.16
S8P8	-1.67	Null		PSH42	.13	Null	Null	P5H2	4.98	6.533(0)	540.02
S8P9	-1.67	Null		PSH41	.32	-4.836(-1)	532.37	P5H1	5.08	7.423(0)	540.57
S8P10	-1.67	Null		PSH40	.52	-5.271(-1)	532.62	P12H1	5.24	7.248(0)	540.95
S8P13	-.98	Null		PSH39	.72	-7.231(-1)	532.54	P12H2	5.33	Null	Null
S8P17	-.03	Null		PSH37	1.18	-1.452(0)	531.87	P12H3	5.43	Null	Null
S8P19	-.03	Null		PSH36	1.39	-1.334(0)	532.46	P12H4	5.53	9.510(0)	542.31
S8P25	-.03	1.128(0)		PSH35	1.59	-1.022(0)	532.32	P12H5	5.63	1.124(1)	543.21
S8P26	-.03	Null		PSH34	1.80	-8.112(-1)	532.66	P12H6	5.72	Null	Null
S8P27	-.03	Null		PSH33	2.00	-2.652(-1)	533.12	P12H7	5.82	1.383(1)	545.74
S8P28	-.03	Null		PSH32	2.15	-2.691(-1)	533.27	P12H8	5.92	1.789(1)	548.57
P5P9	.43	1.051(0)		PSH31	2.24	-8.644(-3)	533.38	P12H9	6.02	Null	Null
P5P24	.56	8.304(-1)		PSH30	2.34	-1.239(-1)	533.60	P12H10	6.12	2.314(1)	552.57
P5P8	.94	1.175(0)		PSH29	2.43	1.015(-1)	533.62	P12H11	6.21	Null	Null
P5P23	1.02	8.556(-1)		PSH28	2.53	1.778(-1)	533.71	P12H12	6.30	2.716(1)	555.90
P5P7	1.45	1.065(0)		PSH27	2.63	3.793(-1)	533.92	P12H13	6.39	2.882(1)	558.18
P5P22	1.53	8.353(-1)		PSH26	2.72	5.053(-1)	534.02	P12H14	6.48	3.026(1)	559.71
P5P21	2.04	8.548(-1)		PSH25	2.82	5.434(-1)	534.08	P12H15	6.56	3.156(1)	561.38
P5P5	2.72	1.087(0)		PSH24	2.91	5.484(-1)	534.15	P12H16	6.66	3.511(1)	564.02
P5P18	2.79	1.049(0)		PSH23	3.02	8.372(-1)	534.35	P12H17	6.74	3.904(1)	567.98
P5P4	3.23	9.891(-1)		PSH22	3.14	Null	Null	P12H18	6.84	3.997(1)	569.76
P5P16	3.31	1.239(0)		PSH21	3.23	9.618(-1)	534.52	P12H19	6.93	4.205(1)	570.27
P5P3	3.73	2.097(0)		PSH20	3.33	6.564(-1)	534.38	P12H20	7.02	3.940(1)	568.94
P5P14	3.87	2.624(0)		PSH19	3.43	1.041(0)	534.57	P12H22	8.01	6.873(1)	597.69
P5P2	4.24	Null		PSH18	3.53	1.353(0)	534.77	P12H23	8.66	8.108(1)	611.47
P5P12	4.34	2.432(0)		PSH17	3.62	2.160(0)	535.19	P12H25	9.92	8.873(1)	624.83
P5P1	4.76	2.530(0)		PSH16	3.72	3.516(0)	536.07	P12H26	10.57	8.772(1)	625.37
P5P10	4.85	2.934(0)		PSH15	3.82	3.789(0)	536.55	P12H28	11.85	8.897(1)	627.63
P12P1	5.47	3.010(0)		PSH14	3.92	4.077(0)	537.00	P12H29	12.49	9.025(1)	629.11
P12P8	9.95	1.118(1)		PSH13	4.01	4.165(0)	537.18	P12H31	13.78	8.072(1)	620.97
P12P10	11.23	Null		PSH12	4.09	3.632(0)	537.11	P12H33	15.06	7.494(1)	615.03
P12P13	13.15	1.295(1)		PSH11	4.14	4.110(0)	537.61	P12H35	16.33	5.392(1)	594.23
P12P16	15.07	9.615(0)		PSH10	4.22	4.476(0)	537.83				

Run 33 Reduced Data Tabulation

Gauge Label	Loc. (in)	Value (PSIA) or (BTU/Ft ² -Sec)	T Surf (DegR)	Gauge Label	Loc. (in)	Value (PSIA) or (BTU/Ft ² -Sec)	T Surf (DegR)	Gauge Label	Loc. (in)	Value (PSIA) or (BTU/Ft ² -Sec)	T Surf (DegR)
L28P1	-26.28	1.145(0)	PSS4	2.89	Null	P5H9	4.31	1.670(0)	536.17		
L28P3	-18.28	1.332(0)	PSS2	4.25	Null	P5H8	4.40	1.819(0)	536.49		
L28P5	-10.28	1.178(0)	L28H3	-27.28	1.477(1)	553.55	P5H7	4.50	2.323(0)	536.91	
S8P2	-1.98	Null	L28H6	-24.28	Null	P5H6	4.59	Null	Null		
S8P3	-1.98	Null	L28H11	-18.28	1.116(1)	548.88	P5H5	4.69	2.499(0)	537.38	
S8P6	-1.67	Null	L28H13	-15.28	1.160(1)	548.52	P5H4	4.79	2.880(0)	537.65	
S8P7	-1.67	Null	L28H18	-9.28	1.030(1)	547.26	P5H3	4.89	2.763(0)	537.75	
S8P8	-1.67	Null	P5H42	.13	Null	P5H2	4.98	3.275(0)	538.03		
S8P9	-1.67	Null	P5H41	.32	-1.404(0)	532.33	P5H1	5.08	3.821(0)	538.38	
S8P10	-1.67	Null	P5H40	.52	-8.208(-1)	533.58	P12H1	5.24	4.436(0)	538.89	
S8P13	-.98	Null	P5H39	.72	-6.409(-1)	533.89	P12H2	5.33	Null	Null	
S8P17	-.03	Null	P5H37	1.18	-7.537(-1)	533.76	P12H3	5.43	Null	Null	
S8P19	-.03	Null	P5H36	1.39	-4.351(-1)	534.06	P12H4	5.53	6.611(0)	540.30	
S8P25	-.03	2.151(0)	P5H35	1.59	-1.068(0)	533.64	P12H5	5.63	7.944(0)	541.18	
S8P26	-.03	1.932(0)	P5H34	1.80	-9.750(-1)	533.67	P12H6	5.72	Null	Null	
S8P27	-.03	Null	P5H33	2.00	-7.842(-1)	533.71	P12H7	5.82	1.051(1)	543.22	
S8P28	-.03	Null	P5H32	2.15	-8.740(-1)	533.80	P12H8	5.92	1.371(1)	545.71	
P5P9	.43	8.059(-1)	P5H31	2.24	Null	P12H9	6.02	1.461(1)	546.61		
P5P24	.56	8.327(-1)	P5H30	2.34	-8.900(-1)	533.74	P12H10	6.12	1.731(1)	548.79	
P5P8	.94	1.249(0)	P5H29	2.43	-2.253(-1)	534.39	P12H11	6.21	Null	Null	
P5P23	1.02	9.311(-1)	P5H28	2.53	-5.200(-1)	533.78	P12H12	6.30	2.119(1)	551.45	
P5P7	1.45	1.108(0)	P5H27	2.63	-9.108(-1)	533.82	P12H13	6.39	2.400(1)	553.91	
P5P22	1.53	8.734(-1)	P5H26	2.72	-8.825(-1)	533.82	P12H14	6.48	2.455(1)	554.31	
P5P21	2.04	8.968(-1)	P5H25	2.82	-9.237(-1)	533.82	P12H15	6.56	2.233(1)	552.91	
P5P5	2.72	1.162(0)	P5H24	2.91	-6.557(-1)	533.91	P12H16	6.66	2.991(1)	558.08	
P5P18	2.79	1.068(0)	P5H23	3.02	-7.706(-1)	533.94	P12H17	6.74	3.356(1)	561.33	
P5P4	3.23	1.085(0)	P5H22	3.14	-1.075(-1)	534.54	P12H18	6.84	3.332(1)	561.70	
P5P16	3.31	1.212(0)	P5H21	3.23	-4.179(-1)	534.20	P12H19	6.93	3.527(1)	563.38	
P5P3	3.73	1.572(0)	P5H20	3.33	-6.999(-1)	534.04	P12H20	7.02	2.759(1)	557.31	
P5P14	3.87	2.772(0)	P5H19	3.43	-5.963(-1)	534.09	P12H22	8.01	6.127(1)	587.52	
P5P2	4.24	Null	P5H18	3.53	-4.438(-1)	534.16	P12H23	8.66	7.611(1)	602.17	
P5P12	4.34	2.796(0)	P5H17	3.62	-2.207(-1)	534.30	P12H25	9.92	8.742(1)	618.72	
P5P1	4.76	2.933(0)	P5H16	3.72	3.263(-1)	534.61	P12H26	10.57	8.624(1)	621.41	
P5P10	4.85	3.391(0)	P5H15	3.82	8.332(-1)	535.03	P12H28	11.85	8.801(1)	625.26	
P12P1	5.47	3.348(0)	P5H14	3.92	1.489(0)	535.56	P12H29	12.49	8.989(1)	627.62	
P12P8	9.95	1.104(1)	P5H13	4.01	1.606(0)	535.80	P12H31	13.78	8.162(1)	620.82	
P12P10	11.23	Null	P5H12	4.09	1.071(0)	535.70	P12H33	15.06	7.555(1)	615.39	
P12P13	13.15	1.297(1)	P5H11	4.14	8.847(-1)	535.51	P12H35	16.33	Null	Null	
P12P16	15.07	9.848(0)	P5H10	4.22	1.786(0)	536.25					

Run 34 Reduced Data Tabulation

Gauge Label	Loc. (in)	Value (PSIA) or (BTU/Ft ² -Sec)	T Surf (DegR)	Gauge Label	Loc. (in)	Value (PSIA) or (BTU/Ft ² -Sec)	T Surf (DegR)	Gauge Label	Loc. (in)	Value (PSIA) or (BTU/Ft ² -Sec)	T Surf (DegR)
L28P1	-26.28	1.175(0)	PSS4	2.89	Null	P5H9	4.31	5.455(1)	586.17		
L28P3	-18.28	1.321(0)	PSS2	4.25	Null	P5H8	4.40	7.153(1)	601.54		
L28P5	-10.28	1.122(0)	L28H3	-27.28	1.531(1)	554.83	P5H7	4.50	7.831(1)	607.32	
S8P2	-1.98	Null	L28H6	-24.28	Null	P5H6	4.59	7.856(1)	608.42		
S8P3	-1.98	Null	L28H11	-18.28	1.136(1)	550.34	P5H5	4.69	8.291(1)	612.29	
S8P6	-1.67	Null	L28H13	-15.28	1.169(1)	549.78	P5H4	4.79	8.167(1)	611.89	
S8P7	-1.67	Null	L28H18	-9.28	1.026(-1)	548.59	P5H3	4.89	8.492(1)	615.80	
S8P8	-1.67	Null	P5H42	.13	Null	P5H2	4.98	8.375(1)	616.15		
S8P9	-1.67	Null	P5H41	.32	6.895(0)	546.62	P5H1	5.08	8.389(1)	616.45	
S8P10	-1.67	Null	P5H40	.52	1.070(1)	548.72	P12H1	5.24	Null	Null	
S8P13	-.98	Null	P5H39	.72	1.020(1)	547.63	P12H2	5.33	Null	Null	
S8P17	-.03	Null	P5H37	1.18	8.731(0)	546.40	P12H3	5.43	Null	Null	
S8P19	-.03	Null	P5H36	1.39	9.240(0)	546.48	P12H4	5.53	Null	Null	
S8P25	-.03	3.205(-1)	P5H35	1.59	8.717(0)	546.27	P12H5	5.63	Null	Null	
S8P26	-.03	3.190(-1)	P5H34	1.80	7.828(0)	545.69	P12H6	5.72	Null	Null	
S8P27	-.03	Null	P5H33	2.00	1.440(1)	547.16	P12H7	5.82	Null	Null	
S8P28	-.03	Null	P5H32	2.15	1.504(1)	550.05	P12H8	5.92	Null	Null	
P5P9	.43	5.714(-1)	P5H31	2.24	1.492(1)	551.05	P12H9	6.02	Null	Null	
P5P24	.56	7.227(-1)	P5H30	2.34	1.222(1)	550.10	P12H10	6.12	Null	Null	
P5P8	.94	1.048(0)	P5H29	2.43	4.936(0)	540.89	P12H11	6.21	Null	Null	
P5P23	1.02	7.656(-1)	P5H28	2.53	1.265(1)	550.52	P12H12	6.30	Null	Null	
P5P7	1.45	9.652(-1)	P5H27	2.63	1.242(1)	551.41	P12H13	6.39	Null	Null	
P5P22	1.53	7.652(-1)	P5H26	2.72	1.311(1)	552.04	P12H14	6.48	Null	Null	
P5P21	2.04	1.417(0)	P5H25	2.82	1.566(1)	552.56	P12H15	6.56	Null	Null	
P5P5	2.72	3.449(0)	P5H24	2.91	1.807(1)	552.70	P12H16	6.66	Null	Null	
P5P18	2.79	3.582(0)	P5H23	3.02	2.424(1)	556.60	P12H17	6.74	Null	Null	
P5P4	3.23	4.902(0)	P5H22	3.14	3.135(1)	561.25	P12H18	6.84	Null	Null	
P5P16	3.31	6.651(0)	P5H21	3.23	3.504(1)	563.78	P12H19	6.93	8.977(1)	634.63	
P5P3	3.73	8.542(0)	P5H20	3.33	3.931(1)	568.14	P12H20	7.02	8.287(1)	628.54	
P5P14	3.87	1.062(1)	P5H19	3.43	4.442(1)	572.33	P12H22	8.01	8.816(1)	636.39	
P5P2	4.24	Null	P5H18	3.53	5.002(1)	577.34	P12H23	8.66	8.897(1)	637.72	
P5P12	4.34	1.111(1)	P5H17	3.62	5.017(1)	578.07	P12H25	9.92	8.529(1)	635.17	
P5P1	4.76	1.301(1)	P5H16	3.72	5.254(1)	581.16	P12H26	10.57	7.923(1)	629.01	
P5P10	4.85	1.431(1)	P5H15	3.82	5.441(1)	583.07	P12H28	11.85	7.160(1)	621.68	
P12P1	5.47	Null	P5H14	3.92	5.964(1)	588.05	P12H29	12.49	6.882(1)	617.53	
P12P8	9.95	1.173(1)	P5H13	4.01	6.301(1)	591.18	P12H31	13.78	4.725(1)	592.81	
P12P10	11.23	Null	P5H12	4.09	5.936(1)	588.46	P12H33	15.06	3.654(1)	579.52	
P12P13	13.15	9.129(0)	P5H11	4.14	7.362(1)	599.33	P12H35	16.33	2.713(1)	568.99	
P12P16	15.07	5.102(0)	P5H10	4.22	6.954(1)	597.63					

Run 35 Reduced Data Tabulation

Gauge Label	Loc. (in)	Value (PSIA) or (BTU/Ft ² -Sec)	T Surf (DegR)	Gauge Label	Loc. (in)	Value (PSIA) or (BTU/Ft ² -Sec)	T Surf (DegR)	Gauge Label	Loc. (in)	Value (PSIA) or (BTU/Ft ² -Sec)	T Surf (DegR)
L28P1	-26.28	1.138(0)	P5S4	2.89	Null	P5H9	4.31	2.804(1)	555.09		
L28P3	-18.28	1.314(0)	P5S2	4.25	Null	P5H8	4.40	3.481(1)	560.94		
L28P5	-10.28	Null	L28H3	-27.28	1.548(1)	549.50	P5H7	4.50	3.870(1)	564.73	
S8P2	-1.98	Null	L28H6	-24.28	1.379(1)	547.76	P5H6	4.59	3.974(1)	565.61	
S8P3	-1.98	Null	L28H11	-18.28	1.176(1)	545.19	P5H5	4.69	4.223(1)	567.81	
S8P6	-1.67	Null	L28H13	-15.28	1.171(1)	544.63	P5H4	4.79	4.348(1)	569.43	
S8P7	-1.67	Null	L28H18	-9.28	1.062(1)	543.56	P5H3	4.89	4.659(1)	572.45	
S8P8	-1.67	Null	P5H42	.13	Null	P5H2	4.98	4.736(1)	573.47		
S8P9	-1.67	Null	P5H41	.32	-1.128(0)	529.03	P5H1	5.08	4.978(1)	575.31	
S8P10	-1.67	Null	P5H40	.52	-5.639(-1)	530.20	P12H1	5.24	5.542(1)	582.52	
S8P13	-.98	Null	P5H39	.72	-4.886(-1)	530.48	P12H2	5.33	7.250(1)	598.64	
S8P17	-.03	Null	P5H37	1.18	7.376(-1)	531.04	P12H3	5.43	Null	Null	
S8P19	-.03	Null	P5H36	1.39	1.353(0)	532.06	P12H4	5.53	7.696(1)	603.28	
S8P25	-.03	2.165(0)	P5H35	1.59	1.280(0)	532.06	P12H5	5.63	8.045(1)	605.90	
S8P26	-.03	1.933(0)	P5H34	1.80	1.809(0)	532.64	P12H6	5.72	4.958(1)	579.49	
S8P27	-.03	Null	P5H33	2.00	2.207(0)	533.20	P12H7	5.82	8.043(1)	607.03	
S8P28	-.03	Null	P5H32	2.15	2.632(0)	533.71	P12H8	5.92	8.853(1)	615.01	
P5P9	.43	6.302(-1)	P5H31	2.24	2.961(0)	534.21	P12H9	6.02	8.530(1)	612.77	
P5P24	.56	8.195(-1)	P5H30	2.34	3.037(0)	534.34	P12H10	6.12	8.628(1)	614.59	
P5P8	.94	1.746(0)	P5H29	2.43	3.468(0)	534.58	P12H11	6.21	Null	Null	
P5P23	1.02	9.745(-1)	P5H28	2.53	4.597(0)	535.10	P12H12	6.30	8.641(1)	616.02	
P5P7	1.45	2.914(0)	P5H27	2.63	4.712(0)	535.34	P12H13	6.39	8.867(1)	618.45	
P5P22	1.53	1.868(0)	P5H26	2.72	6.006(0)	536.10	P12H14	6.48	8.503(1)	615.13	
P5P21	2.04	3.064(0)	P5H25	2.82	7.211(0)	536.96	P12H15	6.56	8.375(1)	614.53	
P5P5	2.72	5.170(0)	P5H24	2.91	7.356(0)	537.06	P12H16	6.66	8.778(1)	619.03	
P5P18	2.79	5.564(0)	P5H23	3.02	1.002(1)	538.74	P12H17	6.74	9.184(1)	623.65	
P5P4	3.23	6.170(0)	P5H22	3.14	1.279(1)	540.37	P12H18	6.84	8.841(1)	620.16	
P5P16	3.31	7.332(0)	P5H21	3.23	1.369(1)	541.48	P12H19	6.93	8.673(1)	618.98	
P5P3	3.73	8.113(0)	P5H20	3.33	1.509(1)	542.52	P12H20	7.02	7.799(1)	611.83	
P5P14	3.87	9.322(0)	P5H19	3.43	1.697(1)	543.93	P12H21	8.01	8.767(1)	624.71	
P5P2	4.24	Null	P5H18	3.53	1.965(1)	546.28	P12H23	8.66	8.915(1)	626.70	
P5P12	4.34	8.933(0)	P5H17	3.62	1.966(1)	547.22	P12H25	9.92	8.460(1)	625.05	
P5P1	4.76	1.043(1)	P5H16	3.72	2.207(1)	548.83	P12H26	10.57	7.964(1)	619.92	
P5P10	4.85	1.156(1)	P5H15	3.82	2.308(1)	549.68	P12H28	11.85	7.355(1)	614.34	
P12P1	5.47	1.233(1)	P5H14	3.92	2.565(1)	552.33	P12H29	12.49	7.031(1)	610.67	
P12P8	9.95	1.147(1)	P5H13	4.01	2.782(1)	554.16	P12H31	13.78	4.870(1)	586.96	
P12P10	11.23	Null	P5H12	4.09	2.614(1)	552.96	P12H33	15.06	3.660(1)	573.54	
P12P13	13.15	9.099(0)	P5H11	4.14	3.051(1)	556.51	P12H35	16.33	2.802(1)	563.76	
P12P16	15.07	5.161(0)	P5H10	4.22	3.180(1)	557.94					

Run 36 Reduced Data Tabulation

Gauge Label	Loc. (in)	Value (PSIA) or (BTU/Ft ² -Sec)	T Surf (DegR)	Gauge Label	Loc. (in)	Value (PSIA) or (BTU/Ft ² -Sec)	T Surf (DegR)	Gauge Label	Loc. (in)	Value (PSIA) or (BTU/Ft ² -Sec)	T Surf (DegR)
L28P1	-26.28	1.117(0)	P5S4	2.89	Null	P5H9	4.31	6.896(1)	604.29		
L28P3	-18.28	1.328(0)	P5S2	4.25	Null	P5H8	4.40	8.097(1)	616.51		
L28P5	-10.28	8.432(-1)	L28H3	-27.28	Null	P5H7	4.50	8.587(1)	621.09		
S8P2	-1.98	Null	L28H6	-24.28	Null	P5H6	4.59	8.483(1)	621.53		
S8P3	-1.98	Null	L28H11	-18.28	1.150(1)	546.95	P5H5	4.69	8.932(1)	625.78	
S8P6	-1.67	Null	L28H13	-15.28	1.172(1)	546.77	P5H4	4.79	8.658(1)	623.64	
S8P7	-1.67	Null	L28H18	-9.28	1.022(1)	545.32	P5H3	4.89	8.924(1)	626.80	
S8P8	-1.67	Null	P5H42	.13	Null	P5H2	4.98	8.732(1)	625.86		
S8P9	-1.67	Null	P5H41	.32	7.636(0)	544.16	P5H1	5.08	8.867(1)	626.82	
S8P10	-1.67	Null	P5H40	.52	1.083(1)	545.37	P12H1	5.24	7.917(1)	610.82	
S8P13	-.98	Null	P5H39	.72	9.901(0)	543.96	P12H2	5.33	9.971(1)	632.30	
S8P17	-.03	Null	P5H37	1.18	1.622(1)	548.60	P12H3	5.43	Null	Null	
S8P19	-.03	Null	P5H36	1.39	1.590(1)	549.32	P12H4	5.53	9.758(1)	613.04	
S8P25	-.03	3.093(-1)	P5H35	1.59	1.490(1)	548.99	P12H5	5.63	9.817(1)	633.67	
S8P26	-.03	2.856(-1)	P5H34	1.80	2.204(1)	551.22	P12H6	5.72	Null	Null	
S8P27	-.03	Null	P5H33	2.00	3.492(1)	558.42	P12H7	5.82	9.438(1)	630.54	
S8P28	-.03	Null	P5H32	2.15	4.231(1)	564.33	P12H8	5.92	1.021(2)	638.36	
P5P9	.43	Null	P5H31	2.24	4.677(1)	568.74	P12H9	6.02	9.699(1)	633.68	
P5P24	.56	7.382(-1)	P5H30	2.34	4.788(1)	571.92	P12H10	6.12	9.816(1)	634.83	
P5P8	.94	3.495(0)	P5H29	2.43	4.576(1)	571.70	P12H11	6.21	Null	Null	
P5P23	1.02	2.066(0)	P5H28	2.53	5.167(1)	576.86	P12H12	6.30	9.171(1)	629.05	
P5P7	1.45	3.512(0)	P5H27	2.63	5.124(1)	578.32	P12H13	6.39	9.853(1)	635.71	
P5P22	1.53	2.815(0)	P5H26	2.72	5.503(1)	582.22	P12H14	6.48	9.246(1)	630.77	
P5P21	2.04	4.278(0)	P5H25	2.82	5.800(1)	586.08	P12H15	6.56	8.983(1)	628.40	
P5P5	2.72	9.983(0)	P5H24	2.91	5.573(1)	584.71	P12H16	6.66	9.525(1)	633.67	
P5P18	2.79	1.044(1)	P5H23	3.02	6.099(1)	590.08	P12H17	6.74	9.990(1)	638.27	
P5P4	3.23	1.182(1)	P5H22	3.14	6.495(1)	593.31	P12H18	6.84	9.490(1)	634.11	
P5P16	3.31	1.298(1)	P5H21	3.23	6.398(1)	593.87	P12H19	6.93	9.395(1)	633.43	
P5P3	3.73	1.425(1)	P5H20	3.33	6.497(1)	595.93	P12H20	7.02	5.723(1)	597.34	
P5P14	3.87	1.510(1)	P5H19	3.43	6.913(1)	600.23	P12H22	8.01	9.067(1)	632.22	
P5P2	4.24	Null	P5H18	3.53	7.133(1)	602.67	P12H23	8.66	8.808(1)	630.23	
P5P12	4.34	1.283(1)	P5H17	3.62	7.039(1)	602.95	P12H25	9.92	8.431(1)	626.96	
P5P1	4.76	1.413(1)	P5H16	3.72	7.264(1)	604.60	P12H26	10.57	7.943(1)	622.03	
P5P10	4.85	1.511(1)	P5H15	3.82	7.052(1)	603.25	P12H28	11.85	6.453(1)	606.15	
P12P1	5.47	1.423(1)	P5H14	3.92	7.627(1)	609.20	P12H29	12.49	5.409(1)	595.02	
P12P8	9.95	1.133(1)	P5H13	4.01	7.952(1)	612.20	P12H31	13.78	3.626(1)	575.10	
P12P10	11.23	Null	P5H12	4.09	7.190(1)	606.16	P12H33	15.06	2.770(1)	565.22	
P12P13	13.15	6.392(0)	P5H11	4.14	8.933(1)	621.91	P12H35	16.33	2.064(1)	557.83	
P12P16	15.07	3.655(0)	P5H10	4.22	8.272(1)	616.86					

Run 37 Reduced Data Tabulation

Gauge Label	Loc. (in)	Value (PSIA) or (BTU/Ft ² -Sec)	T Surf (DegR)	Gauge Label	Loc. (in)	Value (PSIA) or (BTU/Ft ² -Sec)	T Surf (DegR)	Gauge Label	Loc. (in)	Value (PSIA) or (BTU/Ft ² -Sec)	T Surf (DegR)
L28P1	-26.28	1.072(0)		P5S4	2.89	Null		P5H9	4.31	4.889(1)	581.56
L28P3	-18.28	1.340(0)		P5S2	4.25	Null		P5H8	4.40	5.987(1)	591.87
L28P5	-10.28	Null		L28H3	-27.28	1.504(1)	553.89	P5H7	4.50	6.429(1)	596.82
S8P2	-1.98	Null		L28H6	-24.28	Null		P5H6	4.59	6.383(1)	597.02
S8P3	-1.98	Null		L28H11	-18.28	1.161(1)	549.38	P5H5	4.69	6.632(1)	599.73
S8P6	-1.67	Null		L28H13	-15.28	1.177(1)	549.08	P5H4	4.79	6.643(1)	600.76
S8P7	-1.67	Null		L28H18	-9.28	1.044(1)	547.67	P5H3	4.89	6.870(1)	603.72
S8P8	-1.67	Null		P5H42	.13	Null		P5H2	4.98	6.769(1)	603.60
S8P9	-1.67	Null		P5H41	.32	2.163(0)	536.41	P5H1	5.08	6.834(1)	604.58
S8P10	-1.67	Null		P5H40	.52	2.346(0)	536.55	P12H1	5.24	4.913(1)	586.56
S8P13	-.98	Null		P5H39	.72	2.286(0)	536.58	P12H2	5.33	5.520(1)	593.60
S8P17	-.03	Null		P5H37	1.18	3.449(0)	537.72	P12H3	5.43	Null	Null
S8P19	-.03	Null		P5H36	1.39	5.267(0)	538.87	P12H4	5.53	7.515(1)	614.73
S8P25	-.03	2.184(0)		P5H35	1.59	6.644(0)	539.83	P12H5	5.63	7.788(1)	617.11
S8P26	-.03	1.955(0)		P5H34	1.80	9.981(0)	542.06	P12H6	5.72	Null	Null
S8P27	-.03	Null		P5H33	2.00	1.505(1)	545.18	P12H7	5.82	7.541(1)	615.43
S8P28	-.03	Null		P5H32	2.15	1.796(1)	547.46	P12H8	5.92	8.258(1)	622.61
P5P9	.43	1.693(0)		P5H31	2.24	2.052(1)	550.11	P12H9	6.02	7.903(1)	619.85
P5P24	.56	3.081(0)		P5H30	2.34	2.251(1)	551.71	P12H10	6.12	8.014(1)	621.14
P5P8	.94	4.345(0)		P5H29	2.43	2.270(1)	552.24	P12H11	6.21	Null	Null
P5P23	1.02	3.295(0)		P5H28	2.53	2.615(1)	554.77	P12H12	6.30	7.670(1)	618.05
P5P7	1.45	4.783(0)		P5H27	2.63	2.697(1)	555.94	P12H13	6.39	8.147(1)	623.36
P5P22	1.53	4.127(0)		P5H26	2.72	2.964(1)	558.46	P12H14	6.48	7.923(1)	621.34
P5P21	2.04	5.275(0)		P5H25	2.82	3.183(1)	560.88	P12H15	6.56	7.510(1)	617.93
P5P5	2.72	8.968(0)		P5H24	2.91	3.053(1)	560.30	P12H16	6.66	8.041(1)	623.42
P5P18	2.79	8.774(0)		P5H23	3.02	3.454(1)	563.61	P12H17	6.74	8.385(1)	626.84
P5P4	3.23	9.934(0)		P5H22	3.14	3.728(1)	566.11	P12H18	6.84	8.156(1)	625.02
P5P16	3.31	1.049(1)		P5H21	3.23	3.870(1)	567.79	P12H19	6.93	8.031(1)	623.60
P5P3	3.73	1.157(1)		P5H20	3.33	3.995(1)	569.36	P12H20	7.02	5.326(1)	596.07
P5P14	3.87	1.258(1)		P5H19	3.43	4.238(1)	571.66	P12H22	8.01	8.220(1)	626.82
P5P2	4.24	Null		P5H18	3.53	4.411(1)	573.22	P12H23	8.66	8.162(1)	627.02
P5P12	4.34	1.119(1)		P5H17	3.62	4.572(1)	575.41	P12H25	9.92	8.114(1)	625.81
P5P1	4.76	1.278(1)		P5H16	3.72	4.715(1)	577.36	P12H26	10.57	7.534(1)	620.70
P5P10	4.85	1.387(1)		P5H15	3.82	4.761(1)	578.11	P12H28	11.85	6.319(1)	607.24
P12P1	5.47	Null		P5H14	3.92	5.213(1)	582.71	P12H29	12.49	5.322(1)	596.71
P12P8	9.95	1.109(1)		P5H13	4.01	5.499(1)	585.52	P12H31	13.78	3.534(1)	576.95
P12P10	11.23	Null		P5H12	4.09	4.936(1)	580.81	P12H33	15.06	2.669(1)	567.14
P12P13	13.15	6.423(0)		P5H11	4.14	6.092(1)	591.15	P12H35	16.33	2.086(1)	560.03
P12P16	15.07	3.696(0)		P5H10	4.22	6.026(1)	590.95				

Run 38 Reduced Data Tabulation

Gauge Label	Loc. (in)	Value (PSIA) or (BTU/Ft ² -Sec)	T Surf (DegR)	Gauge Label	Loc. (in)	Value (PSIA) or (BTU/Ft ² -Sec)	T Surf (DegR)	Gauge Label	Loc. (in)	Value (PSIA) or (BTU/Ft ² -Sec)	T Surf (DegR)
L28P1	-26.28	1.245(0)		P5S4	2.89	Null		P5H9	4.31	Null	Null
L28P3	-18.28	1.406(0)		P5S2	4.25	Null		P5H8	4.40	7.321(0)	540.16
L28P5	-10.28	Null		L28H3	-27.28	1.573(1)	550.46	P5H7	4.50	Null	Null
S8P2	-1.98	Null		L28H6	-24.28	1.478(1)	549.46	P5H6	4.59	7.209(0)	540.13
S8P3	-1.98	Null		L28H11	-18.28	1.230(1)	546.30	P5H5	4.69	7.108(0)	540.25
S8P6	-1.67	Null		L28H13	-15.28	1.191(1)	545.46	P5H4	4.79	7.196(0)	540.16
S8P7	-1.67	Null		L28H18	-9.28	1.088(1)	544.49	P5H3	4.89	6.706(0)	540.09
S8P8	-1.67	Null		P5H42	.13	Null		P5H2	4.98	7.346(0)	540.15
S8P9	-1.67	Null		P5H41	.32	1.061(0)	533.50	P5H1	5.08	1.052(1)	540.35
S8P10	-1.67	Null		P5H40	.52	3.261(0)	536.92	P12H1	5.24	1.196(1)	541.29
S8P13	-.98	Null		P5H39	.72	6.860(0)	540.64	P12H2	5.33	1.288(1)	542.63
S8P17	-.03	Null		P5H37	1.18	8.143(0)	540.98	P12H3	5.43	Null	Null
S8P19	-.03	Null		P5H36	1.39	8.516(0)	540.87	P12H4	5.53	1.126(1)	544.36
S8P25	-.03	2.203(-1)		P5H35	1.59	7.758(0)	540.64	P12H5	5.63	1.150(1)	544.46
S8P26	-.03	2.158(-1)		P5H34	1.80	7.156(0)	539.92	P12H6	5.72	1.039(1)	543.14
S8P27	-.03	Null		P5H33	2.00	7.840(0)	540.58	P12H7	5.82	1.339(1)	545.47
S8P28	-.03	Null		P5H32	2.15	6.789(0)	540.15	P12H8	5.92	1.921(1)	548.59
P5P9	.43	3.694(-1)		P5H31	2.24	7.872(0)	540.97	P12H9	6.02	2.220(1)	549.87
P5P24	.56	3.002(-1)		P5H30	2.34	7.565(0)	540.61	P12H10	6.12	2.746(1)	553.18
P5P8	.94	8.872(-1)		P5H29	2.43	Null		P12H11	6.21	Null	Null
P5P23	1.02	5.952(-1)		P5H28	2.53	7.537(0)	540.45	P12H12	6.30	3.093(1)	555.13
P5P7	1.45	7.885(-1)		P5H27	2.63	7.490(0)	540.33	P12H13	6.39	3.917(1)	560.74
P5P22	1.53	6.435(-1)		P5H26	2.72	7.609(0)	540.58	P12H14	6.48	3.910(1)	561.52
P5P21	2.04	6.589(-1)		P5H25	2.82	7.749(0)	540.68	P12H15	6.56	4.010(1)	563.48
P5P5	2.72	8.877(-1)		P5H24	2.91	7.092(0)	539.97	P12H16	6.66	4.435(1)	566.90
P5P18	2.79	8.175(-1)		P5H23	3.02	7.517(0)	540.43	P12H17	6.74	4.891(1)	571.09
P5P4	3.23	7.906(-1)		P5H22	3.14	Null		P12H18	6.84	4.993(1)	572.02
P5P16	3.31	8.972(-1)		P5H21	3.23	7.478(0)	540.28	P12H19	6.93	5.151(1)	573.84
P5P3	3.73	1.081(0)		P5H20	3.33	7.417(0)	540.18	P12H20	7.02	5.033(1)	573.52
P5P14	3.87	8.989(-1)		P5H19	3.43	7.574(0)	540.30	P12H22	8.01	7.857(1)	601.91
P5P2	4.24	Null		P5H18	3.53	7.585(0)	540.43	P12H23	8.66	8.657(1)	613.24
P5P12	4.34	7.382(-1)		P5H17	3.62	7.372(0)	540.11	P12H25	9.92	9.515(1)	628.54
P5P1	4.76	8.053(-1)		P5H16	3.72	7.045(0)	539.89	P12H26	10.57	9.075(1)	627.15
P5P10	4.85	1.020(0)		P5H15	3.82	6.901(0)	539.75	P12H28	11.85	8.824(1)	627.32
P12P1	5.47	Null		P5H14	3.92	7.110(0)	540.09	P12H29	12.49	8.720(1)	627.99
P12P8	9.95	1.278(1)		P5H13	4.01	7.571(0)	540.34	P12H31	13.78	7.834(1)	619.19
P12P10	11.23	Null		P5H12	4.09	6.945(0)	539.54	P12H33	15.06	6.339(1)	604.58
P12P13	13.15	1.339(1)		P5H11	4.14	6.682(0)	539.33	P12H35	16.33	4.771(1)	587.14
P12P16	15.07	9.673(0)		P5H10	4.22	7.199(0)	540.10				

Run 39 Reduced Data Tabulation

C-3.

Gauge Label	Loc. (in)	Value (PSIA) or (BTU/Ft ² -Sec)	T Surf (DegR)	Gauge Label	Loc. (in)	Value (PSIA) or (BTU/Ft ² -Sec)	T Surf (DegR)	Gauge Label	Loc. (in)	Value (PSIA) or (BTU/Ft ² -Sec)	T Surf (DegR)
L28P1	-26.28	1.160(0)		P5S4	2.89	Null		P5H9	4.31	4.604(0)	537.69
L28P3	-18.28	1.449(0)		P5S2	4.25	Null		P5H8	4.40	4.768(0)	537.74
L28P5	-10.28	1.917(0)		L28H3	-27.28	1.640(1)	553.29	P5H7	4.50	5.155(0)	538.07
S8P2	-1.98	Null		L28H6	-24.28	Null		P5H6	4.59	5.286(0)	538.29
S8P3	-1.98	Null		L28H11	-18.28	1.227(1)	548.33	P5H5	4.69	5.520(0)	538.54
S8P6	-1.67	Null		L28H13	-15.28	1.190(1)	547.48	P5H4	4.79	5.640(0)	538.82
S8P7	-1.67	Null		L28H18	-9.28	1.135(1)	546.60	P5H3	4.89	5.938(0)	539.10
S8P8	-1.67	Null		PSH42	.13	Null		P5H2	4.98	6.234(0)	539.30
S8P9	-1.67	Null		PSH41	.32	-6.630(-1)	531.73	P5H1	5.08	6.773(0)	539.63
S8P10	-1.67	Null		PSH40	.52	-8.492(-2)	532.83	P12H1	5.24	5.730(0)	539.56
S8P13	-.98	Null		PSH39	.72	1.808(-2)	533.17	P12H2	5.33	6.621(0)	539.30
S8P17	-.03	Null		PSH37	1.18	-2.262(0)	530.95	P12H3	5.43	Null	Null
S8P19	-.03	Null		PSH36	1.39	-1.204(0)	531.77	P12H4	5.53	1.006(1)	541.94
S8P25	-.03	1.172(0)		PSH35	1.59	-1.400(0)	531.62	P12H5	5.63	1.179(1)	543.06
S8P26	-.03	1.075(0)		PSH34	1.80	9.022(-1)	532.13	P12H6	5.72	1.182(1)	542.77
S8P27	-.03	Null		PSH33	2.00	-5.854(-1)	532.51	P12H7	5.82	1.653(1)	545.54
S8P28	-.03	Null		PSH32	2.15	-1.389(-1)	532.76	P12H8	5.92	1.986(1)	548.14
P5P9	.43	3.386(-1)		PSH31	2.24	-3.004(-1)	532.88	P12H9	6.02	2.133(1)	549.10
P5P24	.56	3.348(-1)		PSH30	2.34	-1.707(-1)	532.97	P12H10	6.12	2.497(1)	551.46
P5P8	.94	1.028(0)		PSH29	2.43	9.119(-2)	533.27	P12H11	6.21	Null	Null
P5P23	1.02	7.628(-1)		PSH28	2.53	8.753(-1)	533.44	P12H12	6.30	2.399(1)	551.58
P5P7	1.45	9.445(-1)		PSH27	2.63	1.507(0)	533.76	P12H13	6.39	2.994(1)	555.82
P5P22	1.53	7.240(-1)		PSH26	2.72	2.205(0)	534.16	P12H14	6.48	3.136(1)	557.07
P5P21	2.04	7.510(-1)		PSH25	2.82	2.666(0)	534.60	P12H15	6.56	3.201(1)	558.23
P5P5	2.72	2.003(0)		PSH24	2.91	2.878(0)	534.97	P12H16	6.66	3.405(1)	559.87
P5P18	2.79	2.222(0)		PSH23	3.02	3.227(0)	535.30	P12H17	6.74	3.876(1)	563.29
P5P4	3.23	2.341(0)		PSH22	3.14	3.113(0)	535.51	P12H18	6.84	4.056(1)	564.70
P5P16	3.31	2.612(0)		PSH21	3.23	3.467(0)	535.76	P12H19	6.93	4.102(1)	565.92
P5P3	3.73	2.537(0)		PSH20	3.33	2.674(0)	535.73	P12H20	7.02	4.001(1)	565.77
P5P14	3.87	2.754(0)		PSH19	3.43	3.717(0)	536.28	P12H22	8.01	6.766(1)	592.56
P5P2	4.24	Null		PSH18	3.53	4.107(0)	536.50	P12H23	8.66	7.994(1)	606.92
P5P12	4.34	2.304(0)		PSH17	3.62	3.848(0)	536.50	P12H25	9.92	9.411(1)	627.34
P5P1	4.76	2.385(0)		PSH16	3.72	3.515(0)	536.48	P12H26	10.57	9.201(1)	627.88
P5P10	4.85	2.624(0)		PSH15	3.82	3.671(0)	536.65	P12H28	11.85	9.140(1)	630.62
P12P1	5.47	2.703(0)		PSH14	3.92	4.118(0)	536.93	P12H29	12.49	9.205(1)	632.28
P12P8	9.95	1.250(1)		PSH13	4.01	Null		P12H31	13.78	8.394(1)	624.60
P12P10	11.23	Null		PSH12	4.09	4.445(0)	537.09	P12H33	15.06	6.804(1)	609.47
P12P13	13.15	1.359(1)		PSH11	4.14	4.279(0)	537.26	P12H35	16.33	5.035(1)	591.41
P12P16	15.07	9.668(0)		PSH10	4.22	4.106(0)	537.45				

Run 40 Reduced Data Tabulation

Gauge Label	Loc. (in)	Value (PSIA) or (BTU/Ft ² -Sec)	T Surf (DegR)	Gauge Label	Loc. (in)	Value (PSIA) or (BTU/Ft ² -Sec)	T Surf (DegR)	Gauge Label	Loc. (in)	Value (PSIA) or (BTU/Ft ² -Sec)	T Surf (DegR)
L28P1	-26.28	1.105(0)		P5S4	2.89	Null		P5H9	4.31	2.645(0)	537.61
L28P3	-18.28	1.413(0)		P5S2	4.25	Null		P5H8	4.40	2.767(0)	537.69
L28P5	-10.28	Null		L28H3	-27.28	1.578(1)	554.12	P5H7	4.50	3.020(0)	537.93
S8P2	-1.98	Null		L28H6	-24.28	1.179(1)	545.88	P5H6	4.59	3.094(0)	537.98
S8P3	-1.98	Null		L28H11	-18.28	1.213(1)	550.16	P5H5	4.69	3.194(0)	538.13
S8P6	-1.67	Null		L28H13	-15.28	1.193(1)	549.21	P5H4	4.79	3.361(0)	538.32
S8P7	-1.67	Null		L28H18	-9.28	1.133(1)	548.70	P5H3	4.89	3.646(0)	538.49
S8P8	-1.67	Null		PSH42	.13	Null		P5H2	4.98	3.823(0)	538.68
S8P9	-1.67	Null		PSH41	.32	-1.944(0)	532.51	P5H1	5.08	4.695(0)	539.10
S8P10	-1.67	Null		P5H40	.52	-3.537(-1)	534.31	P12H1	5.24	2.991(0)	538.04
S8P13	-.98	Null		PSH39	.72	-4.486(-2)	534.96	P12H2	5.33	3.550(0)	538.39
S8P17	-.03	Null		PSH37	1.18	-3.039(-1)	535.20	P12H3	5.43	Null	Null
S8P19	-.03	Null		PSH36	1.39	-1.057(0)	534.21	P12H4	5.53	5.347(0)	540.03
S8P25	-.03	2.181(0)		PSH35	1.59	-1.653(0)	533.45	P12H5	5.63	6.262(0)	540.75
S8P26	-.03	1.947(0)		PSH34	1.80	-1.573(0)	533.59	P12H6	5.72	5.955(0)	540.40
S8P27	-.03	Null		PSH33	2.00	-1.376(0)	533.77	P12H7	5.82	7.217(0)	541.50
S8P28	-.03	Null		PSH32	2.15	-1.287(0)	533.92	P12H8	5.92	8.709(0)	542.80
P5P9	.43	1.750(-1)		PSH31	2.24	-1.205(0)	533.98	P12H9	6.02	8.825(0)	543.12
P5P24	.56	2.888(-1)		PSH30	2.34	-1.040(0)	534.08	P12H10	6.12	1.069(1)	544.35
P5P8	.94	1.151(0)		PSH29	2.43	-5.986(-1)	534.64	P12H11	6.21	Null	Null
P5P23	1.02	7.208(-1)		PSH28	2.53	-8.331(-1)	534.26	P12H12	6.30	1.113(1)	544.79
P5P7	1.45	9.979(-1)		PSH27	2.63	-7.715(-1)	534.35	P12H13	6.39	1.343(1)	547.02
P5P22	1.53	8.077(-1)		PSH26	2.72	-5.999(-1)	534.36	P12H14	6.48	1.438(1)	547.92
P5P21	2.04	7.713(-1)		PSH25	2.82	-2.358(-1)	534.54	P12H15	6.56	1.510(1)	548.82
P5P5	2.72	1.161(0)		PSH24	2.91	1.465(-1)	534.77	P12H16	6.66	1.735(1)	550.38
P5P18	2.79	1.469(0)		PSH23	3.02	6.508(-1)	534.99	P12H17	6.74	1.495(1)	547.80
P5P4	3.23	2.539(0)		PSH22	3.14	7.543(-1)	535.21	P12H18	6.84	2.147(1)	553.76
P5P16	3.31	2.966(0)		PSH21	3.23	9.341(-1)	535.51	P12H19	6.93	2.186(1)	554.37
P5P3	3.73	3.006(0)		PSH20	3.33	1.075(0)	535.76	P12H20	7.02	2.148(1)	554.44
P5P14	3.87	3.232(0)		PSH19	3.43	1.406(0)	535.92	P12H22	8.01	4.042(1)	573.36
P5P2	4.24	Null		PSH18	3.53	1.590(0)	536.10	P12H23	8.66	5.768(1)	588.31
P5P12	4.34	2.766(0)		PSH17	3.62	1.779(0)	536.28	P12H25	9.92	8.125(1)	614.24
P5P1	4.76	2.879(0)		PSH16	3.72	1.912(0)	536.39	P12H26	10.57	8.235(1)	618.47
P5P10	4.85	3.243(0)		PSH15	3.82	1.850(0)	536.63	P12H28	11.85	8.424(1)	623.93
P12P1	5.47	2.729(0)		PSH14	3.92	1.928(0)	536.82	P12H29	12.49	8.603(1)	626.99
P12P8	5.95	1.248(1)		PSH13	4.01	2.409(0)	537.05	P12H31	13.78	7.905(1)	621.13
P12P10	11.23	Null		PSH12	4.09	2.319(0)	537.03	P12H33	15.06	6.540(1)	608.28
P12P13	13.15	1.359(1)		PSH11	4.14	2.362(0)	537.22	P12H35	16.33	4.833(1)	591.47
P12P16	15.07	9.741(0)		PSH10	4.22	2.320(0)	537.29				

Run 41 Reduced Data Tabulation

Gauge Label	Loc. (in)	Value (PSIA) or (BTU/Ft ² -Sec)	T Surf (DegR)	Gauge Label	Loc. (in)	Value (PSIA) or (BTU/Ft ² -Sec)	T Surf (DegR)	Gauge Label	Loc. (in)	Value (PSIA) or (BTU/Ft ² -Sec)	T Surf (DegR)
L28P1	-26.28	8.345(-1)		P12P8	9.95	9.354(-1)		P5H11	4.14	8.194(0)	542.29
L28P3	-18.28	1.456(0)		P12P13	13.15	1.053(0)		P5H10	4.22	8.769(0)	543.10
L28P5	-10.28	1.046(0)		P12P16	15.07	1.235(0)		P5H9	4.31	8.744(0)	542.95
S12P2	-1.90	Null		P5S4	2.89	Null		P5H8	4.40	8.552(0)	542.97
S12P3	-1.90	Null		P5S2	4.25	Null		P5H7	4.50	8.882(0)	543.26
S12P4	-1.90	Null		L28H3	-27.28	1.762(1)	553.55	P5H6	4.59	8.466(0)	542.80
S12P7	-1.60	Null		L28H6	-24.28	1.562(1)	551.73	P5H5	4.69	8.689(0)	543.07
S12P8	-1.60	Null		L28H11	-18.28	1.286(1)	548.55	P5H4	4.79	8.840(0)	542.89
S12P9	-1.60	Null		L28H13	-15.28	1.363(1)	548.47	P5H3	4.89	8.522(0)	542.82
S12P10	-1.60	Null		L28H18	-9.28	1.161(1)	546.74	P5H2	4.98	8.624(0)	542.89
S12P13	-.98	Null		P5H42	.13	Null		P5H1	5.08	5.881(0)	539.84
S12P17	-.03	2.165(-1)		P5H41	.32	4.577(0)	541.76	P12H1	5.24	9.903(0)	544.17
S12P19	-.03	Null		P5H40	.52	1.059(0)	545.84	P12H2	5.33	Null	Null
S12P25	-.03	2.835(-1)		P5H39	.72	1.100(1)	545.14	P12H3	5.43	8.692(0)	542.87
S12P26	-.03	2.915(-1)		P5H37	1.18	9.382(0)	543.43	P12H4	5.53	8.773(0)	542.82
S12P27	-.03	2.739(-1)		P5H36	1.39	7.741(0)	541.92	P12H5	5.63	8.729(0)	542.80
S12P28	-.03	Null		P5H35	1.59	9.469(0)	543.67	P12H6	5.72	8.814(0)	542.76
P5P9	.43	6.343(-1)		P5H34	1.80	9.033(0)	543.30	P12H7	5.82	8.335(0)	542.29
P5P24	.56	6.409(-1)		P5H33	2.00	9.142(0)	543.34	P12H8	5.92	9.048(0)	543.25
P5P8	.94	1.073(0)		P5H32	2.15	8.758(0)	542.91	P12H9	6.02	8.773(0)	542.78
P5P23	1.02	7.756(-1)		P5H31	2.24	9.523(0)	543.65	P12H10	6.12	8.856(0)	543.01
P5P7	1.45	9.751(-1)		P5H30	2.34	9.166(0)	543.39	P12H12	6.30	7.272(0)	541.14
P5P22	1.53	8.023(-1)		P5H29	2.43	Null		P12H13	6.39	8.656(0)	542.67
P5P21	2.04	8.062(-1)		P5H28	2.53	8.690(0)	543.18	P12H14	6.48	8.572(0)	542.44
P5P5	2.72	1.025(0)		P5H27	2.63	8.958(0)	543.06	P12H15	6.56	8.698(0)	542.48
P5P18	2.79	Null		P5H26	2.72	9.292(0)	543.39	P12H16	6.66	8.635(0)	542.52
P5P4	3.23	9.439(-1)		P5H25	2.82	9.404(0)	543.53	P12H17	6.74	Null	Null
P5P16	3.31	1.048(0)		P5H24	2.91	8.546(0)	542.61	P12H18	6.84	8.703(0)	542.79
P5P3	3.73	1.053(0)		P5H23	3.02	8.806(0)	543.19	P12H19	6.93	8.649(0)	542.65
P5P14	3.87	1.049(0)		P5H22	3.14	9.577(0)	543.89	P12H20	7.02	8.294(0)	542.18
P5P12	4.34	8.781(-1)		P5H21	3.23	8.607(0)	543.01	P12H22	8.01	9.079(0)	543.28
P5P1	4.76	9.735(-1)		P5H20	3.33	8.540(0)	542.87	P12H23	8.66	9.672(0)	543.68
P5P10	4.85	1.059(0)		P5H19	3.43	8.462(0)	542.49	P12H25	9.92	9.485(0)	543.51
P12P1	5.47	Null		P5H18	3.53	8.272(0)	542.40	P12H26	10.57	9.300(0)	543.23
P12P2	6.11	1.004(0)		P5H17	3.62	8.601(0)	542.82	P12H28	11.85	Null	Null
P12P3	6.76	1.070(0)		P5H16	3.72	Null		P12H29	12.49	9.633(0)	543.60
P12P4	7.39	8.721(-1)		P5H15	3.82	8.213(0)	542.37	P12H31	13.78	8.223(0)	542.05
P12P5	8.03	1.006(0)		P5H14	3.92	8.148(0)	542.24	P12H33	15.06	9.491(0)	543.40
P12P6	8.68	9.743(-1)		P5H13	4.01	8.951(0)	543.02	P12H35	16.33	9.483(0)	543.43
P12P7	9.31	1.092(0)		P5H12	4.09	7.878(0)	542.10				

Run 43 Reduced Data Tabulation

Gauge Label	Loc. (in)	Value (PSIA) or (BTU/Ft ² -Sec)	T Surf (DegR)	Gauge Label	Loc. (in)	Value (PSIA) or (BTU/Ft ² -Sec)	T Surf (DegR)	Gauge Label	Loc. (in)	Value (PSIA) or (BTU/Ft ² -Sec)	T Surf (DegR)
L28P1	-26.28	5.908(-1)		P12P8	9.95	9.445(-1)		P5H11	4.14	1.072(0)	533.84
L28P3	-18.28	1.420(0)		P12P13	13.15	1.134(0)		P5H10	4.22	1.074(0)	533.90
L28P5	-10.28	3.470(-1)		P12P16	15.07	1.217(0)		P5H9	4.31	1.041(0)	533.95
S12P2	-1.90	Null		P5S4	2.89	Null		P5H8	4.40	9.860(-1)	533.99
S12P3	-1.90	Null		P5S2	4.25	Null		P5H7	4.50	1.130(0)	534.08
S12P4	-1.90	Null		L28H3	-27.28	1.753(1)	553.98	P5H6	4.59	1.160(0)	534.07
S12P7	-1.60	Null		L28H6	-24.28	1.590(1)	552.14	P5H5	4.69	1.277(0)	534.15
S12P8	-1.60	Null		L28H11	-18.28	1.313(1)	549.01	P5H4	4.79	1.126(0)	534.11
S12P9	-1.60	Null		L28H13	-15.28	1.368(1)	548.68	P5H3	4.89	1.178(0)	534.15
S12P10	-1.60	Null		L28H18	-9.28	1.208(1)	547.30	P5H2	4.98	1.289(0)	534.30
S12P13	-.98	Null		P5H42	.13	Null		P5H1	5.08	1.556(0)	534.37
S12P17	-.03	8.209(-1)		P5H41	.32	-3.758(-1)	531.74	P12H1	5.24	1.733(0)	534.74
S12P19	-.03	Null		P5H40	.52	-4.255(-1)	531.83	P12H2	5.33	1.676(0)	534.80
S12P25	-.03	8.450(-1)		P5H39	.72	-1.120(0)	531.41	P12H3	5.43	1.526(0)	534.51
S12P26	-.03	8.499(-1)		P5H37	1.18	-1.359(0)	531.15	P12H4	5.53	1.597(0)	534.53
S12P27	-.03	7.605(-1)		P5H36	1.39	-9.931(-1)	532.00	P12H5	5.63	1.300(0)	534.23
S12P28	-.03	Null		P5H35	1.59	-1.104(0)	531.60	P12H6	5.72	1.584(0)	534.56
P5P9	.43	7.206(-1)		P5H34	1.80	-7.798(-1)	531.83	P12H7	5.82	1.369(0)	534.48
P5P24	.56	8.606(-1)		P5H33	2.00	-6.608(-1)	532.09	P12H8	5.92	1.711(0)	534.72
P5P8	.94	1.195(0)		P5H32	2.15	-4.830(-1)	532.33	P12H9	6.02	1.625(0)	534.68
P5P23	1.02	8.831(-1)		P5H31	2.24	-2.858(-1)	532.44	P12H10	6.12	1.521(0)	534.65
P5P7	1.45	1.076(0)		P5H30	2.34	-1.393(-1)	532.62	P12H12	6.30	1.342(0)	534.38
P5P22	1.53	8.736(-1)		P5H29	2.43	-2.514(-2)	532.78	P12H13	6.39	1.685(0)	534.72
P5P21	2.04	9.013(-1)		P5H28	2.53	-2.136(-1)	532.92	P12H14	6.48	1.533(0)	534.72
P5P5	2.72	1.144(0)		P5H27	2.63	-1.318(-1)	532.89	P12H15	6.56	1.824(0)	534.81
P5P18	2.79	Null		P5H26	2.72	-4.418(-1)	533.06	P12H16	6.66	1.861(0)	534.87
P5P4	3.23	1.013(0)		P5H25	2.82	-3.952(-1)	533.08	P12H17	6.74	Null	Null
P5P16	3.31	1.157(0)		P5H24	2.91	-5.674(-1)	533.18	P12H18	6.84	1.948(0)	535.00
P5P3	3.73	1.110(0)		P5H23	3.02	-4.824(-1)	533.22	P12H19	6.93	1.900(0)	535.01
P5P14	3.87	1.175(0)		P5H22	3.14	-1.461(-1)	533.01	P12H20	7.02	1.807(0)	534.87
P5P12	4.34	9.701(-1)		P5H21	3.23	-2.831(-1)	533.41	P12H22	8.01	2.337(0)	535.49
P5P1	4.76	9.629(-1)		P5H20	3.33	-6.062(-1)	533.35	P12H23	8.66	2.545(0)	535.80
P5P10	4.85	1.180(0)		P5H19	3.43	-5.918(-1)	533.47	P12H25	9.92	2.869(0)	536.14
P12P1	5.47	Null		P5H18	3.53	-4.880(-1)	533.37	P12H26	10.57	2.972(0)	536.25
P12P2	6.11	1.042(0)		P5H17	3.62	-8.189(-1)	533.57	P12H28	11.85	Null	Null
P12P3	6.76	1.096(0)		P5H16	3.72	Null		P12H29	12.49	3.771(0)	537.13
P12P4	7.39	8.994(-1)		P5H15	3.82	7.262(-1)	533.63	P12H31	13.78	3.627(0)	536.90
P12P5	8.03	Null		P5H14	3.92	8.030(-1)	533.68	P12H33	15.06	4.541(0)	537.79
P12P6	8.68	9.996(-1)		P5H13	4.01	1.060(0)	533.75	P12H35	16.33	4.657(0)	538.12
P12P7	9.31	1.122(0)		P5H12	4.09	7.788(-1)	533.62				

Run 44 Reduced Data Tabulation

Gauge Label	Loc. (in)	Value (PSIA) or (BTU/Ft ² -Sec)	T Surf (DegR)	Gauge Label	Loc. (in)	Value (PSIA) or (BTU/Ft ² -Sec)	T Surf (DegR)	Gauge Label	Loc. (in)	Value (PSIA) or (BTU/Ft ² -Sec)	T Surf (DegR)
L2BP1	-26.28	2.484(-1)	P12P8	9.95	9.135(-1)	P5H11	4.14	2.416(-1)	534.54		
L2BP3	-18.28	1.388(0)	P12P13	13.15	1.031(0)	P5H10	4.22	2.662(-1)	534.63		
L2BP5	-10.28	1.032(0)	P12P16	15.07	1.165(0)	P5H9	4.31	Null	Null		
S12P2	-1.90	Null	P5S4	2.89	Null	P5H8	4.40	4.699(-1)	534.70		
S12P3	-1.90	Null	P5S2	4.25	Null	P5H7	4.50	4.720(-1)	534.71		
S12P4	-1.90	Null	L2BH3	-27.28	1.666(1)	P5H6	4.59	5.042(-1)	534.70		
S12P7	-1.60	Null	L2BH6	-24.28	1.499(1)	P5H5	4.69	4.711(-1)	534.76		
S12P8	-1.60	Null	L2BH11	-18.28	1.238(1)	P5H4	4.79	5.792(-1)	534.84		
S12P9	-1.60	Null	L2BH13	-15.28	1.303(1)	P5H3	4.89	4.319(-1)	534.77		
S12P10	-1.60	Null	L2BH18	-9.28	1.134(1)	P5H2	4.98	6.742(-1)	534.99		
S12P13	.98	Null	P5H42	.13	Null	P5H1	5.08	1.001(0)	535.19		
S12P17	.03	1.081(0)	P5H41	.32	-5.227(-1)	P12H1	5.24	8.008(-1)	535.15		
S12P19	.03	Null	P5H40	.52	-8.079(-1)	P12H2	5.33	7.904(-1)	535.05		
S12P25	.03	1.042(0)	P5H39	.72	-8.722(-1)	P12H3	5.43	Null	Null		
S12P26	.03	1.072(0)	P5H37	1.18	-1.002(0)	P12H4	5.53	8.496(-1)	535.10		
S12P27	.03	9.718(-1)	P5H36	1.39	-5.658(-1)	P12H5	5.63	6.686(-1)	534.93		
S12P28	.03	Null	P5H35	1.59	-1.230(0)	P12H6	5.72	7.622(-1)	535.11		
P5P9	.43	7.094(-1)	P5H34	1.80	-9.930(-1)	P12H7	5.82	5.808(-1)	535.05		
P5P24	.56	9.154(-1)	P5H33	2.00	-1.129(0)	P12H8	5.92	8.819(-1)	535.22		
P5P8	.94	1.189(0)	P5H32	2.15	-8.912(-1)	P12H9	6.02	9.417(-1)	535.25		
P5P23	1.02	8.520(-1)	P5H31	2.24	-9.056(-1)	P12H10	6.12	8.219(-1)	535.21		
P5P7	1.45	1.056(0)	P5H30	2.34	-7.258(-1)	P12H12	6.30	5.320(-1)	535.07		
P5P22	1.53	Null	P5H29	2.43	-1.429(1)	P12H13	6.39	8.562(-1)	535.30		
P5P21	2.04	Null	P5H28	2.53	-5.513(-1)	P12H14	6.48	8.897(-1)	535.28		
P5P5	2.72	1.135(0)	P5H27	2.63	-4.420(-1)	P12H15	6.56	1.011(0)	535.35		
P5P10	2.79	Null	P5H26	2.72	-2.636(-1)	P12H16	6.66	1.117(0)	535.42		
P5P4	3.23	1.057(0)	P5H25	2.82	-6.406(-1)	P12H17	6.74	Null	Null		
P5P16	3.31	1.151(0)	P5H24	2.91	-2.650(-1)	P12H18	6.84	1.213(0)	535.51		
P5P3	3.73	1.107(0)	P5H23	3.02	-3.888(-1)	P12H19	6.93	1.145(0)	535.48		
P5P14	3.87	1.169(0)	P5H22	3.14	Null	P12H20	7.02	1.106(0)	535.43		
P5P12	4.34	9.752(-1)	P5H21	3.23	2.378(-1)	P12H22	8.01	1.379(0)	535.78		
P5P1	4.76	9.649(-1)	P5H20	3.33	-5.847(-2)	P12H23	8.66	1.587(0)	535.98		
P5P10	4.85	1.164(0)	P5H19	3.43	7.308(-2)	P12H25	9.92	1.724(0)	536.16		
P12P1	5.47	Null	P5H18	3.53	1.280(-2)	P12H26	10.57	1.807(0)	536.25		
P12P2	6.11	1.018(0)	P5H17	3.62	3.421(-2)	P12H28	11.85	Null	Null		
P12P3	6.76	1.050(0)	P5H16	3.72	Null	P12H29	12.49	2.139(0)	536.70		
P12P4	7.39	8.687(-1)	P5H15	3.82	1.140(-1)	P12H31	13.78	2.340(0)	536.72		
P12P5	8.03	1.009(0)	P5H14	3.92	1.276(-1)	P12H33	15.06	2.676(0)	537.11		
P12P6	8.68	9.784(-1)	P5H13	4.01	3.213(-1)	P12H35	16.33	2.766(0)	537.27		
P12P7	9.31	1.032(0)	P5H12	4.09	1.351(-1)	P5H12	534.38				

Run 45 Reduced Data Tabulation

Gauge Label	Loc. (in)	Value (PSIA) or (BTU/Ft ² -Sec)	T Surf (DegR)	Gauge Label	Loc. (in)	Value (PSIA) or (BTU/Ft ² -Sec)	T Surf (DegR)	Gauge Label	Loc. (in)	Value (PSIA) or (BTU/Ft ² -Sec)	T Surf (DegR)
L2BP1	-26.28	-6.915(-2)	P12P8	9.95	9.739(-1)	P5H11	4.14	-2.263(-1)	534.40		
L2BP3	-18.28	1.425(0)	P12P13	13.15	1.182(0)	P5H10	4.22	-3.926(-1)	534.32		
L2BP5	-10.28	2.731(0)	P12P16	15.07	1.248(0)	P5H9	4.31	Null	Null		
S12P2	-1.90	Null	P5S4	2.89	Null	P5H8	4.40	-1.885(-1)	534.39		
S12P3	-1.90	Null	P5S2	4.25	Null	P5H7	4.50	-3.655(-1)	534.36		
S12P4	-1.90	Null	L2BH3	-27.28	1.697(1)	P5H6	4.59	-2.542(-1)	534.43		
S12P7	-1.60	Null	L2BH6	-24.28	1.587(1)	P5H5	4.69	-2.989(-1)	534.48		
S12P8	-1.60	Null	L2BH11	-18.28	1.310(1)	P5H4	4.79	-2.549(-1)	534.41		
S12P9	-1.60	Null	L2BH13	-15.28	1.335(1)	P5H3	4.89	-3.286(-1)	534.52		
S12P10	-1.60	Null	L2BH18	-9.28	1.216(1)	P5H2	4.98	4.784(-2)	534.79		
S12P13	.98	Null	P5H42	.13	Null	P5H1	5.08	3.425(-1)	535.52		
S12P17	.03	1.588(0)	P5H41	.32	-1.712(0)	P12H1	5.24	-3.294(-1)	534.46		
S12P19	.03	Null	P5H40	.52	-1.142(0)	P12H2	5.33	-1.646(-1)	534.52		
S12P25	.03	1.490(0)	P5H39	.72	-8.496(-1)	P12H3	5.43	-1.236(-1)	534.54		
S12P26	.03	1.480(0)	P5H37	1.18	-1.156(0)	P12H4	5.53	-1.819(-1)	534.55		
S12P27	.03	1.433(0)	P5H36	1.39	-6.812(-1)	P12H5	5.63	-1.563(-1)	534.61		
S12P28	.03	Null	P5H35	1.59	-1.084(0)	P12H6	5.72	-1.409(-1)	534.65		
P5P9	.43	7.713(-1)	P5H34	1.80	-1.134(0)	P12H7	5.82	-2.577(-2)	534.73		
P5P24	.56	1.093(0)	P5H33	2.00	-1.160(0)	P12H8	5.92	3.185(-2)	534.77		
P5P8	.94	1.287(0)	P5H32	2.15	-9.455(-1)	P12H9	6.02	7.381(-3)	534.76		
P5P23	1.02	9.435(-1)	P5H31	2.24	-8.104(-1)	P12H10	6.12	2.050(-1)	534.83		
P5P7	1.45	1.129(0)	P5H30	2.34	-7.629(-1)	P12H12	6.30	4.427(-2)	534.84		
P5P22	1.53	9.347(-1)	P5H29	2.43	-2.247(-1)	P12H13	6.39	2.474(-1)	534.98		
P5P21	2.04	9.532(-1)	P5H28	2.53	-4.949(-1)	P12H14	6.48	2.508(-1)	535.01		
P5P5	2.72	1.220(0)	P5H27	2.63	-5.540(-1)	P12H15	6.56	3.137(-1)	535.00		
P5P10	2.79	Null	P5H26	2.72	-5.875(-1)	P12H16	6.66	3.789(-1)	535.08		
P5P4	3.23	1.108(0)	P5H25	2.82	-7.116(-1)	P12H17	6.74	4.792(-2)	534.77		
P5P16	3.31	1.235(0)	P5H24	2.91	-4.525(-1)	P12H18	6.84	4.235(-1)	535.16		
P5P3	3.73	1.174(0)	P5H23	3.02	-5.764(-1)	P12H19	6.93	3.333(-1)	535.16		
P5P14	3.87	1.245(0)	P5H22	3.14	-2.851(-1)	P12H20	7.02	3.031(-1)	535.13		
P5P12	4.34	1.005(0)	P5H21	3.23	-6.624(-1)	P12H22	8.01	4.628(-1)	535.35		
P5P1	4.76	9.483(-1)	P5H20	3.33	-7.270(-1)	P12H23	8.66	8.349(-1)	535.60		
P5P10	4.85	1.229(0)	P5H19	3.43	-5.259(-1)	P12H25	9.92	9.769(-1)	535.76		
P12P1	5.47	Null	P5H18	3.53	-4.668(-1)	P12H26	10.57	9.802(-1)	535.81		
P12P2	6.11	1.090(0)	P5H17	3.62	-6.540(-1)	P12H28	11.85	1.229(0)	536.09		
P12P3	6.76	1.163(0)	P5H16	3.72	Null	P12H29	12.49	1.311(0)	536.18		
P12P4	7.39	9.246(-1)	P5H15	3.82	-5.693(-1)	P12H31	13.78	1.292(0)	536.17		
P12P5	8.03	1.110(0)	P5H14	3.92	-5.265(-1)	P12H33	15.06	1.490(0)	536.44		
P12P6	8.68	1.083(0)	P5H13	4.01	-1.839(-1)	P12H35	16.33	1.640(0)	536.61		
P12P7	9.31	1.156(0)	P5H12	4.09	-5.819(-1)	P5H12	534.13				

Run 46 Reduced Data Tabulation

Gauge Label	Loc. (in)	Value (PSIA) or (BTU/Ft ² -Sec)	T Surf (DegR)	Gauge Label	Loc. (in)	Value (PSIA) or (BTU/Ft ² -Sec)	T Surf (DegR)	Gauge Label	Loc. (in)	Value (PSIA) or (BTU/Ft ² -Sec)	T Surf (DegR)
L28P1	-26.28	-2.626(-1)		P12P8	9.95	9.806(-1)		P5H11	4.14	-5.260(-1)	531.73
L28P3	-18.28	1.386(0)		P12P13	13.15	1.163(0)		P5H10	4.22	-7.483(-1)	531.61
L28P5	-10.28	Null		P12P16	15.07	1.237(0)		P5H9	4.31	Null	Null
S12P2	-1.90	Null		P5S4	2.89	Null		P5H8	4.40	-6.154(-1)	531.70
S12P3	-1.90	Null		P5S2	4.25	Null		P5H7	4.50	-6.205(-1)	531.65
S12P4	-1.90	Null		L28H3	-27.28	1.695(1)	552.82	P5H6	4.59	-6.092(-1)	531.69
S12P7	-1.60	Null		L28H6	-24.28	1.562(1)	551.33	P5H5	4.69	-7.172(-1)	531.70
S12P8	-1.60	Null		L28H11	-18.28	1.348(1)	548.48	P5H4	4.79	-9.828(-1)	531.65
S12P9	-1.60	Null		L28H13	-15.28	1.420(1)	548.51	P5H3	4.89	-5.231(-1)	531.79
S12P10	-1.60	Null		L28H18	-9.28	1.216(1)	546.54	P5H2	4.98	-3.807(-1)	532.02
S12P13	-.98	Null		P5H42	.13	Null		P5H1	5.08	1.727(-1)	532.51
S12P17	-.03	2.023(0)		P5H41	.32	-2.528(0)	529.08	P12H1	5.24	-8.836(-1)	531.55
S12P19	-.03	Null		P5H40	.52	-6.614(-1)	531.17	P12H2	5.33	-5.644(-1)	531.62
S12P25	-.03	1.943(0)		P5H39	.72	-6.337(-1)	531.21	P12H3	5.43	-5.040(-1)	531.68
S12P26	-.03	1.891(0)		P5H37	1.18	-8.121(-1)	531.38	P12H4	5.53	-5.529(-1)	531.67
S12P27	-.03	1.918(0)		P5H36	1.39	-4.933(-1)	532.08	P12H5	5.63	-5.204(-1)	531.69
S12P28	-.03	Null		P5H35	1.59	-1.303(0)	531.18	P12H6	5.72	-4.836(-1)	531.74
P5P9	.43	6.953(-1)		P5H34	1.80	-8.059(-1)	531.29	P12H7	5.82	-5.666(-1)	531.81
P5P24	.56	7.988(-1)		P5H33	2.00	-1.011(0)	531.26	P12H8	5.92	-4.477(-1)	531.84
P5P8	.94	1.372(0)		P5H32	2.15	-9.962(-1)	531.36	P12H9	6.02	-4.659(-1)	531.85
P5P23	1.02	1.006(0)		P5H31	2.24	-9.772(-2)	532.19	P12H10	6.12	-4.720(-1)	531.83
P5P7	1.45	1.181(0)		P5H30	2.34	-1.035(0)	531.47	P12H12	6.30	-4.050(-1)	531.94
P5P22	1.53	9.613(-1)		P5H29	2.43	-1.100(-1)	532.08	P12H13	6.39	-3.118(-1)	532.10
P5P21	2.04	9.539(-1)		P5H28	2.53	-1.231(0)	531.27	P12H14	6.48	-3.775(-1)	532.04
P5P5	2.72	1.220(0)		P5H27	2.63	-6.158(-1)	531.47	P12H15	6.56	-3.060(-1)	532.05
P5P18	2.79	Null		P5H26	2.72	-7.652(-1)	531.50	P12H16	6.66	-2.228(-1)	532.11
P5P4	3.23	1.113(0)		P5H25	2.82	-8.339(-1)	531.42	P12H17	6.74	-1.350(-2)	532.27
P5P16	3.31	1.248(0)		P5H24	2.91	-8.084(-1)	531.49	P12H18	6.84	-4.257(-2)	532.22
P5P3	3.73	1.628(0)		P5H23	3.02	-7.609(-1)	531.51	P12H19	6.93	-9.299(-2)	532.22
P5P14	3.87	1.248(0)		P5H22	3.14	Null		P12H20	7.02	-4.506(-2)	532.26
P5P12	4.34	1.025(0)		P5H21	3.23	-1.150(0)	531.42	P12H22	8.01	-5.030(-2)	532.38
P5P1	4.76	9.611(-1)		P5H20	3.33	-1.006(0)	531.39	P12H23	8.66	2.169(-1)	532.62
P5P10	4.85	1.235(0)		P5H19	3.43	-8.835(-1)	531.43	P12H25	9.92	2.947(-1)	532.72
P12P1	5.47	Null		P5H18	3.53	-5.542(-1)	531.65	P12H26	10.57	4.123(-1)	532.82
P12P2	6.11	1.098(0)		P5H17	3.62	-6.786(-1)	531.53	P12H28	11.85	Null	Null
P12P3	6.76	1.156(0)		P5H16	3.72	-7.195(-1)	531.53	P12H29	12.49	7.284(-1)	533.19
P12P4	7.39	9.278(-1)		P5H15	3.82	-8.840(-1)	531.52	P12H31	13.78	7.234(-1)	533.15
P12P5	8.03	1.101(0)		P5H14	3.92	-7.068(-1)	531.55	P12H33	15.06	9.480(-1)	533.34
P12P6	8.68	1.053(0)		P5H13	4.01	Null		P12H35	16.33	1.067(0)	533.48
P12P7	9.31	1.160(0)		P5H12	4.09	-8.561(-1)	531.46				

Run 47 Reduced Data Tabulation

Gauge Label	Loc. (in)	Value (PSIA) or (BTU/Ft ² -Sec)	T Surf (DegR)	Gauge Label	Loc. (in)	Value (PSIA) or (BTU/Ft ² -Sec)	T Surf (DegR)	Gauge Label	Loc. (in)	Value (PSIA) or (BTU/Ft ² -Sec)	T Surf (DegR)
L28P1	-26.28	-5.176(-1)		P12P8	9.95	7.108(0)		P5H11	4.14	1.895(0)	535.56
L28P3	-18.28	1.350(0)		P12P13	13.15	8.631(0)		P5H10	4.22	1.883(0)	535.49
L28P5	-10.28	2.730(0)		P12P16	15.07	8.234(0)		P5H9	4.31	Null	Null
S12P2	-1.90	Null		P5S4	2.89	Null		P5H8	4.40	2.248(0)	536.10
S12P3	-1.90	Null		P5S2	4.25	Null		P5H6	4.59	2.725(0)	536.66
S12P4	-1.90	Null		L28H3	-27.28	1.585(1)	555.88	P5H5	4.69	2.762(0)	536.98
S12P7	-1.60	Null		L28H6	-24.28	1.420(1)	553.99	P5H4	4.79	3.117(0)	537.20
S12P8	-1.60	Null		L28H11	-18.28	1.223(1)	550.82	P5H3	4.89	3.335(0)	537.25
S12P9	-1.60	Null		L28H13	-15.28	1.306(1)	550.57	P5H2	4.98	3.868(0)	537.86
S12P10	-1.60	Null		L28H18	-9.28	1.119(1)	548.74	P5H1	5.08	4.660(0)	538.55
S12P13	-.98	Null		P5H42	.13	Null		P12H1	5.24	6.181(0)	539.24
S12P17	-.03	1.110(0)		P5H41	.32	-5.773(-1)	532.18	P12H2	5.33	Null	Null
S12P19	-.03	Null		P5H40	.52	-8.971(-1)	532.13	P12H3	5.43	8.215(0)	540.97
S12P25	-.03	1.082(0)		P5H39	.72	-1.181(0)	532.09	P12H4	5.53	1.014(1)	542.67
S12P26	-.03	1.107(0)		P5H37	1.18	-1.200(0)	531.89	P12H5	5.63	1.151(1)	544.13
S12P27	-.03	1.044(0)		P5H36	1.39	-7.604(-1)	532.40	P12H13	6.39	1.999(1)	553.58
S12P28	-.03	Null		P5H35	1.59	-1.115(0)	531.85	P12H16	6.72	1.235(1)	545.17
P5P9	.43	7.360(-1)		P5H34	1.80	-1.124(0)	532.03	P12H7	5.82	1.258(1)	545.54
P5P24	.56	9.329(-1)		P5H33	2.00	-7.145(-1)	532.21	P12H8	5.92	1.540(1)	548.14
P5P8	.94	1.261(0)		P5H32	2.15	-8.349(-1)	532.26	P12H9	6.02	Null	Null
P5P23	1.02	9.006(-1)		P5H31	2.24	-6.648(-1)	532.41	P12H10	6.12	1.763(-1)	550.67
P5P7	1.45	1.067(0)		P5H30	2.34	-7.331(-1)	532.49	P12H12	6.30	1.887(1)	552.24
P5P22	1.53	8.835(-1)		P5H29	2.43	-4.176(-1)	532.70	P12H13	6.39	1.999(1)	553.58
P5P21	2.04	8.743(-1)		P5H28	2.53	-3.269(-1)	532.74	P12H14	6.48	1.959(1)	553.90
P5P5	2.72	1.157(0)		P5H27	2.63	-3.671(-1)	532.82	P12H15	6.56	2.109(1)	554.91
P5P18	2.79	1.151(0)		P5H26	2.72	-4.805(-1)	533.93	P12H16	6.66	2.273(1)	557.20
P5P4	3.23	1.079(0)		P5H25	2.82	-2.789(-1)	533.03	P12H17	6.74	2.617(1)	560.01
P5P16	3.31	1.214(0)		P5H24	2.91	-1.342(-2)	533.18	P12H18	6.84	2.479(1)	559.23
P5P3	3.73	1.904(0)		P5H23	3.02	-2.768(-1)	533.13	P12H19	6.93	2.594(1)	559.96
P5P14	3.87	2.538(0)		P5H22	3.14	-1.014(-1)	533.23	P12H20	7.02	2.550(1)	560.06
P5P12	4.34	2.452(0)		P5H21	3.23	-2.762(-1)	533.22	P12H22	8.01	4.006(1)	576.22
P5P1	4.76	2.664(0)		P5H20	3.33	-2.210(-1)	533.29	P12H23	8.66	4.937(1)	587.33
P5P10	4.85	3.055(0)		P5H19	3.43	-9.447(-2)	533.40	P12H25	9.92	5.562(1)	598.35
P12P1	5.47	Null		P5H18	3.53	1.475(-1)	533.53	P12H26	10.57	5.225(1)	598.06
P12P2	6.11	4.505(0)		P5H17	3.62	6.983(-1)	533.79	P12H28	11.85	6.024(1)	605.82
P12P3	6.76	5.989(0)		P5H16	3.72	1.473(0)	534.40	P12H29	12.49	6.182(1)	608.25
P12P4	7.39	5.957(0)		P5H15	3.82	1.810(0)	534.83	P12H31	13.78	6.010(1)	608.04
P12P5	8.03	7.592(0)		P5H14	3.92	2.107(0)	535.10	P12H33	15.06	6.237(1)	608.90
P12P6	8.68	7.486(0)		P5H13	4.01	1.944(0)	535.37	P12H35	16.33	5.183(1)	600.84
P12P7	9.31	8.344(0)		P5H12	4.09	1.878(0)	535.19				

Run 50 Reduced Data Tabulation

Gauge Label	Loc. (in)	Value (PSIA) or (BTU/Ft ² -Sec)	T Surf (DegR)	Gauge Label	Loc. (in)	Value (PSIA) or (BTU/Ft ² -Sec)	T Surf (DegR)	Gauge Label	Loc. (in)	Value (PSIA) or (BTU/Ft ² -Sec)	T Surf (DegR)
L28P1	-26.28	-4.188(-1)		P12P8	9.95	7.015(0)		P5H11	4.14	1.270(-1)	534.87
L28P3	-18.28	1.357(0)		P12P13	13.15	8.533(0)		P5H10	4.22	2.618(-1)	534.85
L28P5	-10.28	Null		P12P16	15.07	8.031(0)		P5H9	4.31	Null	Null
S12P2	-1.90	Null		P5S4	2.89	Null		P5H8	4.40	1.991(-1)	535.10
S12P3	-1.90	Null		P5S2	4.25	Null		P5H7	4.50	6.302(-2)	535.14
S12P4	-1.90	Null		L28H3	-27.28	1.638(1)	555.64	P5H6	4.59	2.235(-1)	535.28
S12P7	-1.60	Null		L28H6	-24.28	1.484(1)	553.97	P5H5	4.69	3.489(-1)	535.53
S12P8	-1.60	Null		L28H11	-18.28	1.235(1)	550.99	P5H4	4.79	5.478(-1)	535.61
S12P9	-1.60	Null		L28H13	-15.28	1.246(1)	550.37	P5H3	4.89	3.916(-1)	535.64
S12P10	-1.60	Null		L28H18	-9.28	1.102(1)	549.05	P5H2	4.98	8.006(-1)	535.84
S12P13	-0.98	Null		PSH42	.13	Null	Null	P5H1	5.08	7.544(-1)	535.95
S12P17	-.03	2.079(0)		P5H11	.32	-2.277(0)	531.74	P12H1	5.24	2.024(0)	536.50
S12P19	-.03	Null		P5H40	.52	-6.125(-1)	533.95	P12H2	5.33	Null	Null
S12P25	-.03	1.923(0)		P5H39	.72	-4.805(-1)	534.13	P12H3	5.43	3.417(0)	537.16
S12P26	-.03	1.913(0)		P5H37	1.18	-1.046(0)	534.17	P12H4	5.53	4.164(0)	537.56
S12P27	-.03	1.918(0)		P5H36	1.39	-9.458(-1)	534.30	P12H5	5.63	5.178(0)	538.18
S12P28	-.03	Null		P5H35	1.59	-9.925(-1)	534.01	P12H6	5.72	6.387(0)	538.96
P5P9	.43	5.578(-1)		P5H34	1.80	-6.786(-1)	534.06	P12H7	5.82	6.925(0)	539.70
P5P24	.56	7.664(-1)		P5H33	2.00	-9.022(-1)	534.11	P12H8	5.92	9.222(0)	541.31
P5P8	.94	1.346(0)		P5H32	2.15	-7.330(-1)	534.23	P12H9	6.02	9.426(0)	541.84
P5P23	1.02	9.858(-1)		P5H31	2.24	-8.847(-1)	534.18	P12H10	6.12	1.051(1)	542.76
P5P7	1.45	1.101(0)		P5H30	2.34	-8.467(-1)	534.23	P12H12	6.30	1.150(1)	544.01
P5P22	1.53	9.738(-1)		P5H29	2.43	-7.607(-1)	534.19	P12H13	6.39	1.336(1)	545.45
P5P21	2.04	Null		P5H28	2.53	-7.443(-1)	534.22	P12H14	6.48	1.355(1)	545.74
P5P5	2.72	1.207(0)		P5H27	2.63	-6.589(-1)	534.28	P12H15	6.56	1.453(1)	546.64
P5P18	2.79	1.242(0)		P5H26	2.72	-8.681(-1)	534.28	P12H16	6.66	1.539(1)	547.37
P5P4	3.23	1.151(0)		P5H25	2.82	-5.980(-1)	534.31	P12H17	6.74	1.694(1)	548.79
P5P16	3.31	1.236(0)		P5H24	2.91	-4.320(-1)	534.37	P12H18	6.84	1.697(1)	548.99
P5P3	3.73	1.849(0)		P5H23	3.02	-8.635(-1)	534.24	P12H19	6.93	1.774(1)	549.80
P5P14	3.87	1.265(0)		P5H22	3.14	-7.540(-1)	534.12	P12H20	7.02	1.730(1)	549.37
P5P12	4.34	2.463(0)		P5H21	3.23	-8.970(-1)	534.28	P12H22	8.01	3.181(1)	562.38
P5P1	4.76	2.850(0)		P5H20	3.33	-9.635(-1)	534.21	P12H23	8.66	4.055(1)	571.31
P5P10	4.85	3.425(0)		P5H19	3.43	-7.295(-1)	534.25	P12H25	9.92	5.121(1)	583.50
P12P1	5.47	Null		P5H18	3.53	-8.750(-1)	534.25	P12H26	10.57	5.294(1)	587.25
P12P2	6.11	5.358(0)		P5H17	3.62	-7.089(-1)	534.21	P12H28	11.85	5.746(1)	594.58
P12P3	6.76	6.630(0)		P5H16	3.72	-7.848(-1)	534.28	P12H29	12.49	5.947(1)	598.12
P12P4	7.39	6.215(0)		P5H15	3.82	-5.675(-1)	534.38	P12H31	13.78	5.976(1)	598.66
P12P5	8.03	7.568(0)		P5H14	3.92	-3.567(-1)	534.33	P12H33	15.06	5.933(1)	598.98
P12P6	8.68	7.456(0)		P5H13	4.01	1.446(-2)	535.03	P12H35	16.33	5.247(1)	592.16
P12P7	9.31	8.219(0)		P5H12	4.09	-2.503(-1)	534.52				

Run 51 Reduced Data Tabulation

Gauge Label	Loc. (in)	Value (PSIA) or (BTU/Ft ² -Sec)	T Surf (DegR)	Gauge Label	Loc. (in)	Value (PSIA) or (BTU/Ft ² -Sec)	T Surf (DegR)	Gauge Label	Loc. (in)	Value (PSIA) or (BTU/Ft ² -Sec)	T Surf (DegR)
L28P1	-26.28	-4.689(-1)		P12P8	9.95	7.952(0)		P5H11	4.14	8.718(0)	540.31
L28P3	-18.28	1.431(0)		P12P13	13.15	9.116(0)		P5H10	4.22	8.854(0)	540.50
L28P5	-10.28	2.729(0)		P12P16	15.07	8.337(0)		P5H9	4.31	Null	Null
S12P2	-1.90	Null		P5S4	2.89	Null		P5H8	4.40	9.193(0)	540.93
S12P3	-1.90	Null		P5S2	4.25	Null		P5H7	4.50	9.368(0)	541.26
S12P4	-1.90	Null		L28H3	-27.28	1.710(1)	551.37	P5H6	4.59	9.081(0)	540.79
S12P7	-1.60	Null		L28H6	-24.28	1.579(1)	549.86	P5H5	4.69	8.958(0)	540.74
S12P8	-1.60	Null		L28H11	-18.28	1.322(1)	546.65	P5H4	4.79	9.001(0)	540.88
S12P9	-1.60	Null		L28H13	-15.28	1.338(1)	546.06	P5H3	4.89	8.892(0)	540.67
S12P10	-1.60	Null		L28H18	-9.28	1.214(1)	544.89	P5H2	4.98	8.957(0)	540.74
S12P13	-0.98	Null		P5H42	.13	Null	Null	P5H1	5.08	5.413(0)	536.59
S12P17	-.03	2.598(-1)		P5H41	.32	4.300(0)	538.19	P12H1	5.24	1.032(1)	542.58
S12P19	-.03	Null		P5H40	.52	8.894(0)	542.41	P12H2	5.33	1.278(1)	542.13
S12P25	-.03	3.501(-1)		P5H39	.72	9.259(0)	541.39	P12H3	5.43	1.758(1)	544.28
S12P26	-.03	3.625(-1)		P5H37	1.18	9.401(0)	541.39	P12H4	5.53	1.780(1)	546.45
S12P27	-.03	3.469(-1)		P5H36	1.39	9.015(1)	542.08	P12H5	5.63	1.716(1)	546.96
S12P28	-.03	Null		P5H35	1.59	9.421(0)	541.37	P12H6	5.72	1.979(1)	547.67
P5P9	.43	5.594(-1)		P5H34	1.80	9.393(0)	541.06	P12H7	5.82	2.529(1)	550.51
P5P24	.56	6.382(-1)		P5H33	2.00	9.213(0)	541.14	P12H8	5.92	3.346(1)	557.13
P5P8	.94	1.082(0)		P5H32	2.15	9.160(0)	540.68	P12H9	6.02	3.621(1)	559.22
P5P23	1.02	8.008(-1)		P5H31	2.24	9.786(0)	541.52	P12H10	6.12	3.979(1)	562.72
P5P7	1.45	9.792(-1)		P5H30	2.34	9.365(0)	541.26	P12H12	6.30	4.212(1)	565.47
P5P22	1.53	7.387(-1)		P5H29	2.43	9.357(0)	541.01	P12H13	6.39	4.423(1)	568.33
P5P21	2.04	8.300(-1)		P5H28	2.53	9.309(0)	541.09	P12H14	6.48	4.385(1)	569.31
P5P5	2.72	1.078(0)		P5H27	2.63	9.104(0)	540.86	P12H15	6.56	4.117(1)	567.47
P5P18	2.79	1.030(0)		P5H26	2.72	9.568(0)	541.21	P12H16	6.66	4.664(1)	573.17
P5P4	3.23	9.694(-1)		P5H25	2.82	9.651(0)	541.37	P12H17	6.74	5.148(1)	577.58
P5P16	3.31	1.057(0)		P5H24	2.91	9.063(0)	540.61	P12H18	6.84	5.101(1)	577.44
P5P3	3.73	1.034(0)		P5H23	3.02	9.303(0)	541.00	P12H19	6.93	5.142(1)	578.25
P5P14	3.87	1.052(0)		P5H22	3.14	1.031(1)	542.00	P12H20	7.02	5.097(1)	578.40
P5P12	4.34	8.789(-1)		P5H21	3.23	9.085(0)	540.94	P12H22	8.01	6.207(1)	592.41
P5P1	4.76	1.011(0)		P5H20	3.33	9.090(0)	540.81	P12H23	8.66	6.709(1)	599.12
P5P10	4.85	1.069(0)		P5H19	3.43	9.455(0)	541.17	P12H25	9.92	6.694(1)	602.90
P12P1	5.47	Null		P5H18	3.53	7.499(0)	539.05	P12H26	10.57	6.418(1)	601.62
P12P2	6.11	5.387(0)		P5H17	3.62	9.111(0)	540.75	P12H28	11.85	6.472(1)	603.82
P12P3	6.76	8.164(0)		P5H16	3.72	9.380(0)	541.04	P12H29	12.49	6.603(1)	606.24
P12P4	7.39	7.937(0)		P5H15	3.82	9.183(0)	540.91	P12H31	13.78	6.333(1)	603.74
P12P5	8.03	9.567(0)		P5H14	3.92	9.317(0)	540.93	P12H33	15.06	6.211(1)	601.48
P12P6	8.68	8.949(0)		P5H13	4.01	9.379(0)	541.09	P12H35	16.33	5.506(1)	594.20
P12P7	9.31	9.595(0)		P5H12	4.09	8.493(0)	540.14				

Run 52 Reduced Data Tabulation

Gauge Label	Loc. (in)	Value (PSIA) or (BTU/Ft ² -Sec)	T Surf (DegR)	Gauge Label	Loc. (in)	Value (PSIA) or (BTU/Ft ² -Sec)	T Surf (DegR)	Gauge Label	Loc. (in)	Value (PSIA) or (BTU/Ft ² -Sec)	T Surf (DegR)
L28P1	-26.28	-2.438(-1)	P12P8	9.95	7.700(0)	P5H11	4.14	6.535(1)	596.33		
L28P3	-18.28	1.412(0)	P12P13	13.15	6.853(0)	P5H10	4.22	6.401(1)	595.22		
L28P5	-10.28	1.120(0)	P12P16	15.07	3.908(0)	P5H9	4.31	Null	Null		
S12P2	-1.90	Null	P5S4	2.89	Null	P5H8	4.40	6.142(1)	593.80		
S12P3	-1.90	Null	P5S2	4.25	Null	P5H7	4.50	6.394(1)	596.48		
S12P4	-1.90	Null	L28H3	-27.28	1.649(1)	P5H6	4.59	6.201(1)	594.90		
S12P7	-1.60	Null	L28H6	-24.28	1.521(1)	P5H5	4.69	6.328(1)	596.22		
S12P8	-1.60	Null	L28H11	-18.28	1.272(1)	P5H4	4.79	6.388(1)	597.16		
S12P9	-1.60	Null	L28H13	-15.28	1.253(1)	P5H3	4.89	6.271(1)	596.04		
S12P10	-1.60	Null	L28H18	-9.28	1.131(1)	P5H2	4.98	6.359(1)	596.94		
S12P13	.98	Null	P5H42	.13	Null	P5H1	5.08	6.502(1)	591.68		
S12P17	.03	Null	P5H41	.32	3.989(0)	P12H1	5.24	7.023(1)	608.55		
S12P19	.03	Null	P5H40	.52	8.659(0)	P12H2	5.33	8.563(1)	632.34		
S12P25	.03	2.939(-1)	P5H39	.72	8.691(0)	P12H3	5.43	6.206(1)	598.72		
S12P26	.03	3.311(-1)	P5H37	1.18	8.807(0)	P12H4	5.53	6.253(1)	599.27		
S12P27	.03	2.802(-1)	P5H36	1.39	1.037(1)	P12H5	5.63	6.456(1)	600.97		
S12P28	.03	Null	P5H35	1.59	2.440(1)	P12H6	5.72	6.440(1)	601.16		
P5P9	.43	5.181(-1)	P5H34	1.80	3.242(1)	P12H7	5.82	6.216(1)	598.88		
P5P24	.56	6.010(-1)	P5H33	2.00	3.636(1)	P12H8	5.92	6.850(1)	605.87		
P5P8	.94	1.028(0)	P5H32	2.15	4.149(1)	P12H9	6.02	6.471(1)	602.05		
P5P23	1.02	7.782(-1)	P5H31	2.24	4.412(1)	P12H10	6.12	6.577(1)	603.39		
P5P7	1.45	3.720(0)	P5H30	2.34	4.373(1)	P12H12	6.30	6.280(1)	600.53		
P5P22	1.53	1.504(0)	P5H29	2.43	4.469(1)	P12H13	6.39	6.577(1)	603.60		
P5P21	2.04	4.411(0)	P5H28	2.53	4.753(1)	P12H14	6.48	6.271(1)	600.25		
P5P5	2.72	8.735(0)	P5H27	2.63	4.845(1)	P12H15	6.56	6.361(1)	601.35		
P5P18	2.79	8.469(0)	P5H26	2.72	5.240(1)	P12H16	6.66	6.466(1)	602.70		
P5P4	3.23	8.828(0)	P5H25	2.82	5.451(1)	P12H17	6.74	6.864(1)	606.53		
P5P16	3.31	9.057(0)	P5H24	2.91	4.623(1)	P12H18	6.84	6.541(1)	603.51		
P5P3	3.73	9.570(0)	P5H23	3.02	5.422(1)	P12H19	6.93	6.423(1)	602.35		
P5P14	3.87	9.831(0)	P5H22	3.14	6.202(1)	P12H20	7.02	6.065(1)	598.96		
P5P12	4.34	8.224(0)	P5H21	3.23	5.551(1)	P12H22	8.01	6.322(1)	602.73		
P5P1	4.76	8.737(0)	P5H20	3.33	5.680(1)	P12H23	8.66	6.479(1)	605.10		
P5P10	4.85	9.583(0)	P5H19	3.43	5.864(1)	P12H25	9.92	6.404(1)	603.70		
P12P1	5.47	Null	P5H18	3.53	4.910(1)	P12H26	10.57	6.012(1)	599.54		
P12P2	6.11	8.989(0)	P5H17	3.62	5.811(1)	P12H28	11.85	5.781(1)	597.08		
P12P3	6.76	9.056(0)	P5H16	3.72	5.957(1)	P12H29	12.49	5.737(1)	595.98		
P12P4	7.39	7.674(0)	P5H15	3.82	5.842(1)	P12H31	13.78	4.124(1)	579.10		
P12P5	8.03	8.836(0)	P5H14	3.92	5.979(1)	P12H33	15.06	3.081(1)	567.51		
P12P6	8.68	8.343(0)	P5H13	4.01	6.131(1)	P12H35	16.33	2.365(1)	559.48		
P12P7	9.31	8.965(0)	P5H12	4.09	5.538(1)	P5H10					

Run 53 Reduced Data Tabulation

Gauge Label	Loc. (in)	Value (PSIA) or (BTU/Ft ² -Sec)	T Surf (DegR)	Gauge Label	Loc. (in)	Value (PSIA) or (BTU/Ft ² -Sec)	T Surf (DegR)	Gauge Label	Loc. (in)	Value (PSIA) or (BTU/Ft ² -Sec)	T Surf (DegR)
L28P1	-26.28	Null	P12P8	9.95	7.140(0)	P5H11	4.14	3.379(1)	568.18		
L28P3	-18.28	1.318(0)	P12P13	13.15	6.208(0)	P5H10	4.22	3.248(1)	566.91		
L28P5	-10.28	1.082(0)	P12P16	15.07	3.843(0)	P5H9	4.31	Null	Null		
S12P2	-1.90	Null	P5S4	2.89	Null	P5H8	4.40	3.353(1)	568.43		
S12P3	-1.90	Null	P5S2	4.25	Null	P5H7	4.50	3.514(1)	570.31		
S12P4	-1.90	Null	L28H3	-27.28	1.593(1)	P5H6	4.59	3.513(1)	570.21		
S12P7	-1.60	Null	L28H6	-24.28	1.468(1)	P5H5	4.69	3.681(1)	571.68		
S12P8	-1.60	Null	L28H11	-18.28	1.223(1)	P5H4	4.79	3.789(1)	572.87		
S12P9	-1.60	Null	L28H13	-15.28	1.227(1)	P5H3	4.89	3.761(1)	572.58		
S12P10	-1.60	Null	L28H18	-9.28	1.065(1)	P5H2	4.98	3.856(1)	573.80		
S12P13	.98	Null	P5H42	.13	Null	P5H1	5.08	5.088(1)	581.03		
S12P17	.03	Null	P5H41	.32	2.465(0)	P12H1	5.24	5.872(1)	591.67		
S12P19	.03	Null	P5H40	.52	2.295(0)	P12H2	5.33	9.414(1)	606.02		
S12P25	.03	1.343(0)	P5H39	.72	2.282(0)	P12H3	5.43	5.004(1)	581.87		
S12P26	.03	1.284(0)	P5H37	1.18	3.425(0)	P12H4	5.53	4.964(1)	581.88		
S12P27	.03	1.296(0)	P5H36	1.39	5.301(0)	P12H5	5.63	5.163(1)	583.76		
S12P28	.03	Null	P5H35	1.59	7.419(0)	P12H6	5.72	5.276(1)	584.35		
P5P9	.43	1.689(0)	P5H34	1.80	9.655(0)	P12H7	5.82	5.057(1)	582.80		
P5P24	.56	1.767(0)	P5H33	2.00	1.071(1)	P12H8	5.92	5.731(1)	588.96		
P5P8	.94	3.561(0)	P5H32	2.15	1.278(1)	P12H9	6.02	5.486(1)	587.00		
P5P23	1.02	2.441(0)	P5H31	2.24	1.420(1)	P12H10	6.12	5.607(1)	587.92		
P5P7	1.45	4.455(0)	P5H30	2.34	1.452(1)	P12H12	6.30	5.411(1)	586.35		
P5P22	1.53	3.353(0)	P5H29	2.43	1.490(1)	P12H13	6.39	5.737(1)	589.66		
P5P21	2.04	4.110(0)	P5H28	2.53	1.568(1)	P12H14	6.48	5.607(1)	588.44		
P5P5	2.72	5.811(0)	P5H27	2.63	1.658(1)	P12H15	6.56	5.338(1)	586.21		
P5P18	2.79	5.675(0)	P5H26	2.72	1.759(1)	P12H16	6.66	5.710(1)	590.00		
P5P4	3.23	6.208(0)	P5H25	2.82	1.942(1)	P12H17	6.74	6.327(1)	595.49		
P5P16	3.31	6.615(0)	P5H24	2.91	1.886(1)	P12H18	6.84	6.381(1)	596.13		
P5P3	3.73	7.040(0)	P5H23	3.02	2.102(1)	P12H19	6.93	5.966(1)	592.76		
P5P14	3.87	7.611(0)	P5H22	3.14	2.293(1)	P12H20	7.02	5.468(1)	588.52		
P5P12	4.34	6.629(0)	P5H21	3.23	2.210(1)	P12H22	8.01	5.867(1)	593.92		
P5P1	4.76	7.221(0)	P5H20	3.33	2.314(1)	P12H23	8.66	6.105(1)	597.32		
P5P10	4.85	8.075(0)	P5H19	3.43	2.509(1)	P12H25	9.92	6.120(1)	597.84		
P12P1	5.47	Null	P5H18	3.53	2.514(1)	P12H26	10.57	5.712(1)	594.23		
P12P2	6.11	7.931(0)	P5H17	3.62	2.678(1)	P12H28	11.85	5.578(1)	592.71		
P12P3	6.76	8.161(0)	P5H16	3.72	2.792(1)	P12H29	12.49	5.452(1)	591.71		
P12P4	7.39	6.900(0)	P5H15	3.82	2.847(1)	P12H31	13.78	3.872(1)	575.65		
P12P5	8.03	8.158(0)	P5H14	3.92	2.978(1)	P12H33	15.06	2.930(1)	565.77		
P12P6	8.68	7.759(0)	P5H13	4.01	3.071(1)	P12H35	16.33	2.239(1)	558.46		
P12P7	9.31	8.435(0)	P5H12	4.09	2.867(1)	P5H10					

Run 55 Reduced Data Tabulation

Gauge	Loc.	Value	Gauge	Loc.	Value	Gauge	Loc.	Value
Label	(in)	(PSIA) or (BTU/Ft ² -Sec)	Label	(in)	(PSIA) or (BTU/Ft ² -Sec)	Label	(in)	(PSIA) or (BTU/Ft ² -Sec)
		T Surf (DegR)			T Surf (DegR)			T Surf (DegR)
L28P1	-26.28	-2.192(-2)	P12P8	9.95	6.956(0)	P5H11	4.14	2.217(1)
L28P3	-18.28	1.306(0)	P12P13	13.15	6.262(0)	P5H10	4.22	2.376(1)
L28P5	-10.28	-4.555(-1)	P12P16	15.07	3.871(0)	P5H9	4.31	Null
S12P2	-1.90	Null	P5S4	2.89	Null	P5H8	4.40	2.552(1)
S12P3	-1.90	Null	P5S2	4.25	Null	P5H7	4.50	2.714(1)
S12P4	-1.90	Null	L28H3	-27.28	1.504(1)	P5H6	4.59	2.693(1)
S12P7	-1.60	Null	L28H6	-24.28	1.378(1)	P5H5	4.69	2.764(1)
S12P8	-1.60	Null	L28H11	-18.28	1.193(1)	P5H4	4.79	2.893(1)
S12P9	-1.60	Null	L28H13	-15.28	1.230(1)	P5H3	4.89	2.917(1)
S12P10	-1.60	Null	L28H18	-9.28	1.076(1)	P5H2	4.98	3.054(1)
S12P13	.98	Null	P5H42	.13	Null	P5H1	5.08	4.073(1)
S12P17	.03	2.043(0)	P5H41	.32	-7.382(-1)	P12H1	5.24	3.830(1)
S12P19	.03	Null	P5H40	.52	9.302(-2)	P12H2	5.33	Null
S12P25	.03	1.878(0)	P5H39	.72	-6.857(-1)	P12H3	5.43	3.095(1)
S12P26	.03	1.811(0)	P5H37	1.18	-1.275(0)	P12H4	5.53	3.111(1)
S12P27	.03	1.859(0)	P5H36	1.39	-1.246(0)	P12H5	5.63	3.100(1)
S12P28	.03	Null	P5H35	1.59	-8.261(-1)	P12H6	5.72	3.240(1)
P5P9	.43	1.325(0)	P5H34	1.80	7.189(-1)	P12H7	5.82	3.152(1)
P5P24	.56	1.646(0)	P5H33	2.00	2.821(0)	P12H8	5.92	3.506(1)
P5P8	.94	3.641(0)	P5H32	2.15	3.444(0)	P12H9	6.02	3.455(1)
P5P23	1.02	2.491(0)	P5H31	2.24	5.128(0)	P12H10	6.12	3.562(1)
P5P7	1.45	5.084(0)	P5H30	2.34	6.039(0)	P12H12	6.30	3.554(1)
P5P22	1.53	Null	P5H29	2.43	6.408(0)	P12H13	6.39	3.706(1)
P5P21	2.04	Null	P5H28	2.53	7.102(0)	P12H14	6.48	3.485(1)
P5P5	2.72	7.358(0)	P5H27	2.63	7.585(0)	P12H15	6.56	3.647(1)
P5P18	2.79	7.114(0)	P5H26	2.72	8.555(0)	P12H16	6.66	3.728(1)
P5P4	3.23	7.397(0)	P5H25	2.82	9.211(0)	P12H17	6.74	4.177(1)
P5P16	3.31	7.789(0)	P5H24	2.91	9.203(0)	P12H18	6.84	4.189(1)
P5P3	3.73	7.838(0)	P5H23	3.02	9.974(0)	P12H19	6.93	3.952(1)
P5P14	3.87	8.530(0)	P5H22	3.14	1.246(1)	P12H20	7.02	3.699(1)
P5P12	4.34	7.139(0)	P5H21	3.23	1.220(1)	P12H22	8.01	4.293(1)
P5P1	4.76	7.360(0)	P5H20	3.33	1.349(1)	P12H23	8.66	4.666(1)
P5P10	4.85	8.519(0)	P5H19	3.43	1.480(1)	P12H25	9.92	4.800(1)
P12P1	5.47	Null	P5H18	3.53	1.477(1)	P12H26	10.57	4.581(1)
P12P2	6.11	7.964(0)	P5H17	3.62	1.613(1)	P12H28	11.85	4.513(1)
P12P3	6.76	8.158(0)	P5H16	3.72	1.807(1)	P12H29	12.49	4.505(1)
P12P4	7.39	6.399(0)	P5H15	3.82	1.889(1)	P12H31	13.78	3.315(1)
P12P5	8.03	8.048(0)	P5H14	3.92	2.013(1)	P12H33	15.06	2.565(1)
P12P6	8.68	7.582(0)	P5H13	4.01	2.112(1)	P12H35	16.33	1.952(1)
P12P7	9.31	8.324(0)	P5H12	4.09	1.923(1)			559.26

Run 56 Reduced Data Tabulation

Gauge	Loc.	Value	Gauge	Loc.	Value	Gauge	Loc.	Value
Label	(in)	(PSIA) or (BTU/Ft ² -Sec)	Label	(in)	(PSIA) or (BTU/Ft ² -Sec)	Label	(in)	(PSIA) or (BTU/Ft ² -Sec)
		T Surf (DegR)			T Surf (DegR)			T Surf (DegR)
L28P1	-26.28	1.235(0)	P12P8	9.95	4.012(0)	P5H11	4.14	6.847(0)
L28P3	-18.28	1.266(0)	P12P13	13.15	4.735(0)	P5H10	4.22	7.028(0)
L28P5	-10.28	1.238(0)	P12P16	15.07	5.009(0)	P5H9	4.31	Null
S12P2	-1.90	Null	P5S4	2.89	Null	P5H8	4.40	7.499(0)
S12P3	-1.90	Null	P5S2	4.25	Null	P5H7	4.50	7.522(0)
S12P4	-1.90	Null	L28H3	-27.28	1.519(1)	P5H6	4.59	7.111(0)
S12P7	-1.60	Null	L28H6	-24.28	1.396(1)	P5H5	4.69	7.347(0)
S12P8	-1.60	Null	L28H11	-18.28	1.155(1)	P5H4	4.79	7.319(0)
S12P9	-1.60	Null	L28H13	-15.28	1.119(1)	P5H3	4.89	7.072(0)
S12P10	-1.60	Null	L28H18	-9.28	9.984(0)	P5H2	4.98	7.076(0)
S12P13	.98	Null	P5H42	.13	Null	P5H1	5.08	5.664(0)
S12P17	.03	2.018(-1)	P5H41	.32	3.204(0)	P12H1	5.24	1.202(1)
S12P19	.03	Null	P5H40	.52	4.496(0)	P12H2	5.33	Null
S12P25	.03	2.499(-1)	P5H39	.72	9.189(0)	P12H3	5.43	2.154(1)
S12P26	.03	2.826(-1)	P5H37	1.18	8.385(0)	P12H4	5.53	2.183(1)
S12P27	.03	2.620(-1)	P5H36	1.39	8.146(0)	P12H5	5.63	2.144(1)
S12P28	.03	Null	P5H35	1.59	8.135(0)	P12H6	5.72	2.194(1)
P5P9	.43	5.148(-1)	P5H34	1.80	7.875(0)	P12H7	5.82	2.111(1)
P5P24	.56	5.642(-1)	P5H33	2.00	7.867(0)	P12H8	5.92	2.340(1)
P5P8	.94	9.346(-1)	P5H32	2.15	7.623(0)	P12H9	6.02	2.275(1)
P5P23	1.02	6.845(-1)	P5H31	2.24	7.828(0)	P12H10	6.12	2.388(1)
P5P7	1.45	8.682(-1)	P5H30	2.34	8.017(0)	P12H12	6.30	2.410(1)
P5P22	1.53	6.789(-1)	P5H29	2.43	7.522(0)	P12H13	6.39	2.521(1)
P5P21	2.04	7.171(-1)	P5H28	2.53	7.822(0)	P12H14	6.48	2.471(1)
P5P5	2.72	9.142(-1)	P5H27	2.63	7.848(0)	P12H15	6.56	2.522(1)
P5P18	2.79	9.090(-1)	P5H26	2.72	7.734(0)	P12H16	6.66	2.597(1)
P5P4	3.23	8.509(-1)	P5H25	2.82	8.284(0)	P12H17	6.74	2.762(1)
P5P16	3.31	9.146(-1)	P5H24	2.91	7.635(0)	P12H18	6.84	3.201(1)
P5P3	3.73	Null	P5H23	3.02	7.800(0)	P12H19	6.93	2.825(1)
P5P14	3.87	9.086(-1)	P5H22	3.14	8.219(0)	P12H20	7.02	2.635(1)
P5P12	4.34	7.381(-1)	P5H21	3.23	7.604(0)	P12H22	8.01	3.025(1)
P5P1	4.76	9.000(-1)	P5H20	3.33	7.234(0)	P12H23	8.66	3.287(1)
P5P10	4.85	9.609(-1)	P5H19	3.43	7.896(0)	P12H25	9.92	3.332(1)
P12P1	5.47	Null	P5H18	3.53	6.229(0)	P12H26	10.57	3.234(1)
P12P2	6.11	3.503(0)	P5H17	3.62	7.399(0)	P12H28	11.85	3.405(1)
P12P3	6.76	4.361(0)	P5H16	3.72	7.233(0)	P12H29	12.49	3.580(1)
P12P4	7.39	3.889(0)	P5H15	3.82	7.295(0)	P12H31	13.78	3.429(1)
P12P5	8.03	4.619(0)	P5H14	3.92	7.399(0)	P12H33	15.06	3.480(1)
P12P6	8.68	4.537(0)	P5H13	4.01	7.562(0)	P12H35	16.33	3.384(1)
P12P7	9.31	4.814(0)	P5H12	4.09	6.752(0)			575.29

Run 57 Reduced Data Tabulation

Value		Value		Value							
Gauge Label	Loc. (in)	(PSIA) or (BTU/Ft ² -Sec)	T Surf (DegR)	Gauge Label	Loc. (in)	(PSIA) or (BTU/Ft ² -Sec)	T Surf (DegR)	Gauge Label	Loc. (in)	(PSIA) or (BTU/Ft ² -Sec)	T Surf (DegR)
L28P1	-26.28	1.194(0)	P12P8	9.95	3.718(0)	P5H11	4.14	2.436(-1)	P12H1	5.33	533.30
L28P3	-18.28	1.255(0)	P12P13	13.15	4.449(0)	P5H10	4.22	4.775(-1)	P12H2	5.33	533.32
L28P5	-10.28	1.145(0)	P12P16	15.07	4.753(0)	P5H9	4.31	Null	P12H3	Null	Null
S12P2	-1.90	Null	P5S4	2.89	Null	P5H8	4.40	1.111(0)	P12H4	533.72	
S12P3	-1.90	Null	P5S2	4.25	Null	P5H7	4.50	2.128(0)	P12H5	534.30	
S12P4	-1.90	Null	L28H3	-27.28	1.534(1)	P5H6	4.59	2.244(0)	P12H6	534.60	
S12P7	-1.60	Null	L28H6	-24.28	1.394(1)	P5H5	4.69	2.237(0)	P12H7	534.80	
S12P8	-1.60	Null	L28H11	-18.28	1.137(1)	P5H4	4.79	2.261(0)	P12H8	534.93	
S12P9	-1.60	Null	L28H13	-15.28	0.079(1)	P5H3	4.89	2.109(0)	P12H9	534.92	
S12P10	-1.60	Null	L28H18	-9.28	9.934(0)	P5H2	4.98	2.182(0)	P12H10	534.93	
S12P13	-.98	Null	P5H42	.13	Null	P5H1	5.08	2.619(0)	P12H11	535.11	
S12P17	-.03	1.105(0)	P5H41	.32	-4.975(-1)	P12H1	5.24	2.932(0)	P12H12	535.45	
S12P19	-.03	Null	P5H40	.52	-4.363(-1)	P12H2	5.33	Null	P12H3	Null	
S12P25	-.03	1.041(0)	P5H39	.72	-5.272(-1)	P12H4	5.43	Null	P12H5	Null	
S12P26	-.03	1.049(0)	P5H37	1.18	-8.400(-1)	P12H6	5.53	3.837(0)	P12H7	536.28	
S12P27	-.03	9.900(-1)	P5H36	1.39	-1.015(0)	P12H8	5.63	3.878(0)	P12H9	536.54	
S12P28	-.03	Null	P5H35	1.59	-1.077(0)	P12H10	5.72	4.366(0)	P12H11	536.81	
P5P9	.43	5.995(-1)	P5H34	1.80	-1.220(0)	P12H12	5.82	4.169(0)	P12H13	536.82	
P5P24	.56	7.560(-1)	P5H33	2.00	-9.398(-1)	P12H14	5.92	4.761(0)	P12H15	537.48	
P5P8	.94	1.052(0)	P5H32	2.15	-1.182(0)	P12H16	6.02	4.710(0)	P12H17	537.43	
P5P23	1.02	7.709(-1)	P5H31	2.24	-1.018(0)	P12H18	6.12	5.120(0)	P12H19	537.72	
P5P7	1.45	9.505(-1)	P5H30	2.34	-1.128(0)	P12H20	6.30	5.637(0)	P12H21	538.08	
P5P22	1.53	7.865(-1)	P5H29	2.43	-9.633(-1)	P12H22	6.39	5.825(0)	P12H23	538.36	
P5P21	2.04	Null	P5H28	2.53	-6.022(-1)	P12H24	6.48	5.519(0)	P12H25	538.30	
P5P5	2.72	1.004(0)	P5H27	2.63	-5.709(-1)	P12H26	6.56	6.148(0)	P12H27	538.65	
P5P18	2.79	9.773(-1)	P5H26	2.72	-6.258(-1)	P12H28	6.66	6.390(0)	P12H29	538.95	
P5P4	3.23	9.352(-1)	P5H25	2.82	-5.887(-1)	P12H30	6.74	7.161(0)	P12H31	539.62	
P5P16	3.31	1.025(0)	P5H24	2.91	-5.102(-1)	P12H32	6.84	7.251(0)	P12H33	539.66	
P5P3	3.73	1.105(0)	P5H23	3.02	-3.247(-1)	P12H34	6.93	7.493(0)	P12H35	539.92	
P5P14	3.87	1.022(0)	P5H22	3.14	-3.374(-1)	P12H36	7.02	6.960(0)	P12H37	539.50	
P5P12	4.34	1.311(0)	P5H21	3.23	-5.549(-1)	P12H38	8.01	1.168(1)	P12H39	543.91	
P5P1	4.76	2.067(0)	P5H20	3.33	-5.362(-1)	P12H40	8.66	1.507(1)	P12H41	547.14	
P5P10	4.85	2.034(0)	P5H19	3.43	-2.084(-1)	P12H42	9.92	1.779(1)	P12H43	550.46	
P12P1	5.47	Null	P5H18	3.53	Null	P12H44	10.57	1.849(1)	P12H45	551.34	
P12P2	6.11	3.321(0)	P5H17	3.62	1.763(-2)	P12H46	11.85	2.225(1)	P12H47	554.72	
P12P3	6.76	3.785(0)	P5H16	3.72	1.541(-1)	P12H48	12.49	2.408(1)	P12H49	556.66	
P12P4	7.39	3.351(0)	P5H15	3.82	Null	P12H50	13.78	2.451(1)	P12H51	556.93	
P12P5	8.03	4.091(0)	P5H14	3.92	6.515(-2)	P12H52	15.06	2.604(1)	P12H53	558.27	
P12P6	8.68	4.011(0)	P5H13	4.01	9.144(-2)	P12H54	16.33	2.689(1)	P12H55	559.11	
P12P7	9.31	4.434(0)	P5H12	4.09	1.276(-2)	P12H56					

Run 58 Reduced Data Tabulation

Value		Value		Value									
Gauge Label	Loc. (in)	(PSIA) or (BTU/Ft ² -Sec)	T Surf (DegR)	Gauge Label	Loc. (in)	(PSIA) or (BTU/Ft ² -Sec)	T Surf (DegR)	Gauge Label	Loc. (in)	(PSIA) or (BTU/Ft ² -Sec)	T Surf (DegR)		
L28P1	-26.28	1.268(0)	P12P8	9.95	3.927(0)	P5H11	4.14	-6.053(-1)	P12H1	534.19			
L28P3	-18.28	1.294(0)	P12P13	13.15	4.512(0)	P5H10	4.22	-5.819(-1)	P12H2	534.19			
L28P5	-10.28	-5.043(-1)	P12P16	15.07	4.853(0)	P5H9	4.31	Null	P12H3	Null			
S12P2	-1.90	Null	P5S4	2.89	Null	P5H8	4.40	-7.665(-1)	P12H4	534.15			
S12P3	-1.90	Null	P5S2	4.25	Null	P5H7	4.50	-6.740(-1)	P12H5	534.10			
S12P4	-1.90	Null	L28H3	-27.28	1.392(1)	P12H6	4.59	-3.827(-1)	P12H7	534.22			
S12P7	-1.60	Null	L28H6	-24.28	1.312(1)	P12H8	4.69	-9.731(-2)	P12H9	534.46			
S12P8	-1.60	Null	L28H11	-18.28	0.089(1)	P12H10	4.80	P5H4	4.79	2.768(-1)	P12H11	534.77	
S12P9	-1.60	Null	L28H13	-15.28	1.147(1)	P12H12	4.89	5.907(-1)	P12H13	535.11			
S12P10	-1.60	Null	L28H18	-9.28	1.008(1)	P12H14	5.08	3.222(-1)	P12H15	535.36			
S12P13	-.98	Null	P5H42	.13	Null	P12H16	5.18	4.751(-1)	P12H17	535.49			
S12P17	-.03	1.981(0)	P5H41	.32	-2.396(0)	P12H18	5.24	-6.108(-1)	P12H19	534.67			
S12P19	-.03	Null	P5H40	.52	-5.394(-1)	P12H20	5.33	Null	P12H21	Null			
S12P25	-.03	1.900(0)	P5H39	.72	-6.582(-1)	P12H22	5.43	Null	P12H23	Null			
S12P26	-.03	1.868(0)	P5H37	1.18	-8.128(-1)	P12H24	5.53	-5.113(-1)	P12H25	534.40			
S12P27	-.03	1.873(0)	P5H36	1.39	-1.748(-1)	P12H26	5.63	-6.171(-1)	P12H27	534.37			
S12P28	-.03	Null	P5H35	1.59	-3.380(-1)	P12H28	5.72	-3.851(-1)	P12H29	534.45			
P5P9	.43	5.828(-1)	P5H34	1.80	-9.102(-1)	P12H30	5.82	-1.033(-1)	P12H31	534.68			
P5P24	.56	7.098(-1)	P5H33	2.00	-9.640(-1)	P12H32	5.92	1.861(-1)	P12H33	534.85			
P5P8	.94	1.247(0)	P5H32	2.15	-8.271(-1)	P12H34	6.02	2.140(-1)	P12H35	535.02			
P5P23	1.02	9.097(-1)	P5H31	2.24	Null	P12H36	6.12	4.456(-1)	P12H37	535.24			
P5P7	1.45	1.031(0)	P5H30	2.34	-7.104(-1)	P12H38	6.30	7.613(-1)	P12H39	535.73			
P5P22	1.53	8.923(-1)	P5H29	2.43	-7.514(-1)	P12H40	6.39	1.275(0)	P12H41	536.07			
P5P21	2.04	Null	P5H28	2.53	-1.023(0)	P12H42	6.48	1.522(0)	P12H43	536.30			
P5P5	2.72	1.155(0)	P5H27	2.63	-8.389(-1)	P12H44	6.56	1.575(0)	P12H45	536.46			
P5P18	2.79	1.126(0)	P5H26	2.72	-8.437(-1)	P12H46	6.66	1.747(0)	P12H47	536.73			
P5P4	3.23	1.073(0)	P5H25	2.82	-8.531(-1)	P12H48	6.74	2.116(0)	P12H49	537.07			
P5P16	3.31	1.154(0)	P5H24	2.91	-5.842(-1)	P12H50	6.84	2.194(0)	P12H51	537.21			
P5P3	3.73	1.089(0)	P5H23	3.02	-8.505(-1)	P12H52	6.93	2.382(0)	P12H53	537.40			
P5P14	3.87	1.151(0)	P5H22	3.14	-9.955(-1)	P12H54	7.02	2.333(0)	P12H55	537.45			
P5P12	4.34	9.430(-1)	P5H21	3.23	-8.896(-1)	P12H56	7.08	4.234(0)	P12H57	539.77			
P5P1	4.76	1.150(0)	P5H20	3.33	-6.658(-1)	P12H58	7.66	5.896(0)	P12H59	541.72			
P5P10	4.85	2.027(0)	P5H19	3.43	-7.948(-1)	P12H60	9.92	7.738(0)	P12H61	544.05			
P12P1	5.47	Null	P5H18	3.53	-7.393(-1)	P12H62	10.57	8.798(0)	P12H63	545.11			
P12P2	6.11	3.839(0)	P5H17	3.62	-8.553(-1)	P12H64	11.85	1.189(1)	P12H65	548.74			
P12P3	6.76	4.517(0)	P5H16	3.72	-7.744(-1)	P12H66	12.49	1.373(1)	P12H67	551.07			
P12P4	7.39	3.917(0)	P5H15	3.82	-6.033(-1)	P12H68	13.78	1.393(1)	P12H69	551.00			
P12P5	8.03	4.551(0)	P5H14	3.92	-8.441(-1)	P12H70	15.06	1.819(1)	P12H71	555.72			
P12P6	8.68	4.432(0)	P5H13	4.01	-7.625(-1)	P12H72	15.33	1.972(1)	P12H73	557.45			
P12P7	9.31	4.658(0)	P5H12	4.09	-8.850(-1)	P12H74							

Run 59 Reduced Data Tabulation

Gauge Label	Loc. (in)	Value (PSIA) or (BTU/Ft ² -Sec)	T Surf (DegR)	Gauge Label	Loc. (in)	Value (PSIA) or (BTU/Ft ² -Sec)	T Surf (DegR)	Gauge Label	Loc. (in)	Value (PSIA) or (BTU/Ft ² -Sec)	T Surf (DegR)
L28P1	-26.28	1.196(0)	P12P8	9.95	3.968(0)	P5H11	4.14	2.944(0)	537.96		
L28P3	-18.28	1.263(0)	P12P13	13.15	4.290(0)	P5H10	4.22	3.153(0)	538.17		
L28P5	-10.28	1.137(0)	P12P16	15.07	3.497(0)	P5H9	4.31	Null	Null		
S12P2	-1.90	Null	P5S4	2.89	Null	P5H8	4.40	3.320(0)	538.38		
S12P3	-1.90	Null	P5S2	4.25	Null	P5H7	4.50	3.605(0)	538.65		
S12P4	-1.90	Null	L28H3	-27.28	1.525(1)	P5H6	4.59	3.719(0)	538.76		
S12P7	-1.60	Null	L28H6	-24.28	1.430(1)	P5H5	4.69	3.971(0)	538.98		
S12P8	-1.60	Null	L28H11	-18.28	1.159(1)	P5H4	4.79	4.280(0)	539.26		
S12P9	-1.60	Null	L28H13	-15.28	1.073(1)	P5H3	4.89	5.272(0)	540.20		
S12P10	-1.60	Null	L28H18	-9.28	1.019(1)	P5H2	4.98	9.144(0)	543.69		
S12P13	.98	Null	P5H42	.13	Null	P5H1	5.08	1.041(1)	544.79		
S12P17	.03	2.054(0)	P5H41	.32	-2.415(0)	P12H1	5.24	9.729(0)	544.06		
S12P19	.03	Null	P5H40	.52	-5.527(-1)	P12H2	5.33	Null	Null		
S12P25	.03	1.942(0)	P5H39	.72	-6.874(-1)	P12H3	5.43	7.180(0)	542.00		
S12P26	.03	1.846(0)	P5H37	1.18	1.102(-1)	P12H4	5.53	7.068(0)	541.76		
S12P27	.03	1.918(0)	P5H36	1.39	2.562(-1)	P12H5	5.63	6.761(0)	541.51		
S12P28	.03	Null	P5H35	1.59	-2.162(0)	P12H6	5.72	7.109(0)	541.61		
P5P9	.43	4.955(-1)	P5H34	1.80	-2.782(0)	P12H7	5.82	7.175(0)	541.56		
P5P24	.56	6.162(-1)	P5H33	2.00	-2.430(0)	P12H8	5.92	7.363(0)	542.05		
P5P8	.94	1.470(0)	P5H32	2.15	-2.087(0)	P12H9	6.02	7.211(0)	541.97		
P5P23	1.02	8.719(-1)	P5H31	2.24	-2.114(0)	P12H10	6.12	7.310(0)	542.00		
P5P7	1.45	3.157(0)	P5H30	2.34	-2.176(0)	P12H12	6.30	7.539(0)	541.93		
P5P22	1.53	2.240(0)	P5H29	2.43	-1.645(0)	P12H13	6.39	8.045(0)	542.48		
P5P21	2.04	2.842(0)	P5H28	2.53	-1.038(0)	P12H14	6.48	7.860(0)	542.45		
P5P5	2.72	4.439(0)	P5H27	2.63	-1.091(0)	P12H15	6.56	8.059(0)	542.69		
P5P18	2.79	4.513(0)	P5H26	2.72	-1.658(-1)	P12H16	6.66	8.234(0)	542.92		
P5P4	3.23	4.752(0)	P5H25	2.82	-3.385(-1)	P12H17	6.74	9.058(0)	543.52		
P5P16	3.31	5.157(0)	P5H24	2.91	1.714(-1)	P12H18	6.84	8.880(0)	543.48		
P5P3	3.73	5.034(0)	P5H23	3.02	4.583(-1)	P12H19	6.93	8.988(0)	543.56		
P5P14	3.87	5.355(0)	P5H22	3.14	8.310(-1)	P12H20	7.02	8.341(0)	542.95		
P5P12	4.34	4.390(0)	P5H21	3.23	1.362(0)	P12H22	8.01	1.186(1)	545.87		
P5P1	4.76	4.521(0)	P5H20	3.33	1.447(0)	P12H23	8.66	1.468(1)	548.18		
P5P10	4.85	6.383(0)	P5H19	3.43	1.523(0)	P12H25	9.92	1.771(1)	550.48		
P12P1	5.47	Null	P5H18	3.53	1.459(0)	P12H26	10.57	1.844(1)	551.08		
P12P2	6.11	4.870(0)	P5H17	3.62	2.068(0)	P12H28	11.85	2.066(1)	553.12		
P12P3	6.76	4.901(0)	P5H16	3.72	2.335(0)	P12H29	12.49	2.140(1)	554.02		
P12P4	7.39	3.996(0)	P5H15	3.82	2.519(0)	P12H31	13.78	2.049(1)	553.33		
P12P5	8.03	4.538(0)	P5H14	3.92	2.700(0)	P12H33	15.06	1.800(1)	551.32		
P12P6	8.68	4.333(0)	P5H13	4.01	2.898(0)	P12H35	16.33	1.448(1)	548.45		
P12P7	9.31	4.628(0)	P5H12	4.09	2.396(0)	P12H36					

Run 60 Reduced Data Tabulation

Gauge Label	Loc. (in)	Value (PSIA) or (BTU/Ft ² -Sec)	T Surf (DegR)	Gauge Label	Loc. (in)	Value (PSIA) or (BTU/Ft ² -Sec)	T Surf (DegR)	Gauge Label	Loc. (in)	Value (PSIA) or (BTU/Ft ² -Sec)	T Surf (DegR)
L28P1	-26.28	1.322(0)	P12P8	9.95	4.126(0)	P5H11	4.14	3.208(1)	572.92		
L28P3	-18.28	1.287(0)	P12P13	13.15	4.446(0)	P5H10	4.22	3.096(1)	571.52		
L28P5	-10.28	Null	P12P16	15.07	3.737(0)	P5H9	4.31	Null	Null		
S12P2	-1.90	Null	P5S4	2.89	Null	P5H8	4.40	3.151(1)	572.62		
S12P3	-1.90	Null	P5S2	4.25	Null	P5H7	4.50	3.250(1)	573.96		
S12P4	-1.90	Null	L28H3	-27.28	1.537(1)	P5H6	4.59	3.181(1)	573.09		
S12P7	-1.60	Null	L28H6	-24.28	1.434(1)	P5H5	4.69	3.180(1)	573.37		
S12P8	-1.60	Null	L28H11	-18.28	1.137(1)	P5H4	4.79	3.253(1)	574.13		
S12P9	-1.60	Null	L28H13	-15.28	1.118(1)	P5H3	4.89	3.189(1)	573.41		
S12P10	-1.60	Null	L28H18	-9.28	1.049(1)	P5H2	4.98	2.827(1)	569.23		
S12P13	.98	Null	P5H42	.13	Null	P5H1	5.08	6.904(1)	611.91		
S12P17	.03	2.407(-1)	P5H41	.32	3.217(0)	P12H1	5.24	5.259(1)	596.61		
S12P19	.03	Null	P5H40	.52	7.480(0)	P12H2	5.33	Null	Null		
S12P25	.03	2.847(-1)	P5H39	.72	8.957(0)	P12H3	5.43	3.730(1)	580.14		
S12P26	.03	3.168(-1)	P5H37	1.18	8.784(0)	P12H4	5.53	3.532(1)	577.91		
S12P27	.03	2.870(-1)	P5H36	1.39	1.973(1)	P12H5	5.63	3.419(1)	576.72		
S12P28	.03	Null	P5H35	1.59	2.070(1)	P12H6	5.72	3.438(1)	576.66		
P5P9	.43	4.316(-1)	P5H34	1.80	2.135(1)	P12H7	5.82	3.258(1)	574.65		
P5P24	.56	5.019(-1)	P5H33	2.00	2.291(1)	P12H8	5.92	3.582(1)	578.07		
P5P8	.94	1.255(0)	P5H32	2.15	2.352(1)	P12H9	6.02	3.393(1)	576.02		
P5P23	1.02	7.053(-1)	P5H31	2.24	2.574(1)	P12H10	6.12	3.333(1)	575.64		
P5P7	1.45	2.757(0)	P5H30	2.34	2.456(1)	P12H12	6.30	3.345(1)	575.69		
P5P22	1.53	1.881(0)	P5H29	2.43	2.459(1)	P12H13	6.39	3.412(1)	576.37		
P5P21	2.04	2.620(0)	P5H28	2.53	2.525(1)	P12H14	6.48	3.286(1)	574.87		
P5P5	2.72	4.189(0)	P5H27	2.63	2.484(1)	P12H15	6.56	3.288(1)	575.08		
P5P18	2.79	4.187(0)	P5H26	2.72	2.617(1)	P12H16	6.66	3.316(1)	575.46		
P5P4	3.23	4.495(0)	P5H25	2.82	2.747(-1)	P12H17	6.74	3.496(1)	577.37		
P5P16	3.31	4.969(0)	P5H24	2.91	2.509(1)	P12H18	6.84	3.370(1)	576.01		
P5P3	3.73	4.934(0)	P5H23	3.02	2.759(1)	P12H19	6.93	3.308(1)	575.47		
P5P14	3.87	5.211(0)	P5H22	3.14	3.172(1)	P12H20	7.02	2.905(1)	570.81		
P5P12	4.34	4.318(0)	P5H21	3.23	2.858(1)	P12H22	8.01	3.370(1)	576.43		
P5P1	4.76	4.756(0)	P5H20	3.33	2.889(1)	P12H23	8.66	3.499(1)	578.10		
P5P10	4.85	5.047(0)	P5H19	3.43	2.975(1)	P12H25	9.92	3.534(1)	578.02		
P12P1	5.47	Null	P5H18	3.53	2.352(1)	P12H26	10.57	3.363(1)	576.01		
P12P2	6.11	5.055(0)	P5H17	3.62	2.978(1)	P12H28	11.85	3.350(1)	576.00		
P12P3	6.76	5.079(0)	P5H16	3.72	3.096(1)	P12H29	12.49	3.386(1)	576.36		
P12P4	7.39	4.199(0)	P5H15	3.82	3.075(1)	P12H31	13.78	2.862(1)	570.32		
P12P5	8.03	4.703(0)	P5H14	3.92	3.146(1)	P12H33	15.06	2.663(1)	568.25		
P12P6	8.68	4.547(0)	P5H13	4.01	3.181(1)	P12H35	16.33	2.107(1)	561.78		
P12P7	9.31	4.783(0)	P5H12	4.09	2.902(1)	P12H36					

Run 61 Reduced Data Tabulation

Gauge	Loc.	Value (PSIA) or (BTU/Ft ² -Sec)	T Surf	Gauge	Loc.	Value (PSIA) or (BTU/Ft ² -Sec)	T Surf	Gauge	Loc.	Value (PSIA) or (BTU/Ft ² -Sec)	T Surf
Label	(in)	(DegR)		Label	(in)	(DegR)		Label	(in)	(DegR)	
L28P1	-26.28	1.319(0)	P12P8	9.95	1.108(1)	P5H11	4.14	3.126(1)	562.34		
L28P3	-18.28	1.322(0)	P12P13	13.15	8.469(0)	P5H10	4.22	2.862(1)	560.61		
L28P5	-10.28	8.527(-1)	P12P16	15.07	5.085(0)	P5H9	4.31	Null	Null		
S12P2	-1.90	Null	P5S4	2.89	Null	P5H8	4.40	3.350(1)	564.98		
S12P3	-1.90	Null	P5S2	4.25	Null	P5H7	4.50	3.699(1)	568.20		
S12P4	-1.90	Null	L28H3	-27.28	1.536(1)	P5H6	4.59	3.779(1)	569.02		
S12P7	-1.60	Null	L28H6	-24.28	1.457(1)	P5H5	4.69	4.100(1)	571.46		
S12P8	-1.60	Null	L28H11	-18.28	1.235(1)	P5H4	4.79	4.429(1)	574.39		
S12P9	-1.60	Null	L28H13	-15.28	1.178(1)	P5H3	4.89	4.815(1)	576.90		
S12P10	-1.60	Null	L28H18	-9.28	1.097(1)	P5H2	4.98	5.084(1)	583.10		
S12P13	-.98	Null	P5H42	.13	Null	P5H1	5.08	3.698(1)	566.80		
S12P17	-.03	2.004(0)	P5H41	.32	4.810(-1)	P12H1	5.24	7.657(1)	601.77		
S12P19	-.03	Null	P5H40	.52	2.585(-1)	P12H2	5.33	Null	Null		
S12P25	-.03	1.906(0)	P5H39	.72	1.848(-1)	P12H3	5.43	6.608(1)	594.15		
S12P26	-.03	1.843(0)	P5H37	1.18	6.270(-1)	P12H4	5.53	6.560(1)	593.87		
S12P27	-.03	1.880(0)	P5H36	1.39	8.270(-1)	P12H5	5.63	6.625(1)	594.03		
S12P28	-.03	Null	P5H35	1.59	9.068(-1)	P12H6	5.72	6.799(1)	595.98		
P5P9	.43	1.529(0)	P5H34	1.80	9.649(-1)	P12H7	5.82	6.494(1)	594.17		
P5P24	.56	2.143(0)	P5H33	2.00	1.279(0)	P12H8	5.92	7.311(1)	601.62		
P5P8	.94	3.754(0)	P5H32	2.15	1.624(0)	P12H9	6.02	6.897(1)	599.80		
P5P23	1.02	2.712(0)	P5H31	2.24	2.497(0)	P12H10	6.12	6.969(1)	600.98		
P5P7	1.45	3.804(0)	P5H30	2.34	3.168(0)	P12H12	6.30	7.075(1)	603.34		
P5P22	1.53	3.034(0)	P5H29	2.43	3.897(0)	P12H13	6.39	7.250(1)	605.63		
P5P21	2.04	3.185(0)	P5H28	2.53	4.686(0)	P12H14	6.48	7.115(1)	604.85		
P5P5	2.72	5.745(0)	P5H27	2.63	6.213(0)	P12H15	6.56	7.193(1)	605.87		
P5P18	2.79	6.325(0)	P5H26	2.72	7.310(0)	P12H16	6.66	7.407(1)	608.20		
P5P4	3.23	7.055(0)	P5H25	2.82	8.547(0)	P12H17	6.74	7.785(1)	611.89		
P5P16	3.31	8.194(0)	P5H24	2.91	9.779(0)	P12H18	6.84	7.532(1)	610.78		
P5P3	3.73	8.615(0)	P5H23	3.02	1.151(1)	P12H19	6.93	7.503(1)	610.38		
P5P14	3.87	1.178(1)	P5H22	3.14	1.329(1)	P12H20	7.02	6.572(1)	602.37		
P5P12	4.34	9.528(0)	P5H21	3.23	1.295(1)	P12H22	8.01	7.863(1)	617.71		
P5P1	4.76	1.114(1)	P5H20	3.33	1.447(1)	P12H23	8.66	8.028(1)	621.77		
P5P10	4.85	1.540(1)	P5H19	3.43	1.632(1)	P12H25	9.92	7.935(1)	620.98		
P12P1	5.47	Null	P5H18	3.53	1.461(1)	P12H26	10.57	7.335(1)	615.76		
P12P2	6.11	1.268(1)	P5H17	3.62	1.932(1)	P12H28	11.85	6.906(1)	612.91		
P12P3	6.76	1.317(1)	P5H16	3.72	2.137(1)	P12H29	12.49	6.426(1)	608.30		
P12P4	7.39	1.135(1)	P5H15	3.82	1.455(1)	P12H31	13.78	4.301(1)	585.78		
P12P5	8.03	1.324(1)	P5H14	3.92	2.431(1)	P12H33	15.06	3.316(1)	574.83		
P12P6	8.68	1.268(1)	P5H13	4.01	2.613(1)	P12H35	16.33	2.510(1)	565.97		
P12P7	9.31	1.349(1)	P5H12	4.09	2.550(1)	P5H09					

Run 62 Reduced Data Tabulation

Gauge	Loc.	Value (PSIA) or (BTU/Ft ² -Sec)	T Surf	Gauge	Loc.	Value (PSIA) or (BTU/Ft ² -Sec)	T Surf	Gauge	Loc.	Value (PSIA) or (BTU/Ft ² -Sec)	T Surf
Label	(in)	(DegR)		Label	(in)	(DegR)		Label	(in)	(DegR)	
L28P1	-26.28	1.362(0)	P12P8	9.95	1.124(1)	P5H11	4.14	7.727(1)	600.11		
L28P3	-18.28	1.314(0)	P12P13	13.15	8.383(0)	P5H10	4.22	6.845(1)	594.12		
L28P5	-10.28	2.728(0)	P12P16	15.07	2.258(0)	P5H9	4.31	Null	Null		
S12P2	-1.90	Null	P5S4	2.89	Null	P5H8	4.40	7.308(1)	599.48		
S12P3	-1.90	Null	P5S2	4.25	Null	P5H7	4.50	7.769(1)	604.54		
S12P4	-1.90	Null	L28H3	-27.28	1.581(1)	P5H82	4.59	7.670(1)	604.54		
S12P7	-1.60	Null	L28H6	-24.28	1.438(1)	P5H37	4.69	7.837(1)	606.45		
S12P8	-1.60	Null	L28H11	-18.28	1.169(1)	P5H3	4.79	8.016(1)	608.77		
S12P9	-1.60	Null	L28H13	-15.28	1.213(1)	P5H4	4.89	7.976(1)	609.39		
S12P10	-1.60	Null	L28H18	-9.28	1.044(1)	P5H2	4.98	8.337(1)	618.42		
S12P13	-.98	Null	P5H42	.13	Null	P5H1	5.08	6.643(1)	586.36		
S12P17	-.03	2.492(-1)	P5H41	.32	3.127(0)	P12H1	5.24	1.246(2)	650.19		
S12P19	-.03	Null	P5H40	.52	7.522(0)	P12H2	5.33	Null	Null		
S12P25	-.03	3.138(-1)	P5H39	.72	8.655(0)	P12H3	5.43	9.927(1)	627.36		
S12P26	-.03	3.200(-1)	P5H37	1.18	7.817(0)	P12H4	5.53	9.563(1)	624.52		
S12P27	-.03	3.061(-1)	P5H36	1.39	7.827(0)	P12H5	5.63	9.362(1)	622.60		
S12P28	-.03	Null	P5H35	1.59	1.100(1)	P12H6	5.72	9.370(1)	623.89		
P5P9	.43	4.849(-1)	P5H34	1.80	1.546(1)	P12H7	5.82	8.879(1)	619.93		
P5P24	.56	5.466(-1)	P5H33	2.00	1.361(1)	P12H8	5.92	9.898(1)	629.77		
P5P8	.94	9.391(-1)	P5H32	2.15	1.341(1)	P12H9	6.02	9.316(1)	625.21		
P5P23	1.02	7.252(-1)	P5H31	2.24	1.470(1)	P12H10	6.12	9.455(1)	627.05		
P5P7	1.45	2.459(0)	P5H30	2.34	1.443(1)	P12H12	6.30	9.217(1)	625.33		
P5P22	1.53	1.296(0)	P5H29	2.43	1.595(1)	P12H13	6.39	9.392(1)	627.62		
P5P21	2.04	2.548(0)	P5H28	2.53	1.980(1)	P12H14	6.48	9.075(1)	625.23		
P5P5	2.72	4.487(0)	P5H27	2.63	2.380(1)	P12H15	6.56	9.081(1)	625.46		
P5P18	2.79	5.121(0)	P5H26	2.72	2.968(1)	P12H16	6.66	9.231(1)	627.32		
P5P4	3.23	7.203(0)	P5H25	2.82	3.532(1)	P12H17	6.74	9.694(1)	631.48		
P5P16	3.31	8.453(0)	P5H24	2.91	3.625(1)	P12H18	6.84	9.312(1)	628.62		
P5P3	3.73	1.089(1)	P5H23	3.02	3.994(1)	P12H19	6.93	9.148(1)	627.45		
P5P14	3.87	1.643(1)	P5H22	3.14	4.533(1)	P12H20	7.02	7.803(1)	614.91		
P5P12	4.34	1.165(1)	P5H21	3.23	4.541(1)	P12H22	8.01	8.730(1)	627.24		
P5P1	4.76	1.292(1)	P5H20	3.33	4.737(1)	P12H23	8.66	8.836(1)	628.85		
P5P10	4.85	1.451(1)	P5H19	3.43	5.146(1)	P12H25	9.92	8.379(1)	624.82		
P12P1	5.47	Null	P5H18	3.53	4.316(1)	P12H26	10.57	7.851(1)	618.96		
P12P2	6.11	1.462(1)	P5H17	3.62	5.589(1)	P12H28	11.85	7.136(1)	612.05		
P12P3	6.76	1.442(1)	P5H16	3.72	6.059(1)	P12H29	12.49	6.713(1)	606.99		
P12P4	7.39	1.144(1)	P5H15	3.82	2.269(1)	P12H31	13.78	4.587(1)	581.97		
P12P5	8.03	1.379(1)	P5H14	3.92	6.559(1)	P12H33	15.06	3.428(1)	571.07		
P12P6	8.68	1.285(1)	P5H13	4.01	6.689(1)	P12H35	16.33	2.569(1)	561.80		
P12P7	9.31	1.364(1)	P5H12	4.09	6.240(1)	P5H09					

Run 63 Reduced Data Tabulation

Gauge	Loc.	Value (PSIA) or (in)	T Surf (BTU/Ft ² -Sec)	Gauge	Loc.	Value (PSIA) or (in)	T Surf (BTU/Ft ² -Sec)	Gauge	Loc.	Value (PSIA) or (in)	T Surf (BTU/Ft ² -Sec)	
Label			(DegR)	Label			(DegR)	Label			(DegR)	
L28P1	-26.28	7.704(-1)	P12P8	9.95	8.743(-1)	P12P13	13.15	1.067(0)	P5H11	4.14	2.903(-1)	
L28P3	-18.28	1.393(0)	P12P16	15.07	1.131(0)	P5H10	4.22	3.278(-1)	P5H9	4.31	Null	
L28P5	-10.28	1.096(0)	P5S4	2.89	Null	P5H8	4.40	2.058(-1)	P5H6	4.59	3.749(-1)	
S12P2	-1.90	Null	P5S2	4.25	Null	P5H5	4.69	3.938(-1)	P5H4	4.79	4.444(-1)	
S12P3	-1.90	Null	L28H3	-27.28	1.562(1)	555.53	P5H3	4.89	6.803(-1)	P5H7	4.50	3.978(-1)
S12P4	-1.90	Null	L28H6	-24.28	1.407(1)	553.50	P5H2	4.98	8.393(-1)	P5H1	5.08	2.011(0)
S12P7	-1.60	Null	L28H11	-18.28	1.245(1)	550.29	P5H1	5.08	1.094(0)	P12H1	5.24	1.094(0)
S12P8	-1.60	Null	L28H13	-15.28	1.199(1)	550.00	P12H3	5.43	1.054(0)	P12H3	5.53	1.054(0)
S12P9	-1.60	Null	L28H18	-9.28	1.038(1)	548.24	P12H4	5.53	1.014(0)	P12H4	5.63	1.014(0)
S12P10	-1.60	Null	P5H42	.13	Null	P12H5	5.63	9.450(-1)	P12H5	5.72	1.056(0)	
S12P13	-.98	Null	P5H41	.32	-1.319(0)	532.63	P12H6	5.82	8.887(-1)	P12H6	5.92	1.190(0)
S12P17	-.03	1.094(0)	P5H40	.52	-4.833(-1)	534.00	P12H7	6.02	9.504(-1)	P12H7	6.12	9.227(-1)
S12P19	-.03	Null	P5H39	.72	-1.711(-1)	534.74	P12H8	6.30	9.628(-1)	P12H10	6.39	1.173(0)
S12P25	-.03	1.027(0)	P5H17	1.18	-2.096(-1)	534.76	P12H12	6.48	1.196(0)	P12H13	6.48	1.196(0)
S12P26	-.03	1.033(0)	P5H36	1.39	-3.449(-1)	533.93	P12H14	6.56	1.054(0)	P12H15	6.66	1.118(0)
S12P27	-.03	9.672(-1)	P5H35	1.59	-1.771(0)	532.77	P12H16	6.66	1.118(0)	P12H17	6.74	1.096(0)
S12P28	-.03	Null	P5H34	1.80	-1.636(0)	532.88	P12H18	6.84	1.149(0)	P12H19	6.93	1.154(0)
P5P9	.43	2.257(-1)	P5H33	2.00	-1.380(0)	533.15	P12H20	7.02	1.148(0)	P12H21	7.02	1.331(0)
P5P24	.56	2.706(-1)	P5H32	2.15	-1.202(0)	533.38	P12H22	8.01	2.153(0)	P12H23	8.66	1.430(0)
P5P8	.94	9.595(-1)	P5H31	2.24	Null	P12H24	8.66	1.594(0)	P12H25	9.92	1.594(0)	
P5P23	1.02	4.645(-1)	P5H30	2.34	-9.123(-1)	533.73	P12H26	10.57	1.566(0)	P12H26	10.57	1.566(0)
P5P7	1.45	8.898(-1)	P5H29	2.43	Null	P12H28	11.85	Null	P12H29	12.49	1.887(0)	
P5P22	1.53	7.170(-1)	P5H28	2.53	-8.462(-1)	534.00	P12H31	13.78	1.911(0)	P12H31	13.78	1.911(0)
P5P21	2.04	7.231(-1)	P5H27	2.63	-7.671(-1)	534.10	P12H22	15.06	2.153(0)	P12H33	15.06	2.153(0)
P5P5	2.72	9.403(-1)	P5H26	2.72	-6.628(-1)	534.22	P12H35	16.33	2.224(0)	P12H35	16.33	2.224(0)
P5P18	2.79	9.290(-1)	P5H25	2.82	-3.797(-1)	534.36	P12H17	6.74	1.096(0)	P12H17	6.74	1.096(0)
P5P4	3.23	8.777(-1)	P5H24	2.91	-2.633(-1)	534.57	P12H19	6.93	1.154(0)	P12H19	6.93	1.154(0)
P5P16	3.31	9.829(-1)	P5H23	3.02	-3.820(-1)	534.52	P12H20	7.02	1.148(0)	P12H20	7.02	1.148(0)
P5P3	3.73	Null	P5H22	3.14	-2.150(-1)	534.63	P12H22	8.01	1.331(0)	P12H22	8.01	1.331(0)
P5P14	3.87	9.940(-1)	P5H21	3.23	Null	P12H23	8.66	1.430(0)	P12H23	8.66	1.430(0)	
P5P12	4.34	8.219(-1)	P5H20	3.33	-4.174(-2)	534.78	P12H25	9.92	1.594(0)	P12H25	9.92	1.594(0)
P5P1	4.76	8.443(-1)	P5H19	3.43	-1.960(-1)	534.81	P12H26	10.57	1.566(0)	P12H26	10.57	1.566(0)
P5P10	4.85	1.234(0)	P5H18	3.53	-4.497(-2)	534.98	P12H28	11.85	Null	P12H29	12.49	1.887(0)
P12P1	5.47	Null	P5H17	3.62	1.034(-1)	534.96	P12H31	13.78	1.911(0)	P12H31	13.78	1.911(0)
P12P2	6.11	9.837(-1)	P5H16	3.72	-5.081(-2)	534.97	P12H33	15.06	2.153(0)	P12H33	15.06	2.153(0)
P12P3	6.76	1.049(0)	P5H15	3.82	Null	P12H35	16.33	2.224(0)	P12H35	16.33	2.224(0)	
P12P4	7.39	8.692(-1)	P5H14	3.92	1.877(-1)	535.19	P12H17	6.74	1.096(0)	P12H17	6.74	1.096(0)
P12P5	8.03	9.895(-1)	P5H13	4.01	-7.798(-3)	535.08	P12H18	7.02	1.149(0)	P12H18	7.02	1.149(0)
P12P6	8.68	9.568(-1)	P5H12	4.09	1.580(-1)	535.08	P5H12	8.01	Null	P5H12	8.01	Null

Run 65 Reduced Data Tabulation

Gauge	Loc.	Value (PSIA) or (in)	T Surf (BTU/Ft ² -Sec)	Gauge	Loc.	Value (PSIA) or (in)	T Surf (BTU/Ft ² -Sec)	Gauge	Loc.	Value (PSIA) or (in)	T Surf (DegR)	
Label			(DegR)	Label			(DegR)	Label				
L28P1	-26.28	8.559(-1)	P12P8	9.95	8.322(-1)	P12P13	13.15	1.031(0)	P5H11	4.14	6.620(0)	
L28P3	-18.28	1.358(0)	P12P16	15.07	1.104(0)	P5H10	4.22	6.523(0)	P5H9	4.31	Null	
L28P5	-10.28	1.122(0)	P5S4	2.89	Null	P5H8	4.40	6.761(0)	P5H7	4.50	7.105(0)	
S12P2	-1.90	Null	P5S2	4.25	Null	P5H6	4.59	6.796(0)	P5H5	4.69	6.618(0)	
S12P3	-1.90	Null	L28H3	-27.28	1.556(1)	555.32	P5H4	4.79	6.693(0)	P5H4	4.89	6.485(0)
S12P4	-1.90	Null	L28H6	-24.28	1.385(1)	553.54	P5H2	4.98	4.602(0)	P5H2	5.08	4.143(1)
S12P7	-1.60	Null	L28H11	-18.28	1.141(1)	550.09	P12H1	5.24	9.669(0)	P12H1	5.43	7.882(0)
S12P8	-1.60	Null	L28H13	-15.28	1.161(1)	549.88	P12H3	5.43	7.882(0)	P12H3	5.62	7.344(0)
S12P9	-1.60	Null	L28H18	-9.28	1.028(1)	548.25	P12H4	5.53	7.686(0)	P12H4	5.72	7.453(0)
S12P10	-1.60	Null	P5H42	.13	Null	P12H5	5.63	7.344(0)	P12H5	5.82	7.210(0)	
S12P13	-.98	Null	P5H41	.32	7.686(-1)	536.41	P12H7	5.82	7.659(0)	P12H7	5.92	7.659(0)
S12P17	-.03	1.755(-1)	P5H40	.52	1.717(0)	537.96	P12H8	5.92	7.659(0)	P12H8	6.02	7.732(0)
S12P19	-.03	Null	P5H39	.72	3.768(0)	541.08	P12H9	6.02	7.645(0)	P12H9	6.12	7.645(0)
S12P25	-.03	1.871(-1)	P5H37	1.18	7.903(0)	545.03	P12H10	6.12	7.645(0)	P12H10	6.30	7.595(0)
S12P26	-.03	1.886(-1)	P5H36	1.39	8.633(0)	545.32	P12H13	6.39	7.770(0)	P12H13	6.58	7.344(0)
S12P27	-.03	1.698(-1)	P5H35	1.59	7.744(0)	544.61	P12H14	6.48	7.327(0)	P12H14	6.66	544.35
S12P28	-.03	Null	P5H34	1.80	7.524(0)	544.48	P12H15	6.56	7.563(0)	P12H15	6.75	544.36
P5P9	.43	1.825(-1)	P5H33	2.00	7.570(0)	544.55	P12H16	6.66	7.607(0)	P12H16	6.86	544.88
P5P24	.56	1.967(-1)	P5H32	2.15	7.202(0)	544.27	P12H17	6.74	8.009(0)	P12H17	6.93	544.98
P5P8	.94	7.572(-1)	P5H31	2.24	7.688(0)	544.85	P12H18	6.84	7.675(0)	P12H18	7.02	544.60
P5P23	1.02	4.378(-1)	P5H30	2.34	7.433(0)	544.55	P12H19	6.93	7.576(0)	P12H19	7.11	544.48
P5P7	1.45	7.576(-1)	P5H29	2.43	7.235(0)	544.33	P12H20	7.02	7.690(0)	P12H20	7.21	544.76
P5P22	1.53	5.983(-1)	P5H28	2.53	7.504(0)	544.46	P12H22	8.01	Null	P12H22	8.01	Null
P5P21	2.04	6.261(-1)	P5H27	2.63	7.219(0)	544.24	P12H23	8.66	8.146(0)	P12H23	8.66	8.146(0)
P5P5	2.72	8.123(-1)	P5H26	2.72	7.358(0)	544.44	P12H25	9.92	7.996(0)	P12H25	9.92	7.996(0)
P5P18	2.79	7.868(-1)	P5H25	2.82	7.751(0)	544.72	P12H26	10.57	7.786(0)	P12H26	10.57	7.786(0)
P5P4	3.23	7.638(-1)	P5H24	2.91	6.911(0)	543.69	P12H27	8.01	Null	P12H27	8.01	Null
P5P16	3.31	8.444(-1)	P5H23	3.02	7.165(0)	544.21	P12H28	7.02	7.690(0)	P12H28	7.02	7.690(0)
P5P3	3.73	8.355(-1)	P5H22	3.14	7.854(0)	544.84	P12H29	8.66	8.146(0)	P12H29	8.66	8.146(0)
P5P14	3.87	8.436(-1)	P5H21	3.23	6.867(0)	543.92	P12H31	13.78	6.959(0)	P12H31	13.78	6.959(0)
P5P12	4.34	6.947(-1)	P5H20	3.33	7.154(0)	543.98	P12H33	15.06	7.852(0)	P12H33	15.06	7.852(0)
P5P1	4.76	7.406(-1)	P5H19	3.43	7.214(0)	544.28	P12H35	16.33	7.675(0)	P12H35	16.33	7.675(0)
P5P10	4.85	1.025(0)	P5H18	3.53	7.013(0)	544.01	P12H17	3.62	7.050(0)	P12H17	3.62	7.050(0)
P12P1	5.47	Null	P5H17	3.62	7.050(0)	543.96	P12H29	12.49	8.118(0)	P12H29	12.49	8.118(0)
P12P2	6.11	8.441(-1)	P5H16	3.72	7.058(0)	544.06	P12H31	13.78	6.959(0)	P12H31	13.78	6.959(0)
P12P3	6.76	9.162(-1)	P5H15	3.82	Null	P12H33	15.06	7.852(0)	P12H33	15.06	7.852(0)	
P12P4	7.39	7.806(-1)	P5H14	3.92	6.988(0)	543.98						

Gauge Label	Loc. (in)	Value (PSIA) or (BTU/Ft ² -Sec)	T Surf (DegR)	Gauge Label	Loc. (in)	Value (PSIA) or (BTU/Ft ² -Sec)	T Surf (DegR)	Gauge Label	Loc. (in)	Value (PSIA) or (BTU/Ft ² -Sec)	T Surf (DegR)
L28P1	-26.28	8.243(-1)		P12P8	9.95	9.230(-1)		P5H11	4.14	-6.478(-1)	530.75
L28P3	-18.28	1.367(0)		P12P13	13.15	1.136(0)		P5H10	4.22	-6.292(-1)	530.72
L28P5	-10.28	1.161(0)		P12P16	15.07	1.168(0)		P5H9	4.31	Null	Null
S12P2	-1.90	Null		P5S4	2.89	Null		P5H8	4.40	-5.954(-1)	530.72
S12P3	-1.90	Null		P5S2	4.25	Null		P5H7	4.50	-7.017(-1)	530.66
S12P4	-1.90	Null		L28H3	-27.28	1.445(1)	550.57	P5H6	4.59	-5.408(-1)	530.75
S12P7	-1.60	Null		L28H6	-24.28	1.415(1)	549.53	P5H5	4.69	-5.664(-1)	530.79
S12P8	-1.60	Null		L28H11	-18.28	1.166(1)	546.34	P5H4	4.79	-4.556(-1)	530.81
S12P9	-1.60	Null		L28H13	-15.28	1.198(1)	546.42	P5H3	4.89	-2.135(-1)	531.08
S12P10	-1.60	Null		L28H18	-9.28	1.067(1)	544.82	P5H2	4.98	-1.450(-1)	531.42
S12P13	-.98	Null		P5H42	.13	Null		P5H1	5.08	3.837(-1)	531.89
S12P17	-.03	2.072(0)		P5H41	.32	-2.393(0)	527.94	P12H1	5.24	-6.218(-1)	530.72
S12P19	-.03	Null		P5H40	.52	-1.350(0)	529.30	P12H3	5.43	Null	Null
S12P25	-.03	1.889(0)		P5H39	.72	-5.574(-1)	530.39	P12H4	5.53	-6.007(-1)	530.84
S12P26	-.03	1.865(0)		P5H37	1.18	1.665(-1)	531.24	P12H5	5.63	-4.423(-1)	530.93
S12P27	-.03	1.905(0)		P5H36	1.39	1.051(0)	532.06	P12H6	5.72	-5.177(-1)	530.95
S12P28	-.03	Null		P5H35	1.59	-6.240(-1)	531.19	P12H7	5.82	-3.144(-1)	531.03
P5P9	.43	2.727(-1)		P5H34	1.80	-1.828(0)	529.75	P12H8	5.92	-4.813(-1)	530.97
P5P24	.56	3.391(-1)		P5H33	2.00	-1.875(0)	529.30	P12H9	6.02	-3.659(-1)	531.06
P5P8	.94	5.152(-1)		P5H32	2.15	-1.878(0)	529.38	P12H10	6.12	-3.170(-1)	531.07
P5P23	1.02	2.720(-1)		P5H31	2.24	-1.779(0)	529.37	P12H12	6.30	-4.231(-1)	531.16
P5P7	1.45	9.597(-1)		P5H30	2.34	-1.594(0)	529.55	P12H13	6.39	-4.566(-1)	531.16
P5P22	1.53	6.812(-1)		P5H29	2.43	-1.596(0)	529.67	P12H14	6.48	3.260(-2)	531.27
P5P21	2.04	8.853(-1)		P5H28	2.53	-1.275(0)	529.72	P12H15	6.56	-2.596(-1)	531.23
P5P5	2.72	9.961(-1)		P5H27	2.63	-1.332(0)	529.88	P12H16	6.66	-1.707(-1)	531.27
P5P18	2.79	9.286(-1)		P5H26	2.72	-1.428(0)	529.89	P12H17	6.74	-2.889(-1)	531.24
P5P4	3.23	9.043(-1)		P5H25	2.82	-1.223(0)	529.99	P12H18	6.84	-1.965(-1)	531.29
P5P16	3.31	1.034(0)		P5H24	2.91	-8.444(-1)	530.28	P12H19	6.93	-2.214(-1)	531.29
P5P3	3.73	Null		P5H23	3.02	-1.169(0)	530.17	P12H20	7.02	-2.263(-1)	531.35
P5P14	3.87	1.038(0)		P5H22	3.14	-1.056(0)	530.17	P12H22	8.01	Null	Null
P5P12	4.34	8.455(-1)		P5H21	3.23	-8.677(-1)	530.37	P12H23	8.66	1.251(-1)	531.73
P5P1	4.76	7.339(-1)		P5H20	3.33	-7.792(-1)	530.43	P12H25	9.92	2.229(-1)	531.83
P5P10	4.85	1.192(0)		P5H19	3.43	-9.399(-1)	530.41	P12H26	10.57	2.539(-1)	531.86
P12P1	5.47	Null		P5H18	3.53	-7.045(-1)	530.53	P12H28	11.85	Null	Null
P12P2	6.11	1.024(0)		P5H17	3.62	-8.338(-1)	530.45	P12H29	12.49	Null	Null
P12P3	6.76	1.118(0)		P5H16	3.72	-7.739(-1)	530.54	P12H31	13.78	4.670(-1)	532.10
P12P4	7.39	9.172(-1)		P5H15	3.82	Null		P12H33	15.06	5.583(-1)	532.24
P12P5	8.03	1.056(0)		P5H14	3.92	-7.570(-1)	530.55	P12H35	16.33	6.821(-1)	532.34
P12P6	8.68	1.297(0)		P5H13	4.01	-7.534(-1)	530.56				
P12P7	9.31	1.102(0)		P5H12	4.09	-8.427(-1)	530.54				

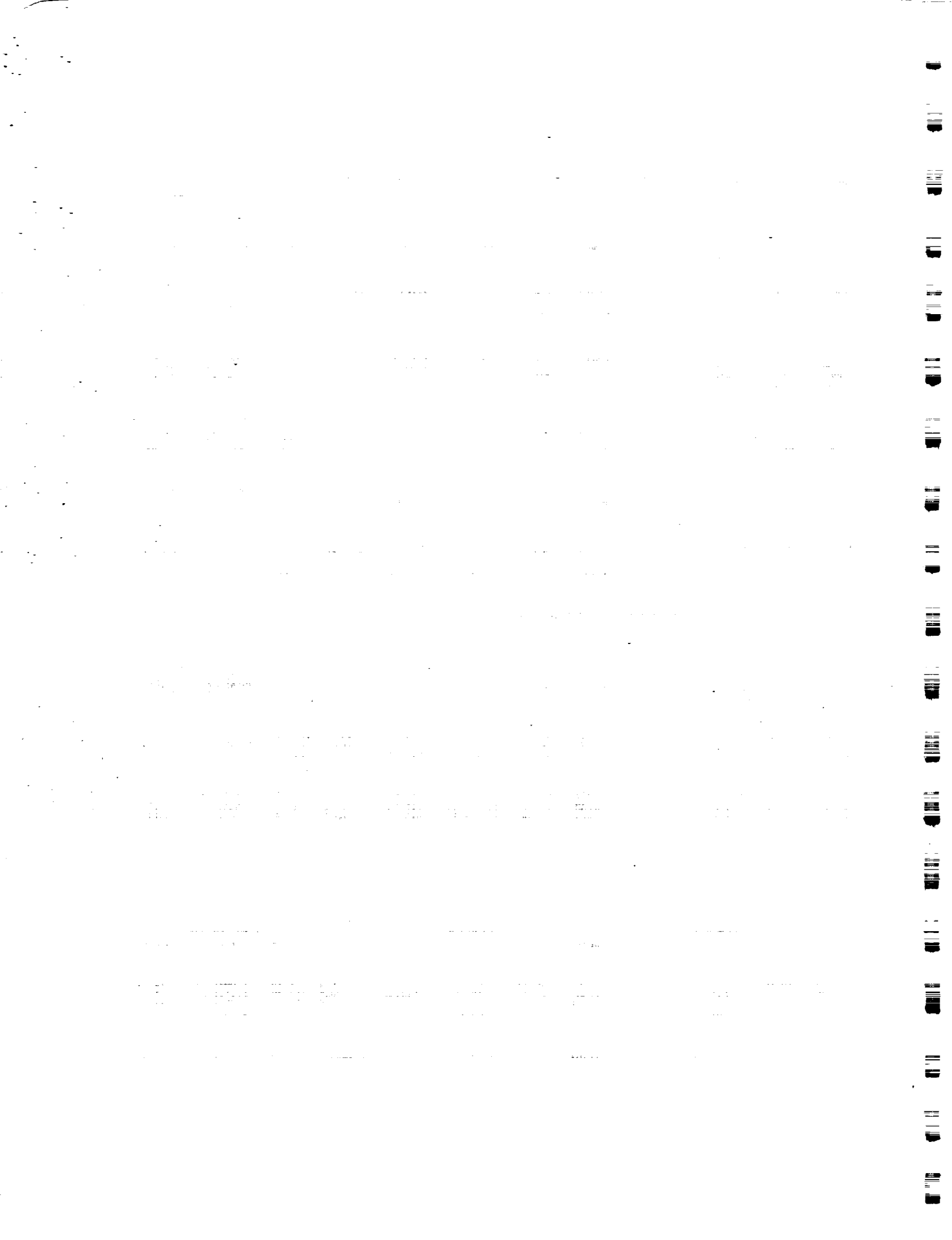
Run 67 Reduced Data Tabulation

Gauge Label	Loc. (in)	Value (PSIA) or (BTU/Ft ² -Sec)	T Surf (DegR)	Gauge Label	Loc. (in)	Value (PSIA) or (BTU/Ft ² -Sec)	T Surf (DegR)	Gauge Label	Loc. (in)	Value (PSIA) or (BTU/Ft ² -Sec)	T Surf (DegR)
L28P1	-26.28	Null		BLP7	.29	2.906(1)		L28H10	-19.28	1.236(1)	545.34
L28P2	-22.28	1.211(0)		BLP8	.35	3.861(1)		L28H11	-18.28	1.194(1)	544.60
L28P3	-18.28	Null		BLP9	.48	3.694(1)		L28H12	-16.28	Null	Null
L28P4	-14.28	7.582(-1)		L28H1	-30.28	Null		L28H13	-15.28	1.202(1)	544.84
L28P5	-10.28	Null		L28H2	-28.28	Null		L28H14	-14.28	1.142(1)	544.39
L28P6	-6.28	1.075(0)		L28H3	-27.28	1.510(1)	548.36	L28H15	-13.28	1.125(1)	544.24
BLP1	.02	7.666(0)		L28H4	-26.28	1.468(1)	547.43	L28H16	-12.28	1.134(1)	544.08
BLP2	.06	1.075(1)		L28H5	-25.28	1.479(1)	547.76	L28H17	-10.28	1.016(1)	543.03
BLP3	.10	1.343(1)		L28H6	-24.28	1.381(1)	547.42	L28H18	-9.28	1.085(1)	543.75
BLP4	.14	1.639(1)		L28H7	-22.28	1.286(1)	546.26	L28H19	-7.28	1.129(1)	543.80
BLP5	.19	1.959(1)		L28H8	-21.28	1.257(1)	545.55	L28H20	-6.28	Null	Null
BLP6	.24	2.373(1)		L28H9	-20.28	1.260(1)	545.57	L28H21	-5.28	Null	Null

Run 68 Reduced Data Tabulation

Gauge Label	Loc. (in)	Value (PSIA) or (BTU/Ft ² -Sec)	T Surf (DegR)	Gauge Label	Loc. (in)	Value (PSIA) or (BTU/Ft ² -Sec)	T Surf (DegR)	Gauge Label	Loc. (in)	Value (PSIA) or (BTU/Ft ² -Sec)	T Surf (DegR)
L28P1	-26.28	Null		BLP7	.54	5.926(1)		L28H10	-19.28	1.172(1)	546.45
L28P2	-22.28	Null		BLP8	.60	4.922(1)		L28H11	-18.28	1.106(1)	545.58
L28P3	-18.28	Null		BLP9	.73	3.995(1)		L28H12	-16.28	Null	Null
L28P4	-14.28	Null		L28H1	-30.28	Null		L28H13	-15.28	1.121(1)	545.66
L28P5	-10.28	Null		L28H2	-28.28	Null		L28H14	-14.28	1.083(1)	545.34
L28P6	-6.28	Null		L28H3	-27.28	1.487(1)	549.87	L28H15	-13.28	1.042(1)	544.98
BLP1	.27	Null		L28H4	-26.28	1.422(1)	548.89	L28H16	-12.28	1.049(1)	544.91
BLP2	.31	Null		L28H5	-25.28	1.432(1)	549.21	L28H17	-10.28	9.304(0)	543.86
BLP3	.35	Null		L28H6	-24.28	1.393(1)	548.88	L28H18	-9.28	1.015(1)	544.43
BLP4	.39	Null		L28H7	-22.28	1.264(1)	547.53	L28H19	-7.28	1.026(1)	544.72
BLP5	.44	5.464(1)		L28H8	-21.28	1.199(1)	546.70	L28H20	-6.28	Null	Null
BLP6	.49	8.707(1)		L28H9	-20.28	1.155(1)	546.50	L28H21	-5.28	Null	Null

Run 69 Reduced Data Tabulation



Appendix B
VELOCITY-PROFILE MEASUREMENTS

Test Conditions

Po =	2.7447X10+3 PSIA	Reservoir Total Pressure
Ho =	1.2530X10+7 (Ft/sec)2	Reservoir Total Enthalpy
To =	1.9825X10+3 degR	Reservoir Total Temperature
M =	6.4843	Freestream Mach Number
U =	4.7350X10+3 Ft/sec	Freestream Velocity
T =	2.2173X10+2 degR	Freestream Temperature
P =	1.0970 PSIA	Freestream Static Pressure
Rho =	4.1520X10-4 Slugs/Ft3	Freestream Density
Mu =	1.8322X10-7 Slugs/Ft-sec	Freestream Viscosity
Re =	1.0730X10+7 1/Ft	Freestream Reynolds Number
Po' =	6.0187X10+1 PSIA	Pitot Pressure
Q =	3.2323X10+1 PSIA	Dynamic Pressure (Rho U^2/288)
Mi =	2.6723	Shock Tube Incident Shock Mach Number
Tw =	5.3840X10+2 degR	Wall Temperature
QoFR=	5.6783X10+1 BTU/Ft2-s	Fay-Riddell Heat Transfer (.25' Diam Cylin.)

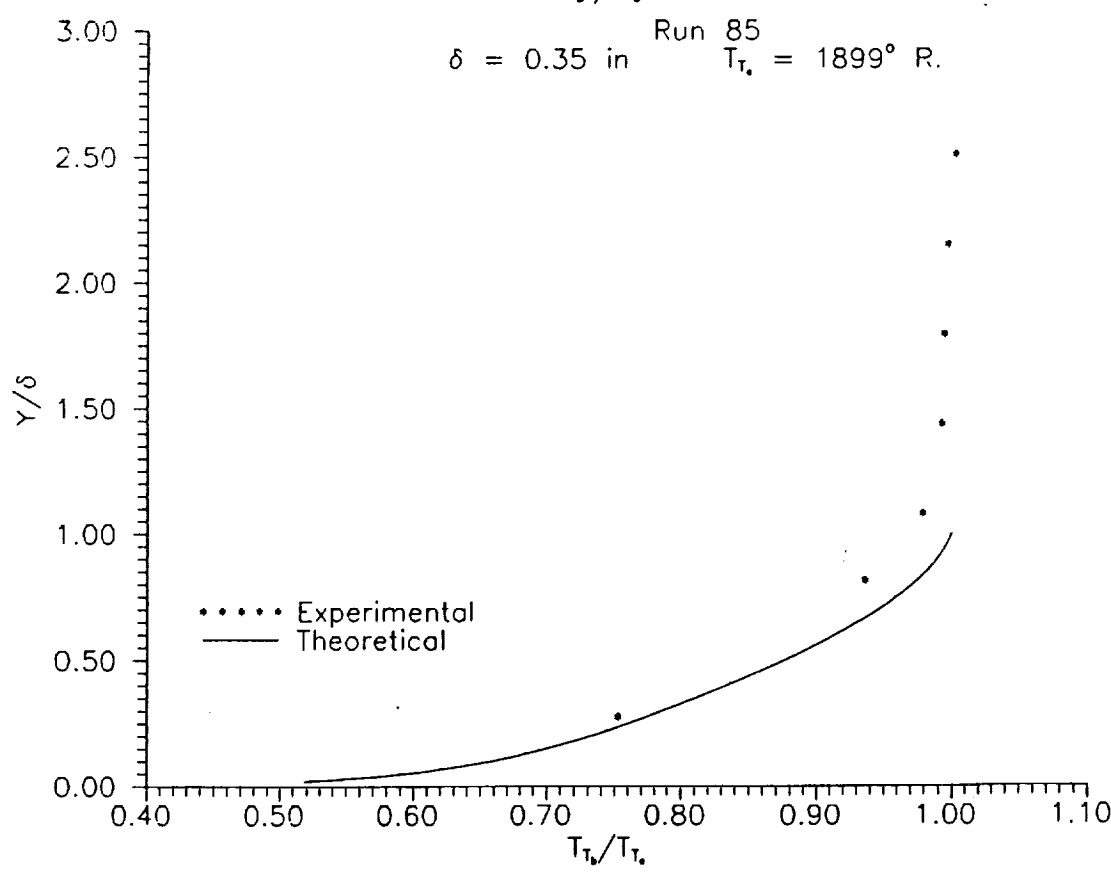
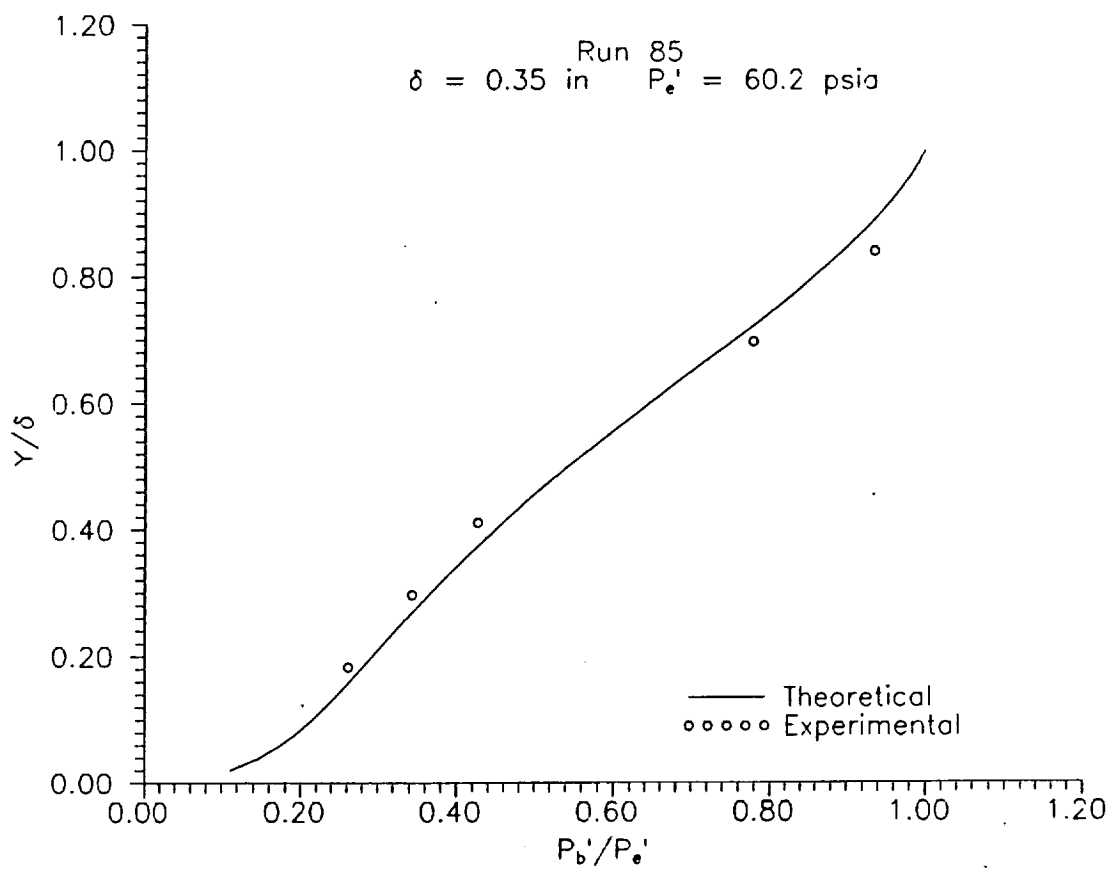
Model Parameter	Value
Plate length (in)	27.0
Run 85	

Gauge#	Location (inches)	Pressure (psia)
BL1	0.024	Null
BL2	0.064	15.780
BL3	0.104	20.700
BL4	0.144	25.700
BL5	0.194	Null
BL6	0.244	46.870
BL7	0.294	56.340
BL8	0.354	Null
BL9	0.414	Null

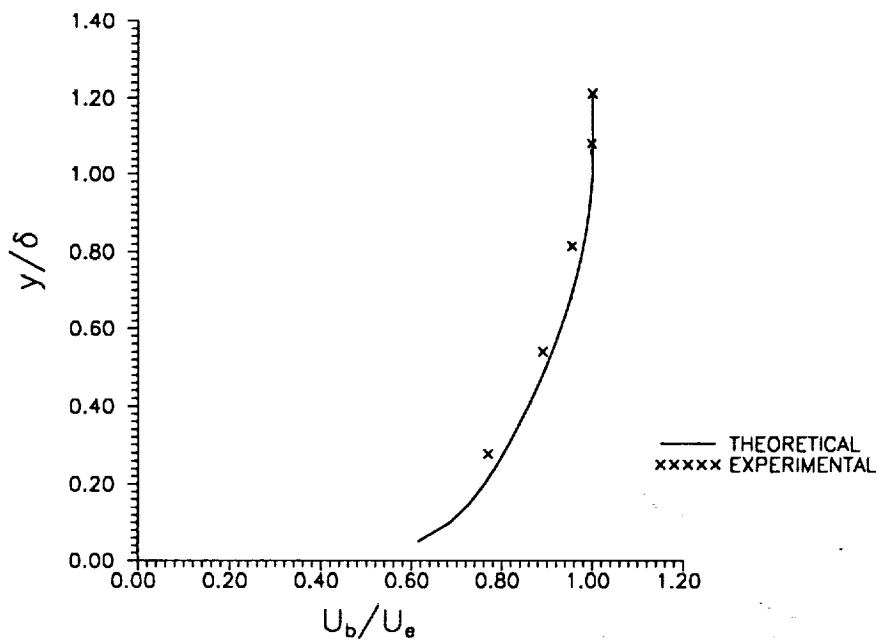
Pressure Data for Run 85

Gauge#	Location (inches)	Temperature deg R
TT1	0.097	1430.0
TT2	0.191	Null
TT3	0.285	1779.0
TT4	0.378	1860.0
TT5	0.503	1886.0
TT6	0.628	1890.0
TT7	0.753	1895.0
TT8	0.878	1905.0
TT9	1.003	1898.0

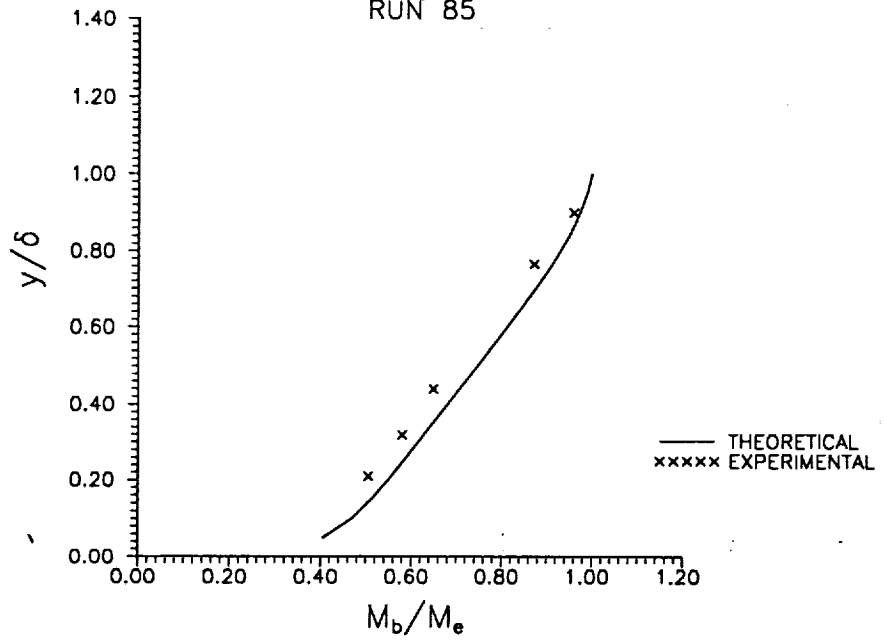
Total Temperature for Run 85



VELOCITY PROFILE
RUN 85



MACH NUMBER PROFILE
RUN 85



Test Conditions

Po =	2.7688X10+3 PSIA	Reservoir Total Pressure
Ho =	1.2078X10+7 (Ft/sec) 2	Reservoir Total Enthalpy
To =	1.9164X10+3 degR	Reservoir Total Temperature
M =	6.4911	Freestream Mach Number
U =	4.6493X10+3 Ft/sec	Freestream Velocity
T =	2.1333X10+2 degR	Freestream Temperature
P =	1.1101 PSIA	Freestream Static Pressure
Rho =	4.3669X10-4 Slugs/Ft ³	Freestream Density
Mu =	1.7667X10-7 Slugs/Ft-sec	Freestream Viscosity
Re =	1.1492X10+7 1/Ft	Freestream Reynolds Number
Po' =	6.1001X10+1 PSIA	Pitot Pressure
Q =	3.2776X10+1 PSIA	Dynamic Pressure (Rho U ² /288)
Mi =	2.6453	Shock Tube Incident Shock Mach Number
Tw =	5.3250X10+2 degR	Wall Temperature
QoFR=	5.4456X10+1 BTU/Ft ² -s	Fay-Riddell Heat Transfer (.25' Diam Cylin.)

Model Parameter Value

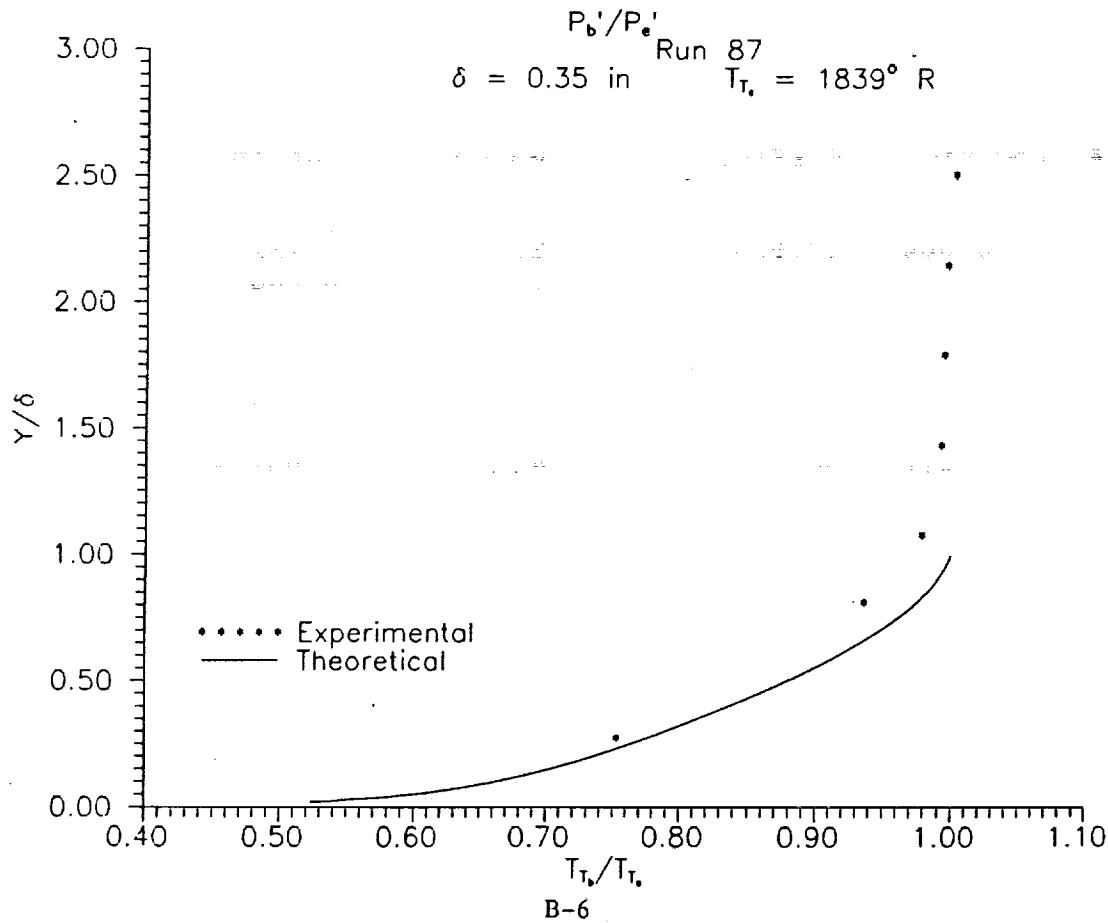
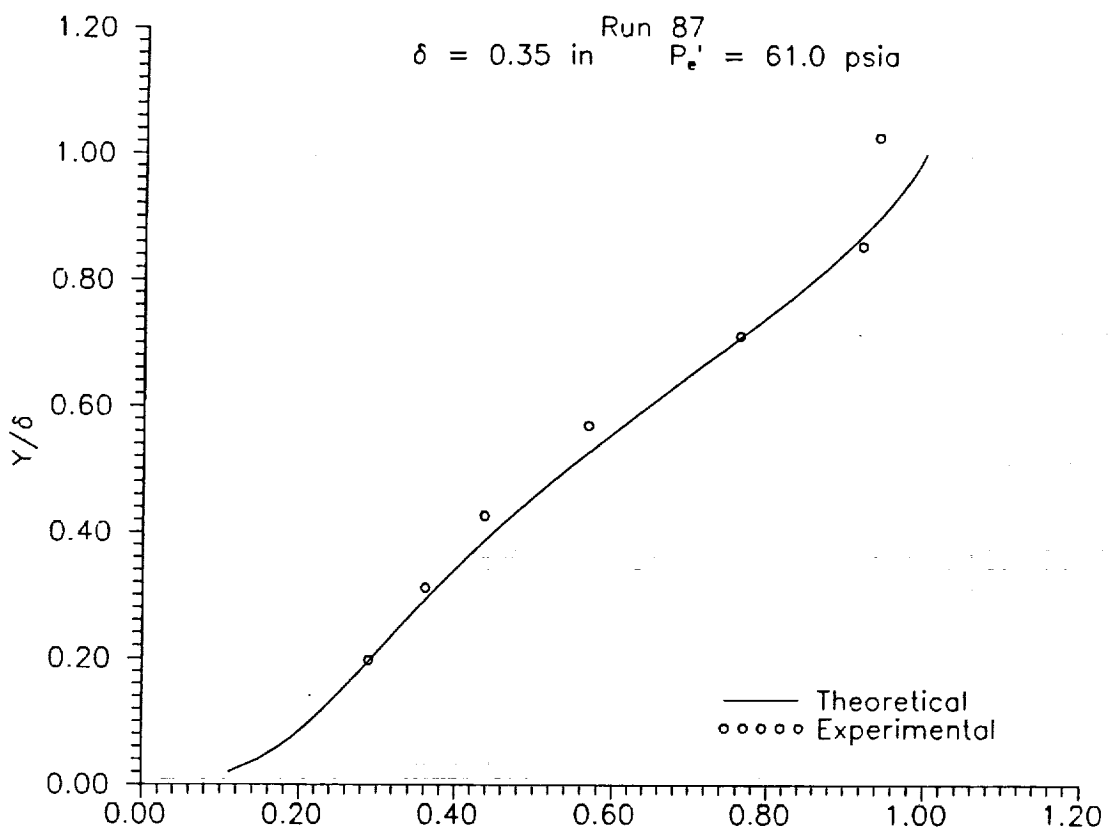
Plate length (in) 27.0

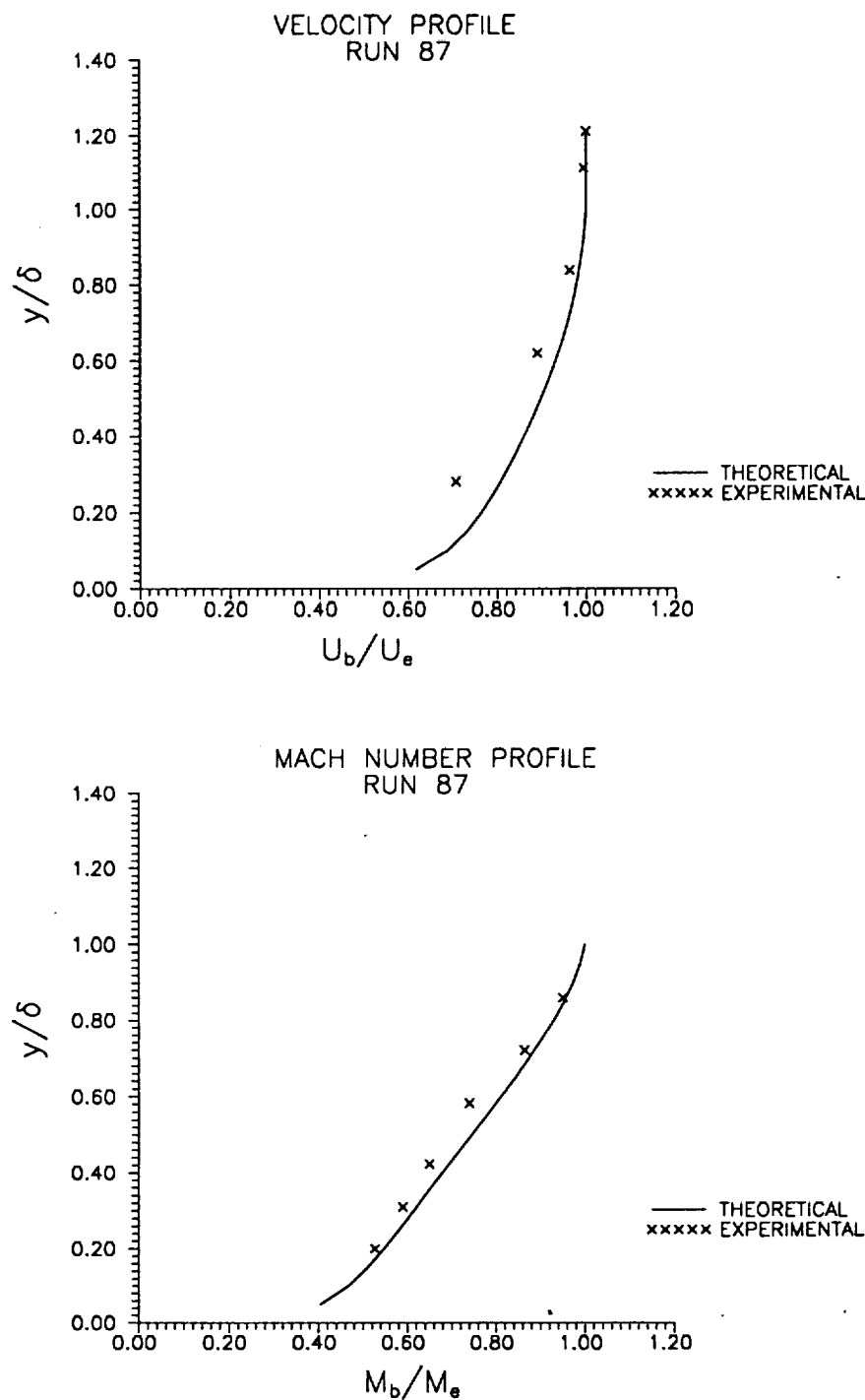
Run 87

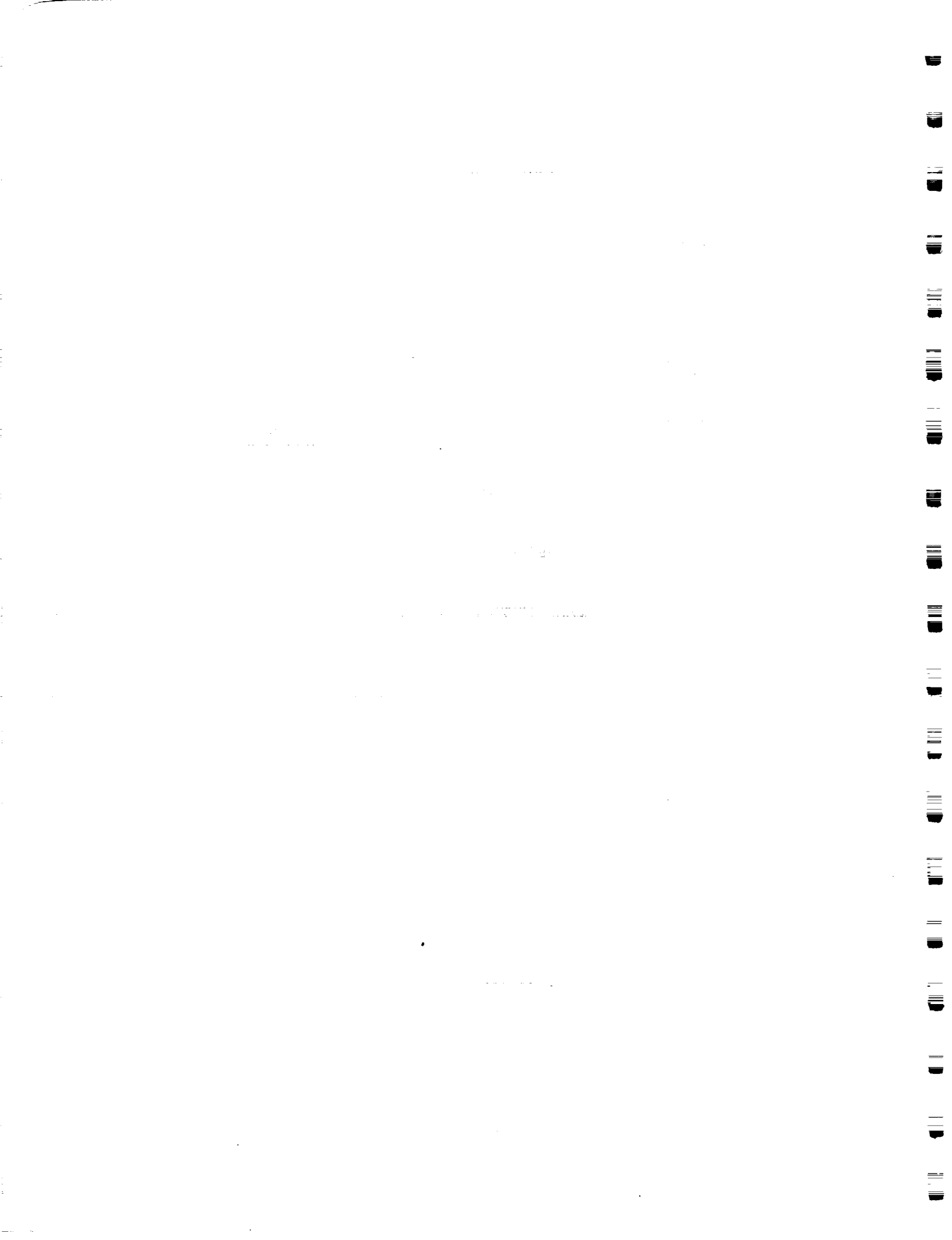
Gauge#	Location (inches)	Pressure (psia)	Gauge#	Location (inches)	Temperature deg R
BL1	0.024	Null	TT1	0.097	1299.0
BL2	0.064	17.630	TT2	0.191	Null
BL3	0.104	22.040	TT3	0.285	1771.0
BL4	0.144	26.680	TT4	0.378	1830.0
BL5	0.194	34.640	TT5	0.503	1837.0
BL6	0.244	46.530	TT6	0.628	1827.0
BL7	0.294	56.160	TT7	0.753	1840.0
BL8	0.354	57.390	TT8	0.878	1849.0
BL9	0.414	Null	TT9	1.003	Null

Pressure Data for Run 87

Total Temperature for Run 87







Appendix C

CUBDAT COMPUTER PROGRAM

Distribution of Program CUBDAT on 5-1/4" Floppy Diskettes

CUBDAT is a program which runs on an IBM PC AT or compatible computer having 640kB of RAM, hard disk, math coprocessor, graphics card and a 5-1/4" high density floppy drive. Under limited conditions, the program may be run from "MAIN_DISK", a bootable diskette which uses COMPAQ PC DOS Version 3.31. However, it is advisable to install the necessary software on the system hard disk and run the program there.

Until recently, program CUBDAT has been distributed to interested parties on a fixed number of 5-1/4", High Density (1.2MB), DOS formatted floppy diskettes. The experience gained as a result of that methodology has led to a more practical approach to handling the continually expanding database and the ability to correct errors detected after distribution. This document will discuss the rationale behind the structure of each diskette and serve as a guide for potential users.

CUBDAT, in its entirety, is delivered on four diskettes whose contents are described at the bottom of this page. However, in general practice, the data files from a single experimental study are delivered on a single diskette with the executable and configuration files needed to access them. In this instance CUBDAT may be run from diskette.

The current complete set of CUBDAT diskettes follows:

1. MAIN_DISK (All executable and configuration files);
 - A. BDYFIXTR
 - B. BICONIC3
 - C. BICONIC4
 - D. BLOWRUFF
 - E. BLUNTBOD
 - F. BLUNTLE
 - G. CURVSURF
 - H. INCIPSEP
 - I. LAMINAR
2. DISK_1 (Subdirectories noted below);
 - A. MRVPAT
 - B. MRVSAND
 - C. NASAFP
 - D. SEP-K90
 - E. SHK-SHK
 - F. SWEPTSKU
 - G. TURBFLO
3. DISK_2 (Subdirectories noted below);
 - A. SLOT_080
 - B. SLOT_120
 - C. SCANT
 - D. SMTHBLW1
 - E. SMTHBLW2
 - F. CONEFLAR
 - G. SHK-COMP
4. DISK_3 (Subdirectories noted below);
 - A. SLOT_080
 - B. SLOT_120
 - C. SCANT
 - D. SMTHBLW1
 - E. SMTHBLW2
 - F. CONEFLAR
 - G. SHK-COMP

Whenever CUBDAT is invoked the default drive and directory are checked for the existence of files "summary.fil" and "summary.mtx". An error message is delivered if either file is missing. The user is then asked to specify in which drive and directory the program is to confine its searches. Unless all files are copied to the hard disk, it is necessary to place the appropriate diskette in the floppy drive. Subsequently, a menu of options is presented which gives the user the ability to select a specific experimental run's data for plotting or tabulation. Reduced data may be stored for pressure, skin friction, force/moment, heat transfer and calorimeter measurements. Test conditions and model configuration parameters may also be displayed for individual runs. The data from a particular run is stored in an ASCII file named "run*.lts" (* = run sequence # w/o leading zeroes). These files are also capable of being "imported" to LOTUS 1-2-3.

A new feature has been incorporated to enable users to plot data from other sources for comparison with reduced data in the database. An external ASCII file named "plot.add" must be included in the directory of the study of interest to provide this capability. The form of "plot.add" is as follows:

1. The initial line contains literal data, not to exceed 75 characters, which is not processed.
2. Two integer entries: Run# and Number of sets of data, N, to follow.
[N.B. Run# < 0 --> all runs. Run#s must be given in numerical order.]
3. For each set of data a single line containing, in order:
 - a. The number of points M to be plotted.
 - b. A type# defining the measurement of interest from the following list:
1=Pressure; 2=CP; 3=Skin Friction; 4=CF; 5=Force & Moment; 6=Heat Transfer;
7=CH; 8=Q/Qo(Fay-Riddell); 9=Calorimeter; 10=CC; 11=Temperature.
c. A symbol# defining the symbol to be drawn from the following list:
0=None; 1=Arrow Up; 2=X; 3=Arrow Down; 4=Square; 5=Arrow Right; 6=Diamond;
7=Arrow Left; 8=Circle; 9=Pentagon; 10=5 Pt Star; 11=Hexagon; 12=6 Pt Star;
13=Asterisk(*); 14=Plus(+); 15=Y; 16=Y Inverted; 17=Up&Down Arrows; 18=Dot.
[N.B. Use a negative value for a symbol only plot.]
 - d. A line# selecting the line type to be used to connect data points from:
1=Solid; 2=Dotted; 3=Dot-Dash; 4=Short Dash; 5=Long Dash.
[N.B. A negative line# causes a double width line to be drawn.]
 - e. Up to eight characters, in single quotes, for the plot legend.
4. M lines containing the x,y coordinates of each point to be plotted.
5. Repeat 3 & 4 until N sets of data have been input.
6. Loop back to 2 until data to be input have been exhausted.

Plotting to the screen employs a Tektronix 4014 emulator for the PC from MicroPlot Systems Inc. The mapping of the 1024 pixels wide by 780 pixels high Tektronix plot window to the size supported by individual PCs is accomplished through a device assignment in the "config.sys" file when the system is booted. The files named "plotdev.xxx", where the extension "xxx" relates to a specific graphics adaptor, are provided for this purpose. To date, only the AT&T 6300 (works with COMPAQ plasma displays), CGA, EGA and Hercules graphics adaptors have been accounted for in the distribution.

In the course of running CUBDAT, files containing graphic information may be produced. These files will be Tektronix compatible and may be directed to the screen for review using the "draw" utility provided. It is invoked by entering the command "draw xxx", where xxx is the name of the file created using CUBDAT. If more than one

plot is present in file xxx, the image on the screen will remain until the "Enter" key is pressed for another page or the "Esc" key is struck to terminate execution. An attempt to print the information in xxx will produce nonsense unless the Tektronix language is supported. Since most current generation laser printers do not "speak" Tektronix, the "tek2ps" utility will convert plot files to PostScript, a more common language. The same file may be converted to PostScript format by entering the command "tek2ps xxx > yyy", where yyy is the name of the translated file to be printed.

MAIN_DISK contains all the programs needed to successfully access and display the reduced data stored in the other diskettes. In addition to CUBDAT, DRAW and TEK2PS, several other programs (filenames with "EXE" extensions) are included. CLR should be used instead of the DOS command CLS to clear the screen and place the prompt at the top of the display. The remaining executable files extract information from the "run*.lts" files and place it on program prescribed or user designated filenames. Each is used by first entering its name and then responding to the prompts.

Optimum use of CUBDAT can be obtained by copying all files from MAIN_DISK into a single subdirectory on the system's hard disk. CALSPAN will be assumed for the purpose of illustration but the user is free to choose any name which is unique to DOS. The "config.sys" file in the system's root directory should be edited to include the lines "files=20", "buffers=40" and "device=calspan\plotdev.?" (see below) to provide the environment required to successfully execute CUBDAT. Always transfer to the CALSPAN subdirectory by entering "cd \calspan" before invoking CUBDAT.

A slight improvement in performance can be obtained by also copying the files from the remaining diskettes into appropriately named subdirectories. If space on the hard disk is limited, CUBDAT can be directed to search for data on the floppy drive.

A list of all filenames delivered on "MAIN_DISK", with remarks enclosed in parentheses, follows:

- ASCIIDAT.EXE (appends selected run info to file ASCIIDAT.OUT)
- AUTOEXEC.BAT (consult your DOS reference manual for file's content)
- BOOTDISK.DOC (enter "TYPE BOOTDISK.DOC" to display useful info)
- CLR.EXE (use instead of "CLS" to clear screen display)
- COMMAND.COM (needed for booting from MAIN_DISK)
- CONFIG.SYS (must contain "DEVICE=PLOTDEV.?" for ?=ATT,CGA,EGA or HGC)
- CUBDAT.EXE (invoke CUBDAT where SUMMARY.FIL and SUMMARY.MTX reside)
- DRAW.EXE (draws plot files created by CUBDAT)
- GETTALL.EXE (appends selected test conditions to ALLPARMS.LTS)
- GETMODEL.EXE (appends run information to MODELSIN.LTS)
- GETTCS.EXE (appends all test conditions to TESTCONS.LIS)
- IBMBIO.COM (system hidden file)
- IBM DOS.COM (system hidden file)
- PLOTDEV.ATT (CONFIG.SYS device name for COMPAQ plasma display)
- PLOTDEV.CGA (CONFIG.SYS device name for Color Graphics Adaptor (CGA))
- PLOTDEV.EGA (CONFIG.SYS device name for Enhanced Graphics Adaptor (EGA))
- PLOTDEV.HGC (CONFIG.SYS device name for Hercules Graphics Card (HGC))
- PSTEK.PRO (required to successfully run TEK2PS.EXE)
- SUMMARY.FIL (used by CUBDAT for valid study (directory) names)
- SUMMARY.MTX (used by CUBDAT for test matrix specifications)
- TABULATE.EXE (tabulates selected calibration type(s) to named file)
- TEK2PS.EXE (translates Tektronix plot files to PostScript)

CUBDAT was created with the intention of providing a useful PC tool for accessing experimental data from Calspan's shock tunnels. In the course of time, the program has evolved based on in-house analysis and reporting needs. It is hoped that use of CUBDAT by others will lead to a greater understanding of the information contained in the data files and foster a dialogue to improve its usefulness. Toward that end, please address your comments to

John R. Moselle (716) 631-6850
Calspan Corporation
P.O. Box 400
Buffalo, NY 14225

**CUBDAT: A CUBRC Program to Access Hypersonic Experimental Database
Compiled from Studies in Calspan Shock Tunnels**

CUBDAT is a program which provides access to reduced data from a number of experimental studies conducted in Calspan's shock tunnels from 1964 to present. Data from each study are stored in ASCII files which are compatible for use with LOTUS 1-2-3. The sequence number, n, of each run performed is part of its associated filename which is of the form "RUNn.LTS". The use of appropriately named subdirectories provides the ability to discriminate data from different experimental series. A file named "CONFIGUR" must also be present in each subdirectory. It defines the single character abbreviations used in place of lengthy descriptions for model parameters related to the experiments. For instance, the phrase "Distance from the Leading Edge" might be represented by the letter "A" in the data files.

Although CUBDAT provides the user with a number of options for the plotting and tabulation of the information within the ASCII files, the ability to use the data in other contexts is essential. Toward this end, added information is provided in the form of:

1. Brief description of file organization;
2. Sample RUNn.LTS file;
3. Sample CONFIGUR file;
4. Plots derived from data in item 2.

When the CUBDAT user requests a display of run test conditions, some parameters which are not contained in the RUNn.LTS files are also reported. Their definitions follow:

H_w = Wall Enthalpy = $C_p \cdot T_w$	$[(\text{Ft/sec})^2]$
CP_f = Converts Pressure to CP = $1/Q$	$[\text{PSIA}^{-1}]$
CH_f = Converts Heat Rate to CH = $778 / (\text{Rho} \cdot U \cdot (H_o - H_w))$	$[(\text{BTU/Ft}^2/\text{sec})^{-1}]$
QoFR= Fay-Riddell* Heat Transfer to 3" Diam. Cylinder	$[\text{BTU/Ft}^2/\text{sec}]$

* Fay, J.A. and Riddell, F.R., "Theory of Stagnation Point Heat Transfer in Dissociated Air," Journal of Aeronautical Sciences, Vol. 25, No. 2

Organization of Information in RUNn.LTS Files

Line(s)	Description of Entry	Units
1	The run sequence number is the initial entry in the file. Lines 2 thru 7 contain the number of entries for the type of measurement [units] indicated:	
2	Pressure	[PSIA]
3	Skin Friction	[PSIA]
4	Force/Moment	[LBF/IN-LBF]
5	Heat Transfer	[BTU/Ft ² /SEC]
6	Calorimeter	[BTU/Ft ² /SEC]
7	Pressure (for separation from data levels in line 2)	[PSIA]

Let N be the total number of entries for all the types of measurement. Then, there follow three groups of N entries whose contents are:

Line(s)	Description of Entry
8,N+7	Group 1 -- Gauge labels within double quotes which may be preceded by a single non-blank character
N+8,2•N+7	Group 2 -- Gauge positions (inches) relative to a reference point provided in report documentation
2•N+8,3•N+7	Group 3 -- Data level in units appropriate to the type of measurement a) Heat transfer measurements may contain a second entry for the temperature at the surface in ⁰ R b) "N" indicates no measurement or nulled data

Thirteen values, one per line, corresponding to some of the conditions during the test follow:

Line(s)	Description of Entry	Units
3•N+8	Mi = Shock Tube Incident Shock Mach#	
3•N+9	Po = Reservoir Total Pressure	[PSIA]
3•N+10	Ho = Reservoir Total Enthalpy	[(Ft/sec) ²]
3•N+11	To = Reservoir Total Temperature	[⁰ R]
3•N+12	M = Freestream Mach#	
3•N+13	U = Freestream Velocity	[Ft/sec]
3•N+14	T = Freestream Temperature	[⁰ R]
3•N+15	P = Freestream Static Pressure	[PSIA]
3•N+16	Q = Dynamic Pressure = ½ • Rho • U ² /144	[PSIA]
3•N+17	Rho = Freestream Density	[Slugs/Ft ³]
3•N+18	Mu = Freestream Viscosity	[Slugs/Ft-sec]
3•N+19	Re = Freestream Reynolds Number	[Ft ⁻¹]
3•N+20	Po' = Pitot Pressure	[PSIA]

The remaining lines in the file contain a single character abbreviation from file CONFIGUR in column one followed by the datum for the associated model parameter.

Organization of Information in RUNn.LTS Files

Sample RUNn.LTS File

Entry	Line#	Comment
59	1	Run# is 59
24	2	24 Pressure gauges
0	3	No Skin Friction data
0	4	No Force/Moment data
32	5	32 H.T. gauges
0	6	No Calorimeter data
0	7	No extra Pressure data

N = 24+32 = 56 Gauge labels follow:

Entry	Line#	Comment
"P 30 "	8	Pressure label
"P 28 "	9	Pressure label
"P 26 "	10	Pressure label
"P 25 "	11	Pressure label
"P 24 "	12	Pressure label
"P 23 "	13	Pressure label
"P 22 "	14	Pressure label
"P 21 "	15	Pressure label
"P 20 "	16	Pressure label
"P 15 "	17	Pressure label
"P 19 "	18	Pressure label
"P 14 "	19	Pressure label
"P 18 "	20	Pressure label
"P 13 "	21	Pressure label
"P 17 "	22	Pressure label
"P 12 "	23	Pressure label
"P 16 "	24	Pressure label
"P 11 "	25	Pressure label
"P 10 "	26	Pressure label
"P 9 "	27	Pressure label
"P 7 "	28	Pressure label
"P 5 "	29	Pressure label
"P 3 "	30	Pressure label
"P 1 "	31	Pressure label
"HT 32 "	32	Heat Transfer label
"HT 31 "	33	Heat Transfer label
"HT 29 "	34	Heat Transfer label
"HT 28 "	35	Heat Transfer label
"HT 25 "	36	Heat Transfer label

Organization of Information in RUNn.LTS Files

"HT 24 "	37	Heat Transfer label
"HT 64 "	38	Heat Transfer label
"HT 65 "	39	Heat Transfer label
"HT 66 "	40	Heat Transfer label
"HT 67 "	41	Heat Transfer label
"HT 68 "	42	Heat Transfer label
"HT 69 "	43	Heat Transfer label
"HT 70 "	44	Heat Transfer label
"HT 10 "	45	Heat Transfer label
"HT 71 "	46	Heat Transfer label
"HT 9 "	47	Heat Transfer label
"HT 7 "	48	Heat Transfer label
"HT 6 "	49	Heat Transfer label
"HT 5 "	50	Heat Transfer label
"HT 4 "	51	Heat Transfer label
"HT 3 "	52	Heat Transfer label
"HT 2 "	53	Heat Transfer label
"HT 1 "	54	Heat Transfer label
"HT 62 "	55	Heat Transfer label
"HT 61 "	56	Heat Transfer label
"HT 59 "	57	Heat Transfer label
"HT 58 "	58	Heat Transfer label
"HT 57 "	59	Heat Transfer label
"HT 56 "	60	Heat Transfer label
"HT 55 "	61	Heat Transfer label
"HT 54 "	62	Heat Transfer label
"HT 53 "	63	Heat Transfer label

56 Gauge positions follow:

Entry	Line#	Comment
0.0000	64	Press. gauge location
0.3750	65	Press. gauge location
0.7500	66	Press. gauge location
0.9375	67	Press. gauge location
1.1250	68	Press. gauge location
1.3125	69	Press. gauge location
1.5000	70	Press. gauge location
1.6875	71	Press. gauge location
1.8125	72	Press. gauge location
1.8750	73	Press. gauge location
1.9375	74	Press. gauge location
2.0000	75	Press. gauge location
2.0625	76	Press. gauge location

Organization of Information in RUNn.LTS Files

2.1250	77	Press. gauge location
2.1875	78	Press. gauge location
2.2500	79	Press. gauge location
2.3125	80	Press. gauge location
2.3750	81	Press. gauge location
2.5000	82	Press. gauge location
2.6875	83	Press. gauge location
3.0625	84	Press. gauge location
3.4375	85	Press. gauge location
3.8125	86	Press. gauge location
4.1875	87	Press. gauge location
1.2600	88	H.T. gauge location
1.3400	89	H.T. gauge location
1.5000	90	H.T. gauge location
1.5800	91	H.T. gauge location
1.8200	92	H.T. gauge location
1.9000	93	H.T. gauge location
2.0250	94	H.T. gauge location
2.0500	95	H.T. gauge location
2.0750	96	H.T. gauge location
2.1000	97	H.T. gauge location
2.1250	98	H.T. gauge location
2.1500	99	H.T. gauge location
2.1750	100	H.T. gauge location
2.1870	101	H.T. gauge location
2.2000	102	H.T. gauge location
2.2080	103	H.T. gauge location
2.2500	104	H.T. gauge location
2.2707	105	H.T. gauge location
2.2916	106	H.T. gauge location
2.3125	107	H.T. gauge location
2.3334	108	H.T. gauge location
2.3543	109	H.T. gauge location
2.3753	110	H.T. gauge location
2.3753	111	H.T. gauge location
2.4553	112	H.T. gauge location
2.6153	113	H.T. gauge location
2.6953	114	H.T. gauge location
2.7753	115	H.T. gauge location
2.8553	116	H.T. gauge location
2.9353	117	H.T. gauge location
3.0153	118	H.T. gauge location
3.0953	119	H.T. gauge location

Organization of Information in RUNn.LTS Files

56 Data levels follow:

Entry		Line#	Comment
"N"		120	Pressure data
2.9817E+00		121	Pressure data
4.8875E+00		122	Pressure data
4.4496E+00		123	Pressure data
2.4228E+00		124	Pressure data
1.2506E+00		125	Pressure data
9.3307E-01		126	Pressure data
2.3393E+00		127	Pressure data
5.2630E+00		128	Pressure data
7.0792E+00		129	Pressure data
1.3301E+01		130	Pressure data
1.7795E+01		131	Pressure data
3.1199E+01		132	Pressure data
4.9766E+01		133	Pressure data
1.0579E+02		134	Pressure data
8.7510E+01		135	Pressure data
6.0132E+01		136	Pressure data
3.1908E+01		137	Pressure data
2.5303E+01		138	Pressure data
2.5834E+01		139	Pressure data
2.1739E+01		140	Pressure data
1.6147E+01		141	Pressure data
9.5870E+00		142	Pressure data
4.3132E+00		143	Pressure data
1.6407E+01	5.5659E+02	144	H.T. & SurfaceT data
8.2543E+00	5.5309E+02	145	H.T. & SurfaceT data
8.0836E+00	5.5710E+02	146	H.T. & SurfaceT data
1.2132E+01	5.6029E+02	147	H.T. & SurfaceT data
4.9894E+01	6.4553E+02	148	H.T. & SurfaceT data
7.9512E+01	7.1050E+02	149	H.T. & SurfaceT data
2.0241E+02	8.3680E+02	150	H.T. & SurfaceT data
"N"		151	H.T. & SurfaceT data
3.0849E+02	8.7951E+02	152	H.T. & SurfaceT data
3.9993E+02	9.1072E+02	153	H.T. & SurfaceT data
4.6382E+02	9.2251E+02	154	H.T. & SurfaceT data
5.5120E+02	9.3979E+02	155	H.T. & SurfaceT data
6.3309E+02	9.5299E+02	156	H.T. & SurfaceT data
7.6012E+02	9.8267E+02	157	H.T. & SurfaceT data
7.3708E+02	9.7058E+02	158	H.T. & SurfaceT data
7.3548E+02	9.5051E+02	159	H.T. & SurfaceT data
5.1358E+02	8.9748E+02	160	H.T. & SurfaceT data

Organization of Information in RUNn.LTS Files

6.0265E+02	9.2167E+02	161	H.T. & SurfaceT data
6.2253E+02	9.2078E+02	162	H.T. & SurfaceT data
4.8431E+02	8.6673E+02	163	H.T. & SurfaceT data
4.3188E+02	8.4131E+02	164	H.T. & SurfaceT data
3.4912E+02	8.0254E+02	165	H.T. & SurfaceT data
3.2089E+02	7.8725E+02	166	H.T. & SurfaceT data
3.4024E+02	7.9381E+02	167	H.T. & SurfaceT data
2.1714E+02	7.2924E+02	168	H.T. & SurfaceT data
2.0662E+02	7.1388E+02	169	H.T. & SurfaceT data
1.7707E+02	6.9167E+02	170	H.T. & SurfaceT data
1.6153E+02	6.8830E+02	171	H.T. & SurfaceT data
1.4524E+02	6.7237E+02	172	H.T. & SurfaceT data
1.4748E+02	6.7381E+02	173	H.T. & SurfaceT data
1.2867E+02	6.5669E+02	174	H.T. & SurfaceT data
1.1740E+02	6.4460E+02	175	H.T. & SurfaceT data

13 Test conditions follow:

Entry	Line#	Comment
3.4120E+00	176	Mi
1.3520E+03	177	Po
1.8554E+07	178	Ho
2.8191E+03	179	To
8.0357E+00	180	M
5.8716E+03	181	U
2.2201E+02	182	T
1.1847E-01	183	P
5.3608E+00	184	Q
4.4783E-05	185	Rho
1.8344E-07	186	Mu
1.4334E+06	187	Re
9.9386E+00	188	Po'

Organization of Information in RUNn.LTS Files

Model parameters follow:

Entry	Line#	Comment
A 15.0	189	Parameter abbreviation, Value
B Blunt	190	Parameter abbreviation, Value
C 22.5	191	Parameter abbreviation, Value
D Yes	192	Parameter abbreviation, Value
E 20	193	Parameter abbreviation, Value
F 50	194	Parameter abbreviation, Value

A possible CONFIGUR file for the above model parameters is shown below.

A	Angle of Attack (Degrees)
B	Nose Type --
C	Model Width (Inches)
D	Angular Trip (Yes/No)
E	Bluntness Ratio (Rn/Rb) (Percent)
F	Heat Transfer Reference Run Number =

